COOL-WATER CARBONATE SEDIMENTOLOGY AND SEQUENCE STRATIGRAPHY OF THE WAITAKI REGION, SOUTH ISLAND, NEW ZEALAND

A thesis submitted in partial fulfilment of the requirements

for the Degree of

Doctor of Philosophy in Geology

in the Department of Geological Sciences,

University of Canterbury

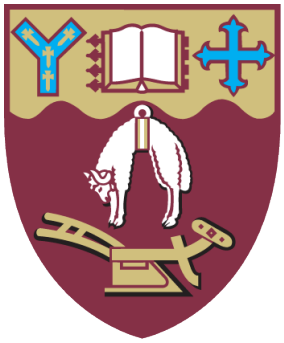

by Nicholas Kim Thompson

2013

Frontispiece

From top, and left to right: Limestone outcrop at Earthquakes; Cross-bedding at Waihao; Karst at Cambells Beach; Rolling countryside of Waitaki; Victorian architecture in Oamaru, made from Ototara Limestone quarried in the Waitaki.

"In all these various formations our coprolites form records of warfare, waged by successive generations of inhabitants of our planet on one another: the imperishable phosphate of lime, derived from their digested skeletons, has become embalmed in the substance and foundations of the everlasting hills; and the general law of Nature which bids all to eat and be eaten in their turn, upon our globe; the carnivores in each period of the world's history fulfilling their destiny office – to check express progress of life, and maintain the balance of creation" (Buckland, 1835)

TABLE OF CONTENTS

LIST OF FIGURES

LIST OF TABLES

ACKNOWLEDGEMENTS

Foremost I thank my supervisors, Kari Bassett and Catherine Reid, for their invaluable advice, ideas, and guidance throughout my research. I gratefully acknowledge funding from the Canterbury Community Trust Doctoral Scholarship, which made this work possible. Additional funding for fieldwork and AAPG Long Beach conference attendance (2011) came from the Mason Trust, Department of Geological Sciences. I am also grateful to financial support from a GSNZ Young Researcher Travel Grant to attend AGU in 2011.

This research involved a range of laboratory work at the University of Canterbury and elsewhere, and I thank the following people for their assistance and input: Rob Spiers, Chris Grimshaw, Travis Horton, Kerry Swanson, Sacha Baldwin-Cunningham and John Southward at the University of Canterbury, and Brent Pooley and Luke Easterbrook at University of Otago. For assistance in the field and helpful discussions, I thank Peir Pufahl (Acadia University, Canada). Thanks go to Nicola and Peter Mountain (Oamaru) for their hospitably and kindness during fieldwork. Sister Mary and Bruce Comfort are thanked for showing me new outcrops and for their interest in my work.

Special thanks go to my office mates Paul Ashwell and Sam McColl for a rewarding and enjoyable work atmosphere, as well as some friendly competition (you earned that whiskey Sam!). Also Nick Riordan, Felix Von Aulock, Sharon Hornblow, and all the students in the Department for making the whole experience more memorable and fun! I thank Murray Matthews for his long hours of proofreading and advice in the final drafts, and Barbara Matthews for encouragement and amazing cooking during my lengthy and productive stays with them at Condell Gardens. I must cite the Canterbury earthquakes for providing additional (and unforgettable) challenges, and for bringing people together. And finally, to my wonderful wife Naomi, for her love, support, boundless encouragement, and unending practical help. I could never have done this without you.

ABSTRACT

In the mid-Cenozoic, New Zealand underwent slow subsidence interspersed with unconformity development, however significant controversy exists around both the extent of submergence below sea level during this period of maximum drowning, as well as the causes of these unconformities. Detailed field observations, combined with extensive petrographic analyses, stable isotopes, cathodoluminescence, and thin section staining were used to develop lithofacies, depositional, and sequence stratigraphic models of the mid-Cenozoic succession in the Waitaki region, South Island, to address these controversies.

Twelve facies types have been described for Late Eocene-Early Miocene sedimentary rocks, leading to the identification of two major (Mid Oligocene & Early Miocene) and one minor (Late Oligocene) sequence boundaries. Surtseyan volcanism in the east produced a palaeohigh, resulting in a submerged rimmed cool-water carbonate platform, with low-lying land to the west. This eastern palaeohigh developed karst during sea-level lowstands, which correlate with silty submarine bored hardgrounds in the west. Glauconitic and phosphatic facies deposited during early marine transgression suggest an authigenic factory supplied by terrigenous clays existed during lowered sea level that was progressively shut down in favour of a carbonate factory as sea level rose and terrigenous supply decreased. The eastern palaeohigh served to nucleate this carbonate factory by raising the sea floor above the influence of siliciclastic sediment supply and providing a shallow substrate for marine colonisation. The higher energy eastern facies display dissolution of aragonitic taxa, while deeper western facies retained an aragonitic assemblage. This early bathymetric high created a barrier to submarine currents, but was gradually reduced by erosion during subsequent lowstands. Calcareous facies were often subjected to minor seafloor cement precipitation to shallow burial diagenesis, while eastern facies developed some meteoric cement during subaerial exposure.

Comparisons between sea-level change in the study area and the New Zealand megasequence indicate eustatic changes as the primary driver of water depth in the Waitaki region until the development of the modern plate boundary in the Early Miocene.

CHAPTER 1 – INTRODUCTION

1. Introduction

The mid-Cenozoic Eocene to Miocene period was a time of major transformation for New Zealand as a result of significant tectonic and oceanographic changes occurring both locally and globally. These changes included climate change, as the world moved from the warmer "greenhouse" conditions of the Mesozoic-Eocene to the present "icehouse" environment accompanied by glaciation of Antarctica and followed by eustatic sea-level falls (Kennett and von der Borch, 1986; Lawver *et al*., 1992; Zachos *et al*., 1992; Jenkins, 1993). New Zealand, meanwhile, had been rifting from Gondwana since the Late Cretaceous (Laird and Bradshaw, 2004), and developing into a thinned block of continental crust which had been eroding without any significant uplift for the first half of the Cenozoic. This resulted in slow subsidence and the creation of an oceanic plateau at the same time as significant unconformity development in the region during the Late Palaeogene (Bradshaw, 1989; Lemarche *et al*., 1997; Sutherland, 1999). This leaves open the question of how much land was exposed above sea level during the Oligocene, if any-which has been a point of contention for many years (Suggate, *et al*., 1978; Campbell and Landis, 2001; Lee *et al*., 2001; Gibbs, 2006). Changes also occurred within oceanographic regimes, resulting in the creation of the Antarctic Circumpolar Current (ACC) (Jenkins, 1974; Barker and Burrell, 1982; Berggren and Prothero, 1992; Diester-Haass and Zahn, 1996; Exon *et al*., 2002), leading some to suggest this as a cause for the regional unconformities rather than Oligocene sea-level change (Carter and Landis, 1972; Carter, 1985; Carter *et al*., 2004). The sedimentary record preserved within the Waitaki region, located in North Otago and South Canterbury, provides the opportunity to learn more

about the effects these tectonic and oceanographic changes had on southern New Zealand and its environment during this time.

The mid-Cenozoic is a very important period in the history of the Waitaki region, although the mechanisms of its development are not yet fully understood. In particular, the existence of mid-Cenozoic unconformities has presented a challenge to understanding the relationship between the surfaces involved in the regional setting (Lever, 2007), and further work is needed to correlate and interpret these enigmatic horizons. The most well-known of these unconformities is the Marshall Paraconformity – a regional mid-Oligocene unconformity found in a number of localities throughout South Island and parts of North Island, New Zealand, and possibly as far away as Australia (Carter and Landis, 1972; Carter, 1985; Lewis, 1992). While the term has been in use since it was first coined, there are a number of other unconformities present above the Marshall in the Late Oligocene (Carter and Landis, 1982; Lewis and Belliss, 1984; Jenkins, 1987), and there has been some argument that the Marshall is no more significant than others found in the strata (Findlay, 1980). Without interpretation of these surfaces, and the lithologies contained between them, it is not possible to understand the effect that global events such as the development of the ACC, and regional processes such as volcanism and tectonic change, have had on this region and, by inference, New Zealand as a whole.

The research reported here addresses some of these uncertainties surrounding sea-level change and unconformity development. It focuses principally on the record within the Waitaki region, and then uses this to determine probable causes of relative sea-level change and how these may be applied to inform events in the greater New Zealand region.

1.1 New Zealand geological setting

The New Zealand landmass began as an accreted part of the Pacific-oriented Gondwana continental margin along with Antarctica and Australia. Prior to the Late Cretaceous, this part of Gondwana was a convergent margin and arc system (Bradshaw, 1989), changing to a zone of extension that led to New Zealand's separation from the Gondwana landmass (Laird and Bradshaw, 2004). This, in turn, led to a period of rifting and development of a passive margin through to the mid-Cenozoic, following which the current plate boundary that runs through New Zealand developed, reversing the period of passive subsidence and establishing the general tectonic regime as it exists today (Fulthorpe *et al*., 1996; Sutherland, 1999). Here the tectonic and palaeoceanographic settings of New Zealand are described, including a more detailed description of the overall mid-Cenozoic first-order megasequence.

1.1.1 Tectonic setting and basin formation

New Zealand is currently a highly tectonically active landmass, resulting from its position astride the major Pacific-Australian plate boundary. Previously, however, this area had been a zone of overall tectonic stability, with passive New Zealand-wide subsidence following its rifting from Gondwana in the mid to Late Cretaceous (Mortimer, 1993; Fulthorpe *et al*., 1996; Lemarche *et al*., 1997; Little *et al*., 1999; Sutherland, 1999; Kamp, 2001). During the Late Palaeozoic through to the Late Cretaceous the tectonic regime was characterised by convergent margin tectonics and probably comprised more than one subduction zone and associated arc system (Bradshaw, 1989). Beginning around 105 Ma, the regime changed to one of crustal extension, with final separation of the subcontinent of Zealandia from Gondwana by ~ 83 Ma (Sutherland, 1999; Laird and Bradshaw, 2004; Davy, 2006). This subcontinent of Zealandia comprises the largely

submerged continental crust, of which the subaerial component makes up the main islands of New Zealand. By the Late Cretaceous a series of low-lying islands had formed, and the accumulation of sediment over the basement had commenced following onset of regional subsidence as rifting continued and the Zealandia landmass moved further from Gondwana (Landis *et al*., 2008). Continued rifting resulted in cooling of the thinned continental crust and the development of a widespread transgression over a 40 My period between the Cretaceous and the Oligocene, with maximum inundation during the Late Oligocene (Carter, 1988). By ~ 45 Ma, a new plate boundary propagated through New Zealand along the current Pacific-Australian plate boundary, and between 45 Ma and 30 Ma the pole of Australia-Pacific rotation had closed in on New Zealand (Sutherland, 1995). Following the Oligocene there was a major change in tectonic regime with the development of the modern strike-slip plate boundary expressed in the current Alpine Fault, ending the transgressive sequence and beginning a general marine regressive sequence during the Miocene (Molnar *et al*., 1975; Carter and Norris, 1976; Norris *et al*., 1978). This thesis focuses primarily on the latest stages of transgression and the period of maximum flooding that was occurring around Zealandia between the Eocene and the Miocene.

1.1.2 Global palaeoceanographic and palaeoclimatologic setting

Palaeogeographic and palaeoclimatic reconstructions indicate an Eocene world which differed markedly from today's, with forests covering much of Antarctica, and palm trees growing in Alaska (Gibbs, 2006). While India had rifted from Gondwana and was colliding with Asia at this time, South America, Australia, and Antarctica were still connected as a remnant Gondwana (Case, 1988). Ocean circulation patterns obviously differed significantly from today's, with high eustatic sea levels (Vail *et al*., 1991; Miller *et al*., 2005). Tectonic changes occurring at the start of the Oligocene brought about the

opening of the passage between Antarctica and Australia and saw the beginning of the first circum-Antarctic current, resulting in the initiation of deep-water circulation (Berggren and Prothero, 1992; Diester-Haass and Zahn, 1996; Nelson and Cooke, 2001; Exon *et al*., 2002). This led to progressive global cooling (Zachos *et al*., 1994) and the development of the ice-sheet now associated with Antarctica (Zachos *et al*., 1992), and with a global drop in sea-level of between 40-75 m around the Eocene to Oligocene boundary (Kominz & Pekar, 2001; Pekar et al 2002; Pekar & Christie-Blick, 2008). This drop in sea level is generally attributed to a marked increase in ice volume in Antarctica (Miller et al., 1991; Zachos et al., 2001; Miller et al., 2005). All of these changes ushered in the oceanic and atmospheric circulation patterns that can be observed today, where icehouse conditions prevail over the greenhouse that existed during the Eocene. It is this transitional period that is the principle focus of this thesis.

Palaeoceanographic and palaeoclimatological effects are principal among the many different, yet inconclusive, proposals put forward as to what may have caused the Marshall Paraconformity (Lever, 2007) - a significant mid-Oligocene unconformity found across the South Island (Carter and Landis, 1972; Carter, 1985; Lewis, 1992). Eustatic sea-level fall as a result of glaciation of the Antarctic continent has been proposed as a likely cause due to the presence of karst surfaces indicative of sub-aerial erosion (Vella, 1967; Loutit and Kennett, 1981). It has been argued, however, that some of the dates of the unconformities at various locations do not correlate well with the onset of this event, as based on eustatic sea-level fall shown in the Vail curves occurring during the hiatus and not at its inception (Vail *et al*., 1977; Fulthorpe *et al.,* 1996; Lever, 2001). It has also been suggested that these hiatus events were non-depositional rather than erosional, attributing the karst features to submarine dissolution and indicating the lack of karst in other locations containing these unconformities (Carter, 1985; 1988; Lewis, 1992). Another possible cause

proposed is non-deposition as the result of the development of the ACC in the Early Oligocene (Carter, 1985; Carter *et al*., 2004). The initial proto-current would have been a shallow flow around the earliest Oligocene with the opening of the Drake Passage, followed by deep circulation occurring by the Late Oligocene (Fulthorpe *et al*., 1996; Pfuhl and McCave, 2005). It has been suggested that this event would have caused a condensing of the stratigraphic record such as is observed in the Canterbury Basin, as well as hardground development, phosphatisation, current-induced sedimentary structures, and even possibly the karsted deposits that have been attributed to subaerial erosion (Carter *et al*., 2004). While this later deep current would have swept the shelf clean, causing erosion of the strata and stopped any new deposition from settling, it has further been proposed that the earlier warm current might have actually helped the deposition of thick limestones during this period without causing any erosion (Stickley *et al*., 2004). Lever (2007) argues that the problem with the development of the ACC being the sole cause of the unconformities is that the same or closely related surfaces would be expected in all locations with the same or very similar age, with evidence of erosion prevalent throughout, but this is not observed.

1.1.3 Mid-Cenozoic tectonic history of New Zealand

The tectonic history of New Zealand during the mid Cenozoic (mid Eocene to mid Miocene) revolves primarily around the development of the Australian-Pacific plate boundary (King, 2000). This boundary began to develop in the mid to Late Eocene around a zone of extension to the south of New Zealand (Molnar *et al*., 1975; Carter and Norris, 1976; Norris *et al*., 1978; King, 2000), following which it began to propagate northward between the Late Eocene and Oligocene, reaching as far as southern Taranaki (Carter and Norris, 1976; King and Thrasher, 1996; King, 2000). This led to the development of a

number of small north-south trending basins through the country (King, 2000). Concurrently, subduction to the north of New Zealand led to the development of reverse faulting in northern New Zealand, which was later to link up with the system developing from the south (Müller *et al*., 2000; Stagpole and Nicol, 2008).

Oligocene New Zealand continued to develop as a passive margin (Ballance, 1993), with active extension prevalent to the south producing subsiding basins (Turnbull *et al*., 1993), while subduction to the north of New Zealand led to the development of arc volcanism (Hayward, 1993). Deformation along the tectonic zone linking the southern extension with the northern subsidence saw the development of major north-south-trending en echelon fault systems (King, 1990; 2000). Further propagation of the southern extensional regime resulted in mild uplift and folding in northeastern South Island (Field *et al*., 1989; Browne, 1995), while uplift was also observed in the Taranaki Region of western North Island (Nelson *et al*., 1994).

By the beginning of the Miocene, transcurrent development of the modern Alpine Fault had begun to develop (Ballance, 1976; Kamp, 1986a; King, 2000; Batt *et al*., 2004; Schellart *et al*., 2006). This new major fault expressed the boundary between the Pacific and Australian plates, cutting across the earlier extensional basins formed during the Eocene and Oligocene (Ballance, 1976; Kamp, 1986a, 1986b). This saw the reactivation of old fault systems along the transfer zone as reverse faults, resulting in uplift and adjacent basin subsidence (Kamp *et al*., 1996; Kamp *et al*., 1999), as well as the development of a zone of compression around central New Zealand, producing a change from carbonate sedimentation to terrigenous facies (Kamp, 1986a; King *et al*., 1999; King, 2000). This tectonic regime continues to the present day.

1.1.4 New Zealand mid-Cenozoic sequence stratigraphic cycle

The New Zealand mid-Cenozoic post-rift cycle, leading up to and immediately following, the period of maximum flooding, can be divided into the following episodes as illustrated in Fig. 1.1 (Carter, 1985; Fulthorpe *et al*., 1996; King *et al*., 1999):

(1) The Cretaceous-Oligocene transgression and passive tectonic setting;

(2) Late Oligocene highstand representing the period of maximum flooding; and

(3) The Miocene-Recent regression and tectonic uplift.

1.1.4.1 Cretaceous-Oligocene transgression

The Cretaceous-Oligocene transgressive sequence represents a relative rise in sea-level associated with subsidence following rifting. Seismic profiling of the Canterbury Basin (Fulthorpe and Carter, 1989; Fulthorpe *et al*., 1996) has shown major reflectors onlapping basement, with a shallow seaward dip in geometry indicative of a ramp morphology; and with some onlap occurring against these reflectors, suggesting that they are sequence boundaries. These sequence boundaries can be traced along continuous surfaces, although faint clinoform reflectors occurring within a few sequences may represent additional systems tracts, indicating that transgression might have been episodic and could have been accompanied by short periods of stillstand or even sea-level fall (Fulthorpe, 1991; Fulthorpe *et al*., 1996).

1.1.4.2 Late Oligocene highstand

Maximum flooding of New Zealand occurred in the Late Oligocene, illustrated by a falling off of terrigenous sediments and the deposition of widespread carbonates all over New Zealand (Fig. 1.1) (Fleming, 1962; Norris *et al*., 1978; Suggate *et al*., 1978). These sediments often form part of a condensed stratigraphic record that can contain a number of

unconformities. Local sea levels during this time are not known accurately, but as Fulthorpe *et al*. (1996) point out, this is crucial to determining the cause of the unconformities and the history of New Zealand during this time.

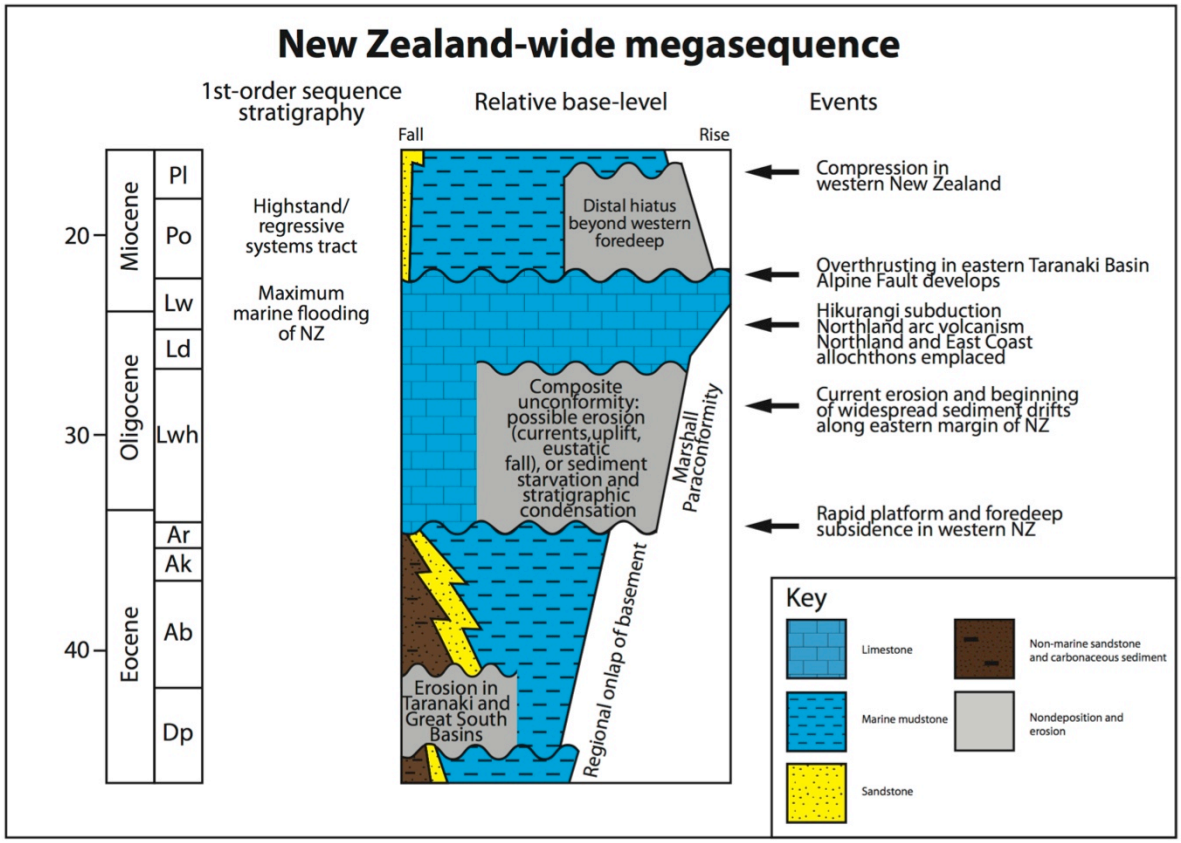

Figure 1.1. Summary stratigraphy illustrating the mid-Cenozoic New Zealand megasequence cycle of transgression, highstand, and regression, as well as the major events and associated sediment types. Modified from King *et al*. (1999).

1.1.4.3 Miocene-Recent regression

The Miocene regression began in response to tectonic uplift caused by the development of the strike-slip Alpine Fault and an associated increase in terrigenous sediment supply (Norris *et al*., 1978). This sediment resulted in eastwards progradation of shelf sediments, beginning in the Late Oligocene or Early Miocene (Fulthorpe *et al*., 1996). Seismic evidence for sediment drifts in offshore Canterbury suggests the existence

of strong current activity during this early phase of deposition, with these drifts contributing to the seaward progradation of the sedimentary succession in some areas of that basin (Fulthorpe and Carter, 1991).

1.1.5 Summary of New Zealand mid Cenozoic Palaeogeography

The mid Cenozoic palaeogeography of New Zealand was significantly different from that seen today, influenced by the tectonic setting and the 1st order megasequence (Sections 1.1.3 and 1.1.4). Fig. 1.2 presents three maps of New Zealand palaeogeography, shown during the mid Eocene, Late Oligocene, and Early Miocene, with the current coastlines overlain for reference. These maps show the water depth changes that occurred across Zealandia throughout this period, and the spatial relationships between the modern basins during this period.

The mid Eocene developed as a period of decreasing siliciclastic supply onto a predominantly shelf setting, with significant land still exposed. Continued transgression through to the Late Oligocene led to extensive (and possibly complete) submergence of the Zealandia landmasses. Shelfal settings were still prominent but with the more distal landmasses the supply of siliclastic sediment was massively reduced to many areas. With the development of the Pacific-Australian plate boundary in the Early Miocene, however, uplift induced by the new compressional regime saw the re-emergence of land and the return of significant siliciclastic supply to the basins of New Zealand.

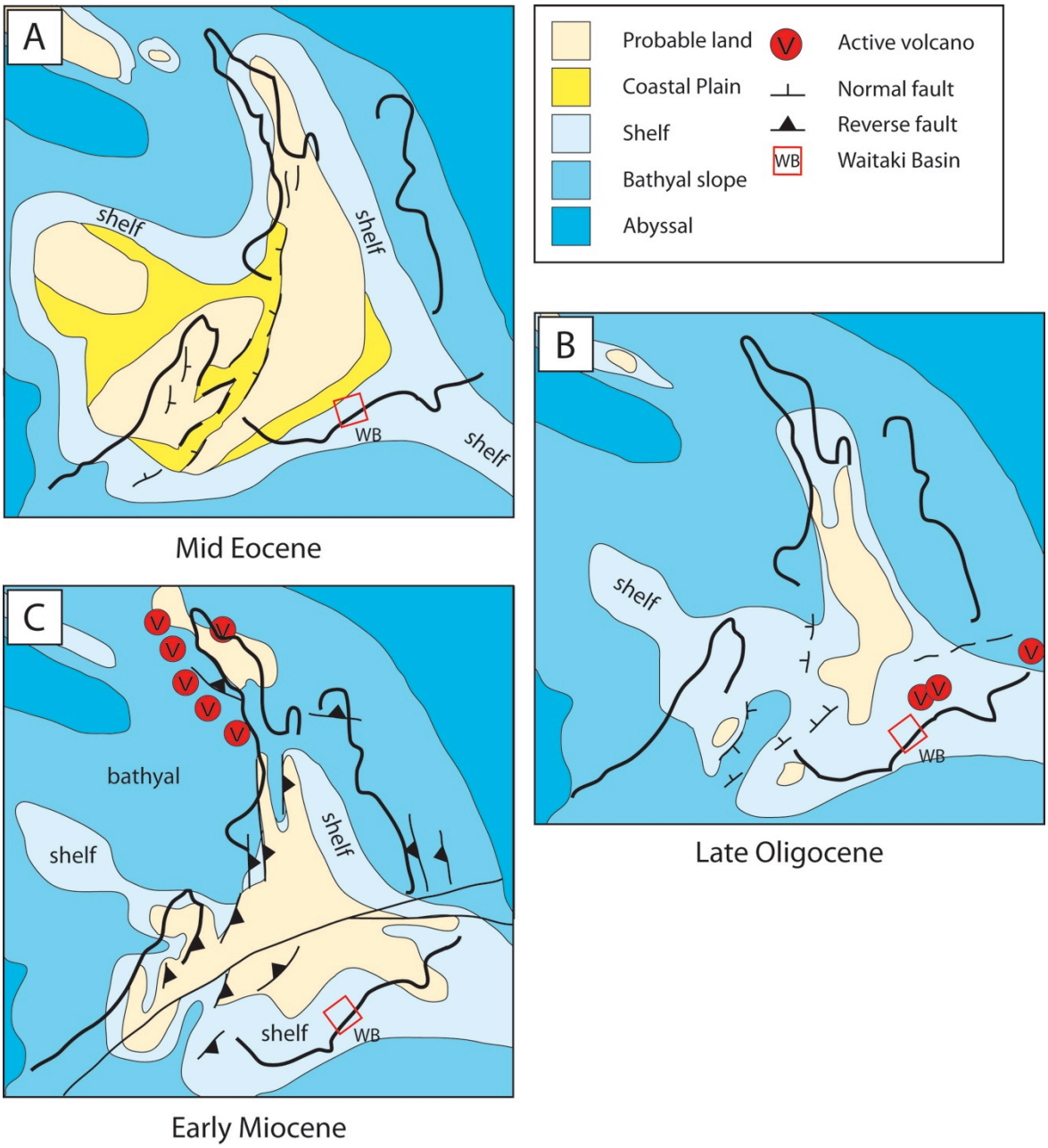

Figure 1.2. New Zealand mid Cenozoic palaeogeographic summary maps. A: Mid Eocene Zealandia, showing extensive subaerial land exposure and the surrounding shelfal settings. B: Late Oligocene Zealandia, illustrating the likely location of land (if any), contrasting with that of the mid Eocene. C: The development of the modern plate boundary through New Zealand saw the re-emergence of land and a return of siliciclastic sediments to the basins. Maps modified from King *et al*. (1999) and King (2000).

1.2 Geology of the Waitaki region

The Waitaki region is located on the east coast of South Island (Fig. 1.3) and contains extensive Cenozoic sedimentary units (Fig. 1.4) preserved in a fault-bounded depression between the Waitaki River to the north and the Kakanui Range to the south (Gage, 1957; Lewis and Belliss, 1984; Forsyth, 2001). The region contains a sedimentary succession formed during the regional transgressive-regressive history of New Zealand, from the Cretaceous to the present. It records the change from terrigenous siliciclastic sedimentary facies to increasingly calcareous and glauconitic marine sedimentary environments, developed alongside localised volcanic edifices. Regional and local unconformities accompanied this change, reflective of a number of different events from subaerial exposure to major submarine current development, culminating in the maximum flooding of the region during the Oligocene. The development of the Pacific-Australian plate boundary and the instigation of the Alpine Fault in the Miocene saw a steady increase of terrigenous sediment once again, and the onset of regional regression.

1.2.1 Waitaki region tectonic setting

The tectonic setting of the Waitaki region is the result of New Zealand-wide subsidence associated with the post-rift extensional regime, with extensional basins formed along the Waihemo Fault system (Laird and Bradshaw, 2004). This was followed by a passive margin phase that saw tectonic depressions form and sedimentary fill accumulate as a result of thermal subsidence during the Late Cretaceous to Oligocene transgressive sequence (Wilson, 1956; Laird, 1996; Forsyth, 2001). In the Late Miocene to Pliocene, regional uplift and deformation began as a result of the propagation of the Australian-Pacific plate boundary. This resulted in significant reactivation of Late Cretaceous faults into thrust systems - a reversal on their previous normal movement (Cooper *et al*., 1987;

Mitchell *et al*., 2009) - and resulted in an increase in siliciclastic sediment supply to the area (Forsyth, 2001).

1.2.2 Waitaki unconformities

The mid-Cenozoic sedimentary succession within the Waitaki region contains at least four significant unconformities. Significant work has been done on these contacts (e.g., Lewis and Belliss, 1984; Carter, 1985; Jenkins, 1987; Lewis, 1989; Fulthorpe *et al*., 1996), but there is still much debate regarding their timing and duration, the exact number of horizons and their inter-relationship, and ultimately their cause (Lever, 2007). They are presented in stratigraphic order within the following Sections.

1.2.3 Basement geology

The Waitaki region is underlain primarily by the Rakaia Terrane, which is a steeply dipping unit exhibiting an increasing schistosity toward the southwest (Bishop *et al.*, 1985; Bradshaw, 1993; Mortimer and Tulloch, 1996; Sutherland, 1999; Turnbull *et al*., 2001). This terrane was formed from Gondwanan-derived turbiditic submarine Permian to Late Triassic quartzofeldspathic sandstone and mudstone, or argillite, on an active continental margin in the accretionary wedge. Carboniferous and Permian age inclusions were sourced from the oceanic substrate onto which these sediments were deposited (MacKinnon, 1983; Roser and Korsch, 1999; Mortimer, 2004).

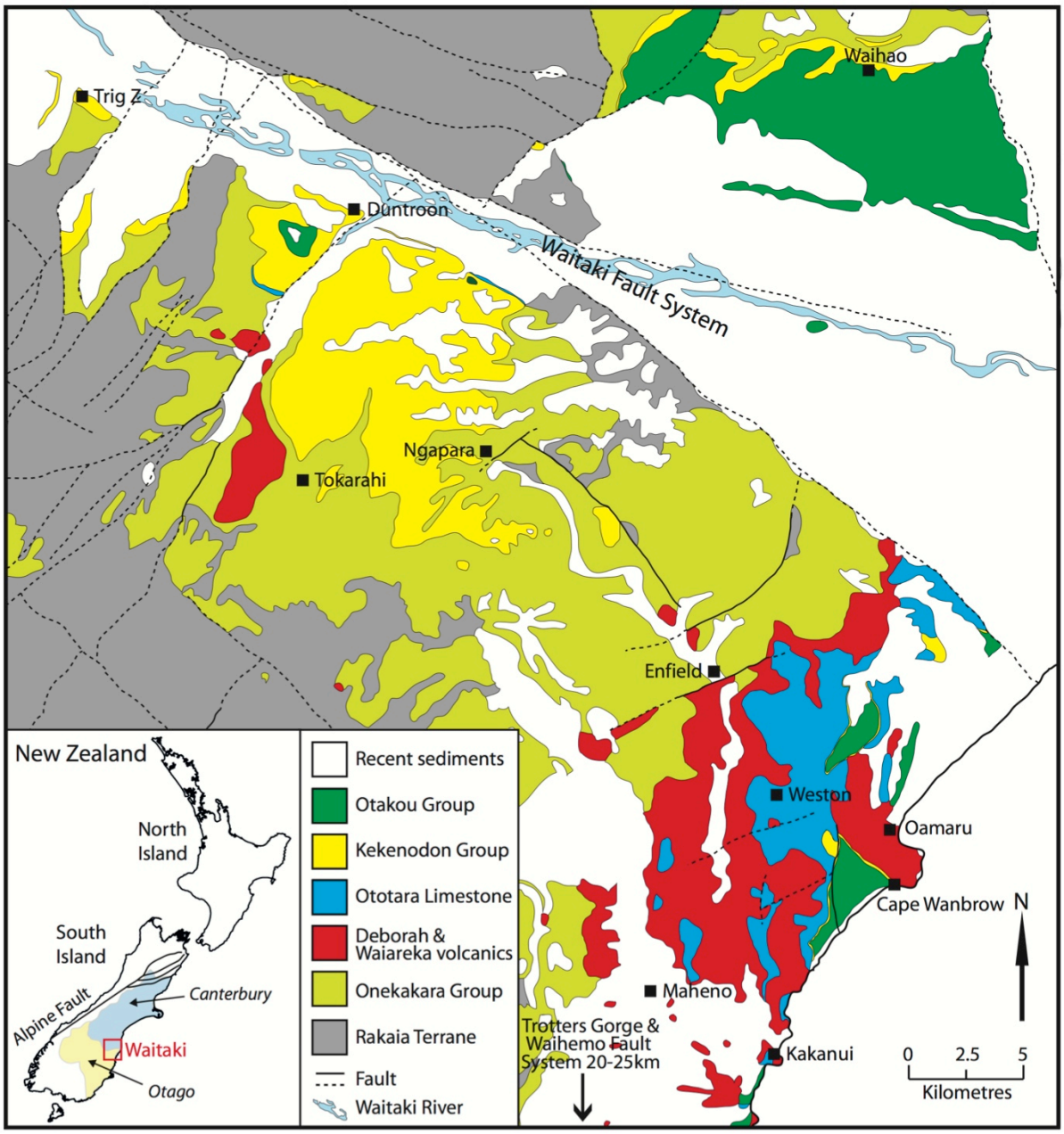

Figure 1.3. Geological map of the study area within the Waitaki region. Note that the units appear as both groups and formations where applicable. Adapted from Forsyth (2001). Inset map shows the location of the Waitaki region within New Zealand.

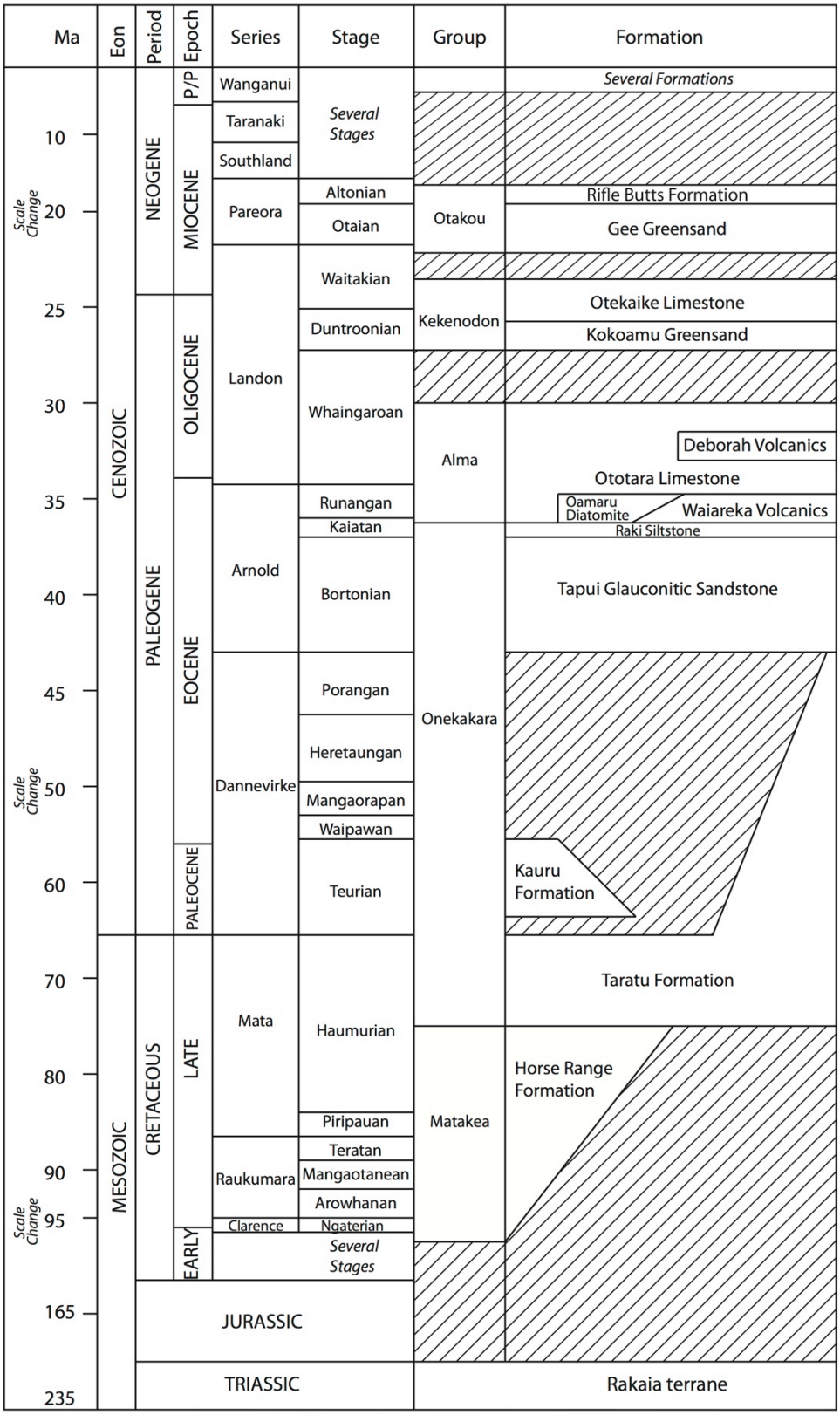

Figure 1.4. Stratigraphic column for the Waitaki region, with specific focus on those formations applicable to this study. Note the scale changes as indicated to the left of the column. Hashed areas represent periods of non-deposition or erosion. Modified from Gage (1957), Edwards (1991) and Cooper (2004).

The degree of metamorphism in this terrane varies spatially, with three textural subdivisions found within and around the study area (Fig. 1.3) (Bishop, 1974; Turnbull *et al*., 2001; Forsyth, 2001). North of the Waitaki Fault System (Fig. 1.3) the rocks retain their primary sedimentary structure, preserving bedding and grain textures. Metamorphic minerals present are very fine-grained. West of the fault system, outside the defined study area, metamorphism becomes more obvious, with flattening of detrital grains and development of a weak cleavage, although bedding is still prominent alongside foliation in outcrop. To the south of the fault system, the basement rocks become well foliated, while still retaining recognisable original structures. Grains become flattened, and metamorphic overgrowths and fine grain development have occurred, with mudstones and sandstones altered to phyllite and meta-sandstone respectively, forming a semischist. These latter two textural groups, south and west of the Waitaki Fault System, form part of the Otago Schist (Forsyth, 2001).

The Otago Schist in the Waitaki region, a semischist, is composed of either alternating layers of quartz-albite and mica-rich laminae, where the former makes up 40 – 60% of the rock; or is massive, with weak foliation comprising 50 – 80% quartz and albite (Mortimer and Roser, 1992).

The unfoliated sandstones and mudstones within the Rakaia Terrane contain quartz, albite, chlorite, muscovite, biotite, and titanite (Forsyth, 2001).

1.2.4 Matakea Group

In the Late Cretaceous, the regional tectonic regime changed from subduction to extension as New Zealand separated from Australia and Antarctica, during which time there was widespread development of grabens within the over-thickened and buoyant crustal block, into which non-marine sediments were deposited (Laird, 1996). This event is

represented in the Waitaki region by the coarse clastic deposits of the Matakea Group, consisting of the Horse Range Formation and the Kyeburn Formation, although only limited exposure of the former falls within the area of study for this thesis. This group is largely confined to structural depressions and is commonly unconformably overlain by the Onekakara Group (Section 1.2.5) (Carter, 1988; Landis *et al*., 2008).

1.2.4.1 Horse Range Formation

The Horse Range Formation is confined to the coastal southeast of the Waitaki region, along the northern edge of the Waihemo Fault around Trotters Gorge and Shag Point (Fig. 1.3**)**, and has been dated as Early to Late Cretaceous based on K-Ar dates obtained from associated ignimbrites (Adams and Raine, 1988). It consists of indurated and poorly-sorted quartz, greywacke and schist conglomerates with minor breccia, sandstone, siltstone and carbonaceous mudstones with thin coal lenses, and lies unconformably over the Rakaia Terrane, with minor rhyolitic ignimbrite (Steiner *et al*., 1959; Douglas, 1970; Adams and Raine, 1988; Mitchell, 1990; Forsyth, 2001). These sediments have been interpreted as having been deposited in a braided river system and associated fans forming along the then normal Waihemo Fault (Steiner *et al*., 1959; Mitchell *et al.*, 2009; Tulloch *et al*., 2009).

1.2.5 Onekakara Group

The Matakea Group underlies the Cenozoic formations in the Waitaki region, and grades into the Onekakara Group - a collection of non-marine to marine sandstones, mudstones, marls and lignite/coal that together represent the beginning of regional transgression that occurred between the Late Cretaceous and the Oligocene (Gage, 1957; Carter, 1988; Field and Browne, 1986; Landis *et al*., 2008), and which may also rest

unconformably on top of basement. The unconformable contact between the Onekakara Group and basement Rakaia Terrane rocks is the result of marine erosion that produced an irregular land surface (Forsyth, 2001).

1.2.5.1 Taratu Formation

The basal non-marine deposits of the Onekakara Group form the Taratu Formation, which has been assigned an age of Late Cretaceous to Eocene (Pole, 1992; 1995). The formation consists of poorly-sorted, quartz-rich pebble conglomerates, sandstones and siltstones with minor lignite and coal lenses; and commonly contains large-scale (≥ 2 m thick) asymptotic cross-beds, where the base of each cross-bed gradually curves into the lower bed (Harrington, 1958; Aitchison, 1988; Forsyth, 2001; Youngson *et al*., 2006) deposited during cyclic deposition within coarse-bed-load, fluvial channels and floodplains (Lindqvist, 1986). Following marine transgression, and prior to deposition of the Tapui Sandstone (Section 1.2.5.4), bottom-scouring storm-waves reworked the upper portion of cross-bedded gravels to produce massive bedding containing sparse glauconite grains (Aitchison, 1988). Preservation thickness of these sediments was controlled by northeast-southwest trending faults active during the period of deposition, and by subsequent erosion (Harrington, 1958). This formation is found along the southern coastline of the study area, and inland along the southern edge of the Waitaki Fault System (Fig. 1.3).

1.2.5.2 Transgressive unconformity (Waipounamu)

The contact between the lower non-marine and upper marine formations represents a time-transgressive unconformity that has been interpreted as being a wave-cut submarine erosive period, termed the Waipounamu Erosion Surface (LeMasurier and Landis, 1996; Landis *et al*., 2008), which can be found in Otago and South Canterbury (Fig. 1.3). This

widespread surface has been argued to represent a ravinement surface formed during marine transgression from the Late Cretaceous to earliest Miocene and resulting from tectonic stability and thermal subsidence (Landis *et al*., 2008).

1.2.5.3 Kauru Formation

The Kauru Formation is a Teurian-stage, non-calcareous, shallow marine succession comprising three members as defined by Gage (1957): Five Forks Glauconitic Sand, Dixon Silt, and Raupo Concretionary Sandstone. The oldest of these, Raupo Concretionary Sandstone, is composed of fine sand-sized quartz and mica, with some glauconite content up-section. It is fossiliferous (principally molluscs) and strongly bioturbated, although it does retain a faint stratification. Parallel with this bedding are concretions of up to 90 cm in diameter in rough beds (Gage, 1957). Dixon Silt is a finely bedded alternating siltstone and mudstone, containing some dispersed traces of glauconite throughout (Gage, 1957). The youngest member, Five Forks Glauconitic Sand, is an evenly bedded, micaceous, glauconitic, medium sandstone. Locally it contacts the lower Dixon Silt on an eroded and bored surface (Gage, 1957). The Kauru Formation has been interpreted as having been deposited slowly in low-energy waters below wave-base, and supplied by fluvial sediment washing off the peneplain (Gage, 1957). This formation is generally found in the south and southwest of the Waitaki region study area (Fig. 1.5).

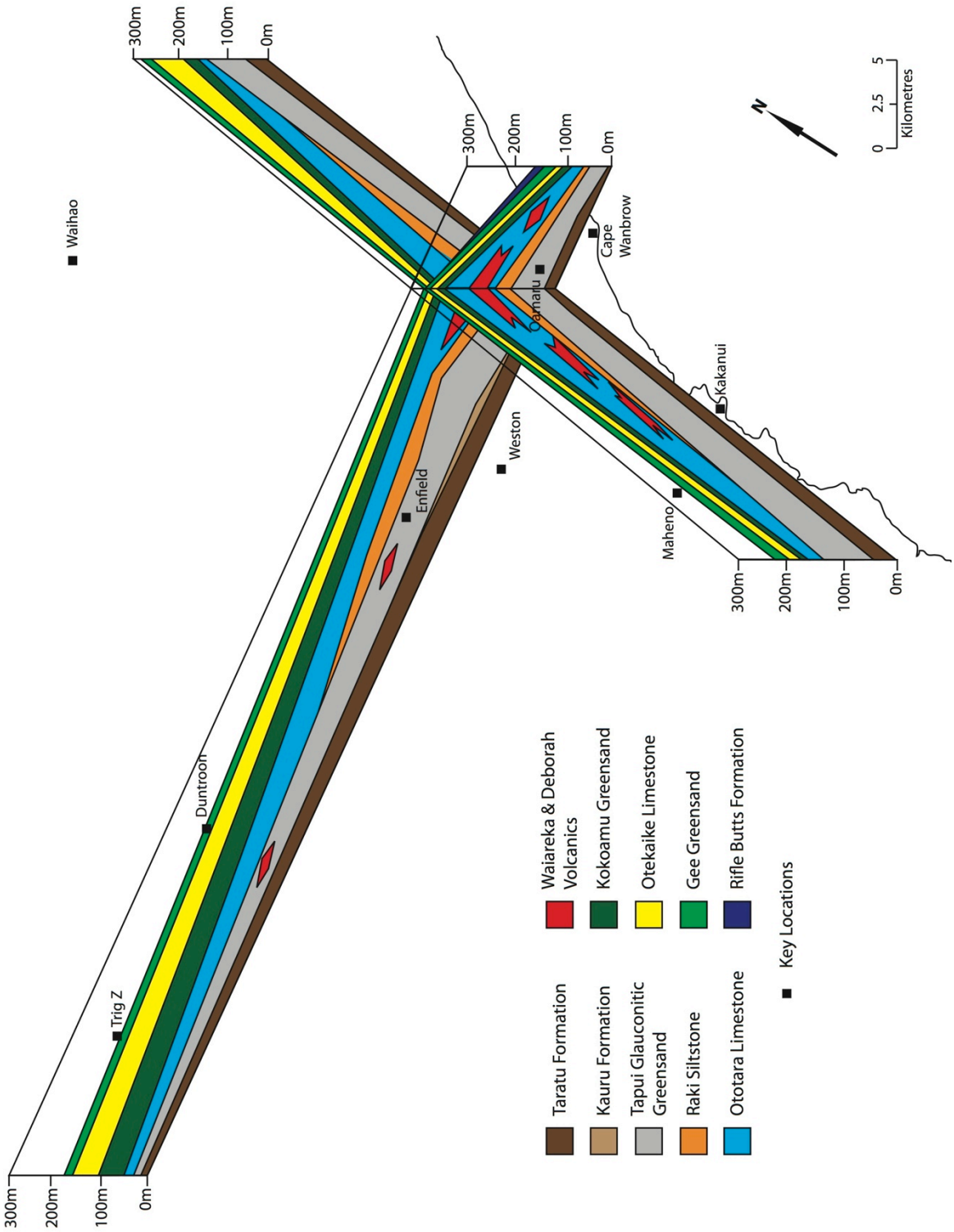

Figure 1.5. Lithostratigraophic thickness fence diagram across the Waitaki study area, derived from thicknesses presented in this chapter. Note the thickness of Ototara Limestone around Oamaru, while the younger Otekaike Limestone thickens towards Duntroon and Trig Z. Volcanic formations are present principally around the modern coastline, with those found inland represented principally by intrusive sills.

1.2.5.4 Tapui Glauconitic Sandstone

Tapui Glauconitic Sandstone is a generally massive, glauconitic or limonitic fine-to-medium sandstone of Bortonian age (Fig. 1.4), found locally up to 150 m thick (Fig. 1.5) (Gage, 1957). Most of these sediments are somewhat calcareous and micaceous, with a usually fine and dispersed carbonaceous content (Gage, 1957). The sandstone lies unconformably on top of Kauru or Taratu Formations in most of the Waitaki region, where glauconite-filled burrows penetrate into the underlying sediments (Gage, 1957). While this unconformable contact with lower sediments appears of significant duration, Gage (1957) suggests that younger sediments from these Formations were likely present, but were eroded during marine transgression prior to development of the Tapui Sandstone.

Near Duntroon, the Tapui Sandstone rests locally on schist basement (Fig. 1.3) (Gage, 1957). The basal 10 m of the formation is dominated by hummocky cross-stratified, coarse glauconitic sandstones, which are increasingly bioturbated up-section, with a decreasing preservation of sedimentary structure (Gage, 1957; Aitchison, 1988). This reflects an increasing water depth in a marine transgression, with the cross-stratified lower sediments deposited within the storm-wave base, while the younger bioturbated sediments record submergence below storm-wave base and subsequent bioturbation (Aitchison, 1988). These sandstones are richly glauconitic (up to 50%), with glauconite grains predominantly vermicular (>75%) with some ovoid and spherical pellets, fossil moulds and internal casts, and some tabular grains (McConchie and Lewis, 1980; Aitchison, 1988). The faunal composition is dominantly molluscs, together with some foraminifera, crustaceans, and shark teeth (Gage, 1957; Glaessner, 1980).

1.2.5.5 Raki Siltstone

Raki Siltstone is a Kaiatan Stage, massive, grey, slightly micaceous siltstone to fine sandstone (Gage, 1957), and lies conformably above the Tapui Glauconitic Sandstone (Fig. 1.4). Its faunal composition comprises oysters and other shell fragments, and carbonaceous fragments (Gage, 1957). Glauconite-filled burrows within the sediment are located within muddy bands up-section (Gage, 1957). Gage (1957) described its mode of deposition as low-energy marine. Exposures of this unit are scarce, but have been found principally along the modern coast within the study area, as well as inland around Ngapara (Figs. 1.3 and 1.5), with a thickness of up to 30 m (Gage, 1957).

1.2.6 Alma Group

Resting conformably on top of the Onekakara Group is Gage's (1957) "Alma Group", comprising Ototara Limestone, Waiareka and Deborah Volcanics, and associated Oamaru Diatomite (Edwards, 1991). This group contains carbonate sediments with interbedded basaltic material (tuffs, sills, dykes and pillow lavas) deposited from the Late Eocene to the Early Oligocene (Gage, 1957). Exposures occur almost exclusively around the modern coastline near Oamaru, with only minor outcrops further inland (Fig. 1.3) (Gage, 1957; Edwards, 1991). It differs from the underlying and overlying groups by being generally free of terrigenous and authigenic influence, while being closely associated with volcanic activity (Gage, 1957). Coombs *et al*. (1986) suggested the term Waiareka-Deborah Volcanics to encompass both Formations, but they will be presented separately in this section for stratigraphic simplicity and for correlation with earlier authors' work - although this term will be used within the thesis where a differentiation between the two units is not necessary.

1.2.6.1 Ototara Limestone

The Ototara Limestone (Mantell, 1850) is an amalgamation of Gage's (1957) Totara and McDonald limestones, as these latter two units are lithologically the same and were only separated by Gage on the basis of the stratigraphic presence of Deborah Volcanics between the two in localised cases (Edwards, 1991; Forsyth, 2001). Ototara Limestone principally occurs in thickest deposits near Oamaru (Edwards, 1991), but it can be found in thinner exposures further inland (Fig. 1.5). The thickest occurrences, west of Oamaru, range between 45 m and 105 m thick, thinning to less than 10 m along the modern coast. Edwards (1991) attributes this variation to the suitability of bathymetric highs for the accumulation of bryozoan growth, and nearby deeper water for the deposition of skeletal material. Bedding is usually indistinct, although conspicuous cross-bedding can be observed in a few locations (Edwards, 1991).

Ototara Limestone is typically interbedded with tuffs of the Waiareka and Deborah Volcanic Formations, and is bounded at its upper surface by a major unconformity (the Marshall Paraconformity) (Section 1.2.6.4) (Gage, 1957). It is commonly identified in the east of the Waitaki region as a massive or indistinctly bedded, grain-supported, bryozoan-rich limestone with little glauconite or terrigenous content, forming the Weston Member and the Flat Top Limestone Member (Gage, 1957). These members are practically identical, and were only distinguished on the basis of stratigraphic location by Gage (1957). Macrofossils are uncommon within this Formation, although bivalves (*Serripecten*) and rare vertebrate (turtle and penguin) fossils have been recorded, particularly in the Everett Brachiopod Limestone Member, a brachiopod-rich coquina near Kakanui (Fig. 1.3) (Gage, 1957; Fordyce, 1979; 1985). These fossiliferous horizons occur principally above richly tuffaceous intervals (Edwards, 1991). A lower member (the Maheno Marl Member) forms a 2 m thick calcareous siltstone over Waiareka tuffs at Maheno (Fig. 1.3) (Gage,

1957). A nodular algal cap bed is located in the coastal area south of Oamaru; while on the south side of Cape Wanbrow this Formation is notable for being composed entirely of algal rhodoliths (Gage, 1957). To the west, the Ototara Limestone makes up the Earthquakes Marl Member, consisting of thinner exposures of massive, moderately soft, light-grey glauconitic, foraminiferal, fine to silty limestone or marl (Gage, 1957).

The Ototara Limestone is of latest Kaiatan to mid-Whaingaroan (Late Eocene to Early Oligocene) age (Gage, 1957; Edwards, 1991; Forsyth, 2001). Strontium dating by Nelson *et al*. (2004) provided ages of between 35.18 and 34.13 Ma at Kakanui River, and 34.9 Ma from the quarry at Weston. It has been interpreted as being of shallow marine origin associated with the formation of numerous rocky reefs, formed by localised volcanic mounts in the east over which bryozoan shoals developed, with deeper quiet-water sediments to the west (Gage, 1957; Lewis and Belliss, 1984; Carter, 1988; Edwards, 1991; Lewis, 1992).

1.2.6.2 Waiareka Volcanics

The Waiareka Volcanic Formation consists mostly of olivine tholeiitic basaltic fine to coarse tuffs, dykes, sills, and pillow lavas, containing augite, hornblende and garnet. It has been assigned an age of late Kaiatan to Runangan (Late Eocene), primarily using foraminifera found in coeval mixed sediment and tuff (Coombs *et al*., 1986; Reay and Sipiera, 1987), confirmed by K-Ar whole-rock dating (Forsyth, 2001). The Waiareka is characterised as primarily pyroclastic and eruptive basalt, and includes lenses of chalk and diatomite (Gage, 1957) derived principally from Surtseyan shallow marine vents and fissures (Coombs *et al*., 1986). These chalk and diatomite sediments form the Oamaru Diatomite (Section 1.2.6.2.1), representing a member of the Waiareka Volcanics (Edwards, 1991). The majority of the igneous material is explosively distributed into agglomerates

and pyroclastic tuff over an area of 50 x 8 km (Gage, 1957). The remainder of the extrusives occur as erupted pillow lavas (formed not only as the result of direct contact with water but also through intrusion into wet sediment), as well as relatively shallow sills and dykes that chilled rapidly upon contact with wet sediment (Uttley, 1918; Benson, 1943; Gage, 1957; Coombs *et al*., 1986).

The Waiareka pyroclastics are focused around the current Waitaki coastline and Oamaru, with a maximum thickness of 200 metres at Cape Wanbrow, and without an exposed basal contact (Forsyth, 2001). The pillow lavas, dykes, and sills are spread more extensively within the region, being found as much in the west of the mapped area as in the east, extending as far inland as Duntroon and Tokarahi (Fig. 1.3) (Forsyth, 2001). At Enfield (Fig. 1.3), a large dyke has been interpreted as the feeder for nearby intrusive basaltic sills (Coombs *at al*., 1986). An olivine tholeiitic sill, found near the village of Tokarahi, intruded into Bortonian Tapui Formation (Middle Eocene) sediment, and is associated with local pillow lavas exposures (Gage, 1957; Forsyth, 2001). A sill is also located at Island Stream, 2.4 km west of Maheno (Gage, 1957).

1.2.6.2.1 Oamaru Diatomite

Oamaru Diatomite is a unit of the Waiareka Volcanics (Edwards, 1991). It is technically not a true diatomite, however, as siliceous content is never greater than 60% and it contains a highly variable diatom content (Edwards, 1991). It is found overlying one of the Waiareka Volcanic pyroclastic members while also underlying, and being a lateral equivalent to, the lower part of the Ototara Limestone (Edwards, 1991). It contains rare macrofossils along with a varying clay and silt content. It has been dated using foraminifera and calcareous nanoplankton to range from Runangan to early Whaingaroan (latest Eocene to earliest Oligocene) (Edwards, 1991; O'Conner, 1999). The diatomite is

found within a strip of 17 x 3 km with a NE/SW trend that runs along the west of the Oamaru area (Fig. 6.1), with thicknesses of 21 – 41 m.

Edwards (1991) interpreted the Oamaru Diatomite as being deposited in an offshore basin, at depths of 75 – 150 m, and in low-energy warm subtropical waters. Low terrigenous input resulted in significant biogenic sediment in a location of nutrient-rich upwelling near the basin's margin.

Formation of Oamaru Diatomite has also been attributed to an increase in substantial amounts of dissolved silica in the water column as a result of the local eruptive activity favouring growth and reproduction of diatoms and sponges, nutrient-rich upwelling waters resulting in plankton blooms, or a combination of these effects (Park, 1918; Gage, 1957; Edwards, 1991).

1.2.6.3 Deborah Volcanics

The Deborah Volcanic Formation contains a variety of eruptives and pyroclastics, including mostly alkaline olivine basaltic tuffs and breccias infused with bombs and lapilli, ultramafic xenoliths (peridotite, eclogite), large xenocrysts, and occasional blocks of schist (Gage, 1957; Dickey Jr, 1968; Reay and Sipiera, 1987; Edwards, 1991). Several intrusive dolerite and basalt masses are also part of this formation (Edwards, 1991). Gage (1957) noted its thickness is greatest near eruptive centres (up to 11 m), before thinning abruptly away from these, usually in a westward direction. Fossil content and K-Ar whole-rock dating places the Deborah Volcanics in the early Whaingaroan (Early Oligocene) (Coombs *et al*., 1986; Reay and Sipiera, 1987; Forsyth, 2001). Bioclastic dykes of hard, tuffaceous limestone, containing some glauconite and detrital quartz, can be found around tuff cones north of Kakanui (Fig. 1.3). These did not form until near the end of the Deborah eruptive phase, and have been interpreted as having continued into the Miocene (Lewis, 1973),

although Dickey Jr (1968) suggests that on the basis of fossil content, these were likely derived from underlying and older material, either the Waiareka volcanics or older Ototara Limestone.

The Deborah Volcanics are located between Kakanui and Weston in a ~ 3.5 km wide strip running up the modern coastline (Fig. 1.3) (Gage, 1957, Edwards, 1991). The Kakanui Mineral Breccia Member, a coarse tuffaceous breccia containing megacrysts, as well as a number of remnant tuff cones, occurs at Kakanui and Gees Point. Around Cape Wanbrow, the Deborah volcanics form a mass of coarse pyroclastics on the north and west flanks of the Cape (Gage, 1957). Gage (1957) further describes a second belt that extends sporadically northwards to the northern arms of Landon Creek. The Deborah volcanics do not occur in the west of the Waitaki region.

1.2.6.4 Marshall Paraconformity

The Marshall Paraconformity forms a significant contact within the Waitaki region. It is characterised by palaeo-hardground and bored surfaces and phosphatised clasts (or locally phosphatised surfaces) with associated faunal assemblages (Lewis and Bellis, 1984; Lewis, 1989); while sequences above often have higher glauconite content. Faunal compositions found in offshore wells have shown that these overlying glauconitic sediments may represent a slightly shallower depositional environment than those below (Carter and Landis, 1972; Fulthorpe *et al*., 1996), allowing for a distinctive surface that can be correlated throughout the region, including the Waitaki region.

Dating of this unconformity has been based almost exclusively on microfaunal evidence, consistently indicating a mid-Oligocene (Whaingaroan) age. Nevertheless, dating performed on other unconformities displaying similar features around South Island, suggests ages ranging between Whaingaroan, Whaingaroan to Duntroonian, and

Whaingaroan to Waitakian (Findlay, 1980). Taking into account the reworking of sediments, the youngest sediments below the unconformity are lower Whaingaroan (Hornibrook, 1966; 1987), while the samples above are nearly exclusively Duntroonian (Hornibrook, 1966; 1987; Jenkins, 1971). The period of time that is missing ranges generally between 2 My (Jenkins, 1987) and 4 My (Hornibrook, 1987), although local hiatuses of up to 15 My are present offshore (Fulthorpe *et al*., 1996). This is of particular importance in the Waitaki region where the Gee Greensand rests directly on top of Ototara Limestone; where Gage (1957) estimated a hiatus of 10 My. This is thought to be the result of a local topographic high (Gage, 1957; Field and Browne, 1989). The only other attempt at dating these unconformities was done by Fulthorpe *et al*. (1996) using strontium isotopes. In their study, samples were collected at only two locations containing the Marshall Paraconformity: Squires Farm – the type section for the Marshall Paraconformity (Carter *et al*., 1982), and McCullough's Bridge. The data gathered from these two locations gave age estimates of ~32.4 to 29 My with a hiatus of 3 – 4 My, relatively consistent with the previous ages given (further strontium dating by Nelson *et al*. (2004) on a number of Oligocene limestones in South Auckland and South Canterbury was intended to constrain the boundaries of the New Zealand ages rather than any particular event or formation).

1.2.7 Kekenodon Group

The Kekenodon Group lies unconformably above the Alma Group, and was first deposited in the Duntroonian to Waitakian Stages (Late Oligocene to earliest Miocene) (Fig. 1.4). This Group is present throughout the Waitaki region, at much greater thicknesses inland than at the coast, and comprises the Kokoamu Greensand grading up into the Otekaike Limestone (Gage, 1957; Forsyth, 2001). The Kekenodon Group has been

interpreted as representing the maximum level of marine transgression in the area and as such is a condensed sequence that contains a number of short and localised unconformities within it (Carter and Landis, 1982; Lewis and Belliss, 1984; Carter, 1985, 1988; Jenkins, 1987; Fulthorpe *et al*., 1996).

1.2.7.1 Kokoamu Greensand

Kokoamu Greensand is a medium to fine sand-sized, locally pebbly, glauconitic, calcareous sandstone that overlies a major bored, phosphatised, and eroded unconformity (see Section 1.2.6.4). The lower contact usually rests on top of Ototara Limestone, although it has also been observed to rest directly on Raki Siltstone (Gage, 1957). Kokoamu Greensand's upper contact grades into the Otekaike Limestone that overlies it (Section 1.2.7.2) (Gage, 1957). In some sections it has been assigned a latest Whaingaroan age at its base (Field and Brown, 1986), although the majority of this formation is Duntroonian in age, based on ostracod dating analyses (Fig. 1.4) (Ayress, 1993). The formation varies in thickness from 15 cm to as much as 50 m (Fig. 1.5), but can be absent entirely in some locations or found only within karst dissolution cavities (Gage, 1957; Hornibrook, 1966). It is often intensely bioturbated in its lower part, while containing abundant calcitic marine macro- and micro-fossils within a more distinctly bedded structure up section (Gage, 1957; Ayress, 1993). The fossil assemblage consists of brachiopods, molluscs, echinoids, barnacles, foraminifera, ostracods, and various mammal bones and teeth (Gage, 1957; MacKinnon *et al*., 1993). Phosphatic nodules are common, especially around the modern coastline (Gage, 1957). Some localities show prominent cross-beds (Batt, 1993).

Kokoamu Greensand is considered to represent the onset of sedimentation following periods of lowered sea level and subaerial exposure in the Waitaki region, prior

to which widespread erosion had taken place (Gage, 1957). Sedimentation was slow and discontinuous with glauconite precipitation forming from iron-bearing terrigenous material (Gage, 1957). Ayress (1993) suggests an outer shelf environment at the base, with a transition to a mid shelf setting further up the formation, based on ostracod assemblages.

1.2.7.2 Otekaike Limestone

Otekaike Limestone is a fossiliferous and glauconitic limestone that exhibits small to large scale cross-bedding in a number of localities, and bands of nodular concretions (Gage, 1957; Ward and Lewis, 1975; Field and Browne, 1986; MacKinnon *et al*., 1993; Graham *et al*., 2000). Its age is usually placed at the very latest Duntroonian to Waitakian (Fig. 1.4) (Gage, 1957). Strontium isotope ratios from macrofossils and foraminifera by Graham *et al*. (2000) place the Otekaike Limestone at Trig Z (Fig. 1.3) at c.25.5 Ma at the base to c. 23.7 Ma at the top. This places the Otekaike at this location in the very latest Duntroonian to mid Waitakian Stages.

Otekaike Limestone's basal contact is often gradational from underlying Kokoamu Greensand, but has been observed to be abrupt in some locations (e.g., near Ngapara), where a bored or eroded surface can be observed (Gage, 1957). At the coast, the formation may lie directly on a phosphatised surface of Ototara Limestone and can contain a layer of phosphatic nodules (Gage, 1957).

Gage (1957) split this formation into four members – the Maerewhenua Glauconitic Limestone Member; the Prydes Gully Nodular Limestone Member; the Miller Member; and the Waitoura Member.

The lowest of these, the Maerewhenua Glauconitic Limestone Member, is a hard and massive glauconitic limestone that grades into a less fossiliferous, hard and yellowish limestone (Gage, 1957). It contains abundant macrofossils, particularly near its base,

including brachiopods, echinoids, and pectens. It extends from inland to the coast, where it contains corals (*Mopsia* and *Isis*) and brachiopods, while the two upper members are confined to the west of the study area (Gage, 1957). The formation is very thin at the coast (either absent or reaching a maximum thickness of 3 m) and thickens markedly to the west (up to 60 m) (Fig. 1.5) (Gage, 1957).

The Prydes Gully Nodular Member is distinctly bedded, and is a fine, creamy-white, nodular limestone with even layers of nodular concretions. The Miller Member is an alternating impure yellow to brown limestone that contains cemented lenses and beds, fine to medium sand-sized, calcareous glauconitic sandstone, with abundant molluscs, brachiopods, and corals (Gage, 1957). Finally, the Waitoura Marl Member is a massive, highly calcareous siltstone, similar to the Miller Member but without the lenses of fossil and nodular concretion material. Gage (1957) observed that the proportion of non-calcareous material (with the exception of glauconite) increases upwards through the entire formation, while the proportion of glauconite progressively lessens.

Arno Limestone, a yellowish-grey, moderately to well-undurated, well-sorted fine quartose grainstone to glauconitic packstone, is exposed in cliff sections to the north of the Waitaki Fault System around Waihao (Riddolls, 1968), where it contains large (up to 2 m thick) cross-beds with extensive scour channels (20 – 120 m wide) (Ward and Lewis, 1975). The cross-beds show a predominantly easterly palaeocurrent direction, whereas the scour channels are oriented principally northwards (Ward, 1973; Ward and Lewis, 1975). Claims that this formation differs significantly from those of North Otago (Ward and Lewis, 1975) were based only on its large cross-bedded and channelised sedimentary structure and its modern geographic location north of the Waitaki River. Although its base is placed slightly older than the Otekaike Limestone, in the late Duntroonian, it is otherwise a correlative unit. Therefore, for the purpose of this study, it is referred to as the

Arno Member of the Otekaike Limestone, representing the Otekaike Limestone in the north of the study area.

Otekaike Limestone was deposited over much of the Waitaki region, with the massive lower members found extensively around Tokarahi and the central study area. It has been interpreted as having formed in a neritic carbonate environment of low but increasing terrigenous supply in sometimes still and relatively clear water (Gage, 1957; Forsyth, 2001). It also shows evidence of interruptions to sedimentation during deposition resulting from sea-level fall, probably without subaerial exposure (Gage, 1957; Forsyth, 2001). Strong current activity is suggested by the existence of extensive cross-bedding in the north (Ward and Lewis, 1975). Palaeoenvironmental estimates (Graham *et al*., 2000) place Otekaike Limestone at a palaeodepth of 50 – 100 m, around the mid continental shelf, at Trig Z (Fig. 1.3) in the west of the Waitaki region.

1.2.7.2.1 Intra-Otekaike Limestone hiatus

Within lower Otekaike Limestone, near the Kokoamu/Otekaike contact, a prominent localised unconformity appears to have developed in some inland Waitaki localities (e.g., Trig Z, Awamoko Creek, Ngapara) during the Waitakian Stage, following deposition of Duntroonian and some Waitakian sediments (Lewis and Belliss, 1984). It appears these surfaces were overlain by thin glauconitic sandstones prior to further limestone deposition. The hiatus is not represented at coastal localities, where the Waitakian sequence is restricted, and it is argued that it may have blended with the Waitakian karst observed on top of the Otekaike Limestone there (see Section 1.2.7.3) (Lewis and Belliss, 1984; Lewis, 1989).

Time spans for this hiatus vary, with a range of 5 – 7 My estimated by Jenkins (1987), although this is disputed by Gage (1988) who suggested it may well be less in

some locations. Hornibrook (1987), however, finds no significant age gap between the Kokoamu Greensand and Otekaike Limestone, even though this unconformity has been sited around this contact in inland locations.

1.2.7.3 Early Miocene unconformity

An unconformity present between Otekaike Limestone and the overlying Gee Greensand (Section 1.2.8.1) can be found in many of the Early Miocene sequences of North Otago and South Canterbury (Batt, 1993). The underlying sediments may be condensed such that the base is made up locally of Alma Group rocks, however, with those of the Kekenodon Group being absent (Gage, 1957). This unconformity is not universally developed across the Waitaki region, and is in fact conformable to the west of the study area near Lake Waitaki, at Awahokomo, where Otekaike Limestone grades into overlying glauconitic sandstones over a 1 m interval (Batt, 1993).

Where it is found, this unconformity is well developed and is an irregular, extensively solution-cavitied surface showing relief of up to 1 m or more at outcrop (Batt, 1993). This has been inferred to be karst formed by subaerial exposure, and contains well-rounded and reworked local and exotic clasts forming basal conglomerates on its surface (Lewis and Belliss, 1984; Batt, 1993).

Batt (1993) used detailed foraminiferal dating to constrain the age of the unconformity as it occurs on the top of Otekaike Limestone to the mid to upper Waitakian Stage using the *Globigerina woodi woodi* and *Globigerina woodi connecta* zones of Jenkins (1971).

It has been suggested by Lewis and Belliss (1984) that this unconformity represents a major event involving subaerial exposure of the region, siting sink holes around Trig Z, Sisters Creek, and elsewhere inland as indicating intra-Waitakian karst. Other authors

disagree, however, through relating suggested inland karst features to submarine erosion and dissolution instead (Gage, 1988). Regardless of the causal nature of this unconformity surface, it does represent a clear break in sedimentation in many areas during the Early Miocene.

1.2.8 Otakou Group

Lying unconformably on top of the Kekenodon Group is the Otakou Group, found within the study area primarily in coastal sections north of Kakanui, and in isolated localities inland (Fig. 1.3) (Gage, 1957; Morgans *et al*., 1999; Forsyth, 2001). Within the study area this Group is represented by Gee Greensand and Rifle Butts Formation, although it is principally Gee Greensand found in the outcrops which is considered in this study (Gage, 1957; Carter and Carter, 1982; Forsyth, 2001).

1.2.8.1 Gee Greensand

Gee Greensand is a highly glauconitic and fossiliferous calcarenite, containing abundant brachiopods and bioturbation. Its distribution extends throughout the Waitaki region, but it is most common in outcrop near the modern coast (Gage, 1957). Thicknesses range from 50 cm to ~ 6 m (Fig. 1.5). It is found on top of Otekaike Limestone in numerous localities (Gage, 1957; Carter and Carter, 1982; Carter, 1988; Field *et al*., 1989; Fulthorpe *et al*., 1996; Forsyth, 2001). The formation's basal contact overlies either Otekaike Limestone or Ototara Limestone and is almost everywhere unconformable, with the nature of the contact ranging from lightly undulating and erosional to karst (Gage, 1957). To the west of the study area Batt (1993) interprets the contact between the Otekaike Limestone and Gee Greensand as being conformable, where Gee Greensand has there been assigned a mid- to late Waitakian age based on foraminiferal analyses.

Gee Greensand usually grades up from nearly pure glauconite at its base to a highly glauconitic, fine calcareous sandstone in upper sections. The formation is generally massive, although indistinct stratification can be enhanced by fossiliferous horizons and calcareous bands (Gage, 1957). Phosphatic nodules and occasional limestone clasts are common in the lower part of the formation at the modern coast (Gage, 1957). Brachiopods and pectens dominate most faunas, although other molluscs, octocorals, shark's teeth, and various mammal bones are present (Gage, 1957). A brachiopod-rich bed can be found at the base of Gee Greensand at Old Rifle Butts. Some localised cross-bedding is present at Gee's Point, onlapping a section of Ototara Limestone with a palaeoflow direction trending north-northeast (Batt, 1993).

Gee Greensand, as described by Gage (1957), is used to describe all glauconitic sands that can be stratigraphically correlated across the Waitaki region. These glauconitic sandstones may be found to have different age limits depending on their location; and while not proven to be a continuous unit in the region, it is assumed that this is likely the case. Deposition of Gee Greensand therefore began and ended at different times at varying locations within the Waitaki region, and thus the boundaries of the unit are not temporally linear. The formation has been assigned a generally Otaian age (Early Miocene), although it is late Waitakian at Landon Creek, Gee's Point, and Campbell's Bay based on foraminiferal analyses (Gage, 1957). Strontium dating of a brachiopod in the Gee Greensand at Gees Point provided an age of 22.14 Ma (Nelson *et al*., 2004).

Gee Greensand's accumulation was slow, with the abundance of autochthonous glauconite and phosphate attributed by previous authors to exposure of the volcanic islands around the modern coast and associated guano deposits (Thomson, 1926; Gage, 1957).

1.2.8.2 Rifle Butts Formation

Rifle Butts Formation lies gradationally on top of Gee Greensand, and is found at its type locality at Old Rifle Butts as a fine-grained, glauconitic, greenish-grey, siliciclastic mudstone, recording a major change in the tectonic regime of Zealandia (Gage, 1957; Lewis and Belliss, 1984). Cemented layers of tabular concretions suggest bedding, but the unit is otherwise unstratified (Gage, 1957).

This Formation contains fossils of foraminifera, ostracods, corals, fish, brachiopods, and abundant molluscs (Gage, 1957). Ostracods have been used to assign this formation to the Altonian Stage (Fig. 1.4) (Ayress, 1993). The Otakou Group is Miocene in age, although offshore it has been found to extend into the Late Pliocene (Field *et al*., 1989), which may indicate the regressive phase following the Kekenodon highstand (e.g., Carter, 1988; Fulthorpe *et al*., 1996). This formation therefore records the development of the modern plate boundary through New Zealand, ending the Oligocene regional transgressive sequence and beginning a regional marine regression sequence (Carter and Norris, 1976; Molnar *et al*., 1975; Norris *et al*., 1978).

1.2.8.3 Mid-Miocene unconformity

The Otakau Group is unconformably overlain everywhere by either non-calcareous Pleistocene or Recent sediments (Gage, 1957). This contact is abrupt in nature, marking a significant hiatus, and is overlain by fine marine siliciclastic sediments that rapidly grade into alluvial facies (Gage, 1957).

1.2.9 Late Miocene to Quaternary

Capping the above sequence are Pleistocene to Pliocene fluvial conglomerates, coal measures, and volcanics, with Quaternary sediments occurring primarily around the larger rivers in the region (Gage, 1957; Forsyth, 2001). These fall outside the scope of this study.

1.3 Lithological nomenclature

This section presents the various lithological terms used throughout this thesis, particularly those for describing carbonate rocks as well as the various components found within them.

1.3.1 Classification of carbonate rocks

The classification system used throughout this thesis in the presentation of new data is based principally on the system developed by Dunham (1962) and modified by Embry and Klovan (1972) (Table 1.1). This system focuses on the relative abundance of allochems and micrite in the rock, but does not distinguish between different carbonate grains. It is based on depositional textures, particularly the grain packing and the relative abundance of micrite versus grains, and any depositional binding of the grains (Boggs, 2001). Those that were not bound together during deposition are then further separated into those that lack lime mud and those that contain it.

As Dunham's classification scheme does not consider the type of grains found within the rock, it is sometimes necessary to add an identifier along with the classification name (e.g. Bryozoan grainstone). This method of identification is used to supplement the Dunham name throughout this thesis.

<table>
<tr><td colspan="5" rowspan="2">ALLOCHTHONOUS LIMESTONE
Original components not organically bound during deposition</td><td colspan="4">AUTOCHTHONOUS LIMESTONE
Original components organically bound</td></tr>
<tr><td colspan="2">By organisms that build a rigid framework</td><td colspan="2">By organisms that encrust and bind</td><td>By organisms that act as baffles</td></tr>
<tr><td colspan="3" rowspan="3">Less than 10% >2 mm components</td><td colspan="2">Greater than 10% >2 mm components</td><td colspan="2" rowspan="2">BOUNDSTONE</td><td rowspan="2">BAFFLE-STONE</td></tr>
<tr><td colspan="2" rowspan="2">Matrix-supported</td><td>>2 mm component-supported</td></tr>
<tr><td colspan="2">Contains lime mud (<0.03 mm)</td><td>No lime mud</td><td rowspan="3">Grain-supported</td><td>FLOAT-STONE</td><td>RUDSTONE</td><td>FRAMESTONE</td><td>BINDSTONE</td></tr>
<tr><td rowspan="2">Mud-supported</td><td rowspan="2">Less than 10% grains (>0.03 mm <2 mm)</td><td>Greater than 10% grains</td><td>PACK-STONE</td><td>GRAIN-STONE</td><td colspan="4" rowspan="2"></td></tr>
<tr><td>MUDSTONE</td><td>WACKE-STONE</td><td colspan="2"></td></tr>
</table>

Table 1.1. The classification of limestones according to depositional textures as used throughout this thesis. Table modified after Dunham (1962) and Embry and Klovan, 1972.

1.3.2 Glauconite nomenclature

Glauconite, a green iron and potassium mica mineral, is commonly associated with low sedimentation rates and unconformities (McRae, 1972; Amorosi, 1995; Kelly and Webb, 1999), and is a common occurrence throughout the Waitaki study area. Therefore it is necessary to make mention here of the different ways that it is described in this study.

Glauconite is used throughout this thesis to refer to the green mineral that is readily observed in both outcrop and thin section. While glauconite can refer to a specific mineral species within a broader spectrum related to the amount of readily expandable layers, it is also often used to refer to the sand-sized grains or alteration found within sedimentary rocks (McRae, 1972). It is this latter type that is used throughout this thesis, as chemical and crystalline analyses of these grains were outside the scope of this study. This terminology can also be expanded to cover grains that have been glauconitised, which refers to their alteration or coating in mineralised glauconite.

A third term is used in this study to denote the facies that contains and can produce significant glauconite. This is here referred to as glaucony, in the sense of a glaucony facies. This is separate to a glauconite sandstone for example, which simply refers to a sandstone that contains glauconite as a principle component, but instead refers to an environment that produces or contains glauconite or the lithology that derives from such, and is an interpretive term, rather than descriptive.

1.4 Project aims and objectives

This thesis presents the results of extensive fieldwork and detailed stratigraphic analysis, as well as numerous thin-section petrographic analyses. By combining these data, and including previous published and unpublished data, the primary aim was to develop a comprehensive mid-Cenozoic sequence stratigraphic model for the Oamaru and inland

area of the Waitaki region of Zealandia, located in North Otago and South Canterbury. This would then provide for a better understanding of sea level change and unconformity development within this area, and to further understanding regarding this period in New Zealand's history.

The primary objectives of this study are:

- To develop a significant outcrop-based collection of stratigraphic sections across the study area within the Waitaki region, such that an accurate lithological dataset can form the basis of this study and enhance future work in the area.
- To establish facies types based on the stratigraphic dataset, combined with extensive petrographic analyses of samples collected throughout the study area.
- To develop a sequence stratigraphic model for the study area, including determination of the sequences and sequence boundaries from the facies and unconformities in the area.
- To determine the nature of the unconformities located in the study area and to determine their causal origin and developmental environment.
- To examine the extent and type of diagenetic processes that occurred in the study area, and to establish how diagenesis affected the preservation of lithologies and fossil assemblages.
- To establish what effect the palaeogeography of the Waitaki region had on facies and unconformity development in conjunction with changing sea levels, as well as how this might be observed within a sequence stratigraphic framework.

- To determine the cause of the significant glauconitic formations developed in the study area during the mid-Cenozoic, and establish if this had a relationship to sea level change.
- To compare the developments observed within the study area to those that are seen elsewhere in New Zealand sedimentary basins during the mid-Cenozoic, and to then determine whether local and/or regional events were the cause of changes observed in the study area. These observations could then be used to enhance the mid-Cenozoic interpretation of New Zealand as a whole.

In order to address these aims and objectives, this thesis is divided into eight further chapters:

- Chapter 2: Stratigraphy
- Chapter 3: Lithofacies
- Chapter 4: Processes of Diagenesis
- Chapter 5: Sequence Stratigraphy
- Chapter 6: Palaeobathymetric Influence on Sequence Stratigraphic Expression
- Chapter 7: Alternating Authigenic and Carbonate Depositional Environments
- Chapter 8: Mid-Cenozoic New Zealand: The Waitaki Region in Context
- Chapter 9: Summary and Conclusions

CHAPTER 2 – STRATIGRAPHY

2. Introduction

This chapter presents the lithostratigraphy and biostratigraphy of the mid-Cenozoic formations found within the study area, developed from fieldwork, and database and literature collations. Of particular interest are the stratigraphic relationships between the formations and how these vary laterally across the study area. These can then be constrained using the biostratigraphic dataset provided here. This is of importance in determining both temporal and spatial changes within and between formations, and forms the basis of lithofacies developments presented in Chapter 3.

2.1 Study area and stratigraphic locations

Extensive fieldwork was carried out within the study area in order to locate and record exposure of mid-Cenozoic sediments, principally those that include the upper Onekakara Group, the Alma Group, the Kekenodon Group and the Otakou Group described in Section 1.2. The locations of those exposures that contain these units, and were used to develop stratigraphic columns for the present project, are presented on a map of the study area in Fig. 2.1. A complete list of outcrop locations investigated in the course of fieldwork, including their geographic coordinates, can be found in Appendix A, while the stratigraphic columns considered throughout this thesis are given in Appendix B.

2.2 Lithostratigraphy

Stratigraphies of the mid-Cenozoic sediments are described here according to three regions within the Waitaki study area:

- “northern” region;

- "western" region; and
- "eastern" region,

as these regions share similar stratigraphic features. The regions are depicted in Fig. 2.1.

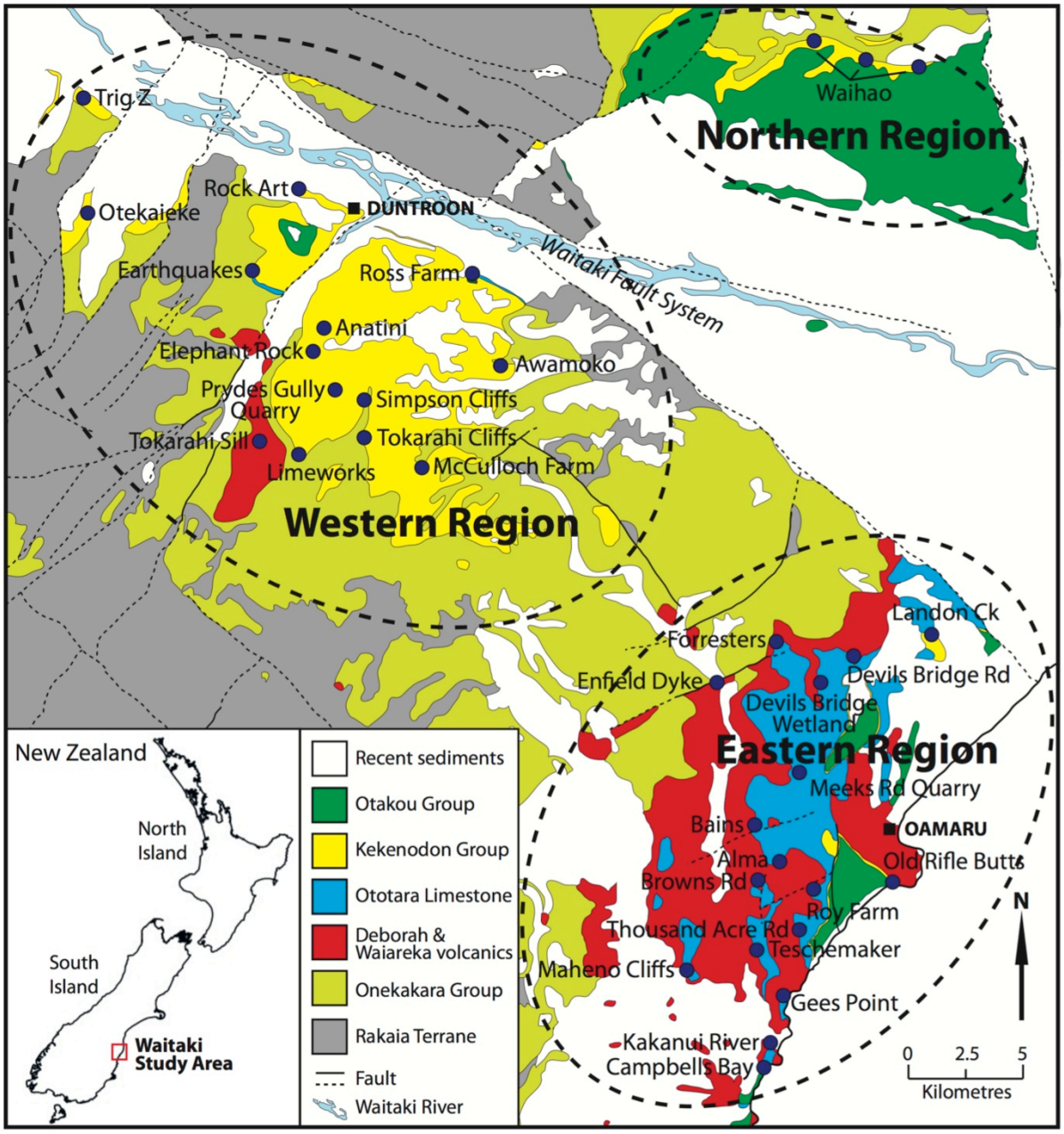

Figure 2.1. Geological map of the study area showing the locations of stratigraphic columns and outcrop analyses used in this thesis. The three 'regions' referred to in this study are also shown here. Adapted from Forsyth (2001).

The nature of the formational contacts within these regions is introduced here also. The northern region includes the Waihao collection of outcrops, the western region all outcrops west of Awamoko, while the eastern region includes those remaining outcrops around Oamaru and along the modern coastline (Fig. 2.1).

2.2.1 Formation spatial variability - overview

Spatial variation across the study area can be briefly summarised as follows.

The Onekakara Group occurs in a number of locations within the Waitaki area, but has limited outcrop exposure and is only observed in the western region (Figs. 2.1 and 2.2). There it occurs as non-calcareous to slightly calcareous sandstones and siltstones with a glauconitic component (Tapui Glauconitic Sandstone and Raki Siltstone).

The overlying Alma Group is found most extensively at the modern coast in the eastern region (Figs. 2.1 and 2.2). The Ototara Limestone (made up of the lower Maheno Marl Member and upper Weston and Flat Top Limestone Members) is found there as a bryozoan-rich, glauconite-poor, usually massive limestone, commonly interbedded with Waiareka-Deborah Volcanics. Towards the west, these eastern Ototara members grade laterally into the Earthquakes Marl Member, which consists of a glauconitic and silty wackestone.

The Kokoamu Greensand, the older of the Kekenodon Group Formations, is a highly glauconitic sandstone throughout the entire basin, although it is significantly thicker in the western region (up to 20 m), while in the east along the coast it is only centimetres thick or entirely absent (Fig. 2.2).

The younger unit, Otekaike Limestone, is a thick (~ 60 m) wackestone to packstone in the western region. To the north it becomes an extensively cross-bedded glauconitic

packstone, although along the coast it is a calcareous, glaucony facies and, like Kokoamu Greensand, very thin (cm scale) to absent (Fig. 2.2).

The overlying Otakou Group, principally Gee Greensand, is more uniform across the study area, with metre-scale outcrop along the coastline as well as inland. Its outcrop is, however, more scarce in both the northern and western regions due to extensive agriculture and its readily erodible nature (Fig. 2.2).

The three regions are discussed separately in the following Sections.

2.2.2 Northern region

The northern region of the study area contains only three locations which together make up the Waihao stratigraphic section (Fig. 2.1). These exposures include Kokoamu Greensand, and an extensive thickness of Otekaike Limestone (Fig. 2.3).

2.2.2.1 Kokoamu Greensand

Kokoamu Greensand is exposed in the northern region at the base of the Waihao section along the river at the easternmost outcrop (Fig. 2.1). There it consists of a 10 m thick, massive, glauconitic (30%), calcareous, fine-grained sandstone, which grades up into overlying Otekaike Limestone (see Section 2.2.2.2). It contains fossils of echinoderm spines, gastropods, and some brachiopod shells, along with *Ophiomorpha* and *Rhizocorallium*. *Ophiomorpha* were identified by their distinctive lighter coloured burrow rim, while *Rhizocorallium* were identified by their near planar orientation with respect to bedding, and their common U-shaped morphology.

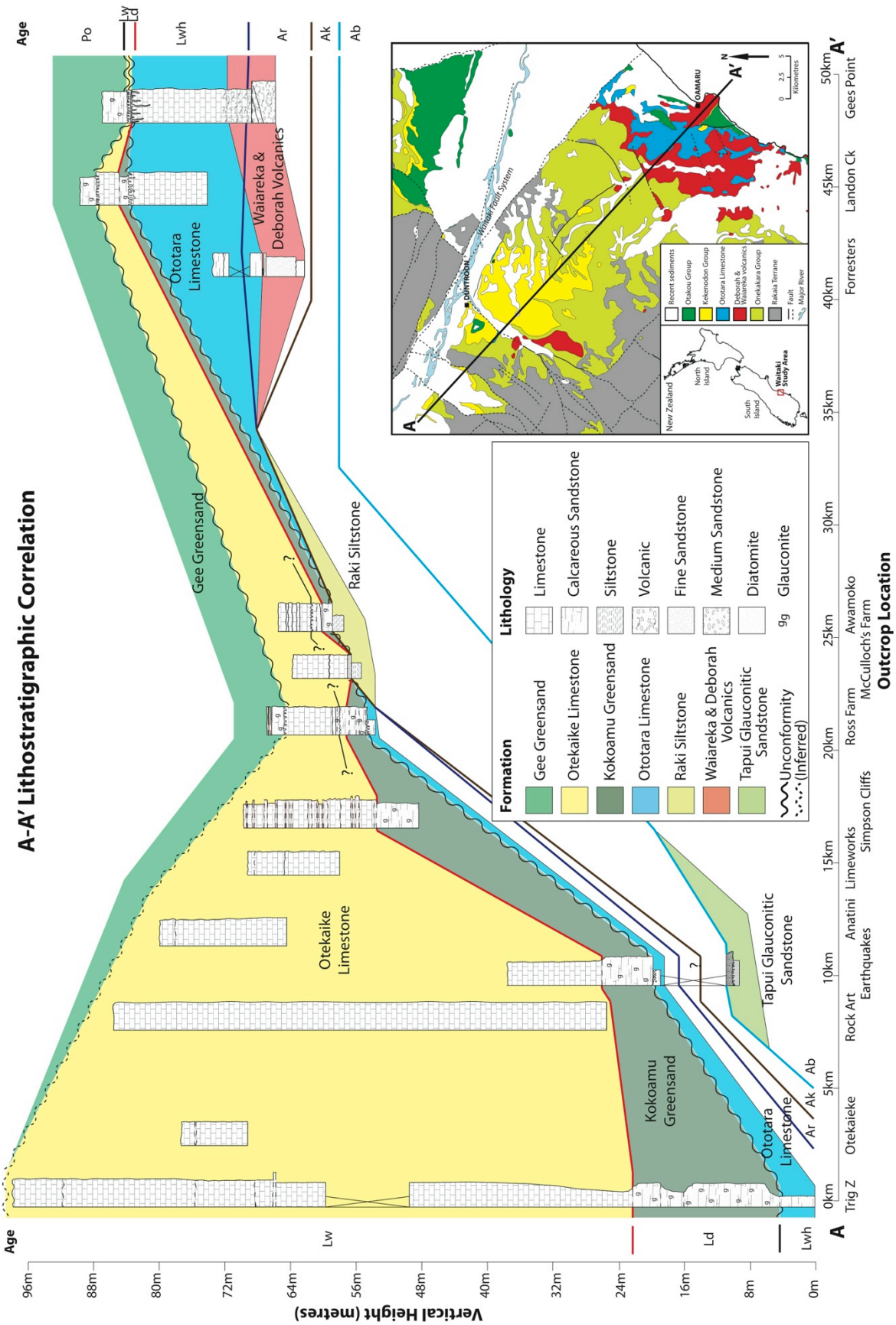

Figure 2.2. Lithostratigraphic correlation section across the study area, from Trig Z to Gees Point, showing the mid-Cenozoic Formations. See inset map for location of section.

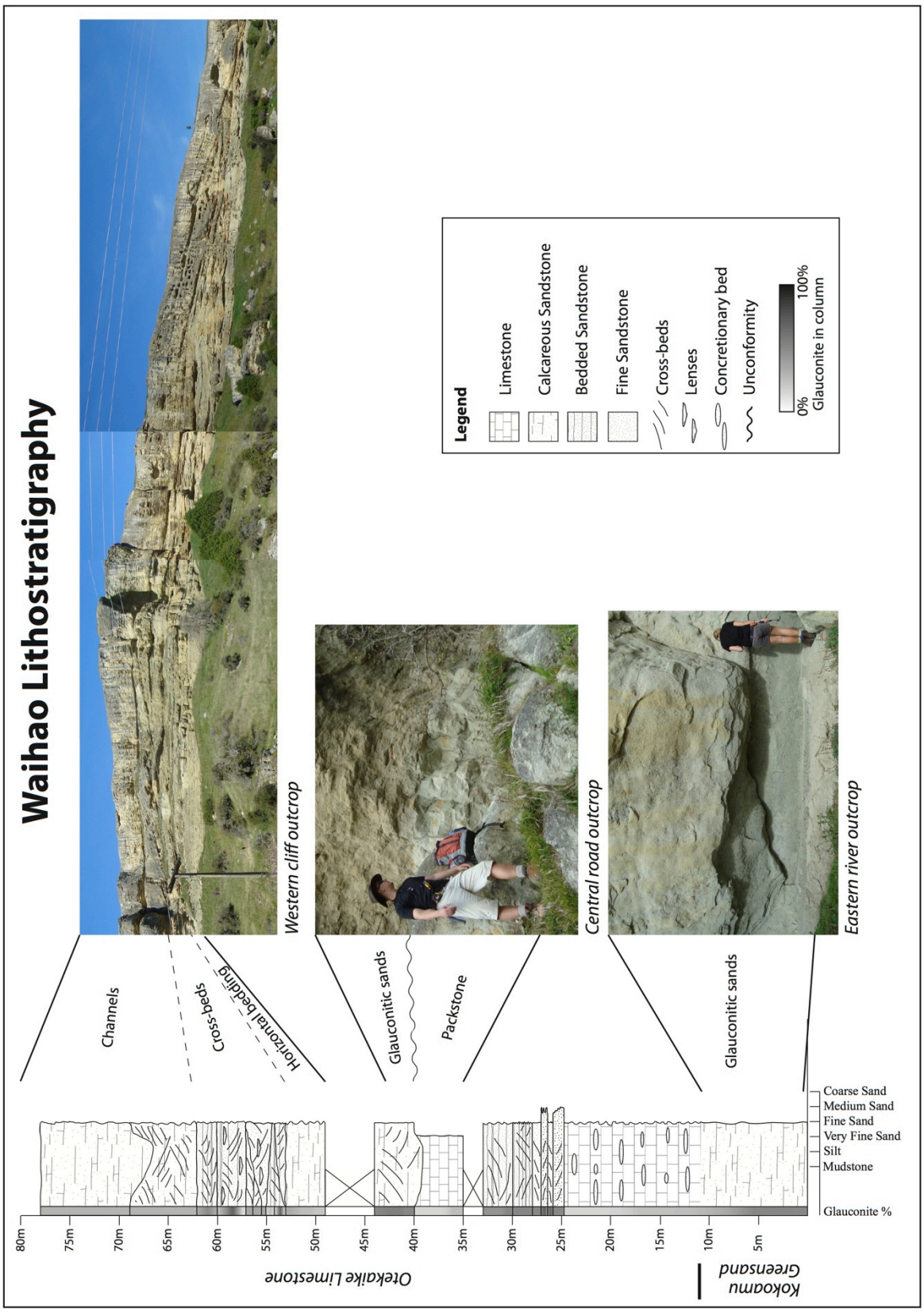

Figure 2.3. Stratigraphy of the Waihao area alongside three outcrop photos from the three different locations. Glauconitic sands of Kokoamu Greensand are at the base of the column, while the central road outcrop shows an undulating unconformity. Lastly the western cliff outcrop contains large cross-beds that underlie decimetre-scale channels.

2.2.2.2 Otekaike Limestone

Otekaike Limestone is the principal formation in the northern region, at Waihao, with a total thickness of nearly 70 m (Fig. 2.3) described here in three sections – lowermost, middle and uppermost outcrops.

Lowermost Otekaike is found near the river outcrop (Fig. 2.3), gradationally above Kokoamu Greensand. At Waihao, this lower Otekaike is similar to the Prydes Gully Limestone Member of the western region (see Section 1.2.7.2), forming a 15 m thick section of discontinuous cemented lenses and beds at cm-scale containing an upwardly decreasing glauconite content. It contains a minor siliciclastic component (2%), as well as numerous echinoderm, gastropod, and brachiopod fossils alongside abundant *Scolicia* (Fig. 2.4). *Scolicia* is identified by its characteristic ribbed texture and common singular trace along bedding (Fig. 2.4). This lithology grades rapidly up into the Alma Member (see Section 1.2.7.2), beginning with ~ 7 m of cross-bedded and cross-laminated fine- to medium-grained glauconitic (up to 50%) beds of 1 – 2 m thickness, with the uppermost bed forming the top of the eastern river section. These beds are fossiliferous, with echinoderms and brachiopod fragments, as well as some large (up to 8 cm diameter) *Scolicia* (Fig. 2.4). An estimated 2 m is missing between this section and the overlying exposure found at the middle outcrop.

Figure 2.4. *Scolicia* traces found at Waihao in Otekaike Limestone.

The middle outcrop consists of two lithologies separated by an undulating sharp contact, and is located on the central road outcrop (Fig. 2.3). The lower of these is a 5 m thick, very fine-grained, friable, glauconite (~ 40%) sandstone, with poorly preserved bedding. It contains a fossil assemblage of brachiopods, small shell fragments, echinoderm spines, and calcareous worm tubes. The intervening undulating contact has a fossil lag of echinoderm, brachiopod, bivalve, and gastropod fragments, as well as some scattered shark teeth together with a few rounded quartz pebbles. The sediments overlying this contact consist of a 4 m thick, fine-grained, poorly sorted, bioturbated, glauconitic, friable, and sandy packstone. The middle outcrop fossil content is the same as that found on the contact surface, plus some coralline algae. From this exposure there is an estimated 10 m of missing outcrop between these sediments and the western cliff-face outcrop (Fig. 2.3).

The uppermost stratigraphy of the Waihao section is located at the eastern cliff outcrop along a 30 m high, laterally extensive cliff section (Fig. 2.3). The lowest unit is a ~ 4 m thick, fine-grained and glauconitic (35%) limestone, with cm-scale poorly preserved bedding, containing a number of echinoderm spines, corals and brachiopod fragments, as well as some moderate bioturbation. Its upper contact is erosive and overlain by 9 m of cross-bedded channel deposits, with significant variation in glauconite content. Bedding found within these cross-beds often shows alternation between highly glauconitic (up to 75% glauconite) and poorly (~ 5%) glauconitic beds. Cross-bed packages often crosscut those stratigraphically below them, forming cross-bedded sections ~ 1 m thick. Palaeocurrent directions trend eastward. The fossil content comprises abundant echinoderm fragments (plate and spines) and small *Lentipecten*, as well as intense *Scolicia* traces. The upper ~ 16 m consists of large channel structures, with channel widths of 20 to 100 m, exhibiting a northward palaeoflow trend. These channels form the top of the

Waihao section. There is no upper contact of Otekaike Limestone with any younger formation.

2.2.3 Western region

The western region contains all of the mid-Cenozoic Formations of interest in the present study, with the exception of the youngest Otakou Group unit - the Rifle Butts Formation. The older Onekakara Group is found exposed only in three locations.

2.2.3.1 Tapui Glauconitic Sandstone

Tapui Glauconitic Sandstone has been located in only one exposure of those recorded in this study, at Earthquakes (Fig. 2.1). There this formation occurs as a deeply weathered, glauconitic sandstone containing quartz pebbles (principally located at the base), lying ~ 10 m below the next exposed sediments of Ototara Limestone. A grass-covered slope has buried any intervening outcrop under which there was assumed by Gage (1957) to be Raki Siltstone. Although Gage (1957) located Tapui Sandstone exposures at outcrops associated with the younger mid-Cenozoic units in two locations mapped here, west of Awamoko and west of McCullochs Farm (Fig. 2.1), these were not found to be currently exposed. It was observed at the Tokarahi Sill (Fig. 2.1), however, where columnar basalt has intruded into Tapui, and where it is a very fine-grained to fine-grained, slightly glauconitic (2 – 4%), locally cross-bedded sandstone.

2.2.3.2 Raki Siltstone

Raki Siltstone was found exposed at two locations in the western region, at Awamoko and McCullochs Farm (Fig. 2.1). At both locations this unit is a weathered, poorly- to non-calcareous, grey, bioturbated, glauconitic siltstone to fine sandstone. As the upper contact is not exposed its true thickness is unknown but, from what is visible, it

would be > 1.5 m. Fossils are not observable in either outcrop or thin section. The upper contact of this unit marks a significant unconformity with either overlying Kokoamu Greensand (Awamoko Creek) or Otekaike Limestone (McCulloch Farm) as described below.

2.2.3.3 Unconformity at top of Raki Siltstone

The upper contacts of Raki Siltstone at Awamoko Creek and McCulloch Farm are shown in Fig. 2.5 (B and C; another unconformity described in Section 2.2.3.6 applies to Figs. A and D).

At Awamoko Creek, Raki Siltstone underlies Kokoamu Greensand and forms a sharp boundary with a slight angular discordance (Fig. 2.5B). Partly eroded *Thalassinoides* burrows with a glauconite sand infill extend only 5 cm downward. These were distinguished from *Ophiomorpha* by the nature of the burrow lining, as these lacked the distinctive (often lighter) burrwo rim, indicating their penetration into a consolidated and harder sediment substrate. There is no obvious fossil lag on top of the contact.

At McCulloch Farm, the Siltstone is capped by well cemented Otekaike Limestone (Fig. 2.5C). *Thalassinoides* are abundant at this contact, although penetration still appears shallow (~ 5 – 10 cm). A lag deposit of whole and fragmented pectens, calcareous worm tubes, scattered and heavily phosphatised cetacean bone, and angular clasts of phosphate, lie on this contact surface.

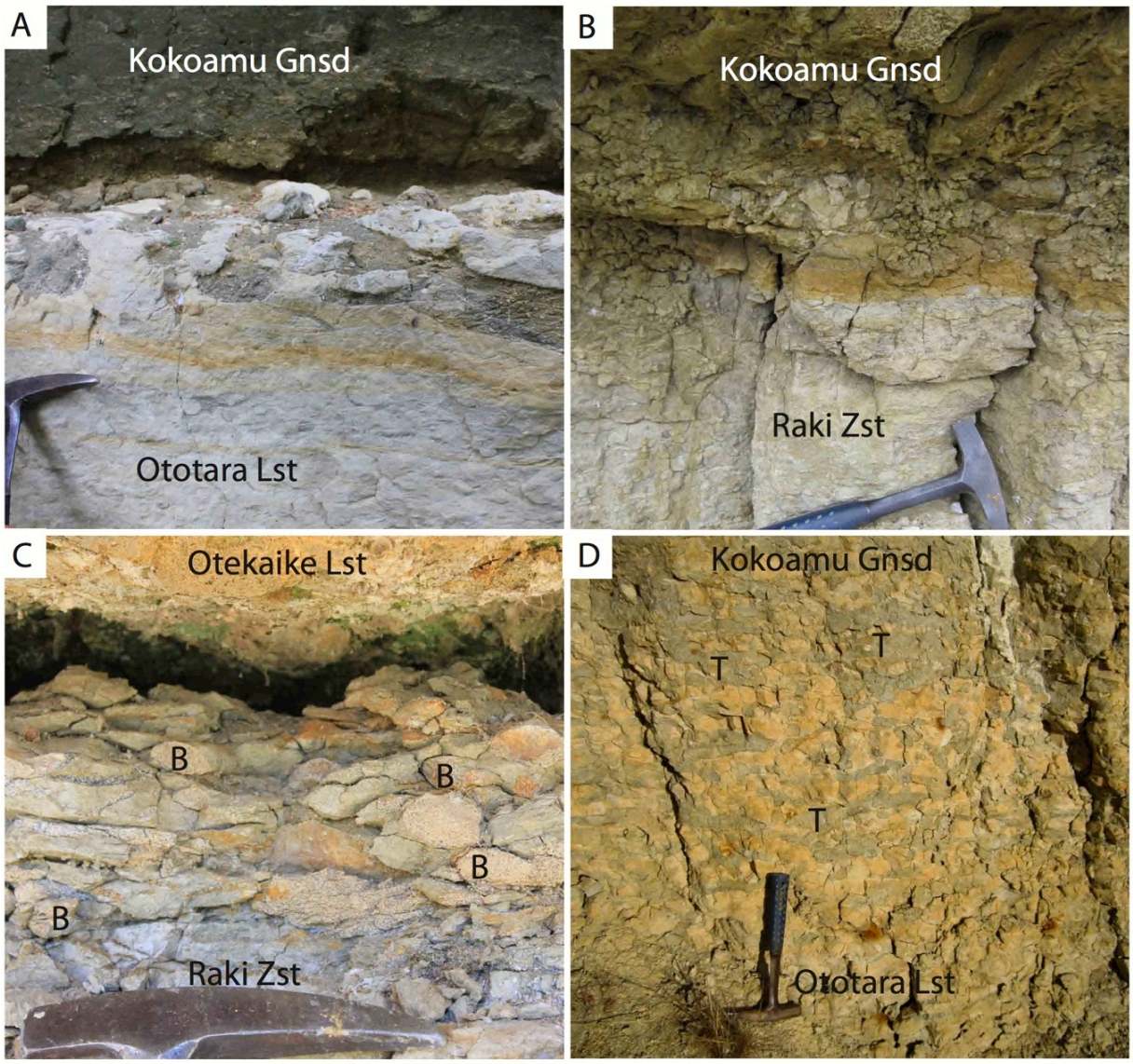

Figure 2.5. Outcrop photos showing the nature of the unconformity above Ototara Limestone and Raki Siltstone in the western Waitaki study area. A: Shallow karst contact between Ototara Limestone and Kokoamu Greensand at Ross Farm. B: Unconformable contact at Awamoko Creek between Raki Siltstone and Kokoamu Greensand. Note that Ototara Limestone is not present here. C: McCulloch Farm, where Raki Silstone is overlain by Otekaike Limestone. Both Ototara Limestone and Kokoamu Greensand are absent. Note burrows through the Raki Siltstone. B = burrow. D: Heavily bored firmground contact at Earthquakes between Ototara Limestone and Kokoamu Greensand. The *Thallasanoides* burrows are filled with Kokoamu Greensand. T = *Thallasanoides*.

2.2.3.4 Waiareka Volcanics

There is limited exposure of the older igneous unit, the Waiareka Volcanics, in the western region; and no exposure of the younger Deborah Volcanics. The only outcrop of Waiareka Volcanics recorded during this study was at Tokarahi Sill (Fig. 2.1), where a ~ 10 m high, columnar-jointed, basaltic sill can be seen intruding into Tapui Glauconitic Sandstone (see Section 2.2.3.1), with associated pillow basalts. The contact between the sediments and the sill show a flaggy, baked margin, while the sill itself shows vertically aligned vesicles. The sediments into which this sill has intruded are likely to be Tapui Glauconitic Sandstone, as suggested by Gage (1957).

2.2.3.5 Ototara Limestone

Otorara Limestone is present in the western region at Trig Z (identified from drill-hole data by Edwards (1971)), Earthquakes, and Ross Farm (Fig. 2.1), and consists solely of the Earthquakes Marl Member (see Section 1.2.6.1). Like the lower Onekakara Group units, this formation is thin (< 4 m thick), and consists of a calcareous, bioturbated, quartzose silty wackestone with no fossils observed in outcrop. *Ophiomorpha* burrows are common, especially at Ross Farm. In the two exposures of this member observed here, Ross Farm and Earthquakes, the upper contact is with Kokoamu Greensand, forming a significant unconformity as described below.

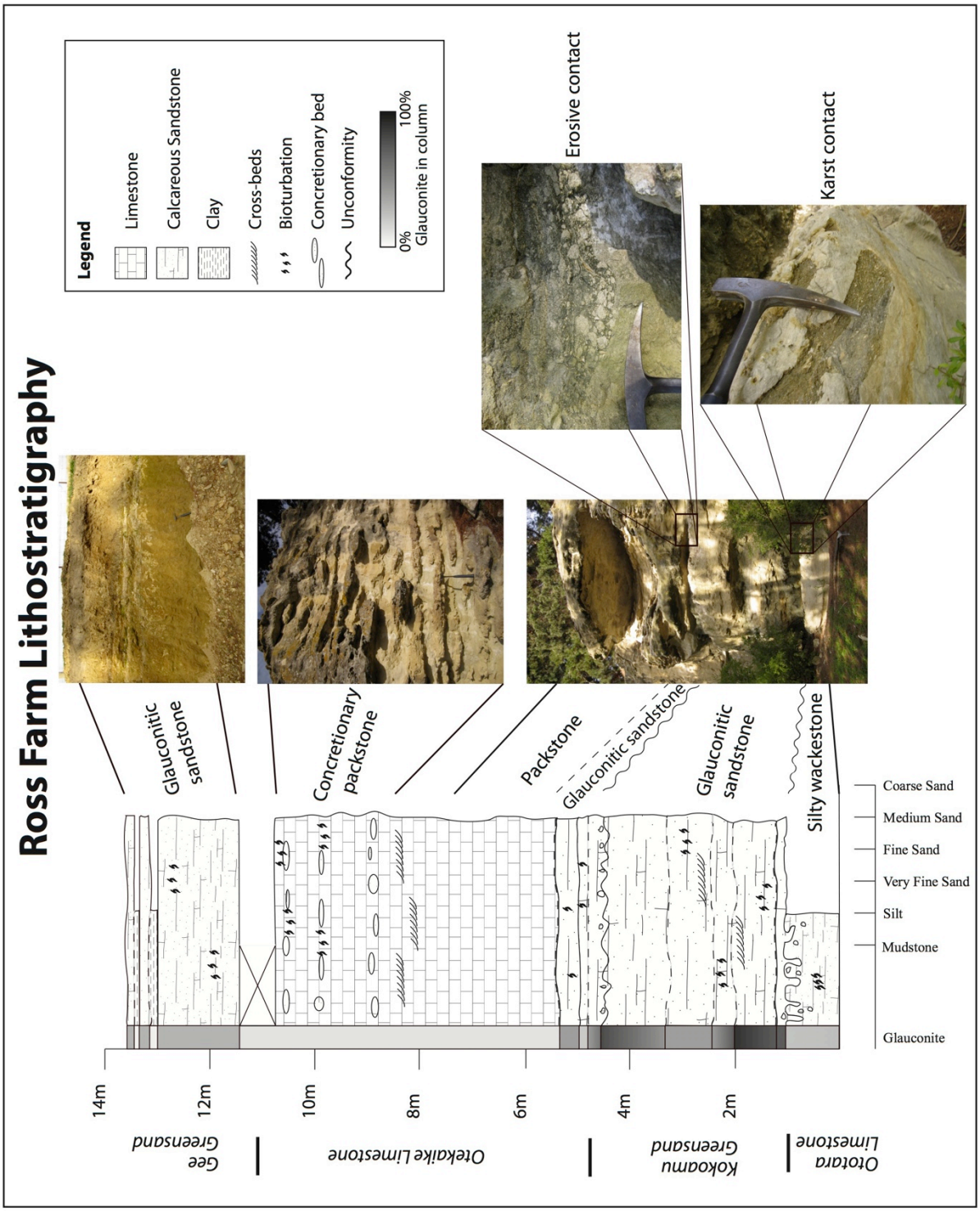

Figure 2.6. Stratigraphy of the Ross Farm outcrop correlated to photos taken at outcrop scale. Annotated is the variation in lithology up the section, along with the Formation names. Note the two unconformities located in the lower section at the Ototara Limestone-Kokoamu Greensand contact, as well as near the Kokoamu Greensand-Otekaike Limestone transition.

2.2.3.6 Unconformity at top of Ototara Limestone

At Earthquakes (Fig. 2.1), the Ototara-Limestone/Kokoamu-Greensand contact is a *Thallasinoides*-burrowed firmground (Fig 2.5D), with the burrows filled with glauconitic sands over a 1 m interval. At Ross Farm, however, this contact appears to be that of a shallow karst, with large cavities filled with highly glauconitic sands of the overlying Kokoamu Greensand (Figs. 2.5A and 2.6).

Data from the drill-hole log at Trig Z (Edwards, 1971) record a gradational contact between Ototara Limestone and overlying Kokoamu Greensand, although it is suggested here that this contact is probably still an unconformity as seen elsewhere in the region - as development of a burrowed firmground may appear gradational in a drill-core.

2.2.3.7 Kokoamu Greensand

Kokoamu Greensand in the western region is relatively uniform, and consists of a bioturbated, calcareous, glauconite sandstone. It occurs in most outcrops in this region, and is usually absent only where the outcrops consists solely of younger units; with one exception at McCulloch Farm (Fig. 2.1) where it is absent between Raki Siltstone and Otekaike Limestone.

Kokoamu Greensand ranges in thickness from up to 20 m at Trig Z, down to as thin as ~ 1.5 m at Awamoko. The lower part of this formation usually contains cross-beds and highly fragmented macrofossils, with a higher glauconite content (up to 90%) than the upper part (25 – 40%) (Fig. 2.6). The upper part contains a more intact fossil assemblage consisting of brachiopods, echinoderm plates and spines, pectinids, and calcareous worm tubes. Bioturbation is present throughout the formation, although is more prevalent in the lower section, and is dominated by *Ophiomorpha* burrows.

While the Kokoamu Greensand contact with overlying Otekaike Limestone can be described as gradational is most areas, there is an unconformable surface near, or at, this transition at Ross Farm and Awamoko (Fig. 2.6). The unconformable horizon observed in this study consists of a slightly undulose surface of less glauconitic limestone that contains small (< 5 cm) limestone clasts above it, on top of which is a calcareous glauconite sandstone which rapidly grades back into Otekaike Limestone. This surface has also been suggested by Jenkins (1987) to exist at Earthquakes (Fig. 2.1), based on a fossil lag recorded in Gage (1957), but this was not confirmed at outcrop during the present study. The Earthquakes contact was instead observed as a rapid gradational contact between a calcareous glauconite sandstone into a less glauconitic limestone. However, whether this apparently unconformable surface at Ross Farm is actually on the Kokoamu Greensand to Otekaike Limestone boundary is difficult to determine in outcrop due to the generally gradational nature usually observed between these two formations – rather, the separation is based partly on a simple reduction in glauconite content between them.

2.2.3.8 Otekaike Limestone

Otekaike Limestone is the dominant formation in the western region, with exposures up to 70 m thick (at Trig Z), thinning down to as little as 6 m further west at Awamoko (Fig. 2.1), although some of the thinner exposures may not be representative of the whole unit. As mentioned earlier (Section 1.2.7.2), Otekaike Limestone comprises five Members (four of which are found in the western region), ranging from muddy glauconitic wackestones to less glauconitic, fossiliferous, and bedded packstones up-section.

The oldest of these Members, the Maerewhenua Glauconitic Limestone Member, is found as a massive glauconitic limestone located at the base of Otekaike Limestone in all outcrops of this region, and appears to be the most extensive member present. At Trig Z it

is more muddy, forming a wackestone with abundant coral Flabellum and localised fossiliferous pockets. Further east (e.g., Ross Farm and Awamoko) it is a packstone (Fig. 2.6). It is at the base of this Member that the upper Kokoamu Greensand localised unconformity is found (at Ross Farm and Awamoko) although, as mentioned in Section 2.2.3.7, this surface may also be present within the lower part of the Otekaike Limestone.

At Trig Z, the Maerewhenua Member is bounded at its upper contact by a concentrated fossil bed (~ 30 cm thick) containing abundant molluscs (gastropods and bivalves), brachiopods, worm tubes, and flabellum corals. In other outcrops in the western region this transition is not so pronounced and is rather more gradational.

The Prydes Gully Nodular Limestone Member is found in most outcrops in the western region, with the exception of Otekaieke, Rock Art, and Earthquakes (Fig. 2.1). Where exposed, it consists of a bedded (cm-scale) limestone with nodular and laterally continuous cemented beds and lenses (Fig. 2.6). The cemented beds tend to have a higher glauconite content than the horizons between them (15 – 25% versus 5 – 15%). The beds also have a more intact fossil assemblage of predominantly pectens, brachiopods, and echinoderms, while the intervening horizons are less fossiliferous and more likely to have a disarticulated fossil content. The overall glauconite content of this member decreases up-section (25 – 5%).

The Miller Member is similar to the Prydes Gully Nodular Limestone Member, except that its cemented horizons are less continuous and consist more of pods of concretions rather than laterally extensive beds. This member sits gradationally on top of the Prydes Gully Member and is distinguished by the change to lenses of concretions, as well as a lower glauconite content (2 – 5%). Its fossil content is similar to that of the Prydes Gully Member.

Lastly, the Waitoura Marl Member was observed only at Trig Z in this study, and while Gage (1957) also records this member at Awamoko it was not identified in the field during this study. At Trig Z this member lies gradationally on top of the Miller Member, and consists of 6 m of highly weathered, slightly glauconitic (10%) packstone. It contains some gastropod and bivalve fossils, which are generally fragmented. In this location the Waitoura Marl Member forms the top of the section.

2.2.3.9 Unconformity at top of Otekaike Limestone

The upper contact of Otekaike Limestone with overlying Gee Greensand is a significant unconformity elsewhere in the study area (see Section 2.2.4.6), but it was not observed anywhere in the western region during this study. Widespread erosion and extensive agricultural modification has obscured any clear occurrences of this contact. Where Gee Greensand is present (Ross Farm) the contact is too poorly preserved for its nature to be clear.

2.2.3.10 Gee Greensand

Gee Greensand was found in only one location in the western region, at Ross Farm (Fig. 2.1), principally due to the agricultural nature of the area, with common grass cover at this stratigraphic level (Fig. 2.6). At Ross Farm it is a moderately weathered and extensively bioturbated, glauconite (~ 30%) sandstone ~ 2 m thick, with *Ophiomorpha* burrows and some brachiopod shells found throughout. This bioturbation and fossil content decreases up-section.

2.2.4 Eastern region

The eastern region of the study area is dominated by the units of the Alma Group (see Section 1.2.6), with only thin exposures of the younger mid-Cenozoic formations overlying these. No units older than the Alma Group were found there during this study.

2.2.4.1 Waiareka and Deborah Volcanics

Waiareka and Deborah Volcanics are located extensively around the eastern region. Pillow lavas can be found at Cape Wanbrow to the northeast of Old Rifle Butts and at Alma (Fig. 2.1), where they form basaltic pillows set in a calcareous matrix containing a number of bryozoan fragments. At Alma the pillow lavas grade into the onlapping Ototara Limestone (see Section 2.2.4.2), with cross-bedded tuff beds and algal-coated basalt clasts within a calcareous matrix, forming a gradational contact between the two formations over a 1 m interval.

Tuff cones can be found at exposures along the modern coastline at Campbells Bay, Kakanui River, Gees Point, and Old Rifle Butts (Fig. 2.1). These cones contain dipping tuffaceous beds, often with a decrease in grainsize towards the rims. At Campbells Bay, concentric bedding can be observed from the cliff, including a change in dip towards the eruptive centre, marking the original cone structure. The cone at Campbells Bay stratigraphically overlies an older cone found further up the Kakanui River, with onlapping Ototara Limestone occurring over both of these features.

Oamaru Diatomite, a member of the Waiareka Volcanics (see Section 1.2.6.2.1), can be found at Forresters and Bains (Fig. 2.1), overlain by volcanic tuffs at the latter. At Forresters the upper contact consists of a zone of slumping and reworking that grades into overlying Weston Member of Ototara Limestone. The Diatomite is rich in diatoms,

radiolarians and siliceous sponge spicules, as well as minor calcareous benthic foraminifera. No macrofossils were observed in outcrop.

At Enfield, a 35 m high, southwest-northeast aligned, vertical basalt dyke intrudes into sediments of indeterminate type. The dyke itself shows a chilled margin. Observations of Gage (1957) indicate this dyke is intruded into sediments of Tapui Glauconitic Sandstone.

2.2.4.2 Ototara Limestone

Ototara Limestone forms the dominant unit in the eastern region, with exposures identified in this study up to 35 m thick. Of the five members of Ototara Limestone (see Section 1.2.6.1), all but the Earthquakes Marl Member are present in this region (the Everett Brachiopod Limestone Member (Gage, 1957) was not examined during the course of this study as its only exposure near Kakanui is no longer publicly accessible). The oldest of the exposed Ototara Limestone members in this region, the basal Maheno Marl Member, is found principally around Maheno (Fig. 2.1) where it forms a 2 m thick, bioturbated, slightly fossiliferous, calcareous wackestone at the base of that exposure.

The two members that make up the principal lithology of Ototara Limestone are the lower Weston Member and the upper Flat Top Limestone Member, consisting of non-glauconitic, bryozoan-rich grainstones found throughout the eastern region. These two members are only differentiated by the occurrence of volcanic units between them (see Section 2.2.4.1), although the lower Weston Member contains a higher abundance of igneous clasts. These members are found in large cliff-forming exposures at Devils Bridge Wetland, Meeks Rd Quarry (exposure only produced by quarrying), Maheno Cliffs, and Teschemaker (Fig. 2.1). At Meeks Rd Quarry, Ototara Limestone contains at least three

lenses of orange to brown clays, up to ~ 40 cm thick, containing bryozoans, brachiopods and minor bioturbation.

The more coastal eastern exposures of Ototara Limestone are thinner (up to 14 m), formed from the younger Flat Top Limestone Member, and found at Landon Creek, Old Rifle Butts, Gees Point, Kakanui River, and Campbells Bay (Fig. 2.1). Here, with the exception of the northernmost exposure at Landon Creek, Ototara Limestone is found onlapping volcanic cones. At Thousand Acre Rd (Fig. 2.1) a 1 m thick tuff is unconformably overlain by 1 m of bryozoan-rich Ototara Limestone. Here there is evidence of cross-bedding in the lower limestone, with the contact showing indications of erosion including blocks of tuff. These onlaps form a transition consisting of a mixed calcareous and igneous horizon (usually no more than 1 m thick; with the thinnest at Old Rifle Butts containing large, 5 – 10 cm, rhodoliths), before returning to a pure Ototara Limestone grainstone lithology. It is in these same easterly exposures, including the outcrop at Landon Creek, that the upper Ototara Limestone contact is exposed underlying Kokoamu Greensand. At all of these locations it consists of a karst horizon, with a locally rubbly surface (Figs. 2.7A-D and 2.8).

At Old Rifle Butts (Fig. 2.1), the top 2 m of Ototara Limestone forms a rhodolith rudstone that overlies the Flat Top Limestone Member, consisting of rounded algal balls set in a bryozoan-rich packstone matrix. The top of this bed marks the upper limit of Ototara Limestone at this location, although its upper contact here is an eroded and undulating contact with Gee Greensand, with no indication of Kekenodon Group units anywhere at this interval. A Rhodolith Rudstone can also be found at Roy Farm (Fig. 2.1) forming the top of the Ototara Limestone exposure there, although no overlying contact could be discerned in the present study.

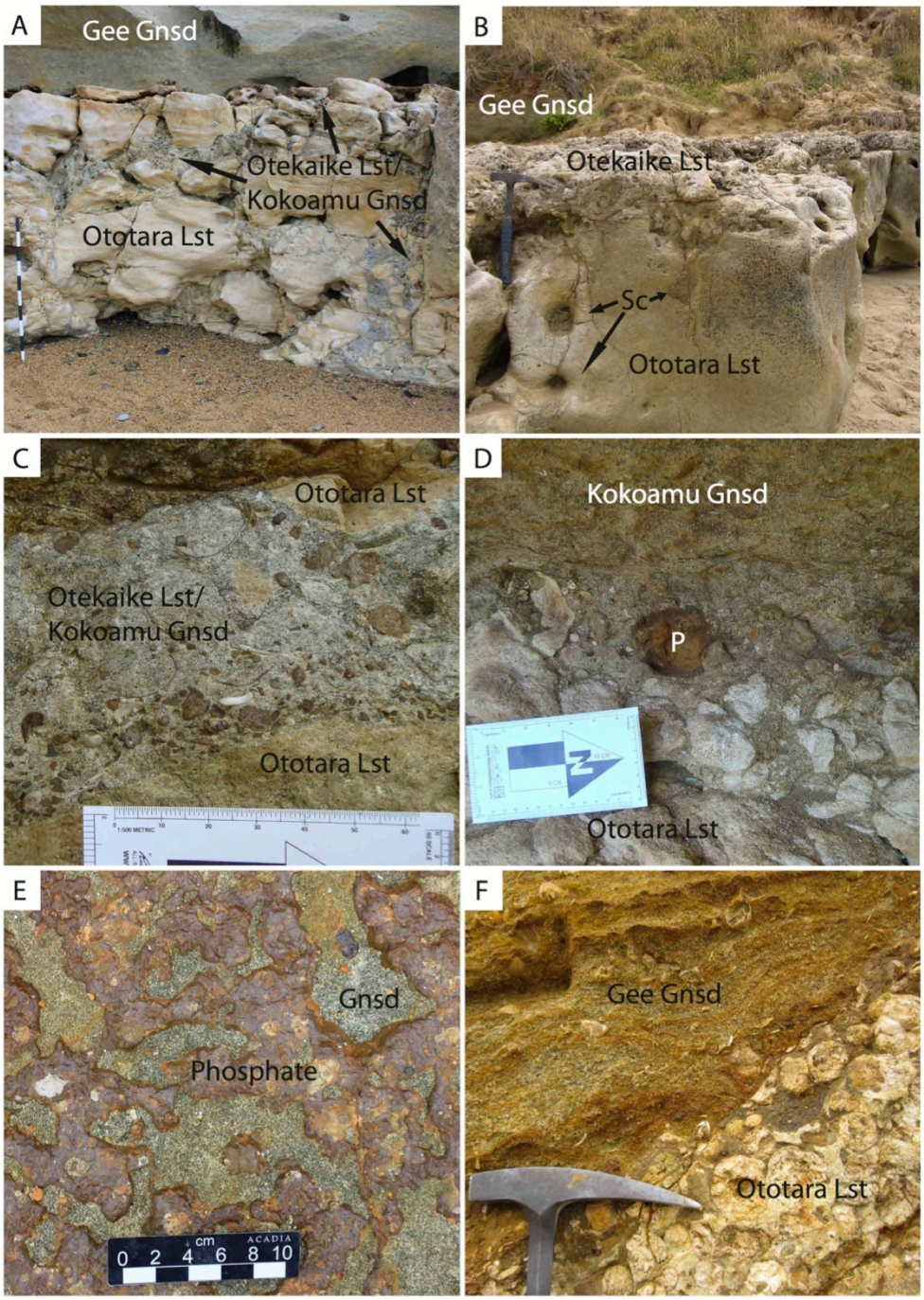

Figure 2.7. Unconformity surface above Ototara Limestone in eastern study area. A: Karst cavities on Ototara Limestone, filled with Otekaike Limestone and Kokoamu Greensand, and overlain by Gee Greensand. B: Karst on Ototara Limestone at Campbells Bay, with thin Kokoamu Greensand and Otekaike Limestone, mostly within dissolution cavities. A second karst filled with Gee Greensand penetrates the older cavities. Sc = solution cavity. C: Karst cavity fill on Ototara Limestone at Gees Point, illustrating brecciated and graded nature. D: Rubbly karst on Ototara Limestone at Landon Creek. P = phosphatised clast. E: Top-down view of phosphatised surface on Ototara Limestone at Gees Point. Gee Greensand filling karst cavities. F: Ototara Limestone upper contact at Old Rifle Butts. This surface has been eroded, and overlain by Gee Greensand.

2.2.4.3 Unconformity at top of Ototara Limestone

The upper Ototara Limestone contact forms a karst surface (Figs. 2.7A-D) in the eastern region, along the modern coastline (Fig. 2.1). Solution cavities generated from the karst surface extend ~ 3 m downward into the bryozoan-rich limestone. These cavities average 15 – 20 cm in diameter, ranging up to 30 cm. Cavity boundaries are sharp with minor undulation, and with some networking between. Cavities are commonly filled with younger Kokoamu Greensand (see Section 2.2.4.4), which is usually very thin where it overlies these karst surfaces, and may also contain Otekaike Limestone (Figs. 2.7A and 2.7B). Phosphatised sub-rounded to angular volcanic and limestone, pebble-sized clasts (up to 5 cm) commonly form concentrations at any depth within the matrix, and occasionally form a clast-supported fill (Fig. 2.7C). At Gees Point the karst surface is sometimes brecciated, with the interstices of the limestone filled with laminated to massive greensand, while locally it exhibits phosphatised coatings (Fig. 2.7E).

2.2.4.4 Kokoamu Greensand

Kokoamu Greensand occurs in only a few of the more coastal sites (Landon Creek, Gees Point, and Campbells Bay; Fig. 2.1), where it is no more than 1 m thick. The thickest occurrence is at Landon Creek where it is a glauconitic (40%), fossiliferous, friable, calcareous sandstone, containing mostly disarticulated brachiopods and echinoids. There it grades rapidly into overlying Otekaike Limestone.

To the south, at Gees Point and Campbells Bay, Kokoamu Greensand is difficult to distinguish from Otekaike Limestone due to the extremely thin (< 20 cm) exposure that forms these two units. In some parts of the Gees Point outcrop Kokoamu Greensand is found only within the karst dissolution cavities at the upper contact of Ototara Limestone, while in others it is entirely absent (Fig. 2.8). At Campbells Bay, Kokoamu Greensand is

again found only within solution cavities as veneers of lithified, fossiliferous, and glauconitic sandstone.

2.2.4.5 Otekaike Limestone

Like Kokoamu Greensand, Otekaike Limestone is found in only three outcrops in the eastern region (Landon Creek, Gees Point, and Campbells Bay; Fig. 2.1). At Landon Creek it forms the thickest eastern exposure at 2 m, and consists of a poorly glauconitic (5%) packstone, containing fragments of echinoderms, bivalves, and brachiopods. At Gees Point and Campbells Bay, Otekaike Limestone forms a very thin veneer (no more than 20 cm thick at Campbells Bay) overlying the Ototara Limestone karst surface. There it forms a lithified, slightly glauconitic packstone containing some bivalve fragments, and some echinoderm plates at thin section scale. In both locations the top of Otekaike Limestone is karst and forms a significant unconformity (see Section 2.2.4.6).

2.2.4.6 Unconformity at top of Otekaike Limestone

As with the unconformity on top of Ototara Limestone, the unconformity between the Otekaike Limestone and Gee Greensand also forms a karst surface in the eastern region (Landon Creek, Campbells Bay and part of Gee's Point; Figs. 2.7A,B,D).

At Old Rifle Butts, and much of the outcrop at Gees Point, this contact is amalgamated with the earlier Ototara unconformity, with the intervening Formations being absent (Fig. 2.7F).

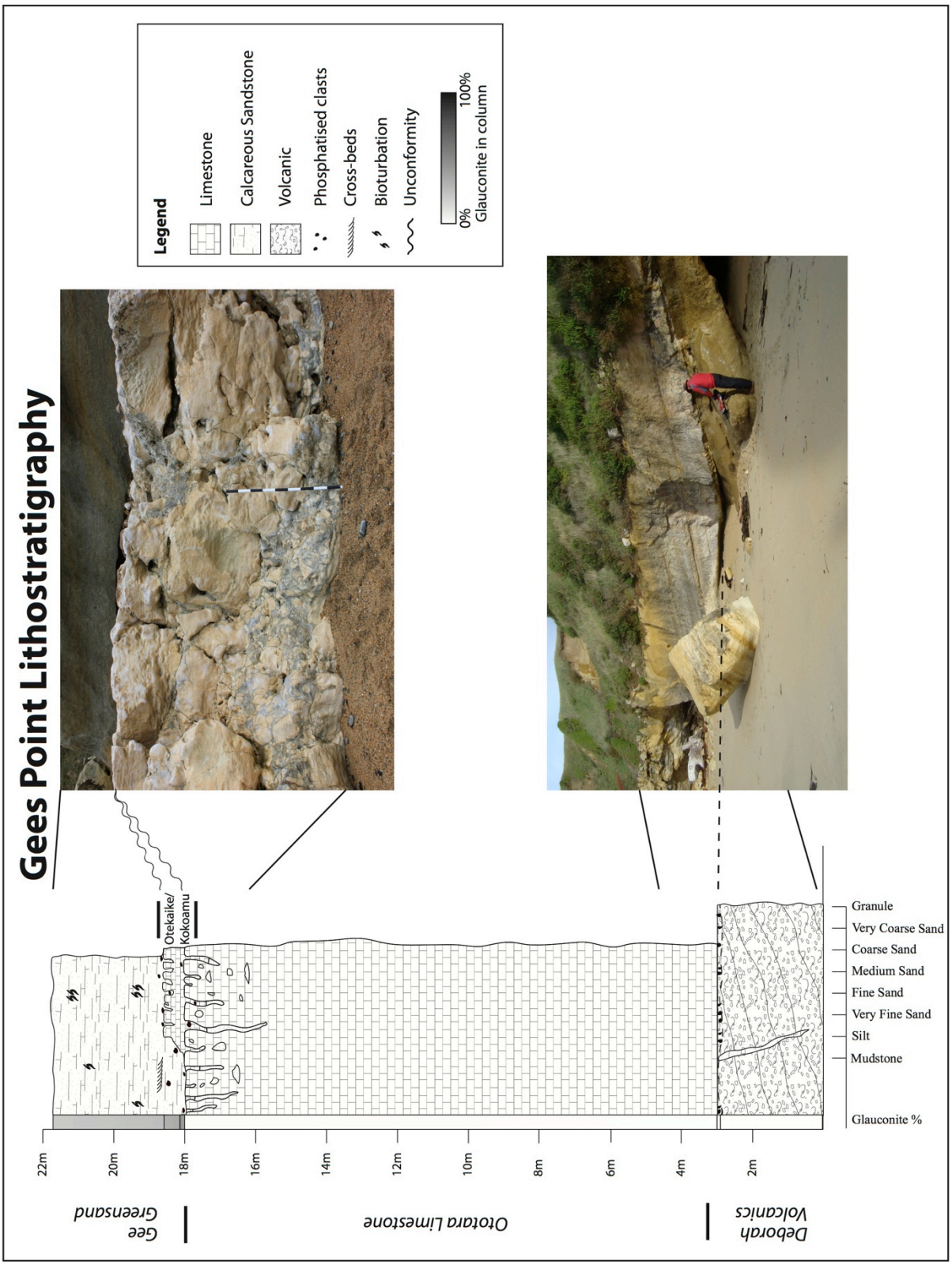

Figure 2.8. Stratigraphy of Gees Point in the eastern region, alongside two outcrop scale photos, illustrating the karst surface that occurs on top of the Ototara Limestone and the thin veneer of Kekenodon Group sediments that overlies it. Also shown is the onlapping of the Ototara Limestone against the flanks of a Deborah Volcanics tuff cone.

At Gee's Point and Campbells Bay, solution cavities developed at this unconformity appear to have re-excavated those produced during karst development following Ototara Limestone deposition, but can be distinguished by fillings of *Melitodes* coral fragments which are abundant at the base of Gee Greensand. Solution cavities are not as deeply penetrating as in the earlier Ototara unconformity (maximum 75 cm) at this location, although at Campbells Bay solution cavities extend to a depth of ~ 3 m.

Phosphatisation does not occur at this unconformity surface except at Gees Point where it is amalgamated with the earlier unconformity on top of Ototara Limestone (Gee Greensand directly overlies Ototara Limestone, without any intervening Kokoamu Greensand or Otekaike Limestone), and the surface is planar and heavily phosphatised (Fig. 2.7E). This surface exhibits numerous phosphatised and non-phosphatised *Melitodes* holdfasts. While this and the earlier Ototara unconformity are amalgamated for the most part at Gee's Point, palaeotopographic lows filled by Otekaike Limestone record a separate development of this surface. At Gee's Point, oncolites are abundant on the exposed surfaces of Otekaike Limestone. Although poorly exposed at the Landon Creek outcrop, this unconformity can be distinguished where Gee Greensand fills small solution cavities within the underlying cemented Otekaike Limestone.

At Old Rifle Butts, this unconformity is again amalgamated with the unconformity on top of Ototara Limestone. There the surface is planar and eroded, however, and phosphate has not developed (Fig. 2.7F). Subaerial exposure associated with either of these unconformities cannot be confirmed as the development of the planar erosion surface has removed any evidence that might have existed.

2.2.4.7 Gee Greensand

Gee Greensand is located along the more coastal outcrops in the eastern region, including Landon Creek, Old Rifle Butts, Gees Point, and Campbells Bay (Fig. 2.1), with its thickest exposure at Old Rifle Butts (~ 7 m). There it has a basal 2 m thick, brachiopod-rich bed containing a high concentration of mostly intact brachiopods set in a calcareous, glauconite (~ 40%) sandstone matrix, which overlies an eroded contact with Ototara Limestone (see Section 2.2.4.2). This then grades into a fine-grained glauconite sandstone, below another 10 cm thick brachiopod bed. Lying gradationally above this last bed is another 4 m of glauconite sandstone containing scattered broken and whole brachiopods, beneath a further 50 cm thick bed containing abundant gastropods and brachiopods. This marks the top of Gee Greensand at Old Rifle Butts, beyond which it grades into the overlying Rifle Butts Formation (see Section 2.2.4.8).

At Landon Creek, Gees Point, and Campbells Bay, Gee Greensand is relatively thin (~ 1 m exposed). At Gees Point its lower section contains abundant phosphatic clasts as well as some localised cross-bedding, while at the southern end of this location it onlaps onto the face of a small normal fault offsetting Ototara Limestone (Fig. 2.8). At all three of these locations it can be found within solution cavities that penetrate the surface of the underlying Otekaike Limestone, while at Gees Point and Campbells Bay the thin nature of the Kekenodon Group means that these solution cavities extend into the Ototara Limestone. *Ophiomorpha* bioturbation is common throughout Gee Greensand.

2.2.4.8 Rifle Butts Formation

The Rifle Butts Formation is found only in the eastern region, at Old Rifle Butts (Fig. 2.1), where it is a grey/blue fine grained, glauconitic, siliciclastic mudstone. Its fossil content consists of a number of aragonitic and calcitic macrofossils (gastropods,

brachiopods, and various bivalves). It grades up from underlying Gee Greensand, and is in turn unconformably capped by Pliocene or younger gravels.

2.3 Biostratigraphy

Biostratigraphic age correlations, based on foraminiferal collections contained in the New Zealand Fossil Record Electronic Database (FRED) and other published faunal content, were used to confirm correlations between lithostratigraphic units and unconformity surfaces (Fig. 2.9). Where biostratigraphic ages were assigned in the database or publications prior to the release of the most recent New Zealand foraminiferal biostratigraphic manual (Hornibrook *et al*., 1989), the age ranges of the microfauna for these records were updated to be consistent with this later text. In most cases, this confirmed or further constrained the age range from older sources, although some records were unable to be resolved as a result of either an insufficient dataset or conflicting recent age ranges for the microfauna provided.

A complete table of results is given in Appendix E, including the dates and names of those who collected each set, while for a complete list of species used in assigning these ages the reader is referred to the database itself: www.fred.org.nz.

Relevant biostratigraphic descriptions for each of the formations and unconformities considered in the present work follow. Biostratigraphic dating results given all relate to results reported in Appendix E.

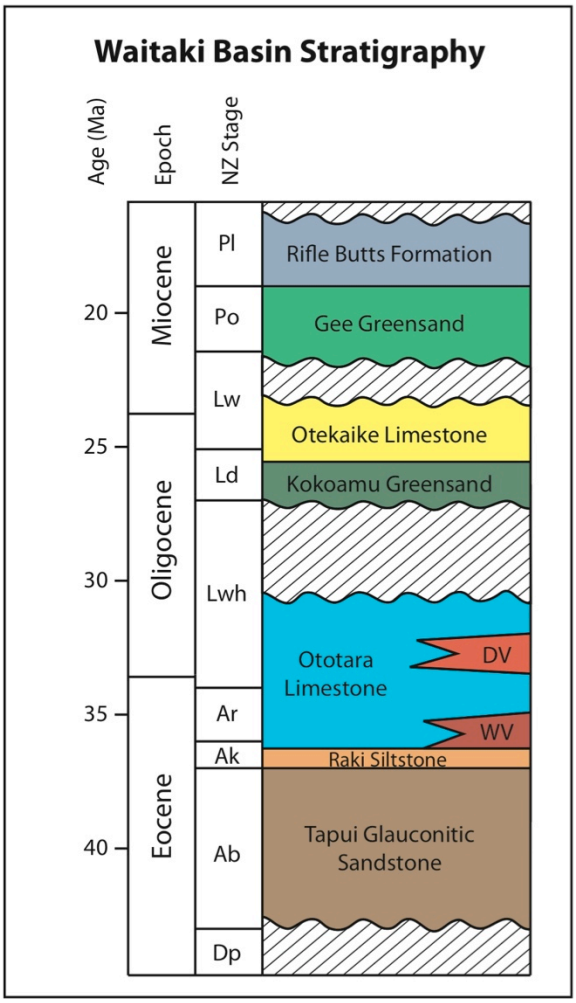

Figure 2.9. Simplified stratigraphic column of the mid-Cenozoic formations used in this study and their assigned ages based on the biostratigraphy presented in this chapter. DV and WV are the Deborah and Waiareka Volcanics, respectively. Dp = Porangan, Ab = Bortonian, Ak = Kaiatan, Ar = Runangan, Lwh = Whaingaroan, Ld = Duntroonian, Lw = Waitakian, Po = Otaian, and Pl = Altonian. Modified from Gage (1957), Forsyth (2001), and Cooper (2004).

2.3.1 Onekakara Group

2.3.1.1 Tapui Glauconitic Sandstone

The first of the Onekakara Group units of interest in this study, the Tapui Glauconitic Sandstone, has been assigned a Bortonian age (43 – 37 Ma) based on foraminiferal and mollusc assemblages (Fig. 2.10). It once served as the Bortonian Stage type locality at Bortons, until this was reassigned to the Hampden Formation at Park Gulch based on the lack of fossil content within the Tapui Sandstone at this location (Gage, 1957;

Fleming, 1959; Hornibrook *et al*., 1989; Cooper, 2004). Benthic foraminifera identified by Finlay and Stache at Maheno and Kakanui (reported in Gage, 1957), when updated using Hornibrook *et al*. (1989), include *Vaginulinopsis hochstetteri*, *Vaginulinopsis spinulosa*, *Cancris compressus*, *Hoeglundina elegens*, and *Bulimina bortonica*, indicating a Bortonian Stage age for this unit.

2.3.1.2 Raki Siltstone

The youngest Onekakara Group unit is Raki Siltstone, which has been assigned to the Kaiatan Stage (37 – 36 Ma) based on its microfauna as it lacks a number of key Bortonian species found in the Tapui Sandstone (Fig. 2.10). Indicative taxa are rare and a Kaiatan age is inferred from *Civicidea pronovozelandicus* and *Sphaeroidina variabilis. Cibicides pseudoconvexus* was found in Raki Siltstone near Kakanui by Parr (in Gage, 1957), and although this species can be found as early as the Teurian in the Chatham Islands, on the mainland it is very rare prior to the Kaiatan (Hornibrook *et al*., 1989). The presence of *Sphaeroidina variabilis*, also near Kakanui, places this formation as no younger than the Kaiatan Stage.

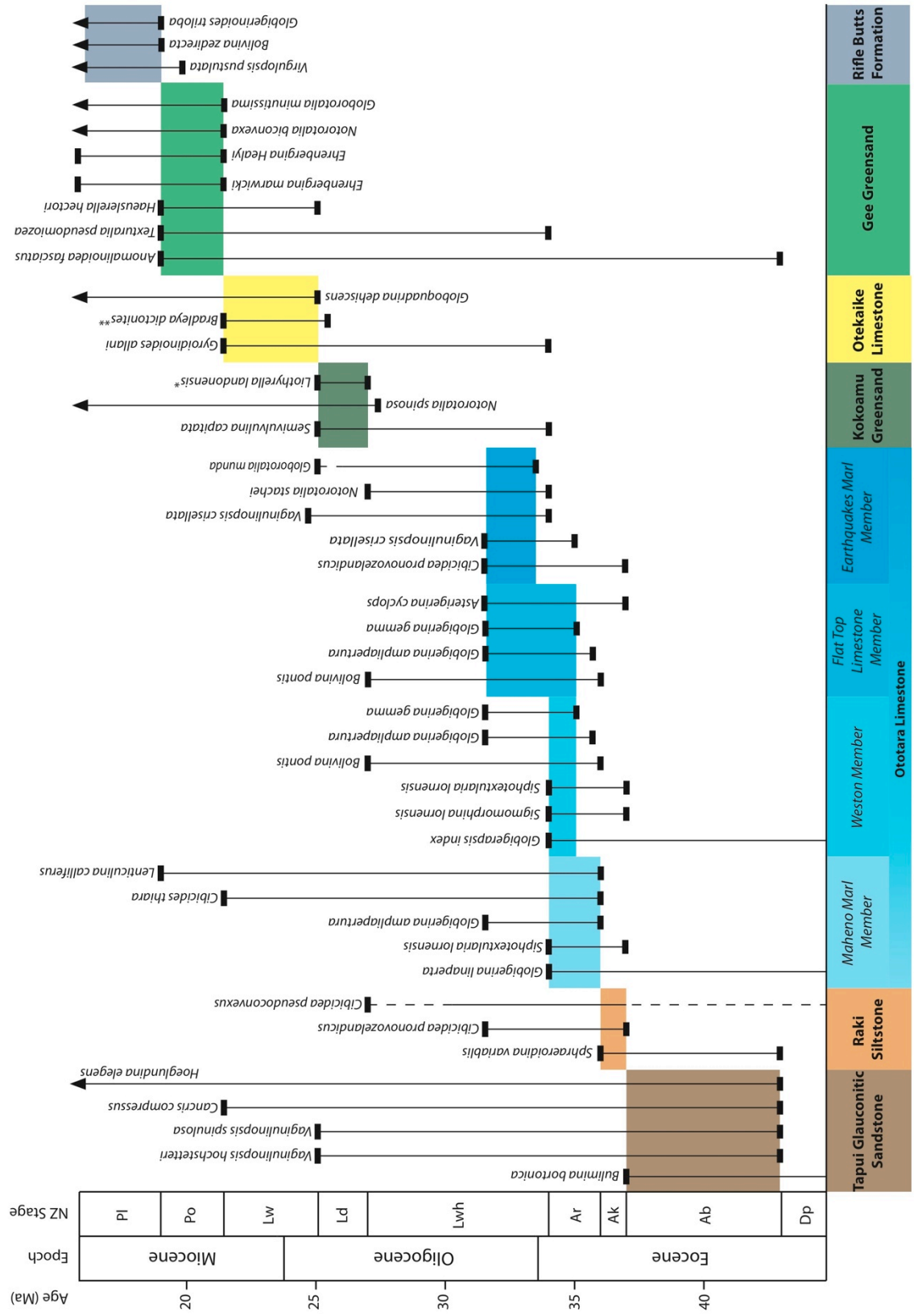

Figure 2.10. Summary biostratigraphy showing the key fossil age ranges for each formation as presented in this chapter. Some ages are not shown where the data is presented from a published source. Solid lines indicate certain ranges, while dashed show uncertainty. *brachiopod; **ostracod.

2.3.2 Alma Group

2.3.2.1 Ototara Limestone

The principal Alma Group unit, Ototara Limestone, has been assigned an age between the late Kaiatan and lower Whaingaroan (37.5 – 30 Ma), based principally on foraminiferal content (Fig. 2.10). However, the age of any particular horizon varies with location and stratigraphic position within the formations.

The Earthquakes Marl Member, found in the western region, shows a lower Whaingaroan age at Ross Farm and Earthquakes. This is based on the presence of *Vaginulinopsis crisellata* (collected by Gage, 1947 and identified by Finlay) and *Globorotalia munda* (from Jenkins, 1971), *Bulimina forticosta*, and *Cibicidea pronovozelandicus* (collected by Hornibrook). At Trig Z it is also assigned to the Whaingaroan Stage due to the presence of *Notorotalia stachei* (from drill-hole data in Edwards, 1971), which is a common marker fossil for this stage.

In the eastern region, Ototara Limestone's biostratigraphy shows a general Kaiatan to Whaingaroan age range, although where key marker taxa are present this can be refined to the lower Whaingaroan based on the presence of *Asterigerina cyclops*.

Exposures with significant thicknesses of Weston and Flat Top Limestone Members, located at Forresters, Bains, Teschemakers and Meeks Rd Quarry, are assigned to the Runangan Stage. This is based on the occurrence of *Globigerina gemma*, *Bolivina pontis*, *Globiferina ampliapertura*, *Globigerapsis index*, *Sigmomorphina lornensis*, and *Siphotextularia lornensis* (collected by Edwards in 1965 and 1966, and identified by Hornibrook).

Also assigned to the Runangan Stage is the exposure of Maheno Marl near Maheno, based on the presence of *Cibicidea thiara*, *Globogerina amplipertura*, and *Lenticulina calliferus*, *Globigerina linaperta* (all from Nazifral, 1976) and *Siphotextularia*

lornensis (collected by Sikumbang, 1976). Other locations, such as Old Rifle Butts, Kakanui River, and Devils Bridge Rd, contain taxa that refine these exposures to the Whaingaroan Stage.

2.3.2.2 Waiareka and Deborah Volcanics

Ages for the other two units in the Alma Group, the Waiareka and Deborah Volcanics, are ca. 40 Ma, and 32.4 – 31.6 Ma, respectively, based on radiometric dating (Coombs *et al*., 1986; Reay and Sipiera, 1987). These ages are consistent with biostratigraphic ages assigning these formations to the late Kaiatan to Runangan, and the lower Whaingaroan, respectively (Forsyth, 2001) (see also Sections 1.2.6.2 and 1.2.6.3).

2.3.2.3 Unconformity at top of Alma Group

From the ages assigned to both the Ototara Limestone and the Kokoamu Greensand within the study area, the unconformity between these two can be assigned to the mid-upper Whaingaroan (see Sections 2.3.2.1 and 2.3.3.1). This is consistent with strontium-isotope dates of 32.4 to 29 Ma presented in Nelson *et al*. (2004) (see Section 1.2.6.4).

2.3.3 Kekenodon Group

2.3.3.1 Kokoamu Greensand

Kokoamu Greensand has been assigned a Duntroonian age (27.3 – 25.2 Ma) derived from foraminiferal analyses (Fig. 2.10), although its extremely thin exposure along the modern coastline in the eastern region means it is often impossible to differentiate from overlying Otekaike Limestone, and therefore tends to show a Duntroonian to Waitakian age range there. At Waihao, in the northern region, Kokoamu Greensand is Duntroonian, with its basal contact at the Whaingaroan-Duntroonian boundary (identified by C.M. Jones in 1993 in the FRED). At Earthquakes, in the western region, this unit was assigned to the

uppermost Whaingaroan to Duntroonian Stages by Hornibrook *et al*. (1989), while at Ross Farm Kokoamu Greensand taken from borings at the Ototara-Kokoamu contact cannot be refined further than the Runangan to Waitakian Stages, probably because of reworking of underlying sediments (in specimens identified by Finlay and Hornibrook).

In a more eastern exposure, at Landon Creek, Kokoamu Greensand is at least uppermost Whaingaroan, based on the presence of *Notorotalia spinosa*, and is assigned to the Duntroonian Stage by the occurrence of the brachiopod *Liothyrella landonensis* (Gage, 1957; Hornibrook, 1966; Hornibrook *et al*., 1989). As previously mentioned, Kokoamu Greensand is almost impossible to differentiate from Otekaike Limestone at the coastline. At Gees Point an age of Duntroonian to Waitakian is assigned based on the presence of *Notorotalia spinosa* and *Semivulvulina capitata*, derived from samples taken out of karst solution cavities by Gage in 1947, and later identified by Finlay. Likewise at Campbells Bay, samples collected from the mixed Kokoamu Greensand and Otekaike Limestone horizon are assigned to the Waitakian stage based on occurrences of *Baggina ampla*, *Globoquadrina dehiscens*, *Haeuslerella decepta*, *H. hectori*, *Cibicides thiara*, *Gyroidinides allani*, *Karreriella novozealandica*, and *Semivulvulina waitakia* (collected by Brown in 1941, identified by Hornibrook, 1989).

It therefore seems that at localities containing thicker packages of Kokoamu Greensand (e.g., Waihao and Earthquakes) a Duntroonian age is likely. Other ages in different locations are probably influenced by reworking or a poor differentiation from overlying Otekaike Limestone.

2.3.3.2 Otekaike Limestone

Otekaike Limestone has been assigned to the upper Duntroonian to Waitakian Stages (26 – 21.7 Ma) (Fig. 2.10), although this varies throughout the study area. In the

most western outcrop, Trig Z, strontium-isotope chronostratigraphy has been combined with foraminiferal and ostracod biostratigraphy to give an uppermost Duntroonian to mid-Waitakian age (ca. 25.5 to 23.7 Ma) (Graham *et al*., 2000). At Earthquakes, Otekaike Limestone has previously been assigned to the mid-Duntroonian to Waitakian from ostracod assemblages (Ayress, 1993), while foraminiferal analyses on a large fallen block by Hornibrook (1986) assigned this section to the Duntroonian Stage. At the Rock Art and Awamoko exposures Otekaike Limestone is assigned to the Waitakian Stage, based on the presence of *Globoquadrina dehiscens* and *Gyroidinoides allani*, identified by Finlay. Otekaike Limestone at Ross Farm and Otekaieke Settlement is also assigned to the Waitakian Stage, based on collections by Jenkins (1971) and Marwick and identified by Finlay, respectively. Foraminiferal analyses at Landon Creek, in the eastern region, by Hornibrook (1966) place Otekaike Limestone in the upper Duntroonian to lower Waitakian, based principally on the absence of *Globoquadrina dehiscens* (age refined from Hornibrook *et al*. (1989)). Ostracod biostratigraphy by Ayress (1993) gave an uncertain age (as samples are difficult to prepare from this formation at Landon Creek) in the upper Duntroonian to Waitakian based on the abundance of *Bradleya dictonites*. As mentioned earlier regarding Kokoamu Greensand, the coastal exposures of these two formations are very thin and thus tend to give a mixed age. At Campbells Bay it has been assigned to the Waitakian Stage by Batt (1993), siting numerous small planktic foraminifera.

2.3.3.3 Unconformity at top of Kekenodon Group

The unconformity between Otekaike Limestone and overlying Gee Greensand is constrained by the ages of the units around it. Batt (1993) placed this unconformity between the First Appearance Datum (FAD) of *Globigerina woodi woodi* in the mid

Waitakian, and the end of the Waitakian marked by the FAD of *Globorotalia minutussima* (Batt, 1993).

2.3.4 Otakou Group

2.3.4.1 Gee Greensand

Gee Greensand has been assigned to an age range between the mid-upper Waitakian and Otaian Stages (23 – 19 Ma), based on foraminiferal analyses by Batt (1993), supported by microfauna in the FRED (Fig. 2.10). Exposure of this formation is limited in the western region, and as such there is sporadic biostratigraphic control there. Outside the study area, towards the west, Batt (1993) assigned Gee Greensand to the mid-late Waitakian Stage across a 1 m thick conformable contact with the underlying Otekaike Limestone.

In the eastern region, at Landon Creek, this formation contains the foraminifera *Ehrenbergina marwicki*, a key marker species for the Otaian Stage and unlikely to be misidentified (Scott, 1973; Morgans *et al*., 1999), placing the unit solely in the Otaian Stage at this location. Further south down the coast, at Gees Point and Campbells Bay, Gee Greensand samples range from the Waitakian to Otaian Stages, defined both from foraminiferal analyses by Batt (1993) as well as earlier collections. A species that confines this unit to the Waitakian is *Globogerina euapertura*, with its Last Appearance Datum (LAD) placed in this stage by Hornibrook *et al*. (1989). However, the presence of *Ehrenbergina marwicki* and *E. willetti* (although questionably not a separate species) confines the Gee with their FAD to the Otaian Stage (collected by Hornibrook and Gage, identification by Hornibrook and Finlay). As both of these species can be found at the base of Gee Greensand, but only *Ehrenbergina* sp. appears further up the unit, it is assumed that

this basal Otaian marker was simply reworked into the mixed basal sediments after the initiation of Greensand deposition in the Waitakian Stage.

At Old Rifle Butts, within the distinct brachiopod-rich bed above Ototara Limestone rhodoliths, Gee Greensand has been assigned to the Otaian Stage, based on the occurrence of *Ehrenbergina healyi*, *E. willetti*, *Notorotalia biconvexa*, *Globorotalia minutissima*, *Texturalia pseudomiozea*, *Haeuslerella hectori*, and *Anomalinoides fasciatus* (collected by Marwick and Jenkins, identified by Hornibrook and Jenkins). A collection by Batt (1993) at this same location contains the early to mid Waitakian species *Globigerina brazieri*, although this can probably be ignored as a reworked sample based on the existence of these other Otaian Stage indicators.

2.3.4.2 Rifle Butts Formation

Gradationally above Gee Greensand, the Rifle Butts Formation has been assigned to the Altonian Stage (19 – 15.9 Ma), based on foraminiferal specimens presented in Gage (1957), collected by Finlay and Reuss at Old Rifle Butts, and collated with Hornibrook *et al*. (1989) (Fig. 2.10). Principally these include *Virgulopsis pustulata*, a species that is abundant in the Altonian Stage along with *Globorotalia miozea*, *Globigerinoides triloba*, and *Bolivina zedirecta*.

2.3.5 Age-normalised stratigraphy

Using the lithostratigraphy combined with the biostratigraphy presented here, an age-normalised cross-section from the western region towards the eastern coastline has been constructed along the same transect used in Fig. 2.2. This shows each lithology with a thickness relative to the likely period of time in which it was depositing at each location. This age-normalised correlation is presented in Fig. 2.11, which highlights periods of non-deposition as well as any lateral variations in deposition through time.

While Fig. 2.11 does indeed appear to highlight periods of non-deposition well, caution must be applied in determining high-resolution changes in deposition at any given time period based on these data, as the biostratigraphy presented here is often only accurate to Stage level. Only in select locations where lithologic boundaries are refined to sub-Stage level can accurate correlations be made.

2.4 Summary

This chapter has presented the lithostratigraphy and biostratigraphy in the Waitaki Region study area for the mid-Cenozoic sedimentary formations. These formations show significant lateral variation across the area, with marked changes in thickness from east to west, particularly of the Kekenodon Group. Two significant unconformities can be correlated across the study area, showing variation between an eastern karst and a western burrowed firmground, while a third less significant erosive surface is also located within the Kekenodon Group.

Biostratigraphic data, while of limited resolution, constrains each formation to at least Stage-level, and confirms the geographic and temporal extent of breaks in deposition. This allows for correlation across the area to determine lateral change through time, and constrains lithologic variations.

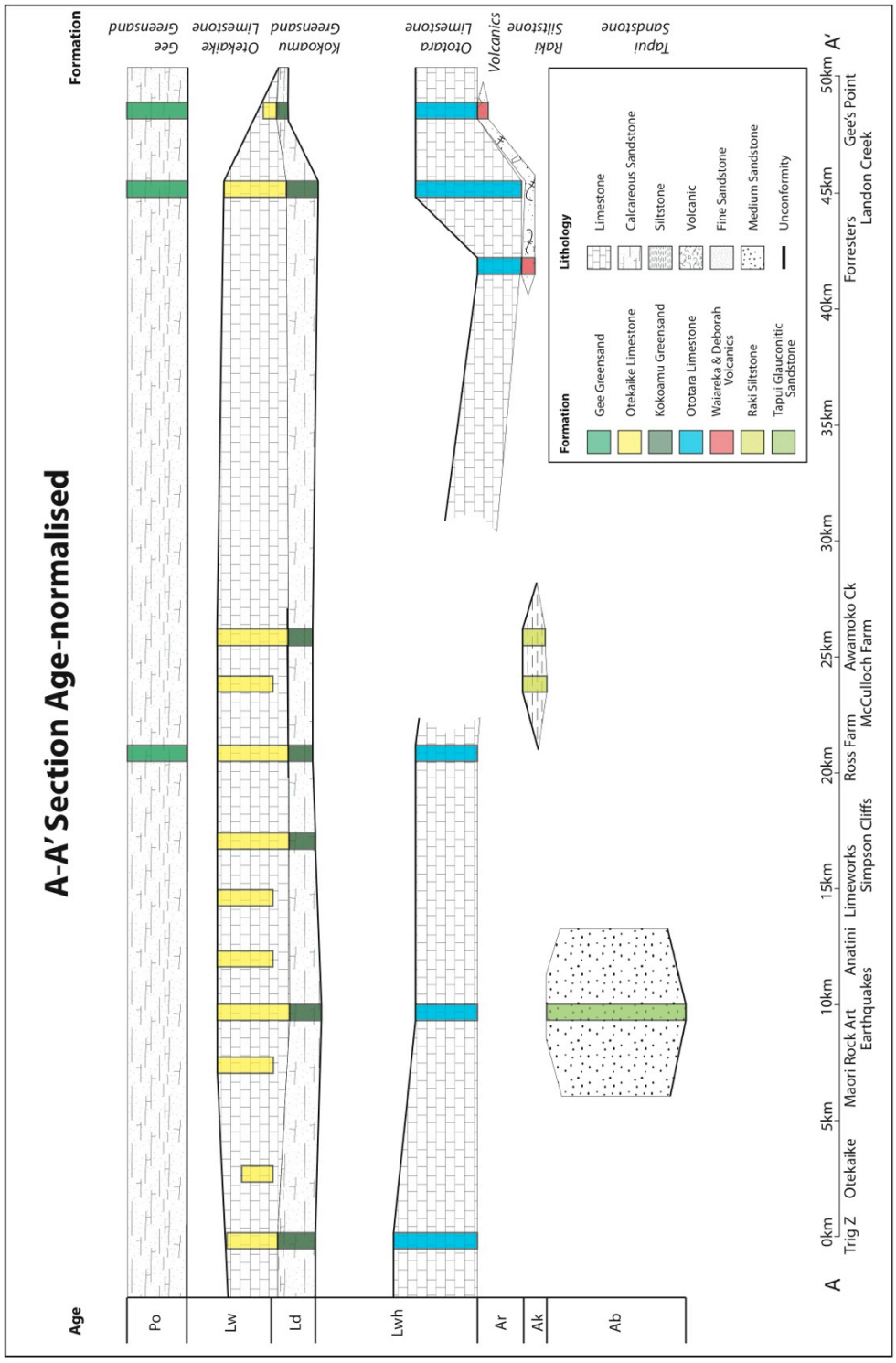

Figure 2.11. Age-normalised stratigraphy from A to A', using the same stratigraphy from Fig. 2.2. This shows each formation across this transect with a thickness dependant on the period of time that it was depositing for, serving to highlight the periods of non-deposition as well as changes through time and space. This was derived using known lithologic ages at various localities and compressing the thickness of the sections to correspond to linear time intervals.

CHAPTER 3 – LITHOFACIES

3. Introduction

The recognition and interpretation of lithofacies is of crucial importance in developing an accurate basin history in a particular region (Reading, 1996; Flügel, 2010). It is essential to address not just the facies of individual beds, samples, or horizons in isolation, but to place them into context with their surroundings in order to interpret their palaeo-environmental setting. This then provides a way to see through the formational nomenclature in a given area and to interpret changes within a formation, as well as across formation boundaries, that may otherwise lie hidden within sometimes arbitrary groupings.

This chapter presents facies derived from both outcrop and petrographic analyses from which each facies' environmental settings are interpreted and placed within the spatial and formational framework found within the study area. These facies are then used as the basis on which to construct a sequence stratigraphic interpretation for the study area as a whole (see Chapter 5), and then to interpret the palaeogeography of the study area through the mid-Cenozoic (Chapter 6)

3.1 Methodology

3.1.1 Outline of methods used

Detailed petrographic analyses of samples, derived from the outcrops within the study area also used for lithostratigraphy (Section 2.2), are an essential tool for determining facies types. These data from both outcrop and petrographic analyses were combined to develop the resultant facies types described below. Facies percentage compositions are given here either as an absolute value or, where the component's composition is significantly variable, a range or average value (with range also given with

the latter). Individual bioclast values totalling the bioclast fraction of the whole facies are given.

3.1.2 Sedimentological descriptions

Detailed sedimentological descriptions were taken in the field at outcrop scale across the study area. Sections were measured from the basal exposure using a tape measure. Features were recorded where they changed, with accuracy depending on outcrop accessibility between centimetre and decimetre scale. Grain size, lithologic composition, texture, colour, mineral variation (particularly glauconite and francolite), fossil content, sedimentary structures and any associated palaeocurrent indicators, and the nature of any contact surfaces were recorded in detail. Particular attention was given to sampling and describing around unconformity surfaces. Where a part of the section could not be physically accessed, it was described on the basis of what could be observed from its nearest accessible point, with samples taken as close as practicable.

Samples were collected from these outcrops (mapped in Fig. 2.1) wherever a change in the nature of the lithology was observed, or from exposures that presented particularly good examples of the various formations. These data were then compiled into stratigraphic logs as presented in Appendix B.

3.1.3 Petrographic methods

Petrographic descriptions of 216 samples collected in the study area were completed using a Leica DM EP Polarising microscope. The full descriptions of each sample are provided in Appendix D.

The thin sections were petrographically analysed for lithological (nature and composition of the matrix/cements, detrital quartz content, authigenic minerals, and any lithics present) and bioclast content (forams, echinoderms, bryozoans, molluscs, brachiopods, coralline red algae, and sponge spicules as well as any other less common forms), including any foraminifera presence and the planktic:benthic ratio for each sample (see Section 3.1.4.1). Quantitative analysis was done by visual estimation of component percentages using comparison charts from Terry and Chilingar (1955), while foram counts were done on a 2cm grid pattern with all forams being counted within the view area at each move of the grid. The nature of any calcite cement was recorded along with any textures that could be discerned (e.g. geopetal, stylolitic). Bioclasts were observed with regard to any reworking textures, particularly abrasion and borings in shell material and the degree to which the material has been broken up or recrystallised. The nature and abundance of any glauconite, such as its maturity, roundness, and its intergrowth with other clasts was recorded. The presence of any phosphatic grains was also recorded.

3.1.4 Classification of water depths

Facies interpretations presented in this chapter include an estimate of depositional depth, defined as inner, mid, or outer shelf to slope. The absolute boundaries between these settings are not well defined in the literature and their positions will also fluctuate with changes in sea level (Boggs, 2001; Flügel, 2010). However in a typical un-rimmed (i.e., open to ocean circulation) cool-water carbonate setting these environments can be loosely divided based on differing environmental elements linked to depth changes. These variations were identified in this study by the lithological and fossil content of each facies, particularly the sediment size, faunal composition, and the foraminiferal ratio.

3.1.4.1 Foraminiferal ratios as depth indicators

Foraminifera are sensitive to changes in sediment size, salinity, temperature, as well as oxygen supply, and can therefore be used as an indicator of depositional depth. This leads to a trend in which deeper water sediments tend to contain higher proportions of planktic forams, as the thickness of the overlying proportion of water is higher thus supplying a greater proportion of these types to the sediment, while colder deeper environments concurrently become increasingly devoid of benthic species (Hayward *et al*., 1999).

However as a result of these same various environmental factors that control foram presence, this method contains some degree of error associated with it (Hayward *et al*., 1999). For example it is possible that increased temperature at deeper depths may allow for an increased benthic presence, or that currents could supply a higher than expected planktic content to a shallower sediment facies. Therefore caution must be used when applying these ratios to depth interpretations.

Foraminiferal ratios have been used in this chapter to provide supporting evidence for palaeodepth determination, but it should be noted that they were not used as the primary or sole indicator as the error associated with both the sample sizes (see Appendix D) and environmental variations does not make this a suitable method in isolation.

3.1.4.2 Inner Shelf

The inner shelf as identified in this chapter is above fair-weather wave base (FWB), and lies near the shoreline (if one exists) in a high-energy environment of tidal movement and constant reworking. It is estimated to lie between 0 – 50 m depth. Lithological textures tend towards grainstones and rudstones (Pedley and Carannante, 2006), as carbonate muds

are reworked down-shelf to calmer and deeper environments. Ratios of foraminifera will be strongly benthic, with little or no planktic tests (<10%) (Hayward *et al*., 1999).

This environment will often have sufficient light levels to allow for coralline algal phototrophs, which can lead to the development of rhodolithic facies, particularly where periodic overturning occurs as a result of turbulence (Pedley and Carannante, 2006). The constant reworking found in this setting tends to make it unlikely that faunas will preserve *in situ*, resulting in fragmented bioclastic assemblages.

3.1.4.3 Mid Shelf

The mid shelf environment extends from below FWB but above storm-wave base (SWB) (Flügel, 2010), and tends to contain facies with a higher mud content than those seen on the inner shelf (e.g., packstones). The depth range is estimated to be between 50 – 100 m for this study, although the variation in the depth window between FWB and SWB can be quite significant (e.g., Boreen and James, 1995).

Foraminiferal ratios have an increased planktic content over that of the inner shelf setting (between 10 – 30% planktic) (Hayward *et al*., 1999). There is also a progressive increase between FWB and SWB in the presence of bivalves and regular echinoids (Pedley and Carannante, 2006).

3.1.4.4 Outer Shelf

The outer shelf tends to lie below SWB, at depth of between 100 – 200 m in this study. Here there is a significant increase in muddy facies as energy levels are lower, producing packstone to wackestone lithologies, although some storm beds can occasionally develop (Flügel, 2010). Planktic foraminiferal ratios tend to contain values between 30 –

65% planktics (Hayward *et al*., 1999). The outer shelf often contains delicate branching fauna that are more suited to this low energy setting (Pedley and Carannante, 2006).

3.1.4.5 Slope

The slope setting is the morphologically steeper section of the continent that begins at the shelf edge and leads down to the basin floor, usually at a much steeper angle than that seen on the shelf (Boggs, 2001). These depths can range to over 1000 m (Boggs, 2001; Flügel, 2010). In this setting muddy sediments dominate, with wackestones to mudstones standard (Flügel, 2010). Foram ratios are dominantly planktic (60 – 100% planktic tests) (Hayward *et al*., 1999).

3.1.5 Glauconite classifications

Glauconite is an important authigenic mineral within the Waitaki study area, occurring within many of the facies types presented in the following sections. The presence of this mineral is quantified here by both maturity, as well as interpretations of its origin. Therefore this section contains definitions of the terms used in this and following chapters.

3.1.5.1 Glauconite maturity

Glauconite itself is a group of hydrated iron and potassium micas that usually occur as sand-sized grains, or alternatively as precipitated mineral pigmentation infilling cracks or replacing other minerals (McRae, 1972; Odin and Matter, 1981). Glauconite precipitates as grains or coatings in an immature form. The maturity of glauconite grains can often be associated with a range of green colouring, with the more immature developing a pale green tint, ranging up to more mature grains that exhibit a much darker green to almost

black colour (James, 1966; McRae, 1972). These colour variations are associated with the amount of iron and potassium within the crystal lattice (Odin and Matter, 1981; Amorosi, 1997). Within this chapter glauconite is presented as immature to mature, based principally on these colour ranges observed within thin-section.

3.1.5.2 Glauconite mobility

Glauconite grains are common on modern continental shelves, occurring most abundantly on the outermost shelf and upper-slope (200 – 300 m) (Odin and Matter, 1981); however in temperate areas is can be found as shallow as 30 m (Porrenga, 1967; McRae, 1972).

Within this study glauconite is usually interpreted to be either autochthonous, allochthonous, or parautochthonous (Fig. 3.1). Autochthonous refers to grains that are found in the precise location in which they formed, while allochthonous grains have been transported to the current location from an area outside the depositional basin. Parautocthonous grains are somewhere between these two types, as they have been remobilised, but are still found within the vicinity of their point of genesis.

Where glauconite has accumulated in areas not conducive to glauconitisation, such as those of non-marine environments or with high sedimentation rates, it is likely to be allochthonous (Amorosi, 1997). Most autochthonous glauconite is confined to the outer-shelf and slope environments (Odin and Fullager, 1988).

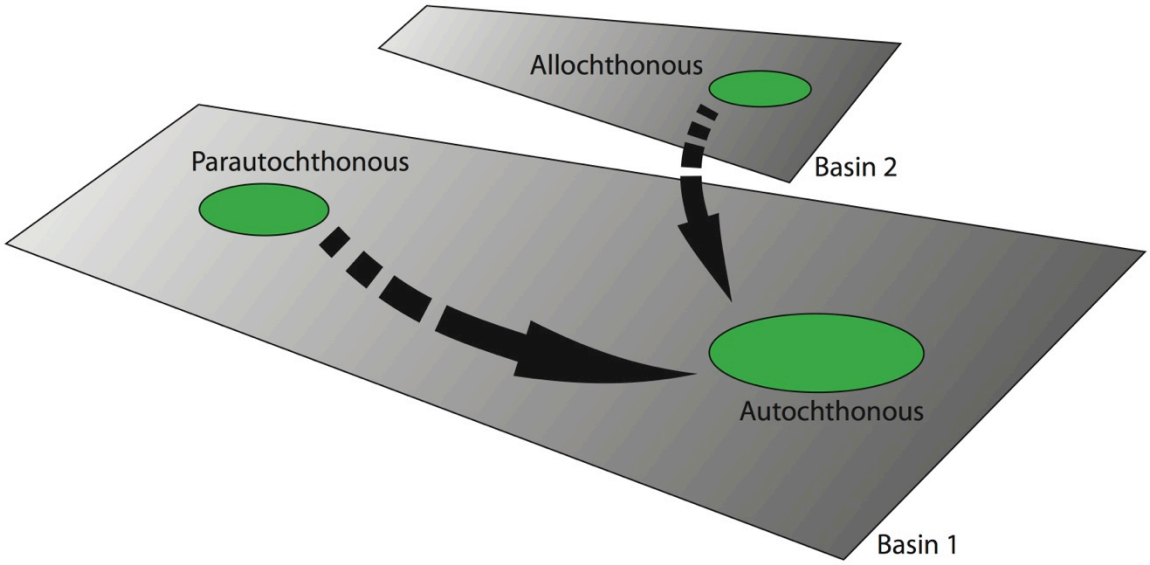

Figure 3.1. Illustration of the three descriptors used to define the remobilisation of glauconite. Autochthonous glauconite is found *in situ*, while allochthonous glauconite is transported from outside the basin to be deposited within basin 1. Parautochthonous glauconite has been reworked, but remains within its basin of genesis.

3.1.6 Ichnofossil types

There are four ichnofossil types identified during this study. These types make an appearance in most of the facies presented below. Each trace fossil type was identified solely in the field at outcrop scale using the morphological features that distinguish each type (Fig. 3.2).

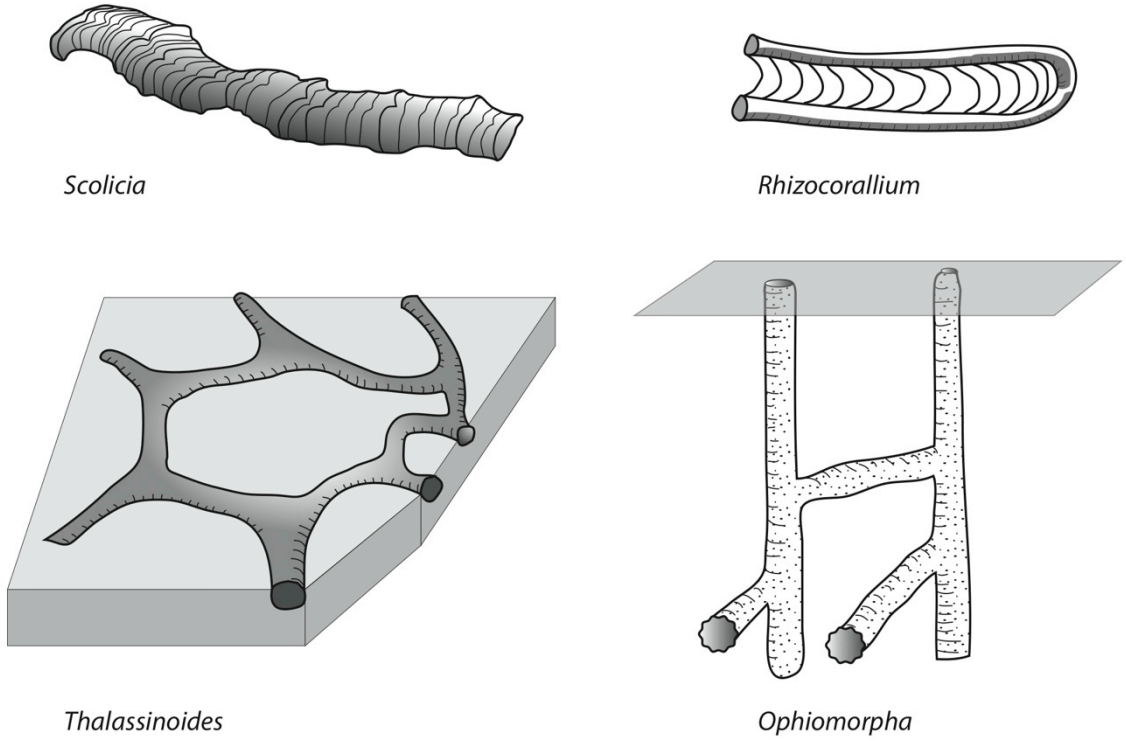

Figure 3.2. Illustrations of the four main trace fossil types identified in this study. *Scolicia* are identified by their wide linear trace with characteristic ribbing running perpendicular to the trace axis. *Rhizocorallium* contains two burrows with linked lineations. *Thalassinoides* and *Ophiomorpha* are similar, however *Ophiomorpha* burrows have a harder, and often alternate colour burrow rim, while *Thalassinoides* does not.

3.2 Sedimentary Facies

Twelve facies (F1 – F12) have been defined (Table 3.1) based on data gathered in the field and detailed petrographic analyses:

F1: Glauconitic Siltstone

F2: Bryozoan Grainstone

F3: Rhodolith Rudstone

F4: Impure Wackestone

F5: Calcareous Greensand

F6: Massive Glauconitic Packstone

F7: Bedded Packstone

F8: Cross-bedded Glauconitic Packstone

F9: Diatomaceous Micrite

F10a: Tuffs; F10b: Pillows

F11: Reworked Volcaniclastic Packstone

F12: Ash/Clay

Each of these is described separately in the following Sections.

3.2.1 Glauconitic Siltstone (F1)

3.2.1.1 Description

The Glauconitic Siltstone facies is a glauconitic, poorly-bedded siltstone (Fig. 3.3). In thin section this facies displays a highly variable matrix of non-calcareous mudstone (17 – 61%). Glauconite content is 30 – 46%, with variable amounts of silt-sized quartz grains (4 – 37%, average 25%). Recognisable biotite lathes, that have been partially glauconitised, comprise < 2% of this facies; and no bioclasts are present.

The mud matrix in the Glauconitic Siltstone facies often appears with a slight alignment of the larger quartz silt grains set within it (Fig. 3.3). Glauconite occurs as mature dark-green, rounded to sub-angular grains showing clear growth rings and glauconitised biotites. These glauconite grains tend to be found in concentrated bands, observable both in outcrop and thin section. The silt-sized quartz grains are angular and well dispersed throughout the facies. Biotite lathes are usually strongly glauconitised, but retain their often-characteristic euhedral shape and sheet-structure, as well as a mild pleochroism in thin section. Hematite occurs commonly in thin sections over both matrix and glauconite grains that may have derived from either alteration or recent weathering.

Poorly preserved and crumbling bedding (~ 2.5 cm thick) can be observed at one outcrop (Awamoko) with a 10°W dip (Fig. 3.3A). Intense bioturbation is also present in the top 5 – 10 cm of this facies at outcrop scale, forming mostly vertical and some horizontal *Thallasinoides* burrows containing preserved internal scratch marks.

3.2.1.2 Distribution

The Glauconitic Siltstone facies is found at the base of two outcrops (Awamoko Creek and McCulloch's Farm) in the western region of the study area, where it represents Raki Siltstone (Fig. 2.1). It may also lie beneath Ototara Limestone at Earthquakes (Gage, 1957).

3.2.1.3 Depositional Environment

An outer-shelf, low-energy setting for the Glauconitic Siltstone facies is inferred on the basis of grain size alone, due to the absence of fossil content. Input of terrigenous clastic silt was likely to have been derived from distant low-lying landmasses of Rakaia Terrane metasediments. The rounded, mature glauconite grains are allochthonous, and were likely to have been deposited in intervals together with minor parautochthonous precipitation (expressed as altered biotites).

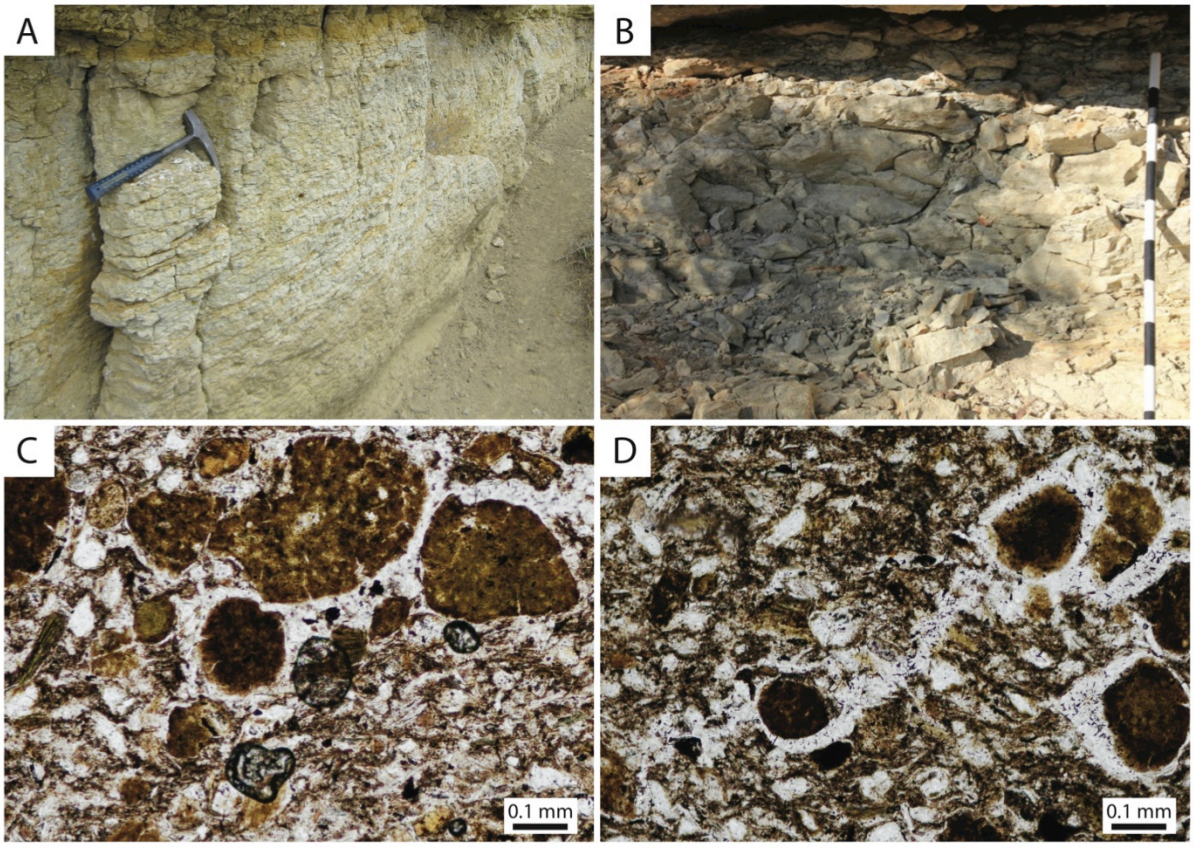

Figure 3.3. Outcrop and thin section photos of the Glauconitic Siltstone (F1) facies. A: Poorly bedded outcrop of this facies at Awamoko. B: Flaggy horizon located at McCulloch Farm. Note metre-stick for scale. C and D: Photomicrographs of this facies from McCulloch Farm, showing the cracked and mature nature of the glauconite set in a quartz silt and mud matrix.

3.2.2 Bryozoan Grainstone (F2)

3.2.2.1 Description

The Bryozoan Grainstone facies is a generally massive, moderately to poorly sorted, grainstone to packstone (Fig. 3.4). Bioclasts make up 37 – 86% of this facies, set within a variable-volume matrix of carbonate mud (4 – 40%). Volcanic lithics locally make up as much as 10% of this facies, while glauconite, phosphate and siliciclastic grains are minimal to absent (< 3%).

The Bryozoan Grainstone facies is distinct in that it appears to be dominated at outcrop by broken branching bryozoans (15 – 52%) (Fig. 3.4A), although in thin section this is more variable (2 – 64%, average 45%). Echinoderm plate and spine fragments make

up another significant component of the bioclasts (1 – 24%). Branching and encrusting coralline red algae fragments locally make up to 24% of the facies, averaging 6%.

Foraminifera make up 1 – 43% of this facies, and are overwhelmingly benthic (usually 70 – 100% benthics), although locally (particularly at Campbells Bay) the benthic:planktic ratio can drop as low as 23%. A higher than average planktic content occurs in conjunction with a higher carbonate mud matrix. Some large benthic foraminifera occur in this facies, notably *Asterocyclina* at Browns Rd (Fig. 3.4D).

Carbonate mud and calcite cement occasionally form geopetal textures within foraminiferal test chambers. Aragonitic bioclasts are generally absent or minimal (< 1%), as are fragments of calcitic bivalves (~ 2%). Traces of brachiopod, possible gastropod, and worm-tube fragments are present in thin section throughout the facies. Abrasion and boring of bioclastic material is moderate to high. Igneous clasts usually consist of crystals of amphibole, biotite, pyroxene, or simply as angular to rounded basalt clasts, most of which show iron weathering. Rounded phosphate grains occur near the top of this facies, while glauconite, although rare, is found as rounded grains and intraclasts within foraminiferal tests. Angular, silt-sized quartz grains occur sporadically throughout the facies.

The Bryozoan Grainstone facies, while generally massive, does show some evidence of bedding, with planar lamination observed at Gee's Point. Bioturbation is not observed at any of the locations described. At outcrop, the fossil content is heavily fragmented, although bryozoans, echinoid plates and spines, occasional large benthic foraminifera, sharks teeth, and calcareous worm tubes can be identified (Fig. 3.4). Furthermore, while brachiopods are rare in thin section, in at least one outcrop (Gee's Point) they can be found moderately disarticulated (and occasionally intact) within fossiliferous beds along with similarly preserved pectens.

3.2.2.2 Distribution

The Bryozoan Grainstone occurs in the eastern region, around the volcanic palaeohighs, and forms a part of Ototara Limestone. It grades to Impure Wackestone (see Section 3.2.4) to the west, as confirmed by biostratigraphic relationships (see Section 2.3.2). Locally, at Old Rifle Butts and Roy Farm, it is overlain by a well-cemented rhodolith bed of the Rhodolith Rudstone (F3) facies (see Section 3.2.3).

3.2.2.3 Depositional Environment

The occurrence of the Bryozoan Grainstone facies in the eastern region, and its association with volcanic palaeohighs, as well as the presence of *Asterocyclina* and red algae, indicates it formed as an extensive inner- to mid-shelf shoal on top of these palaeohighs. Moderate to high energy levels were enough to winnow localised carbonate mud content and to cause biofragmentation, with carbonate mud generally accumulating elsewhere in the basin.

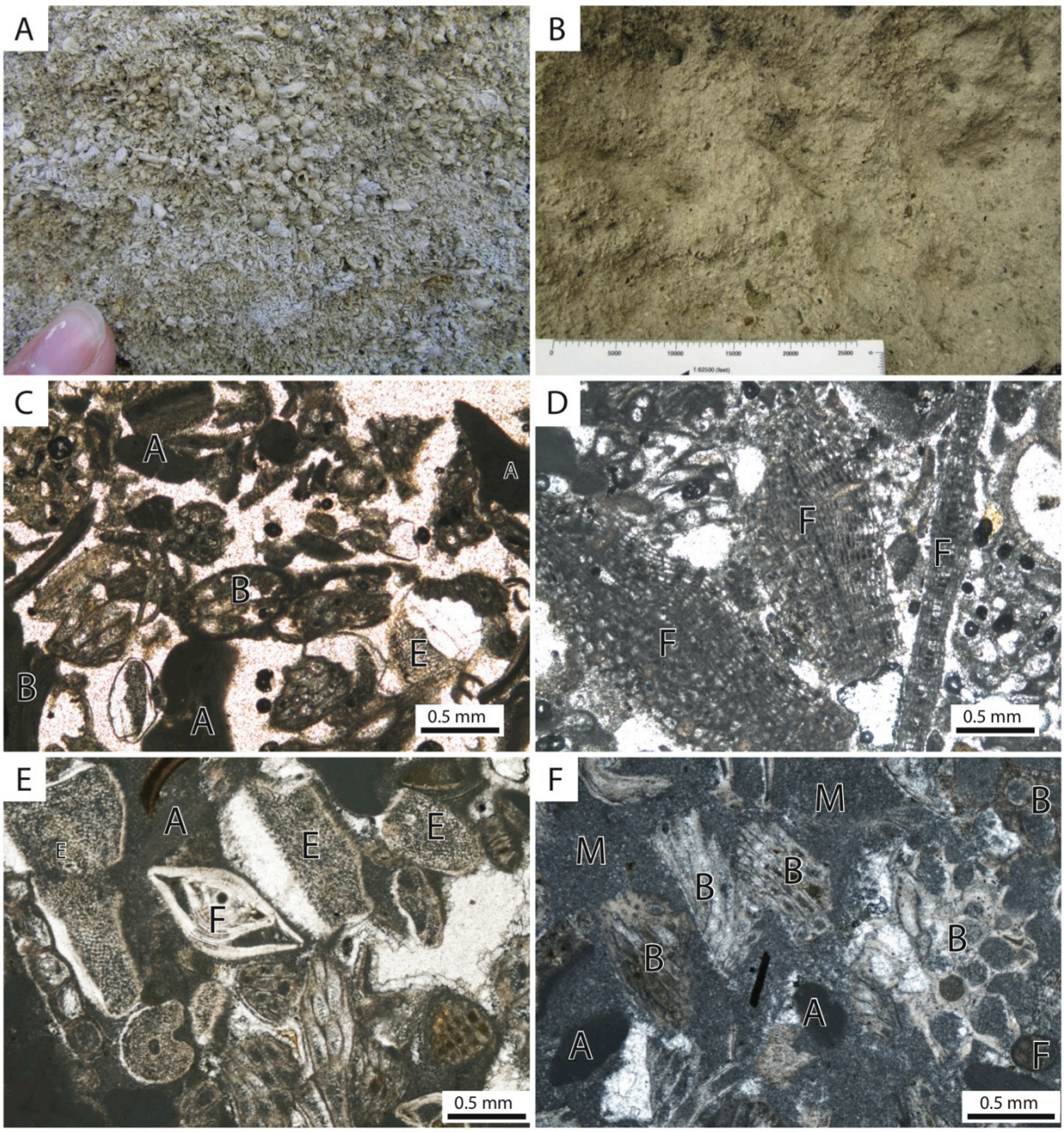

Figure 3.4. Outcrop and thin section photos of the Bryozoan Grainstone (F2) facies illustrating the variation that occurs at different outcrops. All photomicrographs under plain polarised light, except (F) which is under crossed-polarisers. A: Bryozoan-rich grainstone at Alma. B: Bryozoan packstone at Campbells Bay. The scale bar is 13 cm long. C: Grainstone at Landon Creek containing abundant bryozoans (B), some red algal fragments (A), and a small echinoderm plate fragment (E). D: Large benthic foraminifera (F) found at Browns Rd outcrop. E: Packstone with abundant echinoid (E) and bryozoan fragments, along with coralline red algae (A) and a benthic foraminifera test (F). F: Packstone with abundant bryozoan fragments, as well as some algal fragments and a benthic foraminiferal test from Campbells Bay.

3.2.3 Rhodolith Rudstone (F3)

3.2.3.1 Description

The Rhodolith Rudstone facies is a < 2 m thick, well-cemented, clast-supported, moderately sorted rhodolith rudstone (Fig. 3.5). Rhodoliths make up 75% of this facies. The remainder is matrix, consisting mostly of fragmented bioclasts (15%), some carbonate mud (9%), and rare silt-sized quartz grains, glauconite, and phosphate (1%).

The rhodoliths are well-rounded and formed from encrusting red algae, with an average diameter of ~ 5 cm. Geopetal textures occur within the algal interstices, formed from carbonate mud and bioclasts of the matrix (Figs. 3.5C and D). Fenestrate bryozoan fragments make up 7 – 10% of the matrix bioclasts, along with echinoid (5%) and mollusc (1%) fragments. Foraminifera tests make up the remaining 4% of the facies, almost entirely of benthic species, including a number of agglutinated benthic tests along with symbiont-bearing large benthic forams. The bioclasts in the matrix exhibit moderate levels of fragmentation, while abrasion and microborings are at relatively low levels. Glauconite is light to medium green and is present only within bioclastic void space (principally within foraminifera tests).

There are no obvious sedimentary structures apparent in this facies, and no indications of any bioturbation. The rhodoliths are uniformly arranged throughout the bed with no signs of stratification (Figs. 3.5A and B).

3.2.3.2 Distribution

The Rhodolith Rudstone is found proximal to a volcanic high near Old Rifle Butts, above the Bryozoan Grainstone facies (see Section 3.2.2) or sharply contacting volcaniclastics, and forms a part of the upper Ototara Limestone in the eastern region.

3.2.3.3 Depositional Environment

The clast-supported nature of the Rhodolith Rudstone beds, and the absence of binding coralline layers, indicate the rhodoliths have been mobile shortly before final accumulation. It is inferred that the rhodoliths formed on local palaeo-highs at shallow inner-shelf depths, and were remobilised downslope as turbidites and debrites, along with bryozoan material (likely to be derived from the Bryozoan Grainstone facies) during episodic high-energy events or during relative sea-level fall. This is similar to the processes seen at Three Kings Plateau, where shallow skeletal carbonate is reworked into local basins and troughs (Nelson *et al*., 1982).

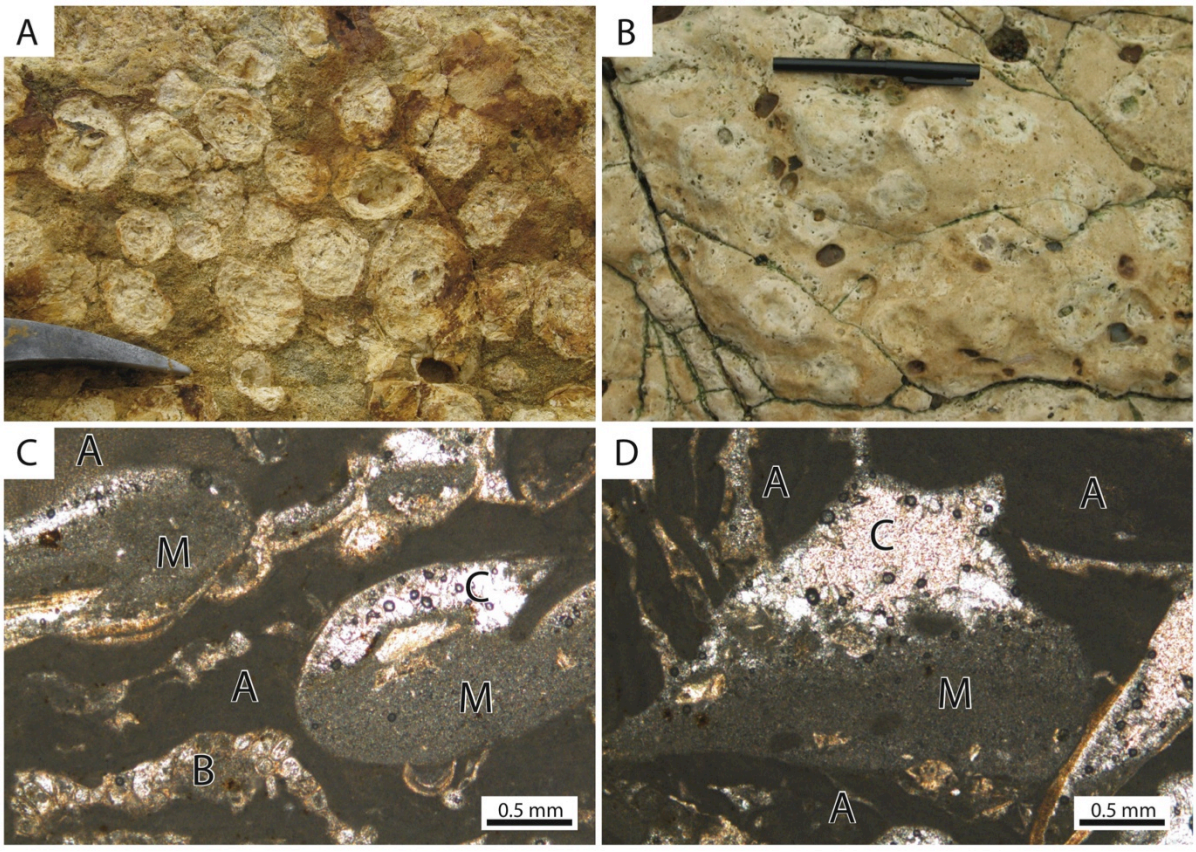

Figure 3.5. Outcrop and thin section photos of the Rhodolith Rudstone (F3) facies. A: Rhodolith Rudstone in a mixed mud and cement matrix at Old Rifle Butts. B: Cemented rhodolith bed overlying volcanic tuffs at Old Rifle Butts. C, D: Algal dominated (A) photomicrographs from the Rhodolith Rudstone at Old Rifle Butts, showing the interstices filled with geopetal mud (M) and cement (C), as well as fragments of bryozoan (B).

3.2.4 Impure Wackestone (F4)

3.2.4.1 Description

The Impure Wackestone facies comprises a friable, massive, bioturbated, moderately to well-sorted glauconitic, calcareous siltstone to impure wackestone (Fig. 3.6). Carbonate mud comprises 28 – 50% of this facies, while silt-sized quartz grains and micas make up another 30 – 40%. Glauconite within this facies makes up 9 – 25% of its composition, while bioclasts comprise a further 5 – 10%.

The carbonate mud matrix is uniform throughout the Impure Wackestone facies, within which the angular, silt-sized (0.01 – 0.05 mm) quartz grains are relatively dispersed, although they can be found in highly concentrated groups in thin section (Fig. 3.6D). Iron staining of clasts and the mud matrix is common. Muscovite is commonly observable in outcrop scale, but was seldom located in thin section, although biotite crystals were commonly observed altering to glauconite in thin section (Fig. 3.6D).

The glauconite content is commonly made up of rounded to sub-rounded medium- to dark-green, cracked grains, as well as some glauconitisation located within and over microfossil tests (foraminifera and radiolarians). Most peloids of glauconite have darker green altered rims (Figs. 3.6C and D). The smaller peloids tend to be more rounded, while larger grains are commonly angular.

Of the bioclasts, foraminifera are the most common in this facies (3 – 19%), and are primarily made up of small planktic species (40 – 88% planktic:benthic ratio). Mollusc fragments of both gastropods and bivalves comprise 3 – 6%, commonly with heavy abrasion and boring of shell fragments. Traces of radiolarians and sponge spicules are present (up to 1%). No discernible sedimentary structures or macrofossils were observed within this facies, although intense *Ophiomorpha* bioturbation traces are present throughout (Figs. 3.6A and B).

3.2.4.2 Distribution

The Impure Wackestone facies is present only in the western region, and forms a part of Ototara Limestone at Ross Farm, Earthquakes, and Trig Z (Fig. 2.1).

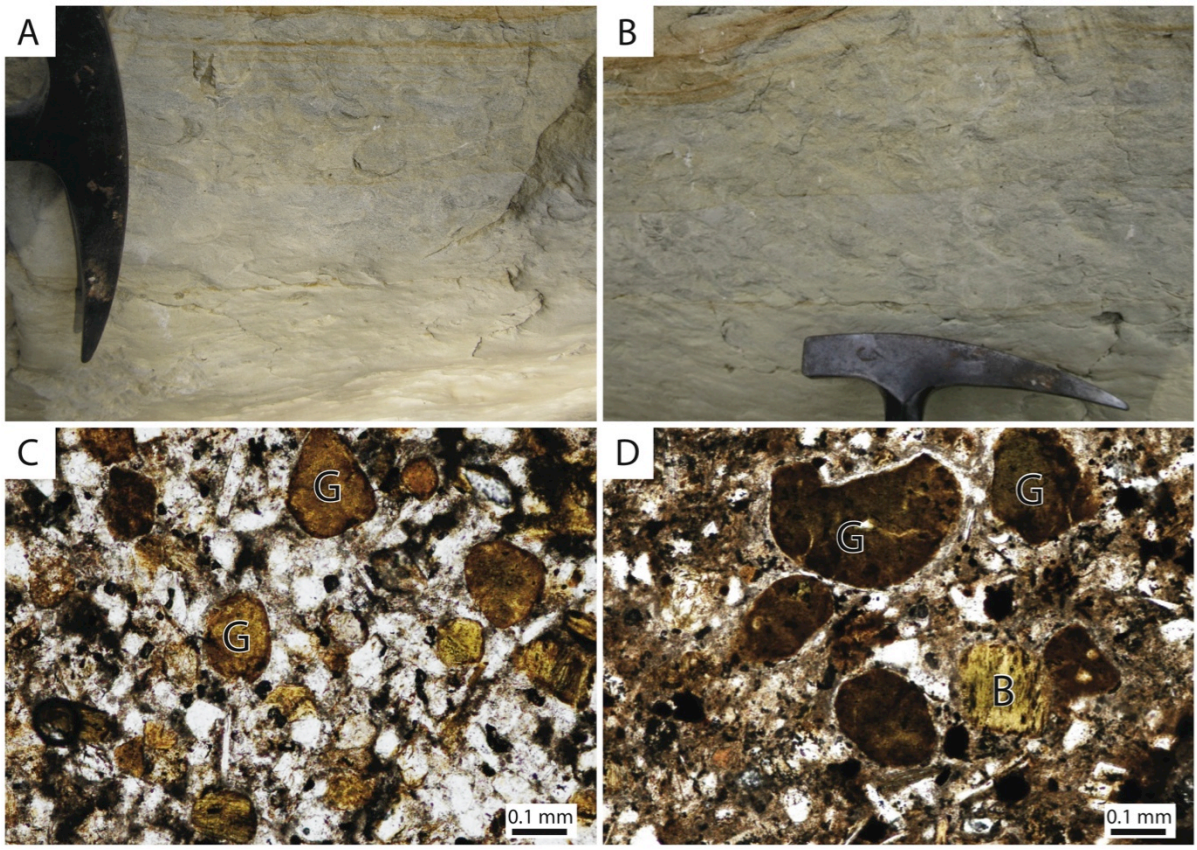

Figure 3.6. Outcrop and thin section photos of the Impure Wackestone (F4) facies. A, B: These photos show the Impure Wackestone facies at Ross Farm, illustrating the high mud content and intense bioturbation (*Ophiomorpha*) prevalent in this facies. C: This photomicrograph, from Ross Farm, shows the high quartz silt content alongside the glauconite grains (G) common in this facies. D: Taken from Earthquakes, this photomicrograph illustrates the often-mature nature of the glauconite grains (G) as well as the presence of occasionally glauconitised biotites (B).

3.2.4.3 Depositional Environment

The Impure Wackestone facies represents deposition in a low-energy, outer-shelf to upper-slope environment, based on grain size coupled with high numbers of planktic foraminifera (e.g., Hayward *et al*., 1999). The planktic content increases westward (from <5% to 50%+), suggesting an increasing depth in that direction. The relatively high

volume of clastic quartz and muscovite implies a distal terrigenous supply of sediment, probably from exposed Rakaia Terrane metasediments to the west, which settled in a deeper part of the basin along with carbonate mud derived from palaeohighs. The mature parautochthonous to allochthonous glauconite grains would have been reworked or transported into this area, while some autochthonous glauconite continued to precipitate within foraminiferal tests, indicating moderate to low sedimentation rates.

3.2.5 Calcareous Greensand (F5)

3.2.5.1 Description

The Calcareous Greensand facies is a generally massive, fossiliferous, calcareous, glauconite, fine- to medium-grained sandstone at its base, grading up to a glauconite grainstone (Fig. 3.7). Its principal component is glauconite grains comprising 20 – 80% (average 46%) of the facies. The bioclast composition ranges similarly: 8 – 76%, average 38%. Carbonate mud content averages 18% (range 1 – 40%). The quartz grain content is generally low, averaging 5% (range 2 – 15%). Phosphate grains average 3% of the facies' components in thin section, although locally can form up to 20% in outcrop. Volcanic clasts make up a further 0 – 2% of this facies.

The variable glauconite concentrations tend to decrease up-section, with highest values located near the base. Glauconite grains exhibit a variety of forms and morphologies, with cracked mature darker-green peloids often filled with, and coated by, more immature pale light-green glauconite precipitant that appears to be 'healing' these cracks. Sympathetic light-green glauconite grain boundaries can often be observed displacing other grains at their contact boundaries (Figs. 3.7D – F), while phosphate grains are often coated in pale-green glauconite. Glauconitisation of biotite crystals, as well as within and around occasional bioclasts (principally echinoderm plates) and carbonate

clasts can be observed (Fig. 3.7C). Quartz silt-sized grains (0.005 – 0.01 mm) are angular, and in thin section are distributed randomly throughout the facies.

The principal bioclastic component is made up of foraminifera, averaging 14% (range 6 – 30%), with variable but evenly dispersed numbers of planktics and benthics, averaging 51% planktic to 49% benthic (planktic range 20 – 83%). The higher planktic ratios are located primarily in the eastern region, with lower values to the west. Echinoderm bioclasts are present in nearly all samples, and include both plates and spines, making up 6% of the facies (range 1 – 26%). Small mollusc fragments, unable to be further identified, range between occasionally absent up to 6%. Brachiopod shell is not usually identifiable as bioclasts, but where observed it comprises up to 7% of the facies and is often clearly punctate. Branching bryozoan fragments occur locally (up to 5%, average 1%), while traces (< 1%) of coralline red algae are also occasionally present. Many of these fossils are fragmented and abraded. Aragonitic forms are commonly phosphatised.

Phosphate grains are usually rounded, and in outcrop phosphate-coated bioturbation traces can occasionally be observed in the lower part of the facies. Furthermore, phosphatised shells, fish scales, and echinoid fragments are present, dominantly in the lower part of the facies where these phosphate grains are most abundant. Occasional reworked (and sometimes phosphatised) volcanic clasts are present where this facies is located proximal to volcanic formations.

Small-to-medium scale trough cross-beds are seen in some outcrops, although they are commonly obliterated by bioturbation (Fig. 3.7A). Bioturbation is often intense, with *Ophiomorpha* the most frequent, with less common occurrences of *Rhizocorallium* and *Scolicia*. Poorly preserved bedding (~ 10 cm thick) can be distinguished locally with phosphatised clast concentrations in the lower part of the facies, principally at Gee's Point.

Intact brachiopods are abundant locally, and at one location (Old Rifle Butts) make up 75% of a fossiliferous bed, although they are usually evenly dispersed throughout the facies. Disarticulated remains of the octocoral *Melitodes* are sometimes abundant where this facies locally overlies a karst horizon. Other macrofossils include gastropods (some phosphatised), echinoid fragments, sharks teeth, pectens, bryozoans, and red algal fragments.

3.2.5.2 Distribution

The Calcareous Greensand facies forms the Kokoamu and Gee Greensands, and is always the particular facies overlying unconformities within the study area. In the eastern region it is sometimes present only as small traces filling karst cavities, or as a thin veneer overlying the karst contact. In the western region, its upper occurrence may be locally fully eroded, or not exposed.

3.2.5.3 Depositional Environment

The Calcareous Greensand facies is interpreted as having been deposited in an inner- to mid-shelf environment of low sedimentation with moderate- to occasional high-energy conditions, based on a combination of grain-size and the presence of the localised cross-beds (e.g., storm events when the facies is within storm wave base). These relatively high-energy conditions may explain the higher ratio of planktic foraminifera than would be expected from this sedimentology, as the local oceanicity may have supplied planktics from outside the area. The substrate where this facies was depositing consisted of a loose mass of moving glauconite sands. These were formed of mature parautochthonous (or allochthonous) glauconite grains together with immature autochthonous glauconite that was formed *in situ*. This sandy substrate would have been subjected to intense

bioturbation during this phase of slow sediment accumulation, with the sedimentology supporting this shallower interpretation.

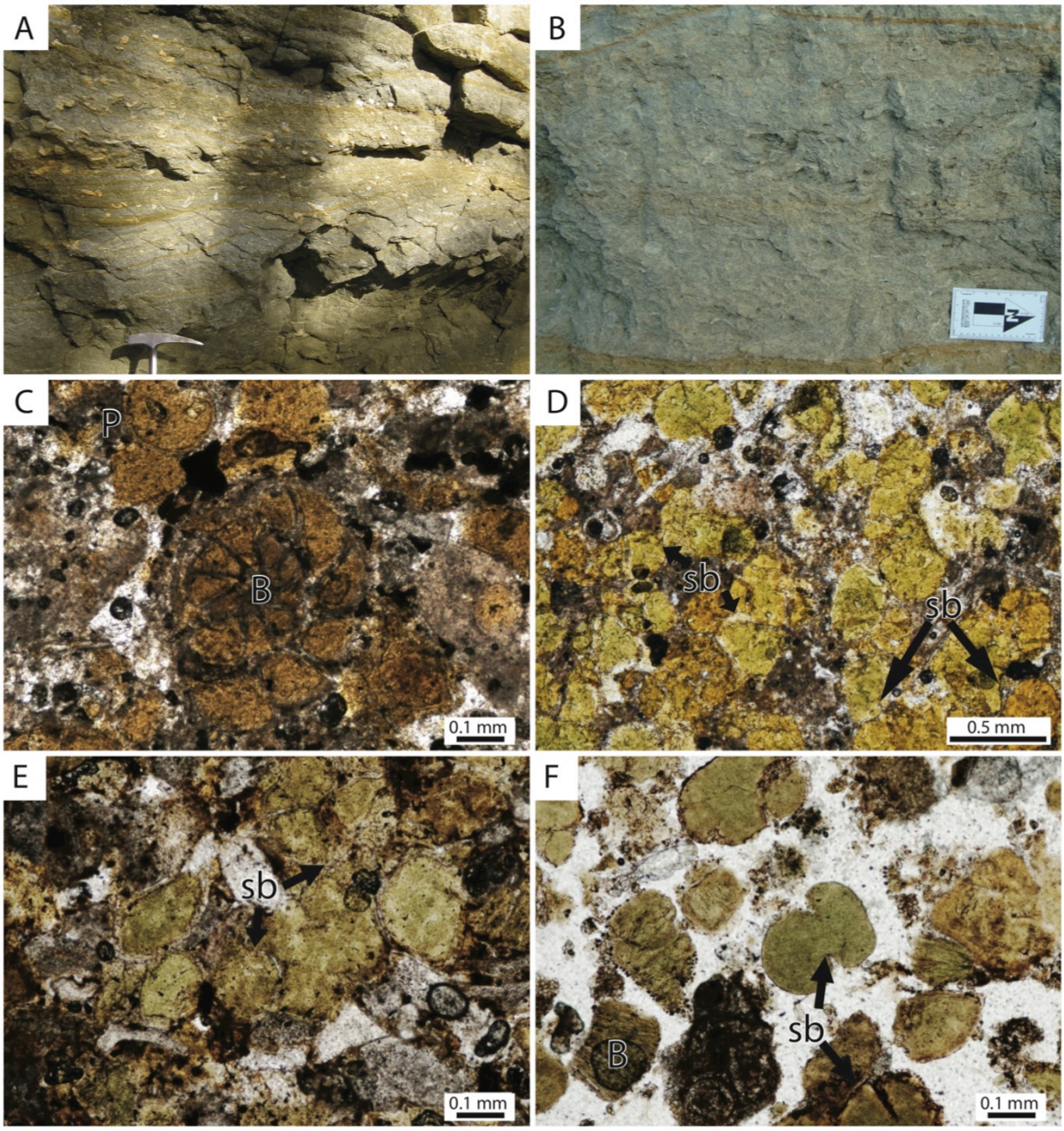

Figure 3.7. Outcrop and thin section-scale photos of the Calcareous Greensand (F5) facies. A: Outcrop at Ross Farm illustrating the very high glauconite content that can be found in this facies, as well as subtle cross-bedding. B: Earthquakes location outcrop, showing intense bioturbation. Scale-card is 15.5 cm long. C: Benthic (B) and Planktic (P) foraminifera from Gees Point, that both contain intraclast glauconite precipitation D: Ross Farm sample, showing sympathetic grain boundaries (sb) amongst relatively immature glauconite grains. E, F: Samples from Awamoko, further illustrating the occurrence of sympathetic glauconite grain boundaries (sb) as well as glauconitised biotite (B).

3.2.6 Massive Glauconitic Packstone (F6)

3.2.6.1 Description

The Massive Glauconitic Packstone facies comprises a massive, glauconitic, fossiliferous, packstone to wackestone and occasional rudstone (Fig. 3.8). Bioclasts make up the largest component of this facies at 53% (range 28 – 84%), while glauconite content averages 13% (range 2 – 32%). Carbonate mud content found in the matrix varies somewhat (5 – 45%, average 20%). Siliciclastic quartz grains constitute an average of 6% of the facies (range 1 – 15%).

Foraminifera comprise the largest identifiable bioclast component of this facies, averaging 18% (range 7 – 47%), and are made up primarily of benthic species (average 64%, range 43 – 82% benthic relative to planktic). Echinoderms make up the other prominent bioclast component (1 – 7%, average 5%), comprising numerous plates with fewer spines (Fig. **3.8**). No large benthic foraminifera species are present. Mollusc shell fragments form a small part of the recognisable bioclast assemblage, averaging only 2% but ranging up to 8% of the facies, but are not identifiable by type. Punctate brachiopod fragments are sometimes observed in thin section, comprising up to 2% of the facies, but are commonly not present. Coralline red algae are rare, and occur only in trace amounts (< 1%). A significant component (average 28%, range 9 – 67%) of the bioclast assemblage in this facies is not identifiable, due to its small size or amorphous state. This is reflected in the fragmentation of bioclasts, abrasion, and micro-borings that are initially moderate, grading to heavy up-section (Fig. 3.8F).

Glauconite occurs as rounded to sub-angular dark-green mature grains, as well as a light-green precipitate within bioclasts, usually foraminifera tests.

Bioturbation in this facies is usually moderate, with *Ophiomorpha* one of the few forms identified at outcrop. Bedding is usually absent or indistinct, although fossiliferous

beds (up to 40 cm thick) do occur at some intervals, notably in the far western region. There are no indications of cross-bedding or other sedimentary structures. Occasional pockets of coralline and shell material may be fish- or ray-feeding structures.

Whole to moderately disarticulated body fossils are usually abundant and varied in outcrop, primarily in the western region, with molluscs (*Lentipecten hochstetteri*, *Serripecten*, *Cucullaea*, *Notocorbula*, *Spissatella*, oysters, gastropods (turritellids, *Sigapatella*, naticids, and scaphopods), brachiopods, calcareous worm tubes, and echinoids common. Aragonitic species are preserved solely in the western region. Mollusc rudstones form as horizons within this facies (notably in the west), comprising poorly sorted, highly fossiliferous, clast-supported rudstones containing most of the taxa listed above.

3.2.6.2 Distribution

The Massive Glauconitic Packstone facies occurs within Otekaike Limestone, although in the western region it represents only the lower part of the formation, which there grades up into the Bedded Packstone facies (see Section 3.2.7). It sits conformably with, and in gradational contact above, the Calcareous Greensand (F5) facies (see Section 3.2.5), and has a thickness of up to 50 m decreasing sharply towards the east.

3.2.6.3 Depositional Environment

Bioclasts, including foraminiferal ratios (e.g., Hayward *et al*., 1999) and mollusc taxa (Beu and Maxwell, 1990), combined with a moderate carbonate mud content, suggest a generally mid- to outer-shelf setting for the Massive Glauconitic Packstone facies. Laterally, its reducing thickness coupled with decreasing mud content towards the east suggests a shallowing trend from west to east across the facies. Energy levels were

moderate, increasing towards the east with increasing biofragmentation and decreasing mud content.

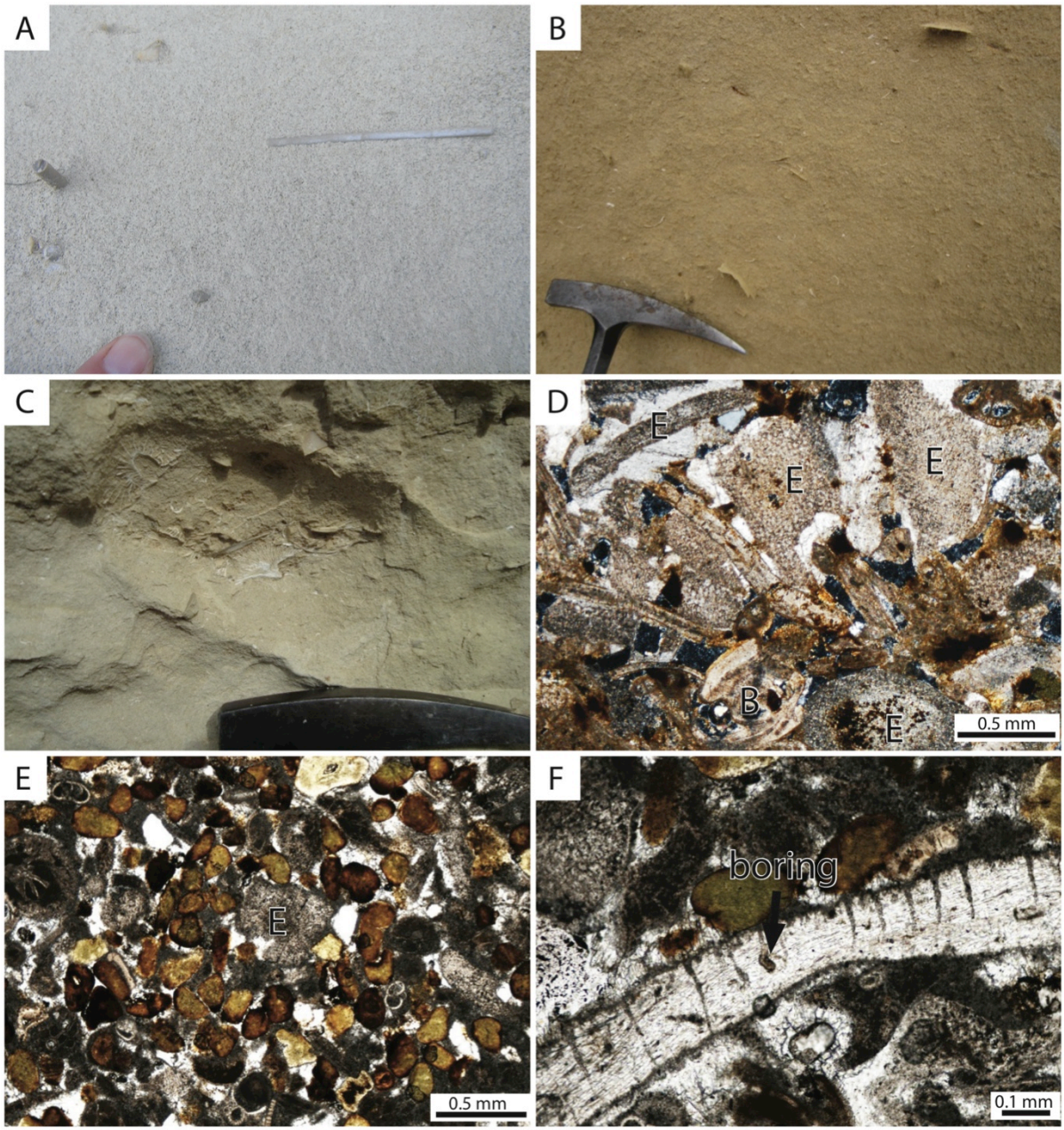

Figure 3.8. Outcrop and thin section photos of the Massive Glauconitic Packstone (F6) facies. A: Cemented outcrop at Simpsons Cliff showing two protruding echinoid spines. B: Outcrop at Otekaieke showing dispersed shell fragments. C: Near the base of the exposure at Trig Z this facies contains small pockets of *Flabellum*. D: Photomicrograph from Landon Creek showing the abundant echinoderm fragments (E) alongside a number of benthic foraminifera (B). E: Gees Point sample showing the abundant relatively mature glauconite grains within this facies, alongside echinoderm plate fragments (E). F: Sample from Gees Point containing a bored punctate brachiopod fragment, with both punctae and boring filled by the mud matrix.

3.2.7 Bedded Packstone (F7)

3.2.7.1 Description

The Bedded Packstone facies is a cemented, medium bedded, fossiliferous packstone to minor wackestone (Fig. 3.9). Bioclasts constitute the major component identified in this facies, at 53% (range 25 – 69%). Carbonate mud is variably present, forming on average 21% of the facies (range 2 – 45%). This variation in carbonate mud usually occurs between alternating beds. Glauconite content is generally low, averaging 7% (range of 2 – 24%); and quartz silt comprises a similar percentage (average 6%, range 1 – 25%). Phosphate is usually absent, but trace phosphate grains are occasionally found (< 1%).

Foraminifera make up most of the identifiable bioclastic component, comprising 16% of this facies (range 5 – 29%). These mostly comprise benthic species, although there is a significant number of planktics present (average benthic:planktic ratio 62%, range 40 – 78%). The ratio of benthic foraminifera taxa increases eastward. No large benthic species were identified, although there were a number of quartz agglutinate biserial tests present. Echinoderms also make up a significant proportion of the bioclasts, averaging 6% (range 1 – 15%). These are primarily fragmented plates with occasional spines. Unidentified bioclasts make up a significant 30% (range 7 – 50%) of the facies, and appear to be mostly small shell fragments. Undifferentiated mollusc bioclasts make up 1 – 5%, while traces of brachiopod shell, reworked coralline red algae and *Graphularia* occur throughout (up to 1%).

Fragmentation of bioclasts is variable between beds, with fossiliferous horizons displaying low fragmentation, while less-fossiliferous beds contain moderate to highly fragmented bioclastic components (Fig. 3.9C). Abrasion and micro-boring of the bioclasts is low to moderate throughout.

Glauconite is present as rounded darker-green mature grains, lighter-green immature precipitate inside bioclast void space, and minor glauconitised biotite (< 5%). Quartz is silt-sized and angular, and is found throughout the facies, as are traces of rounded phosphate grains (Fig. 3.9D). Glauconite, phosphate, and biotite content all tend to decrease upward through this facies.

Cementation alternates between beds of this facies, with average thicknesses of 10 – 30 cm, developing a resistant/non-resistant bedding profile with the cemented beds commonly exhibiting intense, cemented bioturbation networks (Figs. 3.9A and B). Fossiliferous horizons are common (primarily composed of whole echinoderms and brachiopods), and often contain whole-body fossils in the more cemented beds, while less-cemented horizons are more fragmented.

Fossil content is variable, and includes dominantly brachiopods, burrowing intact and disarticulated echinoderms, and large *Lentipecten*. A few scaphopods and gastropods are present locally. Aragonite species can also be found preserved within this facies.

3.2.7.2 Distribution

The Bedded Packstone facies forms the upper part of Otekaike Limestone in the western region, and is not found anywhere in the eastern region. In the northern region it is found in the lower part of Otekaike Limestone.

3.2.7.3 Depositional Environment

Foraminiferal ratios (e.g., Hayward *et al*., 1999) and the variable nature of bioclast preservation indicate the Bedded Packstone facies represents a low-to-moderate-energy, mid- to outer-shelf setting. The presence of many heavily bioturbated beds suggests a well-oxygenated substrate. The alternating mud content of the beds, coupled with the alternation

in bioclast preservation, suggests these beds may have been formed either by a series of storm events or slight fluctuations in relative sea level.

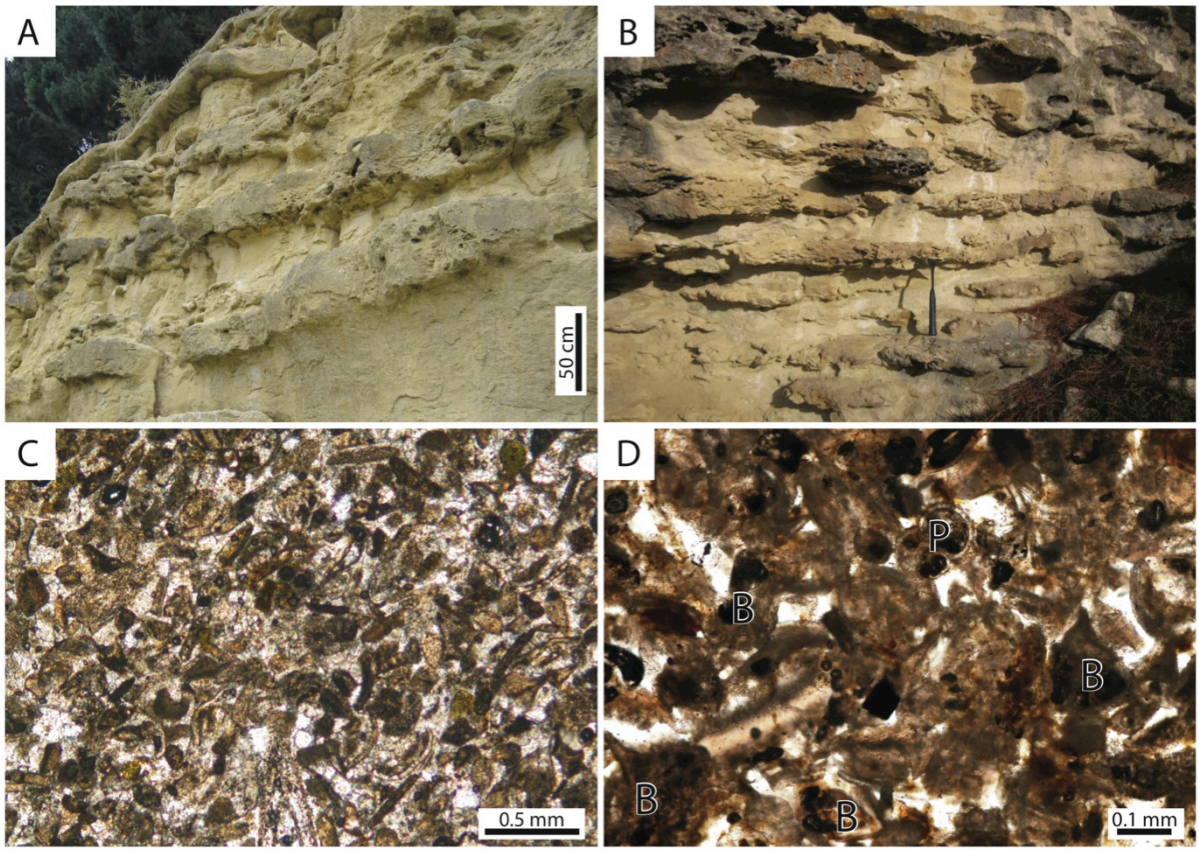

Figure 3.9. Outcrop and thin section photos of the Bedded Packstone (F7) facies. A, B: Bedded outcrop from Awamoko and Ross Farm, respectively. C: Photomicrograph from Simpson Cliffs illustrating the small and fragmented nature of the bioclast assemblage and the lack of glauconite. D: Sample from Trig Z containing a number of benthic (B) foraminiferal tests, as well as a planktic (P) species. Note even at this scale how fragmented the bioclast assemblage is.

3.2.8 Cross-bedded Glauconitic Packstone (F8)

3.2.8.1 Description

The Cross-bedded Glauconitic Packstone facies is a prominently cross-bedded and channelized, bioturbated, moderately to well sorted packstone (Fig. 3.10). Bioclasts make up 38% of this facies (range 25 – 57%). Glauconite content averages 27% (range 4 – 58%), while carbonate mud averages 12 % (range 0 – 30%). Quartz silt comprises 4% of this

facies (range 2 – 20%), alongside traces of biotite, phosphate, and localised igneous crystals (up to 1%).

Glauconite grains are primarily rounded, medium to dark green, and mature, while light-green glauconite precipitation can be found commonly within bioclastic void space, typically foraminifera tests (Fig. 3.10D). The majority of bioclasts are made up of foraminifera (5%, range 6 – 19%) and echinoid plates (3%, range 1 – 14%). Foraminiferal species are predominantly benthic (64%, ranging 24 – 85% benthic relative to planktic) but no large symbiont species were identified. As with the other packstone facies, unidentified bioclasts make up a significant proportion of the facies composition, averaging 17% (range 6 – 20%). Molluscs, including mostly pectens, with some gastropods and pteropods, comprise ~ 1% (occasionally up to 6%) of this facies. Trace fragments of branching bryozoans occur sporadically (< 1%). Abrasion and microborings of bioclasts are very common throughout.

This facies contains trace amounts of angular silt-sized quartz grains which are relatively evenly dispersed, as well as some glauconitised biotites (< 1%). In one sample at Waihao, traces of plagioclase feldspar and amphibole crystals were observed in thin section (< 1%) in conjunction with the highest quartz silt composition identified in this facies (20%). Igneous material was not found in any other samples.

Fragmentation of fossils in this facies is relatively high, with few intact specimens preserved. Identifiable fossils at outcrop commonly include echinoderms (abundant plates and spines), disarticulated brachiopods, and *Lentipecten*.

Large cross-bed sets (up to 2 m thick) dominate this facies and exhibit erosional basal contacts, with large-scale channel structures (20 – 100 m wide) forming the upper part of the facies (Fig. 3.10). Palaeocurrent directions from the cross-beds are towards the east, while the upper channel structures present a more northerly channel orientation.

Glauconite-rich to glauconite-poor alternating thin-bedding is common within cross-beds in conjunction with variable carbonate mud, and accounts for the variation in both of these components. Bioturbation is locally intense, but variably preserved, with *Ophiomorpha*, *Planolites*, and large *Scolicia* identified. *Planolites* are here used to identify ichnofacies that appear planar in nature relative to bedding but contain no other identifying features.

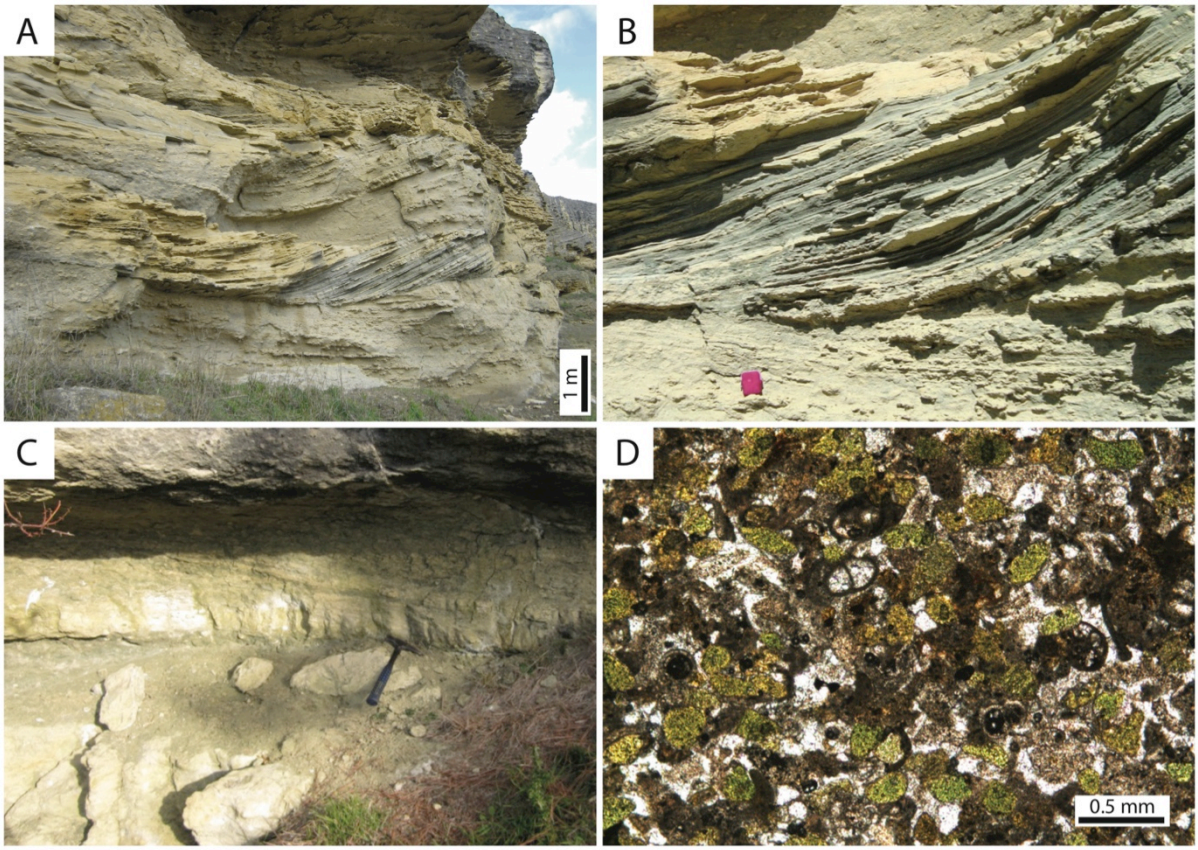

Figure 3.10. Outcrop and thin section photos of the Cross-bedded Glauconitic Packstone (F8) facies. A, B: The two photos illustrate the large-scale nature of the cross-beds found in this facies, as well as the sometimes-high glauconite content of individual or laminae sets. These are located at Waihao. C: Cross-beds found at Ross Farm showing the alternating glauconite contents within the laminae. D: Thin section photomicrograph from Waihao illustrating the more mature glauconite content set alongside a fragmented bioclast assemblage.

3.2.8.2 Distribution

The Cross-bedded Glauconitic Packstone facies is found primarily in the northern region at Waihao, with a localised occurrence at Ross Farm (Fig. 2.1), and is part of the upper section of Otekaike Limestone.

3.2.8.3 Depositional Environment

The Cross-bedded Glauconitic Packstone facies formed on the inner- to mid-shelf environment, based on the taphonomy of the bioclasts and the presence of cross-beds that indicate a high-energy environment. The large-scale cross-bedding and channelling suggest the presence of strong submarine currents. This saw shallow current activity creating dunes, alongside episodic storm events that have previously been inferred (Ward and Lewis, 1975), winnowing carbonate mud while concurrently concentrating glauconite. These events may also have supplied reworked glauconite to these areas.

3.2.9 Diatomaceous Micrite (F9)

3.2.9.1 Description

The Diatomaceous Micrite (F9) facies is a creamy-grey, massive, diatomaceous micrite (Fig. 3.11). It contains 77% calcareous mud (range 50 – 96%). It is mostly bioclast poor, averaging 10% composition (range 1 – 31%). Glauconite grains make up a further 6% (range 1 – 15%), while quartz clasts and grains comprise only 2%, with traces of phosphate (< 1%).

The dominant component of this facies, the calcareous mud matrix, is uniformly dispersed and shows very minor hematite weathering. Bioclasts can only be observed in thin section, and are dominantly whole diatoms and radiolarians comprising 5% of the facies (range < 1 – 17%). There are similar amounts of siliceous sponge spicules (average

4%, maximum 10%) (Figs. 3.11C and D). The number of radiolarians and diatoms may well be higher than the value presented here - the muddy sample matrix prevented more accurate counts. Very few foraminifera are present (average 1% of facies), and tests of both benthic and planktic species were observed. Traces of mollusc shell fragments are occasionally present (< 1%). The remaining bioclasts comprise small, unidentified specimens. One large benthic foram was found at outcrop in the upper part of the facies, alongside a small gastropod shell.

Glauconite occurs as rounded to sub-angular light- to medium-green grains, mostly found on bioclasts as a light-green precipitate in foraminifera tests, as well as around some diatoms and radiolarians (Fig. 3.11D). Quartz is found as silt-sized and angular grains that are evenly dispersed in thin section, but were also observed within one glauconitic siltstone lithic (1 – 2%).

The Diatomaceous Micrite facies is predominantly massive, although at Forresters (Fig. 2.1) a 3.7 m thick section near the top of the facies contains some patches of the diatomaceous micrite facies together with a mostly yellow-brown, poorly sorted, silty clay (Fig. 3.11B). This clay is likely to be derived from the Ash/Clay facies (see Section 3.2.12).

Some nondescript light bioturbation can be found in this facies. Occasional occurrences of lamination are also present.

3.2.9.2 Distribution

The Diatomaceous Micrite facies is found in the eastern region only, proximal to the volcanic palaeohigh, and represents Oamaru Diatomite. It features prominently at two outcrops studied here - Bains and Forresters (Fig. 2.1). It is overlain sharply with the

Volcanics (F10) facies at the Bains locality, and is associated with the Ash/Clay (F12) facies at the Forresters locality.

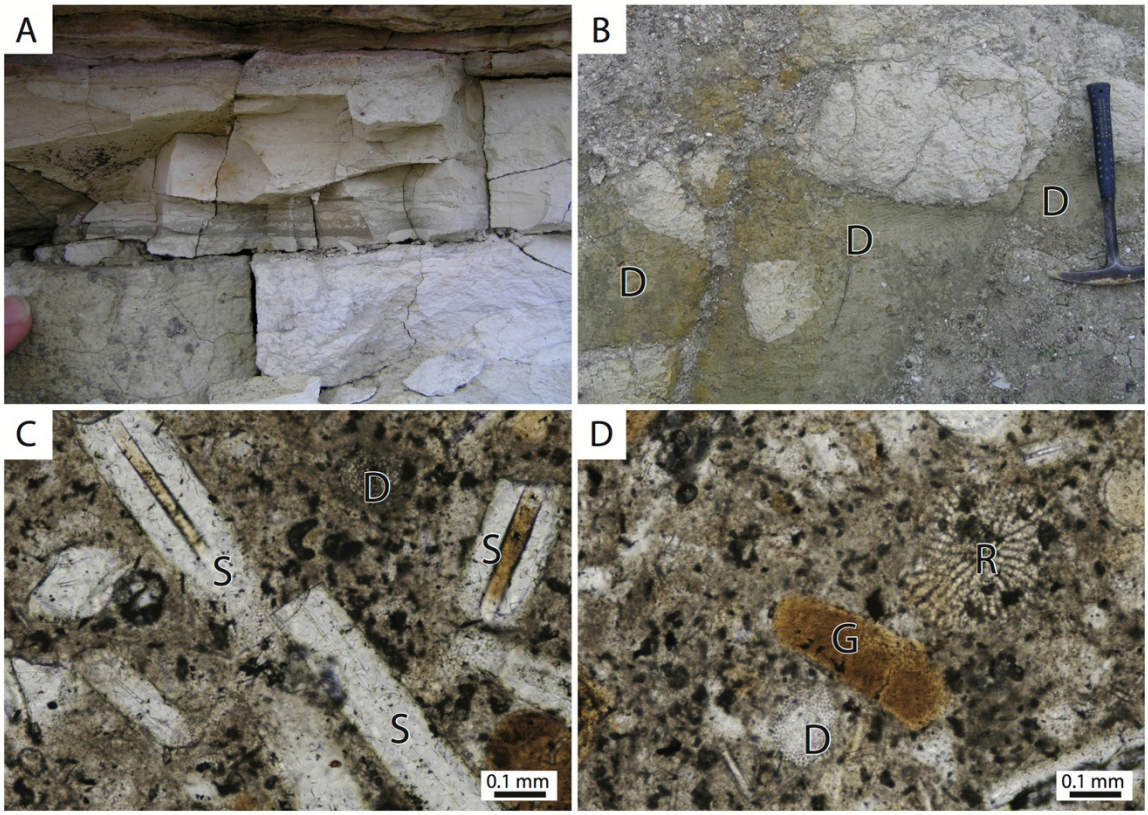

Figure 3.11. Outcrop and thin section photos of the Diatomaceous Micrite (F9) facies. A: Outcrop of this facies at Forresters showing some muddy lamination. B: Bains outcrop where lenses of silty clay are found interspersed with this facies (D). Two small normal faults may be present, and offset the diatomite. C: This sample shows a number of siliceous sponge spicules (S) filled with glauconite, as well as a single diatom (D). D: Radiolarians (R) and diatoms (D) in a muddy matrix, with one elongate glauconite grain (G).

3.2.9.3 Depositional Environment

Edwards (1991) compiled a comprehensive text on Oamaru Diatomite, suggesting deposition under quiet conditions at depths of between 75 and 150 m in warm subtropical waters. Without terrigenous supply, these locations were filled with biogenic remains from plankton blooms produced by nutrient-rich upwelling, likely to have been induced by the associated volcanism. Analyses conducted during the present study seem to agree with this

interpretation, with the sedimentology indicating a quiet, mixed siliceous/carbonate environment. The presence of a mixed horizon with the Ash/Clay (F12) facies (see Section 3.2.12) suggests some localised slumping may have occurred.

3.2.10 Volcanics (F10)

The Volcanics (F10) facies consists of two subfacies: the Volcanic Tuff (F10a) facies; and the Volcanic Pillow (F10b) facies, as described below.

3.2.10.1 Description of Volcanic Tuff (F10a) facies

The Volcanic Tuff (F10a) facies consists of multiple mafic, poorly-sorted, generally crystal-rich, lapilli-bedded tuffs (Figs. 3.12A and B). These beds often contain megacrysts of clinopyroxene, garnet, kaersutite, feldspar, with minor biotite and pyrite, comprising 10 – 75% of the facies in outcrop. Basalt scoria clasts are common (up to 20%), as are ultramafic to mafic enclaves of lherzolite and garnet pyroxenites (up to 10%) (Reay *et al.*, 2002). Crystallised zeolite can sometimes be found locally as a common component (up to 25%). Bioclasts are very rare (< 0.5%).

The tuff beds comprise a generally tuff-matrix-supported, medium- to coarse-grained assemblage (Figs. 3.12A and B). The mafic crystals within these tuffs are euhedral to subhedral, while the occasional larger enclaves in outcrop are usually sub-rounded. Further from the cone centre, the presence of enclaves and large basalt clasts decreases to < 2% of the facies. The very rare bioclast composition is indicated by only two observed benthic foraminifera tests within the entire facies.

This facies is commonly bedded (usually ~ 30 cm thick, but can be up to 1 m thick), expressing an average dip of 20° (Fig. 3.12A). It is often observed to form a gradual curve that defines the morphology of a tuff cone, with a decreasing grainsize

outwards from the centre. Normal grading is observed within the individual tuff beds. Hydrothermal venting and carbonate dykes are often associated with these deposits (Lewis, 1973). Debris flows and load structures are also commonly present (Kakanui River) (Fig. 2.1).

3.2.10.2 Description of Volcanic Pillow (F10b) facies

The Volcanic Pillow (F10b) facies comprises weathered to well-preserved, rounded, basalt pillow lavas, set in a cemented, bryozoan-rich grainstone that fills the interstices between the pillows (Fig. 3.12C and D).

The pillow lavas are generally spherical, although also occur as variations of elongate ellipsoids, the morphology of which appears to be attributable to the pillow's boundary with other pillow lobes (Fig. 3.12C and D). Radial cooling fractures are found in all the observed pillows in outcrop, as are palagonite alteration rinds in conjunction with chilled margins. The bryozoan grainstone found in the pillow interstices contains a dominantly bryozoan bioclast assemblage similar to that of the Bryozoan Grainstone (F2) facies (see Section 3.2.2), containing < 1% glauconite grains, although few foraminifera are present (of which all are benthic).

3.2.10.3 Distribution

Both of these sub-facies are found in the eastern region, while the Volcanic Pillow (F10b) facies is also found sporadically in the west. The Volcanic Tuff (F10a) facies forms the tuff outcrops identified in the eastern region, and represents both the Deborah and Waiareka Volcanics; while the Volcanic Pillow (F10b) facies represents only the Waiareka Volcanics. These facies are usually found stratigraphically associated with the Bryozoan Grainstone facies (see Section 3.2.2).

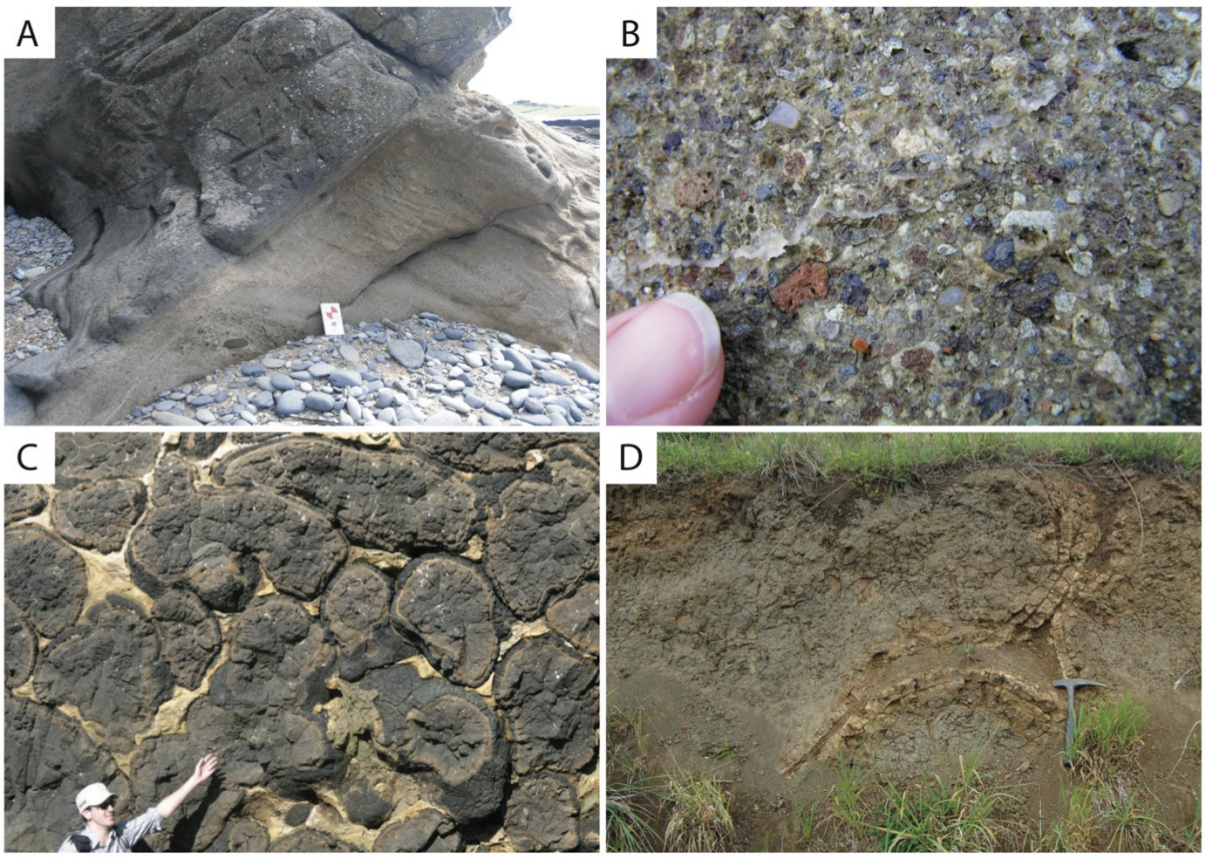

Figure 3.12 Outcrop photos of the Volcanic Tuff (F10a) and Volcanic Pillow (F10b) facies. A: Dipping beds of tuff from the Volcanic Tuff facies on the slop of a cone at Kakanui. The scale card is 15.5 cm long. B: Close up photo at Old Rifle Butts showing the sometimes crystal-rich nature of the Volcanic Tuff facies. C, D: Pillow Lava facies, both pristine and weathered outcrop examples. The matrix is a cemented carbonate grainstone. C is Cape Wanbrow, while D is at Alma.

3.2.10.4 Depositional Environment

The Volcanics facies results from pyroclastic eruptions forming successions of normal-graded tuff beds (Murphy *et al.*, 2008). It represents various volcanics extruded and erupted into a submarine carbonate environment.

The tuffs are the result of monogenetic, Surtseyan-style eruptions forming subaqueous tuff cones over short time periods on a continental shelf. Likewise, the Pillow facies is the result of submarine basaltic lava extruding into carbonate-rich ooze on the seafloor, evidenced by the nature of their carbonate interstices.

3.2.11 Reworked Volcaniclastic Packstone (F11)

3.2.11.1 Description

The Reworked Volcaniclastic Packstone facies is a calcareous, poorly-sorted, volcaniclastic and tuffaceous packstone to calcareous volcanic lithic sandstone (Fig. 3.13). This facies commonly contains large (up to 2 cm diameter) mafic crystals of amphibole, biotite and pyroxene; as well as less common garnets, with occasional angular to sub-angular lithics (2 – 20 cm diameter) of basalt which comprise a total of ~ 45% of the facies (Fig. 3.13). The matrix within which these crystals and clasts are found consists of a mixture of tuff and carbonate mud (together forming ~ 65% composition), together with some bioclasts comprising < 10% of the facies.

The mixed tuff and carbonate mud matrix usually forms an even distribution between clasts and grains in this facies, although where lamination is found carbonate- and tuff-dominated laminae alternate. The mafic crystal components of this facies can be up to 1 cm in diameter, and are made up of roughly equal amounts of euhedral amphiboles, biotites, and pyroxenes. Garnets contribute < 3% of this facies.

Basalt clasts are commonly rounded to sub-rounded, with some showing a vesicular surface. The bioclasts component is made up of fragments of bryozoans (3%), bivalves (1%), echinoids (1%), brachiopods (1%), red algae (1%), and a trace of calcareous worm tubes and foraminifera (< 1%). The remainder of the bioclasts are unidentified.

While this facies is massive in most locations, it is usually relatively thin (0.5 – 1 m). It occasionally contains some tuff/carbonate laminae (< 1 cm thick). The proportion of lithics decreases rapidly up-section.

Whole articulated bivalves are occasionally present locally, as well as some algal rhodoliths that have encrusted over 3 – 5 cm diameter basalt clasts found in relatively concentrated horizons (of up to 20% of the bed). Not all of these basalt clasts are

completely encrusted, however, with some presenting with only superficial or partial coverage. Light bioturbation occurs in the upper part of this facies.

3.2.11.2 Distribution

The Reworked Volcaniclastic Packstone facies defines the transition between the syn-depositional volcanics (Volcanic Deposits facies, Section 3.2.10) and the overlying Bryozoan Grainstone facies located in the eastern region (see Section 3.2.2). As such, this facies is the gradational contact between Ototara Limestone and the Deborah and Waiareka Volcanics.

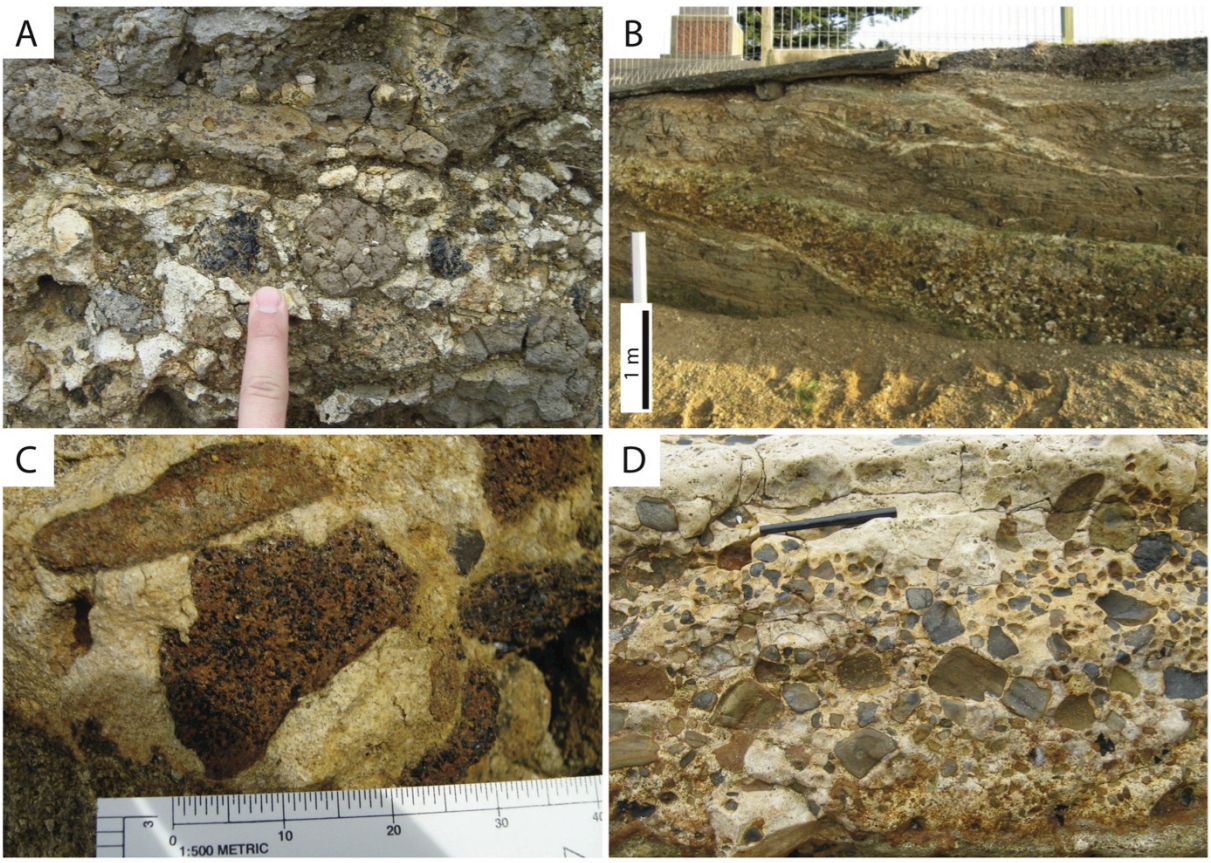

Figure 3.13. Outcrop photos from various locations of the Reworked Volcaniclastic Packstone (F11) facies. A: Rounded and sub-angular igneous clasts set is a calcareous matrix at Alma. B: Dipping beds of this facies at Alma overlying a bed of the Volcanic Tuff (F10a) facies. C: Large sub-angular to sub-rounded igneous clasts in a calcareous matrix at Gees Point. Scale is 8 cm long. D: Mixed igneous assemblage at Old Rifle Butts in a calcareous matrix. Note the rapid decrease in lithics up section. Pen for scale near the centre top of photo.

3.2.11.3 Depositional Environment

The Reworked Volcaniclastic Packstone facies represents the subaqueous reworking of the volcaniclastic sediments around the tuff cones following cessation of submarine eruptive activity and resumption of local carbonate deposition and colonisation of these volcanic highs. The burrows and articulated shells suggest volcanic quiescence with low sedimentation rates, while more fragmentary preservation of shells indicate increased energy and reworking (Cas *et al*., 1989; Murphy *et al*., 2008). Rhodoliths present suggest the cones themselves extended into the photic zone, although they were likely to have been reworked downslope with other lithic and crystal content.

3.2.12 Ash/Clay (F12)

3.2.12.1 Description

The Ash/Clay facies is a thin (< 25 cm thick), massive to laminated, orange to brown, highly weathered, calcareous, silty clay (Fig. 3.14). Clay makes up the bulk of this facies (up to 90%), with some phosphate (up to 6%) and minor glauconite (4%). Bioclast content ranges from absent to ~ 30%. Small amounts of quartz silt and mafic crystals are sometimes present (< 2%).

The dominant component of this facies is the clay, which in outcrop is also moderately calcareous, although the precise proportion of carbonate mud within it is not clear. Echinoderm fragments make up the dominant component of the bioclasts (25% of the facies), with traces of bryozoans found in thin section (2%). Foraminifera are rare (< 1%). Unidentified bioclasts make up the remaining 3% of the facies.

Glauconite and phosphate are found as rounded grains, with the glauconite tending to be dark green and mature. Mafic crystals comprise biotites and some angular opaques. The quartz silt grains are angular and tend to occur in small clusters within the clay matrix.

Hematite alteration and weathering of the matrix and clasts is commonly found in thin section.

This facies is only found as thin beds (up to 25 cm thick), some of which are discontinuous (Fig. 3.14C). Some scattered, branching bryozoan fragments are observable in outcrop, although all other fossil material is only observable in thin section. Some light bioturbation can be found in this facies, as well as a usually poorly preserved, remnant lamination.

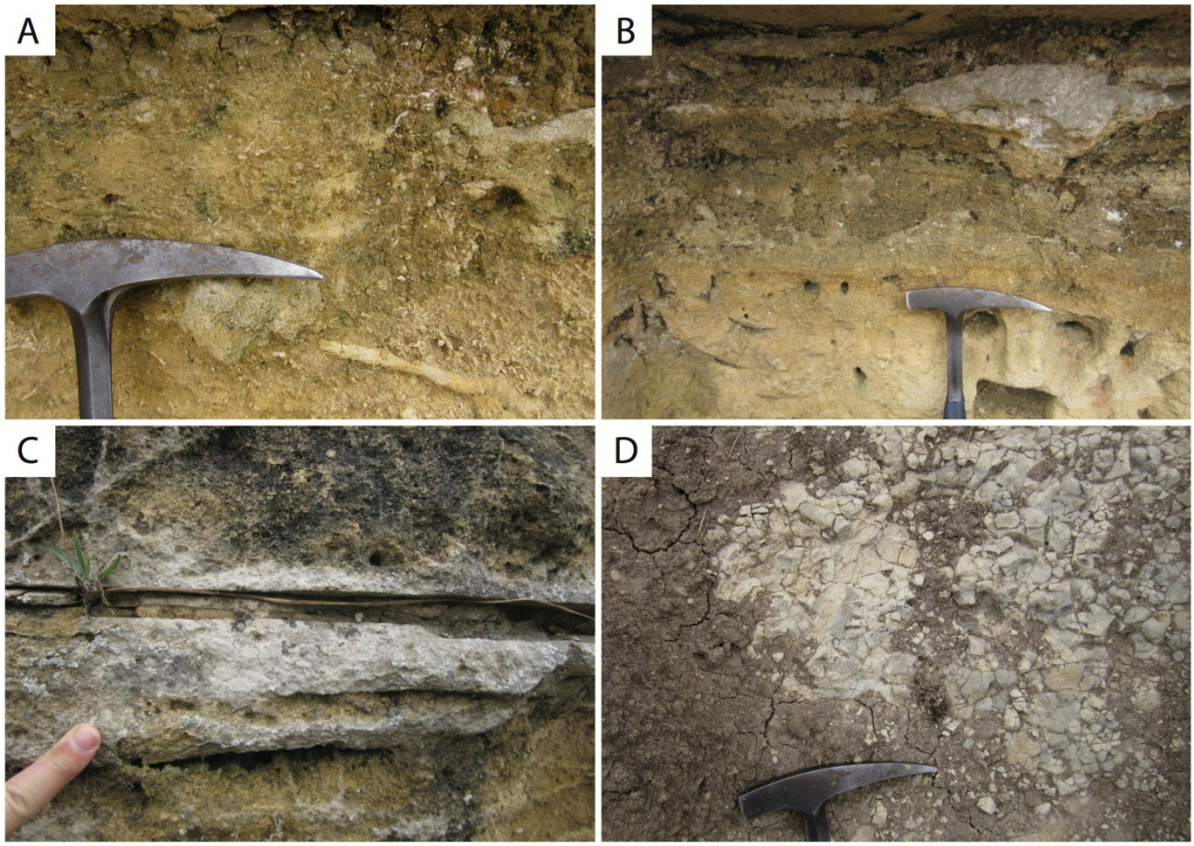

Figure 3.14. Outcrop photos of the Ash/Clay (F12) facies. A, B: show the orange and brown silty clay beds found at Meeks Rd Quarry within the Bryozoan Grainstone (F2) facies. C: Thin lamina at Meeks Rd Quarry of clay within the Bryozoan Grainstone (F2) facies. D: Lense of this facies (light coloured lithology) within the Diatomaceous Micrite (F9) facies at Forresters.

3.2.12.2 Distribution

Lenses and beds of the Ash/Clay facies are found within localized exposures of the Bryozoan Grainstone (see Section 3.2.2) and Volcanics facies (see Section 3.2.10), representing part of Ototara Limestone and the Deborah and Waiareka Volcanics, respectively.

3.2.12.3 Depositional Environment

The thin ash and clay deposits are likely to represent single events depositing ash onto the shelf. They have been weathered to clays (as currently found in outcrop) either around the time of deposition or later. The abundance of echinoderms, in conjunction with a low foraminifera count, suggests low light coupled with high nutrient levels, both of which would result from ash suspended in the water column.

Table 3.1 Summary of the twelve facies presented in this chapter

Facies	Composition	Sedimentary Structures	Occurrence	Depositional Environment
F1: Glauconitic Siltstone	Glauconite-rich (30 – 46%), non-calcareous quartz (~ 25%) siltstone. Glauconite mature.	Massive to poorly bedded, intensely bioturbated at top	Raki Siltstone (west)	Outer shelf, low energy
F2: Bryozoan Grainstone	Bioclastic bryozoan-rich grainstone to packstone. Fragmented bryozoans (~ 45%), echinoderms (1 – 24%), brachiopods, pectinids, coralline red algae (up to 24%); small and large benthic foraminifera, and worm tubes. Some igneous clasts (up to 10%). Glauconite rare.	Local planar lamination, metre scale low-angle lamination, massive (pervasive bioturbation)	Ototara Limestone (east)	Bryozoan inner shelf shoals accumulated about offshore volcanic palaeohighs
F3: Rhodolith Rudstone	Clast supported rhodoliths (~ 5 cm diameter, 75% of facies), in a bryozoan packstone matrix. Bryozoans (7 – 10%), large benthic forams (4%), echinoderms (5%), and pectinids? (1%).	Massive (unit < 2 m thick)	Ototara Limestone (east)	Associated with palaeohighs in the inner shelf; remobilised downslope

Facies	Composition	Sedimentary Structures	Occurrence	Depositional Environment
F4: Impure Wackestone	Quartzose (30 – 40%) glauconitic (9 – 25%) silty wackestone (calcareous mud 28 – 50%). Minor glauconitised biotite. Poorly fossiliferous, forams (3 – 19%), mollusc (3 – 6%, traces of radiolarians and sponge spicules.	Massive, bioturbated (*Ophiomorpha*)	Ototara Limestone (west)	Low energy; outer shelf to upper-slope. Moderate to low sedimentation rate
F5: Calcareous Greensand	Calcareous, glauconitic (20 – 80%, ~ 46%), quartz silt (2 – 15%), phosphate grains (< 3%), trace igneous clasts. Whole brachiopods (up to 60%), foraminifera (~ 14%), echinoderms (~ 6%), pectinids (0 – 6%). Rare bryozoans (1%), traces of coralline algae, gastropods and solitary corals. Local accumulations of fragmented octocorals (*Melitodes*).	Massive, heavily bioturbated (*Ophiomorpha* typical), common small- to medium-scale cross-bedding	Kokoamu and Gee Greensand throughout the mapped area.	Mid-shelf; moderate- to occasional high-energy. Low sedimentation rate
F6: Massive Glauconitic Packstone	Glauconitic (~ 13%) packstone to wackestone and occasional rudstone (carbonate mud ~ 20%); bioclasts (~ 53%) of foraminifera (~ 18%), brachiopods (2%), echinoderms (~ 5%), molluscs (~ 2%). Fossils of aragonitic bivalves, corals, gastropods, brachiopods, and scaphopods, calcareous worm tubes, and echinoderms. Glauconite (~ 13%) and quartz silt (~ 6%).	Massive to indistinctly bedded, moderate bioturbation of *Ophiomorpha*	Otekaike Limestone (entirety of mapped area, lower unit in the west)	Low to moderate energy; mid- to outer-shelf
F7: Bedded Packstone	Fossiliferous cemented-bed packstone; bioclasts (~ 53%), carbonate mud (~ 21%), low glauconite (~ 7%); quartz silt (~ 6%), trace phosphate. Foraminifera (~ 16%), echinoderms (~ 6%), mollusc (1 – 5%), brachiopod (1%). Fossils of brachiopods, burrowing echinoids, *Lentipecten*, *Serripecten*, scaphopod, gastropod, rare coralline red algae. Some aragonite fossils preserved	Bedded (cm-scale) cemented beds, common intense bioturbation	Otekaike Limestone (west)	Low to moderate energy; mid to outer shelf
F8: Cross-bedded Glauconitic Packstone	Glauconitic (~ 27%), fossiliferous packstone; bioclasts (~ 38%), quartz silt (~ 4%), trace phosphate and igneous grains. Foraminifera (~ 5%), and echinoderm (~ 3%) are common bioclasts. Pteropod, bivalve, gastropod all ~ 1%. Rare bryozoans.	Large cross-beds (< 2 m); channels (20 – 100 m across). Heavily bioturbated (*Ophiomorpha*, *Planolites, Scolicia*)	Otekaike Limestone (north), minor occurrence in west	Moderate to high energy; inner to mid shelf. Submarine currents

Facies	Composition	Sedimentary Structures	Occurrence	Depositional Environment
F9: Diatomaceous Micrite	Diatomaceous micrite (~77%). Dominant diatoms, radiolarians, and siliceous sponge spicules (total ~9%). Very few foraminifera, and traces of mollusc fragments (1 – 2%). Minor (~6%) glauconite. Quartz silt (~2%), traces of phosphate	Massive, some mixed lenses. Occasional light bioturbation, rare laminae present	Oamaru Diatomite (east)	Siliceous environments created by volcanic input. Localised slumping
F10a: Tuffs	Mafic lapilli tuff deposits, commonly megacryst-rich (10 – 75%) (amphibole, garnet, feldspar, pyroxene, minor biotite and pyrite) with basalt clasts (up to 20%) and mafic to ultramafic xenoliths (< 10%). Zeolite common (up to 25%). Very rare bioclasts (foraminifera)	Bedded (~ 30 cm) on flanks of tuff cones; carbonate dykes; hydrothermal venting; debris flow and load structures. Normal grading within beds	Deborah and Waiareka Volcanics (east)	Formed from Surtseyan submarine eruptions
F10b: Pillows	Mafic, round pillow lavas in bryozoan-rich carbonate matrix. Palagonite rinds, with radial cooling fractures and chilled margins. Heavily cemented calcareous matrix.	Massive.	Waiareka Volcanics (east and west)	Submarine lava flows into carbonate substrate
F11: Reworked Volcaniclastic Packstone	Calcareous volcaniclastic and tuffaceous packstone. Large mafic crystals (amphibole, garnet, pyroxene), angular basaltic scoria clasts and lithics of tuff (total ~ 45%). Bioclasts (< 10%) of bryozoans (3%), brachiopods (1%), bivalves (1%), echinoderms (1%), and red algae (1%). Traces of calcareous worm tubes and foraminifera. Occasional fossils of rhodoliths, articulated bivalves	Massive to bedded. Occasional tuff/carbonate alternating laminae. Light bioturbation in upper facies	Ototara and Deborah/ Waiareka Volcanics (east)	Reworking of volcanic deposits into carbonate environments, slow sedimentation rates
F12: Ash/Clay	Thin (< 25 cm), massive to laminated, orange to brown, highly weathered, calcareous, silty clay (up to 90%). Fossil content is absent to 30%. Echinoderm fragments form majority (~ 25%) of bioclasts, with rare bryozoans (~ 2%) and foraminifera (< 1%). Bryozoan fossils observable in outcrop. Commonly iron-stained. Minor phosphate (~ 6%) and glauconite (~ 4%). Few quartz silt and mafic crystals (< 2%).	Massive to laminated. Light bioturbation	Interbedded with Ototara Limestone (east) and Waiareka and Deborah Volcanics (east)	Altered ash deposits from a low-light and high-nutrient environment

3.3 Facies Associations

The twelve facies developed in this chapter cover a range of marine environments from high-energy, inner-shelf, through to quiet, upper-slope. These twelve facies can be loosely grouped into facies associations based on both their depositional depth and primary composition as described below and in Table 3.2.

Table 3.2 Summary of facies associations

Facies Association	Facies
Carbonate Inner-shelf	Bryozoan Grainstone (F2) Rhodolith Rudstone (F3) Cross-bedded Glauconitic Packstone (F8)
Carbonate Mid- to Outer-shelf	Calcareous Greensand (F5) Massive Glauconitic Packstone (F6) Bedded Packstone (F7)
Carbonate Outer-shelf to Slope	Impure Wackestone (F4)
Clastic Outer-shelf	Glauconitic Siltstone (F1)
Volcanic	Diatomaceous Micrite (F9) Volcanic Tuff (F10a) Volcanic Pillow (F10b) Reworked Volcaniclastic Packstone (F11) Ash/Clay (F12)

3.3.1 The Carbonate Inner-Shelf Facies Association

The Carbonate Inner-Shelf Facies Association contains the Bryozoan Grainstone (F2), Rhodolith Rudstone (F3) and Cross-bedded Glauconitic Packstone (F8) facies.

Bryozoan Grainstone and Rhodolith Rudstone are found around the eastern volcanic highs and form an inner shelf shoal. These facies are devoid of any significant glauconite content.

The Cross-bedded Glauconitic Packstone is stratigraphically younger than the other two facies, and is located primarily to the north of this shoal and was subjected to high-energy winnowing and reworking of glauconite.

3.3.2 The Carbonate Mid- to Outer-Shelf Facies Association

The Carbonate Mid- to Outer-Shelf Facies Association is made up of the Calcareous Greensand (F5), Massive Glauconitic Packstone (F6), and the Bedded Packstone (F7) facies. This facies association covers a broad range of depth; although further refinement was not possible due to compositional ranges within the facies themselves. There is, however, a deepening trend through the association from Calcareous Greensand, through Massive Glauconitic Packstone, to the Bedded Packstone facies. This is mirrored by a decrease in glauconite content. This facies association is significantly thicker is the western region, thinning eastward.

3.3.3 The Carbonate Outer-Shelf to Slope Facies Association

The Carbonate Outer-Shelf to Slope Facies Association contains only the Impure Wackestone (F4) facies. This facies is found only in the western region, and is made up primarily of mixed carbonate and clastic material, including glauconite. It is here differentiated from the Clastic Outer-Shelf Facies Association (see Section 3.2.4) due to its significant carbonate component, even though it still contains significant clastic silt.

3.3.4 The Clastic Outer-Shelf Facies Association

The Clastic Outer-Shelf Facies Association differs from the Outer-Shelf to Slope Facies Association (see Section 3.2.3) in its lack of carbonate. It consists solely of the

Glauconitic Siltstone (F1) facies - a glauconite-rich, clastic siltstone. This facies association is also found only in the western region.

3.3.5 The Volcanic Facies Association

The Volcanic Facies Association is based principally on the presence of a significant volcanic component, or an interpreted volcanic origin, in each of the facies. It consists of the Diatomaceous Micrite (F9), Volcanic Tuff (F10a), Volcanic Pillow (F10b), Reworked Volcaniclastic Packstone (F11), and Ash/Clay (F12) facies. These facies are found mostly in the eastern region, although the Volcanic Pillow facies is also found to the west.

3.4 Facies Types in Relation to Formations

The facies types presented in this chapter occur within each of the formations presented in Chapters 1 and 2, as discussed in the distribution section of each facies. Fig. 3.15 shows the spatial distribution of the main facies with respect to each of the formations found within the study area.

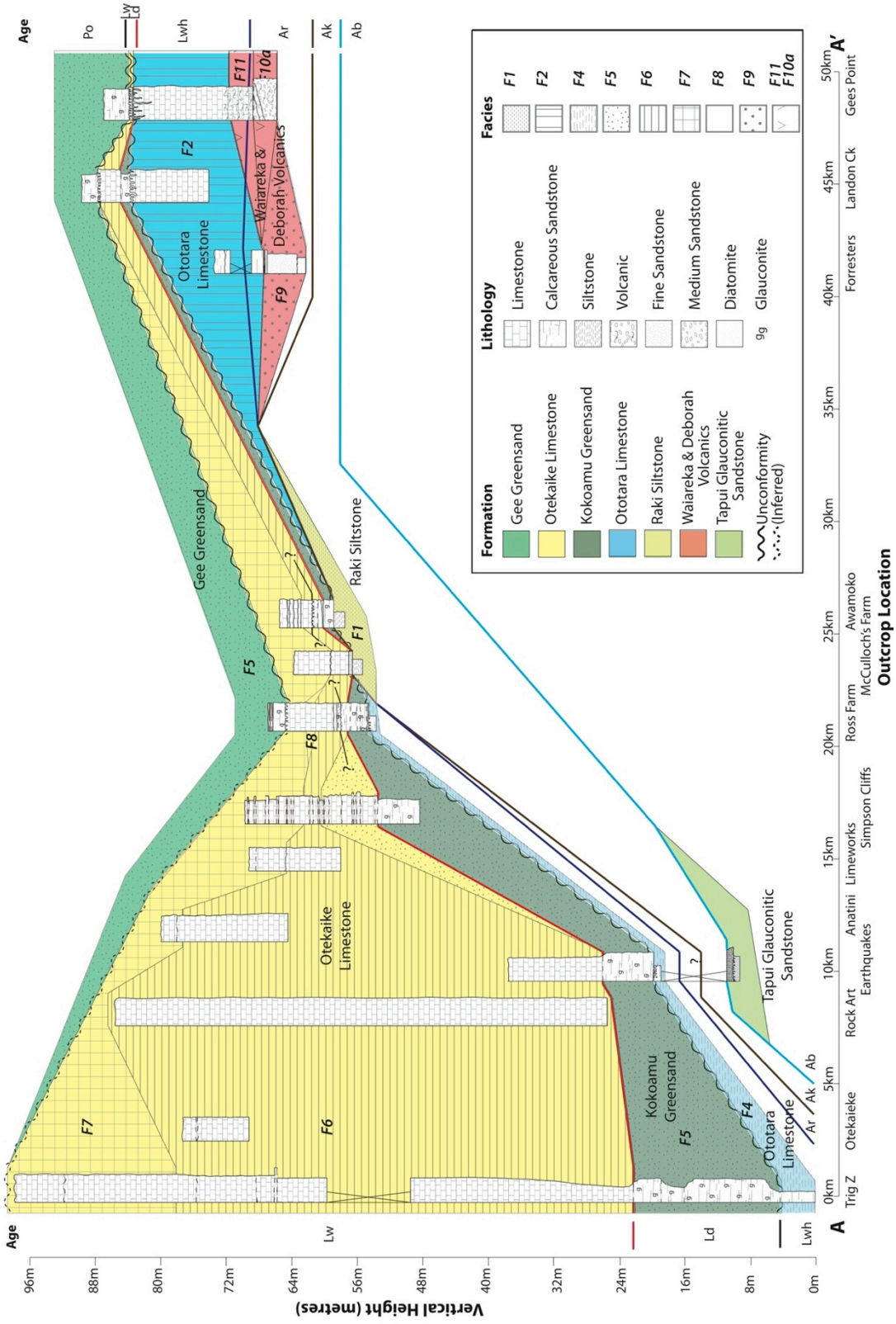

Figure 3.15. Cross section through the study area (A-A'; see Fig. 2.2) showing the different facies types with respect to the formations found in the Waitaki Region. Colours show the formations, while the patterns illustrate the different facies types presented in this chapter.

CHAPTER 4 –PROCESSES OF DIAGENESIS IN THE WAITAKI REGION

4. Introduction

Information on the diagenesis and paragenesis of cool-water carbonates enables understanding of original sediment mineralogy, water temperatures, the syn-depositional environment, the nature of post-depositional processes, and pore-fluid compositions (e.g., Tucker and Wright, 1990; Scholle and Ulmer-Scholle, 2003). Diagenetic processes usually begin as soon as the sediment is formed at the sea floor (James and Choquette, 1990a; Tucker and Wright, 1990), and continue through to burial, with or without meteoric exposure (Fig. 4.1) (Purdy, 1968; James and Choquette, 1990a; Scholle and Ulmer-Scholle, 2003).

Diagenetic processes for cool-water carbonates typically include calcite cement precipitation, calcite and aragonite dissolution, mineral replacement or inversion, recrystallization and compaction (Larsen and Chilingar, 1979; Tucker and Wright, 1990; Scholle and Ulmer-Scholle, 2003). Rock- and sediment-water interactions exert the most important influences on carbonate diagenetic processes, such that as compositions of surface and subsurface fluids change within diagenetic environments, processes occurring in each vary accordingly (Tucker and Wright, 1990).

Sea-floor diagenesis operates over short time frames (up to 1,000 years), but can result in significant dissolution of shell and degraded carbonate grains in the cool-water carbonate realm, especially those composed of aragonite (Scholle and Ulmer-Scholle, 2003; James *et al*., 2005). Meteoric diagenesis occurs during alteration at or near the surface in strata influenced by recently derived meteoric fluids, and can involve extensive dissolution and precipitation of aragonite and high-Mg calcite, with a common result being

the development of karst morphologies (Scholle and Ulmer-Scholle, 2003). The burial diagenetic realm occurs below the zone of active seawater circulation or phreatic mixing, and is often a geologically lengthy process resulting in a general decrease in porosity as a result of physical and chemical compaction accompanied by calcite cement precipitation (Scholle and Ulmer-Scholle, 2003).

Data presented in this chapter are used to determine the degree to which these different diagenetic environments influenced the sediments within the study area, and in what ways. The preservation or alteration of aragonite and high-Mg calcite is of particular importance here, as these mineral phases are not commonly associated with cool-water carbonate-derived rocks following diagenetic removal, and yet aragonitic forms are conspicuous in the Massive Glauconitic Packstone (F6) and Bedded Packstone (F7) facies in the western region, while being largely absent in the other regions (see Section 3.2).

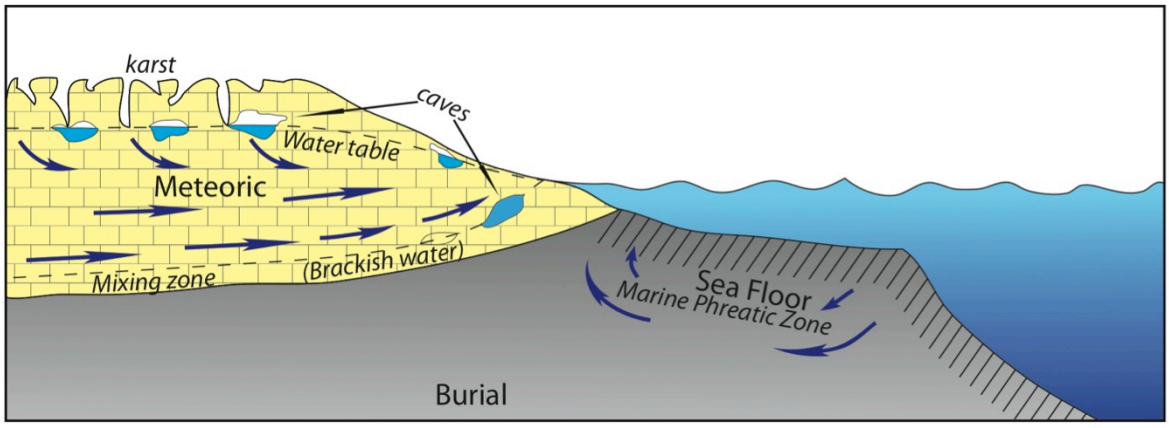

Figure 4.1. Schematic diagram illustrating the three main carbonate diagenetic environments. Variables in local hydrodynamics and the position of the water table can alter the location of the mixing zone of saline and fresh water, and the depth to which it interacts with the marine zone to produce brackish waters. Modified from James and Choquette (1990a) and Scholle and Ulmer-Scholle (2003). Figure is not to scale.

Section 4.1 provides a review of the current understanding of cool-water carbonate diagenesis, with this information being necessary for interpretation of the data gathered

from the Waitaki study area in reconstructing the diagenetic and paragenetic history of the rocks found there.

4.1 New Zealand palaeoceanography and the carbonate realm

While this study refers consistently to the cool-water carbonate realm, it must be acknowledged that a spectrum of mid-Cenozoic limestone types exists in New Zealand (e.g., Nelson *et al*., 1988b). Carbonates here formed mainly under cool to warm-temperate oceanographic conditions (< 20ºC), which became marginally subtropical at times (20 – 23ºC), on open shelf or ramp settings at palaeolatitudes between 60ºS and 35ºS (Nelson, 1978b; Hayton *et al*., 1995; Buening *et al*., 1998). In spite of these variations in depositional conditions, a skeletal-dominated limestone assemblage developed around New Zealand in the mid-Cenozoic, including in the Waitaki study area, with all limestones exhibiting attributes typical of non-tropical carbonates (e.g., Nelson, 1978b, 1988; Nelson *et al*., 1988b; Kamp and Nelson, 1988; Kamp *et al*., 1988; Hayton *et al*., 1995). Both palaeontological evidence and the oxygen-isotope record support these environmental interpretations, suggesting that mean water temperatures around New Zealand were, for the most part, cooler than 20ºC from the Late Eocene to the Early Miocene (e.g., Nelson, 1978b; Hornibrook, 1992; Nelson and Smith, 1996; Buening *et al*., 1998; Nelson and Cooke, 2001).

Within the study area, some subtropical indicators are present, notably as large benthic foraminifera (e.g., *Asterocyclina*) in the Bryozoan Grainstone (F2) facies located in the eastern region (see Fig. 2.1 and Section 3.2.2), and some warm-water mollusc species (see Section 3.2.7**,** and Beu and Maxwell, 1990). The subtropical taxa distribution around New Zealand is, however, usually focused on the western and northern coasts, and is found only occasionally on the east of South Island (Beu and Maxwell, 1990; Buening *et al*., 1998) (see Fig. 1.2 for spatial relationships with New Zealand palaeogeography). These

less-frequent eastern subtropical indicators have therefore been attributed to sporadic north-south migration of a proto-Subtropical Convergence developed in the Early Oligocene, or to localised colonisation of relict volcanic seamounts that warmed local waters (Buening *et al*., 1998; Nelson and Cooke, 2001).

4.2 Cool-water carbonate diagenesis

There are a number of important properties of the cool-water carbonate environment that control the nature of its diagenetic processes. Principal among these is relatively low level of calcium carbonate saturation in temperate seawaters relative to more tropical environments, which leads to a less diverse array of carbonate organisms (Alexandersson, 1978; Leonard *et al*., 1981). Furthermore, lower temperatures limit abiotic precipitation (Nelson, 1988), resulting in little cement precipitation prior to burial (James and Choquette, 1990b; James, 1997). Lower temperatures also result in lower reaction rates which, when coupled with low levels of carbonate saturation, lead to mineral-selective dissolution (Nelson, 1978b; James, 1997; James *et al*., 2005).

The temperate carbonate environment, rather than precipitating extensive calcite cements, tends toward destructive early diagenesis caused by bioerosion, maceration, and partial or total dissolution of skeletal material, which occur with low to negative accumulation rates, low levels of calcium carbonate saturation, and a higher CO_2 content within the water column (Alexandersson, 1978; Young and Nelson, 1988; Smith and Nelson, 1994; James, 1997; Smith and Nelson, 2003). Carbonate mud found in cool-water carbonate sediments is therefore almost always detrital, rather than a precipitate of microcrystalline calcite (micrite) (Scholle and Ulmer-Scholle, 2003).

4.2.2 Sea-floor diagenesis

Within the temperate carbonate realm, the level of calcium carbonate saturation in seawater is reduced relative to more tropical latitudes. Accordingly, the ease with which cementation occurs on the sea floor is also reduced, and carbonate grains (primarily aragonite and high-Mg calcite) become more susceptible to dissolution (Alexandersson, 1978; Rivers *et al*., 2008). Physical breakdown and abrasion of skeletal material is often dependant on hydraulic regime, as well as the taxa from which the carbonate material is derived (Smith and Nelson, 2003). Thus the cool-water carbonate sea-floor diagenetic realm is generally one of destructive diagenesis, involving processes such as grain bioerosion and maceration, in addition to mineral dissolution (Alexandersson, 1979; Nelson, 1988; James, 1997; Smith and Nelson, 2003).

In the sea-floor diagenetic setting, cool-water carbonates are rarely cemented due to the generally destructive character of the environment (Tucker and Wright, 1990) and an often open-ramp morphology that leads to higher energy reworking of shallower sediments (James *et al*., 1994; James, 1997). Marine-cemented temperate limestones can still occur in localised horizons, however, particularly at unconformities associated with shallow water (Nelson and James, 2000). This may be the result of increased water temperatures in these shallower waters, which raised levels of carbonate saturation (Shubber *et al*., 1997), increased energy levels, and escalated exchange of pore fluids (Nelson and James, 2000).

Recent work based on modern and ancient cool-water carbonates (e.g., Brachert and Dullo, 2000; Caron *et al*., 2005; James *et al*., 2005; James *et al*., 2011) has shown that the original sediments may have contained a significantly higher aragonite content than is currently preserved in the rock record. The dominantly low-Mg calcitic record observed today is more likely the result of aragonite and high-Mg removal than a reflection of original sediment mineralogy (Brachert and Dullo, 2005; James *et al*., 2005; Caron and

Nelson, 2009). James *et al*. (2005) further show that seawater at latitudes considered here can be oversaturated with respect to aragonite, and that removal of the aragonitic material was the result of microbial degradation of organic matter and resultant dissolution on the sea floor early in the rock's diagenetic history.

4.2.3 Meteoric diagenesis

The meteoric diagenetic realm is the zone where rainfall-derived groundwater comes into contact with sediment (James and Choquette, 1990a; Tucker and Wright, 1990), commonly leading to dissolution accompanied by precipitation of low-Mg calcite or occasionally dolomite. Subaerial exposure may also cause development of phosphate crusts, iron and aluminium oxides, and clays (Scholle and Ulmer-Scholle, 2003). Meteoric cements tend to have low Fe^{2+} and Mn^{2+} contents (Scholle and Ulmer-Scholle, 2003).

The meteoric setting is subdivided into three areas: the vadose zone, the phreatic zone, and the mixing zone (Fig. 4.2).

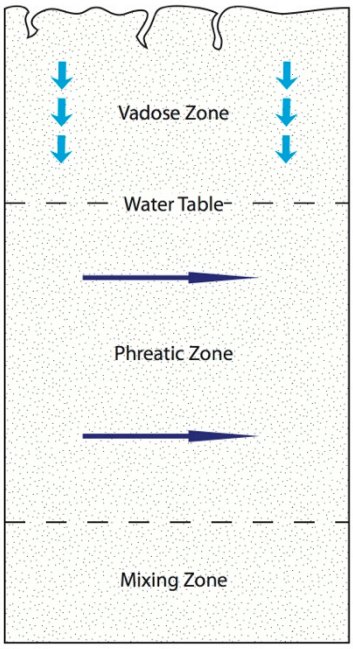

Figure 4.2. The primary environments and settings of carbonate meteoric diagenesis. Modified from James and Choquette (1990a) and Tucker and Wright (1990).

The vadose zone lies above the water table (Fig. 4.2), towards which water flows either through a relatively homogeneous network of pores (e.g., unconsolidated carbonate sediment), or through fractures and cracks created by lithification (James and Choquette, 1990a; Tucker and Wright, 1990). The latter type can lead to the creation of caves and karstic features (Tucker and Wright, 1990). Water entering the rock or sediment in the vadose zone contains dissolved atmospheric CO_2, soil-derived CO_2 (when present), and organic acids, which increase the acidity of the water while also adding organic carbon to it. This leads to the dissolution of unstable aragonite and high-Mg calcite, and may cause the reprecipitation of more stable low-Mg calcite (James and Choquette, 1990a; Tucker and Wright, 1990; Scholle and Ulmer-Scholle, 2003). This reprecipitation often forms meniscus cements and rounded pore-spaces, resulting from the localised distribution of water as droplets in undersaturated sediment (James and Choquette, 1984; Scholle and Ulmer-Scholle, 2003).

The phreatic zone is the horizon where all pore space is filled with fluid below the water table (Tucker and Wright, 1990) (Fig. 4.2). Here the water is actively moving horizontally to subhorizontally towards a local low (e.g., ocean or inland lake). This lens of fresh meteoric water in the phreatic zone extends below sea level to approximately 40 times the height of the water table above mean sea level (as defined by the Ghyben-Herzberg principle) (Todd, 1980). Even a minor elevation of the sediment above sea level can thus result in significant penetration of meteoric waters and associated meteoric diagenesis (James and Choquette, 1990a). Where the zone is close to marine environments, tides and wave action may influence the height of the phreatic zone as the saline base on which the phreatic waters sit rises and falls with changing mean sea level (Tucker and Wright, 1990). The rate of water movement through the phreatic zone has a strong influence on the rate of meteoric diagenesis, and it is common for upper phreatic lenses to

have higher flows while those further below have low-flow to stagnant conditions (Tucker and Wright, 1990). As with the vadose zone, dissolution is often common in the upper phreatic zone, leading to the creation of karstic features near the boundary of the two zones (i.e., the water table) (Scholle and Ulmer-Scholle, 2003). Cements formed in the phreatic zone are relatively uniform, and tend to comprise isopachous or blocky fabrics of equant calcite spar (James and Choquette, 1984; Scholle and Ulmer-Scholle, 2003).

Underlying the phreatic zone is a mixing zone (Fig. 4.2) where saline waters combine with fresh meteoric waters derived from above (Back *et al*., 1979; Tucker and Wright, 1990; Scholle and Ulmer-Scholle, 2003), and where dissolution and dolomitization are common occurrences (Folk and Land, 1975; Tucker and Wright, 1990). This zone tends to be thickest where higher permeability allows better mixing, and also at locations closest to the coast as a result of higher water flow towards the ocean and the influx of saline marine waters (James and Choquette, 1990a).

4.2.4 Karstification

The dissolution of carbonate during meteoric diagenesis results in grain leaching and a net loss of calcium carbonate that can lead to karstification (Esteban and Klappa, 1983; Tucker and Wright, 1990). The length of exposure to the meteoric environment plays a significant role in the development of karst, with a mature karst profile requiring exposure for of the order of one million years to develop (Tucker, 2009). This is further controlled by the magnitude of relative sea-level fall, which influences the depth of meteoric interaction (Tucker, 2009).

The sediment's original mineralogy affects the degree of dissolution or cementation that can take place during this process. Aragonite tends to be least stable in the meteoric setting and is commonly dissolved, while high-Mg calcite will often leach magnesium and

alter to more stable low-Mg calcite, although even this can be dissolved if the waters are undersaturated with respect to calcium carbonate (Tucker, 2009). Thus, in the cool-water carbonate realm, where aragonite and high-Mg calcite are less common, lower levels of readily dissolvable carbonate require more undersaturated waters to dissolve low-Mg calcite, allowing for later calcite precipitation to occur (Tucker and Wright, 1990; Tucker, 2009). This has been observed where, apart from echinoderm-rich calcarenites, temperate sediments tend to remain largely uncemented within the meteoric zone for long periods due to the lack of aragonite to provide carbonate for precipitation (James and Bone, 1989; James and Choquette, 1990a; Nicolaides, 1995).

4.2.5 Burial diagenesis

Burial diagenesis is usually defined as beginning below the depth where sediments are influenced by the zones of sea-floor and meteoric diagenesis (Tucker and Wright, 1990) (Fig. 4.1). This zone involves an array of processes (Table 4.1) that commonly lead to a progressive reduction in porosity as a result of compaction and cementation, with increasing temperature, pressure and porewater salinity (Choquette and James, 1990). This stage of diagenesis is often significantly longer than the other two, commonly millions to hundreds of millions of years in duration (Scholle and Ulmer-Scholle, 2003).

There is little diagenetic alteration below the near-surface (meteoric and sea-floor) diagenetic zones until the onset of compaction in the burial realm. While compaction and cementation usually lead to a reduction in porosity, porosity may actually be gained through dissolution of metastable minerals and earlier diagenetic near-surface-zone cements (Tucker, 2009). Sea-floor diagenetic cements may reduce compaction in the burial zone; while their absence, as commonly found in the cool-water carbonate realm, can increase grain-to-grain contact and subsequent pressure dissolution, liberating more

calcium carbonate for cementation, and significantly reducing porosity (Tucker, 2009). These grain-to-grain compaction processes result in characteristic fabrics, including sutured grain contacts, brittle fracture, dissolution seams, and stylolites (Scholle and Ulmer-Scholle, 2003).

Table 4.1. General processes and their products resulting from burial diagenesis.

Processes	Products
Physical compaction	Reduced thickness, porosity, and permeability; Broken and re-oriented allochems; Compressed textures and structures
Chemical compaction	Reduced thickness, porosity, and permeability; Stylolites and other pressure solution features; Ions for new carbonate cements
Cementation	Mosaic/drusy to very coarse poikilotropic calcite and saddle dolomite (hydrothermal)
Burial dolomitization	Anhedral-crystalline dolomite, often coarse

Source: Adapted from Choquette and James (1990).

Syntaxial overgrowths on echinoderms, where calcite cement has grown around the bioclast with the same crystal alignment as the echinoderm, commonly form during burial diagenesis. They can, however, equally well develop in either the meteoric or sea-floor zone, and are therefore not a useful diagnostic tool for determining cement genesis (Scholle and Ulmer-Scholle, 2003).

Compaction of sediment usually becomes significant at several hundred metres burial depth, at which point pore fluids begin to move upward (Tucker, 2009). This fluid migration results in the onset of calcite spar cementation and, where clays are present, dewatering may supply magnesium to induce dolomitization (Tucker, 2009). As many burial cements are the result of relatively reducing pore-fluids, they tend to have an

elevated Mn^{2+} and Fe^{2+} signature, detectable by both staining for iron and cathodoluminescence (Scholle and Ulmer-Scholle, 2003).

4.3 Methodology

The diagenetic histories of the facies found within the study area (see Section 3.2) were determined through study of the occurrence of calcite cements and fossil mineralogy, together with diagenetic fabrics and their chemical signatures. Diagenetic fabrics were initially recorded from thin sections using standard optical microscope techniques, with a focus on calcite cement fabrics and any indicators of bioclast alteration. Further analyses were performed on a selected number of samples using Alizarin Red S and potassium ferricyanide staining in order to identify the distribution of iron in calcite. Further samples were impregnated with a coloured resin to derive a porosity approximation. Selected samples were then analysed using cathodoluminescence (CL) to determine the occurrence and nature of any phases of cement precipitation.

4.3.1 Carbonate sedimentology and petrography

Using the stratigraphic sections logged in the field (see Appendix B), in conjunction with the facies described in Chapter 3, the presence or absence of calcite cements within the different lithologies was recorded, together with the mineralogy of any fossils present. This was followed by routine carbonate petrographic analyses of 216 samples that were representative of the facies within the study area, recording the amount and nature of cements in each as well as any diagenetic fabrics found, particularly those related to dissolution or replacement of bioclasts. Porosity estimates were carried out by preparing nine thin-section blocks impregnated with blue-coloured resin under vacuum, with visual estimates of porosity and pore-space connectivity within the samples.

4.3.2 Cathodoluminescence

Cathodoluminescence has become an important tool in the investigation of carbonate rocks, particularly in the study of carbonate cements (Machel and Burton, 1991). CL response colours and intensities, and zonation patterns, are governed by activating and quenching elements - principally manganese and iron (Machel and Burton, 1991; Machel *et al*., 1991). The most important activator in calcites is Mn^{2+}, with as little as 10 – 20 ppm needed to produce visual luminescence (Machel and Burton, 1991). Iron (Fe^{2+}) is a common quencher of Mn^{2+}-induced luminescence, with as little as 30 – 35 ppm Fe^{2+} needed to induce this effect (Machel and Burton, 1991). It is therefore usually the ratio of these two elements that controls the intensity of carbonate luminescence responses during CL analyses, although the exact nature of the relationship is not clearly understood (Machel and Burton, 1991; Machel *et al*., 1991).

In the present study, CL imaging of 20 different thin sections, from eight locations, was carried out in order to identify trends in the diagenetic history through the identification of cement responses. The CL equipment comprised a Technosyn cold cathode stage mounted on an Olympus BX41 microscope with a standard vacuum pump, and with a digital camera attached for recording photomicrographs. The operating conditions involved a 0.55mA current, 18kV accelerating voltage, and 30 – 45 s photographic exposure times (dependant on the zoom used: x4 or x20 respectively). Samples were selected for CL imaging on the basis of the presence and proportion of cements observed in thin section. Some formations and facies were not used in this analysis due to their complete lack of cement that made them of limited value for this approach. CL intensities were estimated visually and always by the same observer in one session, coupled with consistent exposure times to allow for accurate comparisons.

The luminescence response from the CL analyses in this study were classed as non-luminescent, dull-luminescence, or bright-luminescence, based on relative observations for the latter two using equivalent time-exposure photomicrographs.

4.3.3 Alizarin Red S and potassium ferricyanide staining

Staining carbonate samples using the Alizarin Red S and potassium ferricyanide staining tests enabled determination of the amount of Fe within calcite, and distinction between calcite and ferroan calcite, as well as between dolomite and ferroan dolomite (Evamy, 1963; Dickson, 1965). The resultant stain colour is indicative of the mineralogy, with pale pink to red for calcite, and an increasing blue component with increasing Fe content (from low-ferrous to high-ferrous) within ferroan calcite. Dolomite appears unstained, while ferroan dolomite is a pale blue to light scarlet. A selection of 18 thin sections was stained from 8 different locations within the study area.

Together, the staining tests and CL studies (Section 4.3.2) provided information on both Fe and Mn content, and thus enable interpretation of the oxidative or reductive nature of the environment of cement development.

4.4 Carbonate cements within the facies

Within the study area, seven of the twelve facies identified were found to contain diagenetic cements, based on outcrop and thin-section analyses, with these occurring almost entirely within facies derived from Ototara Limestone and Otekaike Limestone (refer to Section 3.2 for detailed facies descriptions). The cements are described below in relation to each facies. Results are summarised in Table 4.2 (Section 4.4.9).

4.4.1 Bryozoan Grainstone (F2) cements

The Bryozoan Grainstone (F2) facies is located exclusively around the palaeohigh in the east of the basin, and its diagenetic features are generally uniform throughout.

Thin isopachous calcite rims around the outside of, and sometimes within, bioclasts are commonly seen perpendicular to clast surfaces and oriented towards intragranular void space. This space is occasionally filled with an equant drusy spar mosaic commonly associated with echinoderm fragments (Fig. 4.3A), although some void space is often left unfilled (Fig. 4.3F). Within some bioclasts, an equant spar equicrystalline mosaic may form, often within foraminiferal tests or bryozoan zooecal voids. These spaces sometimes contain isopachous calcite growths that form within the void space of geopetal-textured calcite mud (Fig. 4.3E).

Syntaxial overgrowths on echinoderm plate and spine fragments are common throughout, with these crystals appearing as clear calcite with little indication of a dusty or inclusion-rich texture (Fig. 4.3C). Rare dolomite cements are occasionally present (identified at Landon Creek section). The Bryozoan Grainstone facies is locally heavily cemented in outcrop, particularly below karst surfaces in the eastern region, although cement fabrics at these horizons are not any different from those found elsewhere within this facies.

As the Bryozoan Grainstone facies is often heavily cemented around unconformity surfaces, it was an important formation to target for CL analysis, and analyses were accordingly performed on samples from Gees Point, Landon Creek, Old Rifle Butts, and Roy Farm. Most of the bioclasts at these locations exhibited a bright response; although samples from Roy Farm tended to be predominantly dull, with only some parts of the bioclast presenting a bright-luminescent response. Blocky spar cements in these samples were almost entirely non-luminescent, but often had a brightly luminescing rim (Fig.

4.4B), or occasionally a bright response on spar cement in the centre of intragranular porespace.

Alizarin Red staining of the spar and isopachous cements produced a predominantly pink colour, indicating that these cements are calcitic and Fe-poor (Evamy, 1963; Dickson, 1965). These results suggest that the cements in this facies are Fe- and Mn-depleted. The bright CL response seen on the rims of spar cements may, however, indicate increased Mn^{2+} during the final stage of spar development, with little Fe^{2+} present to quench it.

Carbonate mud or occasionally isopachous intraclast cements observed in bioclast cavities tended to show a dull-luminescent response, with some larger fibrous cements displaying non-luminescence. Alizarin Red staining tended towards a pink (and therefore calcitic) colour, although at Landon Creek one sample stained a pale blue within the carbonate mud matrix, suggesting some Fe present within the detrital muds.

4.4.2 Rhodolith Rudstone (F3) cements

The cement textures observed in the Rhodolith Rudstone facies were very similar to those described for the Bryozoan Grainstone facies. Equant spar drusy mosaics and isopachous rinds of calcite were common (Fig. 4.3B), filling the voids between the clasts, and forming up to 50% of facies composition. Blocky calcite spar was observed between some algae and within bioclasts, commonly abutting onto carbonate muds. Geopetal textures of carbonate mud have their remaining void space filled with isopachous calcite within bioclast voids (Fig. 4.3E). Clear-textured syntaxial overgrowths on echinoid fragments are common (Fig. 4.3E).

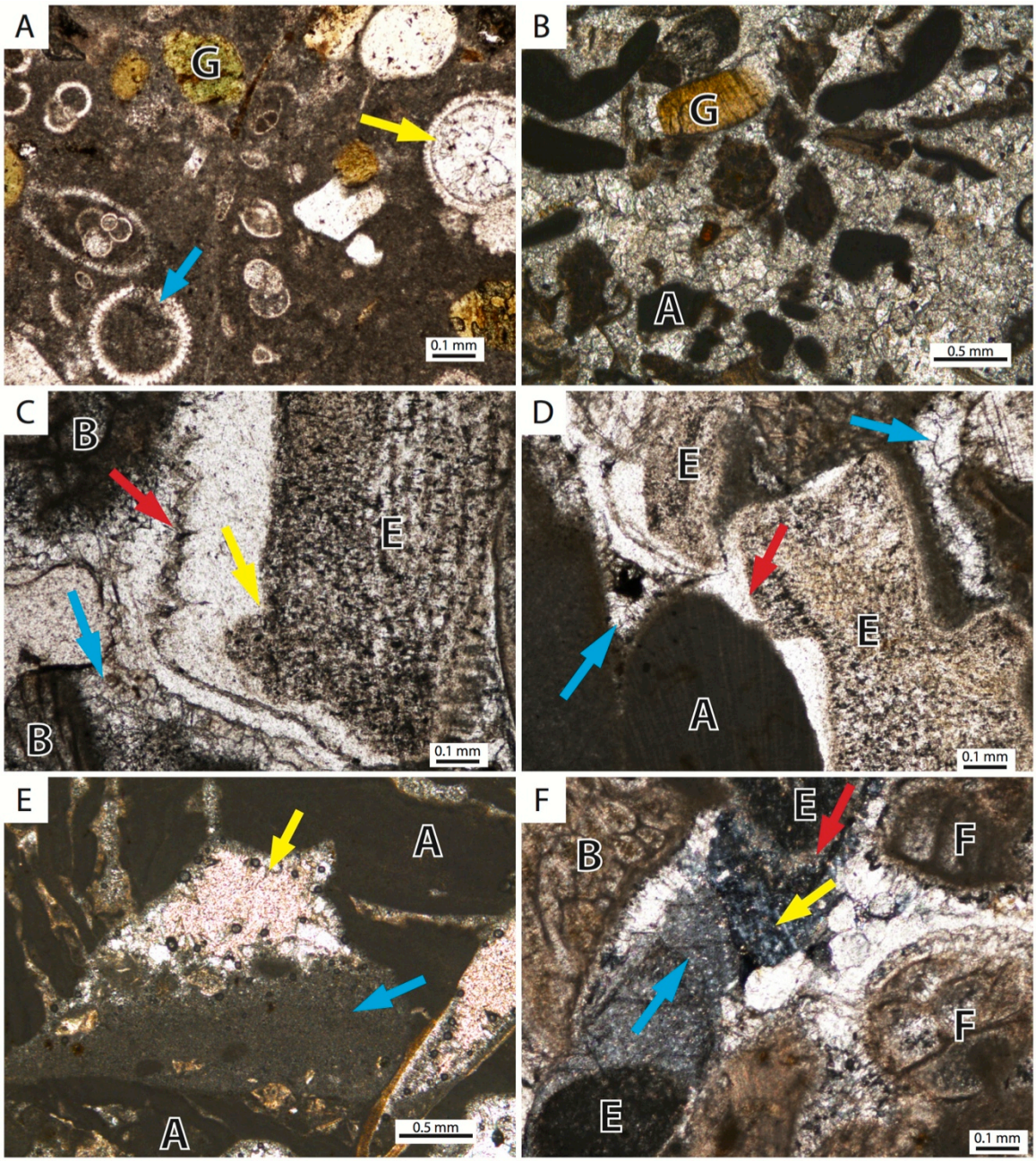

Figure 4.3. Photomicrographs of cement textures in the study area. Abbreviations are (A) Algae, (B) Bryozoan, (E) Echinoderm, (F) Foraminifera, (G) Glauconite. A: Massive Glauconitic Packstone (F6) at Campbells Bay. Foraminifera tests filled by calcite spar (yellow arrow) and carbonate mud (blue arrow). B: Bryozoan Grainstone (F2) at Roy Farm. Calcite spar mosaic, with crystal size increasing away from bioclasts. C, D: Syntaxial overgrowths on echinoderm fragments in Bryozoan Grainstone at Gees Point. Overgrowth edge and blocky cement infill (red arrow). Infill of equant calcite spar (blue arrow). Dissolution rim on echinoderm fragment (yellow arrow). E: Rhodolith Rudstone (F3) at Old Rifle Butts. Geopetal textures filled with blocky calcite spar (yellow arrow) and carbonate mud (blue arrow). F: Bryozoan Grainstone at Gees Point. Sparry cement overgrowths on echinoderm fragments (blue arrow). Small isopachous rims on bioclasts (red arrow). Empty void space (yellow arrow).

Alizarin Red staining produced an entirely pink response in the cements of the Rhodolith Rudstone facies, indicating these are entirely calcitic and do not contain any significant Fe concentrations (Evamy, 1963; Dickson, 1965). CL luminescence in this facies was similar to that of the Bryozoan Grainstone (F2) facies, where non-luminescence in cements was common (although bright responses occurred on the rims of spar and occasionally at the centre of cement-filled intraganular spaces). These two tests indicate that the cements consist of Fe-poor calcite, although the bright CL responses from cement rims and final-stage spar suggest enrichment in Mn^{2+} unhindered by the presence of any Fe^{2+} towards the end of spar precipitation.

4.4.3 Massive Glauconitic Packstone (F6) cements

The Massive Glauconitic Packstone (F6) facies is found throughout the basin and exhibits variable diagenetic features. It is heavily cemented in the eastern region where it is thinnest and located between two karstic unconformities. The cements are composed of equant calcite spar mosaics formed within granular interstices (Fig. 4.3B). Echinoderm fragments are very common and are almost entirely associated with syntaxial overgrowths.

In the northern and western regions of the study area this facies contains less cement. These cements are generally calcite spar within and occasionally around bioclasts, and also tend to be made up of syntaxial overgrowths on echinoderm plates and spines (Fig. 4.3D). Some bioclasts exhibit slim isopachous cement around their rims and occasionally within the tests of foraminifera. Where the facies is more heavily cemented in the west (McCulloch Farm, Anatini, Elephant Rocks), an equant spar drusy mosaic fills the intraclast interstices. In the far west of the study area (Trig Z), where carbonate muds dominate the matrix, this facies does not show any indication of calcite precipitation. As

described in Section 3.2.6, it contains aragonitic taxa in the western region, while in the east the fossil assemblage is entirely calcitic.

The Massive Glauconitic Packstone facies in the Otekaike Limestone at Gees Point and McCulloch Farm showed a dull- to non-luminescent CL response from the bioclasts, although some eroded rims of echinoderm plates were brighter. The carbonate mud matrix in this facies showed a spotted and dull response, inclusive of that within bioclast voids. Blocky spar cements were dull-luminescent and usually contained a thin bright rim, especially where this filled the remaining void space between converging cement growth. Borings into shell fragments sometimes contain blocky spar that had a bright luminescent CL response (Fig. 4.4F).

Alizarin Red staining of this facies showed a variation of Fe content within the cements across the study area. Samples from the western region (McCulloch Farm, Simpson Cliffs) produced a dark blue stain on the spar cement, indicating these cements are ferroan calcite (Evamy, 1963; Dickson, 1965). In the same locations, however, a pink stain formed on the small isopachous rims around bioclasts, indicating that these cements are comprised of Fe-poor calcite, and are likely to be from a different phase to that of the ferrocalcitic spar. Samples from the eastern region (e.g., Gees Point) produced an entirely pink staining on all cements (Fig. 4.5B), both spar and isopachous rinds, suggesting that in this area cement precipitation comprised calcite alone and was not subject to any Fe enrichment (Evamy, 1963; Dickson, 1965). The lack of Fe may have simply derived from the lack of a good Fe supply in the environment.

4.4.4 Bedded Packstone (F7) cements

One of the defining features of the Bedded Packstone (F7) facies is the differing cementation of alternating beds. The less-cemented beds (~ 1% cement) tend to have more

carbonate mud and intact macrofossil concentrations, whereas the more-cemented beds (~ 35% cement) are less muddy, were likely to be more porous at the time of deposition, and contain a more fragmented fossil assemblage. These cemented beds usually contain an equant calcite spar mosaic within the grain interstices, with isopachous cement rinds sometimes formed around the rims of, and inside, bioclasts. Echinoderms exhibit syntaxial overgrowths on all observed examples. Equant blocky calcite cements sometimes fill the void space left by adjoining geopetal textured carbonate mud within some bioclasts.

The bioclasts within the Bedded Packstone facies at both Ross Farm and Simpson Cliffs showed a dull- to non-luminescent CL response very similar to that of the Massive Glauconitic Packstone facies (see Section 4.4.3), and included dull- to bright-luminescence on the eroded rims of echinoid plates (Fig. 4.4H). The cements differed in that their responses were dull throughout, and contained no bright rims (as are common in other facies).

Alizarin Red staining of the Bedded Packstone facies produced a pale to dark blue stain on the spar cements throughout the western region (e.g., Simpson Cliffs, Waihao, and Ross Farm), although isopachous cement rinds on bioclasts developed as a pink stain. It seems, therefore, that isopachous cements are calcitic, while spar cements, including echinoid overgrowths, contain varying amounts of Fe and were precipitated as ferroan calcite (Evamy, 1963; Dickson, 1965).

4.4.5 Cross-bedded Glauconitic Packstone (F8) cements

The Cross-bedded Glauconitic Packstone (F8) facies is highly variable in its level of cementation, from completely uncemented to as high as 50% cement in one sample (Waihao). This variability appears to be linked to glauconite content and grain size, with those horizons rich in glauconite forming poorly or uncemented laminae or beds, while

those with low glauconite content are more cemented. These more-cemented horizons tend to contain a relatively high mud content. The difference between these two lithologies is likely to be the result of an absence of carbonate mud in the glauconitic beds created by winnowing. These variations occur across the whole facies, and are often found within individual cross-beds and cross-bed sets. Echinoderm syntaxial overgrowths are common, as elsewhere in the basin. Where cement has formed it occurs as equant spar, with either an isopachous rind or equicrystalline mosaic, forming both around and within bioclasts.

The CL response from the Cross-bedded Glauconitic Packstone facies at Waihao showed dull- to non-luminescent bioclasts, with eroded rims of echinoderm plates exhibiting a bright response (Fig. 4.4D). The carbonate mud in the matrix and within bioclasts exhibited a spotted and dull response. Blocky spar cements were dull-luminescent, usually with a thin bright response on the outer rim of sparry crystals, occurring especially in the void space between converging cements.

Staining of this facies with Alizarin Red produced a pink stain on isopachous cement rinds around bioclasts, while the spar produced a dark blue stain (Fig. 4.5A). This indicates an early calcite composition in the isopachous cements, with later spar cement being enriched in Fe as a ferroan calcite precipitate (Evamy, 1963; Dickson, 1965).

4.4.6 Volcanic (F10) facies cements

The Volcanic Tuff (F10a) facies contains localised diagenetic zeolite cements, principally observed in outcrop at Kakanui although also observed at Gees Point, Campbells Bay, Alma, and Old Rifle Butts. These cements occur between grains and in pore spaces (see also Murphy *et al*., 2008), comprise up to 20% of the facies in outcrop, and are composed of a light, coarse-grained, crystalline precipitate. Volcanic Pillow (F10b)

facies can also be found within heavily calcite-cemented matrices of Bryozoan Grainstone (F2) facies sediments, where they have not been weathered out.

At Gees Point, the Volcanic Tuff (F10a) facies displays vertical pipes of pink alteration in the tuffs themselves. These occur near the rim of the cone structure, below the onlapping carbonate facies, and are likely to be the product of hydrothermal alteration at, or following, emplacement of the tuffs when hydrothermal fluids were still present.

4.4.7 Reworked Volcaniclastic Packstone (F11) cements

The cementation levels of the Reworked Volcaniclastic Packstone facies are as low as 3%, and proportional to the carbonate content (i.e., the degree to which this facies approaches the host carbonate facies). Those with lower cementation tend to only contain calcite cements within those bioclasts that have been preserved within the facies, usually as a drusy spar mosaic. When a higher level of calcite precipitation has occurred (up to 15%), the interstices between grains (usually bioclasts) contain an equant spar drusy mosaic.

4.4.8 Uncemented facies

The facies not covered thus far in this Section - the Glauconitic Siltstone (F1), Impure Wackestone (F4), Calcareous Greensand (F5), Diatomaceous Micrite (F9), and Ash/Clay (F12) facies - contain no indications of cementation. These facies that show minimal or no diagenetic cementation are lower in calcareous content in favour of higher amounts of quartz, glauconite, or volcanic material than that found in the more cemented calcareous facies.

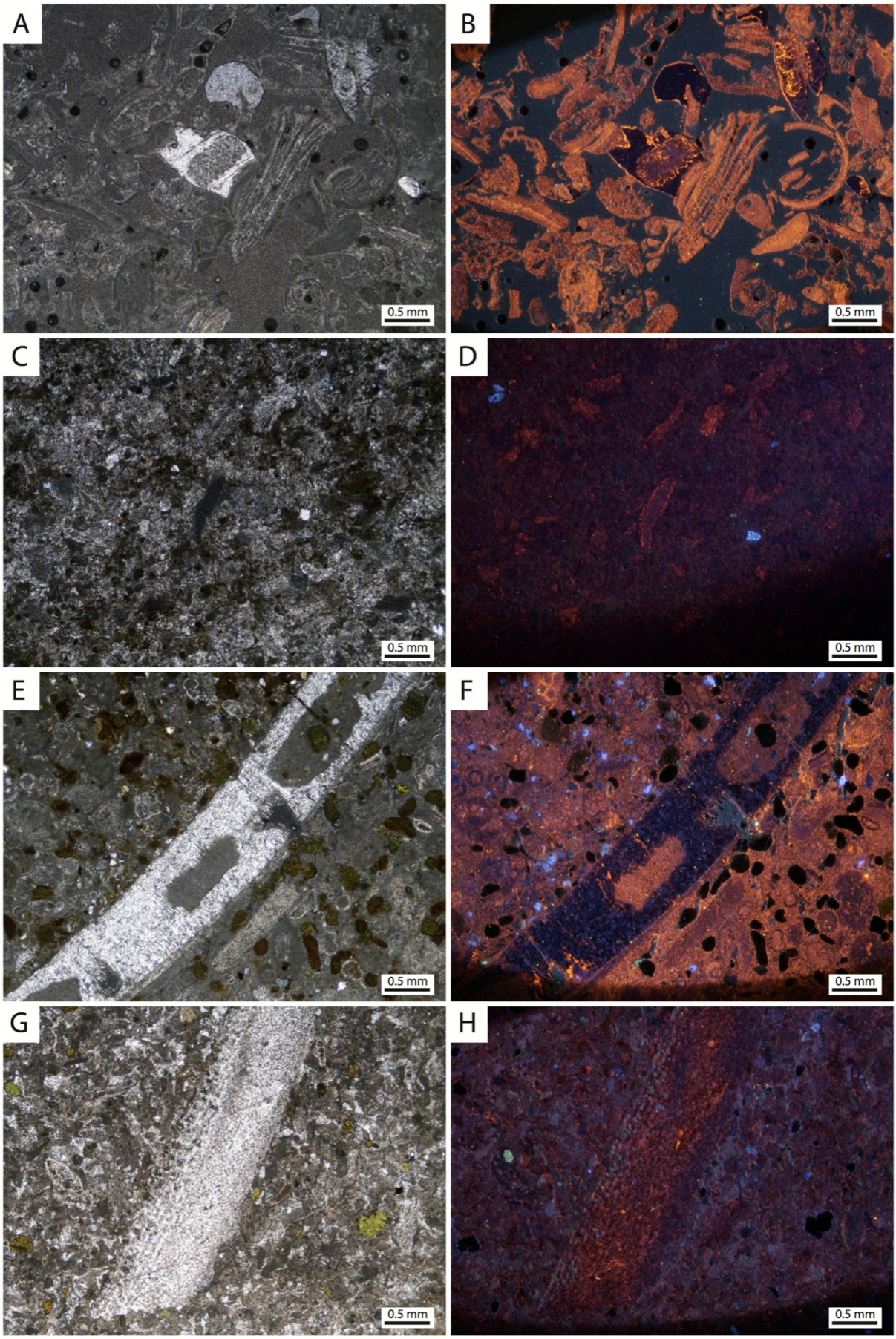
A
0.5 mm
B
0.5 mm
C
0.5 mm
D
0.5 mm
E
0.5 mm
F
0.5 mm
G
0.5 mm
H
0.5 mm

Figure 4.4. Selected cross-polarized light (CPL), plain-polarized (PPL), and carbonate cathodoluminescence (CL) images from four locations, representing three facies. A: CPL image of the Bryozoan Grainstone (F2) facies from Old Rifle Butts, showing a bryozoan- and echinoid-rich grainstone with overgrowth and intraclast cements. B: CL image of (A). Note the bright response from the bioclasts, as well as the non-luminescent syntaxial overgrowth on the central echinoid plate that is rimmed by a bright luminescence. C: Cross-bedded Glauconitic Packstone (F6) facies from Waihao in CPL. D: The CL image of (C) illustrating the generally dull-luminescent response from this facies, aside from the occasionally bright response from echinoid plate rims or minor isopachous cement. E: Massive Glauconitic Packstone (F6) from Gees Point in plain light. This location differs from the sample in (C) and (D) at Waihao as this location is more cemented at outcrop. F: The CL image derived from (E). The dull- to brightly-luminescent response from the micritic matrix is clear, and even appears to be separated by the macrofossil fragment in the centre. Note the boring at centre that has been filled with luminescent sparry cement. G: PPL image from the Bedded Packstone (F7) facies at Ross Farm, with a prominent echinoid plate fragment in the centre. H: The CL image of (G) showing the generally dull-luminescence of the matrix and most bioclast fragments, as well as the brighter rims and occasional internal grains of the echinoid fragment.

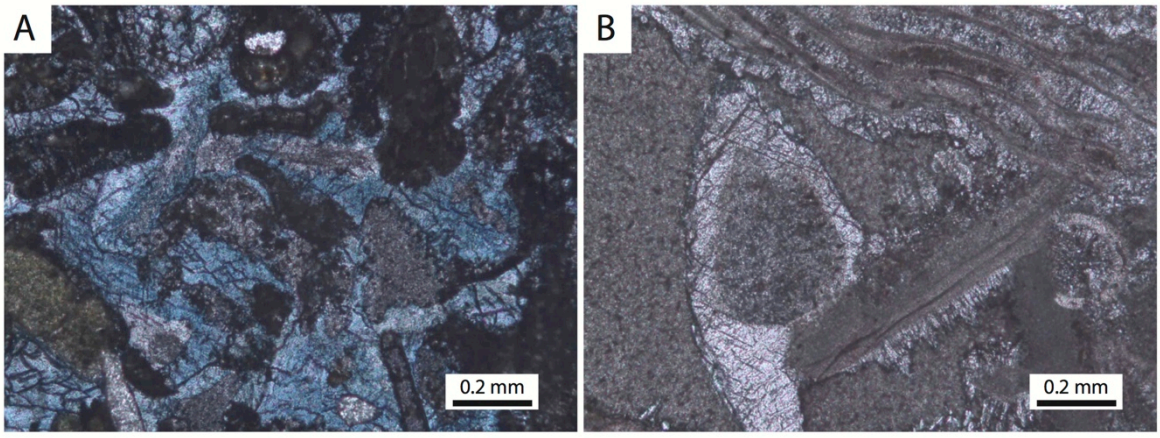

Figure 4.5. Photomicrographs of Alizarin Red stained thin sections showing the two different results obtained within the cements. A: Cross-bedded Glauconitic Packstone (F8) facies from Waihao, showing dark blue stained blocky calcite spar cement. B: Massive Glauconitic Packstone (F6) facies from Gees Point, showing echinoderm plate syntaxial overgrowth and isopachous cements with pink staining.

4.4.9 Summary of facies' diagenetic cement properties

The data presented above for the various facies studied are summarised in Table 4.2 which includes, for each facies, cement types, CL responses, and Alizarin Red staining colours. Fig. 4.6 shows a cartoon-style illustration of the main cement types observed within the study area.

Table 4.2 Summary of facies' cement properties.

Facies	Cement type	CL response	Staining
F1: Glauconitic Siltstone	None	n/a	n/a
F2: Bryozoan Grainstone	Calcite spar as echinoderm syntaxial overgrowths; isopachous rims on bioclasts; rare dolomite rhombs	Non-luminescent response on most cement; bright response on spar rims and youngest void fill	All pink
F3: Rhodolith Rudstone	Calcite spar and isopachous rinds	Non-luminescent response on most cement; bright response on spar rims and youngest void fill	All pink
F4: Impure Wackestone	None	n/a	n/a
F5: Calcareous Greensand	None	n/a	n/a
F6: Massive Glauconitic Packstone	Isopachous rims on bioclasts; calcite spar as syntaxial overgrowths and void fill	Dull response from cements; bright response on spar rims; mottled carbonate mud	Dark blue spar and pink isopachous rims (west); all pink in the east
F7: Bedded Packstone	Isopachous rims on bioclasts; calcite spar as syntaxial overgrowths and void fill	Dull throughout	Pink isopachous rinds; pale to dark blue stain on spar
F8: Cross-bedded Glauconitic Packstone	Isopachous rinds on bioclasts; calcite spar usually as syntaxial overgrowths	Dull response throughout, except bright response from echinoid rims and outer spar rinds.	Dark blue spar, pink isopachous rims

Facies	Cement type	CL response	Staining
F9: Diatomaceous Micrite	None	n/a	n/a
F10: Volcanics	Zeolite and calcite spar; hydrothermal?	Untested	Untested
F11: Reworked Volcaniclastic Packstone	Calcite spar	Untested	Untested
F12: Ash/Clay	None	n/a	n/a

4.5 Bioclast alteration

The principal bioclast alteration fabric observed within the facies of the study area involves dissolution of original mineralogy. This is commonly seen as dissolution of high-Mg calcite on echinoderm plate fragments throughout the study area. These bioclasts commonly show dissolved and eroded rims, often cemented with syntaxial overgrowths (Figs. 4.3C, 4.3D and 4.3F). CL imaging of these fragments produced a bright response on these erosive rims relative to a duller response from the original bioclast itself (see Section 4.4), suggesting a higher Mn^{2+} content relative to Fe^{2+} at the dissolved edge of the bioclast, and indicating likely alteration of the original mineralogy during dissolution of the echinoderm fragments.

In the eastern region, no aragonitic fossils are preserved within any of the facies present, although neomorphisation of originally aragonitic shell fragments is rarely observed. In the far western region, however, significant numbers of aragonitic molluscs have been preserved in outcrop with little indication of replacement or dissolution. These are found within facies that are more carbonate-mud-rich (at Trig Z) and consequently less cemented than those further east. This suggests that if any aragonitic species were present elsewhere in the study area, they have been dissolved and are no longer preserved in the rock record.

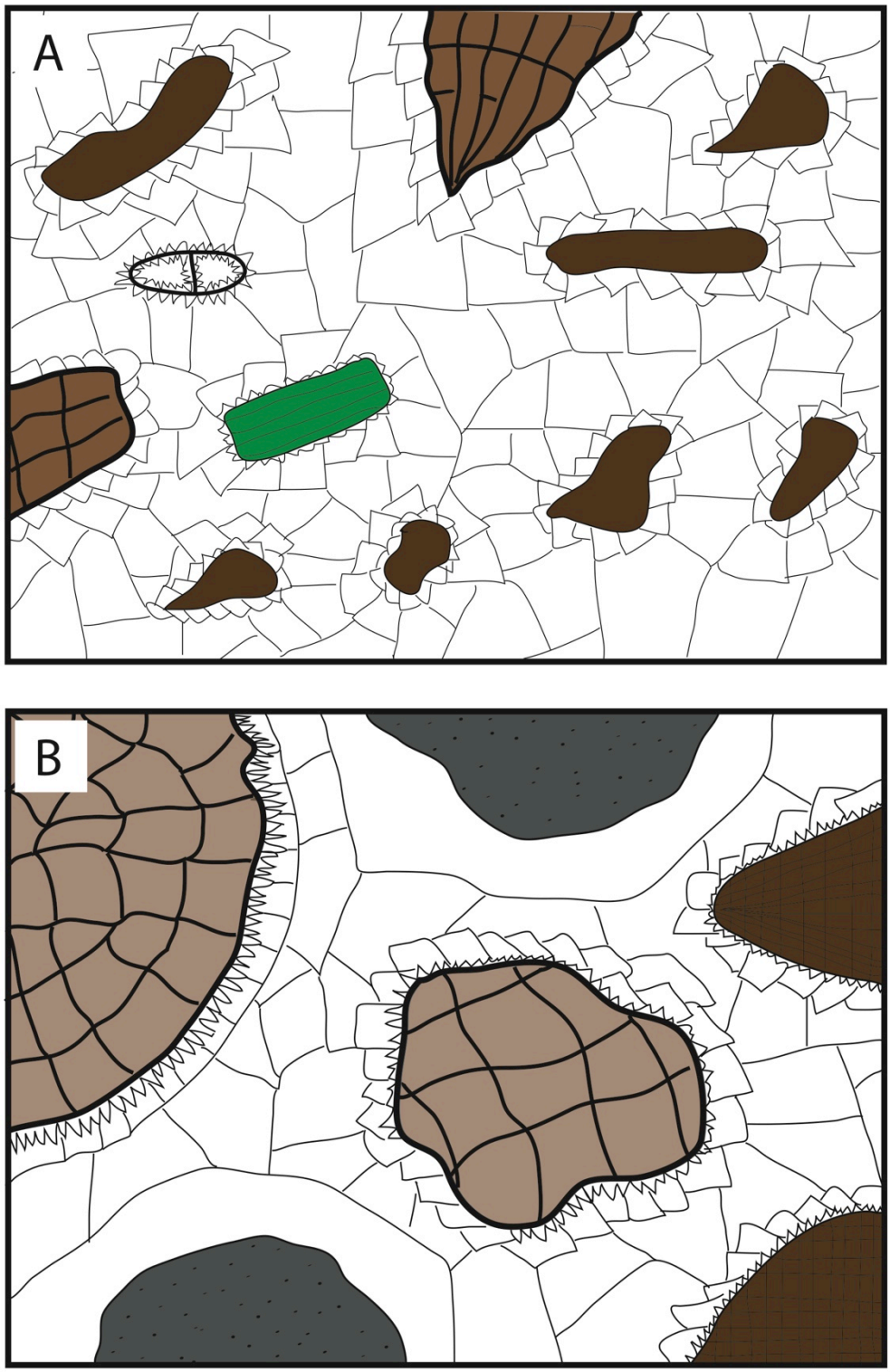

Figure 4.6. Illustration showing the main cement facbrics encountered in the study area and summarised in Table 4.2. A: Principally blocky calcite spar cements around bioclasts, showing increasing crystal size away from clasts. Isopachous cement formed within foram test void space. B: Bioclasts with isopachous cements forming at their rim, with calcite spar filling in the void space between grains. Echinoid fragments (grey) are bounded by single syntaxial cement crystals around each fragment. Spar crystals become larger as the distance increases between grains.

4.6 Porosity and permeability

Porosity and pore connectivity were estimated (Section 4.3.1) for a selection of nine samples from two locations, Gees Point and Ross Farm. At Gees Point, only the Calcareous Greensand (F5) facies was tested with coloured resin to estimate maximum porosity, due to the highly lithified nature and therefore very low porosity of the limestones facies present there (making coloured-resin impregnation impossible). The single sample from the more-cemented lower horizon of the Massive Glauconitic Packstone (F6) facies was highly lithified, and gave a porosity of only 3% with very little interconnectivity between pores. The three samples taken from the upper horizon of Calcareous Greensand (F5) facies (within the Gee Greensand) gave a generally higher porosity of 5 – 20%, with minor to moderate connectivity. In the sample with the lowest porosity, the pore spaces were mainly located within planktic foram tests, and permeability was minimal.

The five Ross Farm samples were taken from the Impure Wackestone (F4), Calcareous Greensand (F5), and the Massive Glauconitic Packstone (F6) facies. The Impure Wackestone sample had a very low porosity (1%), with most of the space taken up with micritic mud and providing no connectivity. The Calcareous Greensand sample showed a porosity of 12%, with some connectivity. Pore spaces tended to be between glauconite grains. A stratigraphically higher sample from this facies, below the Massive Glauconitic Packstone, had a porosity of 20% with well-dispersed pores between glauconite grains and good connectivity. The two samples from the Massive Glauconitic Packstone facies were above and below the local unconformity near the base of this facies found at Ross Farm (see Section 2.2.3.7), with the more cemented sample below this horizon showing a porosity of 10%, and the more friable one above a slightly higher 15%. Pore connectivity was moderate, with pores well dispersed in both of these samples.

There were no indications of squashed pores or deformation of the matrix in samples from any facies. Nor were there any signs of pressure dissolution. It can therefore be assumed that any increase or loss of permeability and porosity was the result of component dissolution or cement precipitation, and not physical compaction. Table 4.3 presents estimates of original pore space derived from comparison between observed porosity and the amount of cements in the matrix. This indicates that in the samples tested there was little change in porosity as a result of diagenetic cementation, however this precludes the samples with high cement volumes, which likely saw significant reduction in original porosity from calcite precipitation.

Table 4.3. Summary of porosity data for selected facies used in this analysiss. Observed present porosity is combined with petrographic data on cement found in the matrix to provide an estimate of the original pore space.

Facies	Original pore space	Diagenetically filled matrix	Present porosity
Impure Wackestone (F4) (Ross Farm)	1%	0%	1%
Calcareous Greensand (F5) (Ross Farm)	12 – 20%	0%	12 – 20%
Massive Glauconitic Packstone (F6) (Ross Farm)	14 – 18%	3 – 5%	10 – 15%
Calcareous Greensand (F5) (Gees Point)	9 – 22%	2 – 4%	5 – 20%
Massive Glauconitic Packstone (F6) (Gees Point)	13%	10%	3%

4.7 Diagenetic history of the Waitaki study area

4.7.1 Environments of calcite cement precipitation

The limestones of the Waitaki region contain spatial and lithological variations in the degree of their diagenetic properties, from poorly-cemented wackestones in the west, to heavily cemented grainstones and rudstones in the east. Calcite cements in the study area are most common within grainstones and packstones, especially those with low carbonate mud contents as occur in the more eastern parts of the basin towards the palaeohigh. This is probably for two inter-related reasons, as follows.

Firstly, those sediments located shallower and closer to the palaeohigh would have been subjected to higher energy environments that not only removed muds or prevented their deposition, but also allowed for a higher fluid flux through the substrate and thus an increased exposure to dissolved calcium carbonate present in pore waters. With increased exposure to calcium-carbonate-saturated seawater, the potential for calcite cement precipitation would have increased in these horizons. Simultaneously, there would have been increasing dissolution of the more soluble high-Mg calcite, aragonitic grains and bioclasts. These higher energy regions would thus also have been where aragonite dissolution was at its highest level. Aragonite preservation is therefore lacking in these shallower, mud-poor facies (see Section 4.7.3). Furthermore, dissolution of aragonite would have increased the dissolved calcium carbonate in the pore fluids, allowing further precipitation of more stable low-Mg calcite cements within the shallower facies.

Secondly, those facies with lower energy levels (typical of the western region), and containing higher carbonate mud contents, would have had a lower flux of pore fluids due to their relatively low pore space and permeability (caused by their smaller grain sizes and the tighter matrices formed during deposition). This would have resulted in less exposure

to dissolved calcium carbonate and therefore a lower concentration, or even complete absence, of calcite cement precipitation, as observed in outcrop (see Section 4.4).

4.7.1.1 Grainstone and rudstone facies

The earliest calcareous facies deposited in the study area are the Ototara Limestone's eastern Bryozoan Grainstone (F2) and Rhodolith Rudstone (F3) facies, and the western Impure Wackestone (F4) facies. Of these three facies, only the eastern two contain apparent diagenetic cements. Both of these facies contain small isopachous rinds that have formed predominantly around bioclasts, with some calcite spar developing within intragranular void space (Fig. 4.6a and b). They are devoid of any aragonitic taxa, and are entirely calcitic. Alizarin Red staining in these facies indicated an absence of Fe, while CL responses suggested that there is also no significant Mn^{2+} present.

The most common of these two eastern facies, the Bryozoan Grainstone, contains some degree of cementation wherever it occurs, although it becomes heavily cemented in its uppermost region (the top ~ 2 m) below the karst unconformity surface at the top of Ototara Limestone. Likewise, the Rhodolith Rudstone, which occurs either at or near this unconformity, is also heavily cemented (see Section 2.2.4.2). Here the cements consist of equant spar drusy mosaic fabric and isopachous rinds, fabrics that could equally well be the result of sea-floor, meteoric, or shallow-burial diagenesis, and are thus not a useful indicator of diagenetic environment.

The depositional environment of the Bryozoan Grainstone facies is one of a winnowed shoal of sand-sized clasts (see Section 3.2.2). In such an environment any original aragonitic taxa were likely to have been lost to early taphonomy and then later to dissolution in the more stable sediment pile, encouraged by the increased fluid flux resulting from its shallow and moderate- to high-energy environment (see Section 4.7.4 for

further discussion). This increased fluid flux would have been enhanced by tidal flows during the lowering of sea level, pumping pore fluids through the sediment (Nelson and James, 2000), and would be particularly prevalent at horizons near the top of these facies that developed on the sea-floor during any sea-level fall.

The dissolution component of aragonite removal was likely to have provided some of the dissolved carbonate required for limited calcite cement precipitation from seawater - although this evidently resulted in only limited isopachous cements and syntaxial overgrowth spar throughout much of the Bryozoan Grainstone facies, with most intragranular void space remaining empty.

The low Fe and Mn contents of the cements in these facies suggest they formed either on the sea floor or in a meteoric environment (Tucker and Wright, 1990), although it is more likely the early cements developed initially on the sea floor. As sea level lowered near the top of these facies, however, deposition would have slowed and then ceased, resulting in increased fluid flow through the same sediment horizon on the sea floor. This may have served to concentrate the cements at this horizon on the sea floor during sea-level fall, rather than operating on a continuously depositing column with sea-floor sediments being continuously buried by new material. This may have resulted in these horizons being completely cemented prior to subaerial exposure.

This process can be seen in modern hardgrounds that tend to exhibit a degree of surficial cementation that grades down into unlithified carbonate (Tucker and Wright, 1990; Wilbur and Neumann, 1993; Scholle and Ulmer-Scholle, 2003). Carbonate sand bodies can also produce a marine cemented subsurface, independent of mobile sand bodies forming in high-energy environments just above it (Keene and Harris, 1995; Nelson and James, 2000). Nelson and James (2000) suggest that marine cement precipitation actually occurs preferentially on temperate carbonate platforms during periods of lower sea level,

as higher temperatures at shallower depths increase carbonate saturation, while at the same time sedimentation rates are lower.

When these horizons at the top of the Bryozoan Grainstone and Rhodolith Rudstone facies were subaerially exposed, the carbonates were likely to have been subjected to some degree of meteoric diagenesis, further enhancing the relatively cemented nature of this part of the facies relative to the older, less-cemented sections further down the sediment column. The very existence of the karst morphology itself indicates that there was certainly meteoric dissolution during this event. It is likely that an increase in dissolved calcium carbonate in the meteoric waters percolating through the sediment would have led to calcite cement precipitation. It is possible, however, that this precipitation could also have occurred in the sea-floor or burial environments.

The dissolved calcium carbonate would have allowed for limited calcite spar precipitation, and may have been responsible for the precipitation of the spar mosaics found at this horizon, although not all intragranular space was filled as a result. Any cements that did form from meteoric fluids probably developed no higher than the phreatic zone - as there are no diagnostic meniscus cements indicative of the vadose zone at these cemented karst horizons.

Where this calcite spar has filled void space within these facies, the cements more proximal to the grains are Fe- and Mn-poor, and can be attributed to either sea-floor or meteoric diagenesis. The spar that is most distal to the grains (i.e. precipitated last within this space), however, showed a bright CL response suggesting an increase in Mn^{2+} relative to Fe^{2+} (supported by staining which indicated low Fe throughout). This, together with the thin, bright-CL responses commonly found on the rims of non-luminescent cements, indicates these late-stage cements were likely to have been produced through a change to reducing conditions, with subsequent enrichment of Mn^{2+} (Nelson *et al*., 1988a; Tucker

and Wright, 1990). A limited burial diagenesis could therefore have occurred, although it is unlikely that these facies underwent any significant burial, as there is a distinct lack of textural evidence for deep burial (such as stylolitic textures, significant burial cements filling all void space, or compaction fabrics). This is further supported by a lack of dull luminescence developed around the bright rim that would be expected under increasing burial temperatures and isotopically light pore waters (Walkden and Berry, 1984; Nelson *et al*., 1988a).

4.7.1.2 Packstone facies

The three packstone facies - the Massive Glauconitic Packstone (F6), Bedded Packstone (F7), and Cross-bedded Glauconitic Packstone (F8) facies - occur predominantly in the western and northern regions, although the Massive Glauconitic Packstone facies can be found in small exposures in the eastern region also (see Section 3.2).

These three facies all contain the same main calcite cement fabrics, comprising isopachous rims around bioclasts (all of which are Fe- and Mn-poor), significant spar made up primarily of echinoderm syntaxial overgrowths, and with some spar mosaics filling intragranular pore space (Fig. 4.6a and b).

The interparticle sparry cements elicited a commonly dull CL response but tended to stain blue, suggesting an increased Fe and Mn content relative to the isopachous rinds. In the eastern region, however, the spar of the Massive Glauconitic Packstone facies is entirely Fe-poor. In both the Massive Glauconitic Packstone and Cross-bedded Packstone facies, the outer rims of these spar cements are commonly high in Mn^{2+} relative to Fe^{2+}, while these rims are absent in the Bedded Packstone facies.

Where these three facies are muddier, particularly in the far west of the study area (where they tend locally towards wackestones) (see Section 3.2), the occurrence of calcite cements diminishes. Horizons within these facies that are glauconite-rich tend to also have minimal calcite cements.

As with the grainstone and rudstone facies (see Section 4.7.1.1), the earliest phase of cement precipitation within the packstone facies was likely to have involved isopachous rims developed around bioclasts, precipitating as Fe- and Mn-poor calcite across the entire study area, most likely in the sea-floor environment during deposition. This diagenetic phase would have been limited by the level of calcium carbonate saturation in the seawater, as well as lower energy levels and porosity found in the western region which reduced fluid flow through the sediment column within these more fine-grained facies.

The calcite spar within the packstone facies differs from the isopachous cements in the western region as it is enriched in both Fe and Mn (with Mn^{2+} being in sufficient quantity not to have its CL response completely quenched by Fe^{2+} present in the calcite). This may indicate this spar cement phase formed in a reducing environment as often occurs during burial diagenesis (see Section 4.2.5).

The western and northern regions contain relatively thick successions of these packstone facies that could have caused shallow burial as sedimentation continued, burying the sediment column beneath them. The fact that this Fe and Mn enrichment is not seen in the thinner eastern region packstone facies suggests that burial diagenesis may well have been responsible for the western and northern calcite spar phase. The Fe-poor calcite spar developed in the Massive Glauconitic Packstone facies in the eastern region may, however, have developed in the meteoric environment during the subsequent sea-level fall recorded by the second karst on top of Otekaike Limestone, of which the Massive Glauconitic Packstone facies is a component in that location (see Section 2.2.4.6). This

process would have been the same as occurred during subaerial exposure of the Bryozoan Grainstone and Rhodolith Rudstone facies (see Section 4.7.1.1).

4.7.1.3 Volcanic facies

Horizons of the Reworked Volcaniclastic Packstone (F11) facies are commonly cemented with calcite, probably as a result of two factors.

Firstly, sedimentation rates would have been very low in the eastern region immediately following the termination of volcanic activity, until carbonate production rates returned to normal. This would have allowed a longer period of exposure of these horizons to calcium carbonate in pore fluids derived from prolonged exposure to seawater during low sedimentation rates.

Secondly, levels of calcium carbonate in solution may well have been increased in these locations due to higher local water temperatures surrounding the recently erupted tuff cones. Evidence for sustained geothermal activity in the tuffs at the perimeters of these cones can be observed at Gees Point and Kakanui (see Sections 3.2.10 and 4.4.6), implying that seawater temperatures immediately proximal to these cones would have been increased by the expulsion of geothermal fluids. This would have caused higher than normal levels of calcite cement precipitation due to increased calcium carbonate saturation in the water column. This could explain the sometimes-heavy calcite cement precipitation observed in this facies. It could also explain the sometimes heavily cemented nature of the Bryozoan Grainstone (F2) facies found between individual pillows in the Pillow (F10b) facies at Cape Wanbrow (see Section 2.2.4.1), where the cooling lava lobes would have facilitated increased calcite precipitation within the porous grainstone (as heated seawater was pumped through it).

4.7.1.4 Uncemented facies

The uncemented facies in the study area tend to exhibit either higher levels of carbonate mud (e.g., Impure Wackestone facies), or contain a significant non-calcareous component (e.g., Calcareous Greensand facies). Facies containing more carbonate mud necessarily have a low porosity and permeability as a result of their smaller grainsize, especially in comparison with the grainstones. This inhibits pore fluid movement and penetration into the sediments, reducing contact with, and flux of, calcium carbonate in solution. The deeper marine environments within which these finer-grained facies deposited were low-energy environments, reducing the amount of fluid flow through the sediment relative to the higher-energy facies in the eastern region.

In contrast, facies containing a significant non-calcareous component tend to be coarser-grained than the deeper muddier facies, but with higher proportions of phosphate and glauconite which can act as chemical inhibitors to calcite precipitation (Berner, 1975; Walter, 1986). Therefore, while porosity and permeability in these facies could have sustained pore-fluid circulation, the grains themselves could have inhibited the kinetics of calcite cement precipitation.

4.7.2 Zeolite cements

Zeolite cements in the study area are associated exclusively with the Volcanic Tuff (F10a) facies. These cements are usually the diagenetic product of ash falls, and are implicated in the alteration of these to clays (Hay, 1966; Ratterman and Surdam, 1981; Pablo-Galan and Chavez-Garcia, 1996). They are derived from the hydration and reaction of pore fluids with volcanic glass, which results in precipitation of zeolites from solution (Surdam and Sheppard, 1978). Salinity plays an important role in this process, so the presence of the tuffs in seawater would have had a significant influence on their

precipitation, such that the process was likely to have occurred on the sea floor after deposition, when saline pore fluids were able to penetrate this facies.

4.7.3 Bioclasts

The cool-water carbonate realm is noted for its more destructive diagenetic nature and its often low diagenetic potential (see Section 4.2), as apparently supported here by bioclasts from the study area.

The dissolution of aragonite and high-Mg calcite is common in this setting, as indicated by the absence of aragonitic taxa in high-energy facies in the eastern region, as well as by the almost universal degradation observed on the edges of high-Mg calcite echinoderm plates prior to calcite overgrowth and cement precipitation. This suggests that the pore waters and/or seawater being flushed through these sediments, following deposition, were undersaturated with respect to aragonite, while being either undersaturated or saturated with respect to calcite, leading to the partial dissolution of the less-stable magnesium-rich calcite and complete dissolution or replacement of aragonite.

Timing of aragonite dissolution in cool-water carbonates is difficult to quantify as it can occur at any stage in a formation's diagenetic history (Caron and Nelson, 2009). It is likely to have occurred on the sea floor not long after deposition, however, as those areas that lack aragonitic taxa also tend to have higher-energy environments and were thus subjected to increased fluid flow and contact with seawater. These two factors would have enhanced both the physical and chemical destruction of aragonite, while the calcitic taxa were less likely to be completely removed under the same conditions.

4.7.4 Aragonite vs. calcite in bioclasts

While the cool-water carbonate realm has traditionally been assumed to be devoid of aragonite, recent work has shown that it may have contained significantly more aragonite and high-Mg calcite than is currently found in the rock record, but is removed as a result of significant dissolution following deposition (Nelson and James, 2000; James *et al*., 2005) (see Section 4.2.2). It appears that this was also the case within the study area, as aragonitic fossils have been preserved in the western region, while only very rare neomorphosed aragonitic shell fragments have been found (in thin section) in the central and more eastern locales.

In the western region (Trig Z and Otekaike outcrops), a number of aragonitic biota are preserved within the Massive Glauconitic Packstone (F6) and Bedded Packstone (F7) facies. There these facies have more carbonate mud within their matrices than their equivalents elsewhere in the basin, and even occur as wackestones in some horizons. This would have lowered porosity and permeability in this part of the basin relative to the more eastern regions, limiting the fluid flux through the sediment following deposition, and thus limiting the potential for aragonite dissolution in these more mud-rich limestones.

In the eastern region, aragonite preservation has not occurred, although rare replacement of original aragonite mineralogy, and thus at least some initial occurrences of aragonitic biota, are apparent. It is therefore likely that aragonitic taxa were present at the time of deposition throughout the basin, and it is only a difference in preservation across the study area that has led to this disparity between east and west.

As suggested by James *et al*. (2005), aragonite dissolution within the cool-water carbonate realm occurs rapidly on the sea floor prior to exposure to the meteoric or burial environments. In those facies that contain diagenetic cements, calcite precipitation has not

significantly occurred on the sea floor, where most cements (by volume) are the result of meteoric or burial diagenesis (see Section 4.7.1).

It is thought to be unusual within cool-water carbonates for sea-floor diagenesis to form the majority of diagenetic cements, as a low calcium carbonate saturation level of seawater and a scarcity of aragonite often inhibit their occurrence (Nelson *et al*., 1988a; Nicolaides and Wallace, 1997; James *et al*., 2011). Their presence here, although limited, could have been enhanced by early sea-floor dissolution of aragonite and high-Mg calcite occurring in the higher-energy facies of the central and eastern parts of the basin, either through the presence of aragonite-undersaturated fluids or microbial action. This would have raised the level of calcium carbonate saturation in the pore fluids, increasing the potential for calcite cement precipitation in these facies.

All of these factors illustrate a relationship between increasing grain size and lower aragonite preservation potential within the study area, where a higher carbonate mud content, as seen in the western outcrops, appears to be related to the increased likelihood of aragonite preservation observed in those locations. This would have led to a preservation bias within the less micritic facies, preserving the more stable low-Mg calcite biota, while removing or replacing the less-stable high-Mg calcite and aragonite biota. This in turn would lead to an underestimation of the original aragonitic biota in cool-water carbonates that is being increasingly recognised in the rock record (e.g., Nelson and James, 2000; Caron *et al*., 2005; James *et al*., 2005).

4.8 Summary

Seven facies within the Waitaki Basin contain significant diagenetic cements. They are primarily located in the eastern half of the study area where grainstones and rudstones stratigraphically overly a volcanic palaeohigh, and in the west within three packstone facies.

Throughout the study area, calcite cement precipitation appears to have occurred initially on the sea floor soon after deposition, particularly in the eastern region. It produced Fe- and Mn-poor isopachous rinds around bioclast components, leaving intragranular pore-space empty. During sea-level fall, decreasing sedimentation rates and an increase in local temperature and energy, enhanced cement precipitation on the sea floor, resulting in development of submarine cemented hardgrounds in the eastern region prior to subaerial exposure. During lowstand, those surfaces were exposed to meteoric processes and underwent dissolution and karst development. Meteoric calcite spar cements were likely to have been precipitated during this time, probably from within the phreatic zone, filling some of the pore-space between grains.

While sea-floor diagenesis appears to be responsible for the initial stages of cement precipitation across the study area (with local meteoric cements produced in the eastern region), later-phase Fe- and Mn-rich sparry ferroan calcite cements were likely to have been precipitated within a reducing burial environment, particularly in the western region where thick sediment accumulations led to burial of older sediments. These ferroan calcite and calcite spar cements filled some, but seldom all, of the remaining pore-space and, together with a lack of diagnostic burial textures, indicate a limited and relatively shallow burial phase.

Facies with little or no calcite cement, found predominantly in the western and northern regions, either exhibit higher carbonate mud contents associated with lower

porosity, or comprise non-calcareous sedimentary grains such as glauconite that do not encourage calcite precipitation. These facies evidently experienced lower fluid flows and were thus not exposed to the same level of dissolved calcium carbonate as in the eastern grainstones.

Dissolution and replacement of originally aragonitic taxa occurred principally in the central and eastern regions of the study area, while aragonitic fossils retained their original mineralogy in the muddier facies within the western region. This suggests a relationship between increasing grain size and decreasing carbonate-mud content that leads to a decrease in aragonite preservation potential across the basin. The early degradation and dissolution of aragonitic taxa in the east may have provided a limited increase in dissolved calcium carbonate in seawater and led to enhanced diagenetic potential of early sea-floor calcite precipitation within the study area.

CHAPTER 5 – SEQUENCE STRATIGRAPHY

5. Introduction

Lithostratigraphic, biostratigraphic and facies data gathered within the Waitaki area during this study enable exploration of water depth histories of the region. This involves combining these datasets in a sequence stratigraphic model, in order to provide a better understanding of relative sea-level change and unconformity development. By recognising sequences, bounded by sequence boundaries, it becomes possible to ascertain the magnitude of water depth changes within each sequence package and to correlate these across the region. Furthermore, by recognising systems tracts, local influences on facies development can be removed - such as palaeotopography or submarine currents, which might otherwise mask the magnitude of eustatic sea-level fluctuations. The recognition of sequences can thus serve to highlight sea-level changes that may have gone unnoticed or simply have been relegated to being understood as local variations.

This approach makes it possible to address questions surrounding the period of maximum submergence within the study area, which can then be related to larger-scale events taking place around New Zealand in the mid-Cenozoic. Furthermore, it allows interpretations regarding the presence, location, and influence of any landmasses on the sedimentary regime within the region, and how these may have changed through this period.

These issues are of principal importance in developing a sequence stratigraphic model, and this chapter therefore focuses primarily on the period between the decline of clastic input into the Waitaki region during the Eocene, through to the renewal of siliciclastic supply initiated during the Early Miocene.

5.1 Methodology and Terminology

This section will cover the sequence stratigraphic theory used in this chapter, as well as the terminology used in presenting the model. Assumptions that were made during interpretation of the data are also included here.

5.1.1 Sequence stratigraphic definitions

Sequence stratigraphy is a method of interpreting stratigraphic data using packages of sequences (Boggs, 2001). Sequences are stratigraphic units composed of relatively conformable successions of strata that are bounded at their top and base by unconformities or related conformities (Mitchum *et al*., 1977). These bounding unconformities are termed sequence boundaries. Sequences as used in this chapter represent one cycle of deposition accumulated during one cycle of relative sea level rise and fall. A sequence therefore contains a complete depositional system, within which are found all the facies that record this cycle of sea level change.

These sequences, and the depositional systems they contain, can be further divided into systems tracts, a term used frequently in this chapter to interpret the changes in sea level observed within each sequence. Four types are recognised within this study: lowstand, transgressive, highstand, and falling stage. A lowstand systems tract (LST) is usually found above a sequence boundary, and form during a time of sea-level lows. They may not be represented by any deposited sediment, as the period of lowstand may have been erosional or non-depositional. Transgressive systems tracts (TST) are found between the LST and the highstand systems tract (HST), and form during sea-level rise. The boundary between this systems tract and that of the HST is usually gradational and can be open to interpretation. A highstand systems tract represents the later period of sea-level rise and the point of highest sea-level within a sequence, and as such are usually found

near the top of a sequence, often below a sequence boundary. A falling stage systems tract (FSST) records the period following the highstand, where sea-level is falling and approaching lowstand. Sediments may or may not be deposited and preserved during this period, but if they are this systems tract is found beneath a sequence boundary and above the HST.

5.1.2 Terminology of sea level and water depth changes

The sequence stratigraphic focus of this chapter is naturally strongly oriented toward interpretation and discussion of changes in water depth and sea level. It is therefore important to define the various terms that are used here, and their basic controls.

The most basic description used here is water depth, which is used to refer to the level of the sea as an absolute datum between the sea surface and the seafloor. These changes are controlled by three main factors, including global sea level, tectonic changes, and also sediment accumulations. The observation of water depth changes makes no inference which of these causes is responsible, and it may very well be all three.

Relative sea-level change refers to changes through time of sea level relative to a previous state, as was the case for water depth, but is controlled only by global sea level and local tectonics. This term does not distinguish which of these causes is in play.

Lastly, the term eustasy, or eustatic sea-level change, is controlled solely by global sea-level changes. This term is interpretive in nature, and cannot necessarily be determined by sequence stratigraphic interpretations in isolation from other data.

5.1.3 Sequence stratigraphic theory and assumptions in temperate carbonates

The sequence stratigraphic method was developed around siliciclastic systems, where sediment is produced outside the shelf and enters the basin based on drainage and

the proximity of landmasses. This can lead to complications when attempting to apply this same methodology to the carbonate system (Caron, 2004). Carbonate systems produce sediment *in situ*, rather than having it transported from elsewhere, and rather than having the supply decreased during sea-level rise, they tend to increase due to the vertical and lateral expansion of accommodation space where sediment can be produced (Schlager, 1999; Caron, 2004). Further, the temperate carbonate environment lacks the barriers seen in tropical settings, and thus sediment produced within the cool-water setting is often shed off the higher energy producing sites and deposited across the basin relative to storm or current energy and sediment grain size (James, *et al*., 1994; Caron, 2004).

Within a sequence stratigraphic framework these characteristics lead to a few assumptions used in this study when developing the sequence stratigraphic model. Firstly, in carbonate systems the period of maximum sediment production and accumulation is during the later TST and the subsequent HST. During periods of lowstand, accommodation space is reduced and energy levels are increased, making sediment production and accumulation difficult. In this latter instance, sediment is transported to deeper parts of the basin. During a highstand, any landmasses are at their most distal to the basin centre, and therefore contribute the lowest amount of terrigenous sediment during this part of the sequence.

5.2 Sequence stratigraphy

The sequence stratigraphic model presented here comprises three primary depositional sequences, separated by two major sequence boundaries, and including one minor boundary. These sequences have been developed primarily from facies data (Chapter 3), supported by lithostratigraphy and biostratigraphy (Chapter 2), and earlier

work (Chapter 1). Sequences are presented according to their sequence number, with systems tracts described accordingly and inclusive of their associated facies.

Each sequence contains a deepening-upward transgressive systems tract (TST) that culminates in a highstand systems tract (HST), followed by a falling stage system tract (FSST) which is rarely preserved in the rock record.

Regional variations within each sequence are based on the three geographically separate areas within the study area, referred to here as the eastern, western, and northern regions (described earlier in Section 2.2, Fig 2.1, and highlighted again in Fig. 5.2). Figure 5.2 includes three section lines (from which Figs. 5.2 – 5.7 are derived). These were chosen in order to give maximum expression to the relationships between the varying facies across the study area, and to highlight the relationships between the three main regions.

5.2.1 Sequence Boundary 1 (SB1)

The sequence stratigraphic model begins with Sequence Boundary 1 (SB1), marked by the unconformable contact between the Matakea Group and the overlying Onekakara Group (see Section 1.2.5). This boundary marks the onset of regional transgression in New Zealand that began in the Late Cretaceous, and is often termed the 'Cretaceous Peneplain' (Gage, 1957; Carter, 1988; Field and Browne, 1986; Landis *et al*., 2008). This surface can often be amalgamated with the transgressive unconformity presented in Section 1.2.5.2, sometimes termed the 'Waipounamu Erosion Surface' (Fig. 5.1) (Landis *et al*., 2008).

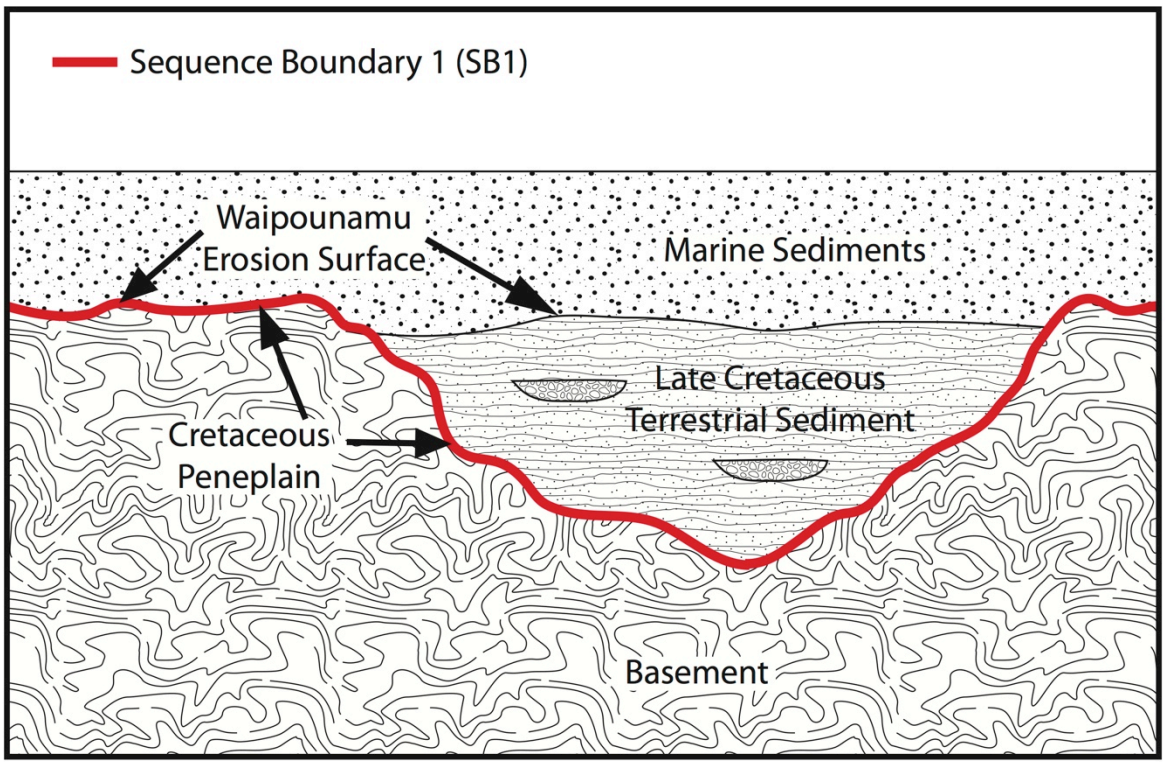

Figure 5.1. Illustration of Sequence Boundary 1 and its relationship to basement rock and the overlying sediments. The Waipounamu Erosion Surface and the Cretaceous Peneplain are shown to illustrate how they interact. Figure adapted from Landis *et al*. (2008).

This surface can be identified in the field as an unconformity with weakly indurated Late Cretaceous sands, gravel, and coal measures overlying deformed Palaeozoic-Mesozoic basement rocks (Fig. 5.1) (LeMasurier and Landis, 1996; Landis *et al*., 2008). These Late Cretaceous sediments underlie the transgressive marine sequence, and often form discontinuous senses in pockets over the basin (Landis *et al*., 2008). Where these Late Cretaceous sediments are absent, marine sediments of the Onekakara Group rest directly on basement (Forsyth, 2001), with this contact representative of SB1 (Fig. 5.1).

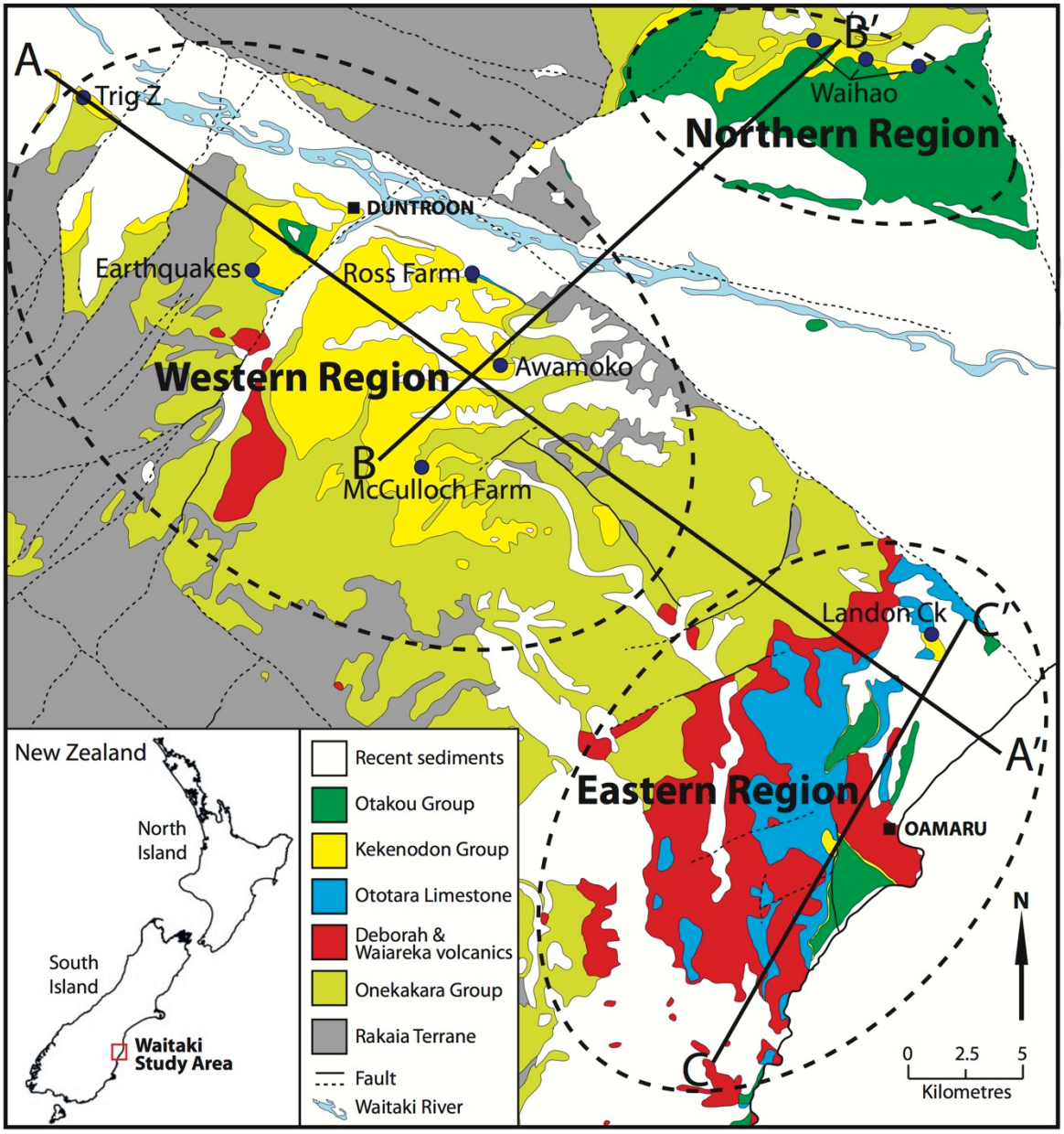

Figure 5.2. Location map of the study area in the Waitaki Region, showing outcrop locations mentioned in this chapter, as well as the relative locations of the three regions referred to throughout. The three section lines shown are used for cross sections presented here. Geological map adapted from Forsyth (2001).

5.2.2 Sequence 1

Sequence 1 is defined as the base of the Onekakara Group, extending through to the top of the Alma Group (see Sections 1.2.5 and 1.2.6).

The lower three formations in the Onekakara Group - Taratu and Kauru Formations, and Tapui Glauconitic Sandstone - do not form part of the facies described in this study (Chapter 3), and their consideration here is based principally on earlier work (Chapter 1). These three formations serve solely to illustrate the early terrestrial to marine transgressional phase of this sequence, and although one unconformity is present within and between these formations, the continuous regional transgressive sequence remains relatively constant.

The facies included in Sequence 1 that follow on from the above three formations are the Glauconitic Siltstone (F1) (Raki Siltstone), Bryozoan Grainstone (F2), Rhodolith Rudstone (F3), Impure Wackestone (F4) (from Ototara Limestone), Diatomaceous Micrite (F9), Volcanic (F10), Reworked Volcaniclastic Packstone (F11), and the Ash/Clay (F12) facies (from Waiareka and Deborah Volcanics). All these facies are from the Alma Group except the Glauconitic Siltstone facies, which is part of the Onekakara Group.

5.2.2.1 Sequence 1 Transgressive Systems Tract

In Sequence 1, the Taratu Formation through to the Raki Siltstone represents a TST, developed between the Haumurian and Kaiatan Stages.

The Taratu and Kauru Formations comprise the non-calcareous, non-marine to marine succession deposited initially on fluvial channels and floodplains, and then reworked during the initial stages of marine transgression up to the beginning of the Eocene (see Sections 1.2.5.1 and 1.2.5.3).

At the onset of the Bortonian Stage, prior to the development of Tapui Glauconitic Sandstone, a wave-cut submarine unconformity developed (see Section 1.2.5.2). This surface is not defined as a sequence boundary in this study, however, as it represents a

ravinement surface developed during marine transgression, rather than a deviation from the regional transgressional pattern (Landis *et al*., 2008).

The Tapui Glauconitic Sandstone itself reflects continuing marine transgression, when the depositional environment moved from within the storm-wave base (SWB) to below it. The Tapui then grades stratigraphically upwards into the Kaiatan Stage Raki Siltstone, and thus into the first of the facies recognised from this study - the Glauconitic Siltstone (F1) from the western region (Fig. 5.2). This facies is the last of the dominantly non-calcareous sediments of this TST, deposited in a quiet outer-shelf setting under a decreasing influx of terrigenous sediment and reworked glauconite (see Section 3.2.1).

As carbonate input increased, Ototara Limestone began to develop in the Runangan through to Whaingaroan Stages, with the deposition of the Bryozoan Grainstone (F2) and Impure Wackestone (F4) facies in the eastern and western regions, respectively (see Sections 3.2.2 and 3.2.4) (Figs. 5.2 and 5.4). The onset of carbonate facies record the last phase of this TST as it reached its maximum depth within the outer-shelf to upper-slope environments in the western region, between the Runangan and early Whaingaroan Stages.

During this period (i.e., Runangan to early Whaingaroan Stages), facies of Ototara Limestone were significantly shallower in the east and were locally interbedded with numerous volcanic tuff cones and associated volcanic facies (e.g., Volcanic (F10) facies). Localised occurrences of bioturbated packstones that form a part of the Bryozoan Grainstone facies can be found beneath some of the volcanic cones in the east (e.g., at Kakanui).

These localised occurrences suggest a mid-shelf setting prevailed locally prior to development of volcanic cones in the area. The shallower carbonate environment created around these local edifices was the result of syn-depositional development with the volcanic facies during the later part of this TST, the structures of which served to provide a

submarine high for marine colonisation by carbonate organisms (see Section 1.2.6.1, and Chapter 6 for further discussion).

5.2.2.2 Sequence 1 Highstand Systems Tract

During the HST of Sequence 1, sea level remained at outer-shelf to upper-slope depths in the western region through to the mid Whaingaroan Stage, with continued deposition of Ototara Limestone.

The deeper-water, western-region Impure Wackestone (F4) facies grades laterally eastwards into the age-equivalent sediments of the eastern region, where the Runangan to mid-Whaingaroan Bryozoan Grainstone (F2) facies dominates the HST of Sequence 1 in that location (Fig. 5.2). This grainstone facies was deposited on an inner-shelf created by the upper Kaiatan through to the lower Whaingaroan Waiareka and Deborah Volcanics. The carbonate sediments were deposited on the flanks of these tuff cones, and inter-bedded with other facies associated with this activity, namely the Diatomaceous Micrite (F9) (from the Oamaru Diatomite), Volcanics (F10), Reworked Volcaniclastic Packstone (F11), and the Ash/Clay (F12) facies (from the Waiareka and Deborah Volcanics) (Fig. 5.7). These facies are mostly localised within and around this eastern volcanic palaeohigh (for further discussion see Chapter 6).

The Rhodolith Rudstone (F3) facies, formed in the photic zone but deposited locally around the volcanic high by high-energy events, further illustrates the shallow calcareous environment produced by this submarine relief (see Section 3.2.3). So while the Bryozoan Grainstone (F2) facies represents a relative shallowing from the earlier Glauconitic Siltstone (F1) facies, this can be attributed to the volcanically induced creation of the eastern palaeohigh. This is in contrast to the western correlative of the Bryozoan

Grainstone facies, the Impure Wackestone (F4) facies, which was unaffected by any local change in bathymetry and was deposited at outer-shelf to upper-slope depths.

During this HST no facies from Sequence 1 were identified in the northern region, although this may well be due to their not being currently exposed.

5.2.2.3 Sequence 1 Falling Stage Systems Tract

There are no facies in the eastern region which can be clearly attributed to a FSST from Sequence 1, because of the influence of the volcanic palaeohigh masking any eustatic sea-level change, coupled with the erosive effect of subsequent subaerial exposure of SB2 (see Section 5.2.3). Nor is there any clear preservation of a FSST within the western region.

In the western region of the study area, however, at the outcrops most proximal to the shallow eastern facies at McCulloch Farm and Awamoko Creek (Fig. 5.2), the older Glauconitic Siltstone (F1) facies forms the top of Sequence 1, without the presence of the younger Bryozoan Grainstone (F2) or Impure Wackestone (F4) facies (found in the eastern or western regions, respectively), suggesting that increased energy levels created by lowered sea level during this FSST may have developed a Regressive Surface of Erosion (RSE). This would have removed not only any record of a FSST, but also any earlier TST and HST facies that may have existed there (Fig. 5.4). This implies that this FSST had an erosional effect on the surficial sediment in the region, or may have acted as an out-of-basin transport mechanism for any material developed in this area during the later phase of Sequence 1.

5.2.3 Sequence Boundary 2 (SB2)

A karst morphology has developed at the top of the Alma Group in the eastern region, clearly indicating subaerial exposure in this area (see Section 2.2.4.3). This is here

defined as Sequence Boundary 2 (SB2), and represents a lowstand systems tract (LST) following Sequence 1.

The subaerial exposure in the eastern region clearly suggests a significant period of erosion extending towards the west (e.g., shallow karst at Ross Farm, Fig. 5.2, see Section 2.2.3.6). This eastern subaerial erosion surface is the lateral equivalent of the heavily burrowed firmground found in the western region (Fig. 5.2) on top of the Alma Group, as confirmed by biostratigraphic and lithostratigraphic relationships (see Chapter 2). It is likely that erosion may have occurred on this surface in the west during the FSST and LST. SB2 is thus the erosive upper contact above the Glauconitic Siltstone (F1), Bryozoan Grainstone (F2), Rhodolith Rudstone (F3), and Impure Wackestone (F4) facies throughout the study area, developed during an area-wide LST.

The sea-level fall between the HST of Sequence 1 and the LST of SB2 was of significant magnitude to take the low-energy, outer-shelf to upper-slope Impure Wackestone facies in the westernmost locations (e.g., Earthquakes; Fig. 5.2) to significantly shallower depths, between inner- to mid-shelf, where deposition ceased and erosion occurred (Fig. 5.2). This is indicated by the presence of the inner- to mid-shelf Calcareous Greensand (F5) facies that was emplaced above this surface during the subsequent TST (see Section 5.2.4.1). The magnitude of this regression is further illustrated by evidence for short-lived shallow subaerial exposure on top of the Impure Wackestone (F4) facies at Ross Farm (Fig. 5.2), in the western region (see Section 3.2.4). The Bryozoan Grainstone facies in the eastern region, which can be as deep as mid-shelf, was subaerially exposed everywhere it is found. The change in water depths seen in the western region, from outer-shelf/upper-slope suggests a relative sea level fall on the order of 100 – 150 m.

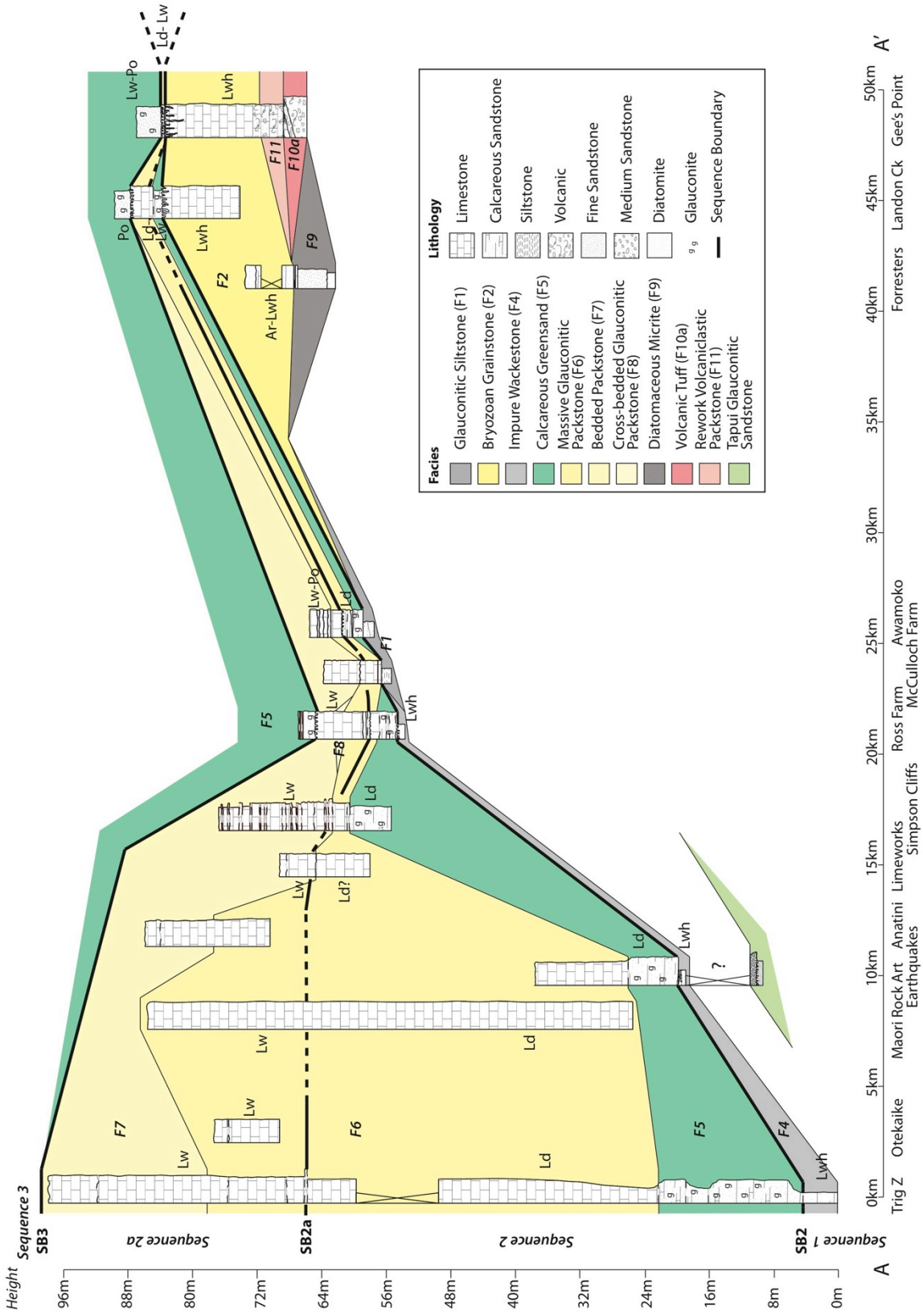

Figure 5.3. Section line through A-A' (Fig. 5.2), showing the sequence and sequence boundary correlations used in the sequence stratigraphic model. Approximate biostratigraphic ages are shown next to each column based on data presented in Chapter 2.

5.2.4 Sequence 2

Sequence 2 comprises two parts, named here as Sequence 2 and Sequence 2a, with an overall trend of transgression, highstand, and regression; and includes the Duntroonian to Waitakian Kokoamu Greensand and Otekaike Limestone. In at least three locations there is evidence for the presence of a small sea-level fall, indicated by the presence of a locally winnowed or erosive surface, occurring mid sequence. This surface is included here as a lower-order LST sequence boundary within the greater Sequence 2, and termed Sequence Boundary 2a (SB2a). The remainder of the TST, HST, and any FSST of Sequence 2 are then placed within the subsequent Sequence 2a, so named as it follows this lower-order LST at SB2a. Sequence Boundary SB2a and Sequence 2a are presented in Sections 5.2.5 and 5.2.6.

5.2.4.1 Sequence 2 Transgressive Systems Tract

Sequence 2 begins above SB2 in the Duntroonian Stage with the deposition of the glauconite-rich, inner- to mid-shelf Calcareous Greensand (F5) facies (see Section 3.2.5) (from the Kokoamu Greensand) which signals the onset of a TST across the study area. The base of this TST was likely diachronous, as accommodation developed gradually across the area, with the karsted surfaces on the eastern volcanic palaeohigh reaching sufficient depths for sediment accumulation only after deposition was well under way in the western region (Figs. 5.4 and 5.7). This implies that the palaeohigh, which had such an effect on the facies distribution in Sequence 1, resulting in inner- to mid-shelf facies in the east and outer-shelf/slope facies in the west, was still prominent (see Section 5.2.2).

In the western and northern regions, the Duntroonian Calcareous Greensand (F5) facies of Kokoamu Greensand indicates a gradual return from an inner- to mid-shelf environment upward through the facies (Figs. 5.3 and 5.5) (see Section 3.2.5). This TST

then continues into the mid- to outer-shelf Massive Glauconitic Packstone (F6) facies, which is predominantly part of Otekaike Limestone that developed from the very latest Duntroonian and into the early Waitakian in the west. This facies change indicates a decrease in energy, together with an increase in sedimentation rates associated with the development of carbonate supply (see Section 3.2.6). This same transition to the Massive Glauconitic Packstone (F6) facies occurred within the Lower- to mid-Duntroonian in the northern region (Figs. 5.5 and 5.6).

This same facies succession between the Calcareous Greensand and the Massive Glauconitic Packstone occurs in the eastern region, although there it is never deposited thicker than 1 m (at Landon Creek; Fig. 5.2), and is often only a thin veneer in coastal outcrops (e.g., Gees Point, Campbells Bay; Fig. 5.2).

5.2.4.2 Sequence 2 Highstand Systems Tract

The HST of Sequence 2 occurs near the base of the Massive Glauconitic Packstone (F6) facies just below SB2a, and was thus likely of mid-shelf depth (Fig. 5.3). It is unlikely this HST lasted for a significant period, as deposition of carbonate facies would be expected to have developed more extensively at this depth than is observed at outcrop, before the development of SB2a.

5.2.4.3 Sequence 2 Falling Stage Systems Tract.

There is no observed record of the FSST within Sequence 2, with any loose sediment deposited during this short sea-level excursion likely to have been eroded during the higher-energy conditions created by the LST of SB2a.

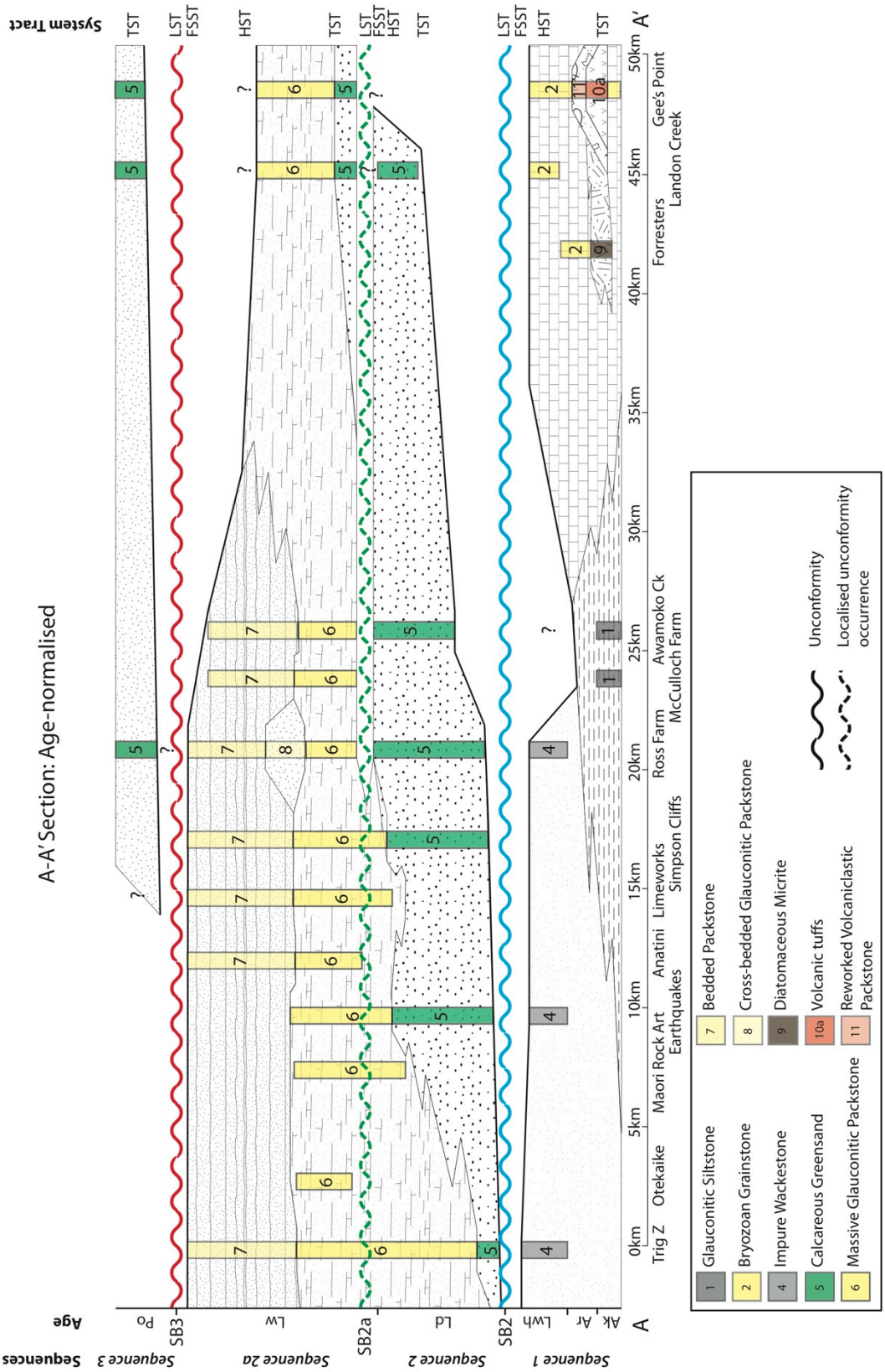

Figure 5.4. Section line through A-A' (Fig. 5.2) showing the facies within each sequence and the sequence boundaries. This section line has been age-normalised, where each facies is represented by the estimated or known period during which it was deposited, with blank periods for non-deposition.

5.2.5 Sequence Boundary 2a (SB2a)

Near the transition between the Calcareous Greensand (F5) facies and the Massive Glauconitic Packstone (F6) facies in the western region, there are a number of surfaces that suggest a minor LST occurred between the late Duntroonian and early Waitakian Stages. These surfaces comprise a fossiliferous rudstone bed (at Trig Z), as well as at least one small rubbly erosive firmground contact (at Ross Farm), and another likely erosive hiatus surface (at Awamoko Creek) (Fig. 5.2). (Some caution must be taken with these surfaces as the low resolution of their ages cannot confirm an exact correlation between them, although their occurrence at similar age and comparable facies intervals within the succession suggest some relationship).

The furthest-west horizon at Trig Z contains a highly fossiliferous bed of whole and broken molluscs and coral (see Section 2.2.3.8), suggesting a period of increased energy relative to the packstone and local wackestone of the Massive Glauconitic Packstone facies it is found within. This occurs similarly at Ross Farm, where a rubbly firmground lies above glauconite sandstones, and where the carbonate content has increased and begun to develop into lithified packstones (see Section 2.2.3.7). This erosive surface, again overlain by a thin layer of glauconite sandstone, suggests a temporary return to higher-energy conditions. Awamoko Creek also contains a rubbly surface overlain by a molluscan fossil lag, again indicating a return to higher-energy conditions relative to the facies beneath. These three surfaces occur around the Duntroonian-Waitakian boundary based on biostratigraphic data from FRED (see Section 2.3.3).

These surfaces suggest that there may have been a small-scale sea-level fall in the early Waitakian Stage that created winnowed beds in the far west, and small, erosive firmgrounds in the centre of the study area where deposition was halted as a result of increased energy levels. This interpretation is supported by an increase in benthic

foraminiferal species (relative to planktics) around the shelly fossil horizon at Trig Z (Fig. 5.2), indicating a slight lowering of sea level at this time. Ostracod species found at Trig Z (Ayress, 2006) further support an excursion to inner shelf, which has been suggested to coincide with this prominent fossil bed.

While these surfaces represent a sea-level fall, and therefore a LST, it is not as significant in either duration or magnitude as the two major unconformities that occurred in the upper Whaingaroan and upper Waitakian Stages (see Section 2.2). There are no signs of subaerial exposure or of any significant change in facies. Furthermore, in some locations the event does not produce a clear surface in outcrop, and often appeared conformable (although some previous authors have recorded similar condensed surfaces around this time interval; see Section 1.2.7.2.1). Although there is some lack of clarity, it is here named as Sequence Boundary 2a (SB2a) - a subset of Sequence 2 - as it is considered prominent enough to indicate an excursion from the general transgression that occurs over the entire span of Sequence 2, while not being of sufficient magnitude to have created an entirely new sequence.

In the eastern region, this LST is likely to have been condensed within the two significant LSTs of SB2 and SB3, where Sequence 2 occurs as a thin veneer rather than a distinct succession (Figs. 5.3 and 5.7). It is likely that if any sediment had been deposited during the previous TST and HST of Sequence 2, it was removed during this event.

In the northern region, the late Duntroonian to early Waitakian is a period of inner- to mid-shelf facies containing a number of basal scour contacts between cross-bed sets, likely providing a record of this period of lowstand (Figs. 5.5 and 5.6). It should be noted that the late Duntroonian Cross-bedded Glauconitic Packstone (F8) facies in the northern region represents a lower sea level than the Duntroonian Massive Glauconitic Packstone (F6) and the Bedded Packstone (F7) facies underlying it. This implies that the development

of this lowstand may have been recorded in the shallower facies in the north before becoming more apparent in the deeper facies in the western region (Fig. 5.6), and that this surface was diachronous.

At Ross Farm and Awamoko Creek (Fig. 5.2), SB2a has a thin veneer of Calcareous Greensand (F5) facies above it before rapidly grading into the Massive Glauconitic Packstone (F6) facies, further supporting the lower magnitude of the LST of SB2a, relative to that of SB2 and SB3.

Taking all the above into account, it is likely that the sea-level fall associated with this LST was of the order of only 15 – 20 m.

5.2.6 Sequence 2a

Sequence 2a continues the overall transgression begun in Sequence 2, returning rapidly to the mid-shelf Massive Glauconitic Packstone (F6) facies of Otekaike Limestone in the western region (see Section 3.2.6) (Figs. 5.3 and 5.4). In the eastern region, both the TST and HST of this sequence developed as a relatively thin sequence no more than 1 m thick, while sometimes being entirely absent. The northern region contains the moderate- to high-energy Cross-bedded Glauconitic Packstone facies throughout this sequence, with the presence of submarine currents probably overprinting the impacts of any eustatic sea level changes (Figs. 5.5 and 5.6).

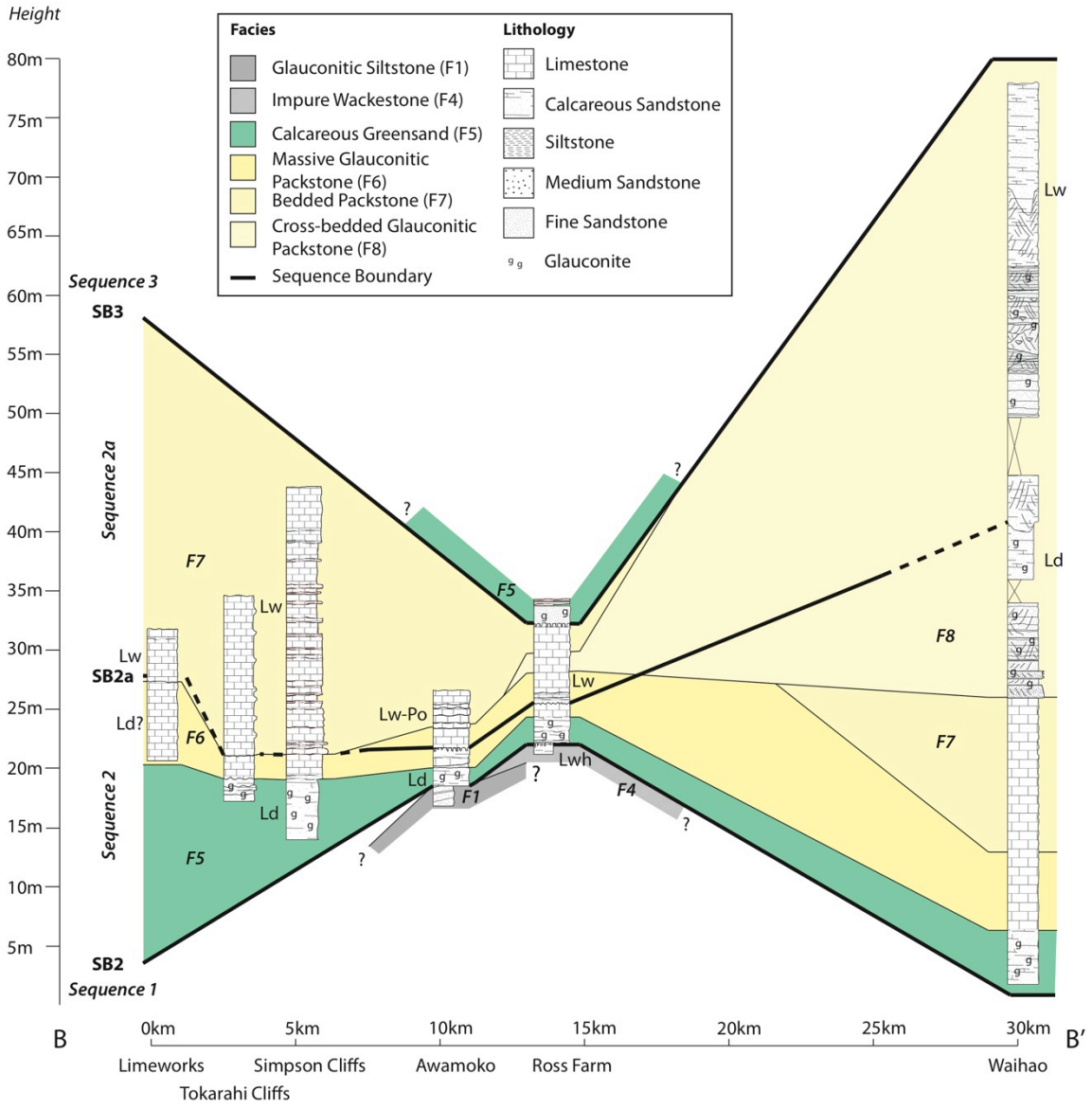

Figure 5.5. Section line through B-B' (Fig. 5.2), showing the facies and each sequence, as well as the sequence boundaries and their known or estimated location. Approximate biostratigraphic ages are shown based on data presented in Chapter 2.

5.2.6.1 Sequence 2a Transgressive Systems Tract

Following the LST of SB2a, the subsequent Sequence 2a TST is represented by the continued deposition of the mid- to outer-shelf Massive Glauconitic Packstone (F6) facies in the western and eastern regions. As with Sequence 2, the deposition of this facies was diachronous, as comparable sea levels gradually arrived across the varying bathymetry of

the study area. This is indicated by the variation in facies thickness observed between east and west, with metres' thickness in the west, while in the east it is no thicker than 0.5 m, and in some cases is absent entirely. While subsequent erosion during the LST of SB3 probably accounts for some reduction in thickness of this succession (see Section 5.2.**7**), the succession at Landon Creek (Fig 5.2), where Sequence 2a is thickest in the eastern region, may provide a good proxy for its original thickness. Thus the disparity observed in thickness during Sequence 2a between the eastern and western regions is likely to be the result of a shorter period favourable for deposition during this TST in the east than in the west.

In the northern region, at Waihao, the Cross-bedded Glauconitic Packstone (F8) facies (Fig. 5.5) represents an inner- to mid-shelf environment, with significantly increased energy from the facies beneath it. A decrease in glauconite content and a lessening of cross-bed activity upward through the facies suggests that it was gradually deepening, and is therefore a part of this TST. The change in energy regime has been attributed to the diminishing effect of the shoal found to the south (in the eastern region) as it is gradually eroded, thus allowing sporadic storm currents to sweep over it and deposit sediment to the north (Ward and Lewis, 1975).

5.2.6.2 Sequence 2a Highstand Systems Tract

The Sequence 2a HST can be placed in the mid-Waitakian at the onset of the Bedded Packstone (F7) facies of Otekaike Limestone in the western region. It is of mid- to outer-shelf depths, marked primarily by a decrease in glauconite content and an increase in carbonate and macrofossil preservation (Fig. 5.4). This suggests that sea level did not return to the depths that occurred during the Sequence 1 HST, where the western region contained outer-shelf to upper-slope facies significantly deeper than those of Sequences 2 and 2a.

This facies does, however, record a series of small water depth fluctuations during this HST, resulting in the development of its characteristic bedding (see Section 3.2.7) - although these events were very small, and do not alter the occurrence of this HST throughout this facies. It is also possible that these bedding features derived from storms or other events, however the lack of any high-energy sedimentological features suggests that this is unlikely.

In the northern region, this HST is marked by the inner- to mid-shelf, channelized, upper portion of the Cross-bedded Glauconitic Packstone (F8) facies, in the mid-Waitakian Stage (Fig. 5.6). The northern Waihao area (Fig. 5.2) was supplied with sediment from the palaeohigh in the eastern region, where the Massive Glauconitic Packstone (F6) is the deepest facies preserved from Sequence 2a, and may therefore be representative of either the TST or HST in this area. Any younger facies from this Sequence in the eastern region would have been removed during subsequent erosion induced by the unconformity at SB3 (see Section 5.2.7).

5.2.6.3 Sequence 2a Falling Stage Systems Tract

The Sequence 2a FSST is not apparent in any of the facies within the study area, and it is likely that if any facies were deposited during sea-level regression, they were later removed either by the development of a RSE, or by high-energy or subaerial environments developed during lowstand.

5.2.7 Sequence Boundary 3 (SB3)

Sequence Boundary 3 (SB3) is observed only in outcrop in the eastern region, and at all locations except Landon Creek (Fig. 5.2) it is either condensed to within centimetres of SB2, or is completely amalgamated with it (Fig. 5.7).

Like SB2, SB3 is also heavily karst or significantly eroded, and was therefore also the result of significant sea-level fall and subsequent subaerial exposure that followed the HST of Sequence 2a (see Section 2.2.4.6). This sequence boundary therefore represents a lowstand, and represents a sea-level fall of the order of 50 – 75 m.

5.2.8 Sequence 3

Sequence 3 contains the Calcareous Greensand (F5) facies from Gee Greensand overlying SB3, which then grades into the increasingly terrigenous mudstones of the Rifle Butts Formation (Fig. 5.7).

5.2.8.1 Sequence 3 Transgressive Systems Tract

The first sediments deposited following the LST of SB3 are the latest Waitakian to Otaian Calcareous Greensand (F5) facies of Gee Greensand that formed as a result of renewed transgression. The base of the Calcareous Greensand facies in the eastern region overlying SB3 contains abundant octocorals and *Melitodes* holdfasts that confirm the presence of a wavecut platform prior to development of this facies during transgression.

This glauconitic facies is thicker in the eastern region than during the TST of Sequence 2 in the same location, although this is more likely to be the result of increased preservation coupled with a lower bathymetric gradient across the study area following two periods of major subaerial erosion on the palaeohigh. Depths in the eastern region reached mid-shelf, although sedimentation rates always remained relatively low, as indicated by the extensive development of this glaucony facies.

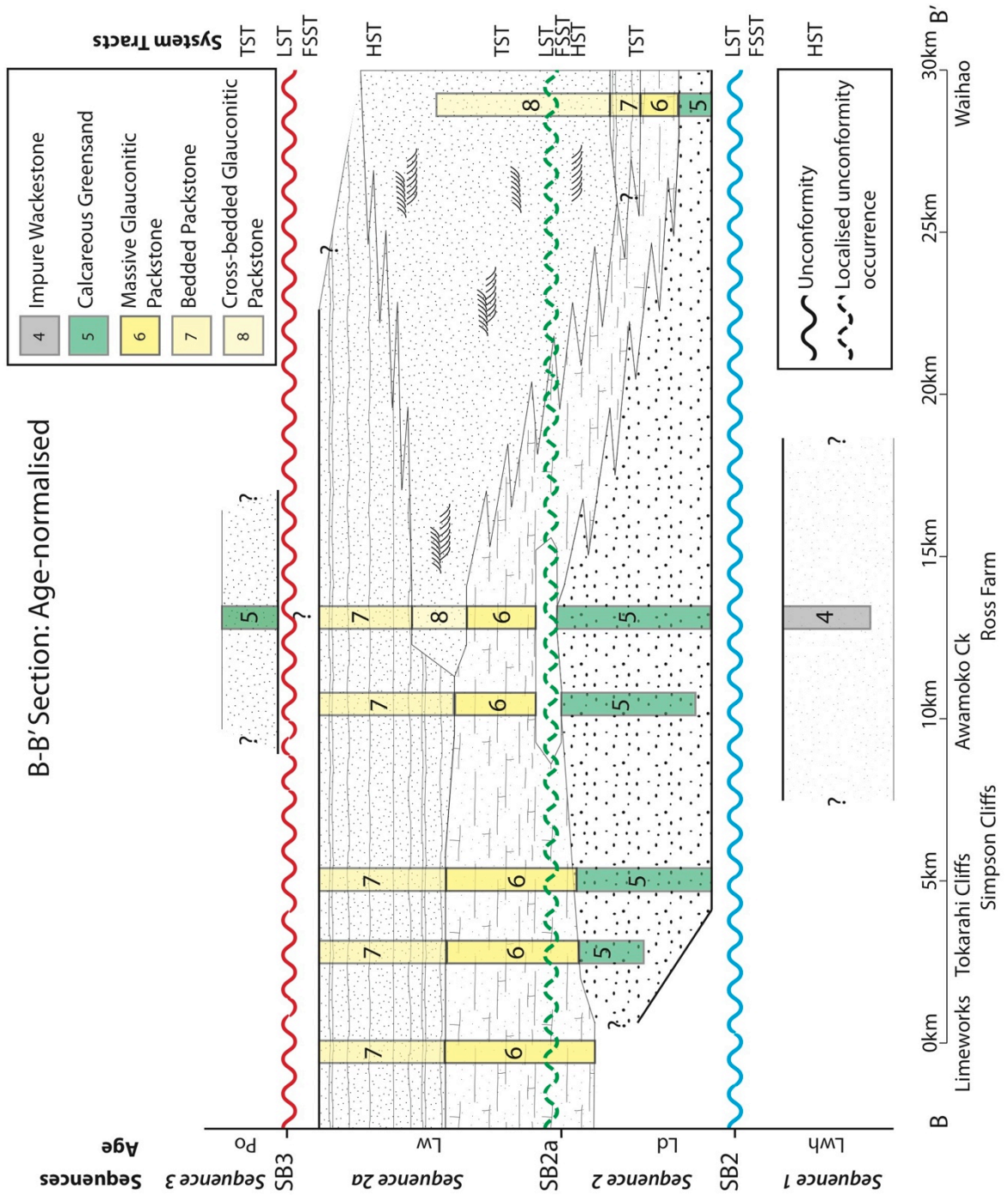

Figure 5.6. Section line through B-B' (Fig. 5.2), showing the sequences and their facies as well as the three sequence boundaries. This section has been age-normalised, where the thickness of each facies is determined by the period of time over which it was deposited.

5.2.8.2 Sequence 3 Highstand Systems Tract

While not forming a distinct facies or surface, the HST of Sequence 3 must be placed at the gradational boundary between the Calcareous Greensand (F5) facies of Gee Greensand and Rifle Butts Formation, located at the Otaian to Altonian Stage boundary. This transition witnessed a significant increase in terrigenous sediment supply and a significant change in depositional regime (see Section 1.2.8.2). Maximum depth at this point probably did not exceed a mid-shelf setting, as implied by the presence of the Calcareous Greensand facies through the Otaian Stage, although it may have reached outer-shelf depths in the western region (no outcrops of this transition in the west were exposed during this study so this cannot be confirmed).

5.2.8.3 Sequence 3 Falling Stage Systems Tract

The gradational change in sediment content from the Calcareous Greensand (F5) facies to the siliciclastic Rifle Butts Formation, at the onset of the Altonian Stage, indicates a change from regional transgression to regression, caused by the development of the modern plate boundary (see Section 1.2.8.2). Sedimentation rates increased with this surge in siliciclastic supply, preserving this record of the FSST within this sequence.

5.2.9 Sequence Boundary 4 (SB4)

A significant and abrupt unconformity forms the top of Sequence 3 and is overlain by much younger, non-calcareous Pleistocene to Recent sediments. This makes up Sequence Boundary 4 and marks the top of the sequence stratigraphic model developed during this study. It represents the continuous regression and uplift that continued onwards from the onset of the FSST of Sequence 3 (see Section 5.2.8.3) as the regional landmass of New Zealand began to emerge from the sea and was subjected to increased levels of subaerial erosion.

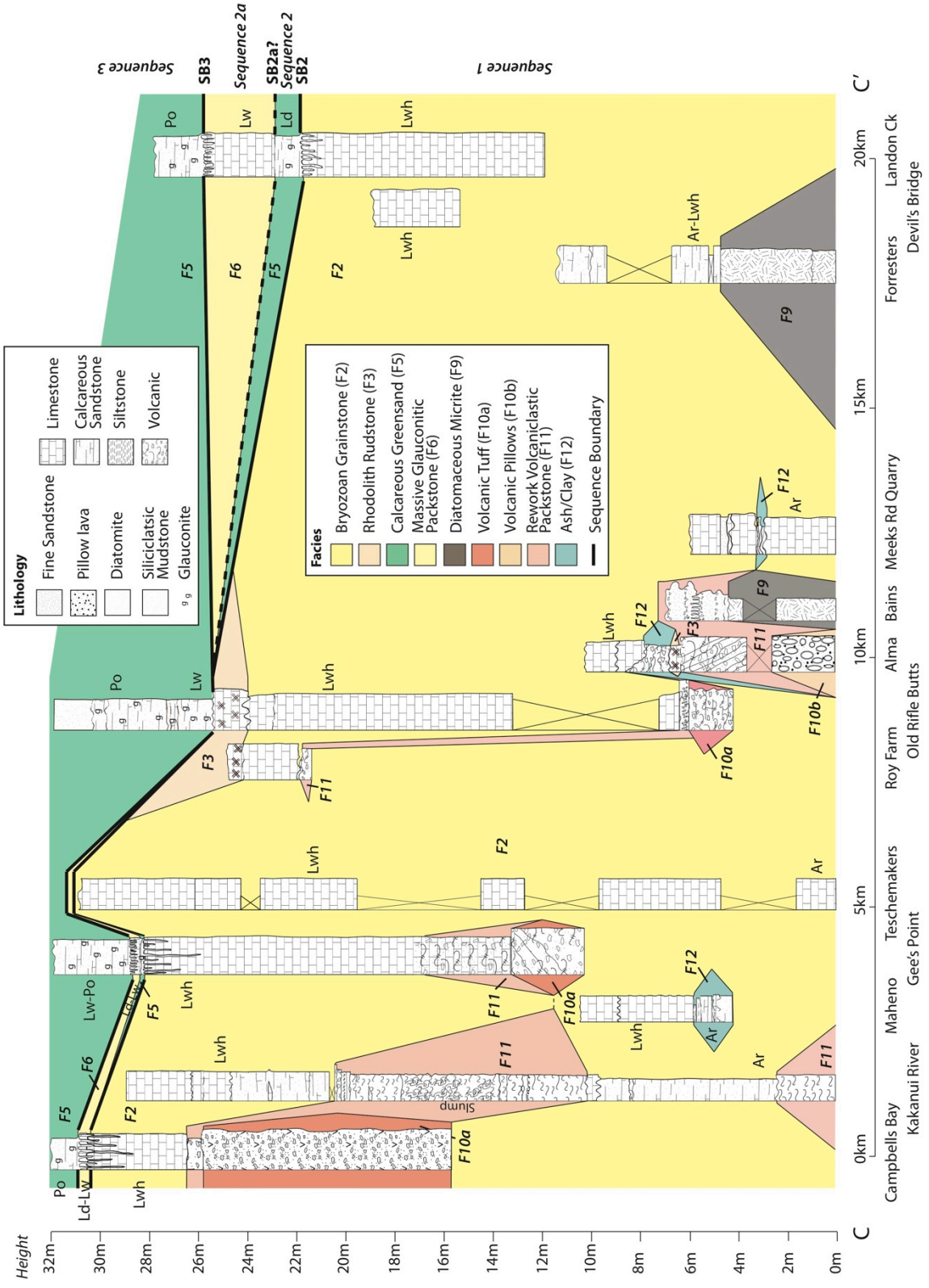

Figure 5.7. Section line through C-C' (Fig. 5.2), showing the sequences and the three sequence boundaries from this sequence stratigraphic model. Biostratigraphic ages are given next to each stratigraphic column where known or estimated based on data presented in Chapter 2.

5.3 Summary and discussion

5.3.1 Chapter summary

The sequence stratigraphic model of the Waitaki study area developed here contains three sequences and four sequence boundaries, with one lower-order sequence boundary. These record a series of transgressive-regressive cycles, beginning in the Late Cretaceous with the regional New Zealand-wide transgression, and continuing through the onset of the modern plate boundary in the Miocene.

Sequence 1 records the change from siliciclastic to carbonate facies, transitioning from a terrestrial fluvial environment to a deep outer-shelf to slope marine setting, as well as the development of an eastern volcanic palaeohigh in the later part of this transgression.

A major upper Whaingaroan sea-level fall occurred at Sequence Boundary 2, of the order of 100 – 150 m, resulting in subaerial exposure over most of the basin and extensive erosion. The development of Sequence 2 represents a Duntroonian to Waitakian transgression, interrupted in the early Waitakian by a small sea-level drop (SB2a), returning almost immediately to mid- and outer-shelf depths with a relative rise in sea level.

A second major sea-level fall occurred at Sequence Boundary 3, again inducing extensive subaerial exposure in the eastern region. This was followed by transgression in Sequence 3, but was then interrupted by the development of the modern plate boundary in the Altonian Stage and the return of significant siliciclastic supply and subsequent relative sea-level fall.

5.3.2 Discussion

The sequence stratigraphic model presented in this chapter can be used to examine two important questions about the Waitaki study area: namely the period of maximum

marine submergence; and the presence, location and influence of any terrestrial features on the sedimentary regime in the region (indicated by siliciclastic supply).

The model contains three principal periods of transgression that correspond to each of the three primary sequences (Sequences 1, 2, and 3). It is during the HST of Sequence 1 that the deepest facies, the Impure Wackestone (F4), was deposited in the western region, at depths that reached down to upper-slope conditions. This facies contains abundant planktic foraminifera and only rare benthic species, while exhibiting no macrofossils in outcrop at any of its exposures. No other facies in the mid-Cenozoic succession within the study area exhibits any indication that depths of this magnitude were reached again.

The correlative shallow Bryozoan Grainstone (F2) and Rhodolith Rudstone (F3) facies found in the eastern region were deposited at shallower depths due to their association with a volcanic palaeohigh, and can be discounted as indicators of maximum depth in the region (nor are they good indicators of siliciclastic supply, as the volcanic high located there is likely to have provided a bathymetric island that siliciclastic sediment would have bypassed). The period of maximum submergence within the Waitaki study area can therefore be placed in the early Whaingaroan Stage, at the end of the first major transgression.

While the Impure Wackestone (F4) facies that developed during the HST of Sequence 1 (within the western region) marks the deepest period within the study area, it is also one of the most siliciclastic-rich, with quartz silt contents comprising up to 40% of its composition (see Section 3.2.4). It is not until Sequence 2 that siliciclastic contents lessen, reaching an average of 5 – 6% in the Calcareous Greensand (F5), Massive Glauconitic (F6) and Bedded Packstone (F7) facies in the western region. This suggests that even though relative sea level within the study area did not reach the same depths as the HST of Sequence 1, the degree of siliciclastic supply was reducing.

The HST of Sequence 2, represented by the mid- to outer-shelf Bedded Packstone (F7) facies, contains an average siliciclastic content of 6% by composition. It is possible that the concentration of quartz silt within the Bedded Packstone is lower than the earlier Impure Wackestone (F4) facies due to the higher degree of *in situ* carbonate production of the former. However even those facies within Sequence 2 which have low sedimentation rates comparable to the Impure Wackestone facies (e.g., Calcareous Greensand Facies), contain similar siliciclastic concentrations. It can be assumed, therefore, that this decrease in siliciclastic supply from Sequence 1 to Sequence 2 was real, although the absolute reduction may be obscured somewhat by the varying sedimentation rates between the facies.

This lowering of terrigenous siliciclastic sediment supply from Sequence 1 through Sequence 2 suggests a decreasing terrigenous influence, and may imply a continuing planation of any proximal landmasses to the west. Further discussion related to siliciclastic sediment supply and the influence of the palaeohigh in the east is discussed in Chapter 6.

CHAPTER 6 – PALAEOBATHYMETRIC INFLUENCE ON SEQUENCE STRATIGRAPHIC EXPRESSION

6. Introduction

The presence of a volcanic palaeohigh in the eastern region makes the sequence stratigraphy of the Waitaki study area more than just a seaward-facing carbonate ramp, as is often the case in the temperate realm (e.g., Burchette and Wright, 1992; Pedley and Carannante, 2006; Massari and D'Alessandro, 2009; Blomeier *et al*., 2010; Bassi and Nebelsick, 2010). This chapter first describes the distributions and interpretations of volcanic and current-induced features within the study area, in order to determine what these features can tell us about the region's changing bathymetry and its effects. It then presents a series of palaeogeographic reconstructions for periods of interest during the region's evolution through the mid-Cenozoic.

These palaeogeographic interpretations enable illustration of the changing palaeobathymetry and morphology of the region, and provide inferences regarding the location and nature of any remaining landmasses west of the study area. It then becomes possible to determine whether the morphology of the study area, so influenced by this eastern volcanic high, caused the development of a carbonate factory.

These interpretations can then be used to explain the temporal and spatial distribution of facies within the study area, which differ from those expected over a simple ramp geometry, and how this influences the expression of the sequence stratigraphic model.

6.1 Volcanic distribution and interpretation summary

The North Otago area contains outcrops of small basaltic volcanoes, scattered over an area of ~ 800 km^2, that formed a subaqueous volcanic field consisting of groups of monogenetic volcanoes (Coombs *et al*., 1986). The volcanic exposures of Waiareka-Deborah Volcanics within the study area form part of this field, and comprise basaltic tuffs, dykes, sills, lava, and breccias (Fig. 6.1). The present study uses earlier work concerning volcanics and volcanism in the Waitaki region (see Section 1.2.6), together with analyses of the volcanic facies (see also Sections 2.2.4.1 and 3.2), to determine the environments of volcanic emplacement and their possible impact on carbonate facies development and local submarine topography.

6.1.1 Waiareka-Deborah Volcanics description and distribution

The Waiareka Volcanic Formation is made up of basaltic fine-to-coarse tuffs, sills, pillow lavas, and dykes, and is of late Kaiatan to Runangan age (Coombs *et al*., 1986; Reay and Sipiera, 1987; Forsyth, 2001). The younger Deborah Volcanic Formation comprises basaltic pyroclastics, tuffs, and breccias, as well as doleritic-to-basaltic intrusives (Gage, 1957; Dickey Jr, 1968; Reay and Sipiera, 1987; Edwards, 1991). Detailed descriptions of these Formations by other authors are given in Sections 1.2.6.2 and 1.2.6.3.

Biostratigraphy and K-Ar dating have constrained the Deborah Volcanics to the early Whaingaroan Stage (Coombs *et al*., 1986; Reay and Sipiera, 1987; Forsyth, 2001). These volcanics form all, or part of, three facies identified in Chapter 3 – the Volcanics (F10) facies, the Reworked Volcaniclastic Packstone (F11) facies, and the Ash/Clay (F12) facies. As such, they are all a part of Sequence 1, described in Section 5.2.2.

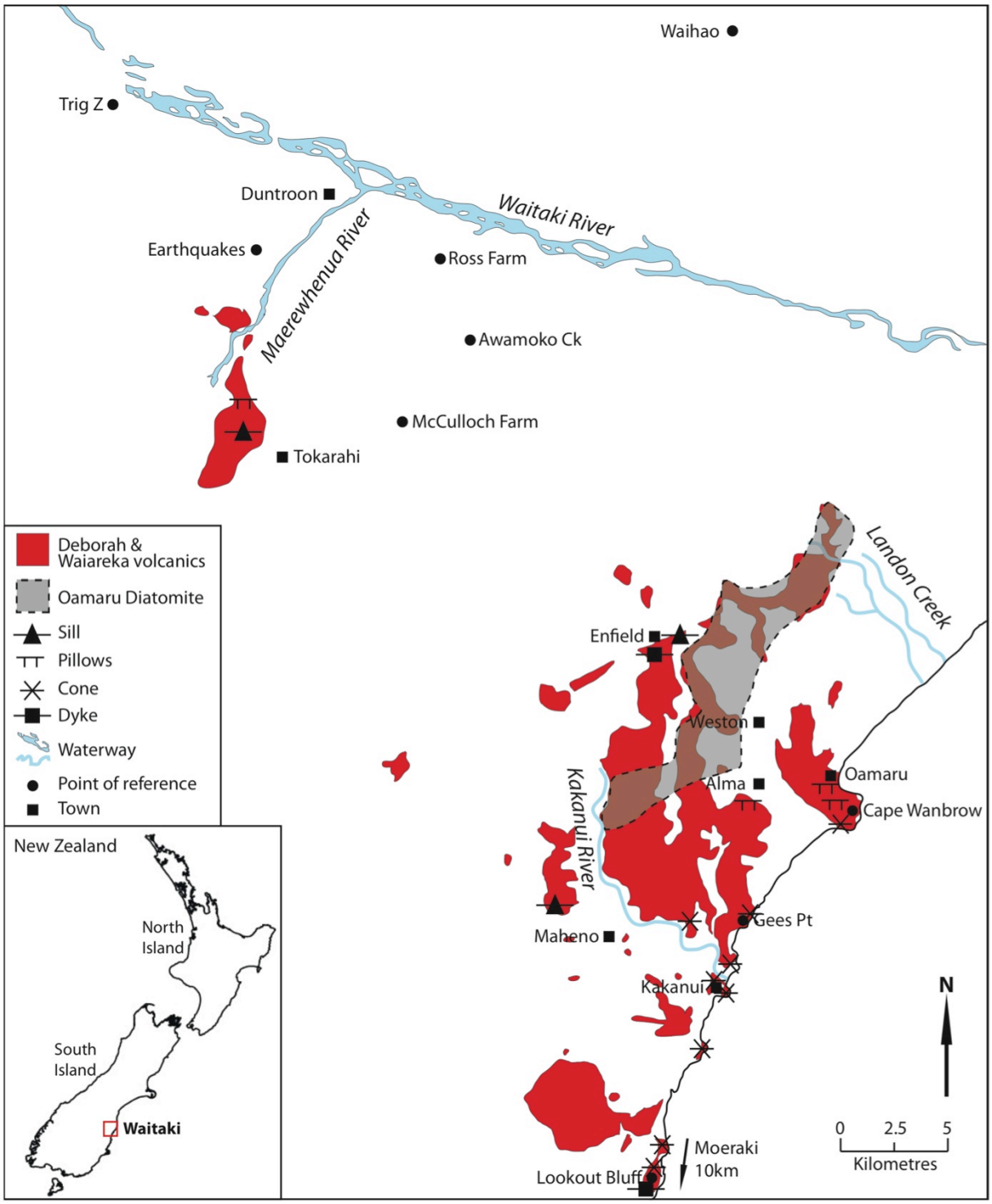

Figure 6.1. Map of the Waitaki Region used in this study, showing the distribution of the Waiareka-Deborah Volcanics and the extent of Oamaru Diatomite. The location of various volcanic features has been added based on observations in the field, as well as studies by Lewis (1973), Cas *et al*. (1989), Reay *et al*. (2002), Maicher (2003), and Murphy *et al*. (2008). Locations of interest referred to in this chapter have also been added. Modified from O'Connor (1999) and Forsyth (2001).

As suggested by Coombs *et al*. (1986), the Waiareka and Deborah Volcanics are here collectively termed the Waiareka-Deborah Volcanics, as a general stratigraphic term for these outcrops and successions. This collective classification is necessary because of difficulties in assigning a specific volcanic or intrusive to either formation in the field without decisive dating. Furthermore, the differentiation of these formations is not necessary for the purpose of this chapter, other than to introduce them and distinguish between locations of earlier and later periods of activity.

The majority of the Waiareka-Deborah Volcanics are distributed into tuffs and tuff-breccias over an area of about 50 x 8 km, derived from widely separated small vents (Fig. 6.1) (Gage, 1957). They mostly comprise the Volcanic Tuff (F10a) facies, and are concentrated around the current Waitaki coastline between Oamaru and Moeraki, with a maximum 200 m thickness around Cape Wanbrow (Fig. 6.1).

The youngest set of vents is concentrated between Kakanui and Weston (Gage, 1957, Edwards, 1991) (Fig. 6.1). Gage (1957) describes a second belt extending northward to Landon Creek, although this was not observed in the field during this study. Pillow lavas, making up the Volcanic Pillow (F10b) facies, are spread extensively throughout the study area, and are as common in the western region as in the east, extending as far inland as Duntroon, accompanied by local dykes and sills (Fig. 6.1) (Forsyth, 2001).

Volcanics located in the western region occurred exclusively during the first period of activity in the Kaiatan to Runangan Stages. These include a large vertical dyke located at Enfield (Coombs *at al*., 1986); while near the township of Tokarahi a sill intrudes into Bortonian sediments of the Tapui Glauconitic Sandstone, and is accompanied by pillow lavas (Fig. 6.1) (Gage, 1957). Another sill is located at Island Stream, 2.4 km west of Maheno (Gage, 1957). A coarse, megacrystic breccia occurs at Kakanui and Gees Point (Fig. 6.1), together with a number of remnant tuff cones; while around Cape Wanbrow

there is a mass of coarse pyroclastics on the northern and western flanks of the hill (Gage, 1957).

6.1.2 Waiareka-Deborah Volcanics interpretation

The tuffs of the Waiareka-Deborah Volcanics commonly show even bedding that is moderately to poorly sorted, and are considered to be the result of deposition on a relatively shallow continental shelf (Coomb *et al*., 1986; Cas *et al*., 1989; Maicher, 2003, Murphy *et al*., 2008), as opposed to an earlier interpretation involving a deeper, low-energy depositional environment (Gage, 1957). These Surtseyan eruptions were likely to have expelled material into the atmosphere from below sea level, after which wave and current action caused mass reworking (Murphy *et al*., 2008). Thin, normal- and reverse-graded beds of the coarser tuffs, as well as convolute-bedding, fluid-escape structures and syndepositional faulting, are the result of high-density current flows and gravity slumps formed during eruption or soon after (Sohn and Chough, 1993; Murphy *et al*., 2008).

Smellie (2001) showed that growing piles of saturated volcaniclastic material become unstable and subject to frequent slumping, with scales ranging from centimetres to several tens of metres (Maicher, 2000). This may be caused by rapid sediment accumulation over steepening and destabilising slopes, and syn-eruptive seismic activity (Maicher, 2003). Near the eruptive centres within the study area, volcanic material is likely to have built up to within wave base, indicated by current-bedding, ripples, cross-bedding and some discordant beds (White, 1996). Cones may occasionally have emerged above sea level for short periods, before rapid subsidence or wave-cut planation post-eruption, as indicated by massively bedded and non-fossiliferous portions of these formations. These features are well exposed along the Kakanui River and at Cape Wanbrow (Fig. 6.1).

In some locations (Kakanui, Lookout Point) these volcanic edifices overlap one another, forming a chain of cones that erupted independently, sometimes separated by tens to hundreds of thousands of years (Fig. 6.1) (Maicher, 2003, Murphy *et al*., 2008). In all cases observed here it appears that once eruptive activity ceased, the cones were colonised by marine organisms, as indicated by the conformable nature of contacts between the Reworked Volcaniclastic Packstone (F11) facies and the overlying Bryozoan Grainstone (F2) facies of Ototara Limestone (Murphy *et al*, 2008; this study). Burrows and hardgrounds between the Volcanics and overlying Ototara Limestone indicate, however, that immediately following volcanic activity there was sometimes a period of sediment starvation (Murphy *et al*., 2008).

6.1.3 Oamaru Diatomite description and distribution

The Oamaru Diatomite, a member of the Waiareka Volcanic Formation (see Section 1.2.6.2.1), makes up the Diatomaceous Micrite (F9) facies (see Section 3.2.9) which was deposited during Sequence 1 (see Section 5.2.2). It has been assigned to the Runangan to early Whaingaroan Stages using foraminifera and nannoplankton (Edwards, 1991; O'Conner, 1999). Lithologically, it is not a true diatomite, as the total siliceous content is never more than 60%, and it contains variable amounts of clay and silt. The Oamaru Diatomite occupies a NE-trending, roughly 50 km^2 area (~ 17 x 3 km) ~ 20 – 40 m thick, located near the modern eastern coastline (Fig. 6.1).

6.1.4 Oamaru Diatomite interpretation

The Oamaru Diatomite was deposited as a carbonate-mud-rich diatomite in quiet, subtropical waters about 75 – 150 m deep (see Section 3.2.9). The prominent siliceous diatom, radiolarian, and sponge-spicule assemblage found in this facies indicates an

increased silica supply in the environment, likely to have been associated with coeval volcanic activity in the eastern region. Substantial amounts of dissolved silica in the water column resulting from local eruptive activity would have favoured extensive growth and reproduction of diatoms and sponges that make up this diatomaceous micrite, enhanced by the presence of nutrient-rich upwelling waters which may have produced localised plankton blooms (Park, 1918; Gage, 1957; Edwards, 1991). Significant biogenic sediment would have formed near the basin's margin, due to a lack of terrigenous siliciclastic sediment supply there.

6.2 Distribution of current-induced facies

A number of locations within the study area show current-induced sedimentary features, most notably at Waihao, north of the Waitaki River (Fig. 6.1). These features tend to fall within the Cross-bedded Glauconitic Packstone (F8) facies described in Section 3.2.8, and form part of Sequences 2 and 2a (see Sections 5.2.4 and 5.2.6). Some smaller, but still prominent, cross-beds can also be found within the Calcareous Greensand (F5) facies in Sequences 2 and 3 (see Sections 3.2.5, 5.2.4, and 5.2.8).

6.2.1 Channelling

Large channels occur only at the Waihao locality (Fig. 6.1), in the Cross-bedded Glauconitic Packstone (F8) facies (Fig. 6.2) (see Section 3.2.8). They have been assigned using the FRED to the Duntroonian and Waitakian stages (see Section 2.3.3). These channels are usually 20 – 100 m wide and 1 – 16 m deep. Many are asymmetrical in cross-section with clear lateral accretion bedforms, suggesting meandering channel morphology (Fig. 6.2).

The levee of each channel is truncated by a younger channel to the west of it. Together with lateral accretion deposits, this indicates a westerly migration of meander bends. Asymmetrical ripples with amplitudes of 1 – 4 cm are found locally, as well as small-scale (< 10 cm) fluidisation features present as disruptions in laminations.

The northerly palaeocurrent direction for channel axes measured in this is based on a small dataset, but Ward and Lewis (1975) also found a dominantly northerly flow direction, based on the cross-bed foresets found within each channel (see Section 6.2.1.1).

6.2.1.1 Cross-bedding

Large-scale cross-bed sets (up to 2 m high) often found filling the large channels at Waihao (see Section 6.2.1), are one of the most prominent features of the Waihao locality in the northern region (Figs. 6.3A and 6.3B**)**. Foreset beds alternate between low-glauconite packstone and highly glauconitic (up to 90%) glauconite sandstone laminations (Fig. 6.3C), and occasionally contain preserved asymmetrical ripples (Fig. 6.3D). The packstones contain whole and fragmented echinoderms, brachiopods, molluscs, cetaceans, and rare bryozoans (Ward and Lewis, 1975; this study). Palaeocurrent measurements made in the field suggest a unimodal easterly flow direction (Fig. 6.4), which is supported by measurements made by Ward and Lewis (1975). Bioturbation is significant within these cross-beds, and includes mostly *Scolicia*, *Planolites*, and *Ophiomorpha* (Ward and Lewis, 1975; this study).

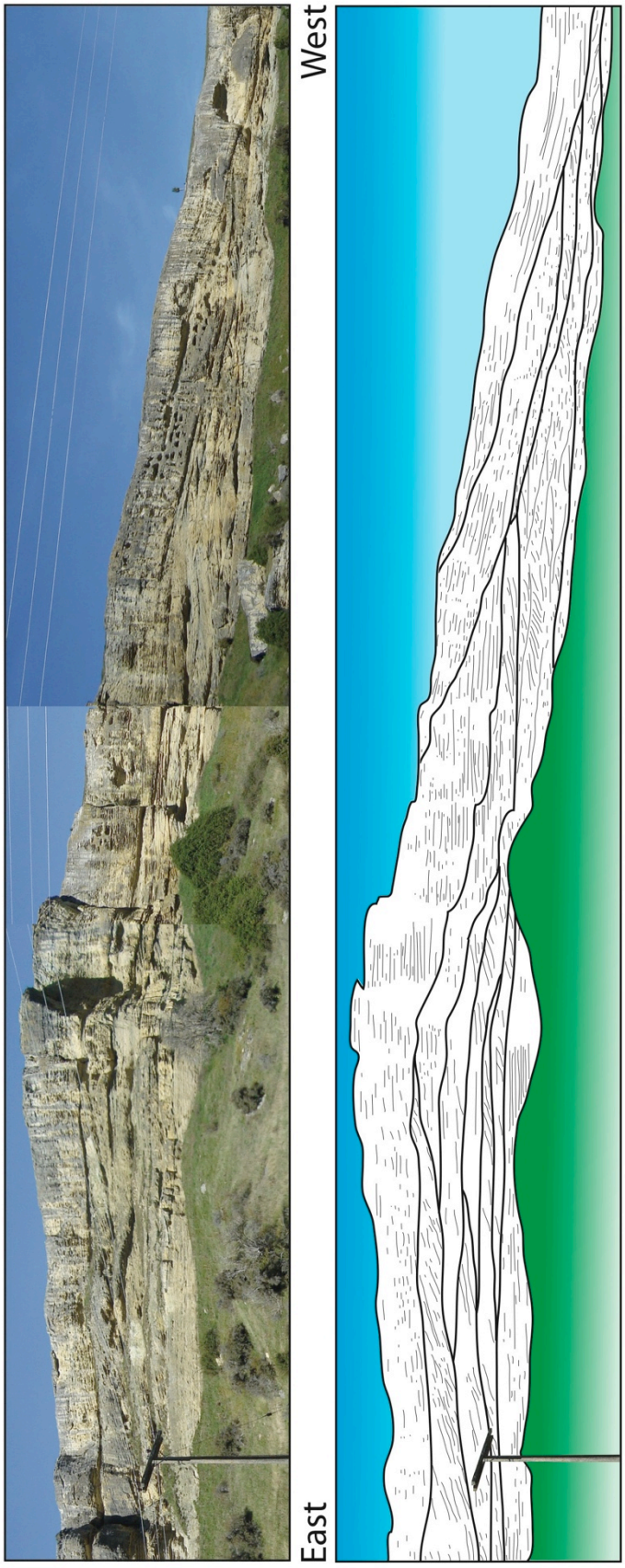

Figure 6.2. Channelling at Waihao in the northern region of the study area, illustrating the levee truncation and the presence of cross-bed foresets within a number of channels.

The Ross Farm locality contains cross-bedding both within the Calcareous Greensand (F5) facies of Kokoamu Greensand and the Cross-bedded Glauconitic Packstone (F8) facies of Otekaike Limestone (Figs. 6.3E and 6.3F). The Calcareous Greensand (F5) cross-beds are small (~ 5 cm) and discontinuous, occurring most prominently in the lower part of the facies. Those within the Cross-bedded Glauconitic Packstone (F8) facies further up-section are larger (~ 80 cm), and very similar in appearance to those found at Waihao with alternating high to low levels of glauconite-forming foreset beds.

The Gees Point locality contains localised cross-bedding in the Calcareous Greensand (F5) facies of Gee Greensand, where there is a small normal fault in the basal Ototara Limestone. Palaeoflow directed measured by Batt (1993) indicate a north to northeast orientation. The cross-bedding occurs where this unit abuts the fault's footwall.

Small-scale and localised cross-bedding occurs in the Calcareous Greensand (F5) facies in other localities within the western region (e.g., Ross Farm, Earthquakes), but these are not as dominant a feature of the facies there as they are in localities that contain the Cross-bedded Glauconitic Packstone (F8) facies.

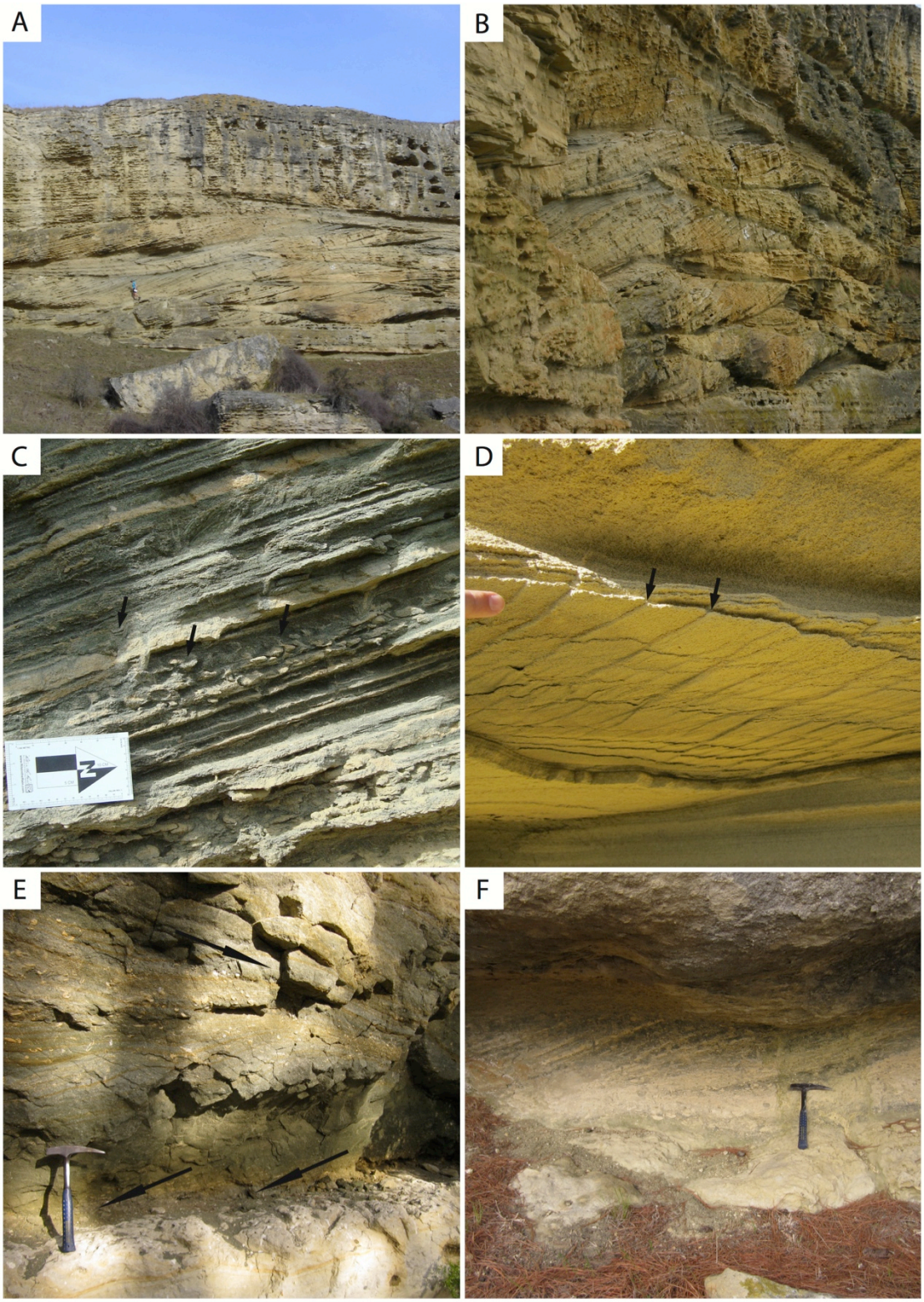

Figure 6.3. Outcrop photos of cross-bedding in study area. A: Large-scale cross-bedding and channel at Waihao. Note figure to centre left for scale; B: Oblique view of cross-beds shown in A; C: Fluid-escape structures, bioturbation, and disrupted laminae (black arrows) at Waihao; D: Asymmetrical ripples at Waihao (black arrows); E: Cross-beds observed in lower Calcareous Greensand (F5) facies at Ross Farm; F: Small lense of Cross-bedded Glauconitic Packstone (F8) facies at Ross farm.

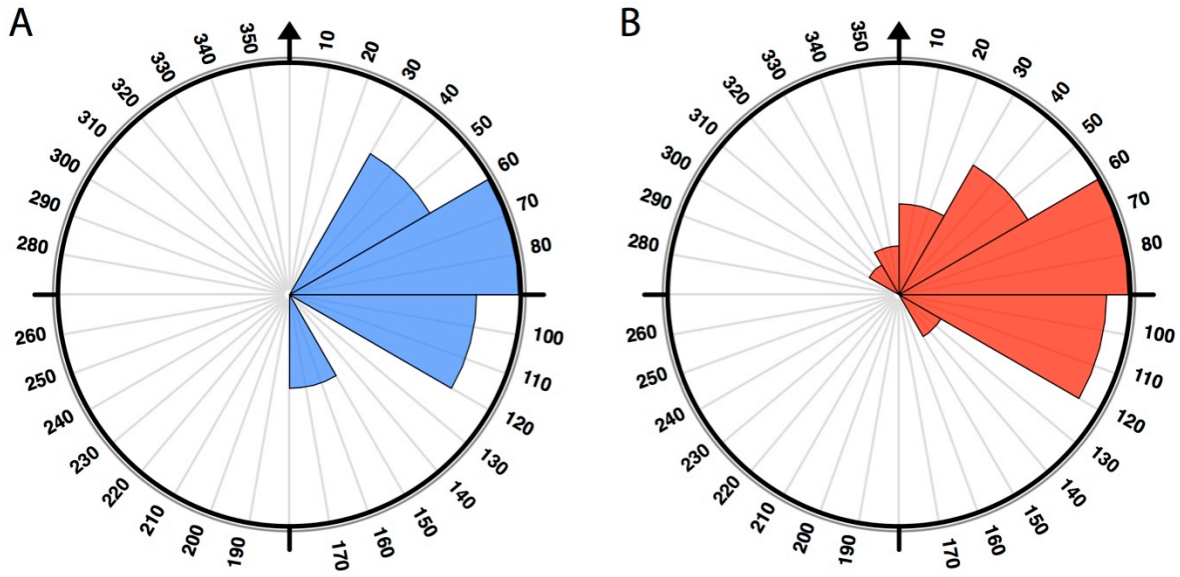

Figure 6.4. Rose histograms given in 30° increments of cross-bed palaeocurrent directions from the Waihao exposure. A: Data collected during this study; B: Data collected by Ward (1973) and Ward and Lewis (1975) from the same location. Combined dataset comprises approximately 115 measurements.

6.3 Palaeogeographic reconstructions

A chronological interpretation of the palaeobathymetry of the study area is presented in this Section, based on facies (Chapter 3) and the sequence stratigraphic model (Chapter 5); together with an examination of how, and in what ways, the geometry of this area changed through the mid-Cenozoic.

Throughout this time period, the siliciclastic content of the facies decreased from west to east (e.g., through the Massive Glauconitic Packstone (F6) facies; see Section 3.2.6). It is therefore likely that any terrigenous supply came from land that lay towards the west, outside the study area (see Section 5.2.2). While the eastern palaeohigh certainly influenced the deposition of siliciclastic sediment by elevating that area out of any terrigenous depositional flow, the western region still records an eastward decrease in terrigenous content within it, beyond any significant influence of the high.

6.3.1 Sequence 1 transgression (Haumurian – Kaiatan)

The TST during Sequence 1 (see Section 5.2.2.1) covers a change from terrestrial fluvial flood plains (Taratu Formation; see Section 1.2.5.1), beginning in the Haumurian Stage, through to a quiet, marine outer-shelf environment (Kauru Formation and the Tapui Glauconitic Sandstone; see Sections 1.2.5.3 and 1.2.5.4). This transgression eventually culminated in the oldest facies identified in this study - the outer-shelf Glauconitic Siltstone (F1) facies found in the western region, deposited during the Kaiatan Stage. During this period there are no indications of localised palaeotopographic variations across the study area, apart from a general eastward-deepening morphology.

As sea levels rose during Sequence 1, the size of siliciclastic grain supply dropped from conglomerates and sandstones, to non-calcareous siltstones, indicating the advance of the shoreline towards the west and the continued lowering of exposed topography (see Section 5.2.2.1). It is likely that the bathymetry of the study area during this time was one of a steepened siliciclastic ramp that deepened to the east away from western landmasses, as there is no indication that the eastern palaeohigh existed prior to the onset of volcanic activity. However it is also possible that the geometry was that of a shelf with clinoform geometry. Once volcanic activity began towards the end of this TST, in the upper Kaiatan Stage, the palaeobathymetry began to be altered, particularly in the east where submarine lava flows and tuff cones were being extruded and erupted (see Section 6.1.1).

6.3.2 Sequence 1 highstand (Runangan – early Whaingaroan)

The Waiareka-Deborah Volcanics (Sections 6.1.1 – 6.1.2), while found in most parts of the study area, are concentrated around the eastern region (Fig. 6.1), and developed principally during the Sequence 1 HST between the Runangan and mid-Whaingaroan Stages (see Section 5.2.2.2). This activity has been interpreted earlier as

having resulted in a palaeohigh or shoal coinciding roughly with the modern eastern coastline (Fig. 6.5) (Gage, 1957; Lewis, 1973; Ward and Lewis, 1975). Significantly lower levels of volcanic activity in the western region, and the absence of Surtseyan tuff cones there, suggest that emplacement of the Waiareka-Deborah Volcanics is likely to have had little influence on western palaeobathymetry.

During this highstand, the eastern region became the site of an extensive cool-water carbonate factory closely associated with the volcanic activity that led to the development of the palaeohigh. This led to the deposition of the inner- to mid-shelf Bryozoan Grainstone (F2) and Rhodolith Rudstone (F3) facies in this area, both of which were devoid of fine-grained carbonate mud, significantly winnowed by the high-energy environment of the shoal. This zone of high relief consisted mostly of a shallow submarine area (Fig. 6.5), probably with variable local topography as a result of the numerous tuff cones making up a large portion of it. Some of these cones were subaerially exposed during eruption (see Section 6.1.2), and there would have been times during this HST when volcanic islands formed around the eastern region.

Further to the west, away from this palaeohigh, there was a deeper, low-energy, mixed siliciclastic-calcareous environment in which the Impure Wackestone (F4) facies formed (see Section 3.2.4). This facies comprises carbonate mud together with significant quantities of siliciclastic silt.

This lateral change across the region from high-energy, shallow facies in the east towards deeper, low-energy facies in the west, indicates that the study area comprised a westward deepening geometry during this highstand (Fig. 6.5).

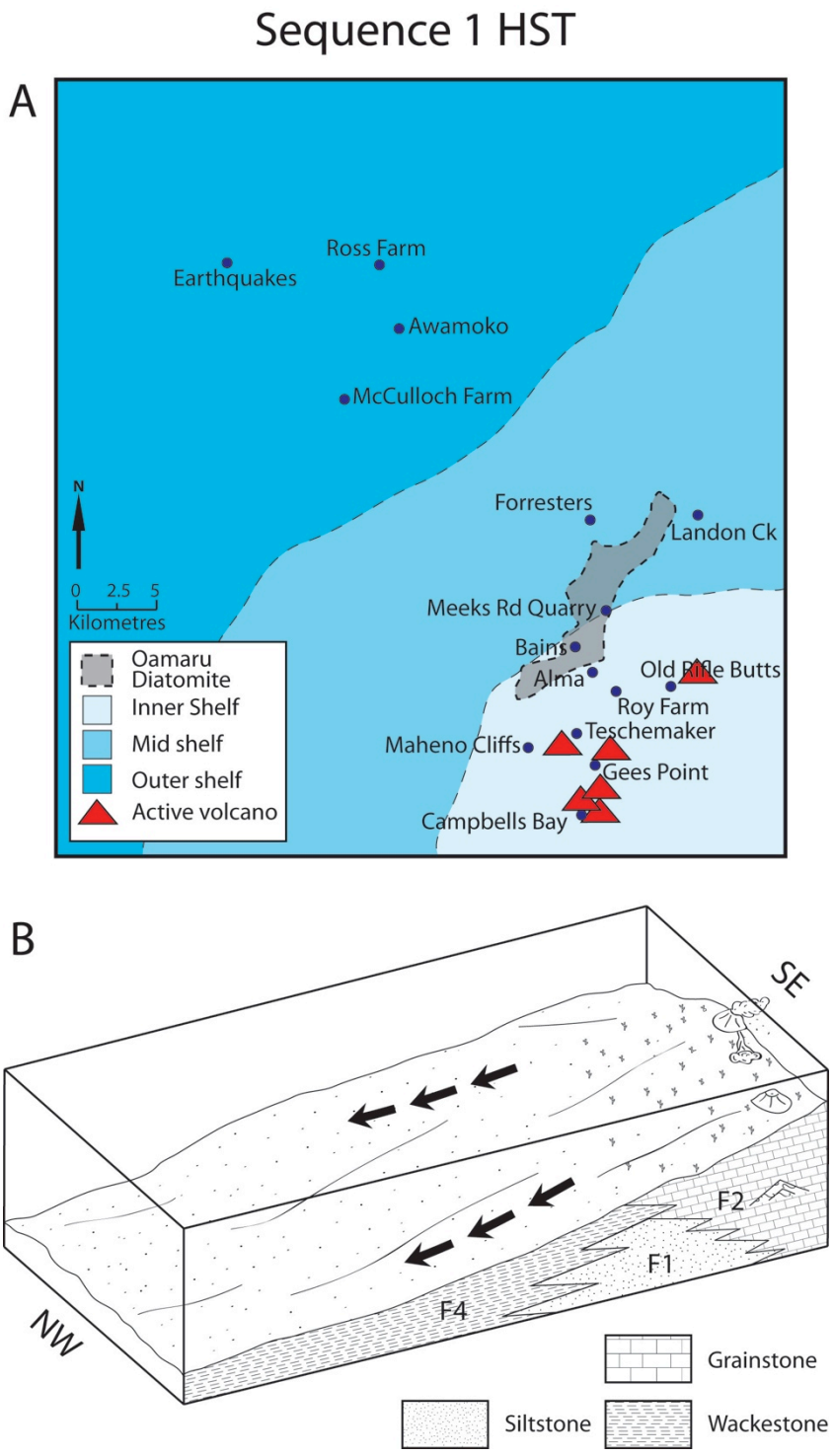

Figure 6.5. Palaeomap and schematic block diagram of the study area during the Sequence 1 HST. A: Map showing the palaeobathymetric variation relative to stratigraphic sections. B: Stylised section showing the eastern palaeohigh shedding carbonate mud downslope towards the deeper western region.

6.3.2.1 Palaeohigh's effect on diatomite distribution

While it was the volcanic activity itself which resulted in the siliceous environment that ultimately formed the Oamaru Diatomite (Section 6.1.3 and 6.1.4), the palaeohigh appears to also have had an influence on where this lithology is found (Fig. 6.1). As observed in the Waiareka-Deborah Volcanics themselves, there was significant wave-induced erosion and planation associated with the build-up of the cones. Finer material would therefore be likely to have settled away from the high-energy regime around these vents, coming to rest in the deeper areas around the palaeohigh. This appears consistent with the approximate distribution of diatomite to the northwest of the palaeohigh (Fig. 6.1), where it was probably deeper than around the built-up vents, while also being protected from the open ocean to the east by the volcanic barrier.

The Diatomaceous Micrite (F9) facies is generally found underlying younger exposures of the Bryozoan Grainstone (F2) facies, suggesting that more siliceous biota flourished in deeper environments prior to significant carbonate colonisation and the establishment of the carbonate factory around the palaeohigh. The growth of the palaeohigh, as a result of carbonate sediment accumulation, would have served to lower relative sea level and extend the shallow area, thus inhibiting accumulation of muddy facies in the eastern region.

These same volcanic-distal Bryozoan Grainstone accumulations can also contain thin lenses of the Ash/Clay (F12) facies (see Section 3.2.12); with these being likely to represent a small influx of fine-grained volcanic material from the vents into the carbonate accumulations, either as a small turbidite or direct ashfall, which then weathered to clay within the sediment column (causing no obvious changes in local sedimentation or biological activity).

6.3.3 Sequence boundary 2 (mid – late Whaingaroan)

During the upper Whaingaroan Stage LST identified as SB2 (see Section 5.2.3), the palaeohigh became subaerially exposed, as indicated by the extensive karst surfaces found in the eastern region as far west as Ross Farm (Fig. 6.6). Further to the west, there is a submarine firmground at Earthquakes, indicative of arrested sedimentation below sea level.

In the westernmost outcrop at Trig Z (Fig. 6.1), drill-core data presented by Edwards (1971) appear to show a conformable relationship at SB2 between Sequences 1 and 2, although the author suggests that a disconformable contact probably exists, like that seen at the nearby Earthquakes outcrop. Volcanic activity prevalent in the eastern region up until the early Whaingaroan, had ceased by that time (see Section 1.2.6.3).

The presence of a shallow karst at Ross Farm, compared to the burrowed firmground at Earthquakes, suggests that either the coastline during this LST may have extended to somewhere between these two outcrops at its farthest extent, or that Ross Farm was an isolated high that became subaerially exposed (Fig. 6.6). The shallower karst at Ross Farm (with solution cavities no deeper than 30 cm) relative to those observed in the east, suggests shorter subaerial erosion there than in the eastern region. This would be expected if Ross Farm were located towards the deeper end of a westward-deepening slope geometry extending from the eastern palaeohigh during this lowstand.

If the east-west depth profile had been relatively uniform, subaerial exposure might have been expected at both McCulloch Farm and Awamoko during SB2, due to their proximity to the subaerially exposed eastern region and the Ross Farm locality. The absence of a karst surface and the presence of *Thalassinoides* burrows at this contact (at both McCulloch Farm and Awamoko) suggest, however, that this surface was submarine. Development of a karst morphology there would also have been less likely due to the non-

calcareous nature of the Glauconitic Siltstone (F1) facies that forms the top of Sequence 1 at these locations. It seems, therefore, that there was some variation in the bathymetry in the centre of the study area which allowed subaerial exposure at Ross Farm, while submarine burrowed surfaces developed around the same time at McCulloch Farm and Awamoko. This subaerial exposure was thus likely to have been localised, and not connected with the exposed eastern shoal (although without any further outcrop exposure of SB2 between the McCulloch Farm/Awamoko outcrops and the eastern region, this cannot be confirmed); with local differences in depths at these SB2 outcrops possibly being the result of a prior bathymetric variation in the sea floor around Ross Farm.

Any Impure Wackestone (F4) facies present on this surface at McCulloch Farm and Awamoko prior to the LST at SB2, is likely to have been thin and would have been eroded off during the FSST of Sequence 1 (Section 5.2.2.3), leaving only the older Glauconitic Siltstone. Such a thin carbonate lithology is most likely to have been due to the outcrops being shallower in the central western region (because of their proximity to subaerially exposed outcrops), with the carbonate mud shedding off the eastern high mostly bypassing these locations as turbidites for the deeper west. This would have resulted in a thinner sequence of Ototara Limestone (likely to be represented by the Impure Wackestone (F4) facies as seen elsewhere in the western region), which may have then been completely eroded off during the FSST and subsequent LST of Sequence 1 and SB2, respectively, explaining their present absence at these outcrops.

Just as erosive removal of sediment appears to have occurred in the central western region, subaerial exposure around the eastern region is likely to have resulted in some planation of the palaeohigh. Significant thicknesses of the dominant Bryozoan Grainstone (F2) facies from the early Whaingaroan Stage remain, however, indicating that erosion was probably not substantial during this first major lowstand. The effect of erosion may have

been reduced by the presence of concentrated sea-floor calcite cementation that occurred at the eastern SB2 surfaces prior to subaerial exposure (see Section 4.7.1.1).

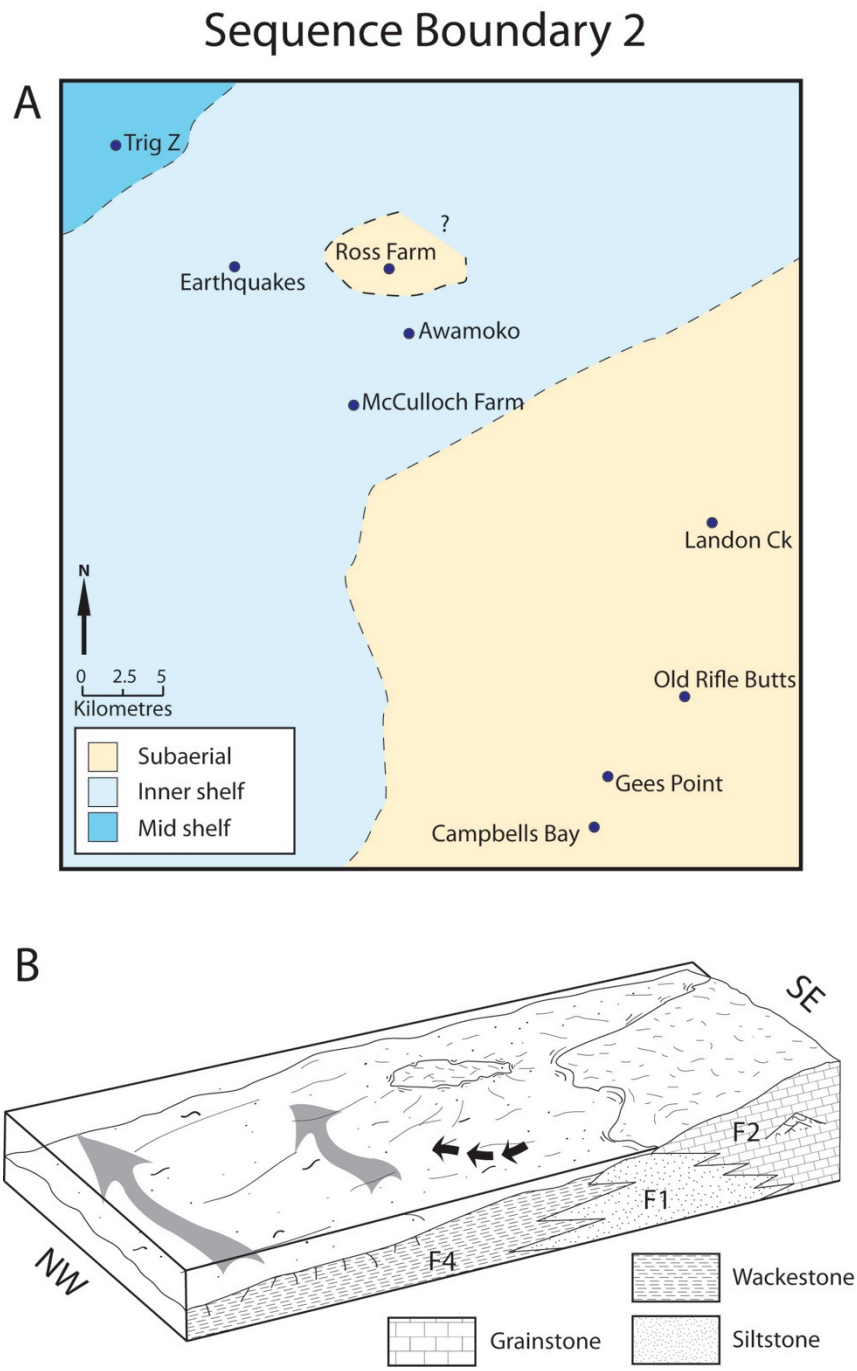

Figure 6.6. Palaeomap and schematic block diagram of the study area during the LST at SB2. A: Map showing the palaeobathymetric variation relative to stratigraphic sections. B: Stylised section showing the extent of subaerial exposure, with those areas still submarine being subjected to an increased energy environment with strong currents and submarine erosion forming burrowed firmgrounds.

6.3.4 Sequence 2 transgression (Duntroonian)

Relatively thick accumulations of the Calcareous Greensand (F5) facies developed through the Duntroonian Stage in the western region, while sedimentation rates were low (see Section 3.2.5), resulting in extensive glauconite accumulation following the earlier lowstand. Minimal sediment accumulation took place during the Duntroonian in the eastern region, however, with only Landon Creek developing any significant sediment during this period (up to 0.5 m). The oldest portions of this facies sometimes contain localised cross-beds indicating a shallower, high-energy environment during the early TST, as at Ross Farm and Earthquakes (Fig. 6.7). The facies then became increasingly calcareous and massive as transgression continued through the Duntroonian. This again illustrates the effect of the westward-deepening sea-floor geometry on this part of the submerged rimmed platform, as the western region reached sufficient depth relative to the palaeohigh to be able to accumulate significantly more sediment than the eastern region during this transgression.

During the onset of the TST in Sequence 2 (see Section 5.2.4.1), the eastern palaeohigh acted as a barrier, possibly explaining the intensely channelled Duntroonian to Waitakian succession at Waihao (Fig. 6.7). The cross-bedding in the Cross-bedded Glauconitic Packstone (F8) facies may be attributable to eastward palaeocurrents moving abundant sediment as slowly migrating submarine sand dunes, while the larger scour-cut channels could represent sporadic north-flowing storm events which brought in glauconitic sediment scoured off the palaeohigh to the south (see Section 6.2.1) (Fig. 6.7).

This eastern barrier would have inhibited free circulation of water flowing northward through the eastern region, except during large storm events. These events, coupled with the already high-energy winnowing environment prevailing in the east during this period, may therefore explain the relatively thin or absent transgressive greensand

facies there during Sequence 2. They would have made sediment accumulation very difficult during the initial shallower stages of the TST, particularly the early phase that followed submersion of the palaeohigh, when the Calcareous Greensand (F5) facies was already being deposited further to the west (e.g. Ross Farm, Earthquakes) (Fig. 6.7).

During this early phase, the eastern palaeohigh was a submarine hardground, as indicated by the presence of numerous *Melitodes* holdfasts present on the surface of SB2 at Gees Point, suggesting that sediment accumulation was minimal for some time following submergence of the high. Easterly flowing currents, observed primarily at Waihao, may have transported sediment eastward, delivering some glauconite to the eastern palaeohigh once it was sufficiently submerged, from the already developing Calcareous Greensand facies deeper in the western region.

6.3.5 Sequence boundary 2a (Duntroonian/Waitakian boundary)

Sequence Boundary 2a is the result of a small lowstand between Sequences 2 and 2a that probably occurred around the Duntroonian/Waitakian Stage boundary (see Section 5.2.5). Given the erosive and rubbly nature of this surface in the western region at Ross Farm and Awamoko (Fig. 6.1), it is likely that this lowstand resulted in increased submarine erosion and non-deposition in these shallower western outcrops. Some of the eastern palaeohigh may, however, have again been subaerially exposed as a result of this sea-level fall, but this cannot be confirmed as there is no identifiable exposure of SB2a in the east.

This lower-order lowstand would have limited the time that the eastern palaeohigh was submerged during the successive TSTs of Sequences 2 and 2a, further reducing sediment accumulation. The served to reduce the suration over which the eastern palaeohigh was at sufficient depth to accumulate sediment, resulting in thinner sequences

there than otherwise might have occurred without this reduced water depth. The SB2a surface itself is likely to have been condensed into the lower SB2 karst horizon in the eastern outcrops proximal to tuff cones, where depths were shallowest, as any sediment accumulation in that area would have been minimal prior to the lowstand of SB2a. Considering the relatively small lowstand that formed this surface (see Section 5.2.5), it is unlikely there was any significant erosion of the eastern palaeohigh itself.

The westward-deepening geometry of the western region resulted in the deepest occurrence of SB2a in the study area (Trig Z), forming only a winnowed fossiliferous rudstone, induced by increased energy and without any erosion being evident (see Section 2.2.3.8).

6.3.6 Sequence 2a highstand (mid Waitakian)

Following the minor SB2a LST, transgression continued with increased carbonate production until highstand in the mid-Waitakian Stage. This HST (Section 5.2.6.2) resulted in extensive calcareous facies development in the northern and western regions during the Waitakian Stage (Bedded Packstone (F7) and Cross-bedded Glauconitic Packstone (F8) facies), while around the palaeohigh in the east there was minimal sediment accumulation (Fig. 6.8). Relative sea level was lower across the study area during this highstand than that occurring during the earlier HST of Sequence 1, based on the change from the muddy Impure Wackestone (F4) facies of Sequence 1 to the shallower mud- and sand-sized Bedded Packstone (F7) facies developed in the same location during this highstand.

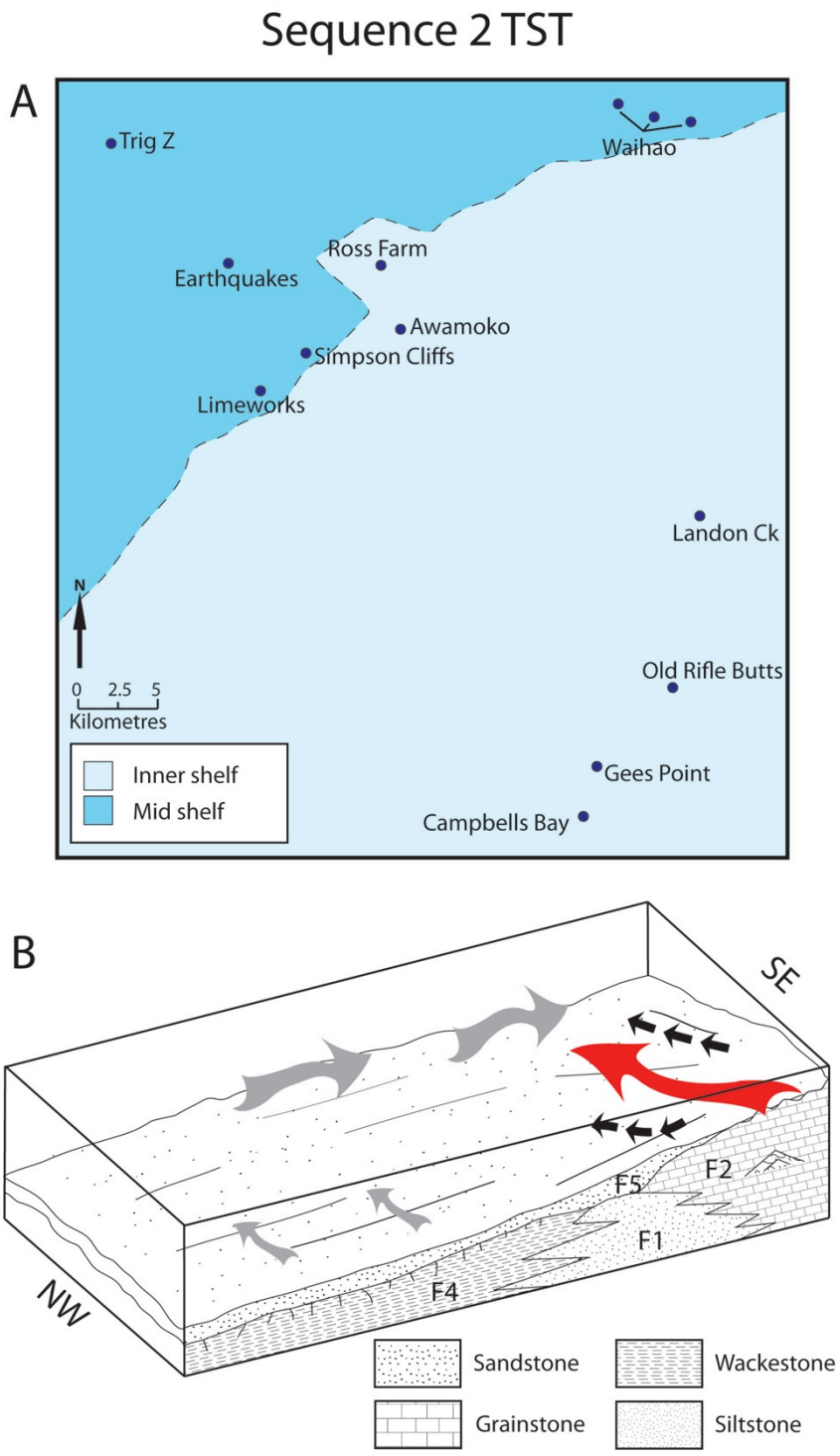

Figure 6.7. Palaeomap and schematic block diagram of the study area during the TST of Sequence 2. A: Map showing the palaeobathymetric variation relative to stratigraphic sections. B: Stylised section showing the reworking of sediment from the eastern palaeohigh towards the north. Red arrow indicates glauconite reworking to the north, while grey arrows show submarine current movement.

This shallower environment enabled the western region to become conducive to more localised carbonate production, rather than being reliant of carbonate supply from the east as during Sequence 1 (Fig. 6.8). The relative decrease in siliciclastic content up through the Massive Glauconitic Packstone and Bedded Packstone facies, is likely to have been the result of this increase in carbonate production, rather than solely a decrease in terrigenous silt supply as sea-level rose.

Siliciclastic supply during this HST did not increase relative to that found in the deeper Impure Wackestone (F4) facies deposited during the HST of Sequence 1. This implies that while relative sea level was lower during this HST, there was a higher volume of carbonate production within the western region than had previously occurred, diluting any siliciclastic supply to the area. Siliciclastic supply was also reduced from that seen at highstand during Sequence 1, when terrigenous sediment and transported carbonate mud made up the majority of sediment in the western region.

Extensive *in situ* carbonate production would have been less likely if siliciclastic supply had remained relatively high, as during Sequence 1 (Nelson, 1988; James, 1997). This relationship between carbonate production and siliciclastic supply was probably the result of continuing planation of any subaerially exposed landmasses to the west of the study area, from which terrigenous sediment was being supplied.

While there was extensive calcareous sediment accumulation in the western region during this HST, the buried eastern volcanic high was likely to have accumulated a thinner sediment succession due to the shallower, high-energy environment there and the effect of storm events (Fig. 6.8). Any sediment removed during these events was likely to have been transported northward towards the Cross-bedded Packstone (F8) facies, resulting in further significant sediment accumulation in that area.

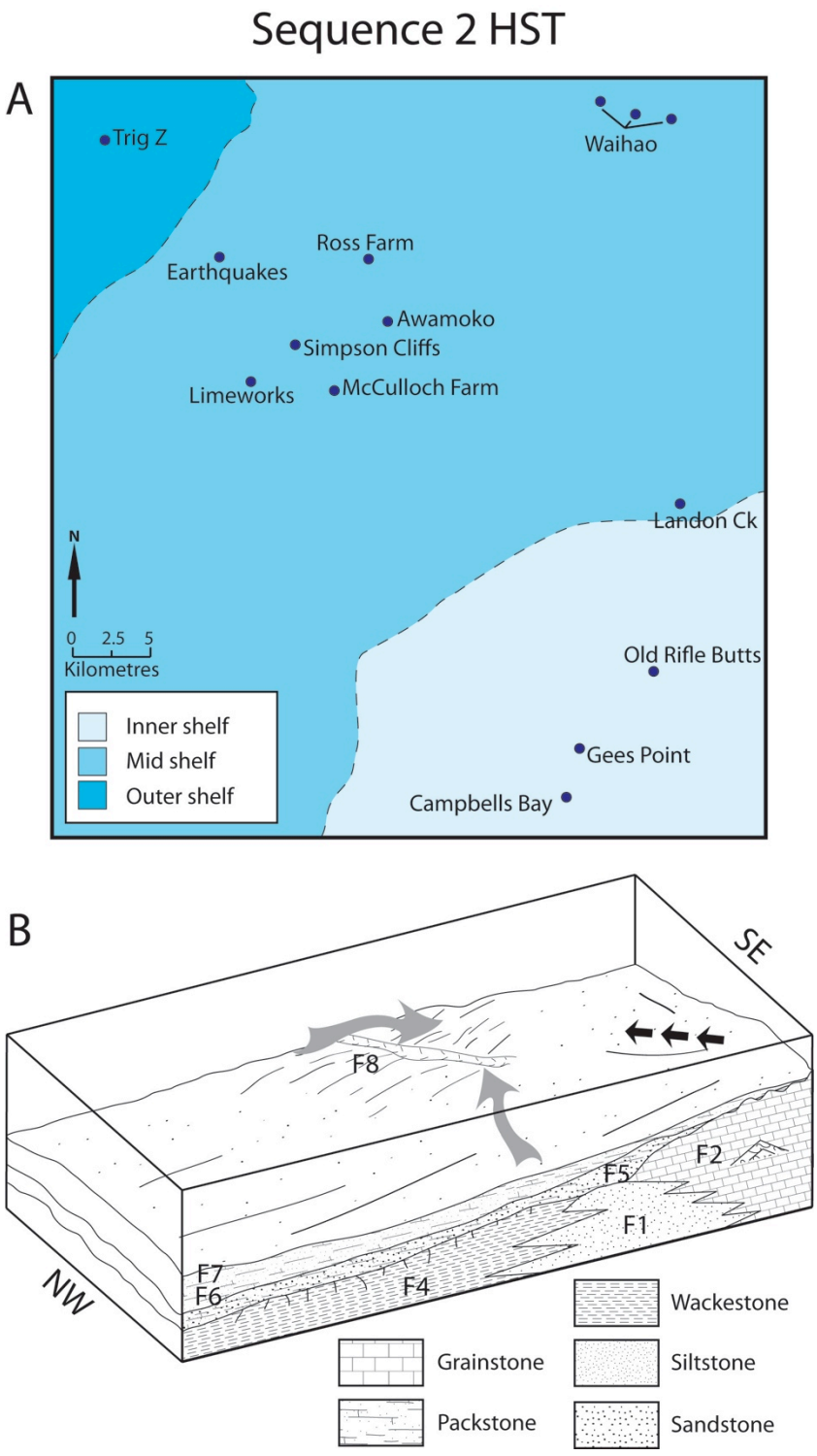

Figure 6.8. Palaeomap and schematic block diagram of the study area during the Sequence 2a HST. A: Map showing the palaeobathymetric variation relative to stratigraphic sections. B: Stylised section showing the eastern palaeohigh shedding carbonate mud down a ramp slope towards the north, where submarine currents are creating channels. Thick accumulations of carbonate sediment are forming in the west.

6.3.7 Sequence boundary 3 (late Waitakian)

The late-Waitakian LST at Sequence Boundary 3 (see Section 5.2.7) induced another significant period of subaerial exposure on the palaeohigh in the eastern region (Fig. 6.9). The nature of the contact in the western region is less certain, as the contact between Sequences 2 and 3 was not directly observable during this study. Batt (1993), however, observed a rapid gradational contact across this sequence boundary just to the west of the study area, implying that deposition may have been more continuous further west.

Across the palaeohigh, the degree of subaerial erosion is comparable with that which occurred during SB2, with solution cavities of a similar depth developed (see Section 2.2.4.6), and the sometimes-complete removal of any sediment accumulated from Sequences 2 and 2a. Lamination and normal grading of Duntroonian and Waitakian glauconitic sediment within the karst solution cavities of SB2, and thin veneers of these same sediments above it, attest to the accumulation of some sediment during Sequences 2 and 2a on the palaeohigh prior to the LST of SB3. However, given the either thin or absent successions at Old Rifle Butts, Campbells Bay and Gees Point, it can be inferred that there was little sediment accumulated during these older sequences, with any accumulation likely to have been eroded during this LST.

The erosive nature of the two subaerial LSTs at SB2 and SB3 imply some lowering of the eastern palaeohigh may have occurred. These events may then have led to a flattening of the basin profile (Fig. 6.9), providing a more uniform surface during Sequence 3 that was less affected by depositional environment variations across the sea floor.

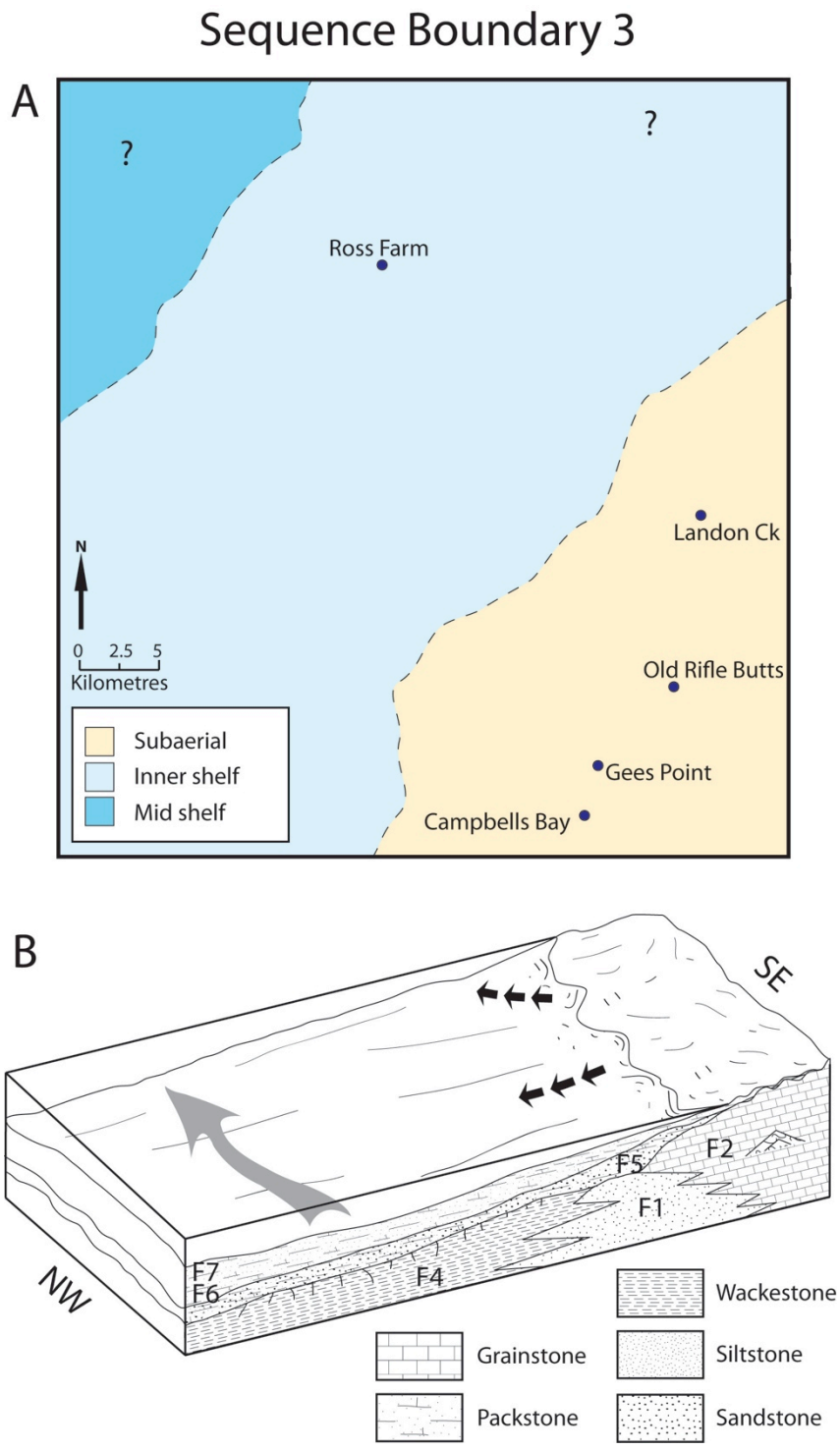

Figure 6.9. Palaeomap and schematic block diagram of the study area during the LST at SB3. A: Map showing the palaeobathymetric variation relative to stratigraphic sections. B: Stylised section showing subaerial exposure on the eastern palaeohigh, and increased submarine energy levels to the west.

6.3.8 Sequence 3 transgression (Otaian)

The Sequence 3 TST, during the Otaian Stage, brought renewed deposition of glauconitic facies (Calcareous Greensand, F5) across the study area (see Section 5.2.8.1), with sediment thicknesses over the eastern palaeohigh being far greater than those seen during Sequences 2 and 2a (Fig. 6.10). This led to similar volumes of these glauconite sandstones accumulating in both the eastern and western regions where, during the previous Sequences, sediment accumulation had favoured either the east or west, but not both.

This supports the likelihood that the geometry of the study area had become more uniform, possibly due to a lowering of the eastern high by planation during successive occurrences of subaerial erosion. This would have allowed more sediment accumulation in the eastern region than had been possible following the earlier LST of SB2, when high-energy conditions prevented significant accumulation. Cross-beds in this facies at Gees Point attest, however, to the still-shallow nature of this eastern region during transgression.

6.3.9 Sequence 3 highstand and falling stage (Altonian)

With the onset of deposition of the Altonian-Stage Rifle Butts Formation (see Section 2.2.4.8), during the Sequence 3 HST (Section 5.2.8.2), an increase in terrigenous sediment occurred for the first time since the Kaiatan Stage. This was the result of a change in tectonic regime and renewed uplift across the region (see Section 1.2.8.2), which massively increased supply of siliciclastic sediment to the basin. This would have subsequently led to the suffocation of any carbonate factory that may have developed with continued transgression in the area. Instead, it resulted in the cessation of sea-level transgression and the onset of relative sea-level fall, induced by regional uplift accompanying the development of the new plate boundary.

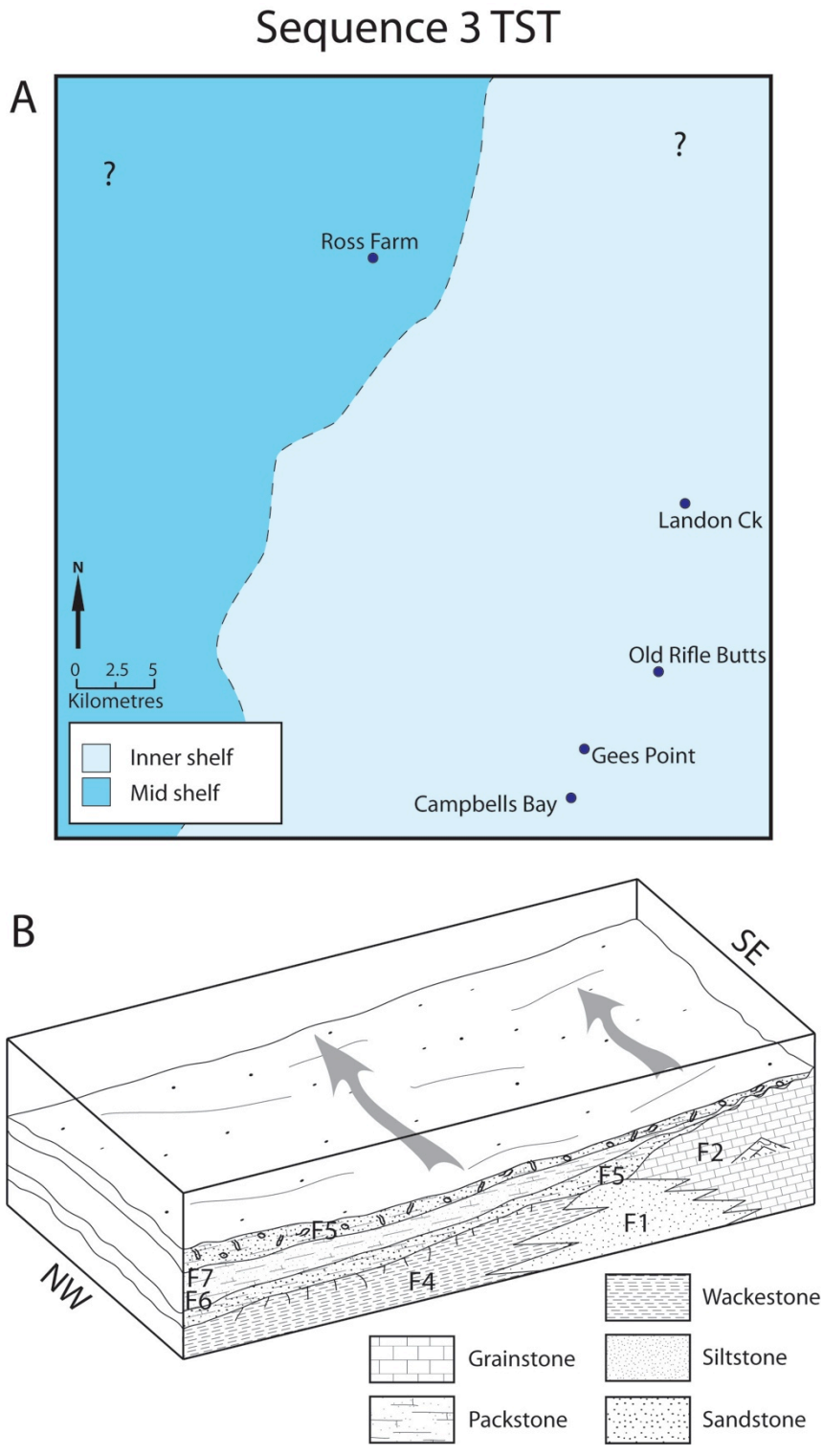

Figure 6.10. Palaeomap and schematic block diagram of the study area during the TST of Sequence 3. A: Map showing the palaeobathymetric variation relative to stratigraphic sections. B: Stylised section showing the more uniform geometry of the sea floor in the study area and simplified submarine current flow, leading to deposition of the Calcareous Greensand (F5) facies across the region.

From this point onwards, the eastern palaeohigh would have eventually become covered by an eastward-prograding shoreline and a seaward-sloping sigmoidal siliciclastic sequence, accompanied by uplift and eventual subaerial exposure. This process can be observed on most shelfal environments around the world during the Oligocene.

6.4 Discussion

6.4.1 Palaeobathymetric influence on facies development

Kamp and Nelson (1988) suggest that sea-floor relief such as that resulting from the volcanic activity occurring between the Kaiatan and Whaingaroan Stages in the eastern region, is highly advantageous for establishment of a cool-water carbonate factory, particularly where terrigenous input is occurrring. These authors point out that this is frequently achieved by active faulting, where parts of the sea-floor are pushed out of surrounding lower-relief areas, providing environments fit for colonisation and carbonate accumulation. This is particularly likely when terrigenous sedimentation rates are unable to maintain pace with the rate of uplift, and thus are not able to smother the factory.

This is illustrated by a mid-Pliocene example in eastern North Island (Kamp *et al*., 1988; Caron *et al*., 2004), where a carbonate factory established itself in shoal areas on and around isolated upthrust antiforms that were separated from the mainland (and thus terrigenous sediment supply) by a forearc basin seaway. There, this resulted in mixed siliciclastic-carbonate facies in the landward direction, while the carbonate factory remained relatively siliciclastic-poor as a result of its position atop a basin high.

This example shares many similarities with the facies developed during the highstand of Sequence 1, where there is certainly a zone of high relief in the eastern region caused by volcanic activity, around which the shallow marine, siliciclastic-poor Bryozoan Grainstone (F2) facies is located. This may explain the stratigraphic gradational contact

between the outer-shelf, non-calcareous Glauconitic Siltstone (F1) facies (deposited during the Kaiatan) that developed into the mixed calcareous-siliciclastic outer-shelf to upper-slope Impure Wackestone (F4) facies between the Runangan and Whaingaroan Stages. Prior to development of the carbonate factory on the eastern high, the western region would have been supplied primarily with siliciclastic sediment until the end of the Kaiatan Stage; but with development of the carbonate factory in the east (indicated by the presence of the Bryozoan Grainstone (F2) facies between the Runangan to early Whaingaroan Stages), detrital carbonate mud began to be supplied downslope to the western region, resulting in development of the Impure Wackestone facies.

This eastern high would therefore also have resulted in a lateral variation in facies, with the mixed-siliciclastic carbonate sediments of the outer-shelf to upper-slope Impure Wackestone facies in the west grading laterally into the Bryozoan Grainstone facies in the east. These different facies suggest that, like examples from Kamp and Nelson (1988) and Caron (2005), this eastern high was isolated from siliciclastic sediment supply, while the deeper and more land-proximal western region accumulated sediment from western terrigenous siliciclastic sources, and as carbonate mud shed downslope from the newly established eastern carbonate factory (Fig. 6.5).

6.4.2 Development of a submerged rimmed platform within the study area

Cool-water carbonates, unlike their tropical counterparts, are dominated by heterozoan assemblages consisting primarily of benthic foraminifera, bryozoans, echinoderms, molluscs and coralline algae (Lees and Buller, 1972; James, 1997; Pedley and Carannante, 2006). Any colonial coral associations are not hermatypic species, so any biological framework structures rarely exceed decimetre-scale relief (Schlager, 2005; Pedley and Carannante, 2006). The resulting lack of reefs to protect against wave and

storm energy causes most cool-water carbonates to develop ramp geometries (Fig. 6.11) (Pomar, 2001; Pedley and Carannante, 2006). Storm events are thus detrimental to a carbonate factory, often leading to partial destruction; while carbonate muds are often carried to the outer ramp where deep-water facies or channel networks are found (Schlager, 2005; Pedley and Carannante, 2006).

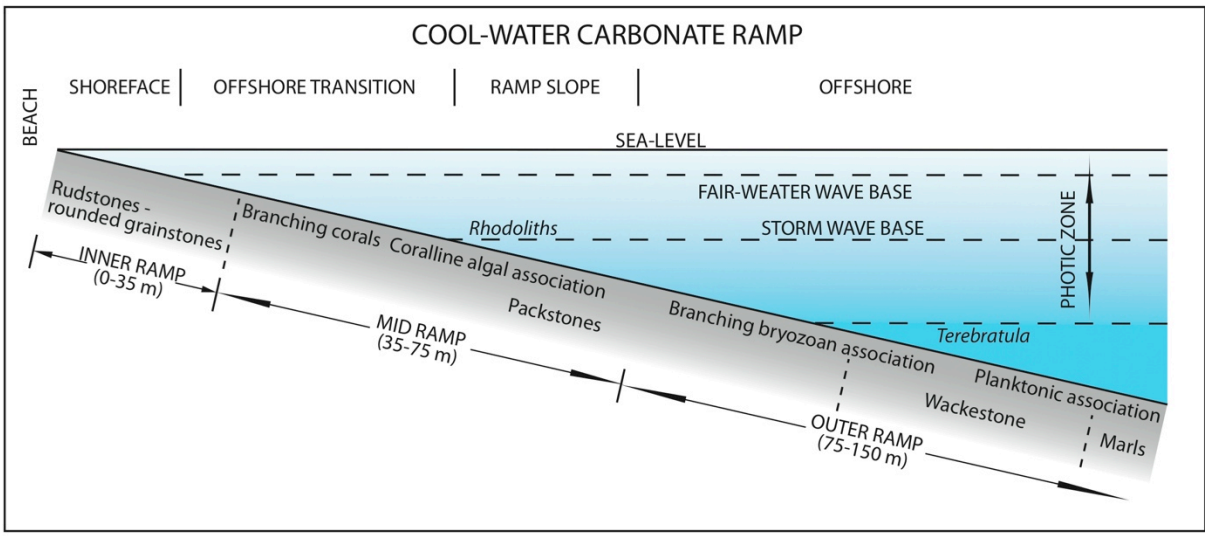

Figure 6.11. Cool-water carbonate ramp profile illustrating biota variation and depth control. Adapted from a Mediterranean Pleistocene example (Reading and Collinson, 1996; Pedley and Grasso, 2002).

Where volcanic seamounts are present, as was clearly the case in the eastern region during the Oligocene, narrow carbonate aprons or haloes can develop, with high sediment mobility and bioclast attrition rates, leading to development of grainstones and packstones (Pedley and Carannante, 2006; James *et al*., 2011). Once sufficient sediment has accumulated for the creation of bioclastic shoals, sheltered 'lagoonal' environments can sometimes develop (Pedley and Carannante, 2006). These volcanic seamounts can locally increase biodiversity in the tuffs to two to three times that of limestones as a result of

increased nutrient supply, and can lead to local warming of waters and a change from heterotrophic to mesotrophic assemblages (James *et al*., 2011).

The sequence stratigraphic model (Chapter 5) and the palaeogeographic reconstructions presented here, illustrate the variations in water depth that occurred across the study area. This variation was first inferred through the Bryozoan Grainstone (F2) and Rhodolith Rudstone (F3 facies being located in the eastern region, while at the same time the more siliciclastic-rich wackestone and packstone facies were deposited (e.g. Impure Wackestone (F4) facies) in the western region. While this lateral facies variation fits within the typical cool-water carbonate-ramp model (Fig. 6.11), the mid- to outer-shelf wackestone and packstone facies found in the western region contain a much higher siliciclastic content relative to those in the east - not what would be expected within a simple ramp setting, where siliciclastic supply would be derived from land exposed near the high-energy facies.

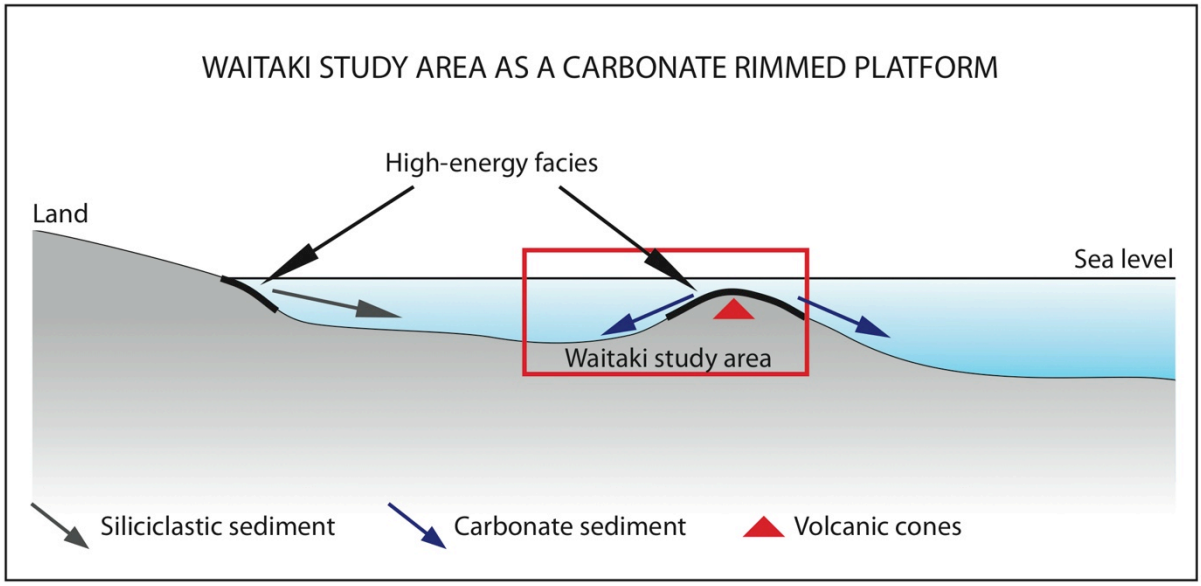

Figure 6.12. Simplified figure illustrating the location of the Waitaki study area within a submerged rimmed platform setting. The supply of carbonate mud from the eastern palaeohigh is shown shedding both east and west, where in the west it mixes with siliciclastic sediment from distal landmasses. Adapted from Schlager (2005).

Therefore, while rimmed platforms are unusual in cool-water carbonates due to their lack of reef-building organisms, the presence of the volcanic structures here allowed for fortuitous development of such a rim by providing a solid topographic high on which carbonate colonisation could take place (Fig. 6.12). The study area thus developed as a submerged rimmed platform, rather than as the more common carbonate ramp, with the highest-energy environments occurring around the eastern region and the volcanic palaeohigh, before steepening to both the east and west into lower-energy and deeper environments (Fig. 6.12). This explains the deepening of facies towards the western region from the eastern high, even though siliciclastic content also increases westward with depth, as the landmasses supplying this sediment were located further west still, and made up the main landmass between which the deeper facies in the western region developed.

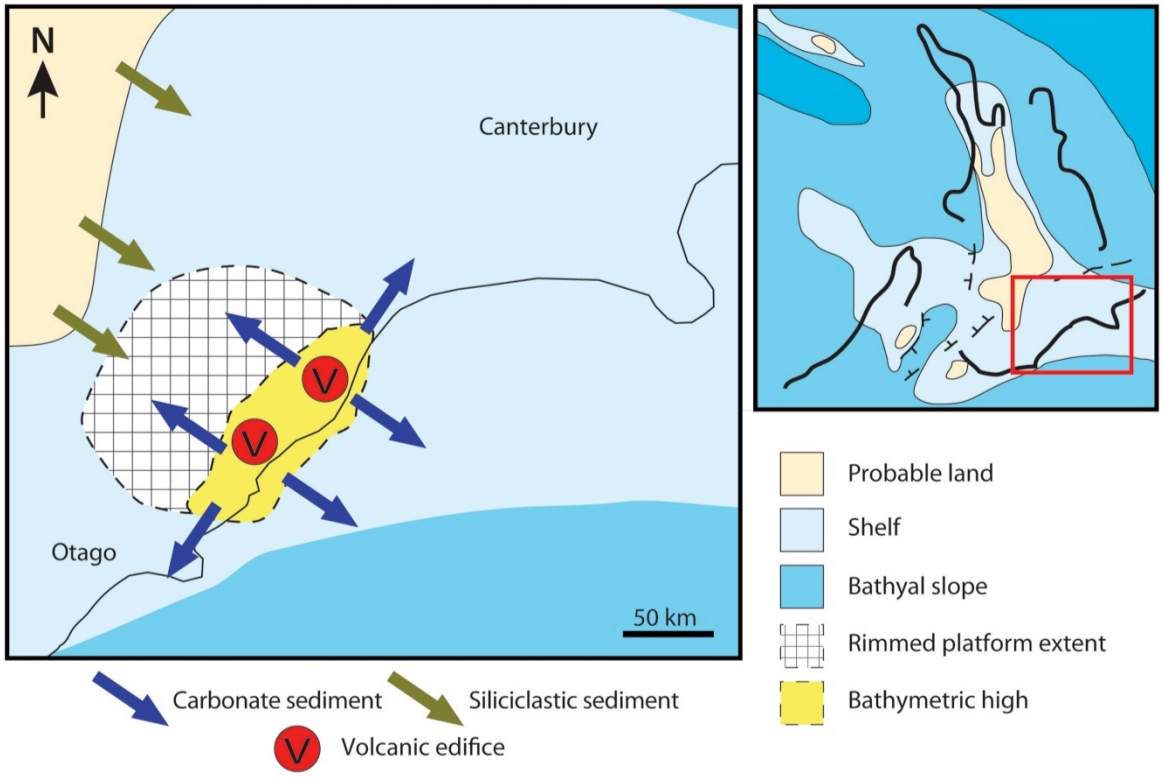

Figure 6.13. Regional scale map showing the likely extent of the rimmed platform present in the study area during the mid Cenozoic.

While locally these facies point to a rimmed platform in the Waitaki area, this feature was unlikely to have extended further out into the wider Canterbury or Otago regions (Fig. 6.13). In those areas we would expect to see more of the classic cool-water carbonate ramp morphology dipping towards the east.

6.5 Chapter summary

The palaeogeography of the study area was defined by the presence of an eastern volcanic-induced palaeohigh which exerted significant influence on the evolution of the basin, eventually resulting in development of a submerged rimmed carbonate platform, of which the study area formed the eastern, westward-dipping section. Volcanic activity occurred throughout the basin, with tuff cones, sills, dykes, and pillow lavas developed between the Kaiatan and early Whaingaroan Stages of Sequence 1. Activity was clearly most dominant in the eastern region, however, where numerous tuff cones were emplaced along the modern coastline. Siliceous sediments were produced and settled in calmer areas around the high, with these areas being both produced by the volcanic activity, and protected from high-energy storm events by its mass.

These igneous formations developed a significant palaeohigh in the eastern region that became the setting for a productive and isolated cool-water carbonate factory, devoid of the terrigenous input seen to the west. The muddier western region facies developed as a result of mixing of siliciclastic sediment (from terrigenous sources further west) with carbonate mud shed downslope from this eastern carbonate factory. A reduction or stagnation in siliciclastic supply, even during lower relative sea levels and higher carbonate production through this succession, suggest that the western landmasses were reduced to very low relief, affecting their ability to supply sediment to the basin.

Two major lowstands resulted in subaerial exposure of the eastern palaeohigh, producing a barrier and causing the funnelling of current activity around it. This barrier was likely to have continued even while submarine, blocking all but the larger currents from the south; while significant storm events that did sweep over it reworked any sediment that had accumulated there and redeposited it to the north.

Furthermore, the sustained high-energy environment in the east, following SB2, limited the ability of the area to accumulate sediment, and resulted in significantly thinner sequences in the Duntroonian and Waitakian Stages. The western region, however, was able to develop significant thicknesses of carbonate sediment due to the lower relative sea level following SB2. Eastward-flowing currents transported sediment through the study area, particularly in the northern region, and may have served to transport some glauconite to the eastern palaeohigh from the already developed Calcareous Greensand (F5) facies in the western region.

These observations demonstrate that the existence of a palaeohigh in a cool-water carbonate environment can have a significant effect on the evolution of the region, altering current and storm patterns, and stimulating entire carbonate factories to develop where they might otherwise not have. Detailed sedimentological analyses and sequence stratigraphic interpretations thus provide useful tools in indicating the existence of such features.

CHAPTER 7 – ALTERNATING CARBONATE AND AUTHIGENIC DEPOSITIONAL ENVIRONMENTS

7. Introduction

Glauconite production is often characteristic of low to negative sedimentation rates, and tends to be associated with condensed sections and unconformities in both siliciclastic and carbonate settings (McRae, 1972; Amorosi, 1995; Kelly and Webb, 1999). Within siliciclastic systems, glauconite-rich deposits are often found within the latter parts of the TST, HST, and associated maximum flooding surfaces (MFS) (McRae, 1972; Amorosi, 1995; Kitamura, 1998; Pekar *et al*., 2003; Banerjee *et al*., 2012). Glauconite precipitation can occur during the LST as long as sedimentation rates are low (McRae, 1972). Phosphate also forms in organic-rich, oxygen-depleted low-sedimentation environments, often associated with condensed surfaces (Glenn *et al*., 1994; Pufahl and Grimm, 2003).

While these condensed surfaces occur in all types of marine settings, the siliciclastic and carbonate (both the tropical and cool-water) realms share certain traits, but also differ in many ways. Siliciclastic systems are formed from detrital sediment transported into the basin, whereas tropical carbonate systems produce grains *in situ* by biological and chemical precipitation. The cool-water carbonate realm combines aspects of both in that it produces sediment *in situ*, almost exclusively through biological rather than chemical means; and, as these sediments are not biologically bound, they are heavily reworked in a manner similar to siliciclastic systems (Schlager, 2003). Cool-water carbonates therefore form similar architectures to siliciclastic systems, consisting of seaward-dipping ramps that lack the protective reefs so common in tropical latitudes.

Within siliciclastic systems, the MFS often signals a decrease in sedimentation rate and development of shelfal condensed surfaces as terrigenous supply is shut off, favouring glauconite production. In contrast, cool-water carbonate factories are able to continue producing sediment down to significant depths under highstand conditions, well below the photic zone, with this often being the most productive period within the sequence (Schalger, 2003). Glauconite and phosphate production have been shown to require an environment of low sedimentation under suboxic reducing conditions (Kelly and Webb, 1999; Pufahl and Grimm, 2003), although this contrasts with analogues of modern cool-water carbonate factories that have been shown to require high oxygen levels, with *in situ* productions rates of up to ~ 10 cm/1000 years (James, 1997; Schlager, 2003). The presence of significant levels of these authigenic minerals is therefore problematic as an indictor of the HST within the cool-water carbonate depositional realm, while they appear to be diagnostic of it within siliciclastic systems.

This Chapter discusses the depositional environment of authigenic mineral formation within the Waitaki study area (Fig. 7.1), particularly concerning production of glauconite and francolite within the cool-water carbonate realm.

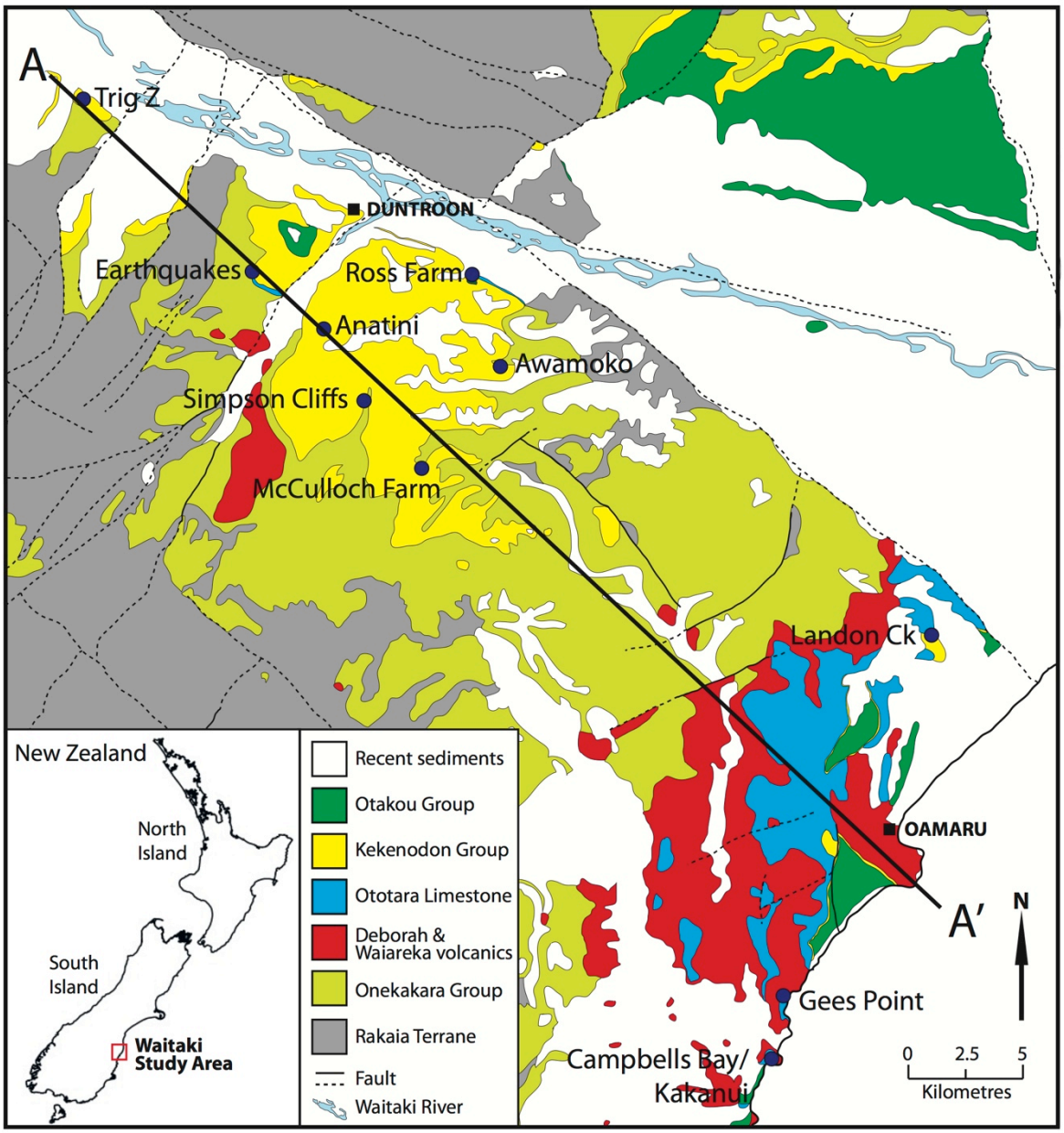

Figure 7.1. Geological map of the Waitaki study area showing stratigraphic locations of interest in this chapter. The cross-section line is that used in Section 7.5 (Fig.7.5**)**. Adapted from Forsyth (2001).

7.1 Authigenic minerals

Glauconite and phosphate are important authigenic minerals within the study area, often occurring together in the Calcareous Greensand (F5) facies found overlying lowstand unconformity surfaces (see Section 3.2.5). This section presents the properties of these minerals, their modes of formation, and occurrences in the modern setting.

7.1.1 Glauconite

7.1.1.1 Properties of glauconite

The term "glauconite" loosely refers to a group of hydrated iron and potassium micas which are found either as sand-sized (100 – 500 μm) grains, or as pigmented minerals infilling cracks and voids or replacing pre-existing minerals (McRae, 1972; Odin and Matter, 1981). Odin and Matter (1981) found that potassium shows significant variability in glauconite, and provides information on grain maturity; with immature, slightly evolved, evolved and highly evolved glauconite containing 2 – 4 %, 4 – 6%, 6 – 8% and > 8% K_2O respectively (Odin and Matter, 1981; Amorosi, 1997).

Glauconite is usually green in colour, ranging from dark green and almost black to a pale greenish-yellow (James, 1966; McRae, 1972). These colour changes are related to the amounts and forms of iron and aluminium present; with colour ranging from a grey or pale-brown in early precursors to the signature green glauconite colour, through to a mature and well-crystallised dark green glauconite mineral (McRae, 1972, and references therein). Therefore these colour changes can be also be used as indicators of grain maturity.

7.1.1.2 Formation of glauconite

Glauconite formation is restricted to sedimentary rocks, and is most commonly found in marine environments (although it has been observed in lacustrine and alluvial settings), where it is both authigenic and allogenic (McRae, 1972).

There are two principal theories concerning mechanisms of glauconite formation:

1. The "layer lattice theory" (Burst, 1958a; 1958b), whereby glauconite production requires a degraded layer silicate lattice, an available source of iron and potassium, and a suitable redox potential. Absorption of potassium and iron by the degraded lattice leads to

a reduction in the number of expandable layers, which in time leads to formation of glauconite (Hower, 1961; McRae, 1972). This process would be halted by burial, supporting the observation that glauconite-dominated environments are generally those with low sedimentation rates (Hower, 1961). It is thought to eliminate any original mineralogy that is not glauconitic in the mature mineral, leaving little trace of its origins (Burst, 1958a; Hower, 1961).

2. The "mechanism of verdissement" (Odin and Matter, 1981; Odin and Fullagar, 1988). The layer lattice theory does not account for development of glauconite between mica and clay sheets (rather than replacing them); the common glauconitisation of granular and hardground calcareous substrates; differing authigenic minerals from the same substrate; the lack of a continuum between aluminous and ferric clay structures; or the geochemical difficulty of losing aluminium while gaining iron. In the verdissement mechanism, glauconite evolution begins and proceeds close to the sediment-water interface within a granular environment, but relatively independent of that environment's mineralogy (Fig. 7.2). In this environment, glauconite crystal growth occurs in pore spaces and may extend across entire grains, imparting an early green colouration (2 – 4% K_2O). During this process, substrate minerals are progressively removed as they are in disequilibrium with the pore-fluid that is precipitating the glauconite, allowing for more pore-space to develop more glauconite. Growth then tends to continue from the centre of the grains, producing cracked grain rims in the more mature and evolved minerals (6 – 8% K_2O). These cracks are finally filled by lower-potassium glauconite precipitation, producing a rounded and highly evolved glauconite grain (K_2O > 8%), as mineralisation occurs preferentially within the cracks rather than on the outer grain surfaces (Odin and Fullagar, 1988).

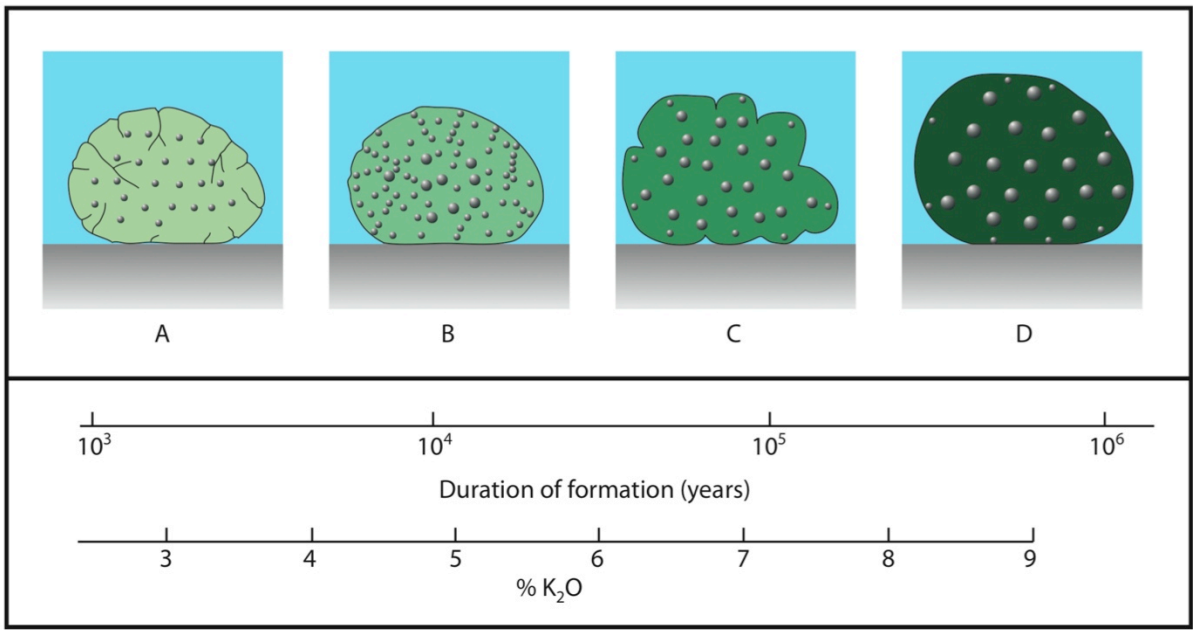

Figure 7.2. The evolution of glauconite within a granular substrate. A: Nascent stage. B: Slightly-evolved stage. C: Evolved stage. D: Highly-evolved stage. The dots represent glauconite minerals, with relative size denoting increased crystal growth. The grain is ~ 5 mm in diameter and lies at the sediment/sea-water interface. Adapted from Odin and Fullagar (1988).

Both theories predict that formation of glauconite will cease if the environment becomes unsuitable, either by burial from open seawater, or sea-level change (Odin and Fullager, 1988). Furthermore, glauconite growth is favoured by the presence of a suitable microenvironment, such as within foraminiferal tests or larger calcareous grains (Odin and Fullager, 1988). Ions necessary for the evolution of glauconite may thus come from both interstitial fluids and seawater, as well as from the substrate itself. While there is still controversy between these two competing theories, both allow for smectitic precursors to the glauconitisation process (Odom, 1984; Baioumy and Boulis, 2012).

The time frames estimated for glauconite evolution vary, with the initial stages appearing quite rapidly, within a few thousand years, although uptake of potassium reduces with time. It can require one million years or more for a highly evolved glauconite grain to develop (Odin and Fullagar, 1988).

7.1.1.3 Modern environments of glauconite production

Glauconite grains are common on many modern continental shelves at water depths of 50 – 500 m (Odin and Fullagar, 1988; Amorosi, 1997), but are most abundant on the outermost shelf and upper-slope at 200 – 300 m depth (Odin and Matter, 1981). Where glauconite has accumulated in areas not conducive to glauconitisation, such as those of non-marine environments or with high sedimentation rates, it is likely to be allochthonous (Amorosi, 1997). Most autochthonous glauconite is confined to the outer-shelf and slope environments (Odin and Fullager, 1988). In temperate areas however, glauconitisation is commonly found at depths as shallow as 30 m (Porrenga, 1967; McRae, 1972).

Glauconitic facies are found at latitudes from 50ºS to 65ºN, indicating no specific climatic conditions are required for its precipitation (Odin and Matter, 1981).

7.1.2 Phosphate

7.1.2.1 Properties of mineralised phosphate

Phosphogenesis in the marine environment is the process of phosphate mineral precipitation within sediments, usually within centimetres of the sediment-water interface (Glenn *et al*., 1994; Föllmi, 1996).

The most common phosphate mineral in early diagenetic marine environments is francolite (e.g., McClellan, 1980; Nathan, 1984; Föllmi, 1996). It has a complex chemical composition as a result of significant substitutions within its structure, and has been approximated empirically by Jarvis *et al*. (1994) as:

$$Ca_{10-a-b}Na_aMg_b(PO_4)_{6-x}(CO_3)_{x-y-z}X(CO_3{\cdot}F)_y(SO_4)_2F_2$$

7.1.2.2 Formation of francolite

Francolite precipitation occurs either directly, through crystallisation onto surfaces of minerals or biological hard parts, or through dissolution and replacement of existing minerals (usually $CaCO_3$) (Föllmi, 1996). These precipitates serve as nuclei for further francolite precipitation until dissolved phosphate is depleted (Föllmi, 1996). Francolite forms authigenically just below the sediment-water interface in an organic-rich environment, with low or negative sedimentation rates at associated hiatus surfaces (Glenn *et al*., 1994; Pufahl and Grimm, 2003). It cannot form too far below the sediment-water interface, or be buried too rapidly (Glenn and Arthur, 1988; Föllmi *et al*., 1991).

Phosphogenesis is often viewed as occurring in two main phases, with the primary period encompassing the physicochemical and biochemical *in situ* processes of precipitation; distinct from the secondary stages of hydraulic and biological reworking of francolite clasts (Baturin, 1971; Glenn *et al*, 1994).

Primary phosphogenesis appears to generally precipitate francolite directly from the dissolved phase, near the sediment-water interface and in the suboxic zone, close to the redox boundary (Glenn *et al*., 1994; Föllmi, 1996). Microbial breakdown of organic matter and release of organic phosphate to pore waters within the sediment is considered the most common mechanism (Fig. 7.3A) (Föllmi, 1996). The interstitial phosphate produced may diffuse up to the sediment/sea-water interface, especially if anaerobic bottom waters are present; with this being dependent on redox-dependant absorption/desorption processes of phosphate into iron and manganese oxyhydroxides, and the ability of microbes to store phosphate under oxic conditions (Gächter *et al*., 1988). Iron oxyhydroxides are significant carriers of inorganic phosphate, and can often be found as aggregated colloidal particles or coatings around suspended clays (Froelich, 1988; Fox, 1990). Phosphate diffusion is also

controlled by sediment accumulation rates, sediment type, and the degree of bioturbation (Föllmi, 1996; and references therein).

In addition to the process of microbial breakdown, dissolved phosphate may also be provided to sediments from iron and manganese oxyhydroxides upon burial or through bioturbation below the redox boundary (Fig. 7.3B) (Föllmi, 1996). Oxyhydroxides produced by hydrothermal and submarine volcanic activity absorb dissolved phosphate from seawater, allowing for later desorption in the sediment substrate (Feely *et al*., 1990; Föllmi, 1996). Less commonly, phosphate can also be directly precipitated at the sediment-water interface from seawater, although this is presumed to include a microbial influence (Föllmi and Garrison, 1991; Föllmi, 1996).

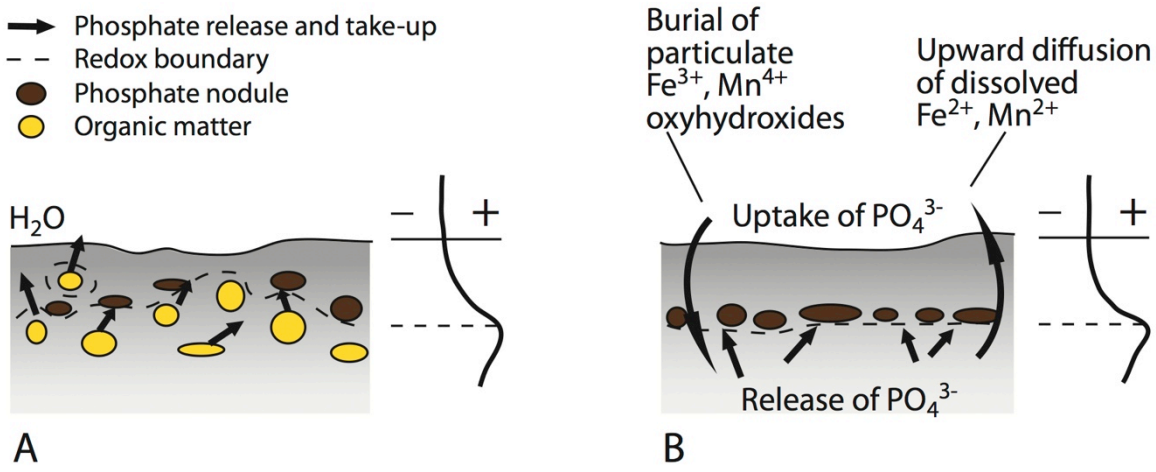

Figure 7.3. Sources of dissolved phosphate alongside curves showing phosphate in pore-water. A: In-vivo and post-mortem release of organic phosphate from *in situ* organic matter, leading to the precipitation of phosphate above the redox boundary. B: Inorganic phosphate release through the redox cycle involving iron and manganese oxyhydroxides. Adapted from Föllmi (1996).

Products of phosphogenesis occur in a number of forms, including primary phosphorite muds, hardgrounds, concretions or nodules, pellets, and lenses or layers within surrounding sediment. Phosphate can also occur as francolite coatings or crusts,

replacement of original lithology, or as precipitate within bioclasts (Glen *et al*., 1994; and references therein). These various forms are often considered as occurring during early sedimentation or diagenesis, with the nodular and cemented forms often observed to deform surrounding laminations, demonstrating their formation during early-stage sea-floor diagenesis (Glenn *et al*., 1994). Most of the ancient occurrences have been associated with condensed horizons, hiatuses and unconformities (Glenn *et al*., 1994).

The secondary stage of phosphogenesis involves transported phosphatic grains, with sediments being dominated by phosphatic pellets, and also containing coated and intraclast grains which show evidence of reworking (Glenn *et al*., 1994).

7.1.2.3 Modern environments of phosphate production

Modern phosphate-rich locations are characterised by current-dominated sedimentary regimes coupled with low sediment accumulation rates (Föllmi, 1996), and with currents being the prime driver behind the rates of sediment aggradation and reworking (Baturin, 1971). These locations are also associated with areas of high productivity in their surface waters, in conjunction with upwelling of phosphate-enriched waters (Föllmi, 1996).

7.2 Methodology

7.2.1 Facies analyses and microscopy

Lithofacies were developed in Chapter 3 using both outcrop and thin-section analyses (Chapters 2 and 3, and Appendix D). The samples collected covered all variations in lithology, and were analysed petrographically. Here, particular attention is paid to the concentration and nature of glauconite and francolite within each facies, both in outcrop and thin section, with a focus on glauconite maturity and grain interaction.

7.2.2 Stable isotopes

Oxygen and carbon isotopic analyses provide a useful tool in assisting with the interpretation of sedimentary environments, especially distinguishing carbonate sediment origins and identifying diagenetic processes (Hudson, 1977; James and Choquette, 1983; Nelson and Smith, 1996). Here this method was used to determine the depositional environment associated with concentrated francolite precipitation following lowstands, in order to confirm whether or not precipitation of francolite occurred on the sea floor.

Nine francolite-coated hand samples were collected from the Calcareous Greensand (F5) facies in Sequence 3 at Gees Point (Fig. 7.1) (see Section 3.2.5 and 5.2.8), all from within the first metre above SB3 (see Section 5.2.7). These nodules comprised francolite-encrusted bioturbation traces, francolite-coated sediment clumps, and dense francolite-dominated nodules.

Mass-spectroscopic analyses for determination of $\delta^{13}C$ and $\delta^{18}O$ values involved ~ 500 µg powdered samples (milled from phosphate nodules using a Dremel Rotary Tool with a diamond-tipped drill bit), composited and loaded in 12 ml exetainer vials, which were then flushed with ultra-high-purity helium using a GC-Pal autosampler connected to a Thermo Finnigan GasBench II. Orthophosphoric acid (~ 100 µl) was added to each helium-filled vial. Carbon dioxide, liberated by the resulting reaction, was injected into a PoraPlot Q gas chromatography column (at 30°C) for gas-phase separation and subsequent elution into a ThermoFisher Delta V Plus mass spectrometer (with helium carrier gas). $\delta^{13}C$ and $\delta^{18}O$ values were determined using the Isodat software package. Precision was assessed by analysis of certified reference materials (NBS18; NBS22) and a pure carbonate internal lab standard (MERCK). Internal and external precisions were better than 0.08 ‰ and 0.25 ‰ for $\delta^{13}C$ and $\delta^{18}O$ respectively. Five sample powders were milled from each hand sample in an effort to constrain the intra-sample isotopic variability. Only

the carbonate fraction of powdered samples, derived from both the francolite mineral itself and the detrital carbonate component of the nodules, was analysed for stable isotopic compositions.

7.3 Results and interpretations of glauconite production

This section presents the variations in glauconite found within the study area, and provides interpretations as to its formational history within the facies.

7.3.1 Lithofacies and glauconite types

Glauconite is abundant in the Glauconitic Siltstone (F1) and Calcareous Greensand (F5) facies, and is a distinct component of the Impure Wackestone (F4), Massive Glauconitic Packstone (F6) and, to a lesser extent, the Cross-bedded Glauconitic Packstone (F8) facies (see Chapters 2 and 3 for full stratigraphic and facies descriptions).

Within the Glauconitic Siltstone (F1) and the Impure Wackestone (F4) facies, the glauconite grains are commonly medium to dark green with a fractured grain boundary present throughout, indicating a relatively evolved nature. These grains are likely parautochthonous to allochthonous, and exhibit weathered and darkened rims, suggesting a degree of reworking prior to deposition. Less common, are lighter green, small glauconite grains and occasional glauconitised micas, which are likely to be the result of *in situ* precipitation. These less-evolved grains are more common in the Impure Wackestone facies of Ototara Limestone than in the older Glauconitic Siltstone facies of Raki Siltstone. These facies thus do not represent a primary environment for significant autochthonous glauconite precipitation.

The glauconite content of the Calcareous Greensand (F5) facies of Kokoamu and Gee Greensands is somewhat different, as it appears to represent two phases of

autochthonous precipitation. The cores of most glauconite peloids are a light to medium green, and often show cracks indicating expansion during growth (Odin and Morton, 1988) or possibly dehydration during evolution (McRae, 1972). This is considered here to be the first phase (phase 1) of glauconite precipitation, consisting of grains of slightly to moderately evolved glauconite, exhibiting common sympathetic boundaries with neighbouring grains. This indicates that they are likely parautochthonous to autochthonous, and probably formed early during development of the facies.

A second phase (phase 2) is commonly found within and around bioclasts, often filling the tests of foraminifera, or less commonly glauconitising echinoderm plate fragments. It shows common pale green rims around the more mature peloids from phase 1, as well as 'healing' within the grain cracks. This phase is likely to represent the later prime producing, or pristine, glauconite facies and, coupled with the presence of the earlier phase of parautochthonous to autochthonous glauconite, suggests that the Calcareous Greensand (F5) facies represents the environment most conducive to glauconite production within the study area.

7.4 Results and interpretations of phosphate production

This section presents the occurrences of the two principal forms of mineral francolite in the study area, followed by the results of stable isotope analyses on francolite nodules.

7.4.1 Lithofacies and phosphate types

Mineral francolite occurs within the Calcareous Greensand (F5) facies on top of two major LST sequence boundaries (SB2 and SB3) (see Section 2.2.4.3 and 2.2.4.6). The francolite found in this study occurs as two types: (1) as single coatings over lithic clasts

and glauconitic grains, burrows, and phosphatised nodules, and (2) as precipitated coatings on amalgamated unconformities at Gees Point (Fig. 7.1). As with the glauconite (see Section 7.3), the phosphate precipitation is found almost entirely above these unconformity surfaces and, in the case of the grains, it is all within the Calcareous Greensand (F5), particularly in the lower part of this facies.

7.4.2 Geochemistry of francolite

Five sample powders were taken from each of the nine hand samples, giving a total of 45 results from the various francolite nodules overlying Sequence Boundary 3 (Appendix F). The five results for each sample were averaged.

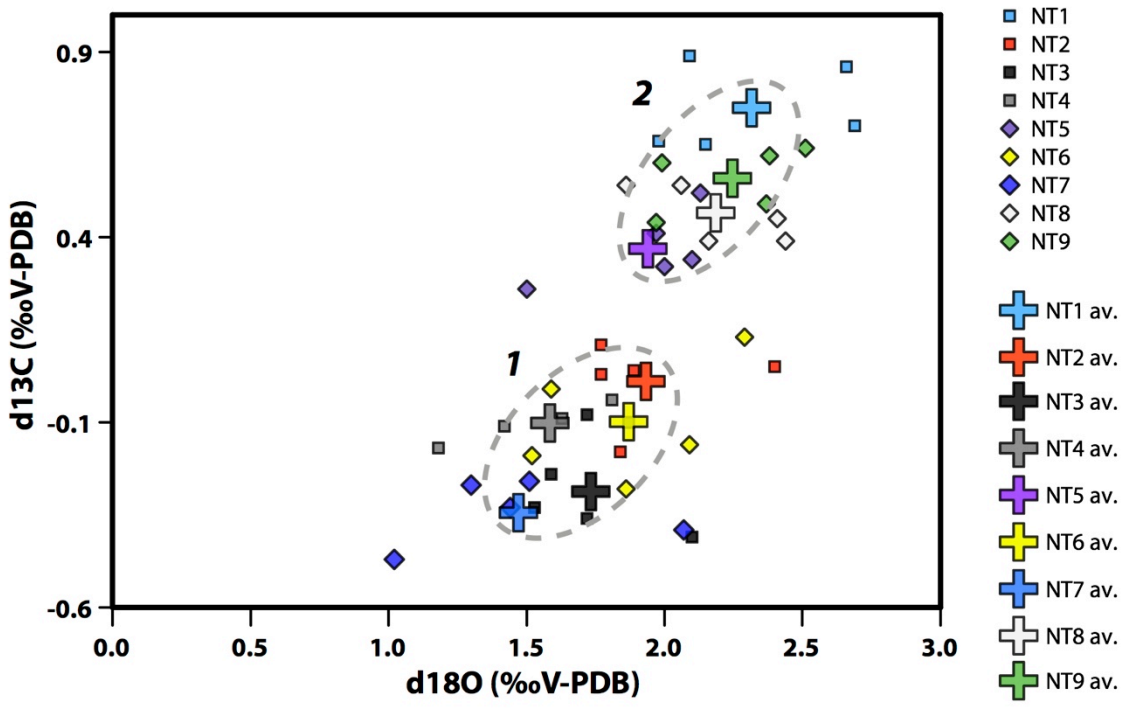

Figure 7.4. $\delta^{13}C$ and $\delta^{18}O$ bivariate plot for the carbonate fraction derived from francolite nodules in the Sequence 3 Calcareous Greensand (F5) facies at Gees Point (Fig. 7.1). All five individual results from each of the nine nodules, as well as the average for each sample, are presented. The averages are shown as two statistically different groupings based on a Student t-test.

The 45 individual and nine averaged results are presented in Fig. 7.4 where $\delta^{13}C$ values are plotted against $\delta^{18}O$. The $\delta^{13}C$ values ranged -0.47 to +0.89 ‰, while $\delta^{18}O$ values ranged 1.02 to 2.69 ‰. Overall, results are tightly clustered within these ranges. Two distinct sub-clusters are apparent (Fig. 7.4) for the averaged results although these have no bearing on the present discussion.

7.5 Sequence stratigraphic context

7.5.1 Glauconite

The Calcareous Greensand (F5) facies formed during the TSTs following the lowstand sequence boundaries (SB2 and SB3, and to a lesser degree after SB2a; see Sections 5.2.4.1, 5.2.5, and 5.2.8.1). The presence of the two glauconite phases within this facies implies therefore that phase-1 glauconite must have begun to precipitate on the sequence boundary during lowstand and early transgression, with deposition and further precipitation of phase-2 glauconite taking place as the TST progressed.

Within the study area, clays were likely to have been supplied to the system during sea-level lowstands, when the shorelines of any low-lying landscapes to the west, comprising Rakaia Terrane, would have been more proximal to the basin (Fig. 7.5B) (see Sections 6.3.1 and 6.4). These landscapes have already demonstrated their ability to produce fine particles for deposition in the older Glauconitic Siltstone and Impure Wackestone facies (see Sections 3.2.1, 3.2.4, and 5.2.2.1). It is likely to have been these clays which supplied material for glauconite precipitation during lowstands, resulting in significant glauconite grain production during these LSTs. Accumulation of these grains was probably minimal, however, as the lowstand Sequence Boundaries represent periods of non-deposition and erosion (see Sections 5.2.3 and 5.2.7). With the onset of transgression, glauconite began to steadily accumulate as the often cross-bedded

Calcareous Greensand (F5) facies (Fig. 7.5C). Glauconite precipitation would have occurred continuously throughout the TST, indicated by the presence of significant autochthonous grains observed within this facies and the deeper Massive Glauconitic Packstone (F6) facies.

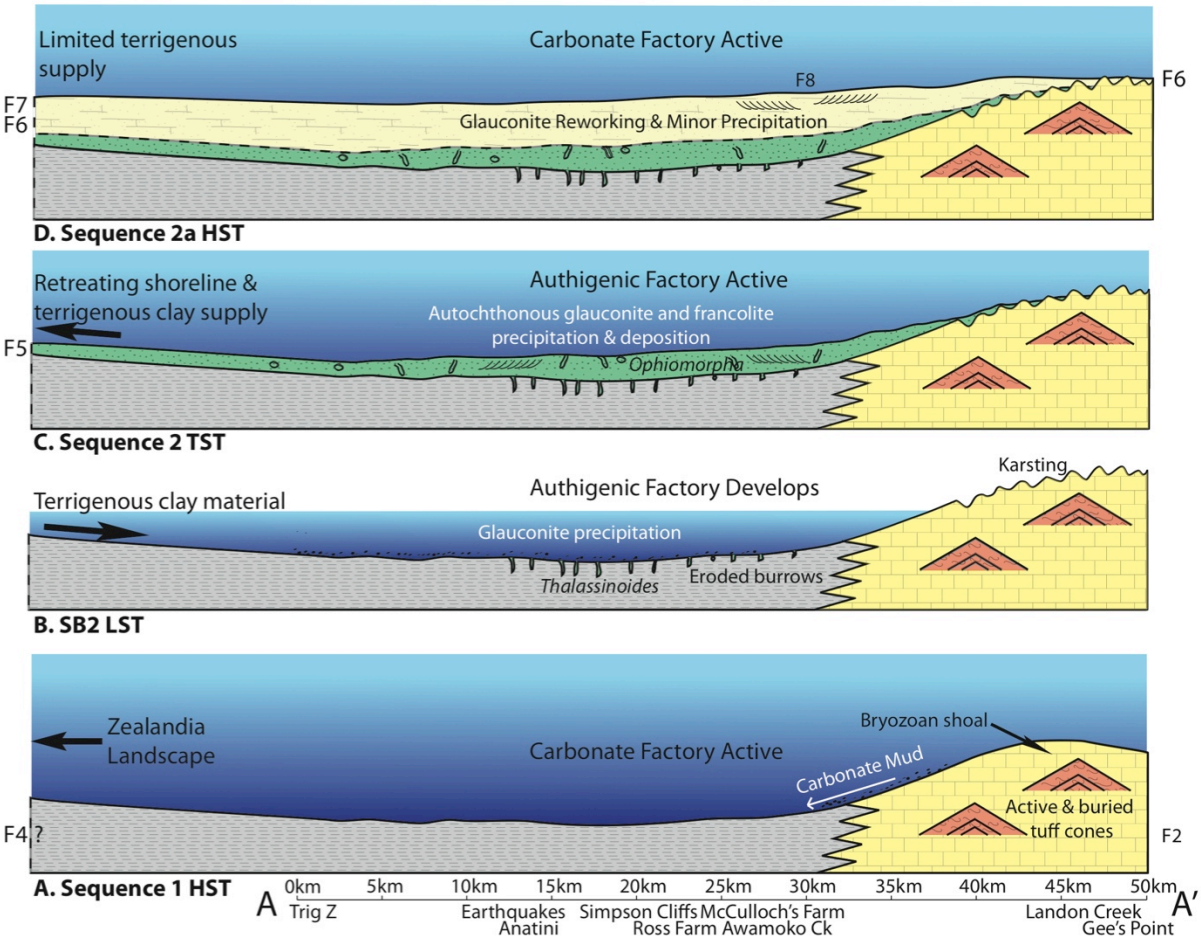

Figure 7.5. Schematic cross-sections through the Waitaki study area, along transect A-A', Fig 7.1, illustrating the alternation between the carbonate and the authigenic factories. A: HST in the mapped area, illustrating the variable depths between the eastern shoal and the deeper west. The carbonate factory was active during this period. B: LST, during which supply of terrigenous clay material is increased to the basin allowing for increased glauconite production. C: TST when clay supply is reduced and energy levels decrease, allowing for the deposition of greensand substrates and further autochthonous glauconite and francolite development. D: A return to a HST and the cessation of authigenic production in favour of the carbonate factory, as a result of the drop in clay material and an increase in sedimentation rates. Sequence 3 repeats the processes presented in B and C, beginning at SB3.

Higher energy levels during lowstand and early transgression would have resulted in local reworking of glauconite grains, with some transportation of grains towards the east being likely, as shown by the eastern palaeoflow indicators present within the Cross-bedded Glauconitic Packstone (F8) facies in the northern region (see Section 6.2.1.1). As transgression continued, local energy levels decreased, allowing increased settling of glauconite grains to accompany further phase-2 precipitation, using both the more-evolved grains of parautochthonous glauconite and reworked bioclastic fragments as nuclei for new glauconite growth.

7.5.2 Phosphate

7.5.2.1 Francolite coatings

Precipitated coatings of francolite occur on top of the karst SB2 surface at Gee's Point, where it is amalgamated with SB3 (see Section 2.2.4.6). Where the Calcareous Greensand (F5) and Massive Glauconitic Packstone (F6) facies sit above the SB2 contact at this location, there is no phosphatic coating (including in a small depression at Gee's Point overlain by the Massive Glauconitic Packstone). Where the Calcareous Greensand facies of Sequence 3 lies directly on top of the Bryozoan Grainstone (F2) facies of Sequence 1, however, a second coating exists over the first.

During lowstand, these sequence boundaries on the eastern palaeohigh were subaerially exposed (Fig. 7.5B), and were clearly not accumulating sediment as they were being subjected to meteoric diagenesis (see Section 4.7.1.1). As sea-level transgression began and these locations were eventually submerged, most began to accumulate sediment (Fig 7.5C). In at least one location (Gee's Point), however, some parts of the SB2 surface remained without any sediment accumulation during Sequences 2 and 2a, a period when high-energy conditions were sweeping this area clear. In these locations, devoid of any

sediment cover, francolite coatings can be found. At other localities where at least some sediment overburden formed, francolite coatings did not form. It seems, therefore, that the coated sequence boundary surfaces are likely to have developed during the TST, HST, and FSST - otherwise these coatings would be expected to have also developed where sediment was accumulating, and not just where the surface was exposed.

7.5.2.2 Francolite nodules

The stable carbon and oxygen isotope francolite nodule data presented in section 7.4.2 is plotted in Fig. 7.6 over fields showing generalised environments of precipitation and diagenesis for New Zealand temperate carbonates (from Nelson and Smith, 1996). Taken from the carbonate portion of francolite nodules (derived out of both the francolite mineral and detrital carbonate mud) from the lower portion of the Sequence 3 Calcareous Greensand (F5) facies (see Section 5.2.8.1), both of these plots show that the carbonate in this facies developed in a temperate seafloor environment and has not been subjected to any diagenetic processes (see Section 4.2). As these carbonate samples were drilled from francolite nodules, including clearly *in situ* bioturbation traces, this places the environment of francolite precipitation within the seafloor environment.

The two distinct isotope ratio groupings (Section 7.4.2, Fig. 7.4) may represent different carbonate sources of the samples (i.e., from francolite and detrital carbonate components), although some samples were simply higher in carbonate than others. The magnitude of differences between the two groups is insignificant in the application here, however, where only gross differences between systems are considered (they coalesce in the scales of Fig. 7.6). Both groups thus fall within the same environmental setting, and are not considered further in the present context.

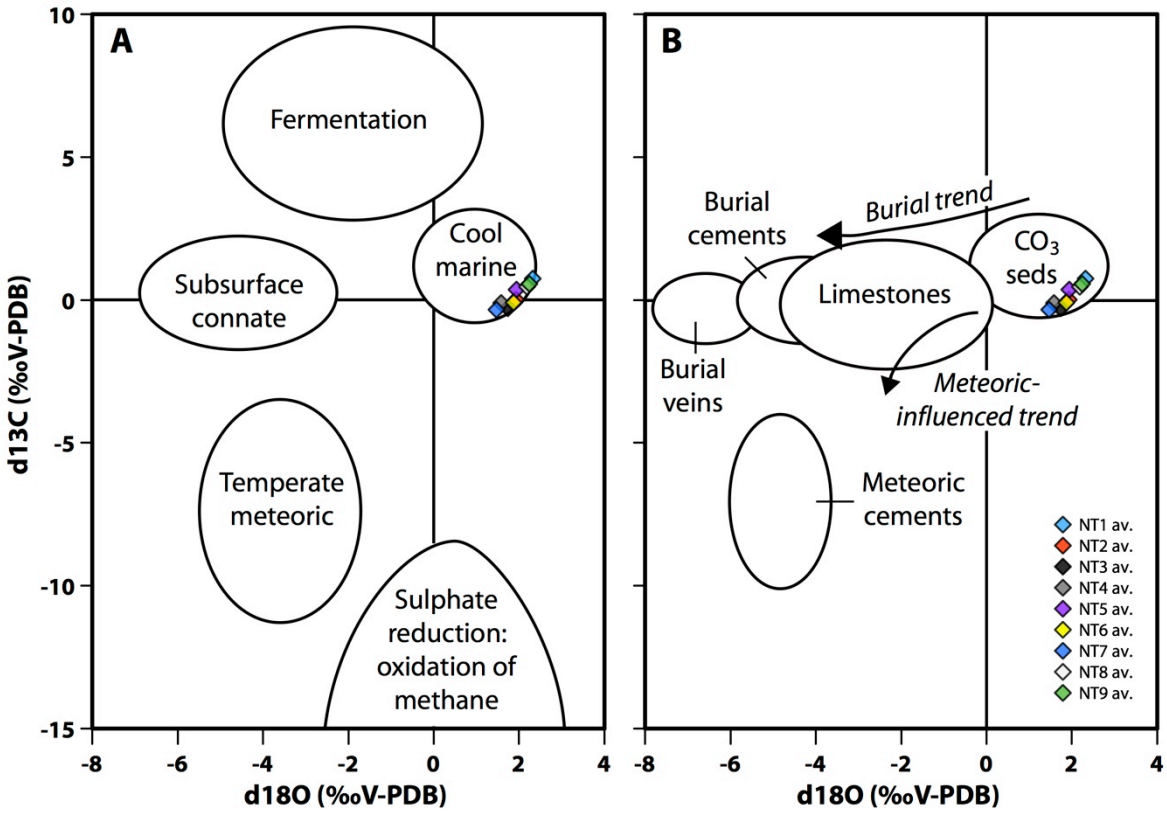

Figure 7.6. Generalised isotope bivariate plots containing the average datapoints from francolite nodules from this study (Section 7.4.2) overlain on inferred environmental and diagenetic categories for New Zealand temperate carbonates. A: Generalised isotope fields of inferred environmental categories for New Zealand carbonate precipitates, showing the francolite nodules developed in the cool marine environment. B: Generalised isotope fields showing the diagenetic trends towards burial and meteoric diagenesis. The francolite data plots in the marine carbonate sediments field, indicating no diagenetic alteration. Generalised plots adapted from Nelson and Smith (1996).

The abundance of francolite nodules present *in situ* in the lower part of the Calcareous Greensand facies in Sequence 3 indicates that their development must have taken place during the shallower parts of the TST, at the same time as significant glauconite precipitation (Fig. 7.5C). Iron and manganese oxyhydroxides, likely to have been supplied from eroding volcanic tuffs, may have further increased the supply of inorganic dissolved phosphate to porewaters during periods of lowered sea level. This would have further increased the rate of francolite precipitation during the early TST. The

higher abundance of francolite nodules in the eastern region supports the possibility of a supply of oxyhydroxides from volcanic material, as these are prevalent in areas proximal to tuff cones. The main period of phosphogenesis must thus be placed within the early TST.

7.5.3 Transition to Carbonate Factory

Increasing sea levels progressively resulted in less glauconite and francolite precipitation and an increase in carbonate production (Fig. 7.5D), whereby the cool-water carbonate factory began to out-produce the authigenic minerals. In the western region of the study area, in deeper palaeoenvironments, a thicker accumulation of Sequence 2 and 2a facies exists (see Sections 5.2.4 and 5.2.6). Here a gradational transition of decreasingly glauconitic to more-calcareous facies is evident - from the Calcareous Greensand (F5) facies, through the overlying Massive Glauconitic Packstone (F6), to the Bedded Packstone (F7) facies (Fig. 7.5D) (see Sections 3.2.5, 3.2.6, and 3.2.7). The latter facies represent the later TST and HST, respectively (see Sections 5.2.6.1 and 5.2.6.2).

It is inferred that with increased sea level during the HST, the supply of terrigenous clay particles and volcanic detritus was limited, while sedimentation rates increased as a result of the higher rates of carbonate production, and thus authigenic glauconite and francolite precipitation was significantly reduced. The conditions were then right for the development of the carbonate factory and the cessation of any further significant authigenic mineral precipitation (Fig. 7.5D).

7.6 Discussion

Glauconite- and francolite-rich facies within the study area are located consistently above lowstand karst surfaces or firmgrounds. The presence of francolite nodules and

glauconite grains often indicates an environment of nil to low sedimentation within an organic-rich, reducing-environment (see Section 7.1). Sea-level lowstands induced high-energy submarine environments and subaerial exposure across the study area (see Sections 5.2.3 and 5.2.7), resulting in regional exposure of low-lying western basement rocks. This allowed the shedding of fine-grained terrigenous clays derived from schistose rocks eastwards into the study area, fuelling glauconite precipitation. Francolite precipitation may have been enhanced during these events by the supply of iron and manganese oxyhydroxides from eroding volcanic tuff cones.

Sea-level lowstand caused the eastern palaeohigh to be subaerially exposed, and thus resulted in the cessation of production at the offshore bryozoan carbonate factory at this location (see Section 5.2.3). Once this area was again submerged during subsequent transgression, glauconite and francolite precipitation began in an environment of low sediment accumulation resulting from the absence of any significant carbonate production (Fig. 7.5B).

Further transgression led to the low-lying western basement landmasses shutting off the supply of precursor clays, oxyhydroxides, and micas needed for glauconitisation and phosphogenesis (Fig. 7.5C). At the same time, flooding of the basin to mid- and outer-shelf depths reinvigorated carbonate production, which then became the dominant sediment-producing factory (Fig. 7.5D), smothering glauconite- and francolite-favourable environments as sedimentation rates increased. These two factories clearly had a gradational relationship, whereby the onset of carbonate production (with conditions that favoured the carbonate factory) inhibited or terminated production from the authigenic factory.

These changes between authigenic and carbonate factories could be recognised in other carbonate settings where lowstand unconformities are found overlain by glauconitic

and phosphatic facies, which then grade into increasingly calcareous, but decreasingly glauconitic, facies associated with increasing water depth. As these facies variations were caused by an increase in terrigenous input, supplying detritus for glauconitisation during these lowstands, the key to this alternation between these two 'factories' is the increase in terrigenous supply to moderate levels. If siliciclastic input had become too high, it would have smothered any authigenic factory, and led to development of dominantly clastic facies. Once depth and the environmental conditions become favourable to carbonate production, however, glauconite will be phased out in favour of more calcareous facies developed by an active carbonate factory - a process that could be recognised by the change from authigenic to carbonate facies.

7.7 Conclusions

The Waitaki study area contains sequences that record glauconitic- and francolite-rich facies developed early in the TST, followed by an increasingly calcareous HST. During the subsequent lowstand and early sea-level transgression, fine-grained, clay-rich terrigenous material, as well as reworked volcanic tuffs, were supplied to the area. This environment favoured precipitation of authigenic glauconitic grains and francolite nodules, and continued through subsequent transgression, with areas proximal to volcanic sediments exhibiting a higher rate of phosphogenesis. Coupled with low sedimentation rates during periods of lowered sea level, these environments favourable to authigenic mineral production are termed the 'authigenic factory'.

As transgression continued and sea level approached highstand, the supply of terrigenous clays and oxyhydroxides was significantly reduced, and glauconite and francolite mineral production decreased, with the system reverting to a carbonate factory. Increased sediment accumulation rates reduced precipitation and maturation of authigenic

minerals. These controls for the production of authigenic components existed at and following lowstand (before instigation of a carbonate factory), with an authigenic factory operating in the absence of significant carbonate production.

Alternation between an authigenic and carbonate factory could be recognised in other carbonate sequences, where glauconitic and phosphatic facies overlying a LST graded into more calcareous facies through a sea-level transgression and subsequent highstand. The key to this process is that terrigenous supply not become too significant, as this would lead to increased sedimentation rates and the smothering of any authigenic glauconite- or phosphate-producing factory, instead producing dominantly clastic facies. Rather, a supply comprising principally fine terrigenous clay for glauconitisation during lowstands favours the establishment of the authigenic factory.

CHAPTER 8 – MID-CENOZOIC NEW ZEALAND: THE WAITAKI REGION IN CONTEXT

8. Introduction

The study area within the Waitaki Basin is only a small part of the larger New Zealand-wide setting, where several regions host mid-Cenozoic sedimentary successions. Each of these regions (identified in Section 8.2.2) records local responses during the regional lead-up to maximum submergence and subsequent re-emergence caused by the 1st order megasequence (see Section 1.1.4**)**. The study area must be placed within this larger context in order to distinguish between events observed in the sequence stratigraphy which are regional and those resulting from local effects, thus identifying features of the Waitaki sequence stratigraphy which apply to the greater New Zealand region.

Current literature describing mid-Cenozoic New Zealand is summarised here, including the tectonic and palaeogeographic setting, and the geology of the seven major regions (see Section 8.2.2) developed over the Zealandia landmass during this period. This information is compared with that developed during the present project for the study area, in order to illuminate insights provided by the Waitaki sequence stratigraphy concerning the palaeogeography and sea-level history of New Zealand. A prime factor here is a correlation of regional sea-level history (recorded in Chapter 5) with syn-depositional sediments in other New Zealand regions, including variations in sediment lithology together with the presence, nature, and age of any local unconformities.

8.1 Tectonic history of Zealandia

Tectonic history is obviously implicated in any comparisons between mid-Cenozoic sediments in the study area and those found elsewhere in New Zealand. An understanding of this history is necessary in reconstructing spatial relationships existing between the various sedimentary basins at the time, and in determining effects of tectonic activity on local sea-level variations. A review of mid-Cenozoic tectonics of New Zealand is therefore provided here.

8.1.1 Mid-Cenozoic tectonic reconstructions of New Zealand

The mid Cenozoic tectonic history of New Zealand, from mid Eocene to mid Miocene, is intimately bound to the development and evolution of the Australian-Pacific plate boundary (King, 2000) (Fig. 8.1 and 8.3). This boundary began to evolve in the mid to Late Eocene within a zone of extension south of New Zealand (Molnar *et al*., 1975; Carter and Norris, 1976; Norris *et al*., 1978; King, 2000). It was followed by gradual propagation northward, reaching southern Taranaki in the Late Eocene to Oligocene (Carter and Norris, 1976; King and Thrasher, 1996; King, 2000).

By the beginning of the Miocene, early transcurrent movement along the modern Alpine Fault had begun (Ballance, 1976; Kamp, 1986a; King, 2000; Batt *et al*., 2004; Schellart *et al*., 2006). This new Alpine Fault cuts across earlier extensional basins formed in the Eocene-Oligocene, indicative of the two different tectonic regimes involved in the evolution of this plate boundary (Ballance, 1976; Kamp, 1986a, 1986b).

The different time-periods are described in the following Sections. For conversions between these international epochs and the New Zealand Stage names used elsewhere in this chapter, refer to Fig. 1.4.

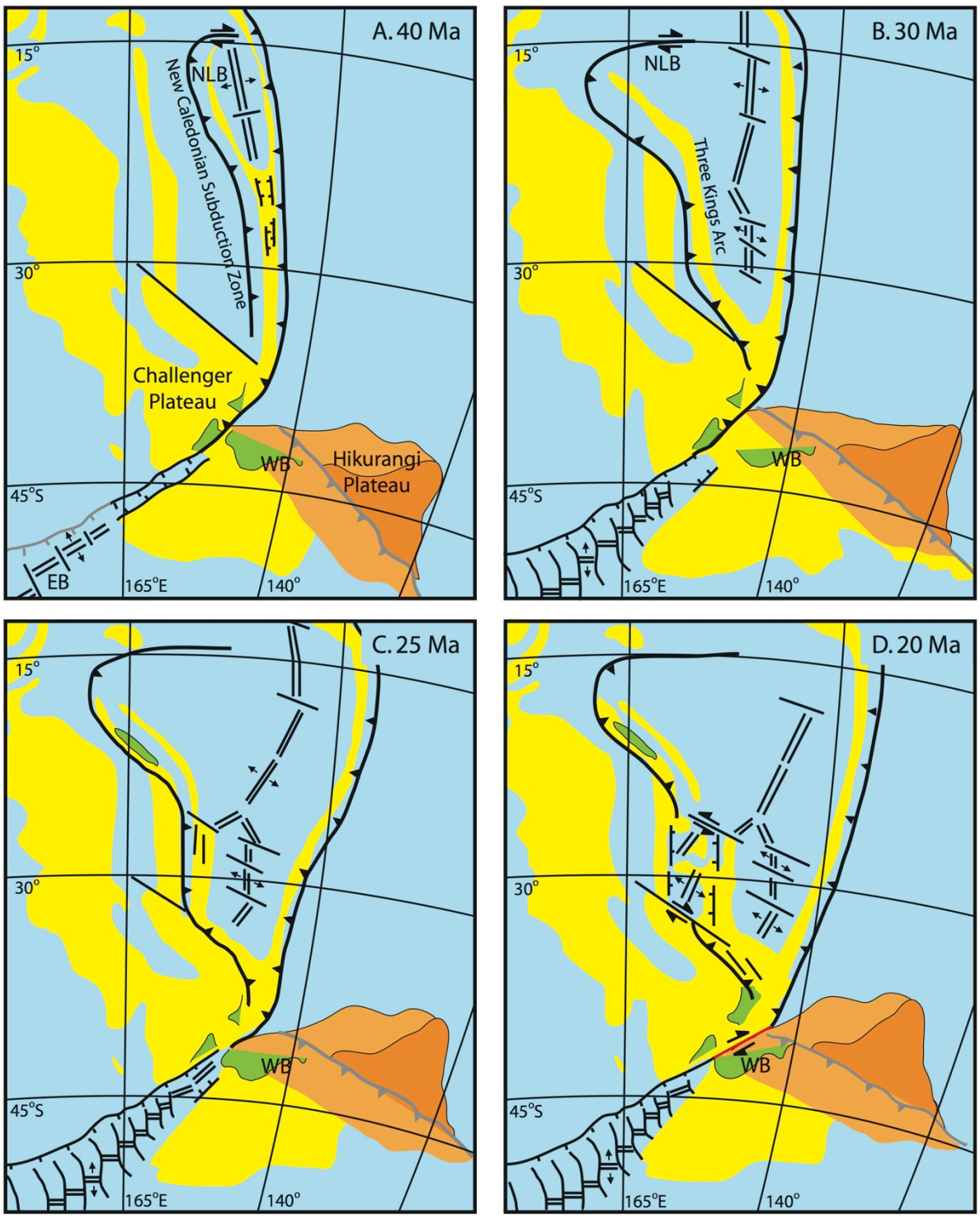

Figure 8.1. Four time-slice maps of the New Zealand region from 40 Ma to 20 Ma, with a focus on the development of the tectonic regime during this period. The darker part of the Hikurangi Plateau is at the surface, while the lighter colour represents the subducted portion. The landmasses are intended to show the approximate location of these areas, and do not provide any comment on the palaeogeography. The red line in (D) is the Alpine Fault, while grey lines represent inactive tectonic features. WB- Waitaki Basin; NLB – North Loyalty Basin; EB – Emerald Basin. Adapted from Schellart *et al*. (2006) and Reyners (2013).

8.1.1.1 Mid Bortonian to mid Runangan (40 – 35 Ma)

Around 45 Ma (Porangan Stage), westward-dipping subduction in the proto-Tonga-Kermadec Trench began to the north of New Zealand, extending into northern New Zealand and leading to development of reverse faulting and shortening in that region (Müller *et al*., 2000; Stagpole and Nicol, 2008). South of New Zealand, the Emerald Basin began to open at 45 Ma (Sutherland, 1995). By 40 Ma (mid Bortonian), this southern spreading centre was well established, leading to initial development of the plate-boundary system northward through New Zealand (Fig. 8.1A) (King, 2000). This change, from northern convergence to southern extension, has been attributed to interference by the western tip of the subducted Hikurangi Plateau, blocking subduction (Reyners, 2013).

From the Bortonian to the Kaiatan Stages, a series of small basins, trending mostly north-south or northeast-southwest, formed in the western Southland (Turnbull *et al*., 1993), West Coast (Nathan *et al*., 1986), south Taranaki (King and Thrasher, 1996), and Waikato (Edbrooke *et al*., 1994) regions. Around Northland, single ENE-trending basins were developing at the same time (Isaac *et al*., 1994). These basins eventually linked up to form a north-trending system through central western New Zealand, the forerunner of the modern plate boundary (King, 2000).

The basins of western New Zealand, including Western Southland, West Coast, and offshore southern Taranaki, all contained extensional regimes and were dominated by normal faulting through to at least the Whaingaroan Stage (King, 2000). Comparatively minor tectonic activity was occurring in the Northland, Waikato and Wanganui, and northern Taranaki regions during this period, giving little indication as to the nature of the proto-plate boundary in these areas (King, 2000). Eastern New Zealand remained relatively stable tectonically, due to its isolation from the development of the western tectonic system (Fig. 8.1A) (King, 2000), remaining so until at least the Whaingaroan (Field *et al*., 1997).

8.1.1.2 Whaingaroan (34 – 28 Ma)

During the Whaingaroan Stage, eastern areas continued to develop as an effectively passive margin (Ballance, 1993); while subsidence was prevalent in western Southland (Turnbull *et al*., 1993), brought on by active extension in the Emerald Basin between 40 and 30 Ma (Fig. 8.1B) (Wood *et al*., 1996). The Pacific-Australian pole of rotation, some distance north of the Emerald Basin, induced much of this extension (Sutherland, 1995). A west-to-southeast-dipping subduction zone to the north of New Zealand continued to propagate southwards, arriving near Northland by 30 Ma (Fig. 8.1B) (Schellart *et al*., 2006), and is associated with the development of arc volcanism in Northland (Hayward, 1993).

The nature of the tectonic zone through the North Island, linking the southern extension with the northern subduction, was likely to have been a zone of deformation, with strain distributed along a series of major north-south-trending en echelon fault systems (King, 1990; 2000). Many of the major basement faults present in these areas may have been accommodating dextral strain throughout the Oligocene (King, 2000). The Waimea Fault near Nelson (Lewis, 1980) and the Taranaki Fault in the Taranaki region (Nelson *et al*., 1994) show evidence for tectonism beginning around 30 Ma, while angular boulder breccia facies suggest the presence of active fault-scarps along the West Coast in the Whaingaroan to Duntroonian Stages (Riordan *et al*., 2012; N. Riordan 2013, pers. comm.).

8.1.1.3 Duntroonian to early Waitakian (27 – 24 Ma)

Between the Whaingaroan and Duntroonian Stages, mild uplift and folding became widespread in northeastern South Island (Field *et al*., 1989; Browne, 1995), resulting from the northeast propagation of extensional basins in the south (Fig. 8.1C) (Nicol, 1992).

Uplift was also occurring at the end of the Whaingaroan west of the Taranaki Fault (Nelson *et al*., 1994), suggesting that the entire northern North Island may have come under compression (King, 2000).

By the end of the Duntroonian Stage, extension in the proto-Norfolk Basin north of New Zealand led to volcanism west of Northland (Mortimer *et al*., 1998; Hayward, 1993), while the East Coast basement block began to develop nappes as the northern subduction zone moved further south (Fig. 8.1C) (Pettinga, 1982; King, 2000). Subsidence rates in the Taranaki Basin accelerated from 25 Ma (King and Thrasher, 1996), with westward and downward displacement on the Taranaki Fault (King, 2000). Faults in Western Southland extending into the Nelson region (e.g., Waimea Fault) became transtensional during this period, as a narrow marine trough developed into the faulted Fiordland area (Turnbull *et al*., 1993).

8.1.1.4 Mid Waitakian to Otaian (23 – 20 Ma)

By the mid Waitakian (ca. 23 Ma), a major change was occurring in the northern and southern parts of the developing plate boundary, resulting in the inception of the modern Alpine Fault (Fig. 8.1D) (Kamp, 1986a; Cooper *et al*., 1987). While the origin of this major fault is vigorously debated (e.g. Kamp, 1986a; Sutherland *et al*., 2000; Reyners, 2013), it is clear throughout the various regions in New Zealand that significant tectonic changes were occurring.

In southern New Zealand, faults began to coalesce into a transfer zone that linked up the southwards-propagating subduction zone. Minor deposition of conglomerates adjacent to the transfer zone began to occur in the West Coast area, and the Buller and Greymouth coalfield areas underwent the beginnings of basin inversion (Kamp *et al*., 1996; Kamp *et al*., 1999). This area was marked by the reactivation of old normal faults as

reverse fault systems, resulting in a pattern of uplift and adjacent basin subsidence (King, 2000). Uplift near the Hope Fault, and thrust faulting in Marlborough, suggest an increase in tectonic activity in this area beginning in the mid Waitakian (Field *et al*., 1989; Lamb and Bibby, 1989).

In central New Zealand, a zone of shortening was accommodated by minor north-south-trending transtensional, transpressional, or strike-slip faults, with the entire central region under compression by the early Otaian Stage (King, 2000). This resulted in the reactivation of former extensional faults as reverse faulting (King, 2000), leading to a major change in sedimentation from carbonate-dominated to terrigenous facies (Kamp, 1986a; King *et al*., 1999). In the Taranaki basin, reverse throw on the Taranaki Fault saw 6 km of vertical displacement and the development of en echelon faulting (King and Thrasher, 1996; King, 2000).

In the Northland and East Coast regions, obduction resulted in allochthon emplacement (Ballance and Spörli, 1979; Hayward, 1993; Isaac *et al*., 1994), with thrust faults and associated debris flow in the central East Coast (Pettinga, 1982). In Northern areas of the East Coast, however, (e.g., Raukumara peninsula) there was significant subsidence and deeper marine sedimentation (Chapman-Smith and Grant-Mackie, 1971). The Three Kings arc was likely to have been contiguous with the newly-developed Northland arc by the Otaian (ca. 22 Ma) (Ballance *et al*, 1982; Isaac *et al*., 1994).

8.2 Mid Cenozoic palaeogeography and depositional environments of New Zealand

In addition to the tectonic setting and its effects on the various regions of New Zealand in the mid-Cenozoic, it is necessary to understand the depositional environments of these regions, including their relative locations with respect to one another through this

period. This section provides a brief review of New Zealand's mid-Cenozoic palaeogeography, followed by a more extensive literature review of the region's spatial and temporal facies development.

8.2.1 Palaeogeography of New Zealand

The Waitaki Basin study area is shown in Fig. 8.2 within the context of three New Zealand palaeogeographic maps modified from King *et al*. (1999) and King (2000). These time-slice maps illustrate the sea-level changes incurred as a result of the regional 1st order megasequence, in conjunction with the evolution of the tectonic setting (see Sections 1.1.4 and 8.1.1). They show that the Middle Eocene (earliest Bortonian Stage) - a period of decreasing siliciclastic input in the study area - exhibited a primarily shelf setting, in close proximity to extensive landmasses that provided a steady supply of terrigenous material. Continuing transgression in the Late Oligocene (Duntroonian to earliest Waitakian Stages) led to maximum submergence of the Zealandia landmass, when a shelf setting was still prominent but landmasses were more distal, reducing the supply of terrigenous sediment and leading to siliciclastic-poor carbonate facies. The Early Miocene (late Waitakian Stage) then saw the propagation of the new plate boundary that led to the re-emergence of land and an increase in terrigenous supply to the shelf setting.

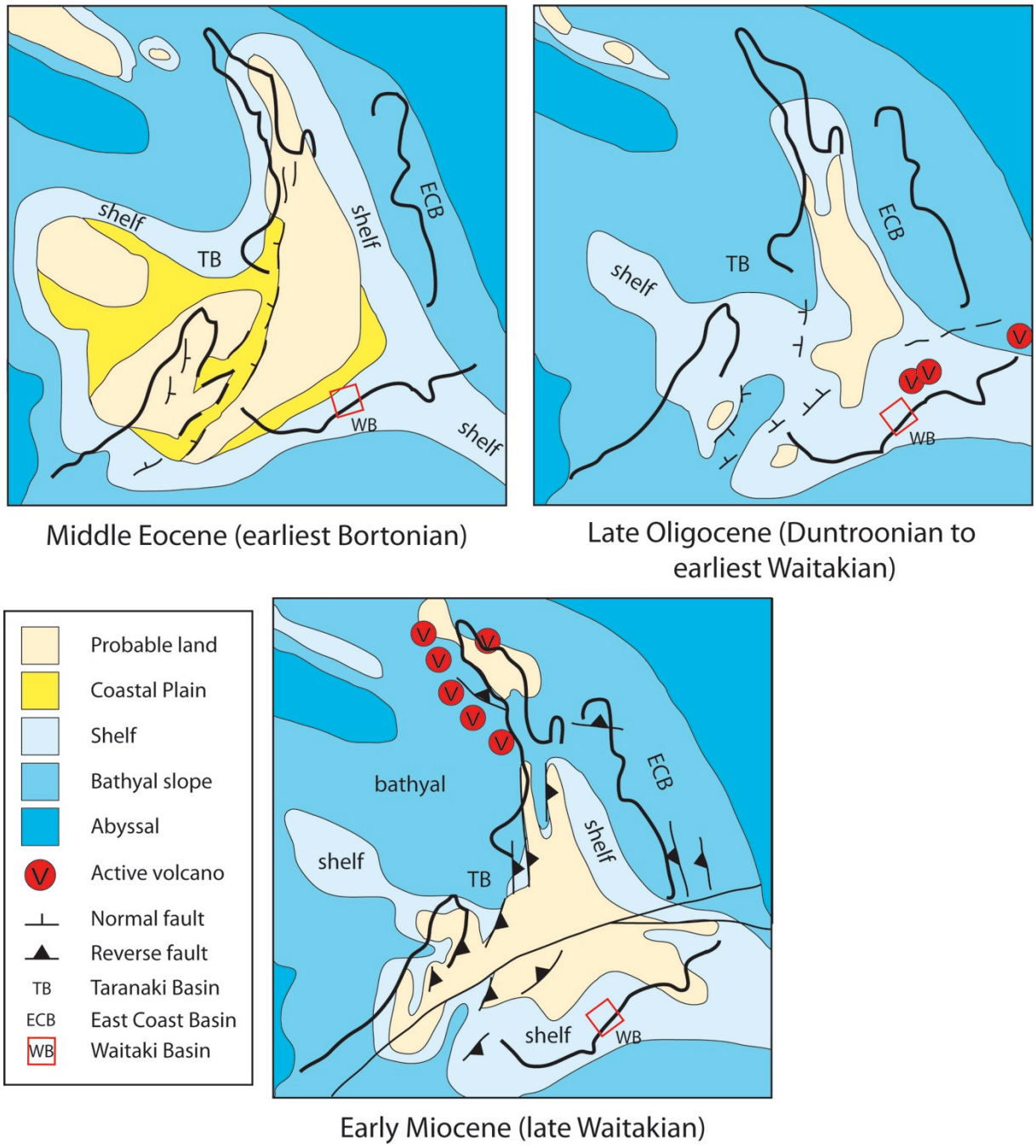

Figure 8.2. New Zealand palaeogeographic reconstructions from the Middle Eocene, Late Oligocene, and Early Miocene epochs, showing the location and estimated sea level during these periods. The Waitaki study area is indicated together with the Taranaki Basin and East Coast Basin. Figures modified from King *et al*. (1999).

8.2.2 New Zealand regional mid Cenozoic summaries

There are seven major regions around New Zealand which contain significant mid-Cenozoic (particularly mid Eocene to Early Miocene) stratigraphic successions, as shown

in Fig. 8.3 - the Northland, Taranaki, Waikato/Wanganui, East Coast, West Coast, Canterbury and Western Southland regions. This section focuses on the lithologies and facies interpretations, and how these varied with location and time. A simplified stratigraphic summary is provided for each region, including unconformities and lithological variations as shown in Fig. 8.4.

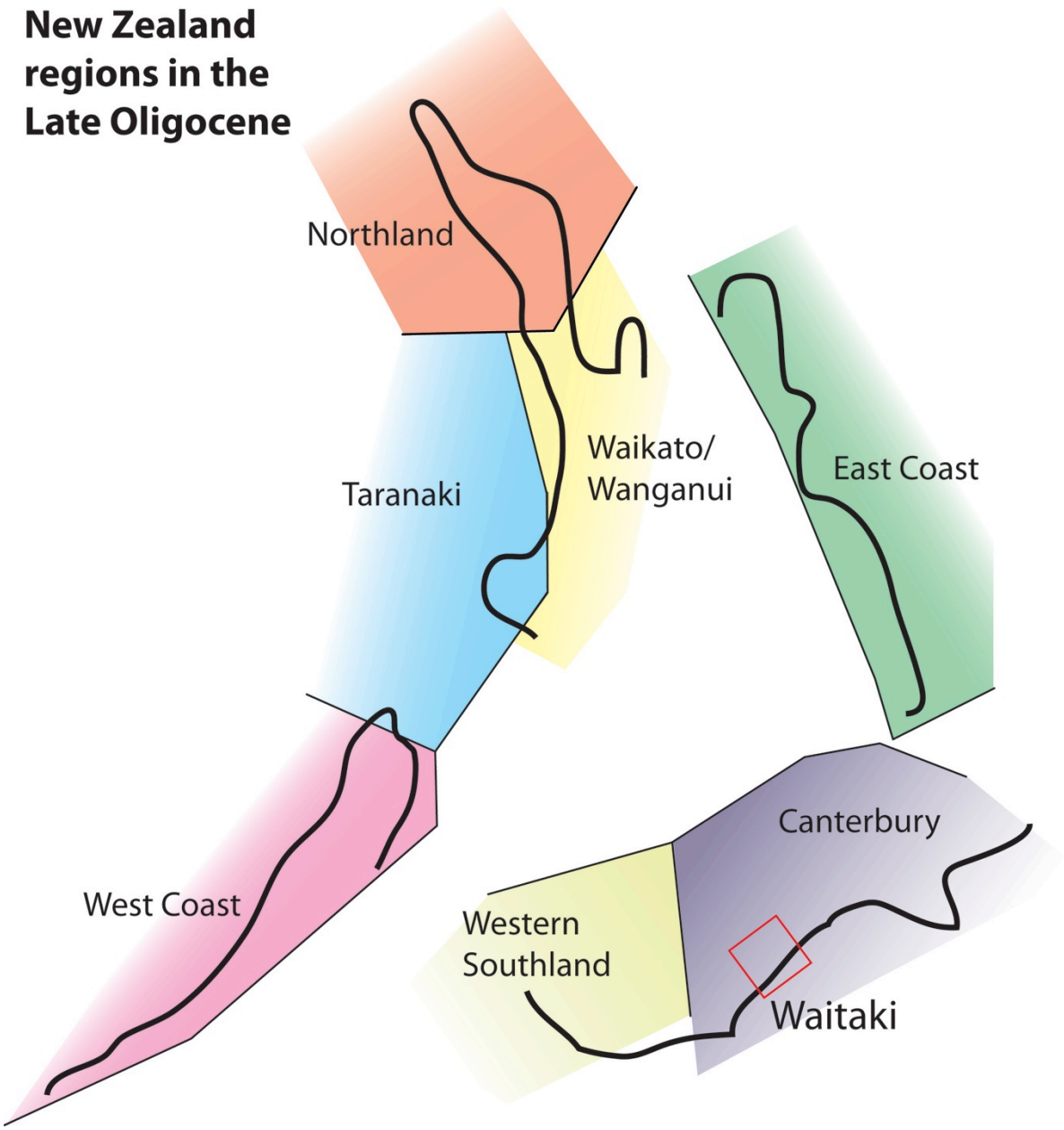

Figure 8.3. The locations of New Zealand regions discussed in this chapter, covering both North Island and South Island. The outlines of New Zealand are given for the Late Oligocene, and are representative of their locations throughout the mid-Cenozoic. The study area is labelled as Waitaki. New Zealand palaeogeographic outlines from King (2000).

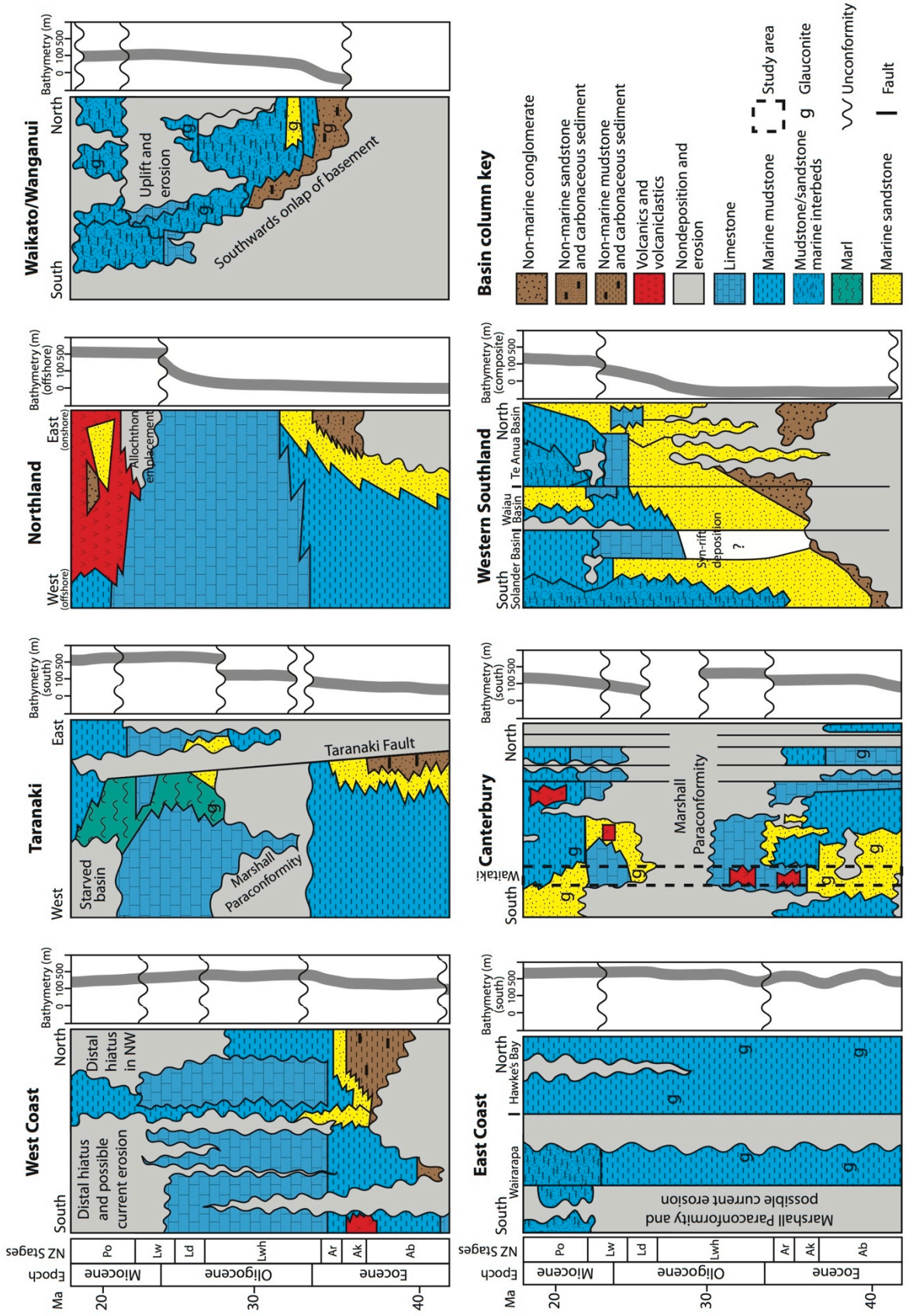

Figure 8.4. Summary stratigraphy and palaeobathymetry of seven New Zealand regions during the mid-Cenozoic. Modified from King *et al*. (1999), Lever (2001), Lever (2007), and references therein.

8.2.2.1 Bortonian to Runangan (43 – 34 Ma)

8.2.2.1.1 Northland region

The sequence for the mid-Cenozoic Northland region (comprising all areas north of present-day Helensville) (Fig. 8.3) begins with the localised Bortonian-Stage Opahi Group, consisting of greensands, mudstones, and some fine argillaceous limestone (Kear, 1964). This is overlain by Runangan to lower Whaingaroan Te Kuiti Group sediments; and, where the Opahi Group is absent, the latter rests on basement (Fig. 8.4) (Hay, 1960, Isaac *et al*., 1994). The Te Kuiti Group contains Arnold Series coal measures (sandstones, coal seams, and carbonaceous mudstones) at its base, grading into transgressive facies of glauconitic sandstones and siltstones with a non-calcareous glauconitic base, to calcareous upper facies (Hay, 1960). Locally these formations may extend to the Whaingaroan Stage.

8.2.2.1.2 Waikato/Wanganui region

The Waikato/Wanganui region covers the area from Helensville (north of Auckland) to the South Taranaki Bight (Fig. 8.3). Here the Runangan to Waitakian Te Kuiti Group shows a trangressional sequence (Fig. 8.4), no greater than 300 m thick (Nelson, 1978a; Suggate *et al*., 1978; White and Waterhouse, 1993; Anastas *et al*., 2006). The Runangan Stage begins with Te Kuiti Group sediments deposited over basement rocks, comprising non-marine to marginal marine deposits of coals and siltstones (Nelson, 1978a). Locally the coal beds are generally of Arnold Series age, but could be as young as Whaingaroan to Duntroonian towards the southeast of the region (Gregg, 1960).

8.2.2.1.3 Taranaki region

The Taranaki region lies mostly offshore on the western side of North Island (Fig. 8.3). The Palaeocene to Early Oligocene stratigraphy of this region forms the Teurian- to

Runangan-Stage marginal-marine Kapuni and marine Moa Groups; with the former being located primarily in the south of the region, while the latter is dominant in the west and northwest (Fig. 8.4) (King and Thrasher, 1996). The Kapuni Group consists of sand-rich shelf and fluvial floodplain facies, while the Moa Group tends towards fine-grained calcareous siltstones and sandstones (King and Thrasher, 1996). By the Bortonian Stage, the area of the Kapuni Group had reduced significantly with increasing transgression, as Moa Group marine sedimentation became dominant over the region, overlying the Kapuni Group. At the same time, the degree of marine influence in the shrinking Kapuni Group increased up-section (King and Thrasher, 1996).

The top of the Kapuni and Moa Groups forms a major unconformity, spanning most of the Eocene and Early Oligocene, due to Late Eocene tectonic influence and subsequent erosion (Fig. 8.4) (King and Thrasher, 1996). This unconformity shows evidence of subaerial exposure, with subsequent deposition of phosphatic pebbles and macrofossil concentrations, and is usually overlain by upper-Whaingaroan greensand, sometimes with two greensand units separated by a limestone member representing the entire Oligocene sequence (King and Thrasher, 1996).

8.2.2.1.4 West Coast region (South Island)

The West Coast region includes what is now the west and northwest of modern South Island (Fig. 8.3). During the Bortonian Stage, a period of gradual marine transgression continued into the mid Oligocene (Fig. 8.4), along with the formation and reactivation of small fault-bounded local basins separated by areas of low-lying land or shallow sea (Nathan *et al*., 1986). This resulted in the central West Coast forming an archipelago by the end of the Runangan Stage, with larger landmasses located to the north

and south (Nathan *et al*., 1986), and only the Karamea Peninsula and several low-lying areas to the south remaining above sea level (Nathan *et al*., 1986).

This transgression is reflected in the formation of the Brunner Coal Measures at the base of the Eocene, conformably overlain by shallow marine sediments including the Rapahoe Group (containing the Kaiata Formation), consisting of carbonaceous mudstone or muddy sandstone (Nathan, 1974; Nathan *et al*., 1986).

8.2.2.1.5 East Coast region (North Island)

The East Coast region includes both onshore and offshore areas along the modern east coast of North Island (Fig. 8.3). In this region, smectitic mudstones and poorly bedded, highly bioturbated calcareous mudstones with beds of glauconitic sandstones (Fig. 8.4) (e.g., Wanstead Formation) developed from the Paleocene to Eocene (Moore and Morgans, 1987; Field *et al*., 1997). These range in age from Teurian to lower Whaingaroan, but are usually no younger than Bortonian (Field *et al*., 1997). Palaeodepths average mid slope, with glauconitic facies representative of shelf deposition (Field *et al*., 1997).

8.2.2.1.6 Canterbury region

The Canterbury region extends from the Marlborough area southwards towards Dunedin (Fig. 8.3). During the Eocene, this region was an area of low relief divided by the Chatham Rise, which was then either a submarine high or a very low-lying peneplain, with outer-neritic to slope conditions to both the north and south (Field *et al*., 1989). Eyre Group units (Piripauan – Whaingaroan) begin with quartzose coal measures (Fig. 8.4) (Broken River Formation), overlain by a number of neritic sandstone, glauconitic sandstone, and mudstone formations (e.g., Waipara Greensand). These are followed by

quartz-rich sandstones and greensand (e.g., Homebush Sandstone and Waiau Greensand), grading into calcareous mudstones (e.g., Ashley Mudstone) (Field *et al*., 1989). These sediments are, in turn, overlain by Bortonian-to-Runangan micritic limestones (e.g., Amuri Limestone) throughout most of the region (Fig. 8.4).

South of the study area, towards Dunedin, the calcareous siltstones of the Hampden Formation developed between the Bortonian and lower Kaiatan stages (Wilson, 1985), while offshore stratigraphy shows neritic facies of latest Bortonian to Whaingaroan age (Crux *et al*., 1984). In the southwest, glauconitic mudstones (Burnside Mudstone) are capped by post-Eocene unconformities (Field *et al*., 1989), while to the west the Runangan Stage is marked by an increase in glauconite and sand (e.g., Feary Greensand and Coleridge Sandstone) (Field *et al*., 1989).

Just north of the present study area, the Waihao Greensand, a glauconitic muddy sandstone, forms the main Bortonian Stage unit (Field *et al*., 1989) with facies ranging from shallow shelf in its lower part and deepening upwards (Maxwell, 1975). It is capped by an unconformity resulting from a fall in relative sea level (Field *et al*., 1989). This was overlain by sandy mudstones, grading to calcareous mudstones, in the Kaiatan to lower Whaingaroan Stages (Ashley Mudstone) (Field *et al*., 1989).

Homebush Sandstone, the main unit of the mid Eocene, reflects shallow marine conditions west of the Chatham Rise and grades up into calcareous quartzose sandstones (e.g., Karetu Sandstone) (Field *et al*., 1989).

8.2.2.1.7 Western Southland region

The Western Southland region lies on the southwestern edge of South Island (Fig. 8.3). Sediments there record an onset of widespread subsidence and sedimentation, with the oldest Eocene sediments deposited during the Bortonian stage, in the north of the

region (Turnbull, 1986), while elsewhere sediments are Kaiatan or Runangan (Turnbull *et al*., 1993). These Eocene sediments consist of three major groupings: the Nightcaps, Annick, and lower Balleny Groups (Turnbull *et al*., 1993). Much of this Eocene succession resembles the Brunner Coal Measures and the Kaiatan mudstone facies found in the West Coast region (See Section 8.2.2.1.4) (Nathan *et al*., 1986; Turnbull *et al*., 1993). The Eocene sedimentary facies of the Western Southland region are indicative of alluvial fan and flood-plain environments, as well as shallow marine and fan delta, fluvial, and lacustrine facies (Turnbull *et al*., 1993).

8.2.2.2 Whaingaroan (34 – 27 Ma)

8.2.2.2.1 Northland region

Regional transgression in Northland (Fig. 8.2) is evident in Whaingaroan-to-Duntroonian Te Kuiti Group limestone facies, which range from offshore and slope in the west (Fig. 8.4**)** (Hornibrook *et al*., 1976) to near-shore in the east, and contain localised greensand interbeds (Hay, 1960). The nearshore facies consist of a crystalline limestone with bryozoan and echinoderm fragments, while the deeper facies form an argillaceous, coccolith-rich, occasionally bedded limestone formed in a non-turbulent subtropical marine setting with minor terrigenous input (Hay, 1960; Carter, 1969). These deeper facies are part of the Northland Allochthon, and are therefore not *in situ* (Ballance and Spörli, 1979).

8.2.2.2.2 Waikato/Wanganui region

Continued deposition of Te Kuiti Group sediments produced the oldest marine beds in the Waikato/Wanganui region, of basal Whaingaroan shallow-water facies (Fig. 8.4) (Suggate *et al*., 1978). Further transgression led to flooding and formation of a series of

north-south limestone seaways bounded by Mesozoic highs to the east and west, with limestone formations thinning to siliciclastic facies onlapping against these highs (Nelson, 1978a; Anastas *et al*., 2006). A hiatus developed in the early Whaingaroan, developing glauconitic sandstones during periods of low deposition (Suggate *et al*., 1978).

8.2.2.2.3 Taranaki region

Oligocene to Early Miocene sedimentation within the Taranaki region formed the basal Whaingaroan to Otaian Ngatoro Group (Fig. 8.4) - a collection of diachronous micritic carbonates that range from basal Whaingaroan to Otaian in the west, to upper Whaingaroan to late Waitakian in the east (King and Thrasher, 1996). Sub-basins formed by local faulting in the Late Eocene appear to be conformable into the Oligocene, marked by a change to a more calcareous lithology (King and Thrasher, 1996). These carbonate facies represent outer-shelf to slope depths (King and Thrasher, 1996).

8.2.2.2.4 West Coast region (South Island)

As terrigenous supply reduced in the West Coast region, sedimentary lithologies became increasingly calcareous (Fig. 8.4) (Nathan *et al*., 1986). These calcareous sediments comprise the Nile Group, including all Oligocene limestones and calcareous formations in the area (Nathan, 1974; Nathan *et al*., 1986).

These Oligocene lithologies form two major facies: a platform facies in the north and south, and a deep basinal facies in the centre of the region (Nathan *et al*., 1986). The platform facies consists mainly of shallow-water bioclastic limestones and is confined to areas where sedimentation is slow, generally with thin sequences (Nathan *et al*., 1986).

Lithologies include bioclastic grainstones, algal packstones and grainstones, sandy limestones, calcareous sandstones, muddy limestones, and calcareous mudstone (Nathan *et al*., 1986). All of these West Coast Oligocene limestones are heavily cemented, with low

porosities as a result of later burial compaction and diagenesis (Nelson, 1978b; Leask, 1980).

Localised unconformity development occurred during the Whaingaroan Stage, although sedimentation was continuous in some parts of the basin at all times (King *et al*., 1999). Unconformable contacts occur near Punakaiki, where karst development, erosion, and rhodolith formation are associated with abrupt shallowing in the lower Whaingaroan (Lever, 2001); while a later local paraconformity of phosphatic nodules and quartz grains developed near the Whaingaroan/Duntroonian boundary at Dolomite Point (Laird, 1988). Near Westport, another Whaingaroan unconformity can be found with up to 4 m of erosion and evidence of rapid shallowing ending in lagoonal mud and sand facies (Lever, 2001).

8.2.2.2.5 East Coast region (North Island)

The Oligocene sediments in the East Coast region generally contain bioturbated, calcareous and massive mudstones, bedded sandstones, and massive, slightly glauconitic limestone, and minor glauconitic fine sandstone (Fig. 8.4) (Field *et al*., 1997). Calcareous content tends to be higher in the north of the region. These formations are commonly Whaingaroan to Duntroonian, with the youngest in the lower Waitakian (Field *et al*., 1997). High percentages of planktic forams indicate slope palaeodepths, although there are indications of a slight regression during this period (Field *et al*., 1997).

8.2.2.2.6 Canterbury region

During the Oligocene, deposition of Runangan to lower Whaingaroan micrite limestone (Amuri Limestone) was unconformably followed by calcareous glauconite sandstones and coarse shelf limestone, indicating continued transgression in the Canterbury region (Fig. 8.4) (Field *et al*., 1989). In the west, the Amuri Limestone is

typically an outer-shelf to slope marl and wackestone, capped by an upper-Whaingaroan unconformity (Field *et al*., 1989). Toward the north, it is siliceous and chalky, while to the south it is expressed as a marl (Field *et al*., 1989). The upper-Whaingaroan unconformity on top of this formation has been interpreted as being a period of erosion and non-deposition (Field *et al*., 1989), and is overlain by shelf-to-slope sandstones (Waipara) to limestones (Kaikoura) (Rattenbury *et al*., 2006).

In the northern Marlborough area, this unconformity is highly glauconitic and burrowed, and has been correlated with the Marshall Paraconformity (Carter, 1985; Field and Browne, 1989; Fulthorpe *et al*., 1996). Non-deposition or erosion spans the Whaingaroan and Duntroonian stages in the south, while localised unconformity development continued in the north during the Duntroonian (Fig. 8.4). Overlying this unconformity are slope-depth packstones (e.g. Spyglass Formation) (Browne, 1995) and some coarser shelf-to-slope depth lithologies in the west of the region (Field *et al*., 1997).

Weka Pass Stone rests unconformably on Amuri Limestone, or conformably on Oligocene Cookson Volcanics (Field *et al*., 1989; Reay, 1993; Field *et al*., 1997). This is a fine-grained and glauconitic sandstone, later overlain by the Whaleback Limestone (Browne, 1995) and interbedded with glauconitic wackestone and mudstone (Field *et al*., 1997).

8.2.2.2.7 Western Southland region

Marine conditions developed in the Western Southland region during the Whaingaroan Stage. There, Upper Balleny Group rocks consist of a fining-up succession of coarse-grained terrigenous sediments, together with thick pelagic marls and chalk (Fig. 8.4) (Carter and Lindqvist, 1975; Turnbull *et al*., 1989). This begins with a basal breccia overlain by thick-bedded sandstones grading into regular-bedded and fining-up sandstones,

capped by chalk and calcareous mudstone (Turnbull *et al*., 1993). The basal breccias are interpreted as being the result of mass flows within a submarine fan on the inner shelf (Carter and Lindqvist, 1975; 1977), while the thick-bedded sandstones were emplaced by mass flows within a proximal fan environment (Carter and Lindqvist, 1975). Upward-grading sandstones, with a slightly glauconitic content, could be the result of a broad fan fringe (Carter and Lindqvist, 1977).

In the east of the region, the Oligocene Waiau Group exhibits less carbonate, and tends to be dominated by mudstones interfingering with numerous basin-edge submarine fans, while limestone-rich shelf sequences formed on the margins of the region (Turnbull *et al*., 1993). In the west, this group contains quartzo-feldspathic and slightly carbonaceous sandstones along with small occurrences of carbonaceous mudstones, conglomerate, and sandy to pebbly impure bioclastic limestones (Turnbull *et al*., 1993). The Te Anau Basin contains localised Whaingaroan unconformities influenced by local tectonics (King *et al*., 1999).

8.2.2.3 Duntroonian to Waitakian (27 – 22 Ma)

8.2.2.3.1 Northland region

The Waitakian to Otaian Waitemata Group developed in Northland following deposition of Te Kuiti Group transgressive marine limestone facies in the Duntroonian (Fig. 8.4), separated from older sediments by an unconformable contact (Ballance, 1976). This group consists mostly of sandstones, but has localised volcaniclastic turbiditic conglomerates (Shane *et al*., 2010), limestones, greensands, and siltstones at its base.

8.2.2.3.2 Waikato/Wanganui region

In the Waikato/Wanganui region during the Duntroonian to Waitakian, terrigenous and glauconitic content within the limestone facies reduced in the upper Te Kuiti Group (Fig. 8.4), indicative of continued transgression (White and Waterhouse, 1993; Anastas *et al*., 2006). Limestones in the seaways typically comprise coarse-grained, biofragmented grainstones and packstones, with little carbonate mud present (Anastas *et al*., 2006). Cross-bedded facies resulting from current flow can also be found within these limestone formations (Anastas *et al*., 2006). A hiatus developed during limestone deposition, producing widespread glauconitic sands during periods of low deposition in the early Duntroonian (Suggate *et al*., 1978). Deposition of the Te Kuiti Group ceased as a result of tectonic uplift, causing erosion and an angular unconformity between this group and the younger sediments deposited above (Suggate *et al*., 1978; King *et al*., 1999).

8.2.2.3.3 Taranaki region

The Duntroonian to Waitakian Ngatoro Group formations indicate outer-shelf to slope marine conditions (Fig. 8.4), sometimes containing sandier lenses representative of turbidite or submarine fan intrusions (King and Thrasher, 1996; Hood *et al*., 2003). Tectonic subsidence accompanied carbonate deposition of this Group, resulting in substantially more transgression at the margins of the region (King and Thrasher, 1996), with this period representing maximum transgression in this area. A angular unconformity at Awakino (northeastern region) represents a Waitakian erosional event, followed by subsidence and onlap (Nelson and Kamp, 2012).

8.2.2.3.4 West Coast region (South Island)

Continued marine transgression led to the drowning of virtually all exposed landmasses along the West Coast between the Duntroonian and early Waitakian (Fig. 8.2) (Nathan *et al*., 1986). Renewed tectonic activity in the mid to late Waitakian accompanied the creation of a significant unconformity separating Oligocene and Miocene formations in most areas (Fig. 8.4) (Nathan *et al*., 1986). While late Waitakian sediments are entirely marine and fairly uniform, land began to emerge some time between the Waitakian and Otaian Stages in the north and south of the basin (Nathan *et al*., 1986). These first emergent areas were the location of the earlier shallow platform facies, interpreted by Nathan *et al*. (1986) as reflecting a probable fall in eustatic sea-level being the cause of this emergence, rather than solely tectonic uplift.

8.2.2.3.5 East Coast region (North Island)

From the Duntroonian to early Waitakian, calcareous slope sediments were continuing to deposit within the East Coast region (Fig. 8.4) (Field *et al*., 1997). Increased tectonic activity during the Waitakian Stage led to extensive faulting and folding, making the vertical and lateral correlation of strata difficult in this area. This period also saw increased large-scale, gravity-induced landslides associated with localised uplift and localised basin formation into the upper Waitakian (Pettinga, 1980; 1982).

8.2.2.3.6 Canterbury region

Canterbury region Duntroonian Stage sediments are generally calcareous, highly glauconitic sandstones (e.g., Omihi Formations and Naseby Greensand) (Fig. 8.4) (Field *et al*., 1989). In the west of the region, these glaucony facies interfinger with some non-marine sediments (Bishop 1974), although all other Duntroonian sediments are marine with an inner-shelf fauna (Field *et al*., 1989).

Waitakian Stage deposition produced grainstones and packstones over much of South Canterbury, with western North Otago developing sandstones and some terrestrial lignites (e.g., Wedderburn Formation) (Field *et al*., 1989). The far west of the region, towards the developing plate boundary, indicates a return to a siliciclastic sedimentation regime during the Waitakian (e.g., Swin Sandstone) (Field *et al*., 1989).

An intra-Waitakian unconformity exists in most of the region, overlain by phosphatic and highly glauconitic greensand near Dunedin (Concord Greensand), and siltstone (Pahau Siltstone) in the north (Andrews, 1968; Field *et al*., 1989). This spatial difference in lithology was the result of a shallow submarine high that extended from Chatham Rise to near Cheviot between the Duntroonian and Waitakian (Fig. 8.2), causing separation of the region into siltstones to the north and greensand/siltstone in the south (Field *et al*., 1989).

8.2.2.3.7 Western Southland region

The calcareous mudstones and chalks of the Western Southland Upper Bellany Group (Fig. 8.4) are indicative of slope depths occasionally interrupted by localised turbidity currents (Carter and Lindqvist, 1977). The western formations contain shallow shelf facies that tend to deepen eastward towards an outer-shelf environment (Turnbull *et al*., 1993).

During the early Waitakian, an erosional unconformity developed (Turnbull *et al*., 1993) together with some localised hiatuses which appeared during the upper Waitakian Stage (Fig. 8.4) (King *et al*., 1999). These surfaces were possibly the result of current-induced non-deposition and/or erosion (King *et al*., 1999).

8.2.2.4 Otaian to Altonian (22 – 16 Ma)

8.2.2.4.1 Northland region

During the Otaian, Northland saw deposition of the Waitemata Group, consisting of conglomerates, breccias, and sandstones developed during allochthon emplacement (Figs. 8.1 and 8.4) (see Section 8.1.1.4) (Ballance, 1976; Suggate *et al*., 1978). This Group formed together with submarine and subaerial volcanics that had been initiated during this period.

8.2.2.4.2 Waikato/Wanganui region

The Otaian Stage Waitemata Group sediments were deposited over the earlier Waitakian unconformity in the Waikato/Wanganui region, with calcareous and glauconite sandstones and occasional limestone lenses developing (Fig. 8.4) (Kear, 1957; Hornibrook and Schofield, 1963; Ballance, 1976; Suggate *et al*., 1978; King *et al*., 1999). These were in turn unconformably overlain by increasingly coarse siliciclastic facies (mudstones, sandstones, and breccias), with localised volcanic material, and are usually non-calcareous (Ballance, 1976; Suggate *et al*., 1978).

8.2.2.4.3 Taranaki region

Otaian Stage and younger sediments in the Taranaki Basin show a regressive and increasingly siliciclastic succession (Wai-iti Group) (Fig. 8.4) comprised of muds, sand-dominated fans and channels, and slope-to-shelf deposits (King and Thrasher, 1996; Kamp *et al*., 2004). The late Otaian Stage saw localised subaerial exposure in the east of the region (Kamp *et al*., 2004). The oldest sand-dominated basin-floor fan sequence is of Altonian to Lillburnian age (Baur, 2012), formed from high sediment supply associated with increased tectonism along the new plate boundary (King and Thrasher, 1996).

8.2.2.4.4 West Coast region (South Island)

During the Otaian Stage, sediments of the West Coast region passed from the earlier Waitakian deep-water limestone facies towards shallow limestones and mudstones. These include some local calcareous mudstones and variable siliciclastic sands (Nathan *et al*., 1986; Laird, 1988). The Waitakian/Otaian contact between earlier limestones and overlying mudstones of the Blue Bottom Group is locally unconformable, with indications of erosion on this surface, with limestone boulders being included within the mudstones above (Lever, 2007).

8.2.2.4.5 East Coast region (North Island)

Increased tectonic activity, beginning in the Waitakian Stage (Fig. 8.4), created concentrations of conglomerate and sandstone within mainly slope mudstone and flysch, with minor units of limestone and tuffs, through to the upper Tongaporutuan Stage (e.g. Tolaga Group) (Fig. 8.4) (Field *et al*., 1997).

8.2.2.4.6 Canterbury region

During the Otaian Stage the Canterbury region underwent an influx of sands (Fig. 8.4) from the west towards the east, extending to eastern onshore Canterbury by the Altonian (Field *et al*., 1989). This was associated with the development of the Alpine Fault at ca. 23 Ma (see Section 8.1.1.4).

8.2.2.4.7 Western Southland region

Regional subsidence continued in Western Southland through the Waitakian and into the Otaian, with a dominantly mudstone composition. This is expressed in the basin-wide Waicoe Formation throughout this period (Fig. 8.4) (Turnbull *et al*., 1993), deposited

as a marine mudstone with lenticular units of sandstone and conglomerates (Turnbull *et al*., 1993).

8.3 Discussion

The sequence stratigraphy of the Waitaki study area presented in Chapter 5 would clearly have been affected by the regional 1st order megasequence of transgression, culminating in the Oligocene, and followed during the Miocene by a sea-level regression associated with propagation of the new plate boundary (see Sections 1.1.4 and 8.1.1.4). Based on this, sedimentary and tectonic histories of the major mid-Cenozoic regions of New Zealand (described above) are here compared in order to allow interpretation of smaller-scale effects which occurred within the study area, and to determine how the sequence stratigraphy developed here may be applied to New Zealand as a whole.

8.3.1 The mid-Cenozoic megasequence and its regional influence

The New Zealand 1st order mid-Cenozoic megasequence (see Section 1.1.4) exhibited a period of regional transgression covering the Cretaceous to the Oligocene, with maximum flooding around New Zealand in the Late Oligocene. Later stages of this transgression can clearly be seen between the Eocene and Oligocene (Fig. 8.4).

The Eocene tended to be a period of subsidence across Zealandia, leading to transgression and flooding of low-lying landmasses, as expressed in a reduction of siliciclastic sediments and fining-upward successions seen in various regions (e.g., West Coast, Canterbury, Northland). This is also evident in the study area, where the Bortonian and Kaiatan Stage facies exhibit a decreasing and fining-upward siliciclastic component (Glauconitic Siltstone (F1) facies, see Sections 3.2.1 and 5.2.2.1).

Carbonate facies start to become dominant as relative sea level rises, and siliciclastic supply drops sufficiently to allow carbonate factory development. The time periods where this occurred varied around New Zealand, depending on proximity to tectonic processes, which affects a region's initial terrestrial topographic elevation, and thus the period of time before siliciclastic supply will be reduced sufficiently for carbonate production to commence (e.g., East Coast vs. Western Southland regions, comparatively shown in Fig. 8.4).

In the study area, significant carbonate production began in the Runangan Stage and carried on into the early Whaingaroan. The carbonate factory was firmly established only around the eastern volcanic high, however, where elevated bathymetry allowed for the colonisation of this platform rim by carbonate biota (e.g., Bryozoan Grainstone (F2) facies, Section 3.2.2), while protecting it from siliciclastic input (see Section 6.4.1). This same palaeobathymetric effect can be seen in the northern Canterbury region, where a volcanic high induced by deposition of the Cookson Volcanics allowed for development and retention of a carbonate factory above an increasing siliciclastic supply into the area (Irvine, 2012).

In the western region of the study area, deeper carbonate facies were deposited (Impure Wackestone (F4) facies, Section 3.2.4), but their siliciclastic content was relatively high, and it is likely that the majority of the carbonate mud component within this facies was supplied downslope from the eastern bryozoan shoals (see Section 6.4.1). Establishment of significant carbonate production in the study area may therefore have been artificially early as a result of this eastern bathymetric anomaly, without which the area might have been similar to other New Zealand regions, such as the West Coast and Taranaki which were proximal to low-lying land masses at the end of the Eocene and earliest Oligocene (see Section 8.1.1.2).

Those New Zealand regions that evolved proximal to the zone of deformation, created by the developing tectonic boundary, tended to have significant quantities of local siliciclastic facies abutting local faults (e.g., West Coast). These occurrences decreased with increasing distance from the developing boundary, with areas such as the East Coast developing deep marine facies with lower occurrences of siliciclastic facies (see Section 8.2.2.1.5). The study area sits somewhere between these two spatial extremes, with a decreasing silt-sized siliciclastic supply throughout the Whaingaroan Stage, but with accumulation at shallower depths than in further distal regions such as the East Coast and North Canterbury.

By the mid Oligocene, carbonate production was becoming uniformly established around New Zealand, although the Western Southland and Waikato/Wanganui regions lagged behind somewhat due to local initial topographic elevation and associated active faulting, which delayed cessation of siliciclastic supply (see Sections 8.2.2.2.2 and 8.2.2.2.7). Carbonate facies development continued until maximum submergence of New Zealand in the Duntroonian to early Waitakian Stages (Fig. 1.1). These Stages represent the period of maximum flooding throughout New Zealand (as a result of the regional 1st order transgression), during which limestones were deposited, at least locally, within every region (Fig. 8.4). The Western Southland region developed its deepest marine facies during this period, with the proximity of land resulting in interfingering with siliciclastic lenses caused by submarine landslides and fans. This transgression is also evident in the West Coast region, in the drowning of all remaining low-lying islands. The Taranaki region shows significant subsidence, resulting in an increase in accommodation space and a change to deep-water facies deposition towards the west. Even the Wanganui/Waikato region saw deposition of marine facies onlapping onto local landmasses during this period.

While most of New Zealand appears to have experienced maximum submergence by the Waitakian Stage, the study area was at its greatest depth earlier, during the early Whaingaroan, as indicated by deposition of the Impure Wackestone (F4) facies in the western region (see Section 5.2.2). During the Duntroonian and Waitakian Stages, the calcareous facies that developed in this western region were somewhat shallower than those of the early Whaingaroan, often with lower relative planktic foraminifera and carbonate mud components, which reduced even more towards the east (Chapter 5). While it is possible that the study area was affected by some degree of mild local tectonic uplift or regional tilting (as was occurring in other areas around New Zealand at this time; e.g., northeastern South Island; see Section 8.1.1.3), it is more likely that the significant thicknesses of sediment developed during this period contributed to the decrease in water depth there. This would explain the overall shallower facies observed in the western region, as opposed to what might otherwise have developed had the regional trend of sea-level transgression been the sole influence on water depth. Thus the deposition of sequences of sediment thicker than those seen in the Whaingaroan, as well as minor distal effects from the Early Miocene uplift associated with the new plate boundary, may have induced a small-to-moderate counter-effect to the regional sea-level transgression seen across the greater New Zealand region, lowering the rate of relative sea-level rise throughout the Duntroonian and Waitakian Stages.

The occurrence of a slight tectonic uplift in the study area during this period is further supported by a relatively uniform siliciclastic content throughout the western region Waitakian Stage carbonate facies, even though carbonate production rates were increasing (Massive Glauconitic Packstone (F6) and Bedded Packstone (F7) facies; see Sections 1.2.7.2, 3.2.6, and 3.2.7), suggesting that siliciclastic supply may also have been increasing slightly. There may have been a degree of tectonic uplift in the region to the west of the

study area, which led to increased terrigenous sediment supply from landmasses that had previously supplied terrigenous sediment through to the Whaingaroan. Such tectonic changes, occurring prior to the development of the Alpine Fault, may be attributable to changes in the zone of deformation around the evolving plate boundary (Fig. 8.1). This would suggest that regions both proximal and distal to the developing plate boundary were tectonically influenced by it to some degree, although this influence was probably minor in the study area, where the relatively shallower facies developed during the Duntroonian to Waitakian Stages are primarily attributed to the accumulation of thick carbonate sequences during this period.

The upper Waitakian Stage developed as a period of significant environmental change throughout New Zealand, principally induced by propagation of the new Alpine Fault and the substantial uplift associated with it, supplying increasing volumes of siliciclastic material to regions nearby. This period brought siltstone and mudstone facies to most New Zealand regions, intensifying through the Otaian and into the Altonian Stages. It was during this period that the second significant unconformity (SB3) developed in the study area (see Section 5.2.7, and Section 8.3.2.2 for further discussion). While siliciclastic sediment supply increased in most areas, however, localised subsidence (e.g., western Taranaki and offshore Northland) saw some areas retain or develop deeper-water facies.

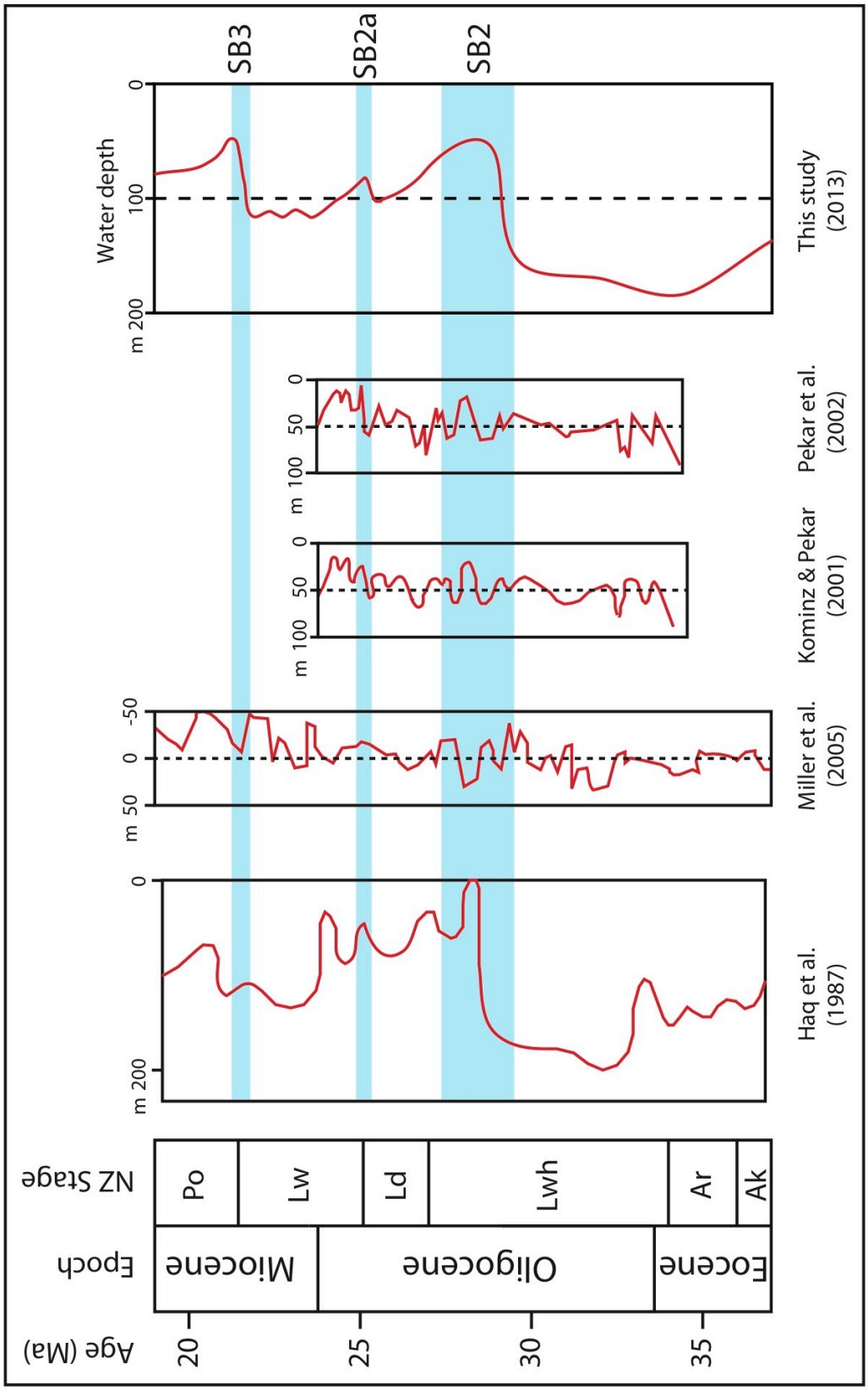

Figure 8.5. Comparison of sea level curves between this study and Haq *et al.* (1987), Kominz and Pekar (2001), Pekar *et al*. (2002), and Miller *et al*. (2005). The three sequence boundaries developed in this study are highlighted in blue.

This upper Waitakian to Otaian Stage relative sea-level rise can be seen on the sea level curves of Haq *et al.* (1987) and Miller *et al*. (2005) (Fig. 8.5), although the rises during this period are separated by a period of sea level fall in the early Otaian. With the deposition of the Calcareous Greensand (F5) facies of Sequence 3 (see Sections 3.2.5 and 5.2.8.1) in the study area suggesting a continued period of transgression, it is likely that local small-scale tectonic uplift may have played a role in countering eustatic sea-level rise. By the Altonian Stage, however, siliciclastic sediment supply had significantly increased, as terrigenous material from the new plate boundary began to reach the Waitaki region in sufficient volume to prohibit reestablishment of the carbonate factory and to fill accommodation space. This led to relative sea-level fall, especially when coupled with the increasing effect of tectonic uplift derived from the plate boundary and its widening stress field through the Miocene.

8.3.2 Lowstands: The varying influence of tectonic and eustatic sea-level

The study area contains two significant unconformities which both show evidence of subaerial exposure in the eastern region resulting from sea-level lowstands (see Sections 5.2.3 and 5.2.7). These occurred in the mid-to-late Whaingaroan and the mid Waitakian to basal Otaian (mid Oligocene and Early Miocene) (see Section 2.3.2.3 and 2.3.3.3).

8.3.2.1 Sequence Boundary 2 (SB2) lowstand

The first unconformity (SB2, Section 5.2.3) has been correlated with the regional Marshall Paraconformity and, as such, has a contentious regional and local genesis (see Section 1.1.2). The two main contending interpretations of this unconformity's development involve either a period of glacio-eustatic sea-level fall resulting from Antarctic glaciation (Vella, 1967; Loutit and Kennett, 1981), and/or a period of non-

deposition resulting from the development of the Antarctic Circumpolar Current (Carter, 1985; Carter *et al*., 2004).

If it had simply been a period of non-deposition, the karst dissolution prevalent in the eastern region would not be expected, as it certainly indicates a period of relative sea-level fall and exposure in that area. While such karst features have sometimes been attributed to submarine dissolution rather than subaerial exposure (Carter, 1985; 1988; Lewis, 1992), the outcrop and facies analyses (Chapters 2 and 3), and the resultant sequence stratigraphic model (Chapter 5), suggest that this could not be the case here.

It is clear, therefore, that this surface (SB2) is the result of relative sea-level fall in the study area during the mid to late Whaingaroan, but its cause is not so clear. Attempts have been made in the past to link the various occurrences of this surface around New Zealand to a comparable sea-level fall shown in the Vail curve (Vail *et al*., 1977). Dates for the development of some of these surfaces do not correlate well with this event, however, sometimes falling within the hiatus rather than at its inception (e.g. Fulthorpe *et al.,* 1996; Lever, 2001). Fig. 8.5 shows more recent sea-level curves, where eustatic sea-level falls can be seen in all the curves within the region of SB2. However the magnitude and timing of these falls does not coincide with the onset of regression as seen in this study.

If this sea-level fall was not principally the result of eustatic regression in the study area, the only other likely explanation would be local or regional tectonic uplift. The Whaingaroan Stage was generally a period of subsidence and passive margin development, although there were localised occurrences of active faulting and strain propagation from the slowly emergent tectonic zone spreading through Zealandia at the time (see Section 8.1.1.2). Many of these events occurred in areas on the western side of the tectonic zone (e.g., Nelson, Taranaki, West Coast), developing a series of north-south faults

accommodating dextral strain. While it is possible that this western strain development could have affected the study area, it seems unlikely given that there is little indication of significant Whaingaroan faulting in the region. If tectonic uplift was accountable for the mid Whaingaroan sea-level fall there (of the order of 100 – 150 m at SB2), tectonically induced disturbance or faulting would be likely to be apparent within syn-depositional sediments and the surface developed as a result, and it is not. Furthermore, while local effects such as an apparent angular unconformity at Campbells Bay (Lewis and Belliss, 1984) might be cited, these are not widespread and could simply be the result of topographic relief associated with the volcanic field and the palaeohigh, rather than more widespread tectonic uplift. Regional tectonic uplift being a prime cause of this surface in the study area can therefore reasonably be discounted. However there may have been some influence from tectonic occurrences that contributed to the magnitude of the upper Whaingaroan regression, as the more recent curves presented in Fig. 8.5 do not account for the full sea level changes recorded within the study area.

It seems, therefore, that this surface must be attributed principally to the eustatic sea-level falls recorded in the late Whaingaroan Stage, with some lesser contribution from tectonic influence. The earlier onset of SB2 in the study area could be attributed to erosion of mid Oligocene sediment during subaerial exposure and increased energy levels during this period. In other New Zealand regions more proximal to the developing tectonic zone in the western side of New Zealand, however, the record of this sea-level fall might be obscured by the greater influence of local tectonic activity, whether from uplift or basin subsidence. Unconformities of this age can be found in these tectonically active areas during the Whaingaroan Stage (e.g., West Coast, Section 8.2.2.2.4), indicating that this sea-level change was also recorded there, although their occurrence is often localised, with other areas in the region showing a period of continuous deposition. This may reflect the

variable depths found in these areas being brought about by sub-basin creation as a result of localised faulting, resulting in different depositional effects during this eustatic sea-level fall.

Regions in the east of New Zealand (e.g., Canterbury and the East Coast) contain clearer signals of eustatic change due to their distance from the tectonic zone, although areas of significant depth relative to the study area (e.g., northern East Coast) were less likely to be affected by this lowstand, as they remained sufficiently submerged for sedimentation to continue.

8.3.2.2 Sequence Boundary 3 (SB3) lowstand

The second unconformity in the study area (SB3) developed in the late Waitakian to Waitakian/Otaian Stage boundary (Early Miocene). As with SB2, this sequence boundary has been interpreted as resulting from relative sea-level fall and resulting lowstand (see Section 5.2.7). Pekar *et al*. (2006) show a sea-level fall on the order of 75 m for the Waitakian/Otaian Stage boundary, which relates well to the lowstand presented here as SB3. Alongside this, the Alpine Fault and the new Pacific-Australian plate boundary propagated through New Zealand in this time period, initiating a period of tectonic uplift and increased siliciclastic supply to the region (see Section 8.1.1.4).

Unconformities occur in all seven of New Zealand's regions around Waitakian-Otaian boundary (Fig. 8.4), although there is local variation in the timing of their development. Tectonic uplift caused late Waitakian erosion and angular unconformities in the Waikato/Wanganui, Taranaki, West Coast and East Coast regions, and locally in the Canterbury and Western Southland regions (see Section 8.2.2.3). Western Southland and the West Coast also contain hiatuses that may have resulted from current-induced erosion. Areas proximal to the new plate boundary tended either towards uplift and the influx of

significant siliciclastic sediment, or towards localised subsidence and relative sea-level transgression; although these sea-level change signatures are dominated by tectonic faulting and not necessarily by eustatic sea-level change.

While some degree of tectonic influence in the study area during the Waitakian Stage is likely to have occurred (see Section 8.3.1), it would have occurred alongside eustatic sea-level rise (Fig. 8.5), as well as by the significant increases in sediment thickness observed during this period. As with SB2, there is little indication of significant tectonic-induced faulting within the study area associated with SB3, apart from a small normal fault at Gees Point (see Section 2.2.4.7), which could well have been derived from local karst development or minor brittle deformation. The occurrence of these surfaces around New Zealand, and their timing with the inception of the Alpine Fault are, however, strong indicators that tectonic influence was the cause of this lowstand - a likely result of far-field crustal deformation extending from the main zone of deformation located to the west of the study area.

It therefore seems likely that this LST at SB3 was primarily the result of tectonic uplift affecting the study area. This may, however, also have been accompanied by some degree of eustatic sea-level fall (Fig. 8.5). A shallowing of depositional facies in the late Waitakian Stage correlating with SB3 can also be observed throughout the West Coast region, where it has also been attributed to a period of eustatic sea-level fall during this period (see Section 8.2.2.3.4). This could then account for the relative sea-level rise that followed SB3 during Sequence 3 (see Section 5.2.8). Without any change in eustatic sea level in the study area through this period, it becomes problematic to attribute this sea-level regression at SB3 solely to tectonic uplift, to be immediately followed by a relative sea-level rise of at least the same magnitude during the Otaian Stage.

It seems, therefore, that the study area remained marginally within the main zone of deformation and faulting associated with the development of the Alpine Fault until the Altonian Stage when the Rifle Butts Formation was deposited. This formation is associated with a significant increase in siliciclastic sediment supply (see Section 1.2.8.2), when the influence from the evolving plate boundary began to significantly alter the depositional record in the study area.

8.3.2.3 Eustatic or tectonic influence?

Comparisons of unconformity developments in the study area and the main New Zealand regions, as described above, indicate that a region's proximity to the plate boundary and its associated zone of deformation played an important role in the recording of any eustatic sea-level influences.

Regions strongly affected by subsidence and uplift, resulting from the propagation of the plate boundary, tended to develop a local record reflecting relative sea-level change induced by these events (Fig. 8.6). Regions more distal to the tectonic zone, however, often show a higher-resolution signature of lower-order sea-level fluctuations. The study area appears to record eustatic sea-level changes that overprint small local tectonic influences during the Whaingaroan Stage, with it being outside any significant deformational zone derived from the developing plate boundary during this time (Fig. 8.6). Subsequent deposition between the Duntroonian to Waitakian Stages was not as deep as during the early Whaingaroan, however, though this period involved maximum submergence elsewhere in New Zealand. This would have been the result of a combination of moderate tectonic uplift in the study area coupled with subsequent deposition of thicker sequences of carbonate sediment, which together provided a counter-effect to the eustatic sea-level rise recorded elsewhere (Fig. 8.6).

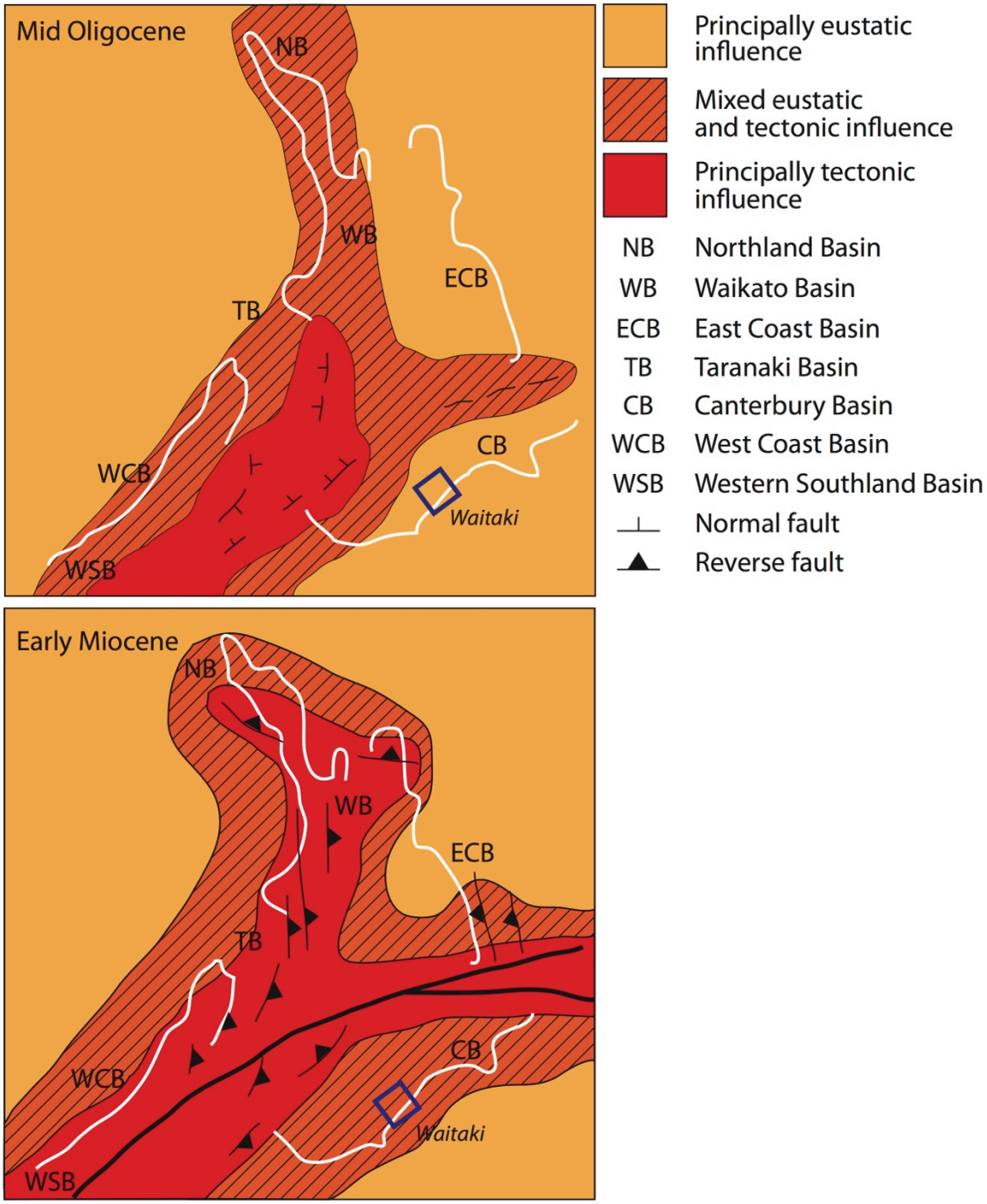

Figure 8.6. Diagram showing the influences on relative sea level change across Zealandia during the mid Oligocene and Early Miocene. Tectonic influences are limited before the large scale development of the Alpine Fault in the Miocene, after which most areas are affected by some degree of tectonic activity. Palaeogeography adapted from King *et al*. (1999).

At the inception of the Alpine Fault (ca. 23 Ma), unconformities developed around New Zealand that showed signs of erosion and lowering of sea level. The same features

can be seen in the study area (SB3). Some degree of tectonic uplift is likely to have taken place in the Waitaki area as a result of the changing tectonic setting, leading to a regional shallowing effect. This was accompanied by a eustatic sea-level fall around the same time, with a subsequent sea-level rise in the Otaian overprinting any continuing tectonic uplift until at least the Altonian Stage. With continued development of the Alpine Fault and the Pacific-Australian plate boundary in the Altonian and onwards, however, the dominance of eustatic sea-level effects in the area changed, and regional regression became increasingly a tectonically-induced occurrence (Fig. 8.6).

8.3.3 Extent of land submergence in New Zealand in the mid-Cenozoic

Throughout the mid-Cenozoic the lithologies within the study area showed a varying but relatively constant presence of terrigenous supply. This occurs especially during lowstands, when clay glauconite-precursors are supplied in abundance to develop the Calcareous Glauconite (F5) facies. Furthermore, quartz silts are found in a number of facies, particularly those from the Late Eocene and Early Oligocene.

This suggests firstly that landmasses were present through to at least the mid-Late Oligocene, when less glauconitic and silty facies became common. However, with a second major lowstand during the Late Oligocene and Early Miocene, glauconite facies again dominate. This demonstrates that with a moderate lowering of sea-level, terrigenous sediments are again supplied to the basin suggesting that even if landmasses to the west of the Waitaki region were completely submerged, they were very shallow. However the results of this study cannot conclude one way or another if land remained subaerial throughout the entire mid-Cenozoic 'drowning' of New Zealand, only that they were present and likely existed as subaerial islands to shallow shoals.

8.4 Conclusion

The mid-Cenozoic period in New Zealand witnessed the steady propagation of the Pacific-Australia plate boundary, set against the background of a marine transgressive 1st order megasequence through to the Early Miocene. The eventual development of the modern tectonic setting in the Miocene was followed by regional regression that led to significant siliciclastic sediment supply derived from uplifting basement blocks.

In the Late Eocene and Early Oligocene, the study area experienced this transgressive megasequence as a decrease in siliciclastic sediment supply and development of increasingly calcareous facies. A carbonate factory developed in this setting over a bathymetric high induced by eastern volcanic cone emplacement while siliciclastic supply was still high. This resulted in the establishment of carbonate facies within the study area earlier than they might otherwise have developed, as the area would likely have been similar to other regions proximal to the developing tectonic zone. Furthermore, the period of maximum relative sea level within the study area occurred in the Early Oligocene, while maximum submergence in the New Zealand megasequence did not occur until the Late Oligocene.

Tectonic influence affected the study area in the Late Oligocene, exhibited as minor tectonic uplift and the deposition of a thick carbonate sequence, differing from the relative sea-level rise that resulted in the period of maximum flooding elsewhere in New Zealand, such that during this period the study area did not reach the relative depths seen during the Early Oligocene. With the development of the Alpine Fault in the Early Miocene, it is likely that the lowstand that developed at the same time in the study area, and elsewhere in New Zealand, was the result of an increase in tectonic uplift occurring around the same time as a minor eustatic sea-level fall. This was followed by a period of relative sea-level transgression and the development of calcareous glauconite sandstones across the study

area in the Early Miocene, before increased tectonic influence again induced a period of sea-level fall that led to the end of eustatic influence on relative sea level.

Comparisons between the two major sequence boundaries in the Waitaki study area and similar unconformities in other regions around New Zealand imply that regional proximity to the developing plate boundary influenced how eustatic sea-level changes were recorded in the sedimentary record. Regions proximal to this tectonic zone, particularly those on the western side of New Zealand, tended towards a local sea-level record that often reflected these events, while more distal regions have a better overall record of eustatic sea-level changes occurring across the region.

The study area appears to have been controlled primarily by eustatic sea-level variations between the Eocene and the Early Oligocene, and was therefore not heavily influenced by this developing tectonic zone. Increasing tectonic influence led to a shallower depositional environment in the Late Oligocene, however, while other regions in New Zealand were subjected to a period of maximum submergence reflecting the regional 1st order megasequence. This situation changed only once the newly developing Alpine Fault extended its stress field outwards (in the Early Miocene) to induce uplift in the study area, coupled with a significant increase in siliciclastic supply derived from newly uplifted basement blocks, smothering carbonate production and filling accommodation space. Regional regression was thus set in motion from that point on, as recorded in the development of siliciclastic facies in the Waitaki region and around New Zealand as a whole.

CHAPTER 9 – SUMMARY AND CONCLUSIONS

9. Summary of chapter conclusions

The aim of this project was primarily to address aspects of controversy surrounding the extent of submarine drowning in the mid-Cenozoic, and to assess the possible causes of unconformity development in the Waitaki study area, South Island, New Zealand. Individual objectives set for the project are described in Section 1.3.

Extensive stratigraphic outcrop and thin-section petrographic analyses were used, together with stable-isotope, cathodoluminescence, and thin-section staining methodology, to develop lithofacies, depositional, and sequence stratigraphic models of the mid-Cenozoic succession in the Waitaki area. Results and interpretations were combined to investigate environmental causes of unconformities and to link them to local and regional processes, including palaeogeography, evolving tectonic influence, and eustatic sea-level changes. From there, it was possible to determine the effect of palaeobathymetry on local facies distribution and relationships, as well as the observed alternation between carbonate and authigenic facies. Finally, a comparison between the study area and the regional mid-Cenozoic sedimentary record around New Zealand allowed for a determination of the relative degrees to which local and regional events were the causes of changes observed in the study area.

9.1 Lithostratigraphy, biostratigraphy, and facies types

Twelve lithofacies were developed using both outcrop-based fieldwork and extensive analyses of over 200 thin sections. All mid-Cenozoic formations in the study area show significant lateral variation, including substantial changes in thickness from east to west within the study area, particularly in the Duntroonian to Waitakian Kekenodon

Group. Two major unconformities which developed in the upper Whaingaroan and upper Waitakian Stages can be correlated across the region, and show a change from karst morphology in the east to a burrowed firmground in the west. A third minor erosive surface was also found within localised Late Oligocene exposures.

Biostratigraphic analyses based on the Fossil Record Electronic Database (FRED) were used to constrain each formation and facies to at least New Zealand Stage level, confirming correlations between eastern and western facies and unconformity surfaces that vary significantly throughout the region. Of particular importance was the confirmation that the eastern karst horizons could be correlated with the burrowed firmgrounds to the west of the study area.

The twelve facies developed here cover a range of marine environments, from high-energy, inner-shelf, through to quiet, upper-slope settings, which existed between the Kaiatan and Otaian Stages. These facies were grouped within five Facies Associations loosely based on their depth of deposition and primary composition.

The Clastic Outer-Shelf Facies Association comprises the Glauconitic Siltstone (F1) facies. This is a non-calcareous and glauconite-rich clastic siltstone deposited in the west of the study area at outer-shelf depths during the Kaiatan Stage.

The Carbonate Inner-Shelf Facies Association includes the Bryozoan Grainstone (F2), Rhodolith Rudstone (F3), and Cross-bedded Glauconitic Packstone (F8) facies. Of these, F2 and F3 are located in the east, and deposited on an inner-shelf high between the Runangan and Whaingaroan Stages. The Cross-bedded Glauconitic Packstone facies developed principally in the north of the study area, and was subjected to high-energy winnowing and reworking by easterly palaeocurrents.

Three facies make up the Carbonate Mid- to Outer-Shelf Facies Association between the Duntroonian and Otaian Stages. The Calcareous Greensand (F5) facies is the

shallowest of these and occurs across the study area, where it deposited as inner- to mid-shelf calcareous glauconite sands. It often grades into the Massive Glauconitic Packstone (F6) and Bedded Packstone (F7) facies, which becomes decreasingly glauconitic with higher carbonate contents. These three facies are often found in succession and signal deepening water. The thickest sediment accumulations are located in the west of the study area.

The Carbonate Outer-Shelf to Slope Facies Association contains only the Impure Wackestone (F4) facies in the west of the study area, deposited during the early Whaingaroan Stage. This facies comprises a mixed siliciclastic and carbonate composition developed at outer-shelf to upper-slope depths.

The Volcanic Facies Association is located principally in the east of the study area and contains four facies: the Diatomaceous Micrite (F9), Volcanic Tuff (F10a) and Volcanic Pillow (F10b), Reworked Volcaniclastic Packstone (F11), and Ash/Clay (F12) facies. These developed between the Kaiatan and Whaingaroan Stages in close association with the Bryozoan Grainstone (F2) and Rhodolith Rudstone (F3) facies in the east.

9.2 Diagenetic history

Seven of the facies described here contain significant diagenetic cements, principally located in the east of the study area, below the unconformities. These cements were analysed using the petrographic dataset, enhanced with cathodoluminescence and Alizarin Red S staining, in order to determine the diagenetic history of the Waitaki region.

Results indicate that sea-floor diagenesis occurred throughout the area soon after deposition, particularly in the east. The cements developed as Fe- and Mn-poor isopachous rinds around bioclast components, often leaving empty intragranular porespace. Sea-level falls resulted in decreasing sedimentation rates which locally increased temperature and

energy, serving to concentrate sea-floor cement precipitation at non-depositional horizons, prior to subaerial exposure in the east. During lowstand, these surfaces were subjected to meteoric diagenesis in the phreatic zone that precipitated calcite spar, filling some intragranular porespace.

Iron- and manganese-rich sparry ferroan calcite cements precipitated later during burial, particularly within the thick sequences in the west of the study area. These ferroan calcite and calcite blocky spar cements filled some, but seldom all, remaining porespace, indicating only a limited degree of shallow burial.

Those facies with little or no calcite cements, located mostly in the west and north of the study area, tend either to contain higher carbonate mud relative to the uncemented samples and exhibit low porosities, or are composed mostly of non-calcareous sedimentary grains which inhibit calcite nucleation. These facies did not experience the higher fluid flux associated with the high-energy grainstone facies in the east.

Dissolution and replacement of originally aragonitic taxa appear to have occurred in the east of the study area among the high-energy grainstone and rudstone facies, while to the west a number of aragonitic fossils are preserved in the muddier facies. This suggests a relationship between increasing grain size and decreasing carbonate-mud content that leads to a decrease in aragonite preservation potential. This dissolution and degradation of the eastern aragonitic taxa may have enhanced early sea-floor diagenesis by providing a limited increase in dissolved calcium carbonate within pore-waters.

9.3 Sequence stratigraphy

A sequence stratigraphic model of the Waitaki study area was developed using outcrop-based lithostratigraphy, biostratigraphy and facies types. The model included three sequences and four sequence boundaries, including one lower-order sequence boundary. It

records a series of transgressive-regressive cycles beginning in the Late Cretaceous, and continuing until the onset of the modern plate boundary in the Miocene.

The first sequence records a change from siliciclastic to carbonate facies, transitioning from a terrestrial fluvial environment through to an outer-shelf to upper-slope marine setting. This sequence highlighted the existence of an eastern palaeohigh developed between the Kaiatan and Whaingaroan Stages.

A major upper Whaingaroan Stage sea-level fall marks a sequence boundary following this transgression, of the order of 100 – 150 m. This induced subaerial exposure in the east, while deeper western facies developed a firmground.

The second sequence records transgression during the Duntroonian and Waitakian Stages, which was interrupted briefly by an early Waitakian Stage sea-level fall. A more major sea-level regression then occurred in the upper Waitakian that led to a second period of subaerial exposure on the eastern palaeohigh. This was followed by transgression in the Otaian Stage, with a significant increase in siliciclastic sediment by the Altonian, leading to further sea-level regression.

Of the three periods of highstand within the study area, it was the first sequence ending in the early Whaingaroan that reached the greatest depths, indicated by deposition of the outer-shelf to upper-slope Impure Wackestone facies. Later transgressions did not reach the same depth, thus constraining the period of maximum submergence of the study area to the early Whaingaroan Stage.

The Impure Wackestone facies indicates significant siliciclastic input into the basin in the early Whaingaoran. While siliciclastic content decreased through later Duntroonian and Waitakian facies, average quartz silt content was still 5 – 6% throughout this period in the west of the study area, while to the north easterly palaeocurrents found in high-energy facies also contain a moderate siliciclastic component. These two factors indicate the

presence of a landmass to the west of the study area which, while reduced by the Waitakian Stage, was still supplying sediment to the area and was therefore likely to still be emergent.

9.4 Palaeobathymetry and sequence stratigraphic expression

The palaeogeography of the study area was defined by the presence of an eastern volcanic-induced high which exerted significant influence on the evolution of the region, eventually resulting in development of a submerged rimmed carbonate platform of which the study area formed the eastern, westward-dipping section. Extensive volcanic activity, and creation of numerous tuff cones in the east between the Kaiatan and early Whaingaroan Stages, encouraged production of siliceous sediments that settled in calm areas north of the high, protected by this barrier from submarine current activity.

This eastern palaeohigh became the setting for a productive carbonate factory between the Runangan and early Whaingaroan Stages by providing an elevated area devoid of terrigenous sediment supplied from the west. Detrital carbonate sediment was then supplied westward from the high to deposit with siliciclastic silts, forming the Impure Wackestone facies.

During the two major lowstands identified in the sequence stratigraphic model, the eastern high was likely to have provided a barrier to submarine current activity, resulting in a funnelling effect around it. This effect may have continued while submarine, blocking all but the larger currents from the south (although significant storm events that swept over it would have reworked any sediment accumulated there and redeposited it northwards). The sustained high-energy environment, found on the eastern high during the shallower second sequence, limited sediment accumulation in that area and led to a much thinner sequence in the east than in the west of the study area.

It is concluded that the existence of a palaeohigh in a cool-water carbonate environment may have significant effects on the evolution of a region, altering current and storm patterns, and stimulating carbonate-factory development where it might otherwise not have developed.

9.5 Alternating authigenic and carbonate production

The study area contains glauconitic- and francolite-rich facies developed during early transgression, followed by increasingly calcareous facies through to highstand. Lowstand and early sea-level transgression brought fine-grained, clay-rich terrigenous material to the area from the western landmass. This environment favoured precipitation of authigenic glauconitic grains and francolite nodules - which continued through transgression, with areas proximal to volcanic sediments exhibiting a higher rate of phosphogenesis. Coupled with low sedimentation rates during periods of lowered sea level, these environments were favourable to authigenic mineral production (as "authigenic factories").

As transgression continued and sea level approached highstand, the supply of terrigenous clays was reduced and effectively shut off by sea-level transgression inducing shoreline advancement, and glauconite and francolite mineral production decreased, with the system reverting to a carbonate factory. The restart of the carbonate factory further enhances the dilution of the already reduced clay supply. Increased sediment accumulation rates reduced precipitation and maturation of authigenic minerals. These controls for the production of authigenic components existed at and following lowstand (before instigation of a carbonate factory), with an authigenic factory operating in the absence of significant carbonate production.

Alternation between authigenic and carbonate factories may be recognised in carbonate sequences elsewhere, where glauconitic and phosphatic facies overlying a sea-level lowstand grade into more calcareous facies through sea-level transgression and into highstand. The key factor in this process is that terrigenous supply must not become too significant, as this would lead to increased sedimentation rates and the smothering of any authigenic glauconite or phosphate production, and lead to the deposition of clastic facies. Rather, a moderate supply of terrigenous clay for glauconitisation during lowstands favours the establishment of an authigenic factory.

9.6 Mid-Cenozoic New Zealand and the Waitaki area in context

The Waitaki study area shows a decrease in siliciclastic sediment supply, and development of increasingly calcareous facies, in the Late Eocene and Early Oligocene. The eastern carbonate factory developed in this setting over a bathymetric high while siliciclastic supply was still high. This resulted in the establishment of carbonate facies within the study area earlier than they might otherwise have developed, as the Waitaki area is likely to have otherwise been similar to other New Zealand regions more proximal to the developing tectonic zone at the Pacific-Australian plate boundary.

The deposition of a thick carbonate sequence in the Late Oligocene, as well as possible minor tectonic influence, affected the study area by counteracting relative sea-level rise (which resulted in a period of maximum flooding elsewhere in New Zealand), such that during this period the study area did not reach depths approached during the Early Oligocene. With the development of the Alpine Fault in the Early Miocene, it is likely that the lowstand which developed in the study area then was the result of an increase in tectonic uplift, accompanied by a minor eustatic sea-level fall. This was followed by a period of eustatic sea-level transgression and development of calcareous

glauconite sandstones in the Early Miocene, before increased tectonic uplift induced relative sea-level fall and the end of eustatic influence on relative sea level.

Comparisons between the two major sequence boundaries in the study area, and with similar unconformities in other New Zealand regions, imply that proximity to the developing plate boundary influenced how eustatic sea-level changes were recorded in the sedimentary record. Regions proximal to this zone of deformation, particularly those around western New Zealand, contain a local sea-level record that often reflects these tectonic events, while more distal regions contain a better overall record of eustatic sea-level change.

The study area appears to have been strongly influenced by eustatic sea-level change between the Eocene and the Early Oligocene, and was therefore not heavily influenced by the developing plate boundary. Increasing tectonic influence led to moderate uplift and a shallower depositional environment in the Late Oligocene however, while other regions in New Zealand recorded a period of maximum submergence reflecting the regional 1st order megasequence. This changed once the developing Alpine Fault had extended its stress field outwards in the Early Miocene to induce uplift in the study area, coupled with a significant increase in siliciclastic supply derived from newly uplifted basement blocks, smothering carbonate production and filling accommodation space. Regional regression was thus set in motion, as recorded in the development of siliciclastic facies in the Waitaki region and around New Zealand as a whole.

9.7 Future directions

The Waitaki region is clearly an interesting area for study of mid-Cenozoic sedimentary successions, with potential for improving understanding of local and regional New Zealand history, and there remains much that can still be done. Particular areas that

warrant further investigation include enhanced age control, additional detailed palaeoenvironmental determination, and added constraint on the degree of diagenesis in the area.

The ages of both the facies types identified in this study, and the sequence boundaries that separate them, could be enhanced by further detailed and focused biostratigraphic analyses within each specific facies across the study area. Detailed palaeontological study would further enhance depth control and palaeoenvironmental variation within and between each facies identified here.

Strontium isotope dating, particularly around the two major unconformities, would provide absolute ages, enhancing correlation of facies and unconformable surfaces in the region. This would allow for improved comparison with other New Zealand regions.

Variations in glauconite maturity presented here would be enhanced by further extensive geochemical analyses, particularly concerning the K_2O content of these grains within all facies around the Waitaki area, and in other similar mid-Cenozoic New Zealand successions. This would provide additional quantification to the categories and processes presented here.

Finally, detailed electron microprobe and stable isotope geochemistry of calcareous cements within all facies could be used to further develop the diagenetic processes identified in this study.

REFERENCES

Adams, C.J. and Raine, J.I. (1988) Age of Cretaceous silicic volcanism at Kyeburn, Central Otago, and Palmerston, eastern Otago, South Island, New Zealand. *New Zealand Journal of Geology and Geophysics*, **31**, 471-475.

Aitchison, J.C. (1988) An Eocene storm-generated littoral placer, northeast Otago. *New Zealand Journal of Geology and Geophysics*, **31**:3, 381-383.

Alexandersson, E.T. (1978) Destructive diagenesis of carbonate sediments in the eastern Skagerrak, North Sea. *Geology*, **6**:6, 324-327.

Alexandersson, E.T. (1979) Marine maceration of skeletal carbonates in Skagerrak, North Sea. *Sedimentology*, **26**, 845-852.

Amorosi, A. (1995) Glaucony and sequence stratigraphy: A conceptual framework of distribution in siliciclastic sequences. *Journal of Sedimentary Research*, **B65**:4, 419-425.

Amorosi, A. (1997) Detecting compositional, spatial, and temporal attributes of glaucony: a tool for provenance research. *Sedimentary Geology*, **109**, 135-153.

Anastas, A.S., Dalrymple, R.W., James, N.P. and Nelson, C.S. (2006) Lithofacies and dynamics of a cool-water carbonate seaway: mid-Tertiary, Te Kuiti Group, New Zealand. *Geological Society, London, Special Publications*, **255**, 245-268.

Andrews, P.B. (1968) Patterns of sedimentation during early Otaian (Early Miocene) time in North Canterbury, New Zealand. *New Zealand Journal of Geology and Geophysics*, **11**, 711-752.

Ayress, M.A. (1993) Ostracod biostratigraphy and palaeoecology of the Kokoamu Greensand and Otekaike Limestone (Late Oligocene to Early Miocene), North Otago and South Canterbury, New Zealand. *Alcheringa: An Australasian Journal of Palaeontology*, **17**:2, 125-151.

Ayress, M.A. (2006) Ostracod biostratigraphy of the Oligocene-Miocene (upper Waitakian to lower Otaian) in southern New Zealand. *New Zealand Journal of Geology and Geophysics*, **49**:3, 359-373.

Back, W., Hanshaw, B.B., Pyle, T.E., Plummer, L.M. and Wiedie, A.E. (1979) Geochemical significance of ground-water discharge and carbonate solution to the formation of Caleta Xei Ha, Quintana Roo, Mexico. *Water Resources Research*, **15**, 1531-1535.

Baioumy, H. and Boulis, S. (2012) Non-pelletal glauconite from Campanian Qusseir Formation, Egypt: Implication for glauconitization. *Sedimentary Geology*, **249-250**, 1-9.

Ballance, P.F. (1976) Stratigraphy and bibliography of the Waitemata Group of Auckland, New Zealand. *New Zealand Journal of Geology and Geophysics*, **19**:6, 897-932.

Ballance, P.F. (1993) The paleo-Pacific, post-subduction, passive margin thermal relaxation sequence (Late Cretaceous-Paleogene) of the drifting New Zealand continent. In: *South Pacific Sedimentary Basin – Sedimentary Basins of the World, 2* (Ed. P.F. Ballance). Elsevier, Amsterdam, pp. 93-110.

Ballance, P.F. and Spörli, K.B. (1979) Northland Allochthon. *Journal of the Royal Society of New Zealand*, **9**:2, 259-275.

Ballance, P.F., Pettinga, J.R. and Webb, C. (1982) A model of Cenozoic evolution of northern New Zealand and adjacent areas of the southwest Pacific. *Tectonophysics*, **87**, 37-48.

Banerjee, S., Chattoraj, S.L., Saraswati, P.K., Dasgupta, S. and Sarkar, U. (2012) Substrate control on formation and maturation of glauconites in the Middle Miocene Harudi Formation, western Kutch, India. *Marine and Petroleum Geology*, **30**:1, 144-160.

Barker, P.F. and Burrell, J. (1982) The influence upon Southern Ocean circulation, sedimentation, and climate of the opening of the Drake Passage. In: *Antarctic Geoscience* (Ed. C. Craddock), University of Wisconsin Press, 377-385.

Bassi, D. and Nebelsick, J.H. (2010) Components, facies and ramps: Redefining Upper Oligocene shallow water carbonates using coralline red algae and larger foraminifera (Venetian area, northeast Italy). *Palaeogeography, Palaeoclimatology, Palaeoecology*, **295**, 258-280.

Baturin, G.N. (1971) Stages of phosphorite formation on the ocean floor, *Nature*, **232**, 61-62.

Batt, G.E. (1993) Aspects of an Early Miocene Unconformity in North Otago and South Canterbury. Unpublished BSc (Hons) thesis, University of Otago, Dunedin.

Batt, G.E., Baldwin, S.L., Cottam, M.A., Fitzgerald, P.G., Brandon, M.T. and Spell, T.L. (2004) Cenozoic plate boundary evolution in the South Island of New Zealand: New thermochronological constraints. *Tectonics*, **23**:4, 1-17.

Baur, J. (2012) Regional seismic attribute analysis and tectonostratigraphy of offshore south-western Taranaki Basin, New Zealand. Unpublished PhD Thesis, Victoria University of Wellington.

Benson, W.N. (1943) The basic igneous rocks of Eastern Otago and their tectonic environment, part IV. *Transactions of the Royal Society of New Zealand*, **73**, 116-138.

Berggren, W.A. and Prothero, D.R. (1992) Eocene-Oligocene climatic and biotic evolution: an overview, In: *Eocene-Oligocene climatic and biotic evolution.* (Eds D.R. Prothero and W.A. Berggren), Princeton University Press, 1-28.

Berner, R.A. (1975) The role of magnesium in the crystal growth of calcite and aragonite from seawater. *Geochimica et Cosmoschimica Acta*, **39**, 489-504.

Beu, A.G. and Maxwell, P.A. (1990) Cenozoic Mollusca of New Zealand. *New Zealand Geological Survey Paleontological Bulletin* **58**, New Zealand Geological Survey, Lower Hutt, pp. 518.

Bishop, D.G. (1974) Tertiary and Quaternary geology of the Naseby and Kyeburn areas, Central Otago. *New Zealand Journal of Geology and Geophysics*, **17**, 19-39.

Bishop, D.G., Laird, M.G. and Landis, C.A. (1985) Provisional terrane map of South Island, New Zealand. In: *Tectonostratigraphic Terranes of the Circum-Pacific region, Circum-Pacific Council for Energy and Mineral Resources Earth Science Series 1* (Ed. D. Howell), Circum-Pacific Council for Energy and Mineral Resources, Houston, pp. 515-521.

Blomeier, D., Dustira, A., Forke, H. and Scheibner, C. (2010) Environmental change in the Early Permian of NE Svalbard: from a warm-water carbonate platform (Gipshuken Formation) to a temperate, mixed siliciclastic-carbonate ramp (Kapp Starostin Formation). *Facies*, **57**:3, 493-523.

Boreen, T.D. and James, N.P. (1995) Stratigraphic sedimentology of Tertiary cool-water limestones, SE Australia. *Journal of Sedimentary Research*, **65**, 142.

Brachert, T. and Dullo, W. (2000) Shallow burial diagenesis of skeletal carbonates: selective loss of aragonite shell material (Miocene to Recent, Queensland Plateau and Queensland Trough, NE Australia) – implications for shallow cool-water carbonates. *Sedimentary Geology*, **136**:3-4, 169-187.

Bradshaw, J.D. (1989) Cretaceous geotectonic patterns in the New Zealand region. *Tectonics*, **8**, 803-820.

Bradshaw, J.D. (1993) A review of the Median Tectonic Zone: terrane boundaries and terrane amalgamation near the Median Tectonic Line. *New Zealand Journal of Geology and Geophysics*, **36**, 117-125.

Browne, G.H. (1995) Sedimentation patterns during the Neogene in Marlborough, New Zealand. *New Zealand Journal of Geology and Geophysics*, **25**, 459-483.

Buening, N., Carlson, S.J., Spero, H.J. and Lee, D.E. (1998) Evidence for the Early Oligocene formation of a proto-Subtropical Convergence from oxygen isotope records of New Zealand Paleogene brachiopods. *Palaeogeography, Palaeoclimatology, Palaeoecology*, **138**, 43-68.

Burchette, T. and Wright, V. (1992) Carbonate ramp depositional systems. *Sedimentary Geology*, **79**:1-4, 3-57.

Burst, J.F. (1958a) "Glauconite" pellets: their mineral nature and applications to stratigraphic interpretations. *Bulletin of the American Association of Petroleum Geologists*, **42**, 310-327.

Burst, J.F. (1958b) Mineral heterogeneity in "glauconite" pellets. *American Mineralogist*, **43**, 481-497.

Campbell, H.J. and Landis, C.A. (2001) New Zealand awash. *New Zealand Geographic*, **51**, 6-7.

Caron, V. and Nelson, C. (2009) Diversity of neomorphic fabrics in New Zealand Plio-Pleistocene cool-water limestones: insights into aragonite alteration pathways and controls. *Journal of Sedimentary Research*, **79**:4, 226-246.

Caron, V., Nelson, C.S. and Kamp, P.J.J. (2004) Contrasting carbonate depositional systems for Pliocene cool-water limestones cropping out in central Hawke's Bay, New Zealand. *New Zealand Journal of Geology and Geophysics*, **47**:4, 697-717.

Caron, V., Nelson, C.S. and Kamp, P.J.J. (2005) Sequence stratigraphic context of syndepositional diagenesis in cool-water shelf carbonates: Pliocene limestones, New Zealand. *Journal of Sedimentary Research*, **75**, 231-250.

Carter, L. (1969) The Mahurangi Limestone from Puketotara Peninsula, Northland, New Zealand. *New Zealand Journal of Geology and Geophysics*, **12**:1, 104-118.

Carter, R.M. (1985) The mid-Oligocene Marshall Paraconformity, New Zealand. Coincidence with global eustatic sea-level fall or rise? *The Journal of Geology*, **93**:3, 359-371.

Carter, R.M. (1988) Post-breakup stratigraphy (Kaikoura Synthem; Cretaceous-Cenozoic) of the continental margin off southeastern of New Zealand. *New Zealand Journal of Geology and Geophysics*, **31**, 405-429.

Carter, R.M. and Carter, L. (1982) The Motunau Fault and other structures at the southern edge of the Australian-Pacific plate boundary, offshore Marlborough, New Zealand. *Tectonophysics*, **88**, 133-159.

Carter, R.M. and Landis, C.A. (1972) Correlative unconformities in southern Australasia. *Nature*, **237**, 12-13.

Carter, R.M. and Landis, C.A. (1982) Oligocene unconformities in the South Island. *Journal of the Royal Society of New Zealand*, **12**, 42-46.

Carter, R.M. and Lindqvist, J.K. (1975) Sealers Bay submarine fan complex, Oligocene, southern New Zealand. *Sedimentology*, **22**, 465-483.

Carter, R.M. and Lindqvist, J.K. (1977) Balleny Group, Chalky Island, southern New Zealand: an inferred Oligocene submarine canyon and fan. *Pacific Geology*, **12**, 1-46.

Carter, R.M. and Norris, R.J. (1976) Cenozoic history of southern New Zealand: an accord between geological observations and plate-tectonic predictions. *Earth and Planetary Science Letters*, **31**, 85-94.

Carter, R.M., Lindqvist, J.K. and Norris, R.J. (1982) Oligocene unconformities and nodular phosphate-hardground horizons in western Southland and northern West Coast. *Journal of the Royal Society of New Zealand*, **12**, 11-46.

Carter, R.M., McCave, I.N. and Carter, L. (2004) Leg 181 synthesis: fronts, flows, drifts, volcanoes, and the evolution of the southwestern gateway to the Pacific Ocean, eastern New Zealand. *Proceedings of the Ocean Drilling Program, Scientific Results*, **181**.

Cas, R.A., Landis, C.A. and Fordysce, R.E. (1989) A monogenetic, Surtla-type, Surtseyan volcano from the Eocene-Oligocene Waiareka-Deborah volcanics, Otago, New Zealand: a model. *Bulletin of Volcanology*, **51**, 281-298.

Case, J. (1988) Palaeogene floras from Seymour Island, Antarctic Peninsula. *In:* Geology and palaeontology of Seymour Island, Antarctic Peninsula (Eds R.M. Feldman and W.O. Woodburne), Geological Society of America Memoir **169**, pp. 523-530.

Chapman-Smith, M. and Grant-Mackie, J.A. (1971) Geology of the Whangaparaoa area, eastern Bay of Plenty. *New Zealand Journal of Geology and Geophysics*, **14**, 3-38.

Choqueete, P.W. and James, N.P. (1990) The burial diagenetic environment. In: *Diagenesis* (Eds I.A. McIlreath and D.W. Morrow), St John's Geological Association of Canada, Ottawa, pp. 75-112.

Coombs, D.S., Cas, R.A., Kawachi, Y., Landis, C.A., McDonough, W.F. and Reay, A. (1986) Cenozoic volcanism in north, east and Central Otago. *Royal Society of New Zealand Bulletin*, **23**. Royal Society of New Zealand, Wellington.

Cooper, A.F., Barreiro, B.A., Kimbrough, D.L. and Mattison, J.M. (1987) Lamprophyre dike intrusion and the age of the Alpine Fault, New Zealand. *Geology*, **15**, 941-944.

Cooper, R.A. (ed.) (2004) The New Zealand Geological Timescale. Institute of Geological and Nuclear Sciences Monograph **22**, 284 pp.

Cooper, A.F., Barreiro, B.A., Kimbrough, D.L. and Mattinson, J.M. (1987) Lamprophyre dike intrusion and the age of the Alpine Fault, New Zealand. *Geology*, **15**, 941-944.

Crux, J.A., Eaton, G.L. and Sturrock, S.J. (1984) Biostratigraphy of the Clipper-1 well, offshore New Zealand. *Petroleum Report Series,* PR**1044**, New Zealand Ministry of Commerce, Wellington, PPL 38202.

Davy, B.W. (2006) Bollons seamount and early New Zealand – Antarctic seafloor spreading. *Geochemistry, Geophysics, Geosystems*, **7**:6.

Dickey Jr, J. (1968) Observations on the Deborah Volcanic Formation near Kakanui, New Zealand. *New Zealand Journal of Geology and Geophysics*, **11**: 5, 1159-1162.

Dickson, J.A.D. (1965) A modified technique for carbonates in thin section. *Nature*, **205**:4971, 587.

Diester-Haass, L. and Zahn, R. (1996) The Eocene-Oligocene transition in the Southern Ocean: history of water masses, circulation, and biological productivity inferred from high resolution records of stable isotopes and benthic foraminiferal abundances (ODP Site 689). *Geology*, **24**, 16-20.

Douglas, B.J. (1970) Geology between southern Horse Range and Shag Point/Katiki. Unpublished DipSci thesis, University of Otago, Dunedin.

Dunham, R.J. (1962) Classification of carbonate rocks according to depositional texture. In: *Classification of Carbonate Rocks* (Ed. W.E. Ham). *AAPG Memoir 1*, p. 108–121.

Edbrooke, S.W., Sykes, R. and Pocknall, D.T. (1994) Geology of the Waikato Coal Measures, Waikato Coal Region, New Zealand. *Institute of Geological & Nuclear Sciences Monograph* **6**. Institute of Geological & Nuclear Sciences, Lower Hutt.

Edwards, A.R. (1971) Report on five stratigraphic holes drilled in North Otago, 1968. In: *New Zealand Geological Survey Report* **49**, Lower Hutt.

Edwards, A.R. (1991) The Oamaru Diatomite. *New Zealand Geological Survey Paleontological Bulletin*, **64**, Department of Industrial and Scientific Research, Lower Hutt, 260 pp.

Embry, A.F. and Klovan, J.E. (1972) Absolute water depth limits of late Devonian paleoecological zones. *Geol. Rundschau*, **61**, 672-686.

Esteban, M. and Klappa, C.F. (1983) Subaerial exposure. In: *Carbonate Depositional Environments* (Eds P.A. Scholle, D.G. Bebout and C.H. Moore). *AAPG Memoir* 33, Tulsa, p. 1-54.

Evamy, B.D. (1963) The application of a chemical staining technique to a study of dedolomitisation. *Sedimentology*, **2**, 164-170.

Exon, N., Kennett, J., Malone, M., Brinkhuis, H., Chaproniere, G., Ennyu, A., Fothergill, P., Fuller, M., Grauert, M., Hill, P., Janecek, T., Kelly, C., Latimer, J., McGonigal, K., Nees, S., Ninnemann, U., Nuernberg, D., Pekar, S., Pellaton, C., Pfuhl, H., Robert, C., Röhl, U., Schellenberg, S., Shevenell, A., Stickley, C., Suzuki, N., Touchard, Y., Wei, W. and White, T. (2002) Drilling reveals climatic consequences of Tasmanian gateway opening. *EOS*, **83**:23, 253-259.

Feely, R.A., Massoth, G.J., Baker, E.T., Cowen, J.P., Lamb, M.F. and Krogslund, K.A. (1990) The effect of hydrothermal processes on midwater phosphorus distributions in the northeast Pacific. *Earth and Planetary Science Letters*, **96**, 305-318.

Field, B.D. and Browne, G.H. (1986) Lithostratigraphy of Cretaceous and Tertiary rocks, Southern Canterbury, New Zealand. *New Zealand Geological Survey Record,* **14**, Department of Industrial and Scientific Research, Wellington.

Field, B.D., Browne, G.H., Davy, B., Herzer, R.H., Hoskins, R.H., Raine, J.I., Wilson, G.J., Sewell, R.J., Smale, D. and Watters, W.A. (1989) Cretaceous and Cenozoic sedimentary basins and geological evolution of the Canterbury region, South Island, New Zealand. *New Zealand Geological Survey Basin Studies 2*. Department of Scientific and Industrial Research, Wellington.

Field, B.D., Uruski, C.I. *et al*. (1997) Cretaceous-Cenozoic geology and petroleum systems of the East Coast Region, New Zealand. *Institute of Geological and Nuclear Sciences Monograph,* **19**, Institute of Geological & Nuclear Sciences Limited, Lower Hutt.

Findlay, R.H. (1980) The Marshall Paraconformity (Note). *New Zealand Journal of Geology and Geophysics*, **23**, 125-133.

Fleming, C.A. (1959) Océanie. Fascicule 4. New Zealand. *Lexique Stratigraphique International*, **6**, Centre National de al Recherche Scientifique, Paris. 527 pp.

Fleming, C.A. (1962) New Zealand biogeography: a palaeontologists approach. *Tuatara*, **10**, 53-108.

Flügel, E. (2010) Microfacies of Carbonate Rocks: analysis, interpretation and application. Springer-Verlag, Berlin, 984 pp.

Folk, R.L. and Land, L.S. (1975) Mg/Ca ratio and salinity, two controls over crystallization of dolomite. *Bulletin of the American Association of Petroleum Geologists*, **59**, 60-68.

Föllmi, K. (1996) The phosphorous cycle, phosphogenesis and marine phosphate-rich deposits. *Earth Science Reviews*, **40**, 55-124.

Föllmi, K.B. and Garrison, R.E. (1991) Phosphatic sediments, ordinary or extraordinary deposits? The example of the Miocene Monterey Formation (California). In: *Controversies in Modern Geology* (Eds D.W. Müller, J.A. McKenzie and H. Weissert), *Academic Press*, London, pp. 55-84.

Föllmi, K.B., Garrison, R.E. and Grimm, K.A. (1991) Stratification in phosphatic sediments: Illustrations from the Neogene of California. In: *Cycles and Events in Stratigraphy* (Eds G. Einsele, W. Ricken), Springer-Verlag, Berlin, pp. 492-507.

Fordyce, R.E. (1979) Records of two Paleogene turtles and notes on other Tertiary reptilian remains from New Zealand. *New Zealand Journal of Geology and Geophysics*, **22**, 737-741.

Fordyce, R.E. (1985) Late Eocene archaeocete whale (Archaeoceti: Dorudontinae) from Waihao, South Canterbury, New Zealand. *New Zealand Journal of Geology and Geophysics*, **28**, 351-357.

Forsyth, P.J. (2001) Geology of the Waitaki area, 1:250,000 Geological Map 19. Institute of Geological and Nuclear Sciences. 1 sheet + 64 pp.

Fox, L.E. (1990) Geochemistry of dissolved phosphate in the Sepik River and Estuary, New Guinea. *Geochimica et Cosmoschimica Acta*, **54**, 1019-1024.

Froelich, P.N. (1988) Kinetic control of dissolved phosphate in natural rivers and estuaries: a primer on the phosphate buffer mechanism. *Limnology and Oceanography*, **33**, 649-668.

Fulthorpe, C.S. (1991) Geological controls on seismic sequence resolution. *Geology*, **19**:1, 61-65.

Fulthorpe, C.S. and Carter, R.M. (1989) Test of seismic sequence methodology on a southern hemisphere passive margin: the Canterbury Basin, New Zealand. *Marine Petroleum Geology*, **6**, 348-359.

Fulthorpe, C. S., Carter, R.M., Miller, K.G. and Wilson, J. (1996) Marshall Paraconformity: a mid-Oligocene record of inception of the Antarctic circumpolar current and coeval glacio-eustatic lowstand? *Marine and Petroleum Geology*, **13**:1, 61-77.

Gächter, R., Meyer, J.S. and Mares, A. (1988) Contribution of bacteria to release and fixation of phosphorus in lake sediments. *Limnology and Oceanography*, **33**, 1542-1558.

Gage, M. (1957) The Geology of the Waitaki Subdivision. *New Zealand Geological Survey Bulletin*, **55**, Department of Industrial and Scientific Research, Wellington, 135 pp.

Gage, M. (1988) Mid-Tertiary unconformities in north Otago – A review and assessment. *Journal of the Royal Society of New Zealand*, **18**, 119-125.

Gibbs, G. (2006) Ghosts of Gondwana. Craig Potton Publishing, Nelson. 232 pp.

Glaessner, M.F. (1980) New Cretaceous and Tertiary crabs (Crustacea: Brachyura) from Australia and New Zealand. *Transactions of the Royal Society of South Australia*, **104**, 171-192.

Glenie, R.C., Schofield, J.C. and Ward, W.T. (1968) Tertiary sea levels in Australia and New Zealand. *Palaeogeography, Palaeoclimatology, Palaeoecology*, **5**, 141-163.

Glenn, C.R. and Arthur, M.A. (1988) Petrology and major element geochemistry of Peru Margin phosphorites and associated diagenetic minerals: Authigenesis in modern organic-rich sediments. *Marine Geology*, **80**, 287-307.

Glenn, C.R., Föllmi, K.B., Riggs, S.R., Baturin, G.N., Grimm, K.A., Trappe, J., Abed, A.M., Galli-Oliver, C., Garrison, R.E., Ilyin, A.V., Jehl, C., Rohrlich, V., Sadaqah, R.M.Y., Schidlowski, M., Sheldon, R.E. and Siegmund, H. (1994) Phosphorus and phosphorites: Sedimentology and environments of formation. *Eclogae Geologicae Helveticae*, **87**, 747-788.

Graham, I.J., Morgans, H.E.G., Waghorn, D.B., Trotter, J.A. and Whitford, D.J. (2000) Strontium isotope stratigraphy of the Oligocene-Miocene Otekaike Limestone (Trig Z section) in southern New Zealand: Age of the Duntroonian/Waitakian Stage boundary. *New Zealand Journal of Geology and Geophysics*, **43**:3, 335-347.

Greg, D.R. (1960) The geology of Tongariro Subdivision. *Bulletin of the New Zealand Geological Survey*, **40**.

Harrington, H.J. (1958) Geology of the Kaitangata Coalfield. *New Zealand Department of Scientific and Industrial Research Geological Survey Bulletin*, **59**.

Hay, R.F. (1960) The geology of the Mangakahia Subdivision. *Bulletin of the New Zealand Geological Survey*, **59**.

Hay, R.L. (1966) Zeolites and zeolitic reactions in sedimentary rocks. *Geological Society of America Special Paper*, **85**, 130 pp.

Hayton, S., Nelson, C.S. and Hood, S.D. (1995) A skeletal assemblage classification system for non-tropical carbonate deposits based on New Zealand Cenozoic limestones. *Sedimentary Geology*, **100**, 123-141.

Hayward, B.W. (1986) A guide to palaeoenvironment assessment using New Zealand Cenozoic foraminiferal faunas. *New Zealand Geological Survey Report PAL*, **109.**

Hayward, B.W. (1993) The tempestuous 10 million year life of a double arc and intra-arc basin – New Zealand's Northland Basin in the Early Miocene. In: *South Pacific Sedimentary Basins* (Ed. P.F., Ballance). Sedimentary Basins of the World 2. Elsevier, Amsterdam, pp. 113-142.

Hayward, B.W., Grenfell, H.R., Reid, C.M., Hayward, K.A. (1999) Recent New Zealand shallow-water benthic foraminifera: Taxonomy, ecological distribution, biogeography, and use in paleoenvironmental assessment. *New Zealand Geological Survey Bulletin,* **75**, 258 pp.

Hood, S.D., Nelson, C.S. and Kamp, P.J.J. (2003) Petrogenesis of diachronous mixed siliciclastic-carbonate megafacies in the cool-water Oligocene Tikorangi Formation, Taranaki Basin, New Zealand. *New Zealand Journal of Geology and Geophysics*, **46**, 387-405.

Hornibrook, N. de B. (1966) The stratigraphy of Landon (or Boundary) Creek, Oamaru. *New Zealand Journal of Geology and Geophysics*, **9**, 458-470.

Hornibrook, N. de B. (1987) Mid-Tertiary unconformities in the Waitaki Subdivision, North Otago – a comment. *Journal of the Royal Society of New Zealand*, **17**, 181-184.

Hornibrook, N. de B. (1992) New Zealand Cenozoic marine paleoclimates: a review based on the distribution of some shallow water and terrestrial biota. In: *Pacific Neogene Environment, Evolution, and Events* (Eds. T. Tsuchi and J.C. Ingle). University of Tokyo Press, Tokyo, pp. 83-106.

Hornibrook, N. de B. and Schofield, J.C. (1963) Stratigraphic relations of the Waitemata Group of the lower Waikato District. *New Zealand Journal of Geology and Geophysics*, **6**, 38-51.

Hornibrook, N. de B., Edwards, A.R., Mildenhall, D.C., Webb, P.N. and Wilson, G.J. (1976) Major displacements in Northland, New Zealand; micropaleontology and stratigraphy of Waimamaku 1 and 2 wells. *New Zealand Journal of Geology and Geophysics*, **19**:2, 233-263.

Hornibrook, N. de B., Brazier, R.C. and Strong, C.P. (1989) Manual of New Zealand Permian to Pleistocene foraminiferal biostratigraphy. *New Zealand Geological Survey Paleontological Bulletin*, **56**, 175 pp.

Hower, J. (1961) Some factors concerning the nature and origin of glauconite. *American Mineralogist*, **46**, 313-334.

Hudson, J.D. (1977) Stable isotopes and limestone lithification. *Journal of the Geological Society of London*, **133**, 637-660.

Irvine, J.R.M. (2012) Sedimentology, stratigraphy and palaeogeography of Oligocene to Miocene rocks of North Canterbury-Marlborough. Unpublished MSc thesis, University of Canterbury, Christchurch.

Isaac, M.J., Herzer, R.H., Brook, F.J. and Hayward, B.W. (1994) Cretaceous and Cenozoic sedimentary basins of Northland, New Zealand. *Institute of Geological and Nuclear Sciences Monograph 8*, 203 pp.

James, H.L. (1966) *Chemistry of the iron-rich sedimentary rocks*. U.S. Government Print Office, Washington D.C., 66 pp.

James, N.P. (1997) The cool-water carbonate depositional realm. In: *Cool-water Carbonates* (Eds. N.P. James and J.A.D. Clarke), *SEPM Special Publication*, **56**, 1-22.

James, N.P. and Bone, Y. (1989) Petrogenesis of Cenozoic, temperate water calcarenites, South Australia: a model for meteoric/shallow burial diagenesis of shallow water calcite sediments. *Journal of Sedimentary Petrology*, **59**, 191-203.

James, N.P. and Choquette, P.W. (1983) Diagenesis 5. Limestones: introduction. *Geoscience Canada*, **10**, 159-161.

James, N.P. and Choquette, P.W. (1984) Diagenesis 9. Limestones – the meteoric diagenetic environment. *Geoscience Canada*, **11**, 161-194.

James, N.P. and Choquette, P.W. (1990a) The meteoric diagenetic environment. In: *Diagenesis* (Eds I.A. McIlreath and D.W. Morrow), St John's Geological Association of Canada, Ottawa, pp. 35-74.

James, N.P. and Choquette, P.W. (1990b) The sea floor diagenetic environment. In: *Diagenesis* (Eds I.A. McIlreath and D.W. Morrow), St John's Geological Association of Canada, Ottawa, pp. 13-34.

James. N.P. and Clarke, J.A.D. (Eds) (1997) *Cool-water Carbonates*. *SEPM Special Publication*, **56**, 440 pp.

James, N.P., Boreen, T.D., Bone, Y. and Feary, D.A. (1994) Holocene carbonate sedimentation on the west Eucla Shelf, Great Australian Bight: a shaved shelf. *Sedimentary Geology*, **90**, 161-177.

James, N.P., Bone, Y. and Kyser, T.K. (2005) Where has all the aragonite gone? Mineralogy of Holocene neritic cool-water carbonates, Southern Australia. *Journal of Sedimentary Research*, **75**, 454-463.

James, N.P., Jones, B., Nelson, C.S., Campbell, H.J. and Titjen, J. (2011) Cenozoic temperate and sub-tropical carbonate sedimentation on an oceanic volcano – Chatham Islands, New Zealand. *Sedimentology*, **58**, 1007-1029.

Jarvis, I., Burnett, W.C., Nathan, Y., Almbaydin, F., Attia, K.M., Castro, L.N., Flicoteaux, R., Hilmy, M.E., Husain, V., Qutawna, A.A., Serjani, A. and Zanin, Y.N. (1994) Phosphorite geochemistry: state-of-the-art and environmental concerns. In: *Concepts and Controversies in Phosphogenesis* (Ed. K.B. Föllmi), *Eclogae Geologicae Helveticae*, **87**, 643-700.

Jenkins, D.G. (1971) New Zealand Cenozoic planktonic foraminifera. *New Zealand Geological Survey Palaeontological Bulletin*, **42**, 278 pp.

Jenkins, D.G. (1974) Initiation of the proto-circum-Antarctic current. *Science*, **252**, 371-373.

Jenkins, D.G. (1987) Oligo-Micocene unconformities in North Otago and the Tasman Sea. *Journal of the Royal Society of New Zealand*, **17**, 177-180.

Jenkins, D.G. (1993) The evolution of the Cenozoic southern high- and mid-latitude planktonic foraminiferal faunas. In: *Antarctic palaeoenvironment: A perspective on global change, part two* (Eds P.J. Kennett and D.A. Warnke), *American Geophysical Union, Antarctic Research Service*, **60**, 175-194.

Kamp, P.J.J. (1986a) The mid-Cenozoic Challenger Rift system of western New Zealand and its implications for the age of Alpine Fault inception. *Geological Society of America Bulletin*, **97**, 255-281.

Kamp, P.J.J. (1986b) Late Cretaceous-Cenozoic tectonic development of the southwest Pacific region. *Tectonophysics*, **121**, 225-251.

Kamp, P.J.J. (2001) Possible Jurassic age for part of Rakaia Terrane: implications for tectonic development of the Torlesse accretionary prism. *New Zealand Journal of Geology and Geophysics*, **44**, 185-203.

Kamp, P.J.J. and Nelson, C.S. (1987) Tectonic and sea-level controls on non-tropical limestones in New Zealand. *Geology*, **15**, 610-613.

Kamp, P.J.J. and Nelson, C.S. (1988) Nature and occurrence of modern Neogene active margin limestones in New Zealand. *New Zealand Journal of Geology and Geophysics*, **31**, 1-20.

Kamp, P.J.J., Harmsen, F.J., Nelson, C.S., and Boyle, S.F. (1988) Barnacle-dominated limestone with giant cross-beds in a non-tropical, tide swept, Pliocene forearc seaway, Hawke's Bay, New Zealand. *Sedimentary Geology*, **60**, 173–195.

Kamp, P.J.J., Webster, K. and Nathan, S. (1996) Thermal history analysis by integrated modelling of apatite fission track and vitrinite reflectance data: application to an inverted basin (Buller Coalfield, New Zealand). *Basin Research*, **8**, 383-402.

Kamp, P.J.J., Whitehouse, I.W.S. and Newman, J. (1999) Constraints on the thermal and tectonic evolution of Greymouth Coalfield. *New Zealand Journal of Geology and Geophysics*, **42**, 447-467.

Kamp, P.J.J., Vonk, A.J., Bland, K.J., Hansen, R.J., Hendy, A.J.W., McIntyre, A.P., Ngatai, M., Cartwright, S.J., Hayton, S. and Nelson, C.S. (2004) Neogene stratigraphic architecture and tectonic evolution of Wanganui, King Country, and eastern Taranaki Basins, New Zealand. *New Zealand Journal of Geology and Geophysics*, **47**:4, 625-644.

Kear, D. (1957) Stratigraphy of the Kaawa-Ohuka coastal area, west Auckland. *New Zealand Journal of Science and Technology*, **B38**, 826-842.

Kear, D. (1964) Kaitaia drillhole, near Kaitaia, Northland. *New Zealand Journal of Geology and Geophysics*, **7**, 903-910.

Keene, J.B. and Harris, P.T. (1995) Submarine cementation in tide-generated bioclastic sand dunes: epicontinental sea-way, Toreres Strait, north-east Australia. *International Association of Sedimentology Special Publication*, **24**, 225-236.

Kelly, J. and Webb, J. (1999) The genesis of glaucony in the Oligo-Miocene Torguay Group, southeastern Australia: petrographic and geochemical evidence. *Sedimentary Geology*, **125**, 99-114.

Kennett, J.P. and von der Borch, C.C. (1986) Southwest Pacific Cenozoic palaeoceanography. In: *Initial Report DSDP 90* (Eds J.P. Kennett and C.C. von der Borch, C.C.), *US Government Printing Office*, Washington, pp. 1493-1517.

King, P.R. (1990) Polyphase evolution of the Taranki Basin, New Zealand: changes in sedimentary and structural style. Ministry of Commerce (199), 1989 New Zealand Oil Expolration Conference Proceedings. Petroleum and Geothermal Unit, Energy and Resources Division, Ministry of Commerce. Pp. 134-150.

King, P.R. (2000) Tectonic reconstructions of New Zealand: 40 Ma to the present. *New Zealand Journal of Geology and Geophysics*, **43**:4, 611-638.

King, P.R. and Thrasher, G.P. (1996) Cretaceous-Cenozoic geology and petroleum systems of the Taranaki Basin, New Zealand. *Institute of Geological and Nuclear Sciences monograph*, **13**. Institute of Geological and Nuclear Sciences Limited, Lower Hutt, pp. 243.

King, P.R., Naish, T.R., Browne, G.H., Field, B.D. and Edbrooke, S.W. (1999) Cretaceous to Recent sedimentary patterns in New Zealand. *Institute of Geological and Nuclear Sciences folio series* **1**:1999.1.

Kitamura, A. (1998) Glaucony and carbonate grains as indicators of the condensed section: Omma Formation, Japan. *Sedimentary Geology*, **122**, 151-163.

Kominz, M.A. and Pekar, S.F. (2001) Oligocene eustacy from two-dimensional sequence stratigraphic backstripping. *Geological Society of America Bulletin*, **113**, 291-304.

Laird M.G. (1988) Punakaiki, Sheet S37 Geological map of New Zealand 1:63 360. Department of Scientific and Industrial Research, Wellington. 1 sheet + 48 pp.

Laird, M.G. (1996) Mid and early late Cretaceous break-up basins of the South Island, New Zealand. In: *Mesozoic geology of the eastern Australian Plate, extended abstract*, **43**, *Geological Society of Australia*, pp. 329-336.

Laird, M.G. and Bradshaw, J.D. (2004) The break-up of a long-term relationship: the Cretaceous separation of New Zealand from Gondwana. *Gondwana Research*, **7**, 273-286.

Lamb, S.H. and Bibby, H.M. (1989) The last 25 Ma of rotational deformation in part of the New Zealand plate-boundary zone. *Journal of Structural Geology*, **11**, 473-492.

Landis, C.A., Campbell, H.J., Begg, J.G., Mildenhall, D.C., Paterson, A.M. and Trewick, S.A. (2008) The Waipounamu Erosion Surface: questioning the antiquity of the New Zealand land surface and terrestrial fauna and flora. *Geological Magazine*, **145**, 173-197.

Larson, G. and Chilingar, G.V. (Eds) (1979) *Diagenesis in Sediments and Sedimentary Rocks*, Developments in Sedimentology, **25A**, Elsevier, Amsterdam, pp. 579.

Lawver, L.A., Gahagan, L.M. and Coffin, M.F. (1992) The development of paleoseaways around Antarctica. In: *The Antarctic palaeoenvironment: A perspective on global change, part one* (Eds J.P. Kennett and D.A. Warnke). *American Geophysical Union, Antarctic Research Service.* **56**, 7-30.

Leask, W. (1980) Basin analysis of Tertiary strata in Golden Bay, Nelson. *Unpublished M.Sc. thesis*, Victoria University of Wellington.

Lee, D.E., Lee, W.G. and Mortimer, N. (2001) Where and why have all the flowers gone? Depletion and turnover in the New Zealand Cenozoic angiosperm flora in relation to palaeogeography and climate. *Australian Journal of Botany*, **49**, 341-356.

Lees, A. and Buller, A.T. (1972) Modern temperate water and warm water shelf carbonate sediments contrasted. *Marine Geology*, **13**, 1767-1773.

Lemarche, G., Collot, J., Wood, R.A., Sosson, M., Sutherland, R. and Delteil, J. (1997) The Oligocene-Miocene Pacific-Australia plate boundary, south of New Zealand: Evolution from oceanic spreading to strike-slip faulting. *Earth and Planetary Science Letters*, **148**, 129-139.

LeMasurier, W.E. and Landis, C.A. (1996) Mantle-plume activity recorded by low-relief erosion surface in West Antarctica and New Zealand. *Geological Society of America Bulletin*, **108**, 1450-1466.

Leonard, J.E., Cameron, B., Pilkey, O.H. and Friedman, G.M. (1981) Evaluation of cold-water carbonates as a possible paleoclimatic indicator. *Sedimentary Geology*, **28**, 1-28.

Lever, H. (2001) An Eocene to early Oligocene unconformity-bounded sequence in the Punakaiki-Westport area, West Coast, South Island, New Zealand. *New Zealand Journal of Geology and Geophysics*, **44**:2, 355-363.

Lever, H. (2007) Review of unconformities in the Late Eocene and Early Miocene successions of the South Island, New Zealand: Ages, correlations, and causes. *New Zealand Journal of Geology and Geophysics*, **50**:3, 245-261.

Lewis, D.W. (1973) Polyphase limestone dikes in the Oamaru Region, New Zealand. *Journal of Sedimentary Research*, **43**: 4, 1031-1045.

Lewis, D.W. (1989) Mid-Tertiary unconformities in North Otago revisited. *Journal of the Royal Society of New Zealand*, **19**, 113-116.

Lewis, D.W. (1992) Anatomy of an unconformity on mid-Oligocene Amuri Limestone, Canterbury, New Zealand. *New Zealand Journal of Geology and Geophysics*, **35**:4, 463-475.

Lewis, D.W. and Belliss, S.E. (1984) Mid Tertiary Unconformities in the Waitaki Subdivision, North Otago. *Journal of the Royal Society of New Zealand*, **14**:3, 251-276.

Lewis, K.B. (1980) Quarternary sedimentation on the Hikurangi oblique-subduction and transform margin, New Zealand. *International Association of Sedimentologists Special Publication*, **4**, 171-184.

Lindqvist, J.K. (1986) Teredinid-bored Araucariaceae logs preserved in shoreface sediments, Wangaloa Formation (Paleocene), Otago, New Zealand. *New Zealand Journal of Geology and Geophysics*, **29**:2, 253-261.

Little, T.A., Mortimer, N. and McWilliams, M. (1999) An Episodic Cretaceous Cooling Model for the Otago-Marlborough Schist, New Zealand, Based on $^{40}Ar/^{39}Ar$ White Mica Ages. *New Zealand Journal of Geology and Geophysics*, **42**, 305-326.

Loutit, T.S. and Kennett, J.P. (1981) New Zealand and Australian Cenozoic sedimentary cycles and global sea-level changes. *American Association of Petroleum Geologists Bulletin*, **65**, 1586-1601.

Machel H.G. and Burton E.A. (1991) Factors governing cathodoluminescence in calcite and dolomite and their implications for studies of carbonate diagenesis. In: *Luminescence Microscopy and Spectroscopy: Qualitative and Quantitative Applications* (Eds C.E. Barker and O.C. Kopp). *SEPM Short Course*, **25**, 37-57.

Machel, H.G., Mason, R.A., Mariano, A.N. and Mucci, A. (1991) Causes and measurements of luminescence in calcite and dolomite. In: *Luminescence Microscopy and Spectroscopy: Qualitative and Quantitative Applications* (Eds C.E. Barker and O.C. Kopp). *SEPM Short Course*, **25**, 9-26.

MacKinnon, D.I., Beus, S.S. and Lee, D.E. (1993) Brachiopod fauna of the Kokoamu Greensand (Oligocene), New Zealand. *New Zealand Journal of Geology and Geophysics*, **36**, 327-347.

MacKinnon, T.C. (1983) Origin of the Torlesse Terrane and coeval rocks. *Geological Society of America Bulletin*, **94**, 967-985.

Maicher, D. (2000) Architecture and development of a shallow marine tuff cone at Lookout Bluff, New Zealand. In: *International Maar Conference*, Terra Nostra, Daun/Vulkaneifel, pp. 309-317.

Maicher, D. (2003) A cluster of Surtseyan volcanoes at Lookout Bluff, north Otago, New Zealand; aspects of edifice spacing and time. In: *Explosive subaqueous volcanism* (Eds J.D.L. White, J.L. Smellie, and D.A. Clague), *Geophysical Monograph* **140**, 167–178.

Mantell, G.A. (1850) Notice of the remains of *Dinornis* and other birds. With note on fossiliferous deposits of the Middle Island of New Zealand, by E Forbes. *Quarterly Journal of the Geological Society*, **6**, 319-343.

Massari, F. and D'Alessandro, A. (2009) Icehouse, cool-water carbonate ramps: the case of the Upper Pliocene Capodarso Fm (Sicily): role of trace fossils in the reconstruction of growth stages of prograding wedges. *Facies*, **56**, 47-58.

Maxwell, P.A. (1975) Studies on New Zealand Cenozoic mollusca, including the Eocene mollusca of McCollough's Bridge, Waihao River, South Canterbury. Unpublished PhD thesis, University of Canterbury, Christchurch.

McClellan, G.H. (1980) Mineralogy of carbonate flourapatites. *Journal of the Geological Society of London*, **137**, 675-681.

McConchie, D.M. and Lewis, D.W. (1980) Varieties of glauconite in Late Cretaceous and early Tertiary rocks of the South Island of New Zealand and new proposals for classification. *New Zealand Journal of Geology and Geophysics*, **23**, 413-438.

McRae, S. (1972) Glauconite. *Earth-Science Reviews*, **8**:4, 397-440.

Miller, K.G., Wright, J.D. and Fairbanks, R.G. (1991) Unlocking the ice house: Oligocene-Miocene oxygen isotopes, eustacy, and margin erosion. *Journal of Geophysical Research*, **96**, 6829-6848.

Miller, K.G., Kominz, M.A., Browning, J.V., Wright, J.D., Mountain, G.S., Katz, M.E., Sugarman, P.J., Cramer, B.S., Christie-Blick, N. and Pekar, S.F. (2005) The Phanerozoic record of global sea-level change. *Science*, **312**, 1293-1298.

Mitchell, M. (1990) The northern exposures of the Horse Range Formation, Trotters Gorge, East Otago. Unpublished BSc (Hons) thesis, University of Otago, Dunedin.

Mitchell, M., Craw, D., Landis, C.A. and Frew, R. (2009) Stratigraphy, provenance, and diagenesis of the Cretaceous Horse Range Formation, east Otago, New Zealand. *New Zealand Journal of Geology and Geophysics*, **52**, 171-183.

Mitchum, R.M. Jr., Vail, P.R. and Sangree, J.B. (1977) Seismic stratigraphy and global change of sea level, Part 6: Stratigraphic interpretation of seismic refelction patterns in depositional sequences. In: *Seismic stratigraphy – Applications to hydrocarbon exploration*. (Ed. Payton, C.E.) *American Association of Petroleum Geologists Memoir* **26**, 117-133.

Moore, P.R. and Morgans, H.E.G. (1987) Two new reference sections for the Wanstead Formation (Paleocene-Eocene) in Southern Hawkes Bay. *New Zealand Geological Survey record*, **20**, 81-87.

Molnar, P., Atwater, T., Mammerycx, J. and Smith, S.M. (1975) Magnetic anomalies, bathymetry and tectonic evolution of the South Pacific since the late Cretaceous. *Geophysical Journal International*, 40(3), 383-420.

Morgans, H.E.G., Edwards, A.R., Scott, G.H., Graham, I.J., Kamp, P.J.J., Mumme, T.C., Wilson, G.J. and Wilson G.S. (1999) Integrated Stratigraphy of the Waitakian-Otaian Stage Boundary stratotype, Early Miocene, New Zealand. *New Zealand Journal of Geology and Geophysics*, **42**, 581-614.

Mortimer, N. (1993) Jurassic Tectonic History of the Otago Schist. *Tectonics*, **12**, 237-244.

Mortimer, N. (2004) New Zealand's geological foundations. *Gondwana Research*, **7**:1, 261-272.

Mortimer, N. and Roser, B.P. (1992) Geochemical evidence for the Caples-Torlesse boundary in the Otago Schist. *Journal of the Geological Society of London*, **149**, 967-977.

Mortimer, N. and Tulloch, A. (1996) A Mesozoic basement of New Zealand. *Mesozoic Geology of the Eastern Australian Plate Conference (Abstract) Geological Society of Australia*, **43**, 391-399.

Mortimer, N., Herzer, R.H., Gans, P.B., Parkinson, D.L. and Seward, D. (1998) Basement geology from Three King Ridge to West Norfolk Ridge, southwest Pacific Ocean: evidence from petrology, geochemistry and isotopic dating of dredge samples. *Marine Geology*, **148**, 135-162.

Müller, R.D., Gaina, C., Tikku, A., Mihut, D., Cande, S.C. and Stock, J.M. (2000) Mesozoic/Cenozoic tectonic events around Australia. *Geophysical Monographs*, **121**, 161-188.

Murphy, B., Corcoran, P. and Moore, L. (2008) Subaqueous eruption and shallow-water reworking of a small-volume Surtseyan edifice at Kakanui, New Zealand. *Canadian Journal of Earth Sciences*, **45**:12, 1469-1485.

Nathan, S. (1974) Stratigraphic nomenclature for the Cretaceous-Lower Quaternary rocks of Buller and north Westland, West Coast, South Island, New Zealand. *New Zealand Journal of Geology and Geophysics*, **17**:2, 423-445.

Nathan, S., Anderson, H.J., Cook, R.A., Herzer, R.H., Hoskins, R.H., Raine, J.I. and Smale, D. (1986) Cretaceous and Cenozoic sedimentary basins of the West Coast Region, South Island, New Zealand. *New Zealand Geological Survey Basin Studies*, **1**.

Nathan, Y. (1984) The mineralogy and geochemistry of phosphorites. In: *Phosphate Minerals* (Eds J.O. Nriagu, J.O. and P.B. Moore), Springer-Verlag, Berlin, pp. 275-291.

Nelson, C.S. (1978a) Stratigraphy and paleontology of the Oligocene Te Kuiti Group, Waitomo County, South Auckland, New Zealand. *New Zealand Journal of Geology and Geophysics*, **21**:5, 553-594.

Nelson, C. S. (1978b) Temperate shelf carbonate sediments in the Cenozoic of New Zealand. *Sedimentology*, **25**, 737-771.

Nelson, C. S. (1988) An introductory perspective on non-tropical carbonates. *Sedimentary Geology*. **60,** 3-12.

Nelson, C.S. and Smith, A.M. (1996) Stable oxygen and carbon isotope compositional fields for skeletal and diagenetic components in New Zealand Cenozoic nontropical carbonate sediments and limestones: a synthesis and review. *New Zealand Journal of Geology and Geophysics*, **39**, 93-107.

Nelson, C.S. and James, N.P. (2000) Marine cements in mid-Tertiary cool-water shelf limestones of New Zealand and southern Australia. *Sedimentology*, **47**:3, 609-629.

Nelson, C.S. and Cooke, P.J. (2001) History of oceanic front development in the New Zealand sector of the Southern Ocean during the Cenozoic – a synthesis. *New Zealand Journal of Geology and Geophysics*, **44**, 535-553.

Nelson, C.S. and Kamp, P.J.J. (2012) Oligocene-Miocene sedimentary record, eastern Taranaki Basin margin. *In*: Fieldtrip Guides, Geosciences 2012 Conference, Hamilton, New Zealand (compiled by A. Pittari). *Geoscience Society of New Zealand Miscellaneous Publication*, **134B**, 63 pp.

Nelosn, C.S., Hancock, G.E. and Kamp, P.J.J. (1982) Shelf to basin, temperate skeletal carbonate sediments, Three Kings Plateau, New Zealand. *Journal of Sedimentary Petrology*, **52**:3, 717-732.

Nelson, C.S., Harris, G.J. and Young, H.R. (1988a) Burial-dominated cementation in non-tropical carbonates of the Oligocene Te Kuiti Group, New Zealand. *Sedimentary Geology*, **60**, 233-250.

Nelson, C.S., Keane, S.L. and Head, P.S. (1988b) Non-tropical carbonate deposits on the modern New Zealand shelf. *Sedimentary Geology*, **60**, 71-94.

Nelson, C.S., Kamp, P.J.J. and Young, H.R. (1994) Sedimentology and petrology of mass-emplaced limestone (Orahiri Limestone) on a late Oligocene shelf, western North Island, and tectonic implications for eastern margin development of Taranaki Basin. *New Zealand Journal of Geology and Geophysics*, **37**, 269-285.

Nelson, C.S., Lee, D., Maxwell, P., Maas, R., Kamp, P.J.J. and Cooke, S. (2004) Strontium isotope dating of the New Zealand Oligocene. *New Zealand Journal of Geology and Geophysics*, **47**:4, 719-730.

Nicol, A. (1992) Tectonic structures developed in Oligocene limestones: implications for New Zealand plate boundary deformation in North Canterbury. *New Zealand Journal of Geology and Geophysics*, **35**, 353-362.

Nicolaides, S. (1995) Cementation in Oligo-Miocene non-tropical shelf limestones, Otway Basin, Australia. *Sedimentary Geology*, **95**, 97-122.

Nicolaides, S. and Wallace, M.W. (1997) Pressure-dissolution and cementation in an Oligocene-Miocene non-tropical limestone (Clifton Formation), Otway Basin, Australia. In: *Cool-water Carbonates* (Eds. James, N.P. and Clark, J.D.A.), SEPM, Special Publication **56**, 127-140.

Norris, R.J., Carter, R.M. and Turnbull, I.M. (1978) Cainozoic sedimentation in basins adjacent to a major continental transform boundary in southern New Zealand. *Journal of the Geological Society of London*, **135**, 191-205.

O'Conner, B. (1999) Radiolaria from the Late Eocene Oamaru Diatomite, South Island, New Zealand. *Micropaleontology*, **45**:1, 1-55.

Odin, G.S. and Matter, A. (1981) De glauconiarum origine. *Sedimentology*, **28**, 611-641.

Odin, G.S. and Morton, A.C. (1988) Authigenic green particles from marine environments. In: *Diagenesis II. Developments in Sedimentology* (Eds G.V. Chilingarian, and K.H. Wolf), **43**, Elsevier, Amsterdam, pp. 213-264.

Odin, G.S. and Fullagar, P.D. (1988) Geological significance of the glaucony facies. In: *Green Marine Clays: Developments in Sedimentology* (Ed. G.S. Odin), Elsevier, Amsterdam, pp. 295-332.

Odom, I.E. (1984) Glauconite and celadonite minerals. In: *Reviews in Mineralogy: Micas* (Ed. S.W. Bailey), **13**, pp.545-572.

Pablo-Galán, L. de and Chávez-García, M. de L. (1996) Diagenesis of Oligocene vitric tuffs to zeolites, Mexican Volcanic Belt. *Clays and Clay Minerals*, **44**:3, 324-338.

Park, J. (1918) The geology of the Oamaru District, North Otago (Eastern Otago Division). *New Zealand Geological Survey Bulletin*, **20**.

Pedley, H.M. and Grasso, M. (2002) Lithofacies modelling and sequence stratigraphy in microtidal cool-water carbonates: a case study from the Pleistocene of Sicily, Italy. *Sedimentology*, **49**, 533-553.

Pedley, M. and Crannante, G. (2006) Cool-water carbonate ramps: a review. *Geological Society of London Special Publication*, **255**:1, 1-9.

Pekar, S.F. and Christie-Blick, N. (2008) Resolving apparent conflicts between oceanographic and Antarctic climate records and evidence for a decrease in pCO_2 during the Oligocene through early Miocene (34-16 Ma). *Palaeogeography, Palaeoclimatology, Palaeoecology*, **260**, 41-49.

Pekar, S.F., Christie-Blick, N., Kominz, M.A. and Miller, K.G. (2002) Calibration between eustatic estimates from backstripping and oxygen isotopic records for the Oligocene. *Geology*, **30**, 903-906.

Pekar, S.F., Christie-Blick, N., Miller, K.G. and Kominz, M.A. (2003) Quantitative constraints on the origin of stratigraphic architechture at passive continental margins; Oligocene sedimentation in New Jersey, U.S.A.. *Journal of Sedimentary Research*, **73**, 227-245.

Pekar, S.F., DeConto, R.M., and Harwood, D.M. (2006) Resolving a late Oligocene conundrum: Deep-sea warming and Antarctic glaciation. *Palaeogeography, Palaeoclimatology, Palaeoecology*, **231**, 29-40.

Pettinga, J.R. (1980) Geology and landslides of the eastern Te Aute district, southern Hawke's Bay. Unpublished PhD thesis, University of Auckland, Auckland.

Pettinga, J.R. (1982) Upper Cenozoic structural history, coastal Hawke's Bay, New Zealand. *New Zealand Journal of Geology and Geophysics*, **25**, 149-191.

Pfuhl, H.A. and McCave, I.N. (2005) Evidence for Late Oligocene establishment of the Antarctic Circumpolar Current. *Earth and Planetary Science Letters*, **235**, 715-728.

Pole, M. (1992) Cretaceous macrofloras of eastern Otago, New Zealand: Angiosperms. *Australian Journal of Botany*, **40**, 169-206.

Pole, M. (1995) Late Cretaceous macrofloras of eastern Otago, New Zealand: Gymnosperms. *Australian Systematic Botany*, **8**, 1067-1106.

Pomar, L. (2001) Types of carbonate platforms: a generic approach. *Basin Research*, **13**, 313-334.

Porrenga, D.H. (1967) Glauconite and chamosite as depth indicators in the marine environment. *Marine Geology*, **5**, 495-501.

Pufahl, P. and Grimm, K. (2003) Coated phosphate grains: Proxy for physical, chemical, and ecological changes in seawater. *Geology*, **31**:9, 801-804.

Purdy, E.G. (1968) Carbonate diagenesis: An environment survey. *Geologica Romana*, **7**, 183-228.

Rattenbury M.S., Townsend D. and Johnston, M.R. (2006) Geology of the Kaikoura area, 1:250,000 Geological Map **13**. Institute of Geological & Nuclear Sciences, Lower Hutt. 1 folded map + 70 pp.

Ratterman, N.G. and Surdam, R.C. (1981) Zeolite mineral reactions in a tuff in the Laney Member of the Green River Formation, Wyoming. *Clays and Clay Minerals*, **29**:5, 365-377.

Reading, H.G. (Ed.) (1996) Sedimentary environments: processes, facies, and stratigraphy. Blackwell Science Ltd, Oxford.

Reading, H.G. and Collinson, J.D. (1996) Clastic coasts. In: *Sedimentary Environments: Processes, Facies and Stratigraphy* (Ed H.G. Reading), Blackwell, Chichester, pp. 154-231.

Reay, A. and Sipiera, P.P. (1987) Mantle Xenoliths from the New Zealand region. In: *Mantle Xenoliths* (Ed. P.H. Nixon), John Wiley & Sons Ltd, Chichester.

Reay, A., Chappell, D. and Garden, B. (2002) A new garnet-bearing mineral breccia from North Otago, New Zealand. *New Zealand Journal of Geology and Geophysics*, **45**, 461-466.

Reay, M.B. (1993) Geology of the middle part of the Clarence valley. Scale 1:50 000. *Institute of Geological and Nuclear Sciences geological map 10*. Institute of Geological and Nuclear Sciences, Lower Hutt.

Reyners, M. (2013) The central role of the Hikurangi Plateau in the Cenozoic tectonics of New Zealand and the Southwest Pacific. *Earth and Planetary Science Letters*, **361**, 460-468.

Riddolls, B.W. (1968) The stratigraphy of part of South Canterbury, New Zealand. *Exeter University Geological Society Magazine*, **1**, 24-28.

Riordan, N., Reid, C. and Bassett, K. (2012) Oligo-Miocene, mixed carbonate-clastic sedimentation along a submarine fault scarp, Nile Group, North Westland, New Zealand. *Geoscience Society of New Zealand 2012 Conference Abstracts*.

Rivers, J., James, N. and Kyser, T. (2008) Early diagenesis of carbonates on a cool-water carbonate shelf, Southern Australia. *Journal of Sedimentary Research*, **78**:12, 784-802.

Roser, B.P. and Korsch, R.J. (1999) Geochemical characterisation, evolution and source of a Mesozoic accretionary wedge: the Torlesse terrane, New Zealand. *Geological Magazine*, **136**, 493-512.

Schlager, W. (2003) Benthic carbonate factories of the Phanerozoic. *International Journal of Earth Sciences*, **92**:4, 445-464.

Schlager, W. (2005) *Carbonate sedimentology and sequence stratigraphy* (Vol. 8). SEPM Society for Sedimentary Geology.

Schellart, W.P., Lister, G.S. and Toy, V.G. (2006) A Late Cretaceous and Cenozoic reconstruction of the Southwest Pacific region: Tectonics controlled by subduction and slab rollback processes. *Earth-Science Reviews*, **76**, 191-233.

Scholle, P.A. and Ulmer-Scholle, D. (2003) A Color Guide to the Petrography of Carbonate Rocks: Grains, textures, porosity, diagenesis. *American Association of Petroleum Geologists*, **77**.

Scott, G.H. (1973) *Ehrenbergina* (Foraminiferida): Variability and application to Lower Miocene biostratigraphy in New Zealand. *New Zealand Journal of Geology and Geophysics*, **16**, 52-67.

Shane, P., Strachan, L.J. and Smith, I. (2010) Redefining the Waitemata Basin, New Zealand: A new tectonic, magmatic, and basin evolution model at a subduction terminus in the SW Pacific. *Geochemistry, Geophysics, Geosystems*, **11**.

Shubber, B., Bone, Y., James, N.P. and McGowran, B. (1997) Warming-upward cycles in mid-Tertiary cool-water limestones, St. Vincent Basin, South Australia. In: *Cool-water Carbonates* (Eds. N.P. James and J.A.D. Clarke). *SEPM Special Publication*, **56**, 237-249.

Smellie, J.L. (2001) Lithofacies architecture and construction of volcanoes erupted in englacial lakes: Icefall Nunatak, Mount Murphy, eastern Marie Byrd Land, Antarctica. *Special Publication of the International Association of Sedimentologists*, **30**, 9-34.

Smith, A.M. and Nelson, C.S. (1994) Selectivity in sea-floor processes – taphonomy of bryozoans. In: *Biology and Palaeobiology of Bryozoans* (Eds P.J. Hayward, J.S. Ryland and P.D. Taylor). Olsen and Olsen, Denmark, pp. 177-180.

Sohn, Y.K. and Chough, S.K. (1993) The Udo tuff cone, Chju Island, South Korea: transformation of pyroclastic fall into debris fall and grain flow on a steep volcanic slope. *Sedimentology*, **40**, 769-786.

Stagpole, V. and Nicol, A. (2008) Regional structure and kinematic history of a large subduction back thrust: Taranaki Fault, New Zealand. *Journal of Geophysical Research*, **113**, B01403.

Steiner, A., Brown, D.A. and White A. J.R. (1959) Occurrence of ignimbrite in the Shag valley, north-east Otago. *New Zealand Journal of Geology and Geophysics*, **2**, 380-384.

Stickley, C.E., Brinkhuis, H., Schellenberg, A.A., Sluijs, A., Roehl, U., Fuller, M., Grauert, M., Huber, M., Warnaar, J. and Williams, G.L. (2004) Timing and nature of the deepening of the Tasmanian Gateway. *Paleoceanography*, **19**:4, 18.

Suggate, R.P., Stevens, G.R. and Te Punga, M.T. (Eds.) (1978) *The Geology of New Zealand: Volume II*. Government Printer, Wellington, 820 pp.

Surdam, R.C. and Sheppard, R.A. (1978) Zeolites in saline, alkaline-lake deposits. In: *Natural Zeolites: Occurrence, Properties, Use* (Eds L.B. Sand and F.A. Mumpton). Pergamon Press, New York pp. 145-174.

Sutherland, R. (1995) The Australia-Pacific boundary and Cenozoic plate motions in the Southwest Pacific: some constraints from GEOSAT data. *Tectonics*, **14**, 819-831.

Sutherland, R. (1999) Basement geology and tectonic development of the greater New Zealand region: an interpretation from regional magnetic data. *Tectonophysics*, **308**, 341-362.

Sutherland, R., Davey, F. and Beavan, J. (2000) Plate boundary deformation in South Island, New Zealand, is related to inherited lithospheric structure. *Earth and Planetary Science Letters*, **177**, 141-151.

Terry, R.D. and Chilingar, G.V. (1955) Summary of "Concerning some additional aids in studying sedimentary formations", by M.S. Shvestov. *Journal of Sedimentary Petrology*, **40**:2, p.229-234.

Thomson, J.A. (1926) Marine phosphatic horizons. *New Zealand Journal of Science and Technology*, **8**:3, 143-160.

Todd, D.K. (1980) *Groundwater Hydrology*. London, John Wiley & Sons, 535 pp.

Tucker, M. (2009) Carbonate diagenesis and sequence stratigraphy. *Sedimentology Review:1*. Wiley-Blackwell, Hoboken, pp. 51-72.

Tucker, M.E. and Wright, V.P. (1990) Carbonate Sedimentology. Blackwell Scientific Publications, Oxford, 482 pp.

Tulloch, A.J., Ramezani, J., Mortimer, N., Mortensen, J., Van Den Bogaard, P. and Maas, R. (2009) Cretaceous felsic volcanism in New Zealand and Lord Howe Rise (Zealandia) as a precursor to final Gondwana break-up. *Geological Society, London, Special Publications*, **321**, 89-118.

Turnbull, I.M. (1986) Geological map of New Zealand, 1:50 000l, sheet D42BD and D43. Department of Scientific and Industrial Research, Wellington. 1 sheet + 40 pp.

Turnbull, I.M., Lindqvist, J.K., Norris, R.J., Carter, R.M., Cave, M.O., Sykes, R. and Hyden, F.M. (1989) Lithostratigraphic nomenclature of the Cretaceous and Tertiary sedimentary rocks of Western Southland, New Zealand. *New Zealand Geological Survey Record*, **31**.

Turnbull, I.M., Uruski, C.I. *et al.* (1993) Cretaceous and Cenozoic sedimentary basins of western Southland, South Island, New Zealand. *Institute of Geological and Nuclear*

Sciences Monograph 1. Institute of Geological and Nuclear Sciences Limited, Lower Hutt, pp. 86.

Turnbull, I.M., Mortimer, N. and Craw, D. (2001) Textural zones in the Haast Schist – a reappraisal. *New Zealand Journal of Geology and Geophysics*, **44**, 171-183.

Uttley, G.H. (1918) The volcanic rocks of Oamaru. *Transactions of the New Zealand Institute*, **50**, 106-117.

Vail, P.R., Mitchum, R.M.J., Todd, R.G., Widmier, J.M., Thompson, S. III, Sangree, J.B., and Bubb, J.N. (1977) Seismic stratigraphy and global changes of sea level. *AAPG Memoir*, **26**.

Vail, P.R., Audemard, F., Bowring, S.A., Eisner, P.N. and Perez-Cruz, C. (1991) The stratigraphic signatures of tectonics eustacy and sedimentology – an overview. In: *Cycles and Events in Stratigraphy* (Eds G. Einsele, W. Ricken and A. Seiacher), Springer-Verlag, Berlin, pp. 617-659.

Vella, P., (1967) Eocene and Oligocene sedimentary cycles in New Zealand. *New Zealand Journal of Geology and Geophysics*, **10**, 119-145.

Walkden, G.M. and Berry, J.R. (1984) Syntaxial overgrowths in muddy crinoidal limestones: cathodoluminescence sheds new light on an old problem. *Sedimentology*, **31**, 251-267.

Walter, L.M. (1986) Relative efficiency of carbonate dissolution and precipitation during diagenesis: a progress report on the role of solution chemistry. In: *Roles of Organic Matter is Sediment Diagenesis* (Ed. D.L. Gautier), *Special Publication of the Society for Economic Paleontology and Mineralogy,* **38**, pp. 1-11.

Ward, D.M. (1973) Paleoenvironment of the Arno Limestone (Waitakian Age), Waihao district, South Canterbury. Unpublished BSc (Hons) thesis, University of Canterbury, Christchurch.

Ward, D.M. and Lewis, D.W. (1975) Palaeoenvironmental implications of storm-scoured, ichnofossilifeous mid-Tertiary limestones, Waihao district, South Canterbury, New Zealand. *New Zealand Journal of Geology and Geophysics*, **18**, 881-908.

White, J.D.L. (1996) Pre-emergent construction of a lacustrine basaltic volcano, Pahvant Butte, Utah (USA). *Bulletin of Volcanology*, **58**, 249-262.

White, P. and Waterhouse, B. (1993) Lithostratigraphy of the Te Kuiti Group: a revision. *New Zealand Journal of Geology and Geophysics*, **36**:2, 255-266.

Wilbur, R.J. and Neumann, A.C. (1993) Effects of submarine cementation on microfabrics and physical properties of carbonate slope deposits, northern Bahamas. In: *Carbonate Microfabrics* (Eds R. Rezak and D.L. Lavoie), Springer-Verlag, New York, pp. 79-94.

Wilson, D.D. (1956) The Late Cretaceous and early Tertiary transgression in South Island, New Zealand. *New Zealand Journal of Science and Technology* **37**, 610–622.

Wilson, I.R. (1985) Galleon-1 geological completion report. *Petroleum Report 1146*, New Zealand Geological Survey Open Petroleum Report.

Wood, R.A., Lamarche, G., Herzer, R.H., Delteil, J. and Davy, B.W. (1996) Paleogene seafloor spreading in the southeast Tasman Sea. *Tectonics*, **15**, 966-975.

Young, H.R. and Nelson, C.S. (1988) Endolithic biodegradation of cool-water skeletal carbonates on Scott Shelf, northwestern Vancouver Island, Canada. *Sedimentary Geology*, **60**, 251-267.

Youngson, J.H., Craw, D. and Falconer, D.M. (2006) Evolution of Cretaceous-Cenozoic quartz pebble conglomerate gold placers during formation and inversion, southern New Zealand. *Ore Geology Reviews*, **28**:4, 451-474.

Zachos, J.C., Breza, J.R. and Wise, S.W. (1992) Early Oligocene ice-sheet expansion on Antarctica: Stable-isotope and sedimentological evidence from Kerguelen Plateau, Southern Indian Ocean. *Geology*, **20**, 569-573.

Zachos, J.C., Stott, L.D. and Lohmann, K.C. (1994) Evolution of early Cenozoic marine temperatures. *Paleoceanography*, **9**, 353-387.

Zachos, J.C., Shackleton, N.J., Revenaugh, J.S., Palike, H. and Flower, B.P. (2001) Climate response to orbital forcing across the Oligocene-Miocene boundary. *Science*, **292**, 274-278.

APPENDICES

APPENDIX A – STRATIGRAPHIC COLUMN DATABASE

This appendix contains a summary table of the locations within the Waitaki study area where stratigraphic data was recorded and a detailed stratigraphic column compiled (Appendix B). Coordinates are supplied in World Geodetic System 1984. Elevations are provided, where obtained, in metres.

Column ID	Location Name	Latitude	Longitude	Elevation
NT 09/01	Waihao	44 47 29.792 S	170 56 09.916 E	81 m
NT 09/02	Rock Art	44 50 34.117 S	170 38 42.026 E	151 m
NT 09/03	Earthquakes	44 52 27.281 S	170 37 16.444 E	240 m
NT 09/04	Landon Creek	45 01 46.578 S	170 59 36.752 E	72 m
NT 09/06	Gee's Point	45 10 01.702 S	170 54 34.452 E	10 m
NT 09/07	Alma	45 06 29.598 S	170 55 05.907 E	22 m
NT 09/08	Prydes Gully Quarry	44 55 42.109 S	170 40 10.099 E	Unknown
NT 09/09	Tokarahi-Ngapara Rd Cliffs	44 56 10.402 S	170 41 14.096 E	238 m
NT 09/10	Anatini	44 54 05.597 S	170 39 34.313 E	254 m
NT 09/11	Raupo Creek	45 03 14.950 S	170 44 57.111 E	96 m
NT 09/12	Fuchsia Creek	45 04 32.352 S	170 42 16.653 E	195 m
NT 09/13	Fuchsia Creek Road-cut	45 04 03.944 S	170 43 30.831 E	148 m
NT 09/14	Trig Z	44 48 17.461 S	170 31 50.844 E	209 m
NT 10/02	Campbells Bay	45 11 39.995 S	170 53 45.981 E	1 m
NT 10/03	Kakanui River mouth	45 11 21.009 S	170 53 57.012 E	2 m
NT 10/04	Old Rifle Butts	45 07 32.003 S	170 57 59.019 E	2 m
NT 10/06	Awamoko Creek	44 55 05.007 S	170 45 30.021 E	200 m
NT 10/07	Tokarahi Cliffs	44 56 37.984 S	170 40 42.992 E	240 m
NT 10/08	Tokarahi Sill	44 56 25.010 S	170 37 04.017 E	259 m
NT 10/09	Elephant Rocks	44 53 39.616 S	170 39 30.005 E	222 m
NT 10/13	Browns Road	45 06 50.005 S	170 54 26.978 E	46 m
NT 10/14	Simpson Cliffs	44 55 49.546 S	170 40 50.182 E	205 m
NT 10/15	Roy Farm	45 07 25.351 S	170 55 29.168 E	50 m
NT 10/16	Forresters	45 01 43.356 S	170 54 22.527 E	163 m
NT 10/17	Bains	45 06 04.006 S	170 53 14.894 E	118 m
NT 10/18	Teschemaker Volcanics	45 09 45.101 S	170 52 40.946 E	21 m
NT 10/19	Kakanui River Section	45 11 13.619 S	170 53 45.956 E	3 m
NT 10/20	Teschemaker	45 09 04.760 S	170 53 31.710 E	32 m
NT 10/21	Ross Farm	44 52 49.179 S	170 44 27.054 E	173 m
NT 10/22	McCulloch Farm	44 57 20.120 S	170 42 48.910 E	256 m
NT 10/23	Limeworks	44 57 04.473 S	170 38 35.032 E	291 m
NT 10/24	Thousand Acre Rd	45 08 31.635 S	170 55 06.382 E	35 m
NT 10/25	Maheno	45 09 24.785 S	170 50 58.675 E	34 m
NT 10/27	Otekaieke Settlement	44 51 18.389 S	170 31 54.327 E	245 m
NT 10/28	Meek Rd Quarry	45 04 48.161 S	170 54 54.008 E	78 m
NT 10/29	Devil's Bridge Roadcut	45 02 04.932 S	170 56 57.236 E	122 m
NT 10/30	Devil's Bridge Wetland	45 02 28.836 S	170 56 13.905 E	115 m

APPENDIX B – STRATIGRAPHIC COLUMNS

This Appendix presents stratigraphic columns from all locations within the Waitaki study area, as presented in Appendix A. Attached to each are the locations of samples taken, including summary graphs to represent the varying sample compositions from petrographic analyses.

Notes: Stratigraphic height varies between sections. Not all samples presented have been petrographically analysed.

Legend

Lithologies

- Limestone
- Calcareous Sst
- Sandy Zst
- Siltstone
- FG sandstone
- MG sandstone
- CG sandstone
- Conglomerate
- Diatomite
- Schist
- Banded tuff
- Tuff breccia
- Columnar jointing
- Pillow lava

Fossils

- Algae
- Benthic foraminifera
- Bivalves
- Bioturbation
- Brachiopods
- Bryozoans
- Cetacean
- Corals
- Echinoderm plates
- Echinoderm spines
- Echinoderm (whole)
- Fossils (broken)
- Fossils (undiff.)
- Gastropods
- Oyster
- Scaphopod
- Sea-pens
- Shark teeth
- Worm tubes

Sedimentary structures

- Channels
- Cross-beds
- Flame structures
- Hinted bedding
- Laminations
- Local scour
- Low angle cross-beds
- Normal grading
- Ripples
- Rip-up clasts
- Veining
- Vesicles
- Wavy laminations

Lithologic features

- Volcanic clasts
- Concretions
- Sediment lense

Glauconite Content

0% — 100%

Thin Section Component Graphs

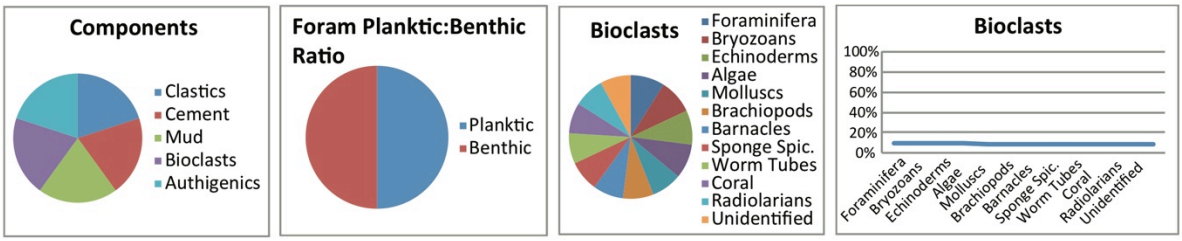

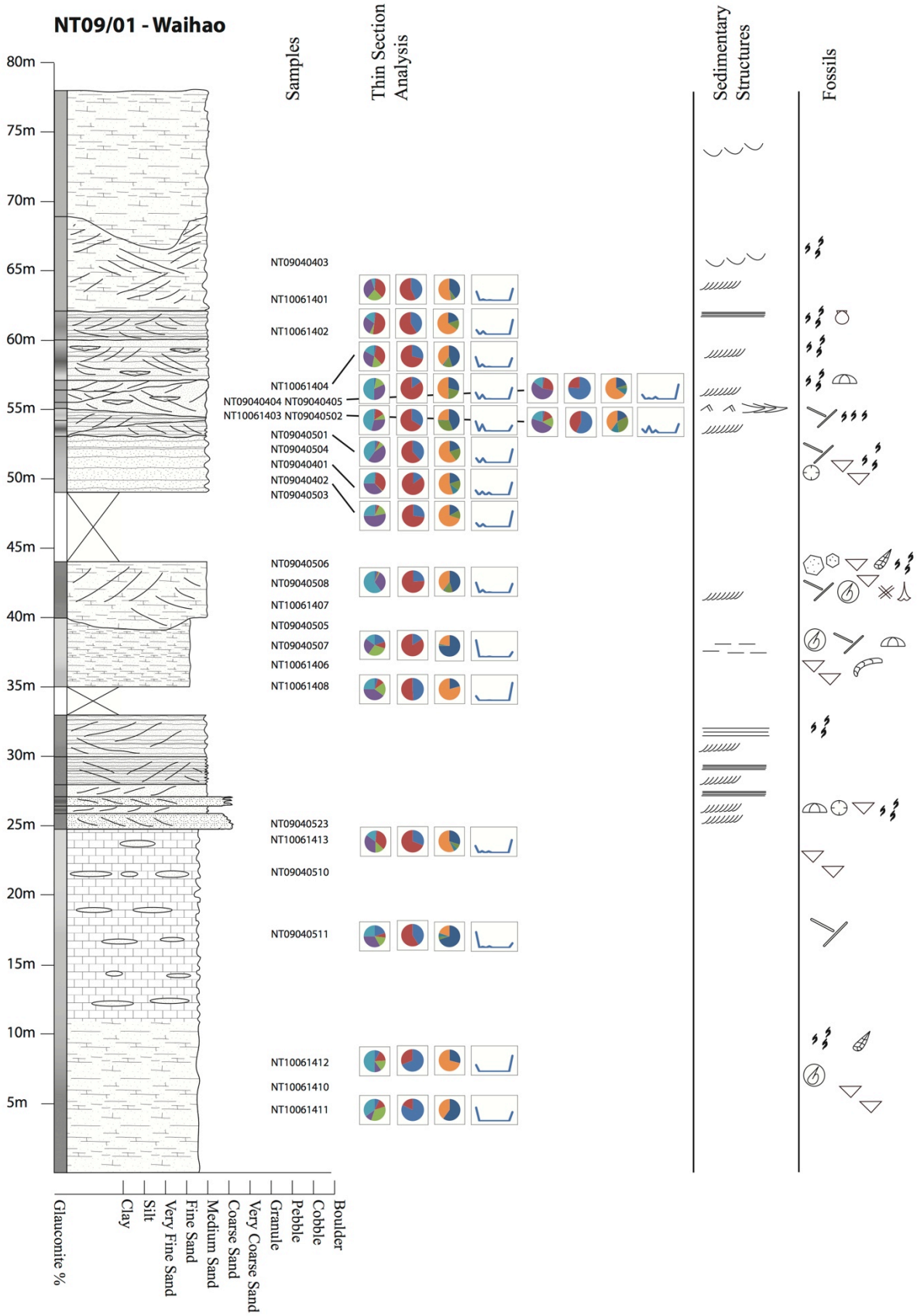
NT09/01 - Waihao
80m
75m
70m
65m
60m
55m
50m
45m
40m
35m
30m
25m
20m
15m
10m
5m
Samples
Thin Section Analysis
Sedimentary Structures
Fossils
NT09040403
NT10061401
NT10061402
NT10061404
NT09040404 NT09040405
NT10061403 NT09040502
NT09040501
NT09040504
NT09040401
NT09040402
NT09040503
NT09040506
NT09040508
NT10061407
NT09040505
NT09040507
NT10061406
NT10061408
NT09040523
NT10061413
NT09040510
NT09040511
NT10061412
NT10061410
NT10061411
Glauconite %
Clay
Silt
Very Fine Sand
Fine Sand
Medium Sand
Coarse Sand
Very Coarse Sand
Granule
Pebble
Cobble
Boulder

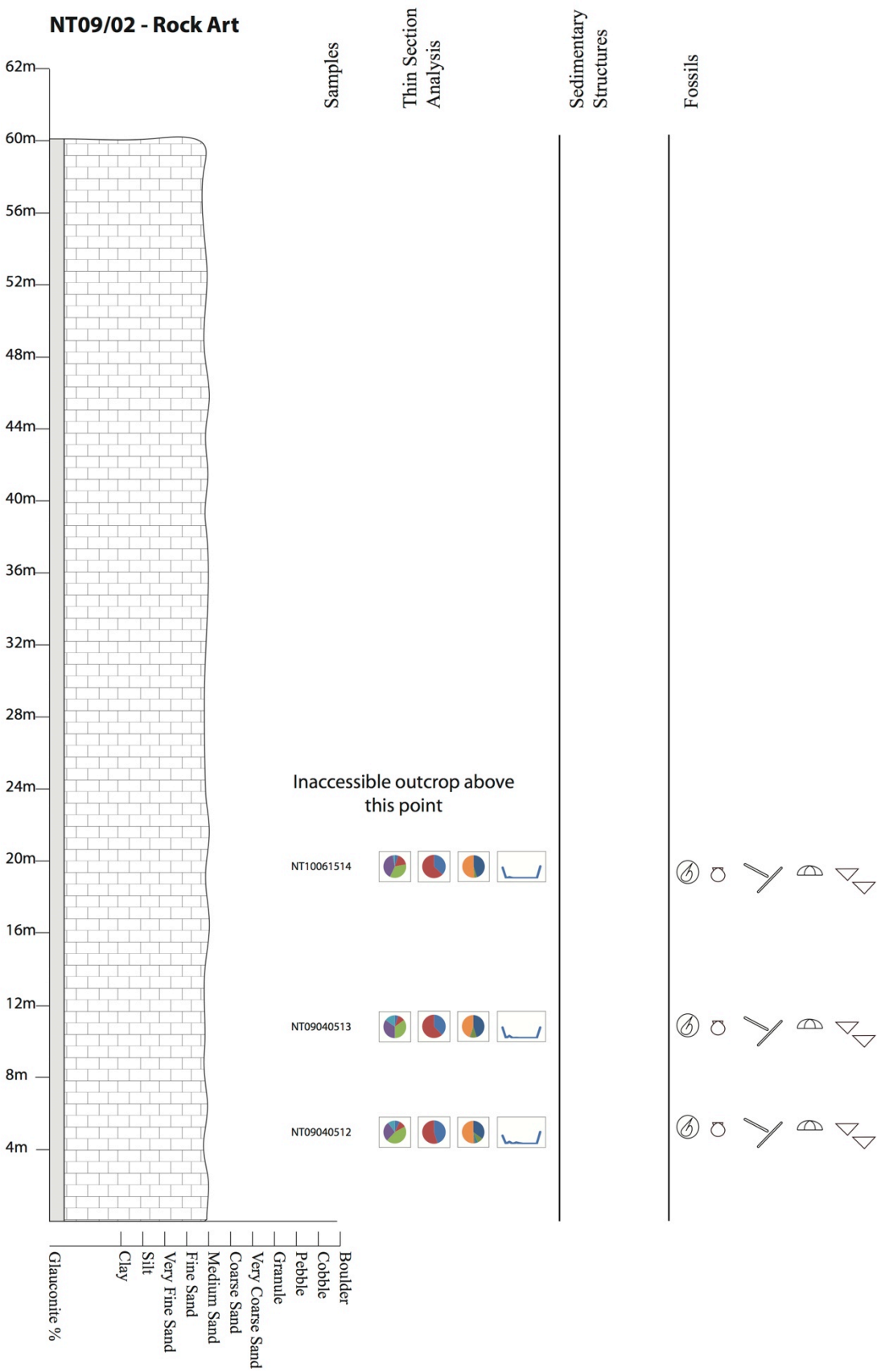
NT09/02 - Rock Art
Samples
Thin Section Analysis
Sedimentary Structures
Fossils
62m
60m
56m
52m
48m
44m
40m
36m
32m
28m
24m
20m
16m
12m
8m
4m
Inaccessible outcrop above this point
NT10061514
NT09040513
NT09040512
Glauconite %
Clay
Silt
Very Fine Sand
Fine Sand
Medium Sand
Coarse Sand
Very Coarse Sand
Granule
Pebble
Cobble
Boulder

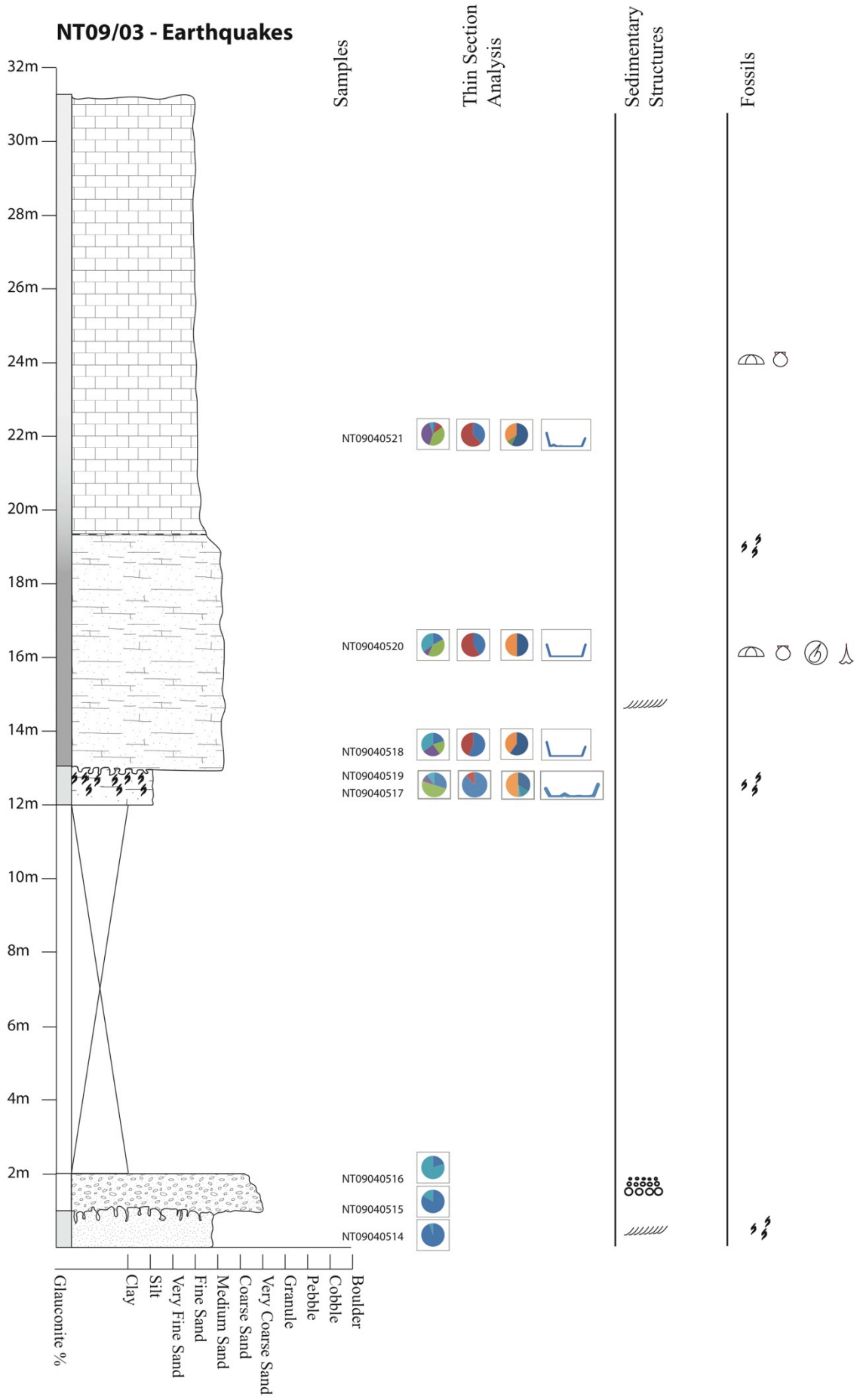
NT09/03 - Earthquakes
32m
30m
28m
26m
24m
22m
20m
18m
16m
14m
12m
10m
8m
6m
4m
2m
Samples
Thin Section Analysis
Sedimentary Structures
Fossils
NT09040521
NT09040520
NT09040518
NT09040519
NT09040517
NT09040516
NT09040515
NT09040514
Glauconite %
Clay
Silt
Very Fine Sand
Fine Sand
Medium Sand
Coarse Sand
Very Coarse Sand
Granule
Pebble
Cobble
Boulder

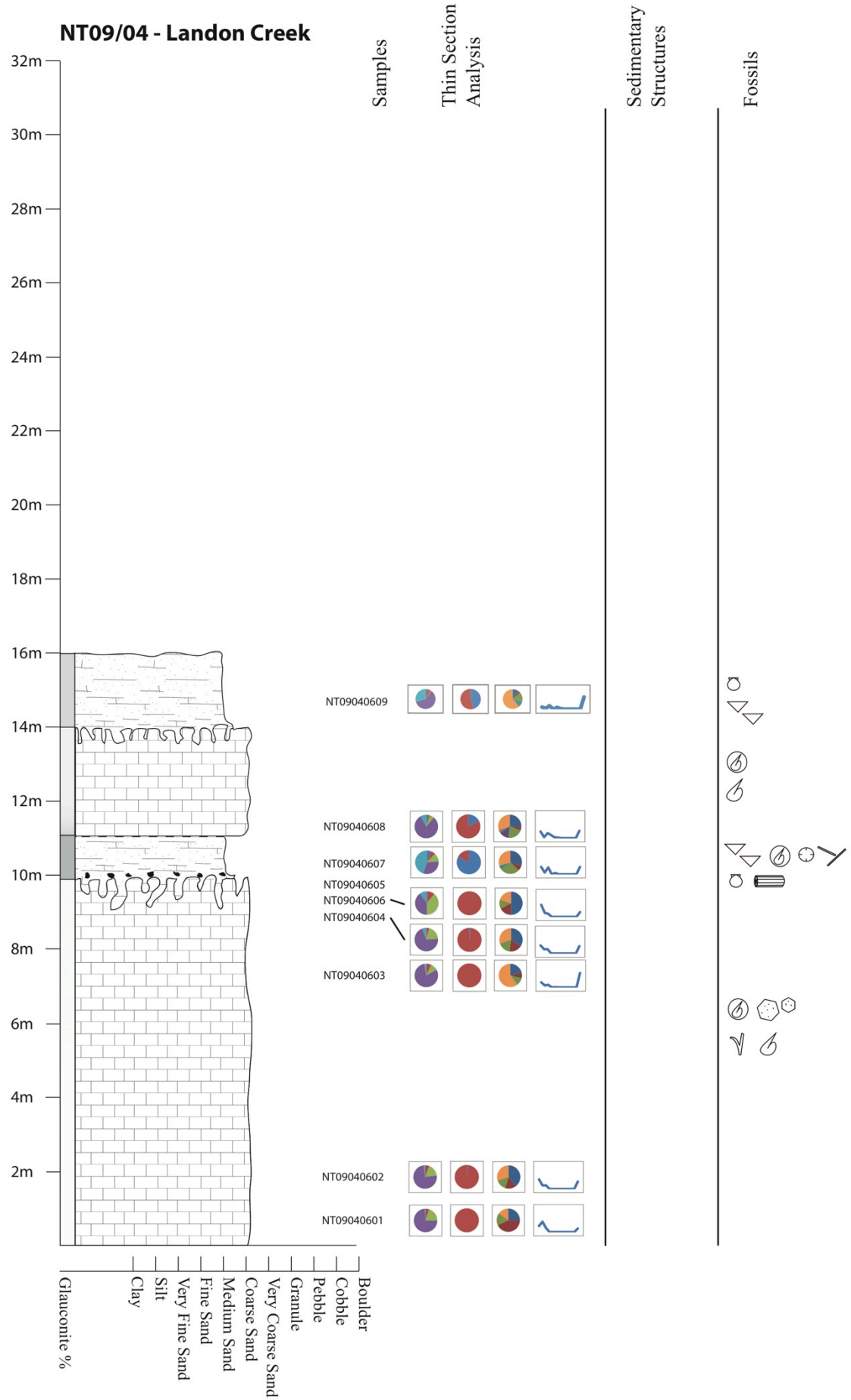
NT09/04 - Landon Creek
Samples
Thin Section Analysis
Sedimentary Structures
Fossils
32m
30m
28m
26m
24m
22m
20m
18m
16m
14m
12m
10m
8m
6m
4m
2m
NT09040609
NT09040608
NT09040607
NT09040605
NT09040606
NT09040604
NT09040603
NT09040602
NT09040601
Glauconite %
Clay
Silt
Very Fine Sand
Fine Sand
Medium Sand
Coarse Sand
Very Coarse Sand
Granule
Pebble
Cobble
Boulder

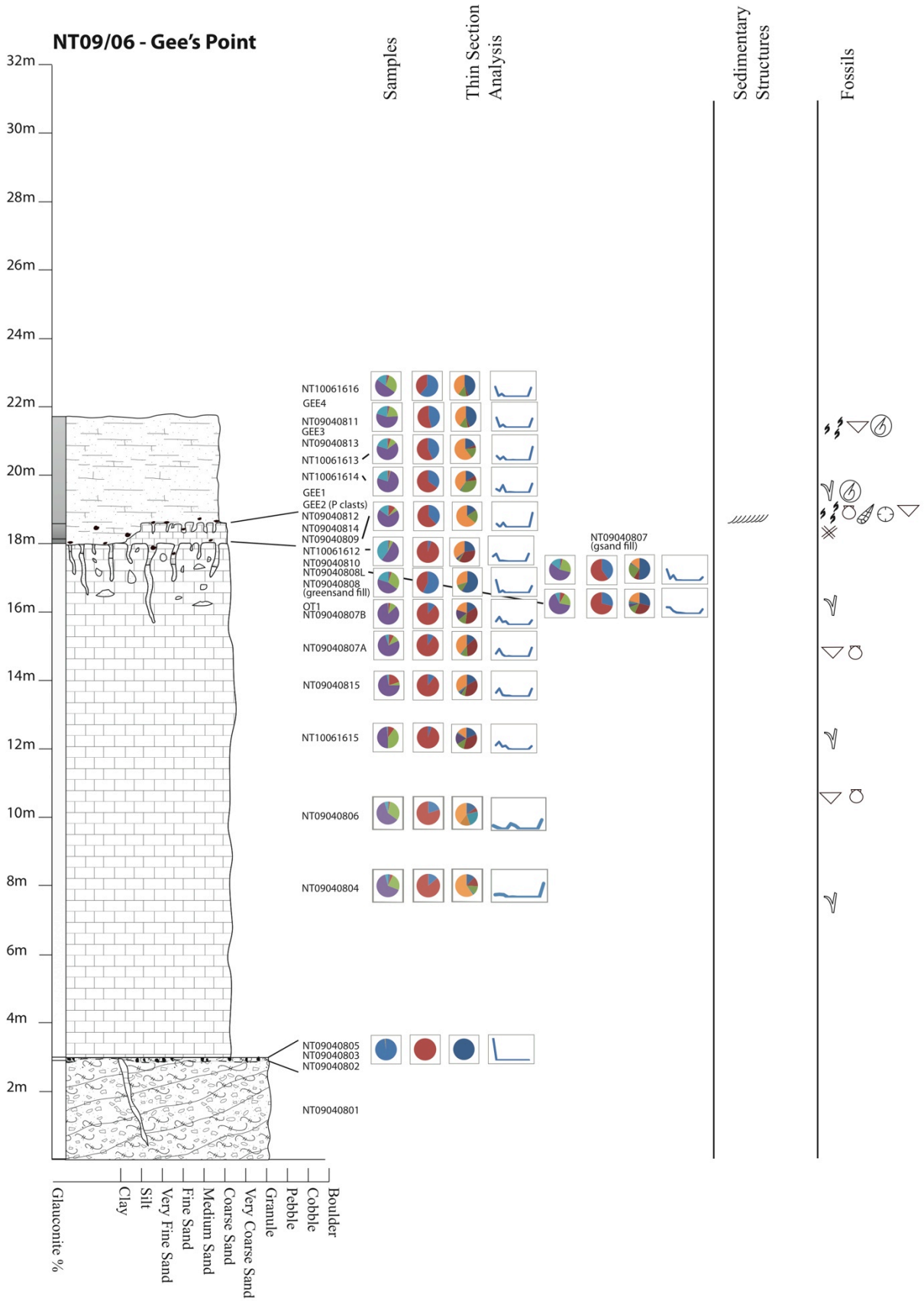
NT09/06 - Gee's Point
Samples
Thin Section Analysis
Sedimentary Structures
Fossils
32m
30m
28m
26m
24m
22m
20m
18m
16m
14m
12m
10m
8m
6m
4m
2m
NT10061616
GEE4
NT09040811
GEE3
NT09040813
NT10061613
NT10061614
GEE1
GEE2 (P clasts)
NT09040812
NT09040814
NT09040809
NT10061612
NT09040810
NT09040808L
NT09040808 (greensand fill)
OT1
NT09040807B
NT09040807A
NT09040815
NT10061615
NT09040806
NT09040804
NT09040805
NT09040803
NT09040802
NT09040801
NT09040807 (gsand fill)
Glauconite %
Clay
Silt
Very Fine Sand
Fine Sand
Medium Sand
Coarse Sand
Very Coarse Sand
Granule
Pebble
Cobble
Boulder

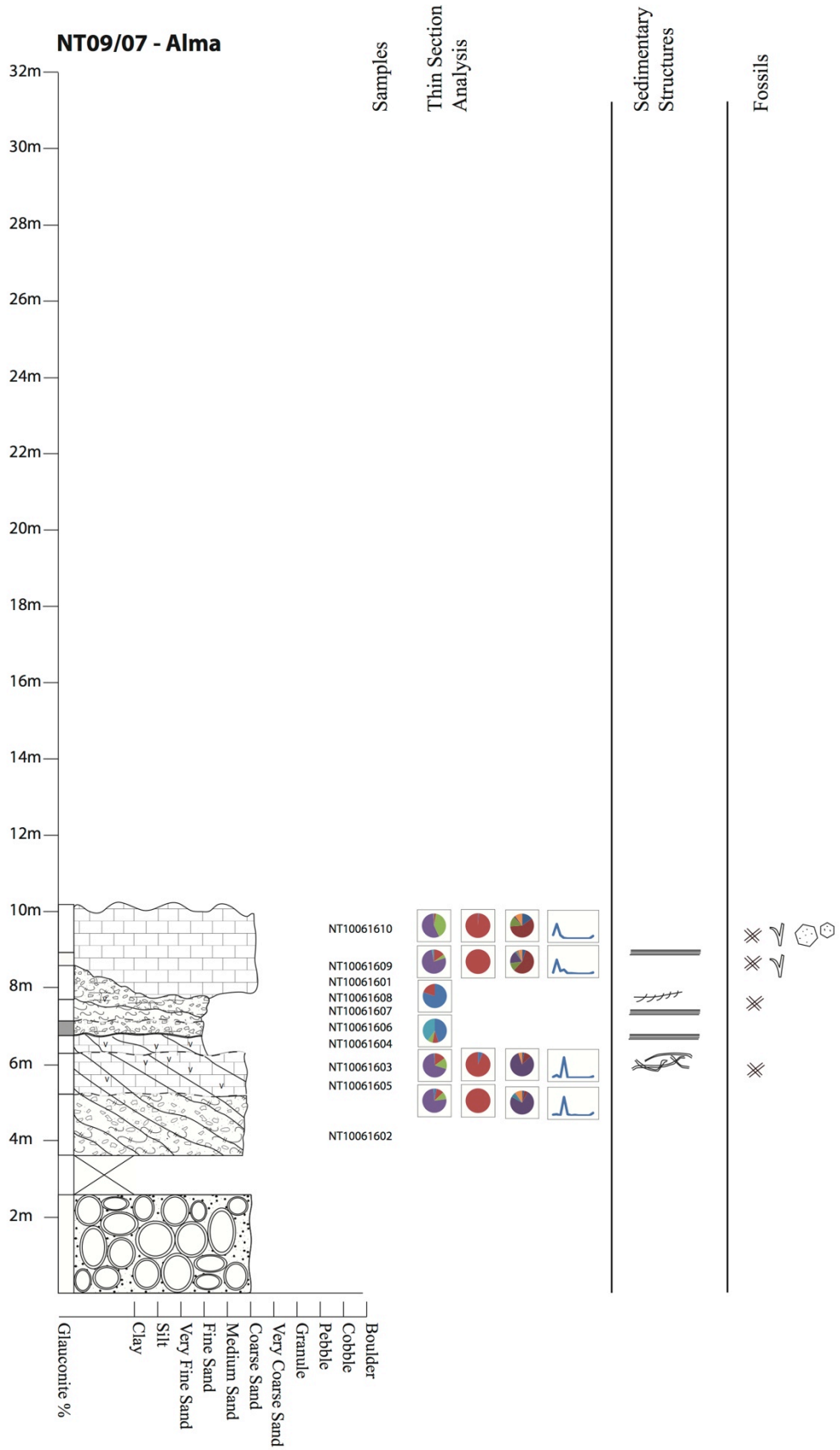
NT09/07 - Alma
Samples
Thin Section Analysis
Sedimentary Structures
Fossils
32m
30m
28m
26m
24m
22m
20m
18m
16m
14m
12m
10m
8m
6m
4m
2m
NT10061610
NT10061609
NT10061601
NT10061608
NT10061607
NT10061606
NT10061604
NT10061603
NT10061605
NT10061602
Glauconite %
Clay
Silt
Very Fine Sand
Fine Sand
Medium Sand
Coarse Sand
Very Coarse Sand
Granule
Pebble
Cobble
Boulder

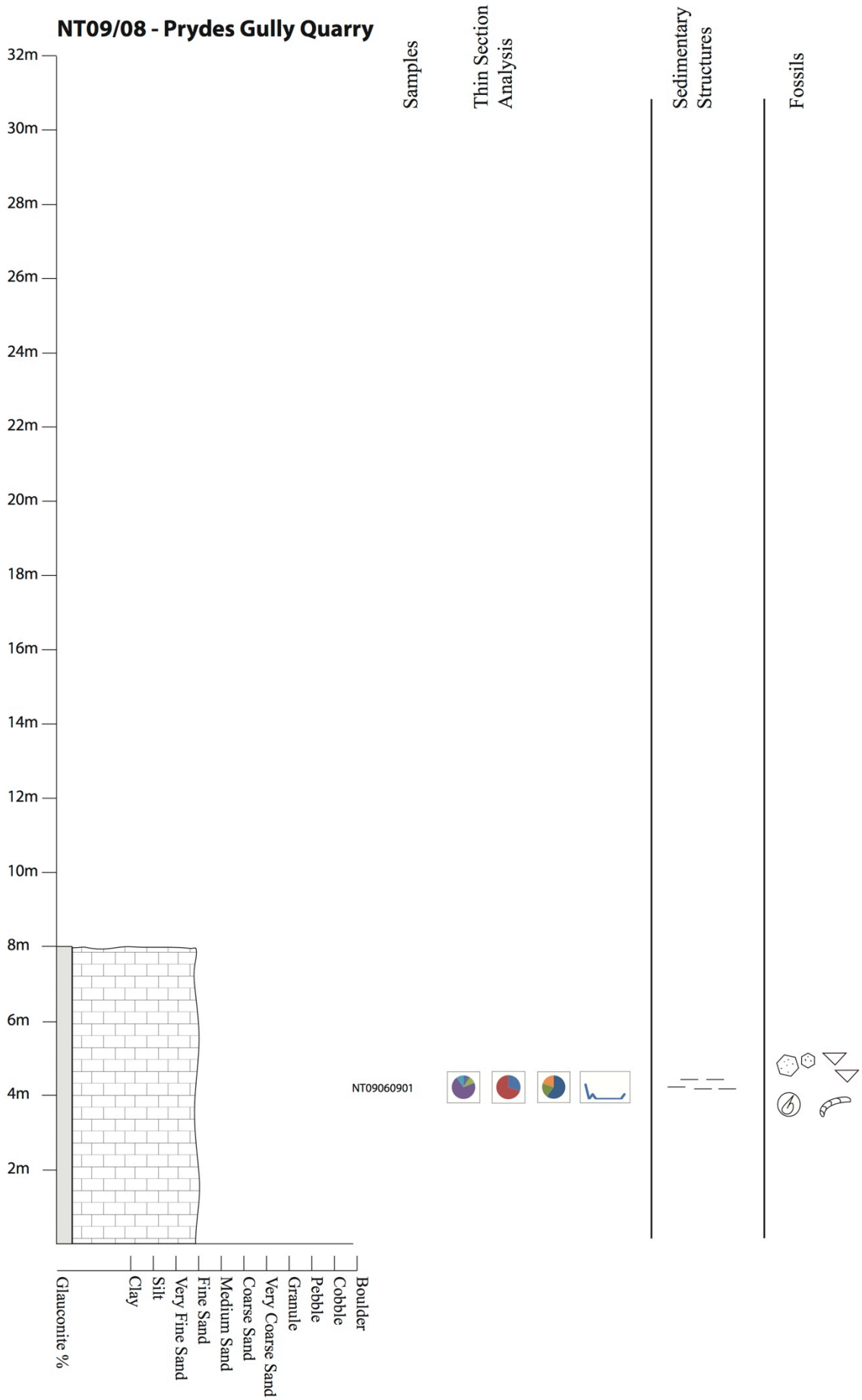
NT09/08 - Prydes Gully Quarry
32m
30m
28m
26m
24m
22m
20m
18m
16m
14m
12m
10m
8m
6m
4m
2m
Samples
Thin Section Analysis
Sedimentary Structures
Fossils
NT09060901
Glauconite %
Clay
Silt
Very Fine Sand
Fine Sand
Medium Sand
Coarse Sand
Very Coarse Sand
Granule
Pebble
Cobble
Boulder

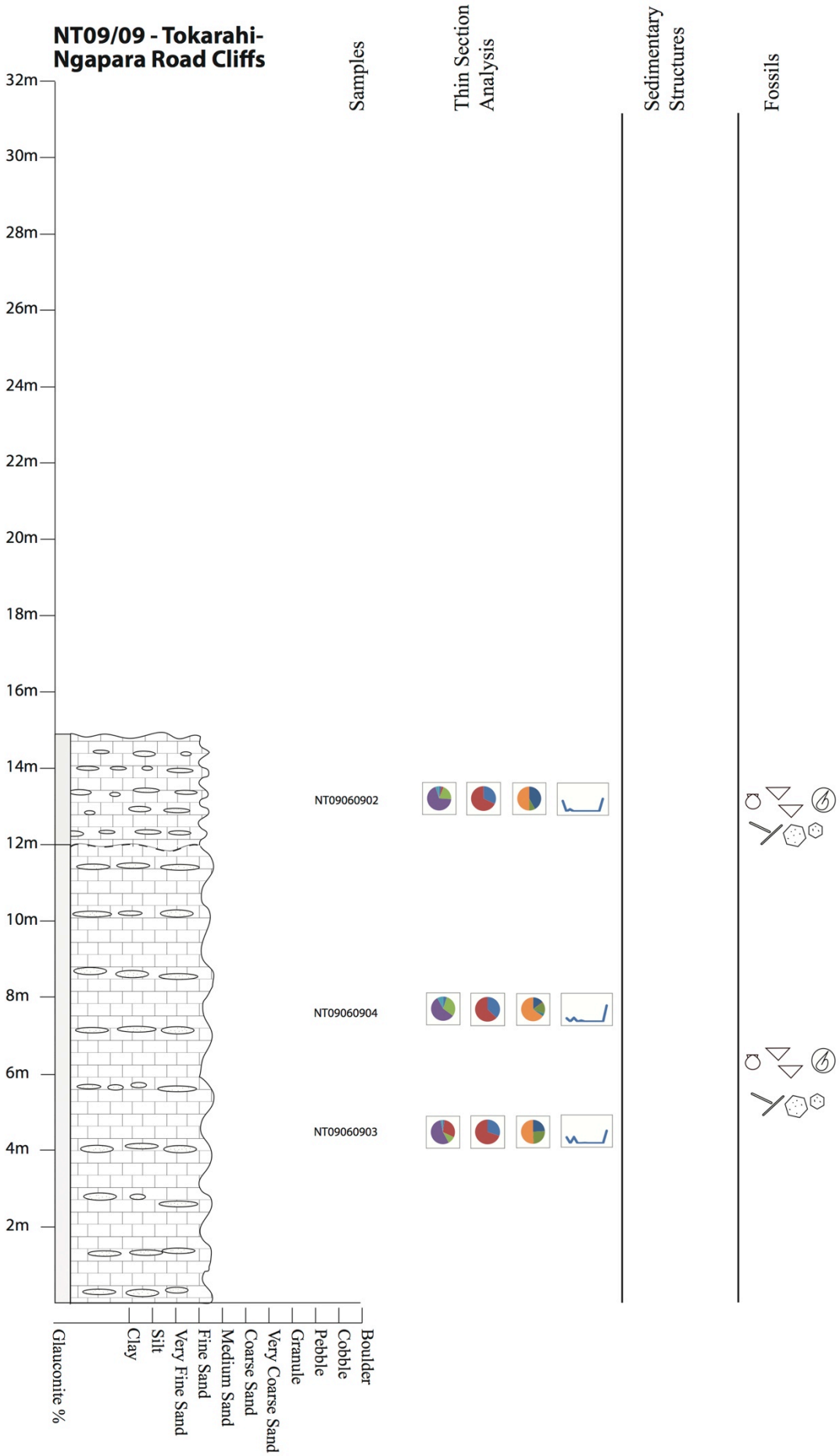
NT09/09 - Tokarahi-Ngapara Road Cliffs
Samples
Thin Section Analysis
Sedimentary Structures
Fossils
32m
30m
28m
26m
24m
22m
20m
18m
16m
14m
12m
10m
8m
6m
4m
2m
NT09060902
NT09060904
NT09060903
Glauconite %
Clay
Silt
Very Fine Sand
Fine Sand
Medium Sand
Coarse Sand
Very Coarse Sand
Granule
Pebble
Cobble
Boulder

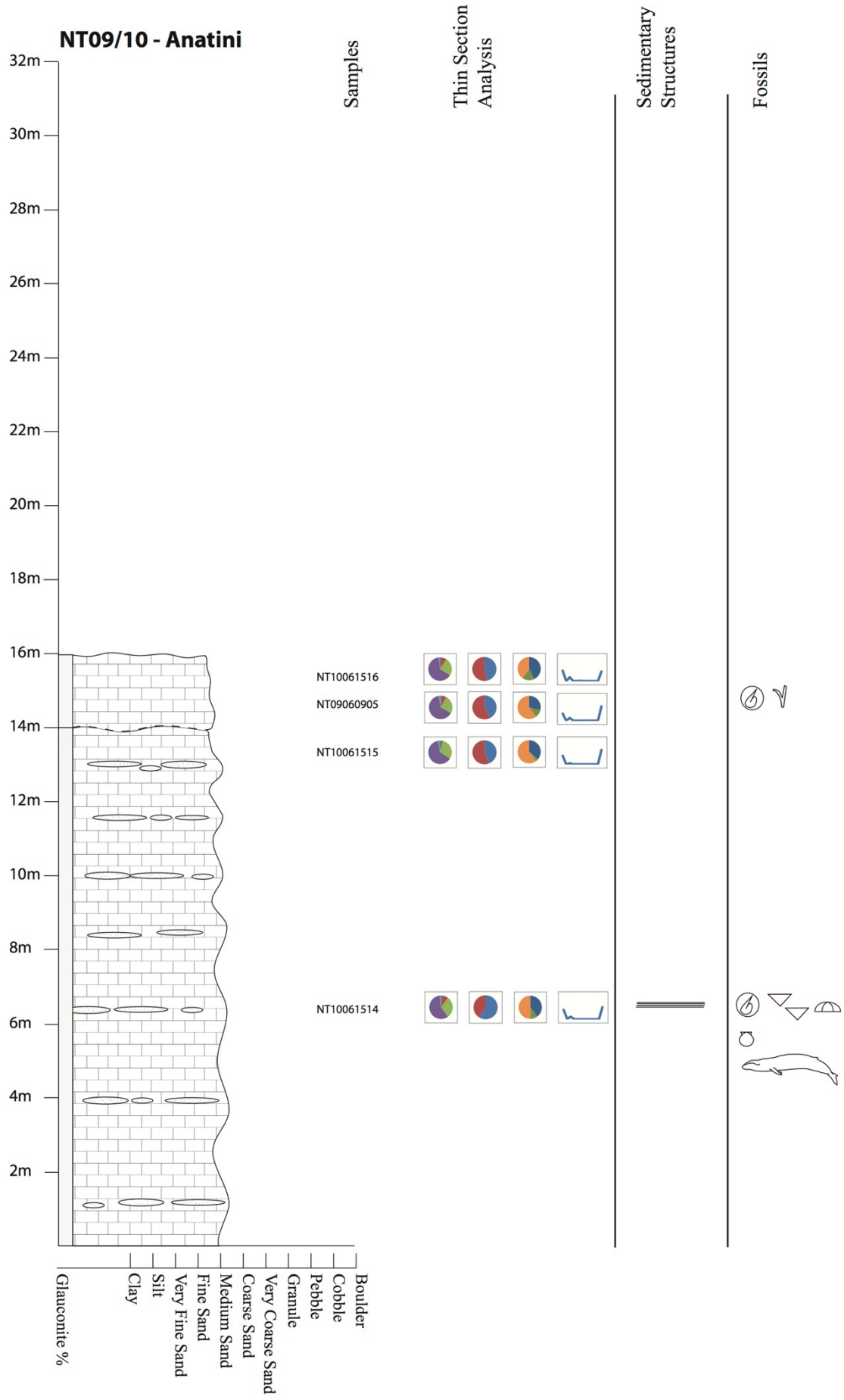
NT09/10 - Anatini
32m
30m
28m
26m
24m
22m
20m
18m
16m
14m
12m
10m
8m
6m
4m
2m
Samples
Thin Section Analysis
Sedimentary Structures
Fossils
NT10061516
NT09060905
NT10061515
NT10061514
Glauconite %
Clay
Silt
Very Fine Sand
Fine Sand
Medium Sand
Coarse Sand
Very Coarse Sand
Granule
Pebble
Cobble
Boulder

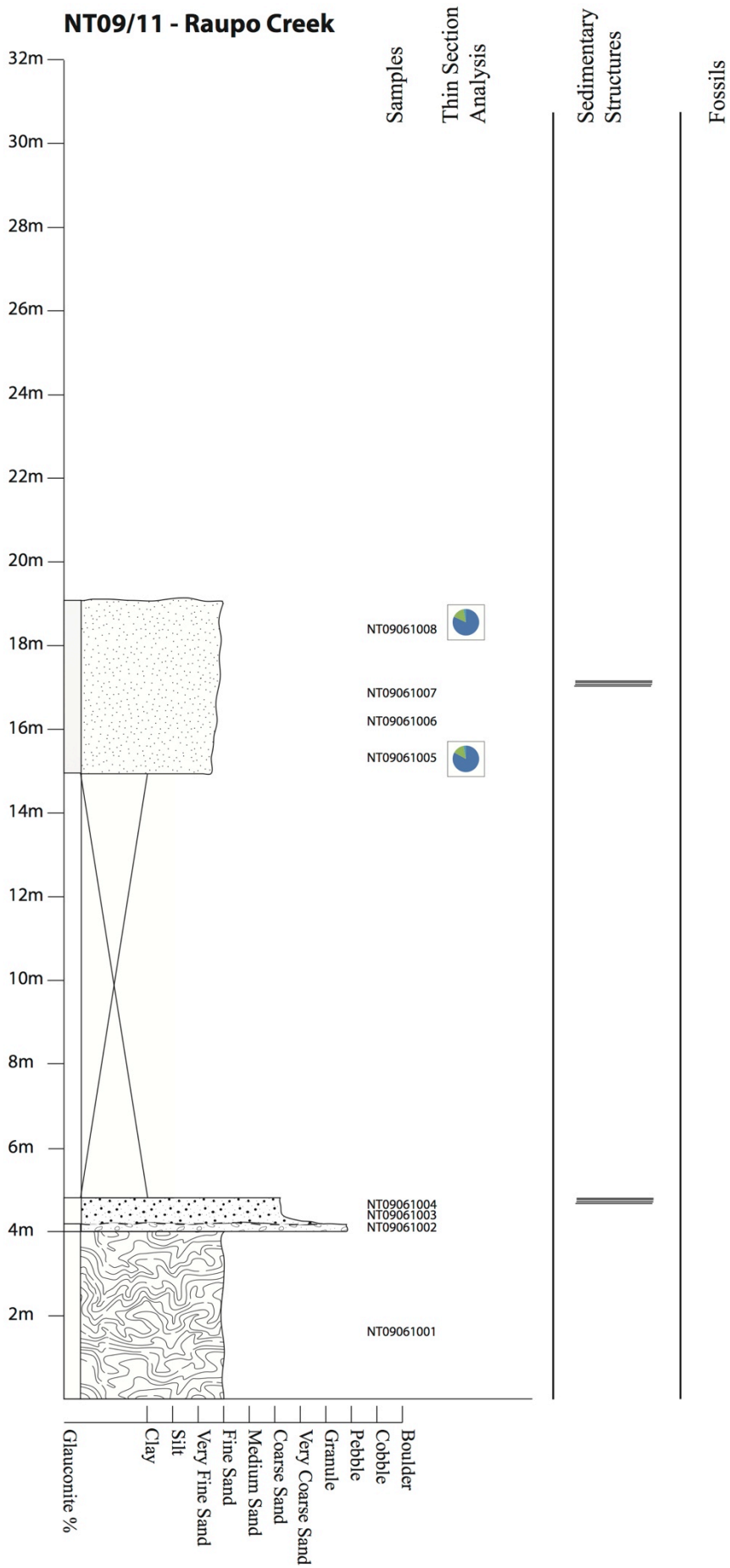
NT09/11 - Raupo Creek
32m
30m
28m
26m
24m
22m
20m
18m
16m
14m
12m
10m
8m
6m
4m
2m
Samples
Thin Section Analysis
Sedimentary Structures
Fossils
NT09061008
NT09061007
NT09061006
NT09061005
NT09061004
NT09061003
NT09061002
NT09061001
Glauconite %
Clay
Silt
Very Fine Sand
Fine Sand
Medium Sand
Coarse Sand
Very Coarse Sand
Granule
Pebble
Cobble
Boulder

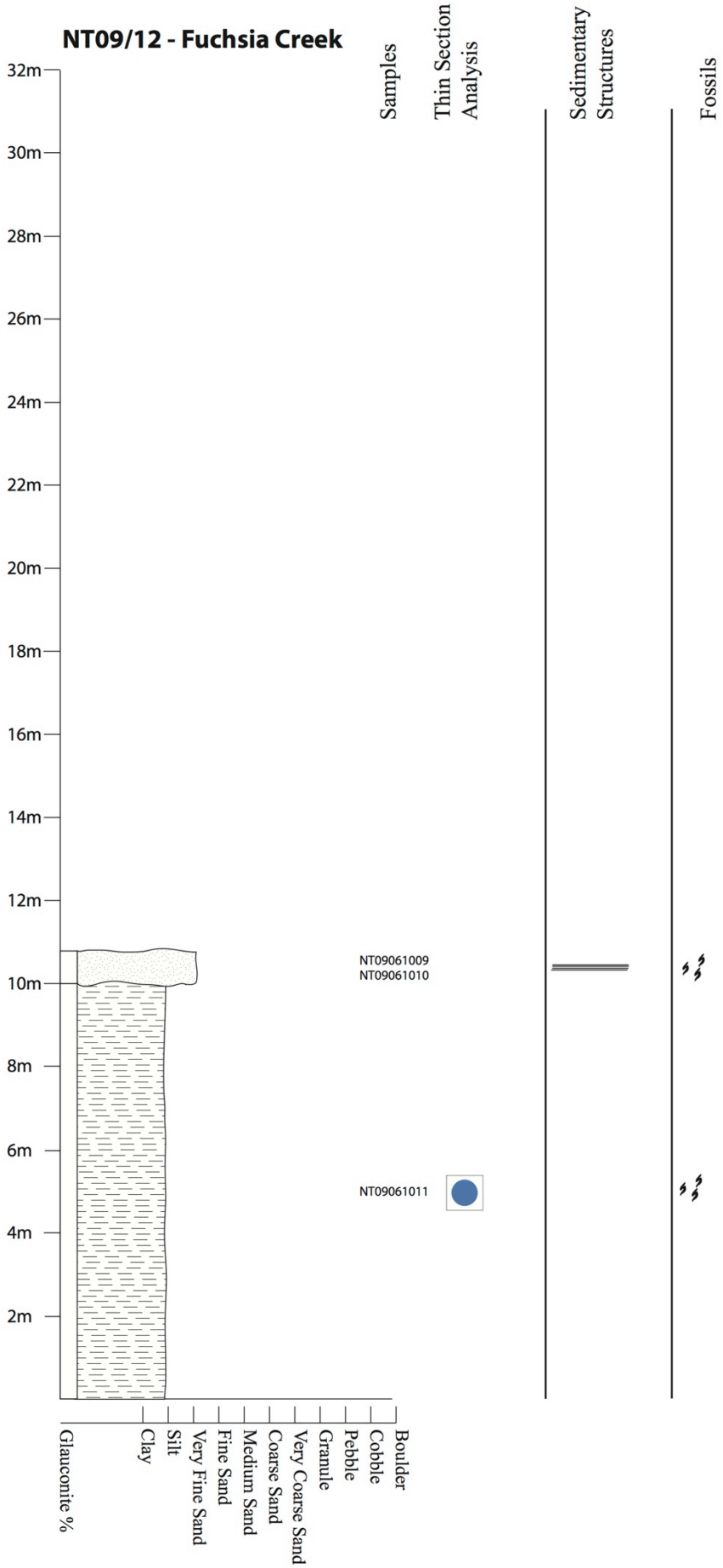
NT09/12 - Fuchsia Creek
32m
30m
28m
26m
24m
22m
20m
18m
16m
14m
12m
10m
8m
6m
4m
2m
Samples
Thin Section Analysis
Sedimentary Structures
Fossils
NT09061009
NT09061010
NT09061011
Glauconite %
Clay
Silt
Very Fine Sand
Fine Sand
Medium Sand
Coarse Sand
Very Coarse Sand
Granule
Pebble
Cobble
Boulder

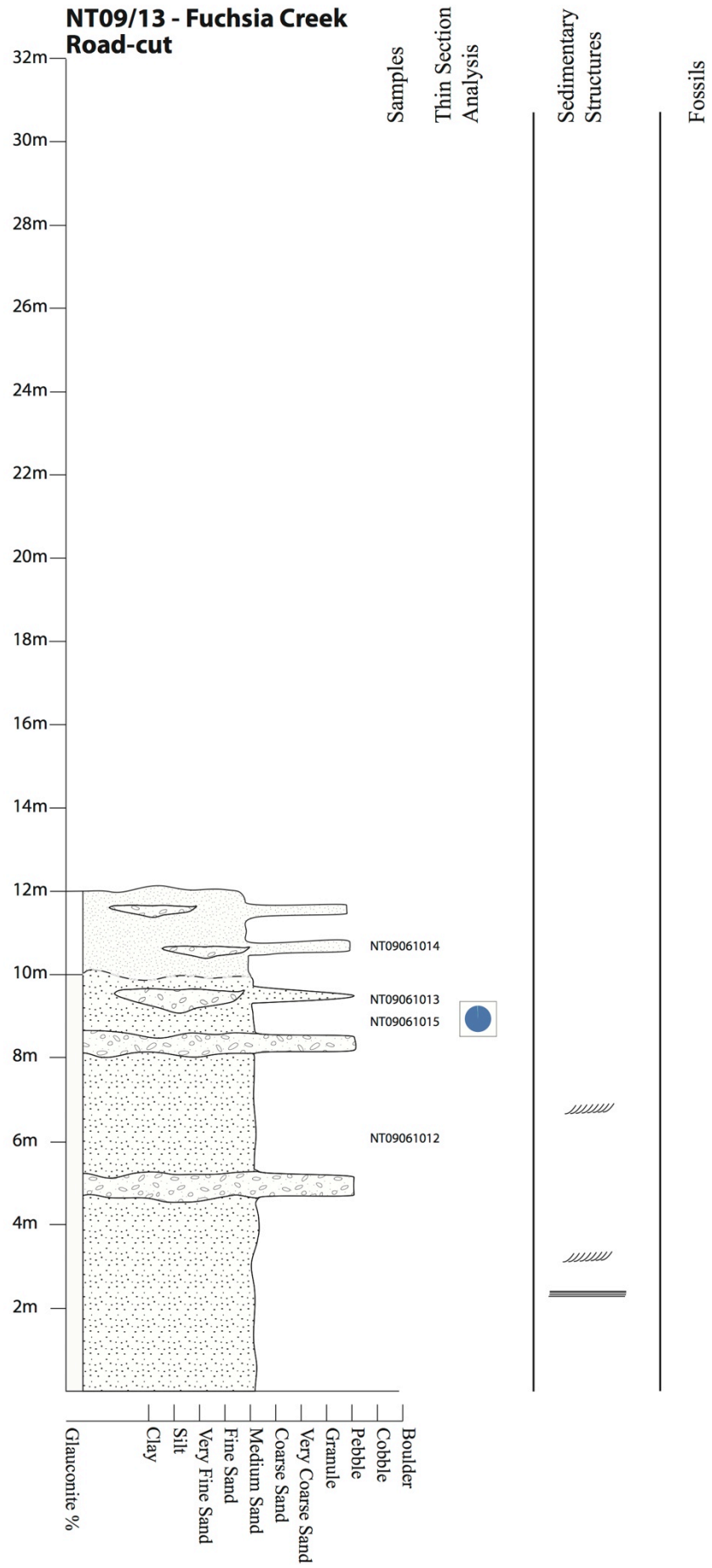
NT09/13 - Fuchsia Creek Road-cut
32m
30m
28m
26m
24m
22m
20m
18m
16m
14m
12m
10m
8m
6m
4m
2m
Samples
Thin Section Analysis
Sedimentary Structures
Fossils
NT09061014
NT09061013
NT09061015
NT09061012
Glauconite %
Clay
Silt
Very Fine Sand
Fine Sand
Medium Sand
Coarse Sand
Very Coarse Sand
Granule
Pebble
Cobble
Boulder

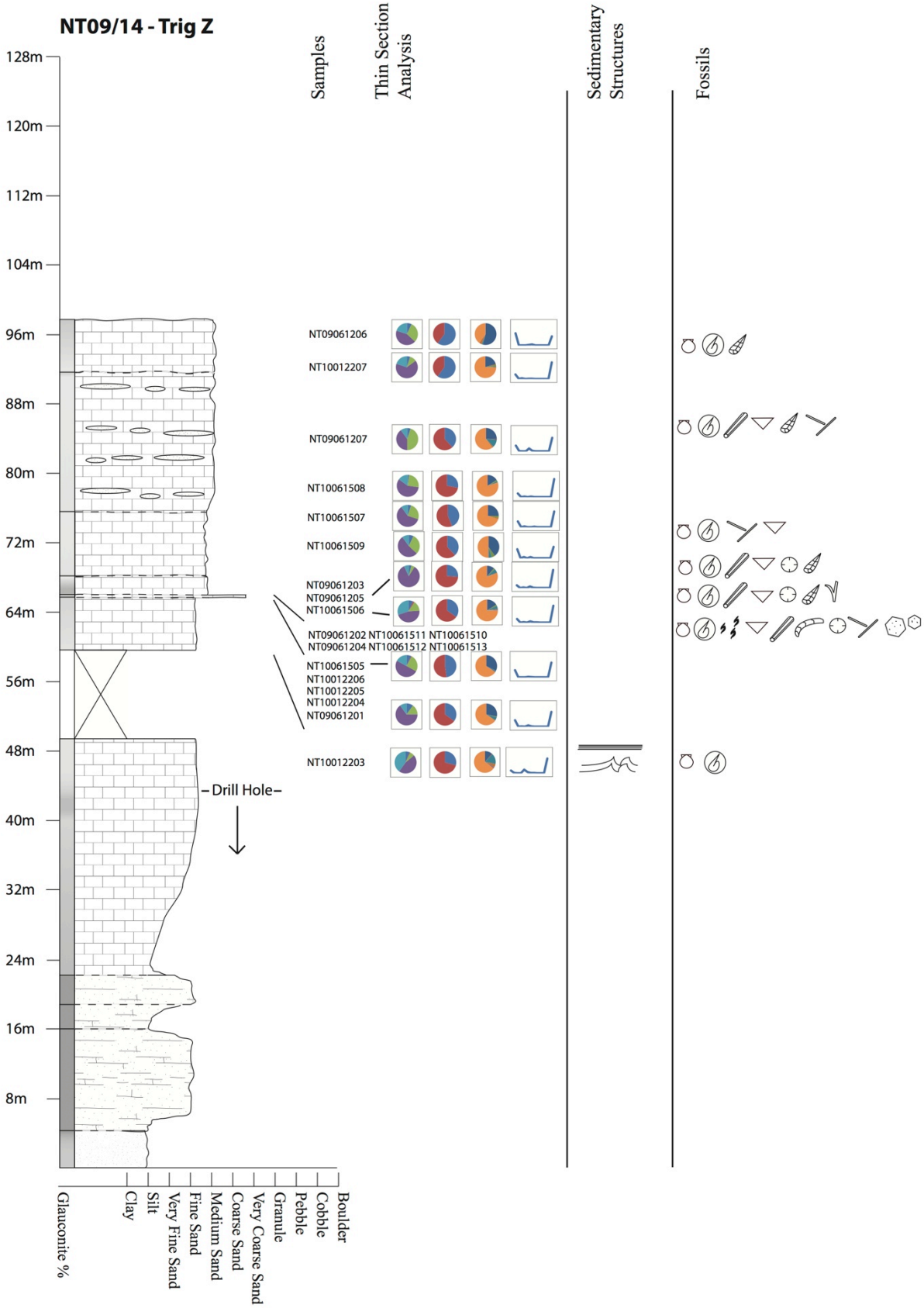
NT09/14 - Trig Z
128m
120m
112m
104m
96m
88m
80m
72m
64m
56m
48m
40m
32m
24m
16m
8m
Samples
Thin Section Analysis
Sedimentary Structures
Fossils
NT09061206
NT10012207
NT09061207
NT10061508
NT10061507
NT10061509
NT09061203
NT09061205
NT10061506
NT09061202 NT10061511 NT10061510
NT09061204 NT10061512 NT10061513
NT10061505
NT10012206
NT10012205
NT10012204
NT09061201
NT10012203
Drill Hole
Glauconite %
Clay
Silt
Very Fine Sand
Fine Sand
Medium Sand
Coarse Sand
Very Coarse Sand
Granule
Pebble
Cobble
Boulder

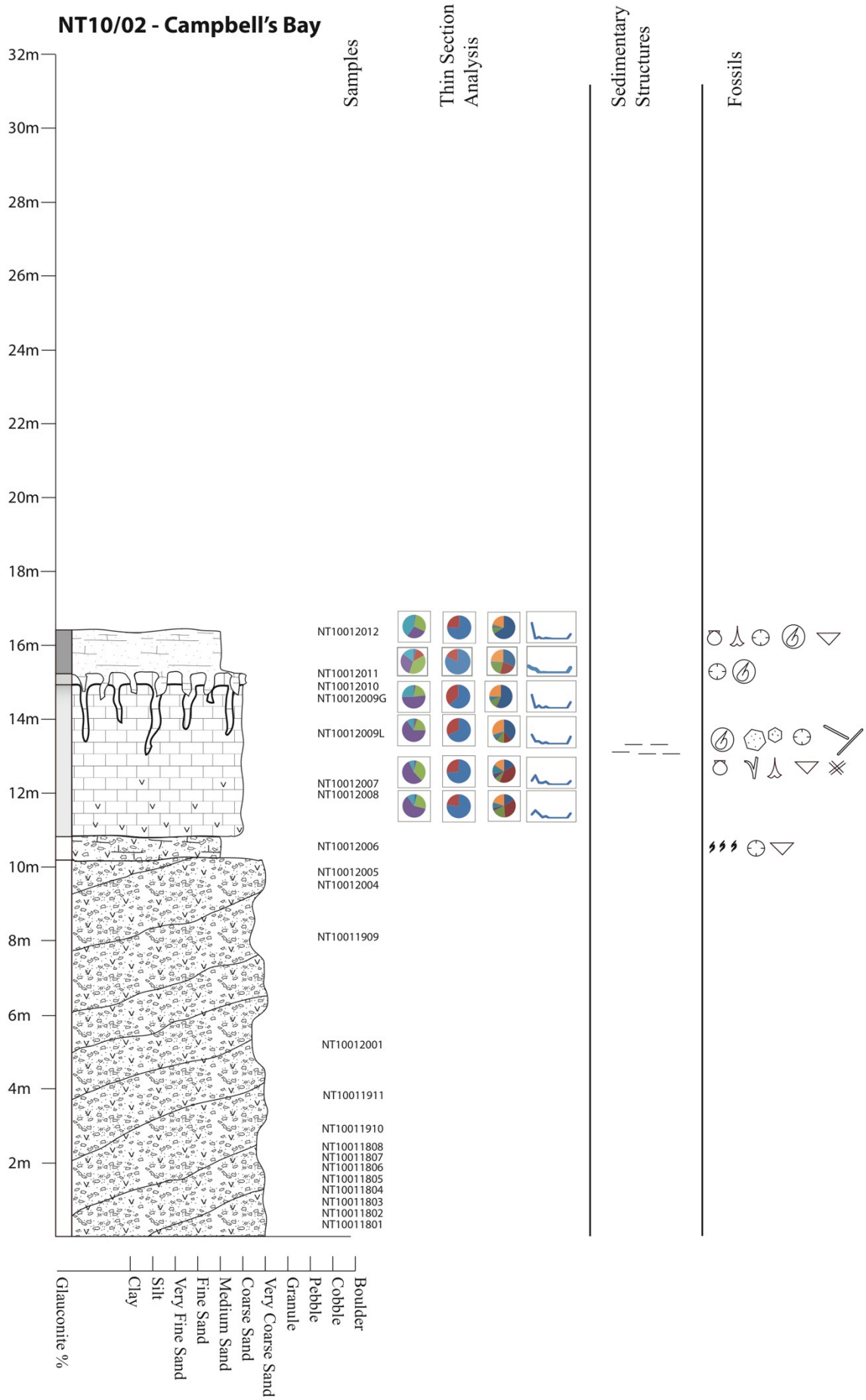
NT10/02 - Campbell's Bay
32m
30m
28m
26m
24m
22m
20m
18m
16m
14m
12m
10m
8m
6m
4m
2m
Samples
Thin Section Analysis
Sedimentary Structures
Fossils
NT10012012
NT10012011
NT10012010
NT10012009G
NT10012009L
NT10012007
NT10012008
NT10012006
NT10012005
NT10012004
NT10011909
NT10012001
NT10011911
NT10011910
NT10011808
NT10011807
NT10011806
NT10011805
NT10011804
NT10011803
NT10011802
NT10011801
Glauconite %
Clay
Silt
Very Fine Sand
Fine Sand
Medium Sand
Coarse Sand
Very Coarse Sand
Granule
Pebble
Cobble
Boulder

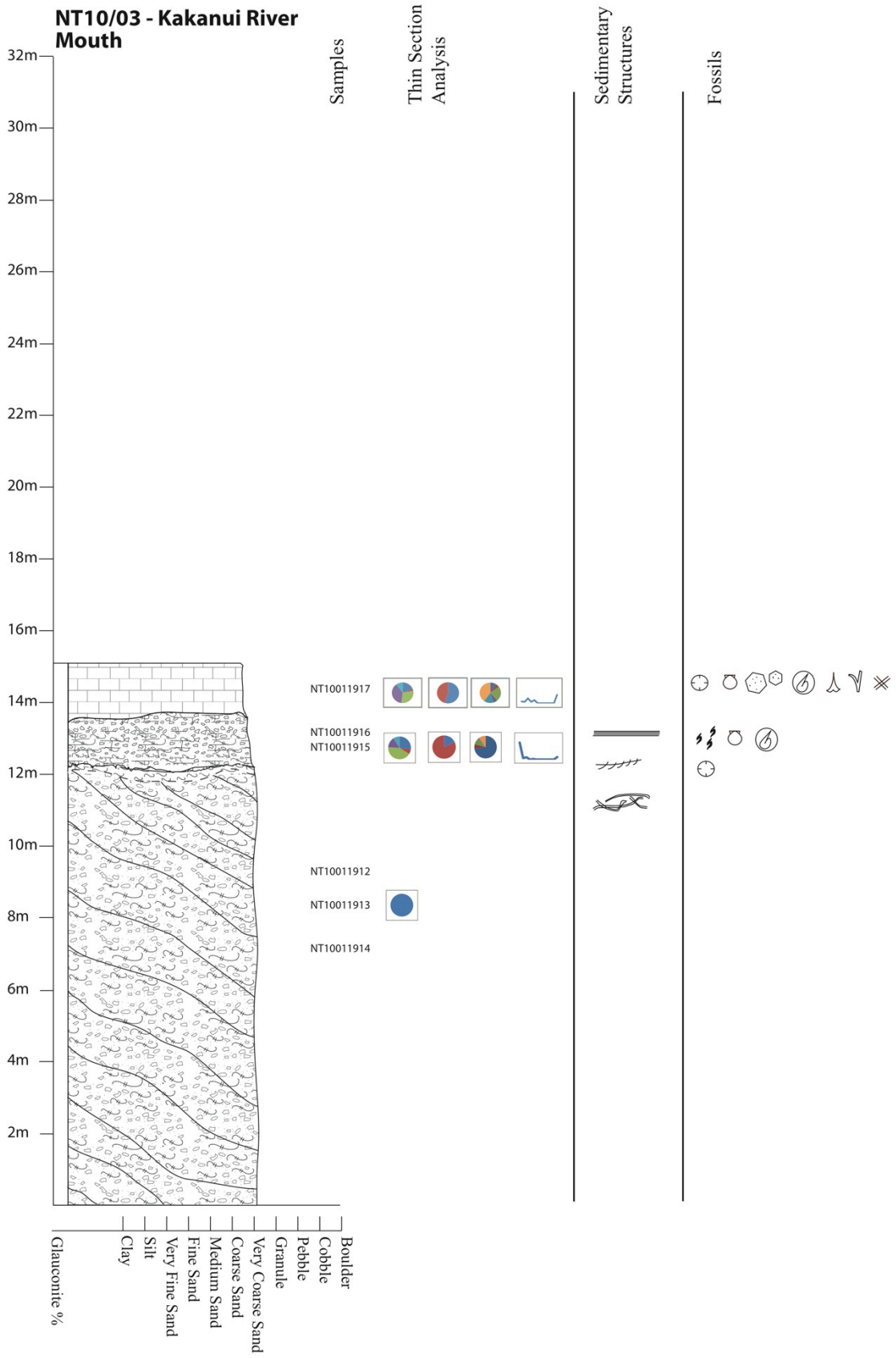
NT10/03 - Kakanui River Mouth
32m
30m
28m
26m
24m
22m
20m
18m
16m
14m
12m
10m
8m
6m
4m
2m
Samples
Thin Section Analysis
Sedimentary Structures
Fossils
NT10011917
NT10011916
NT10011915
NT10011912
NT10011913
NT10011914
Glauconite %
Clay
Silt
Very Fine Sand
Fine Sand
Medium Sand
Coarse Sand
Very Coarse Sand
Granule
Pebble
Cobble
Boulder

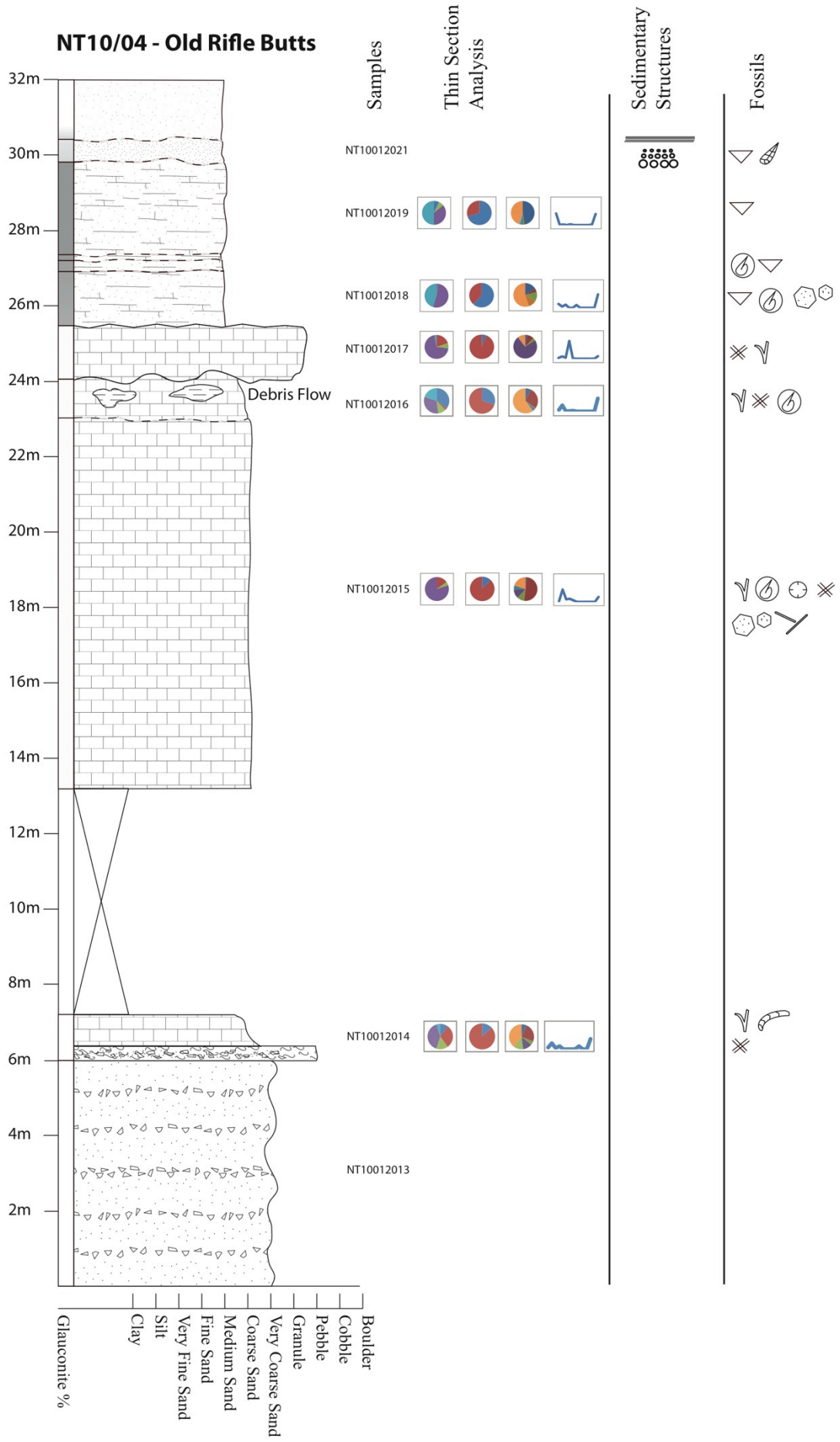
NT10/04 - Old Rifle Butts
32m
30m
28m
26m
24m
22m
20m
18m
16m
14m
12m
10m
8m
6m
4m
2m
Debris Flow
Samples
Thin Section Analysis
Sedimentary Structures
Fossils
NT10012021
NT10012019
NT10012018
NT10012017
NT10012016
NT10012015
NT10012014
NT10012013
Glauconite %
Clay
Silt
Very Fine Sand
Fine Sand
Medium Sand
Coarse Sand
Very Coarse Sand
Granule
Pebble
Cobble
Boulder

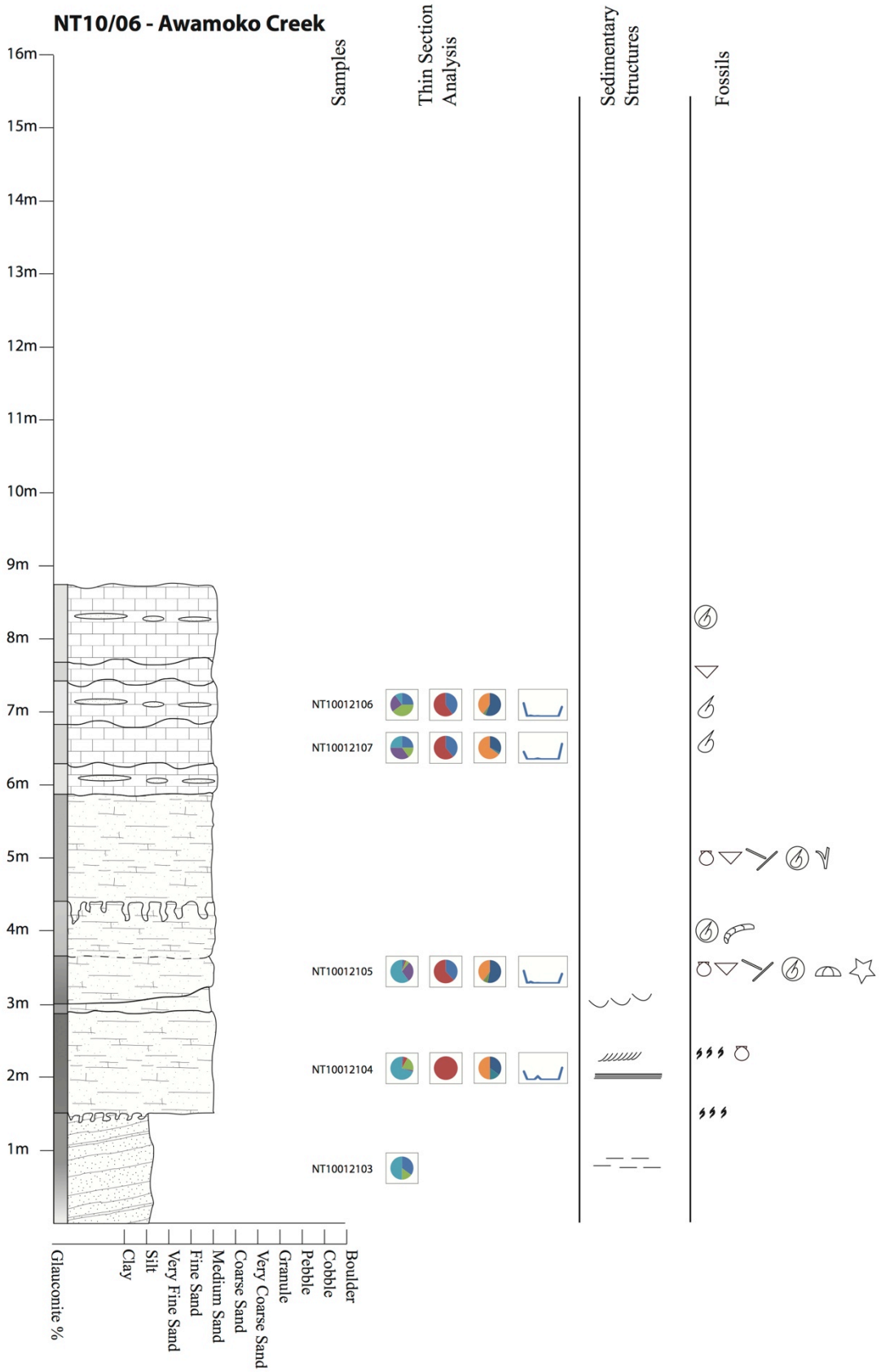
NT10/06 - Awamoko Creek
Samples
Thin Section Analysis
Sedimentary Structures
Fossils
16m
15m
14m
13m
12m
11m
10m
9m
8m
7m
6m
5m
4m
3m
2m
1m
NT10012106
NT10012107
NT10012105
NT10012104
NT10012103
Glauconite %
Clay
Silt
Very Fine Sand
Fine Sand
Medium Sand
Coarse Sand
Very Coarse Sand
Granule
Pebble
Cobble
Boulder

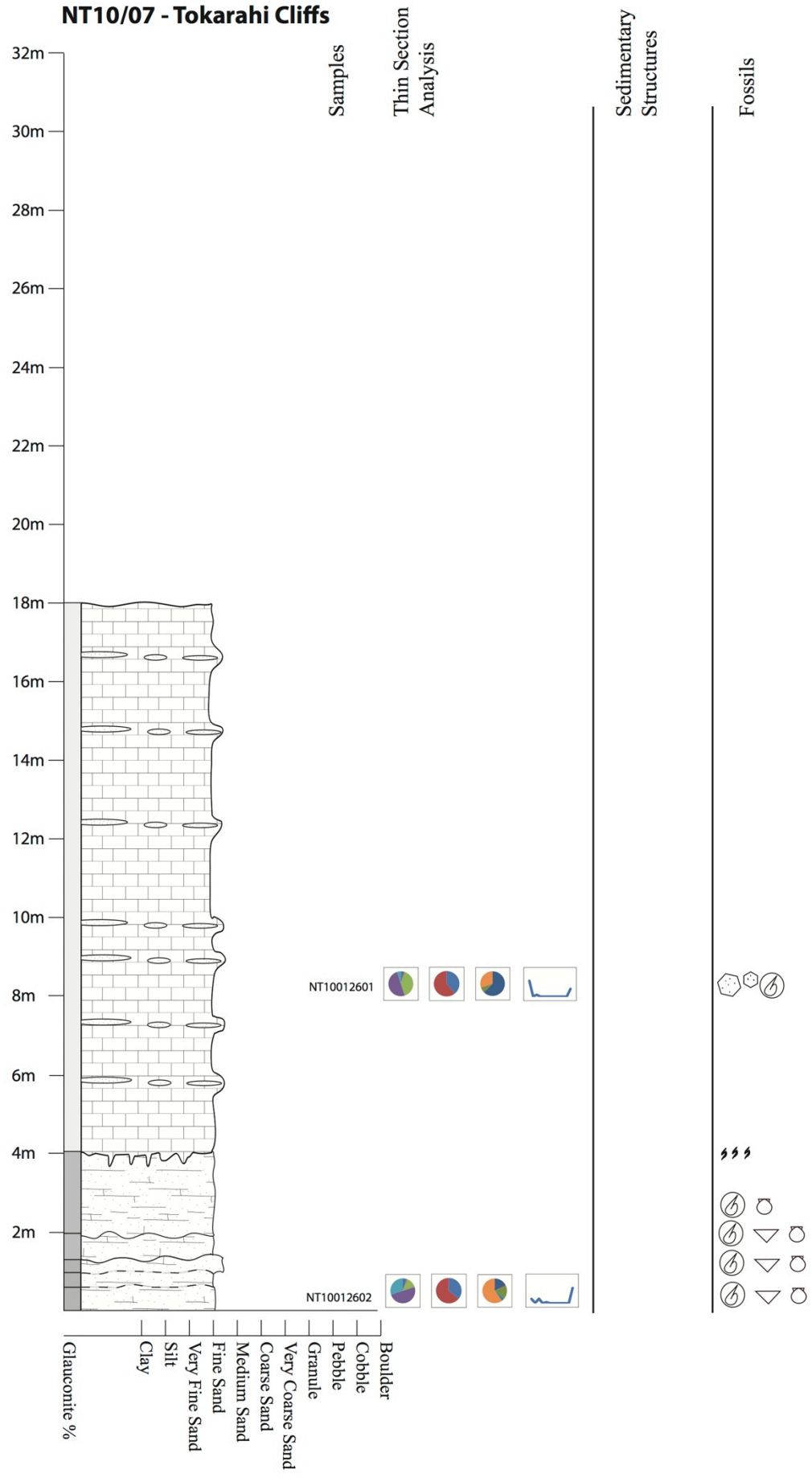
NT10/07 - Tokarahi Cliffs
32m
30m
28m
26m
24m
22m
20m
18m
16m
14m
12m
10m
8m
6m
4m
2m
Samples
Thin Section Analysis
Sedimentary Structures
Fossils
NT10012601
NT10012602
Glauconite %
Clay
Silt
Very Fine Sand
Fine Sand
Medium Sand
Coarse Sand
Very Coarse Sand
Granule
Pebble
Cobble
Boulder

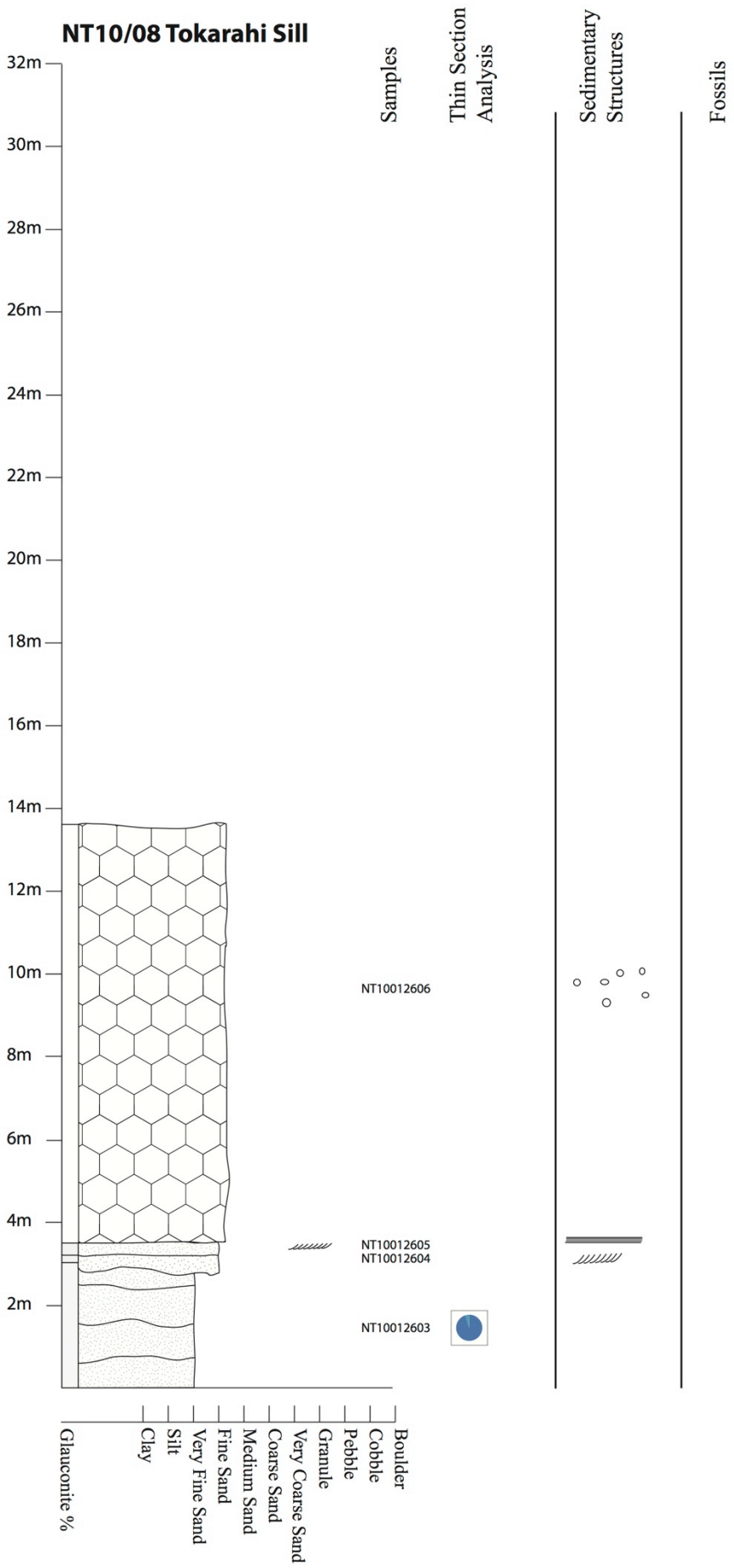
NT10/08 Tokarahi Sill
32m
30m
28m
26m
24m
22m
20m
18m
16m
14m
12m
10m
8m
6m
4m
2m
Samples
Thin Section Analysis
Sedimentary Structures
Fossils
NT10012606
NT10012605
NT10012604
NT10012603
Glauconite %
Clay
Silt
Very Fine Sand
Fine Sand
Medium Sand
Coarse Sand
Very Coarse Sand
Granule
Pebble
Cobble
Boulder

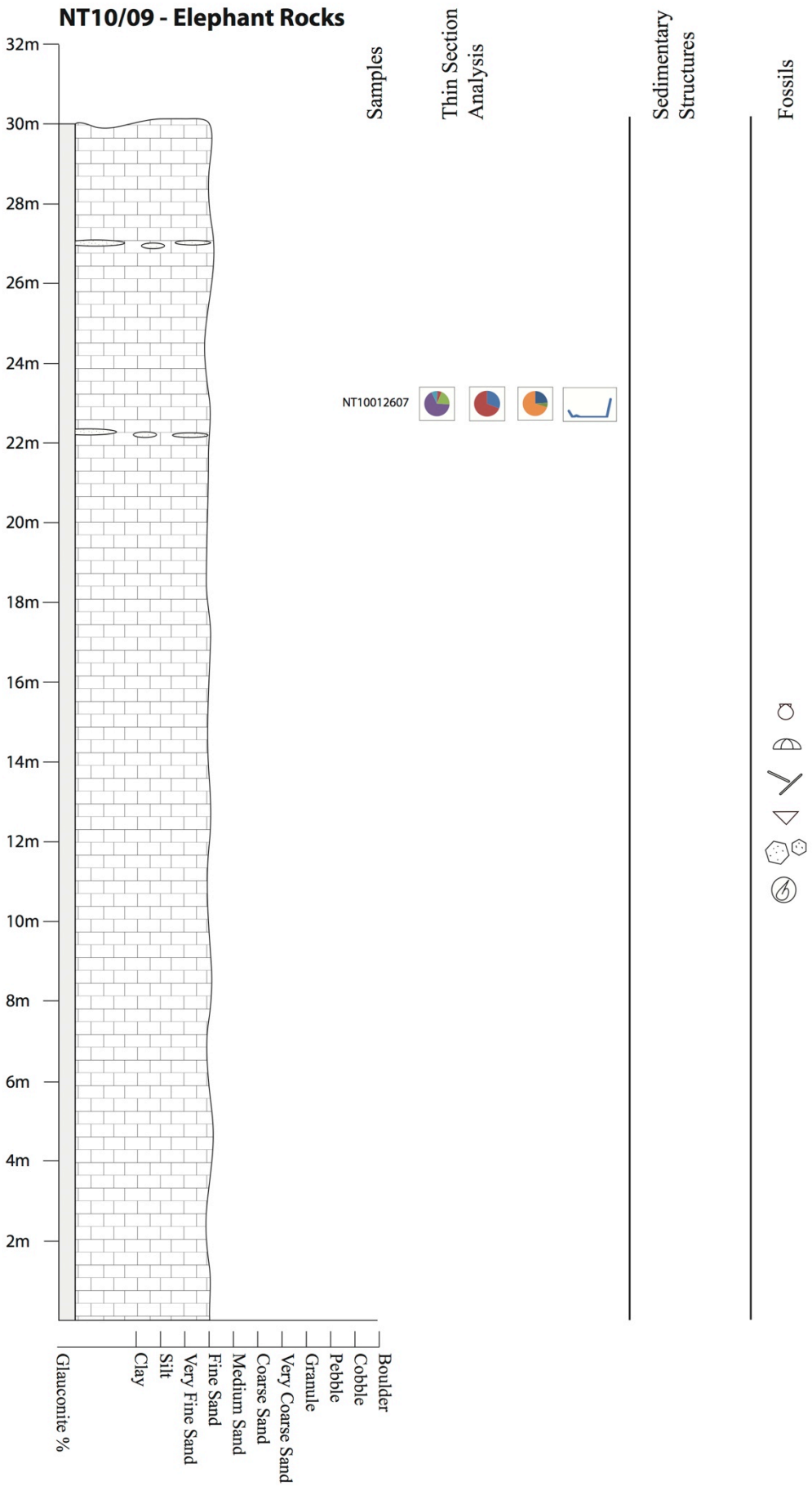
NT10/09 - Elephant Rocks
32m
30m
28m
26m
24m
22m
20m
18m
16m
14m
12m
10m
8m
6m
4m
2m
Samples
Thin Section Analysis
Sedimentary Structures
Fossils
NT10012607
Glauconite %
Clay
Silt
Very Fine Sand
Fine Sand
Medium Sand
Coarse Sand
Very Coarse Sand
Granule
Pebble
Cobble
Boulder

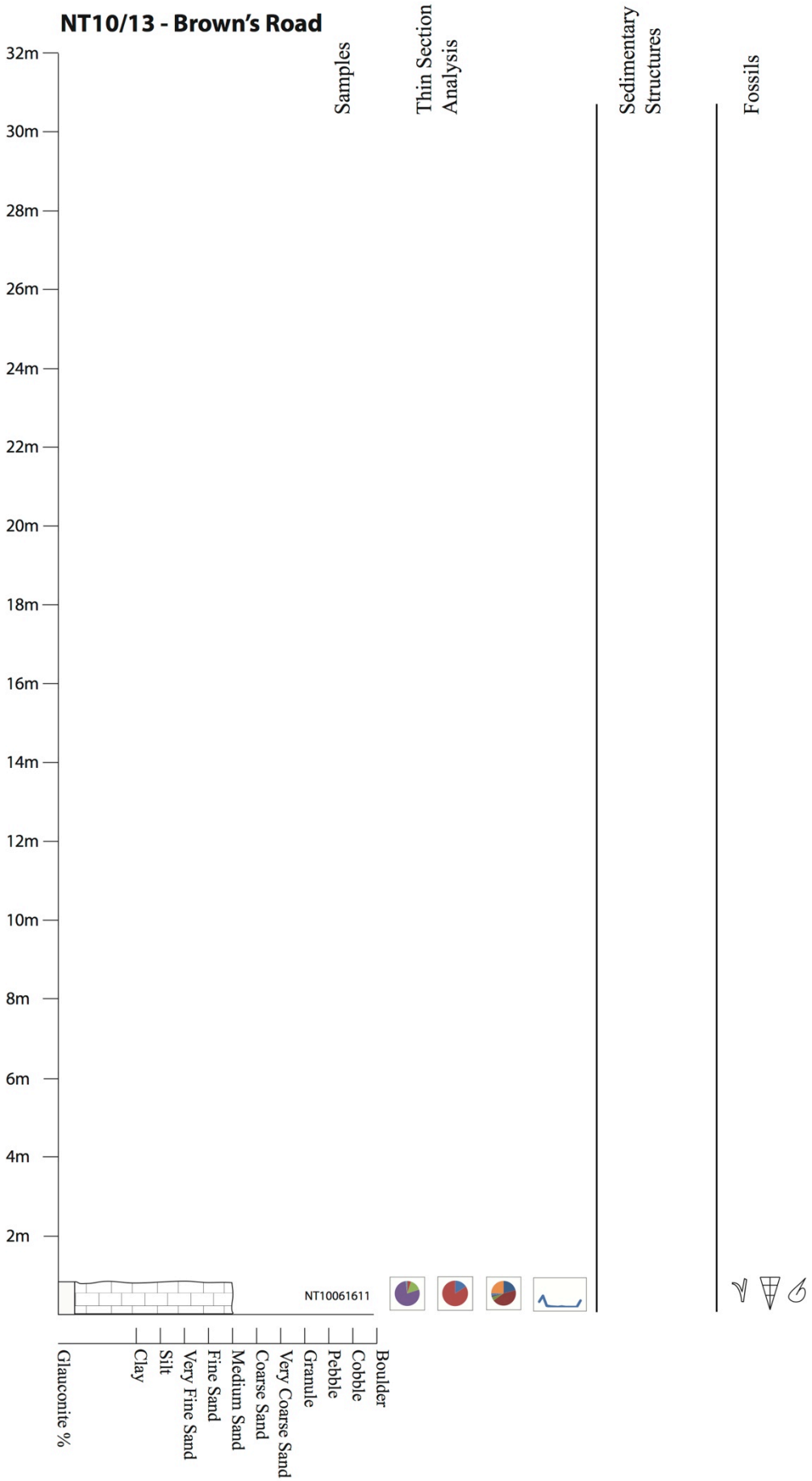
NT10/13 - Brown's Road
32m
30m
28m
26m
24m
22m
20m
18m
16m
14m
12m
10m
8m
6m
4m
2m
Samples
Thin Section Analysis
Sedimentary Structures
Fossils
NT10061611
Glauconite %
Clay
Silt
Very Fine Sand
Fine Sand
Medium Sand
Coarse Sand
Very Coarse Sand
Granule
Pebble
Cobble
Boulder

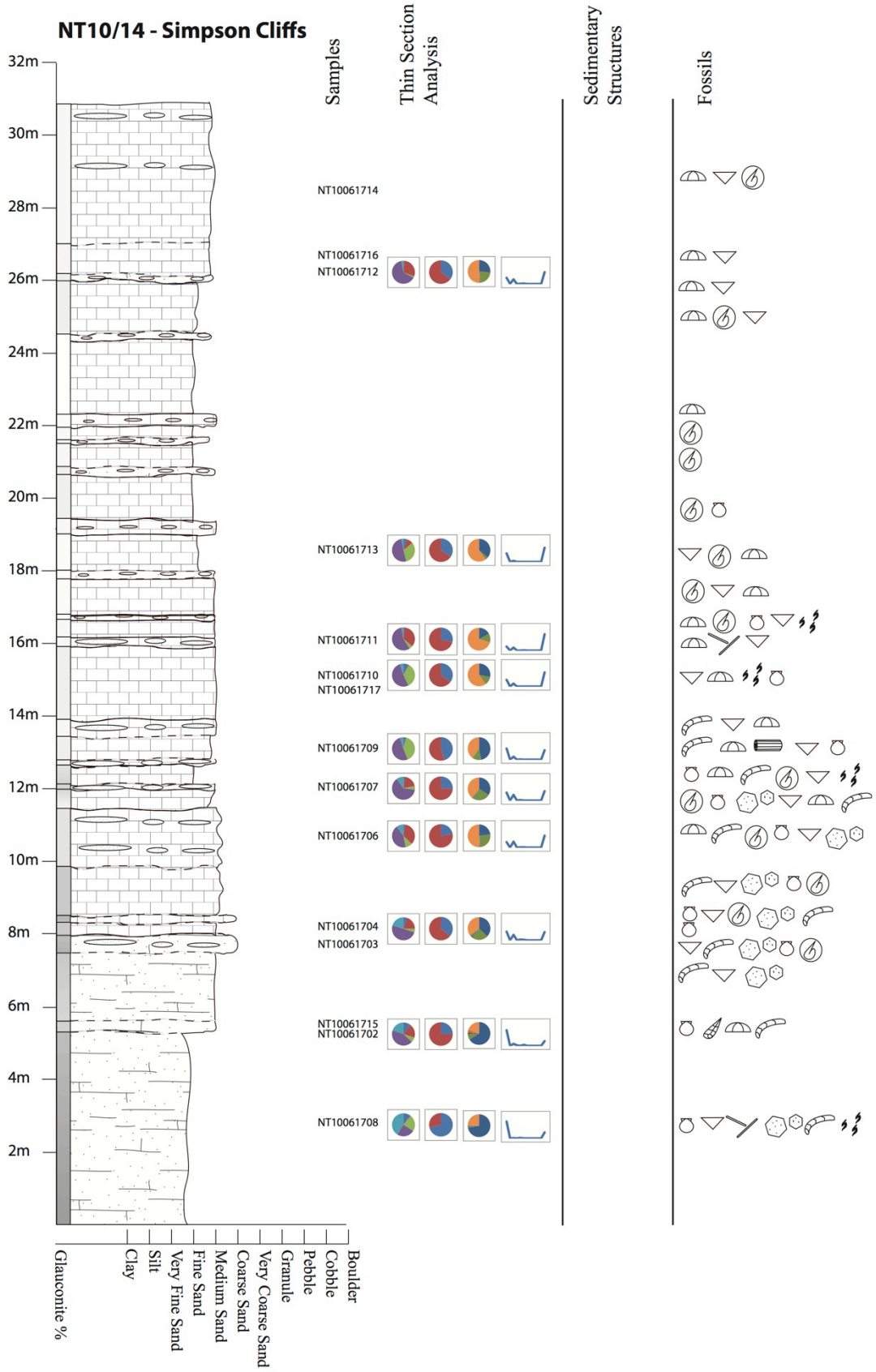
NT10/14 - Simpson Cliffs
32m
30m
28m
26m
24m
22m
20m
18m
16m
14m
12m
10m
8m
6m
4m
2m
Samples
Thin Section Analysis
Sedimentary Structures
Fossils
NT10061714
NT10061716
NT10061712
NT10061713
NT10061711
NT10061710
NT10061717
NT10061709
NT10061707
NT10061706
NT10061704
NT10061703
NT10061715
NT10061702
NT10061708
Glauconite %
Clay
Silt
Very Fine Sand
Fine Sand
Medium Sand
Coarse Sand
Very Coarse Sand
Granule
Pebble
Cobble
Boulder

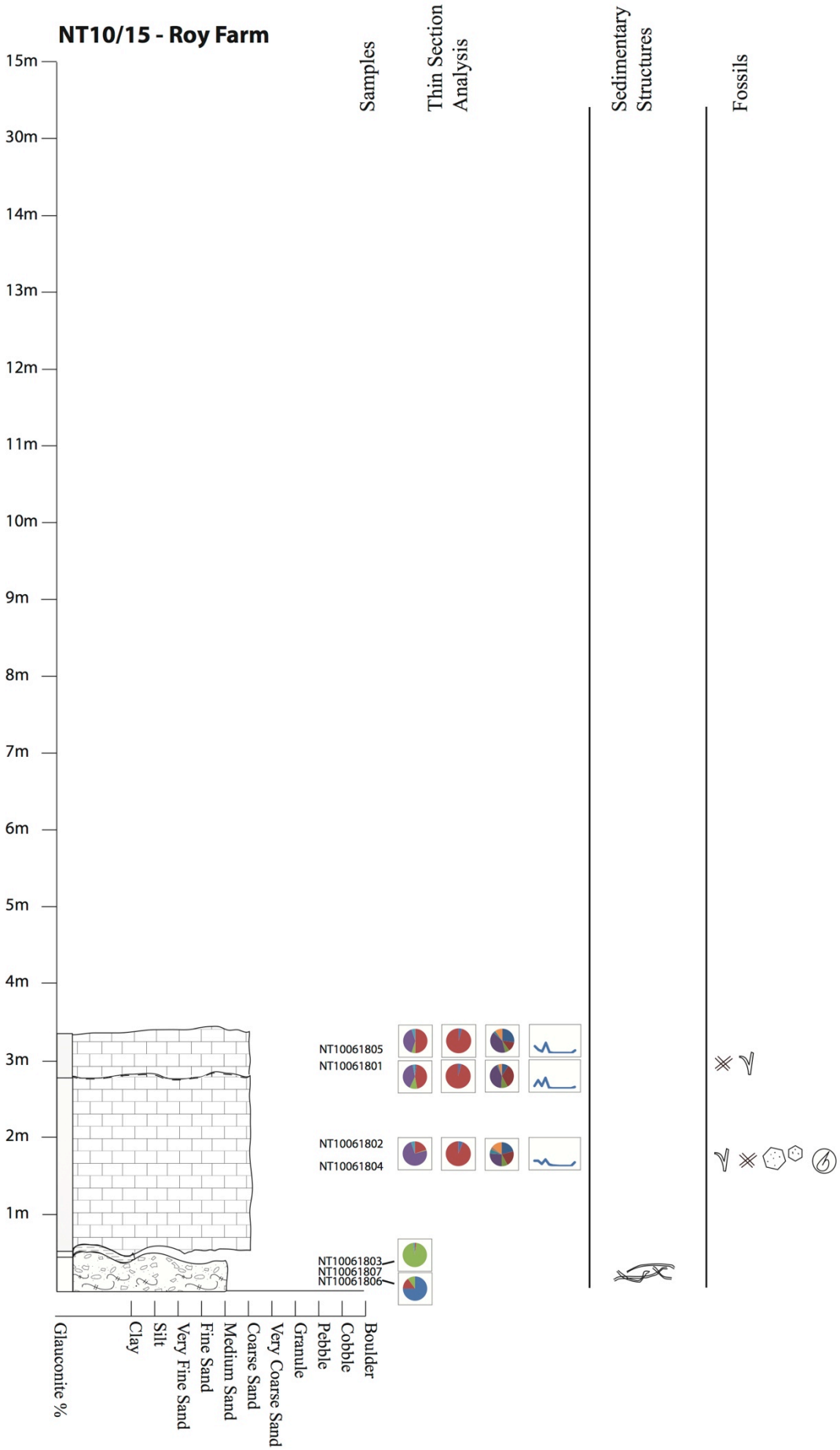
NT10/15 - Roy Farm
Samples
Thin Section Analysis
Sedimentary Structures
Fossils
15m
30m
14m
13m
12m
11m
10m
9m
8m
7m
6m
5m
4m
3m
2m
1m
NT10061805
NT10061801
NT10061802
NT10061804
NT10061803
NT10061807
NT10061806
Glauconite %
Clay
Silt
Very Fine Sand
Fine Sand
Medium Sand
Coarse Sand
Very Coarse Sand
Granule
Pebble
Cobble
Boulder

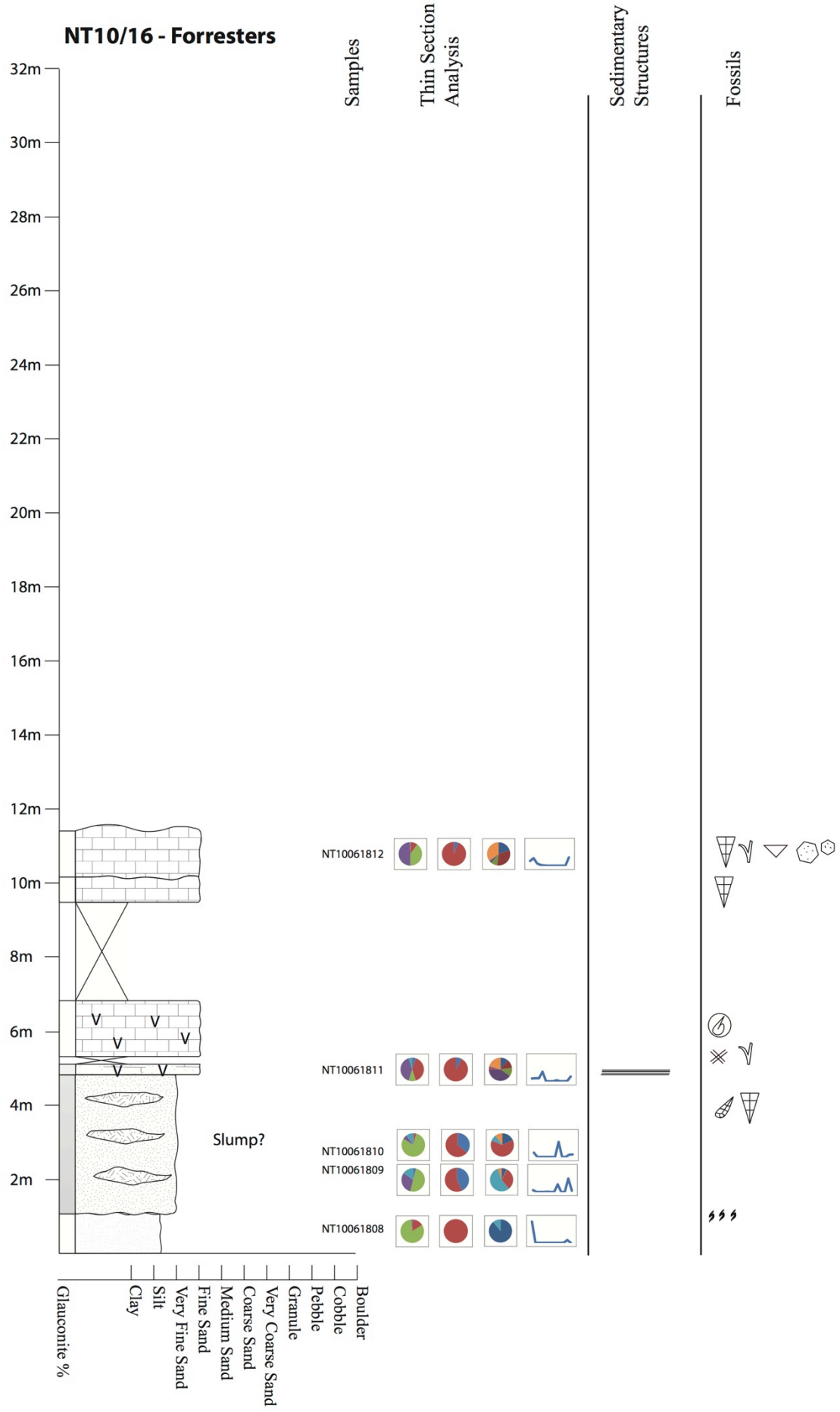
NT10/16 - Forresters
Samples
Thin Section Analysis
Sedimentary Structures
Fossils
32m
30m
28m
26m
24m
22m
20m
18m
16m
14m
12m
10m
8m
6m
4m
2m
NT10061812
NT10061811
NT10061810
NT10061809
NT10061808
Slump?
Glauconite %
Clay
Silt
Very Fine Sand
Fine Sand
Medium Sand
Coarse Sand
Very Coarse Sand
Granule
Pebble
Cobble
Boulder

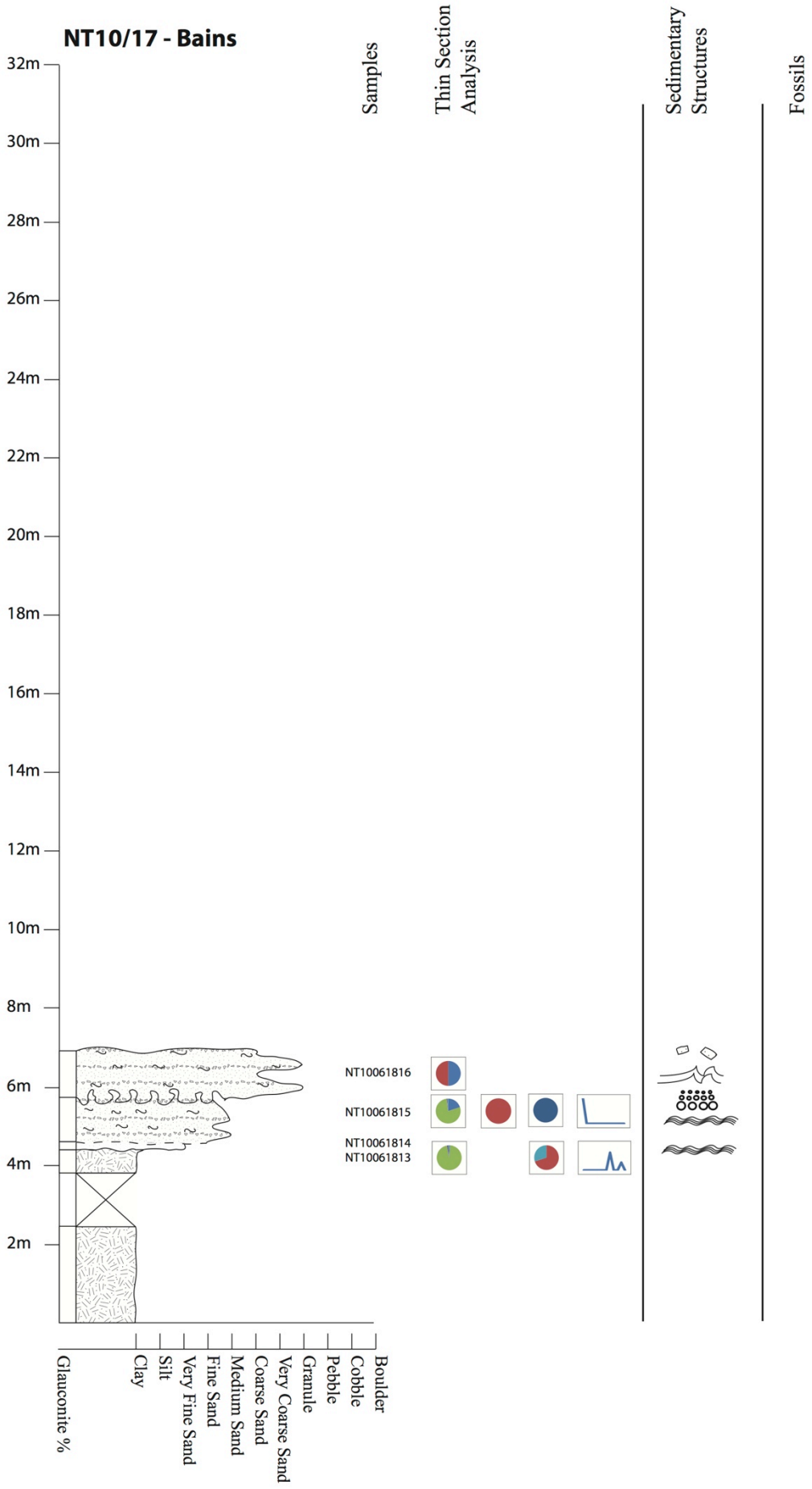
NT10/17 - Bains
32m
30m
28m
26m
24m
22m
20m
18m
16m
14m
12m
10m
8m
6m
4m
2m
Samples
Thin Section Analysis
Sedimentary Structures
Fossils
NT10061816
NT10061815
NT10061814
NT10061813
Glauconite %
Clay
Silt
Very Fine Sand
Fine Sand
Medium Sand
Coarse Sand
Very Coarse Sand
Granule
Pebble
Cobble
Boulder

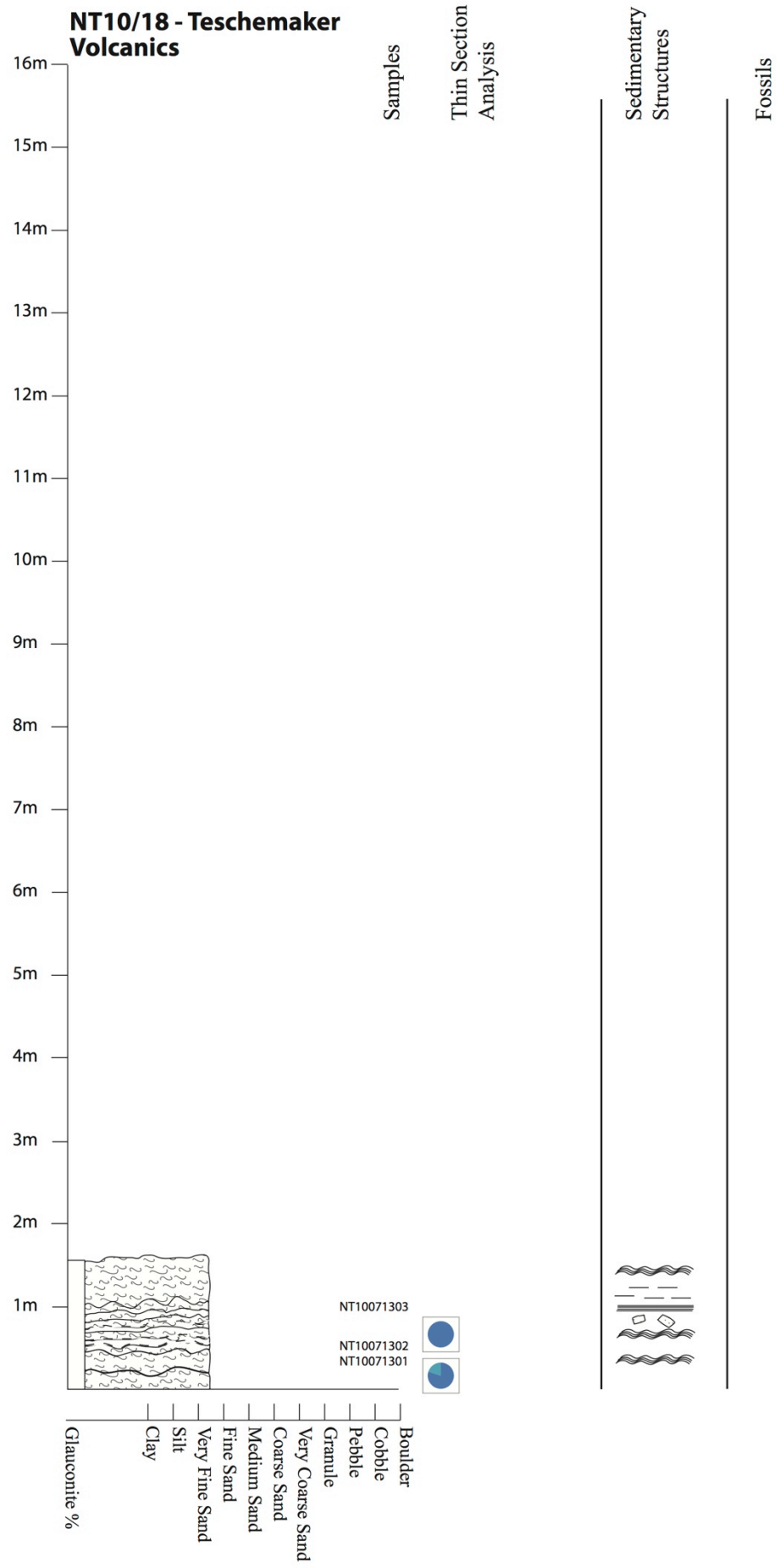
NT10/18 - Teschemaker Volcanics
16m
15m
14m
13m
12m
11m
10m
9m
8m
7m
6m
5m
4m
3m
2m
1m
Samples
Thin Section Analysis
Sedimentary Structures
Fossils
NT10071303
NT10071302
NT10071301
Glauconite %
Clay
Silt
Very Fine Sand
Fine Sand
Medium Sand
Coarse Sand
Very Coarse Sand
Granule
Pebble
Cobble
Boulder

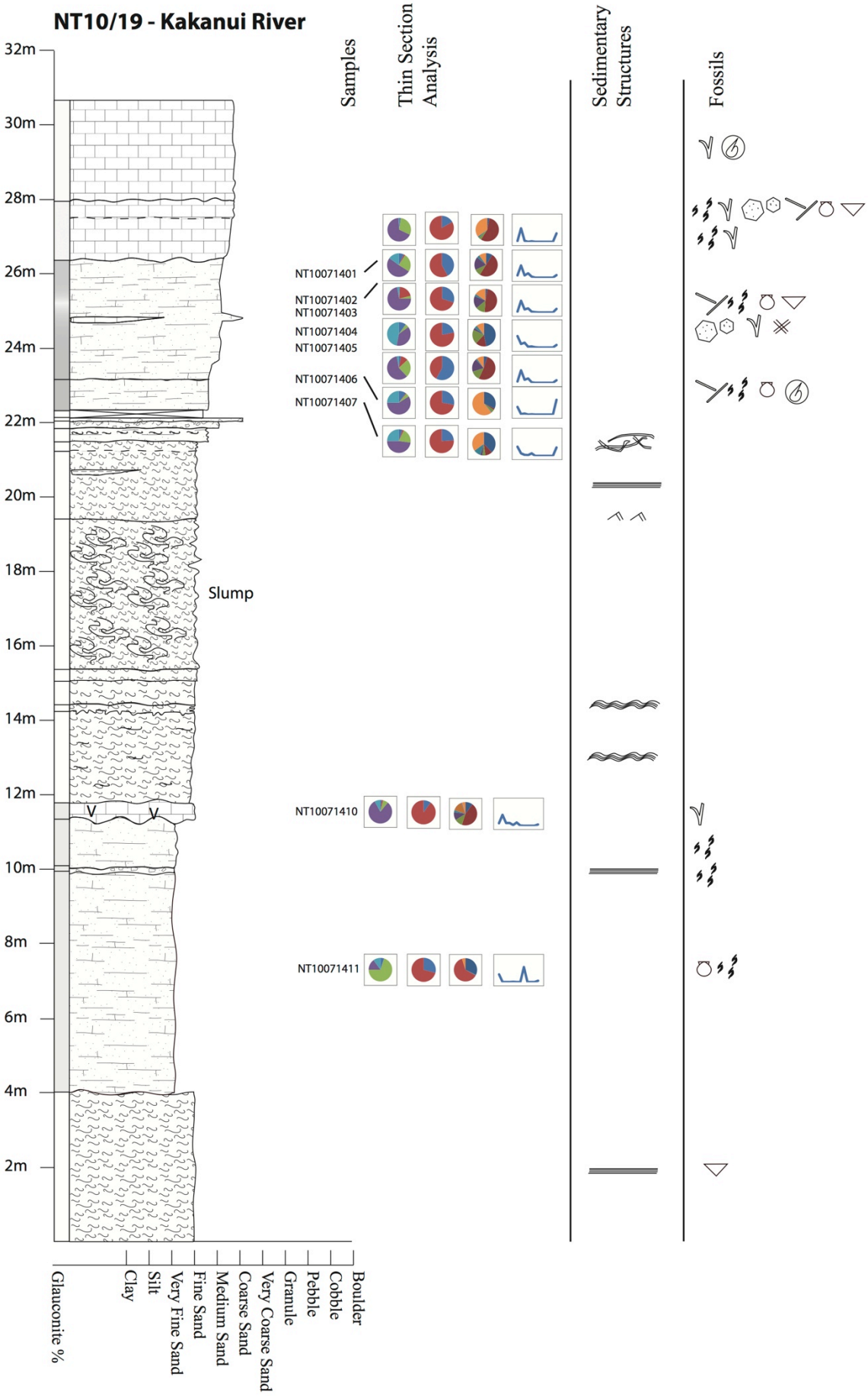
NT10/19 - Kakanui River
32m
30m
28m
26m
24m
22m
20m
18m
16m
14m
12m
10m
8m
6m
4m
2m
Slump
Samples
Thin Section Analysis
Sedimentary Structures
Fossils
NT10071401
NT10071402
NT10071403
NT10071404
NT10071405
NT10071406
NT10071407
NT10071410
NT10071411
Glauconite %
Clay
Silt
Very Fine Sand
Fine Sand
Medium Sand
Coarse Sand
Very Coarse Sand
Granule
Pebble
Cobble
Boulder

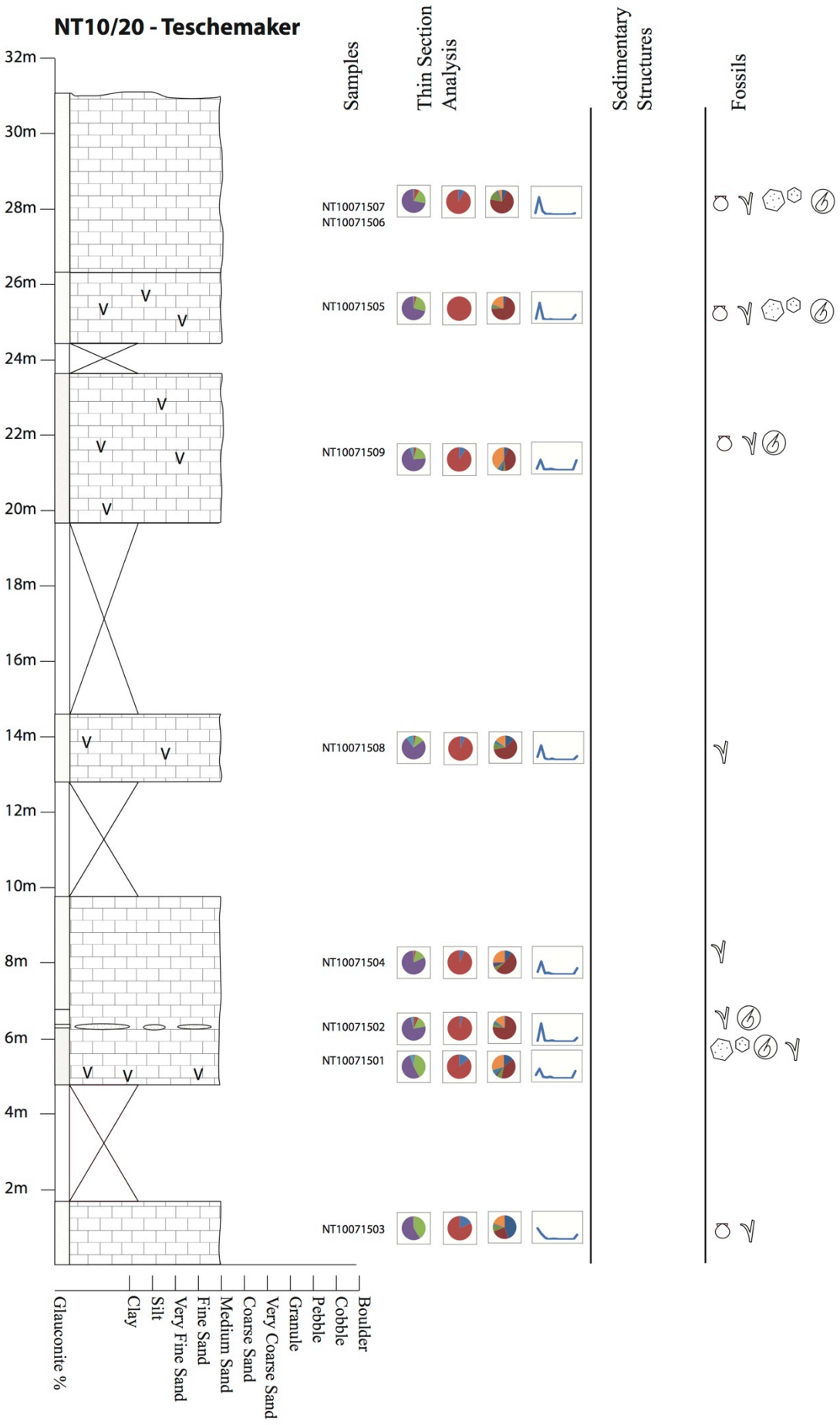
NT10/20 - Teschemaker
32m
30m
28m
26m
24m
22m
20m
18m
16m
14m
12m
10m
8m
6m
4m
2m
Samples
Thin Section Analysis
Sedimentary Structures
Fossils
NT10071507
NT10071506
NT10071505
NT10071509
NT10071508
NT10071504
NT10071502
NT10071501
NT10071503
Glauconite %
Clay
Silt
Very Fine Sand
Fine Sand
Medium Sand
Coarse Sand
Very Coarse Sand
Granule
Pebble
Cobble
Boulder

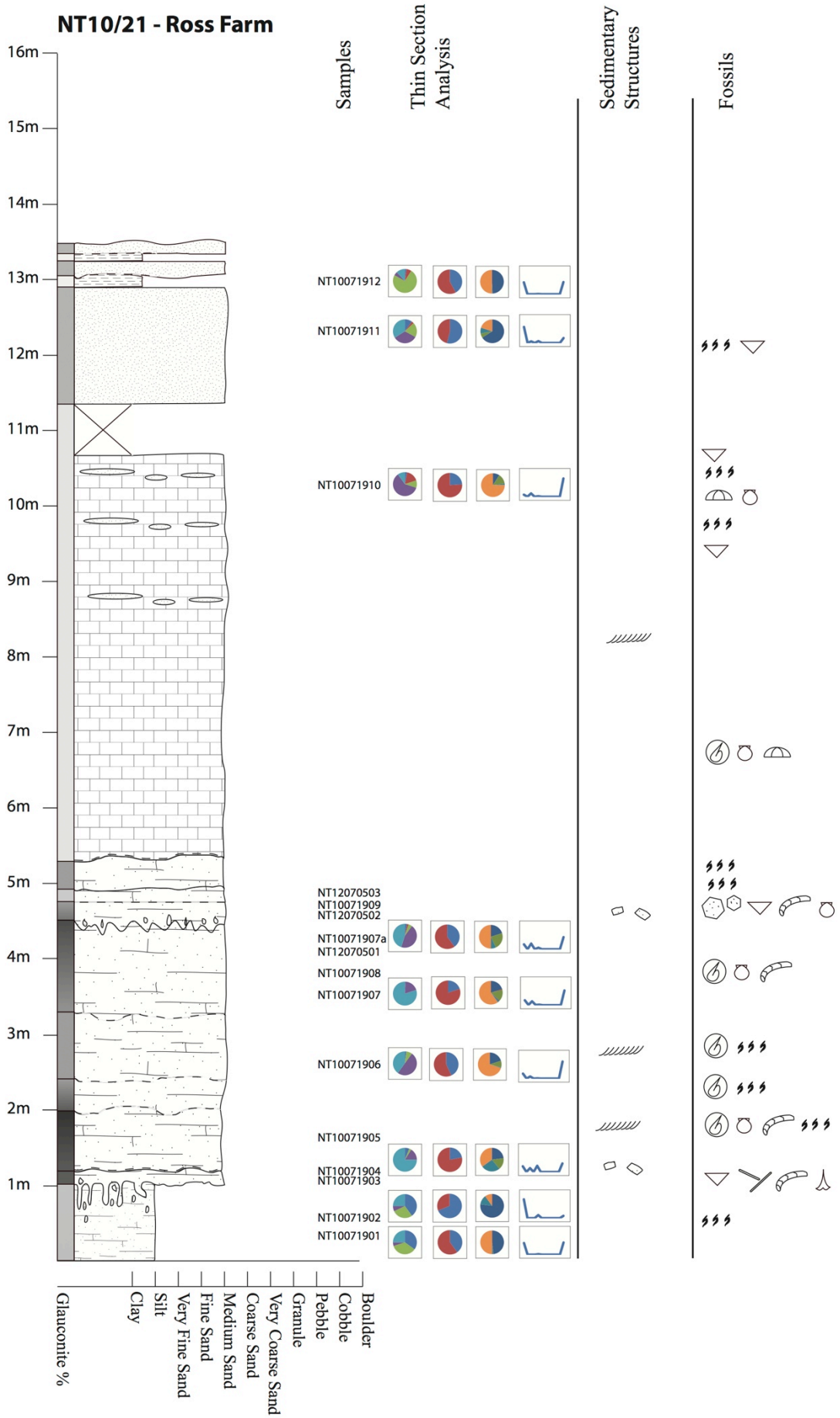
NT10/21 - Ross Farm
16m
15m
14m
13m
12m
11m
10m
9m
8m
7m
6m
5m
4m
3m
2m
1m
Samples
Thin Section Analysis
Sedimentary Structures
Fossils
NT10071912
NT10071911
NT10071910
NT12070503
NT10071909
NT12070502
NT10071907a
NT12070501
NT10071908
NT10071907
NT10071906
NT10071905
NT10071904
NT10071903
NT10071902
NT10071901
Glauconite %
Clay
Silt
Very Fine Sand
Fine Sand
Medium Sand
Coarse Sand
Very Coarse Sand
Granule
Pebble
Cobble
Boulder

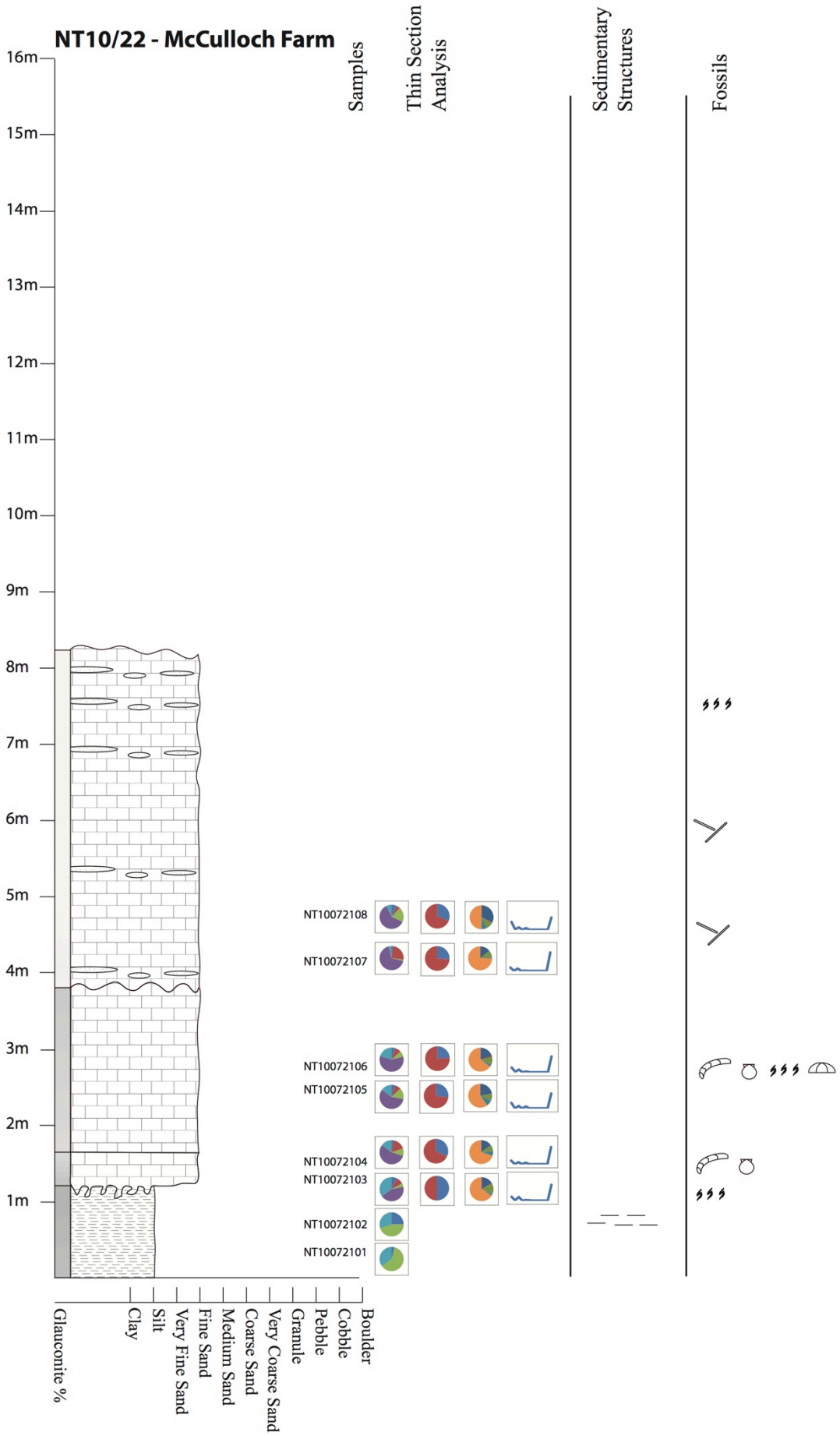
NT10/22 - McCulloch Farm
16m
15m
14m
13m
12m
11m
10m
9m
8m
7m
6m
5m
4m
3m
2m
1m
Samples
Thin Section Analysis
Sedimentary Structures
Fossils
NT10072108
NT10072107
NT10072106
NT10072105
NT10072104
NT10072103
NT10072102
NT10072101
Glauconite %
Clay
Silt
Very Fine Sand
Fine Sand
Medium Sand
Coarse Sand
Very Coarse Sand
Granule
Pebble
Cobble
Boulder

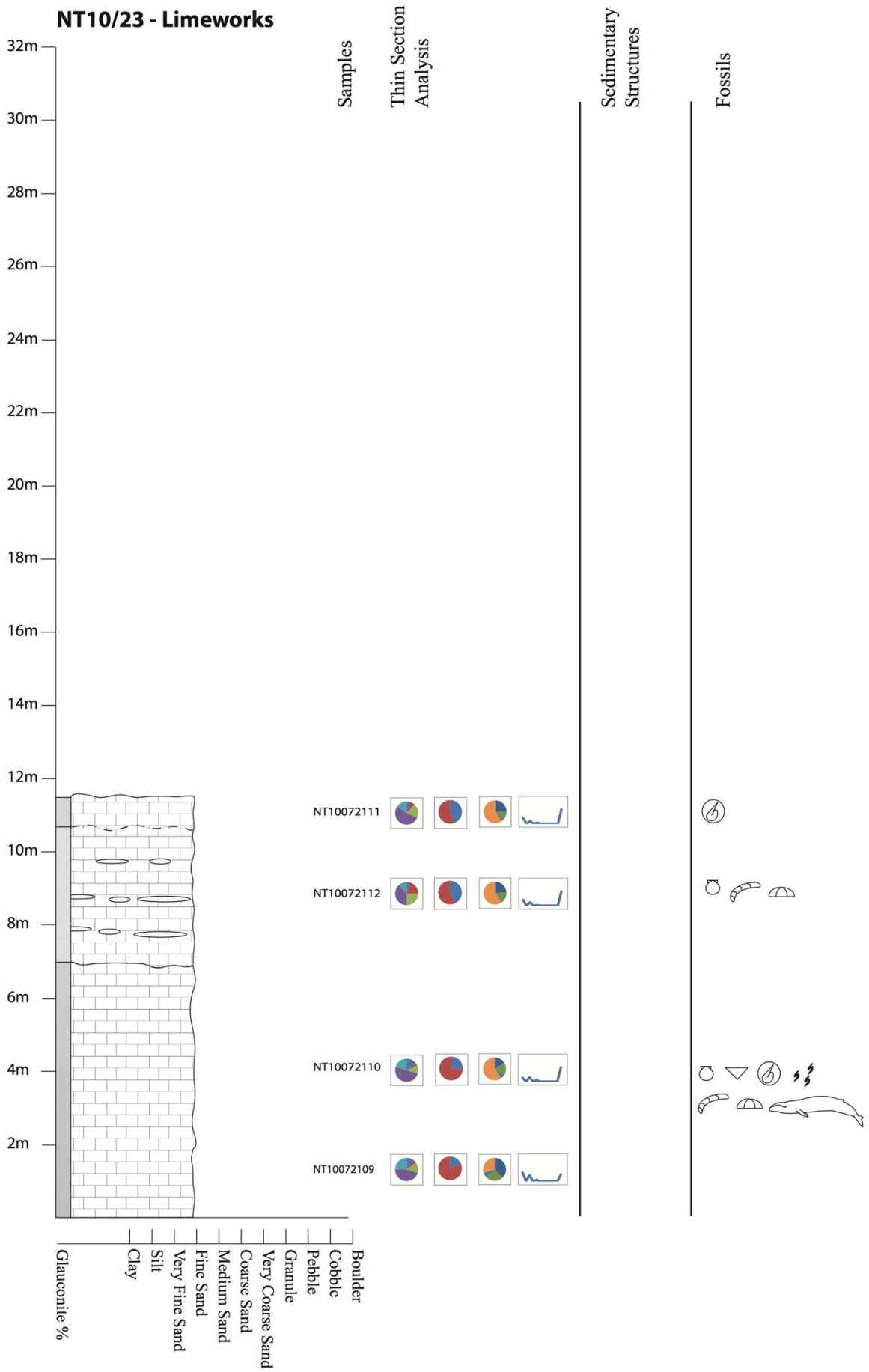
NT10/23 - Limeworks
32m
30m
28m
26m
24m
22m
20m
18m
16m
14m
12m
10m
8m
6m
4m
2m
Samples
Thin Section Analysis
Sedimentary Structures
Fossils
NT10072111
NT10072112
NT10072110
NT10072109
Glauconite %
Clay
Silt
Very Fine Sand
Fine Sand
Medium Sand
Coarse Sand
Very Coarse Sand
Granule
Pebble
Cobble
Boulder

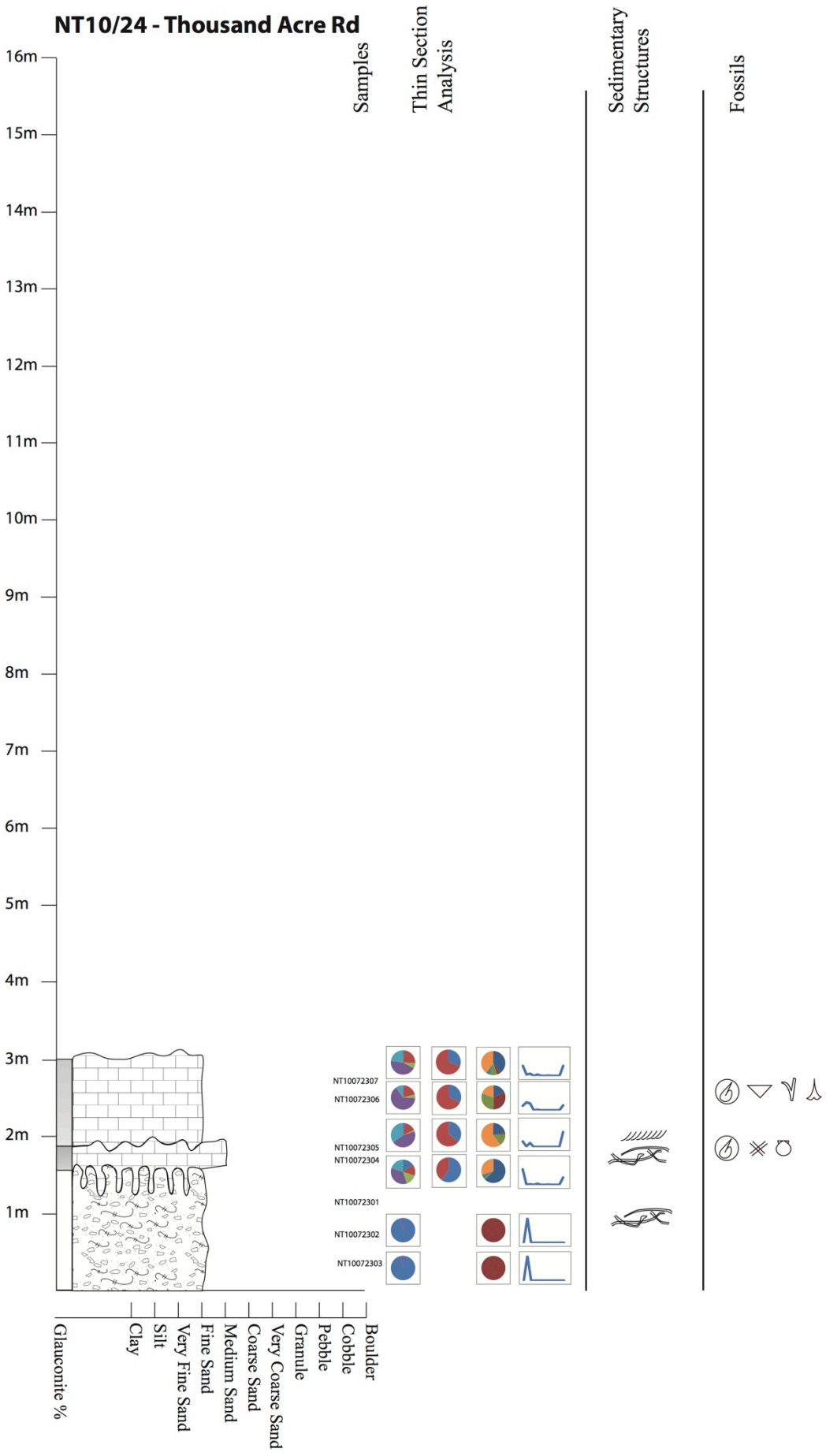
NT10/24 - Thousand Acre Rd
16m
15m
14m
13m
12m
11m
10m
9m
8m
7m
6m
5m
4m
3m
2m
1m
Samples
Thin Section Analysis
Sedimentary Structures
Fossils
NT10072307
NT10072306
NT10072305
NT10072304
NT10072301
NT10072302
NT10072303
Glauconite %
Clay
Silt
Very Fine Sand
Fine Sand
Medium Sand
Coarse Sand
Very Coarse Sand
Granule
Pebble
Cobble
Boulder

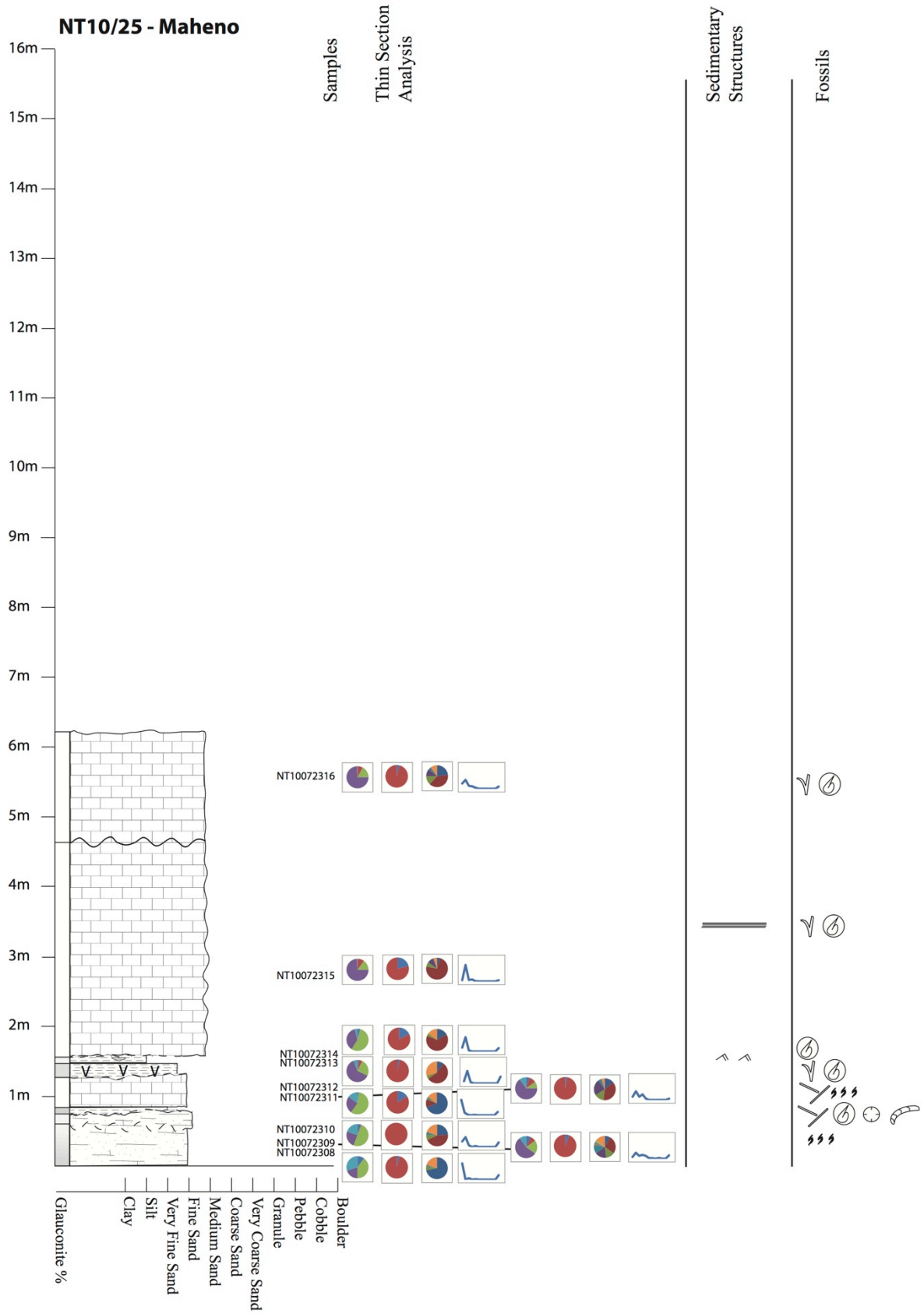
NT10/25 - Maheno
16m
15m
14m
13m
12m
11m
10m
9m
8m
7m
6m
5m
4m
3m
2m
1m
Samples
Thin Section Analysis
Sedimentary Structures
Fossils
NT10072316
NT10072315
NT10072314
NT10072313
NT10072312
NT10072311
NT10072310
NT10072309
NT10072308
Glauconite %
Clay
Silt
Very Fine Sand
Fine Sand
Medium Sand
Coarse Sand
Very Coarse Sand
Granule
Pebble
Cobble
Boulder

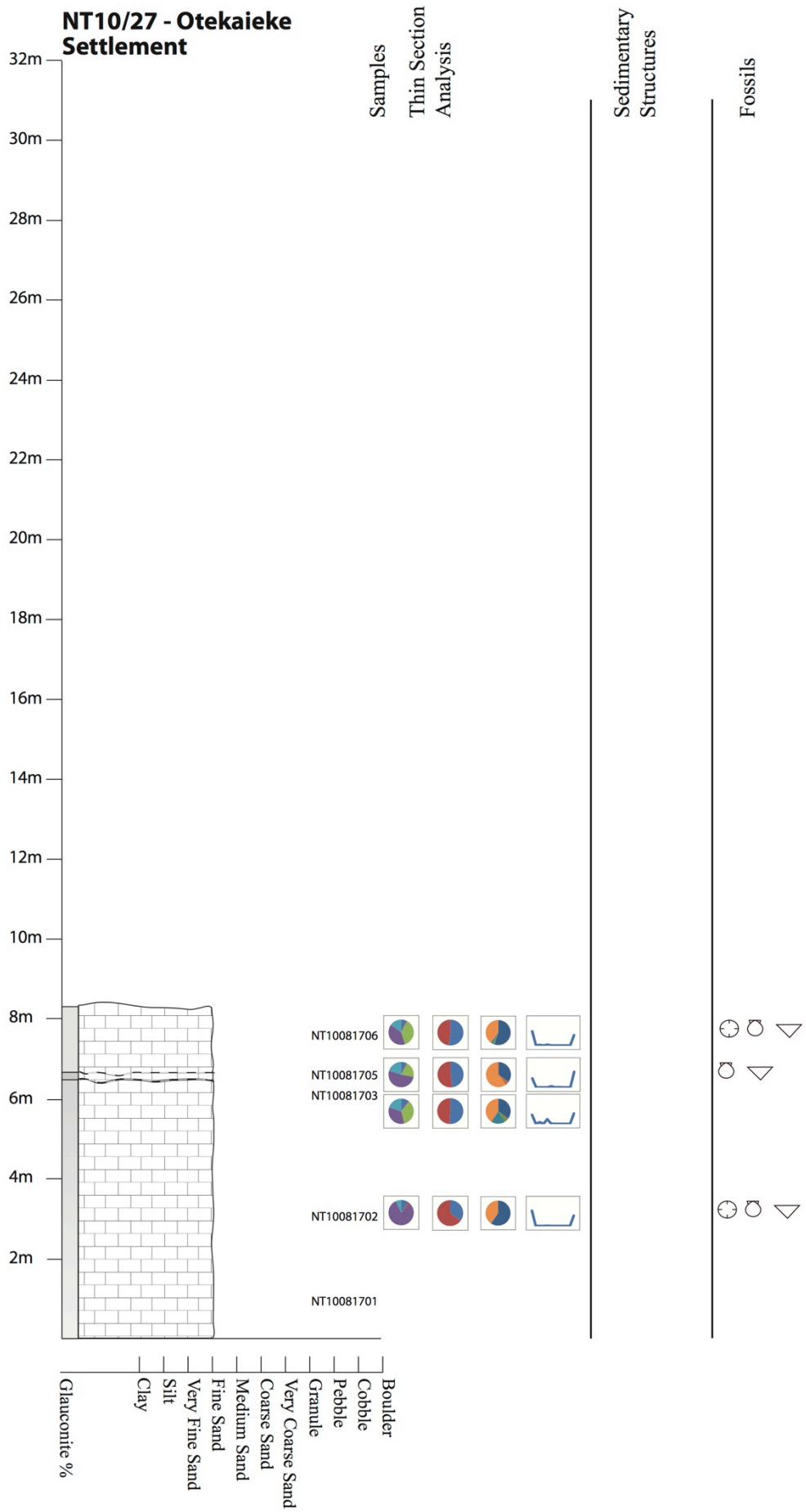
NT10/27 - Otekaieke Settlement
32m
30m
28m
26m
24m
22m
20m
18m
16m
14m
12m
10m
8m
6m
4m
2m
Samples
Thin Section Analysis
Sedimentary Structures
Fossils
NT10081706
NT10081705
NT10081703
NT10081702
NT10081701
Glauconite %
Clay
Silt
Very Fine Sand
Fine Sand
Medium Sand
Coarse Sand
Very Coarse Sand
Granule
Pebble
Cobble
Boulder

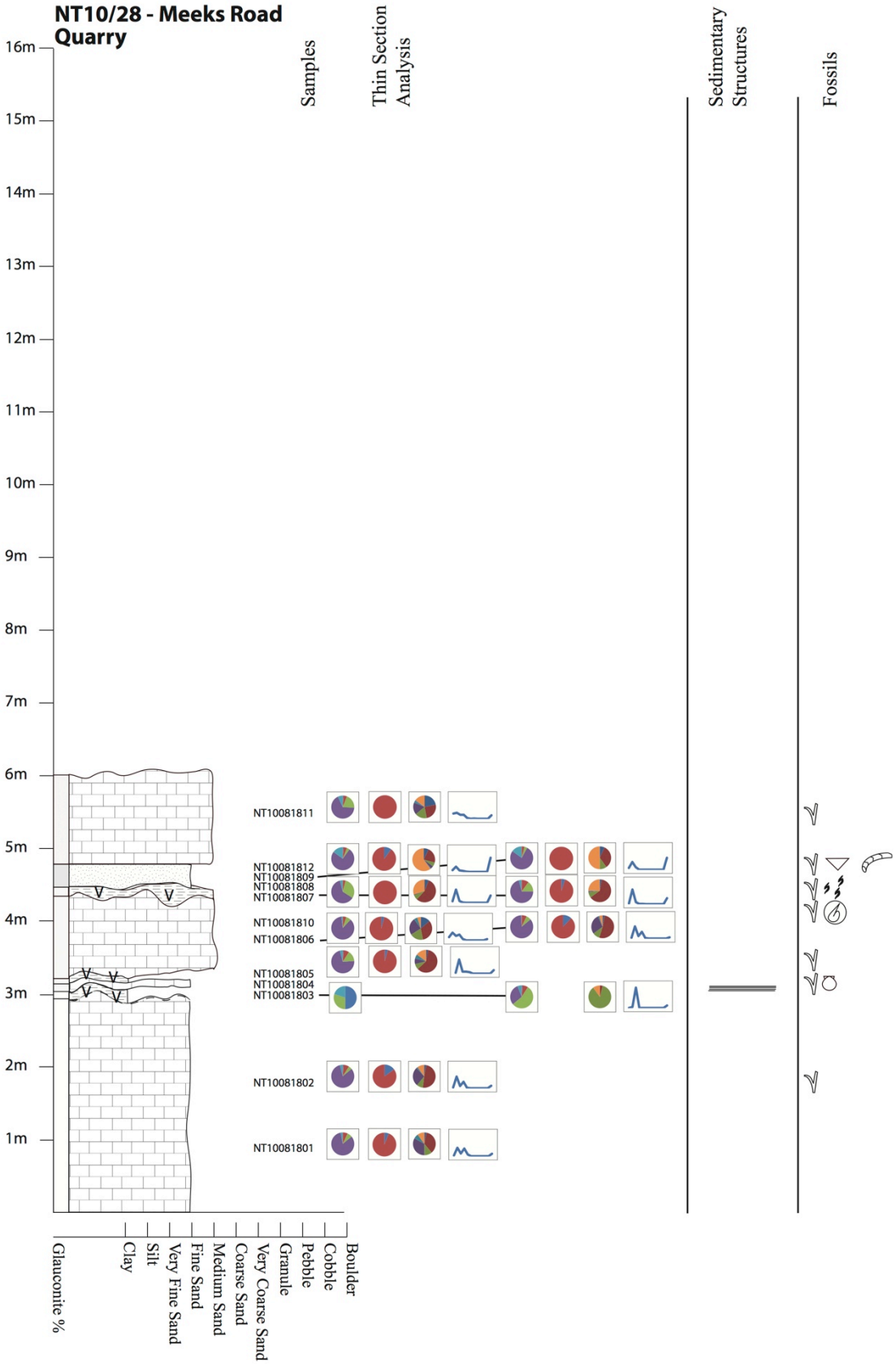
NT10/28 - Meeks Road Quarry
16m
15m
14m
13m
12m
11m
10m
9m
8m
7m
6m
5m
4m
3m
2m
1m
Samples
Thin Section Analysis
Sedimentary Structures
Fossils
NT10081811
NT10081812
NT10081809
NT10081808
NT10081807
NT10081810
NT10081806
NT10081805
NT10081804
NT10081803
NT10081802
NT10081801
Glauconite %
Clay
Silt
Very Fine Sand
Fine Sand
Medium Sand
Coarse Sand
Very Coarse Sand
Granule
Pebble
Cobble
Boulder

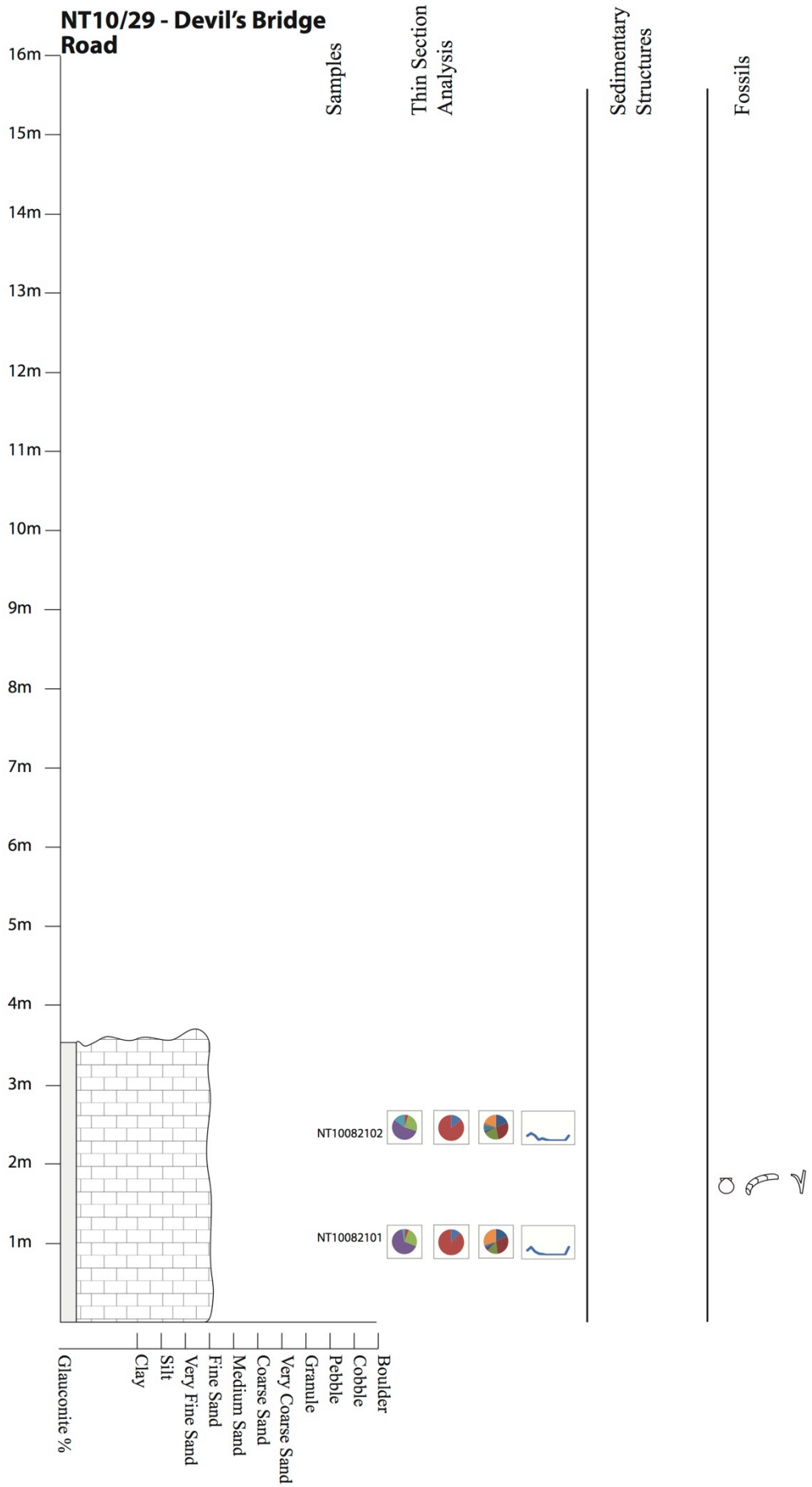
NT10/29 - Devil's Bridge Road
16m
15m
14m
13m
12m
11m
10m
9m
8m
7m
6m
5m
4m
3m
2m
1m
Samples
Thin Section Analysis
Sedimentary Structures
Fossils
NT10082102
NT10082101
Glauconite %
Clay
Silt
Very Fine Sand
Fine Sand
Medium Sand
Coarse Sand
Very Coarse Sand
Granule
Pebble
Cobble
Boulder

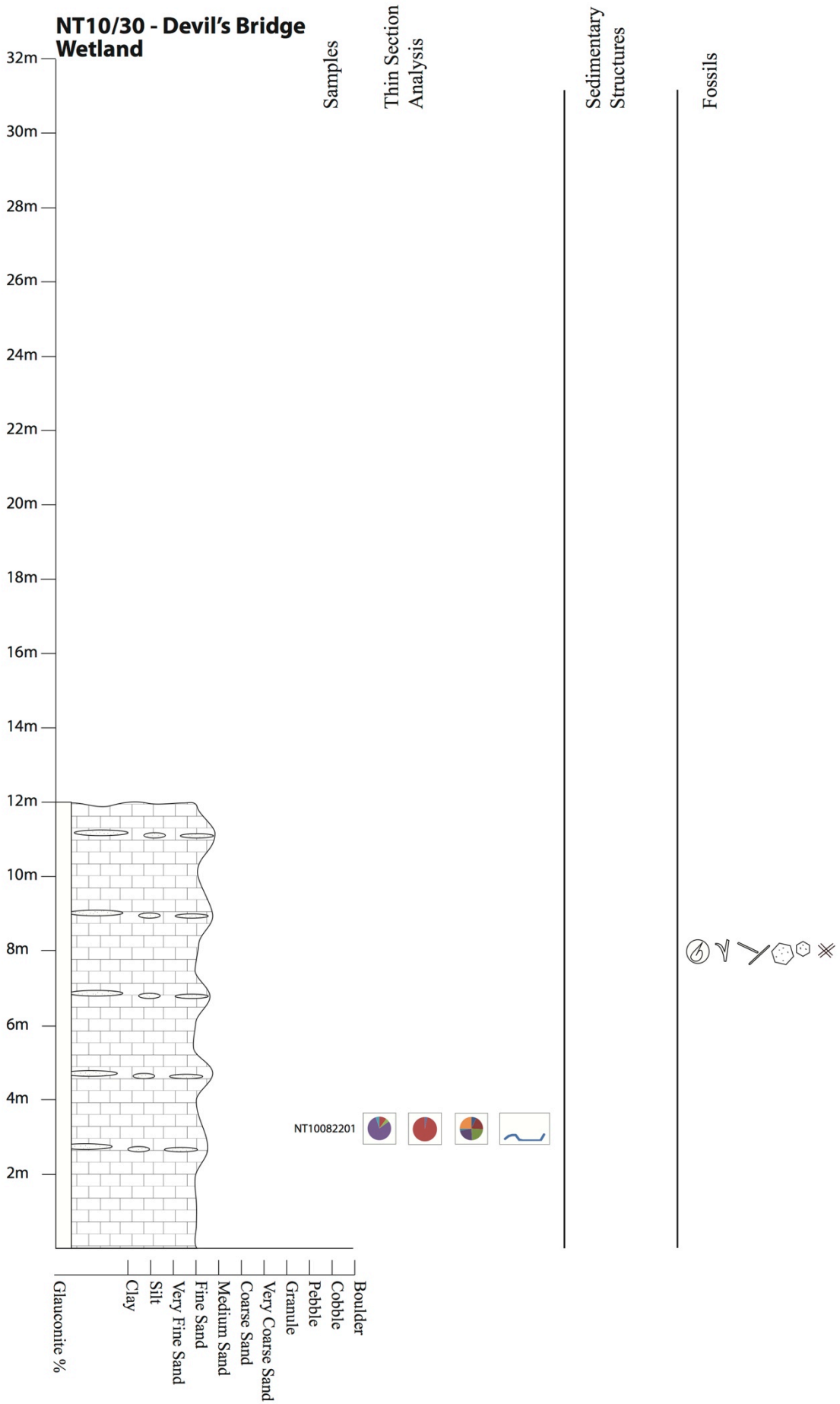
NT10/30 - Devil's Bridge Wetland
32m
30m
28m
26m
24m
22m
20m
18m
16m
14m
12m
10m
8m
6m
4m
2m
Samples
Thin Section Analysis
Sedimentary Structures
Fossils
NT10082201
Glauconite %
Clay
Silt
Very Fine Sand
Fine Sand
Medium Sand
Coarse Sand
Very Coarse Sand
Granule
Pebble
Cobble
Boulder

APPENDIX C – SAMPLE DATABASE

This appendix contains a list of all samples collected during the course of this study. Each sample is collated with the stratigraphic location from which it was collected (Appendices A and B), as well as the formation it derives from. A column is presented showing whether the sample was thin sectioned, as well as any notes on the sample that usually pertain to the resultant thin section.

Column ID	Sample ID	Formation	Thin Section	Notes
NT 09/01	NT09040401	Otekaike Limestone	Y	
	NT09040402	Otekaike Limestone	Y	Loose seds in resin
	NT09040403	Otekaike Limestone		
	NT09040404	Otekaike Limestone	Y	Loose seds in resin
	NT09040405	Otekaike Limestone	Y	
	NT09040501	Otekaike Limestone	Y	Loose seds in resin
	NT09040502	Otekaike Limestone	Y	Loose seds in resin
	NT09040503	Otekaike Limestone		
	NT09040504	Otekaike Limestone		
	NT09040505	Otekaike Limestone		
	NT09040506	Otekaike Limestone		
	NT09040507	Otekaike Limestone	Y	
	NT09040508	Otekaike Limestone	Y	Loose seds in resin
	NT09040510	Otekaike Limestone		
	NT09040511	Otekaike Limestone	Y	Loose seds in resin
	NT10061401	Otekaike Limestone	Y	
	NT10061402	Otekaike Limestone	Y	
	NT10061403	Otekaike Limestone	Y	Loose seds in resin
	NT10061404	Otekaike Limestone	Y	
	NT10061406	Otekaike Limestone		
	NT10061407	Otekaike Limestone		
	NT10061408	Otekaike Limestone	Y	
	NT10061410	Otekaike Limestone		
	NT10061411	Otekaike Limestone	Y	
	NT10061412	Otekaike Limestone	Y	
	NT10061413	Otekaike Limestone	Y	
NT 09/02	NT09040512	Otekaike Limestone	Y	
	NT09040513	Otekaike Limestone	Y	
	NT10061514	Otekaike Limestone	Y	
NT 09/03	NT09040514	Tapui Sandstone	Y	Loose seds in resin
	NT09040515	Tapui Sandstone	Y	Loose seds in resin
	NT09040516	Tapui Sandstone?	Y	Loose seds in resin

Column ID	Sample ID	Formation	Thin Section	Notes
	NT09040517	Ototara Limestone	Y	
	NT09040518	Kokoamu Greensand	Y	Loose seds in resin
NT 09/03	NT09040519	unknown		Shark tooth
	NT09040520	Kokoamu Greensand	Y	Loose seds in resin
	NT09040521	Otekaike Limestone	Y	
	NT09040601	Ototara Limestone	Y	
	NT09040602	Ototara Limestone	Y	
	NT09040603	Ototara Limestone	Y	
	NT09040604	Ototara Limestone	Y	Karst clast
NT 09/04	NT09040605	unknown		Sea-pen fossil
	NT09040606	Ototara Limestone	Y	Karst clast
	NT09040607	Kokoamu Greensand	Y	Loose seds in resin
	NT09040608	Otekaike Limestone	Y	
	NT09040609	Gee Greensand	Y	Loose seds in resin
	NT09040610	Tapui Sandstone?		Baked country rock
NT 09/05	NT09040611	Waiareka Volcanics		Outer dyke
	NT09040612	Waiareka Volcanics		Inner dyke
	NT09040801	Deborah Volcanics		
	NT09040802	unknown		Sea-pen fossil
	NT09040803	Deborah Volcanics		
	NT09040804	Ototara Limestone	Y	
	NT09040805	Deborah Volcanics	Y	Clast from cavity
	NT09040806	Ototara Limestone	Y	Shelly horizon
	NT09040807	Ototara/Kokoamu	Y	Two thin sections (A & B)
	NT09040808	Ototara/Kokoamu	Y	Two thin sections (L & G)
	NT09040809	Kokoamu Greensand	Y	Above phosphate layer
NT 09/06	NT09040810	Kokoamu Greensand		
	NT09040811	Gee Greensand	Y	
	NT09040812	Kokoamu Greensand?		Phosphate clast
	NT09040813	Gee Greensand		Mafic clast
	NT09040814	Kokoamu Greensand?		Phosphate coated clast
	NT09040815	Ototara Limestone	Y	Heavily cemented
	NT10061612	Ototara Limestone	Y	Phosphatic contact
	NT10061613	Gee Greensand	Y	Southern Bay
	NT10061614	Gee Greensand	Y	Southern Bay
	NT10061615	Ototara Limestone	Y	Southern bay
	NT10061616	Gee Greensand	Y	
	OT1	Ototara Limestone	Y	
	Gee1	Gee Greensand	Y	
	Gee2A	Gee Greensand	Y	Phosphate coated clasts

Column ID	Sample ID	Formation	Thin Section	Notes
NT 09/06	Gee3	Gee Greensand	Y	
	Gee4	Gee Greensand	Y	Phosphate coated clasts
NT 09/07	NT10061601	Ototara Limestone		Encrusting bryozoan
	NT10061602	Waiareka Volcanics		
	NT10061603	Waiareka Volcanics	Y	
	NT10061604	Waiareka Volcanics		Loose seds in resin
	NT10061605	Waiareka Volcanics	Y	
	NT10061606	Waiareka Volcanics	Y	Tuff
	NT10061607	Waiareka Volcanics		
	NT10061608	Waiareka Volcanics	Y	Loose seds in resin
	NT10061609	Ototara Limestone	Y	
	NT10061610	Ototara Limestone	Y	
NT 09/08	NT09060901	Otekaike Limestone	Y	
NT 09/09	NT09060902	Otekaike Limestone	Y	Cemented bed
	NT09060903	Otekaike Limestone	Y	Cemented bed
	NT09060904	Otekaike Limestone	Y	
NT 09/10	NT09060905	Otekaike Limestone	Y	Nodule
	NT10061514A	Otekaike Limestone	Y	
	NT10061515	Otekaike Limestone	Y	Two slides
	NT10061516	Otekaike Limestone	Y	
NT 09/11	NT09061001	Otago Schist		
	NT09061002	Taratu Formation		
	NT09061003	Taratu Formation		
	NT09061004	Tapui Sandstone?		
	NT09061005	Tapui Sandstone?	Y	Loose seds in resin
	NT09061006	Tapui Sandstone?		
	NT09061007	Tapui Sandstone?		
	NT09061008	Tapui Sandstone?	Y	Loose seds in resin
NT 09/12	NT09061009	Tapui Sandstone?		
	NT09061010	Tapui Sandstone?		
	NT09061011	Tapui Sandstone?	Y	Loose seds in resin
NT 09/13	NT09061012	Tapui Sandstone?		
	NT09061013	Tapui Sandstone?		Conglomerate
	NT09061014	Tapui Sandstone?		
	NT09061015	Tapui Sandstone?	Y	Loose seds in resin
NT 09/14	NT09061201	Otekaike Limestone	Y	
	NT09061202	Otekaike Limestone		Fossils
	NT09061203	Otekaike Limestone		Sea-pen fossil
	NT09061204	Otekaike Limestone		Fossils
	NT09061205	Otekaike Limestone	Y	Fossils above shell bed
	NT09061206	Otekaike Limestone	Y	

Column ID	Sample ID	Formation	Thin Section	Notes
	NT09061207	Otekaike Limestone	Y	
	NT10012201	unknown	Y	Loose seds in resin
	NT10012202	unknown	Y	
	NT10012203	unknown	Y	
	NT10012204	Otekaike Limestone		Sample from ground
	NT10012205	Otekaike Limestone		
	NT10012206	unknown		Greensand from cave
	NT10012207	Otekaike Limestone	Y	
NT 09/14	NT10061501	Otekaike Limestone	Y	Loose seds in resin
	NT10061502	unknown		
	NT10061503	Otekaike Limestone	Y	Loose seds in resin
	NT10061504	Otekaike Limestone	Y	Loose seds in resin
	NT10061505	Otekaike Limestone	Y	Loose seds in resin
	NT10061506	Otekaike Limestone	Y	Loose seds in resin
	NT10061507	Otekaike Limestone	Y	
	NT10061508	Otekaike Limestone	Y	
	NT10061509	Otekaike Limestone	Y	
	NT10061510	Otekaike Limestone		Fossils
	NT10061511	Otekaike Limestone		Above shell bed
	NT10061512	Otekaike Limestone		Above shell bed
	NT10061513	Otekaike Limestone		Fossils above shell bed
	NT10011801	Deborah Volcanics		Scoria xenoliths
	NT10011802	Deborah Volcanics		
	NT10011803	Deborah Volcanics		Xenoliths
	NT10011804	Deborah Volcanics		Xenoliths
	NT10011805	Deborah Volcanics		
	NT10011806	Deborah Volcanics		
	NT10011807	Deborah Volcanics		
	NT10011808	Deborah Volcanics		Large crystal
	NT10011901	Deborah Volcanics		Megacrysts
NT 10/02	NT10011902	Deborah Volcanics		Megacrysts
	NT10011903	Deborah Volcanics		Megacrysts
	NT10011904	Deborah Volcanics		
	NT10011905	Deborah Volcanics		Megacrysts
	NT10011906	Deborah Volcanics		Megacrysts
	NT10011907	Deborah Volcanics		
	NT10011908	Deborah Volcanics		
	NT10011909	Deborah Volcanics		Tuff
	NT10011910	Deborah Volcanics		Tuff
	NT10011911	Deborah Volcanics		Tuff
	NT10012001	Deborah Volcanics		Zeolite tuff

Column ID	Sample ID	Formation	Thin Section	Notes
NT 10/02	NT10012002	Deborah Volcanics		Weathered tuff
	NT10012003	Deborah Volcanics		Tuff
	NT10012004	Deborah Volcanics		Tuff
	NT10012005	Deborah Volcanics		Tuff
	NT10012006	Ototara Limestone		Tuffaceous limestone
	NT10012007	Ototara Limestone	Y	
	NT10012008	Ototara Limestone	Y	
	NT10012009	Ototara/Kokoamu	Y	Karst contact
	NT10012010	Kokoamu Greensand		Phosphate clast
	NT10012011	Otekaike Limestone	Y	
	NT10012012	Gee Greensand	Y	Loose seds in resin
NT 10/03	NT10011912	Deborah Volcanics		Xenoliths
	NT10011913	Deborah Volcanics	Y	Weathered tuff
	NT10011914	Deborah Volcanics		Platey mineral
	NT10011915	Deborah Volcanics	Y	
	NT10011916	Ototara Limestone		
	NT10011917	Ototara Limestone	Y	
NT 10/04	NT10012013	Deborah Volcanics		
	NT10012014	Ototara Limestone	Y	
	NT10012015	Ototara Limestone	Y	
	NT10012016	Ototara Limestone	Y	Loose seds in resin
	NT10012017	Ototara Limestone	Y	Rhodoliths
	NT10012018	Gee Greensand	Y	Brachiopod-rich
	NT10012019	Gee Greensand	Y	
	NT10012021	Gee Greensand		
NT 10/05	NT10012101	Waiareka Volcanics		Pillow lava
	NT10012102	Waiareka Volcanics		Pillow lava
NT 10/06	NT10012103	Raki Siltstone	Y	
	NT10012104	Kokoamu Greensand	Y	Loose seds in resin
	NT10012105	Otekaike Limestone	Y	
	NT10012106	Otekaike Limestone	Y	
	NT10012107	Otekaike Limestone	Y	
NT 10/07	NT10012601	Otekaike Limestone	Y	
	NT10012602	Otekaike Limestone	Y	Loose seds in resin
NT 10/08	NT10012603	Tapui Sandstone?	Y	Loose seds in resin
	NT10012604	Tapui Sandstone?		
	NT10012605	Tapui Sandstone?		
	NT10012606	Waiareka Volcanics		Columnar basalt
NT 10/09	NT10012607	Otekaike Limestone	Y	
NT 10/13	NT10061611	Ototara Limestone	Y	
NT 10/14	NT10061702	Otekaike Limestone	Y	

Column ID	Sample ID	Formation	Thin Section	Notes
	NT10061703	Otekaike Limestone		
	NT10061704	Otekaike Limestone	Y	
	NT10061705	Otekaike Limestone		
	NT10061706	Otekaike Limestone	Y	
	NT10061707	Otekaike Limestone	Y	
	NT10061708	Kokoamu Greensand	Y	Loose seds in resin
	NT10061709	Otekaike Limestone	Y	
NT 10/14	NT10061710	Otekaike Limestone	Y	
	NT10061711	Otekaike Limestone	Y	
	NT10061712	Otekaike Limestone	Y	
	NT10061713	Otekaike Limestone	Y	
	NT10061714	Otekaike Limestone		
	NT10061715	Otekaike Limestone		Brachiopods
	NT10061716	Otekaike Limestone		Brachiopods
	NT10061717	Otekaike Limestone		Brachiopods
	NT10061801	Ototara Limestone		Rhodoliths
	NT10061802	Ototara Limestone	Y	Heavy cement
	NT10061803	Ototara Limestone	Y	Chalk/clay
NT 10/15	NT10061804	Ototara Limestone	Y	Heavy cement
	NT10061805	Ototara Limestone	Y	Rhodoliths
	NT10061806	Deborah Volcanics	Y	Tuff lapilli
	NT10061807	Deborah Volcanics		
	NT10061808	Raki Siltstone?	Y	Bioturbated silt
	NT10061809	Oamaru Diatomite	Y	Loose seds in resin
NT 10/16	NT10061810	Oamaru Diatomite	Y	
	NT10061811	Ototara Limestone?	Y	Tuffaceous packstone
	NT10061812	Ototara Limestone?	Y	Tuffaceous packstone
	NT10061813	Oamaru Diatomite	Y	
NT 10/17	NT10061814	Oamaru Diatomite?		
	NT10061815	Waiareka Volcanics?	Y	
	NT10061816	Waiareka Volcanics?	Y	
	NT10071301	Waiareka Volcanics	Y	Loose seds in resin
NT 10/18	NT10071302	Waiareka Volcanics	Y	
	NT10071303	Waiareka Volcanics		Tuff
	NT10071401	Ototara Limestone	Y	Loose seds in resin
	NT10071402	Ototara Limestone	Y	
	NT10071403	Ototara Limestone	Y	
NT 10/19	NT10071404	Ototara Limestone	Y	Loose seds in resin
	NT10071405	Ototara Limestone	Y	
	NT10071406	Ototara Limestone	Y	Loose seds in resin
	NT10071407	Ototara Limestone	Y	Loose seds in resin

Column ID	Sample ID	Formation	Thin Section	Notes
NT 10/19	NT10071408	Deborah Volcanics?	Y	Loose seds in resin
	NT10071409	Deborah Volcanics	Y	Tuff lamina
	NT10071410	Ototara Limestone	Y	Mafic fragments
	NT10071411	Ototara Limestone	Y	Soft
NT 10/20	NT10071501	Ototara Limestone	Y	
	NT10071502	Ototara Limestone	Y	
	NT10071503	Ototara Limestone	Y	
	NT10071504	Ototara Limestone	Y	
	NT10071505	Ototara Limestone	Y	
	NT10071506	Ototara Limestone		Crystal clast
	NT10071507	Ototara Limestone	Y	
	NT10071508	Ototara Limestone	Y	Loose seds in resin
	NT10071509	Ototara Limestone?	Y	
NT 10/21	NT10071901	Ototara Limestone	Y	
	NT10071902	Ototara Limestone	Y	
	NT10071903	Kokoamu Greensand		Fossil fragments
	NT10071904	Kokoamu Greensand	Y	Loose seds in resin
	NT10071905	Kokoamu Greensand		
	NT10071906	Kokoamu Greensand	Y	Loose seds in resin
	NT10071907	Otekaike Limestone	Y	Two thin sections
	NT10071908	Otekaike Limestone		Lentipecten
	NT10071909	Otekaike Limestone?		
	NT10071910	Otekaike Limestone	Y	
	NT10071911	Gee Greensand	Y	Loose seds in resin
	NT10071912	Gee Greensand	Y	Loose seds in resin
	NT12070501	Otekaike Limestone	Y	Below firmground
	NT12070502	Otekaike Limestone	Y	Above firmground
	NT12070503	Otekaike Limestone	Y	Above firmground
	NT12070504	Kokoamu/Otekaike	Y	Above firmground
NT 10/22	NT10072101	Raki Siltstone	Y	Loose seds in resin
	NT10072102	Raki Siltstone	Y	
	NT10072103	Otekaike Limestone?	Y	Slab fallen off contact
	NT10072104	Otekaike Limestone	Y	
	NT10072105	Otekaike Limestone	Y	
	NT10072106	Otekaike Limestone	Y	
	NT10072107	Otekaike Limestone	Y	
	NT10072108	Otekaike Limestone	Y	
NT 10/23	NT10072109	Otekaike Limestone	Y	Fossils
	NT10072110	Otekaike Limestone	Y	
	NT10072111	Otekaike Limestone	Y	
	NT10072112	Otekaike Limestone	Y	

Column ID	Sample ID	Formation	Thin Section	Notes
NT 10/24	NT10072301	Deborah Volcanics		
	NT10072302	Deborah Volcanics	Y	Loose seds in resin
	NT10072303	Deborah Volcanics	Y	Loose seds in resin
	NT10072304	Ototara Limestone	Y	
	NT10072305	Ototara Limestone	Y	Loose seds in resin
	NT10072306	Ototara Limestone	Y	
	NT10072307	Ototara Limestone	Y	
NT 10/25	NT10072308	Ototara Limestone	Y	
	NT10072309	Ototara Limestone	Y	
	NT10072310	Ototara Limestone	Y	Loose seds in resin
	NT10072311	Ototara Limestone	Y	
	NT10072312	Ototara Limestone	Y	Loose seds in resin
	NT10072313	Ototara Limestone	Y	Loose seds in resin
	NT10072314	Ototara Limestone	Y	Loose seds in resin
	NT10072315	Ototara Limestone	Y	
	NT10072316	Ototara Limestone	Y	
NT 10/27	NT10081701	Otekaike Limestone		
	NT10081702	Otekaike Limestone	Y	Loose seds in resin
	NT10081703	Otekaike Limestone	Y	Loose seds in resin
	NT10081705	Otekaike Limestone	Y	Loose seds in resin
	NT10081706	Otekaike Limestone	Y	
NT 10/28	NT10081801	Ototara Limestone	Y	
	NT10081802	Ototara Limestone	Y	
	NT10081803	Deborah Volcanics?	Y	Loose seds in resin
	NT10081804	Deborah Volcanics?	Y	Loose seds in resin
	NT10081805	Ototara Limestone	Y	
	NT10081806	Ototara Limestone	Y	
	NT10081807	Ototara Limestone	Y	Loose seds in resin
	NT10081808	Ototara Limestone	Y	Loose seds in resin
	NT10081809	Ototara Limestone	Y	Loose seds in resin
	NT10081810	Ototara Limestone	Y	
	NT10081811	Ototara Limestone	Y	Bioturbation infill
	NT10081812	Ototara Limestone	Y	Loose seds in resin
NT 10/29	NT10082101	Ototara Limestone	Y	
	NT10082102	Ototara Limestone	Y	
NT 10/30	NT10082201	Ototara Limestone	Y	Cemented bed

APPENDIX D – SAMPLE PETROGRAPHIC DATABASE

This appendix presents petrographic descriptions from all samples thin sectioned during this study (Appendix C), presented in order of their stratigraphic location (Appendix A). Some samples contain additional hand specimen descriptions. Descriptions are divided into five main components:

- Clastics
- Cements
- Mud
- Bioclasts
- Authigenics

Where applicable the authigenic and clastic components have been further subdivided within this section.

The bioclasts have been identified by type where possible, with their percentage provided as a fraction of both the sample's bioclastic composition, as well as a percentage of those identified within the sample (i.e. excluding the unidentified bioclast component). A count (including absolute numbers) of both planktic and benthic foraminiferal tests is also provided, with a percentage ratio presented.

Lastly, notes on various features identified in the thin section are also presented here.

Stratigraphic Column:	NT09/01		
Sample Number:	NT09040401	**Location:**	Waihao
Date Collected:	4/4/09	**Formation:**	Otekaike Lst

Hand Specimen Description

Colour	**Induration**	**Bedding and Sedimentary Structures**		**Grainsize**
Whitish-Green	Friable			Fine
Grain or matrix supported	**Sorting**	**Roundness**	**Sphericity - shape**	**Biologic binding**
Grain	Well			No
Textural Name:	**Packstone**	**Notes:**	Trace fossils (burrowing - burrows are less glauconitic and white), glauconite (40%), mud pods	

Thin Section Description

Matrix	**Percentage /100**
Clastics: Quartz, biotite	2%
Cement	35%
Mud	1%
Bioclasts	37%
Authigenic minerals: Glauconite	25%

Foraminifera	**Percentage /100**
Planktic	15% (n=16)
Benthic	85% (n=88)

Bioclasts	**Percentage of identified/total**
Foraminifera	44%/20%
Bryozoans	0%/0%
Echinoderms	33%/15%
Algae	0%/0%
Molluscs	22%/10%
Brachiopods	0%/0%
Barnacles	0%/0%
Sponge spicules	0%/0%
Worm Tubes	0%/0%
Unidentified bioclasts	55%

Notes from thin section:	Glauconite is oxidised in some grains. Vast majority of benthic forams are hyaline. Echinoids commonly have calcite overgrows formed in optical continuity. Few pteropods(?). Molluscs appear to be mostly bivalves, with some gastropod fragments. Few are any larger than the biggest forams.

Stratigraphic Column:	NT09/01		
Sample Number:	NT09040402	**Location:**	Waihao
Date Collected:	4/4/09	**Formation:**	Otekaike Lst

Hand Specimen Description

Colour	Induration	Bedding and Sedimentary Structures		Grainsize
Yellowish-cream	Friable			Fine
Grain or matrix supported	**Sorting**	**Roundness**	**Sphericity - shape**	**Biologic binding**
Grain	Well			No
Textural Name:	**Packstone**	**Notes:**		

Thin Section Description

Matrix	Percentage /100
Clastics: Quartz (angular - sub-rounded), some minor biotite.	3%
Cement	4%
Mud	15%
Bioclasts	53%
Authigenic minerals: Glauconite (90%), hematite (10%)	25%

Foraminifera	Percentage /100
Planktic	27% (n=35)
Benthic	73% (n=95)

Bioclasts	Percentage of identified/total
Foraminifera	55%/17%
Bryozoans	0%/0%
Echinoderms	44%/13%
Algae	0%/0%
Molluscs	0%/0%
Brachiopods	0%/0%
Barnacles	0%/0%
Sponge spicules	1%/<1%
Worm Tubes	0%/0%
Unidentified bioclasts	70%

Notes from thin section:	Loose sediments in resin. Blocky calcite cement observed around echinoid fragments, although may be underestimated due to nature of slide and lack of matrix. Rounded glauconite grains, with some glauconitised biotites. Minor hematite alteration of matrix and within foram tests. Benthics are coiled (planar, trochospiral), uniserial, and biserial. Tests are microcrystalline with some hyalines. Shell fragments, forming part of the unidentified bioclasts, show signs of boring.

Stratigraphic Column:	NT09/01		
Sample Number:	NT09040404	**Location:**	Waihao Downs
Date Collected:	4/4/2009	**Formation:**	Otekaike Lst

Hand Specimen Description

Colour	**Induration**	**Bedding and Sedimentary Structures**		**Grainsize**
Brownish-green	Friable			Fine
Grain or matrix supported	**Sorting**	**Roundness**	**Sphericity - shape**	**Biologic binding**
Matrix	Well			No
Textural Name:	**Wackestone**	**Notes:**		

Thin Section Description

Matrix	**Percentage /100**
Clastics: Quartz (sub-rounded - sub-angular)	3%
Cement	Trace
Mud	15%
Bioclasts	32%
Authigenic minerals: Glauconite	50%

Foraminifera	**Percentage /100**
Planktic	15% (n=9)
Benthic	85% (n=51)

Bioclasts	**Percentage of identified/total**
Foraminifera	59%/29%
Bryozoans	0%/0%
Echinoderms	40%/20%
Algae	0%/0%
Molluscs	1%/1%
Brachiopods	0%/0%
Barnacles	0%/0%
Sponge spicules	0%/0%
Worm Tubes	0%/0%
Unidentified bioclasts	50%

Notes from thin section:	Loose sediment in resin. Almost no matrix preserved in this slide. Some very minor spar observed still attached to a couple of echinoid fragments as overgrowth. Micrite estimate taken from the more intact sediment portions as assumed to be representative. Glauconite grains are rounded to sub-rounded. Estimate for glauconite grains may be slightly high due to its ability to remain in the slide as loose sediment. Some intraclast growth, but only in small amounts. Some glauconitised biotites. Benthics are coiled (planar, trochospiral), biserial, and uniserial. One possible milliolid? Tests are mostly microcrystalline with a few hyalines. One possible quartz agglutinate benthic test. Shell fragments show some boring. Most unidentified bioclastics are shell fragments. It is possible that the benthics are overrepresented with respect to the planktics as they are more robust and may have preserved better in a slide of this nature.

Stratigraphic Column:	NT09/01		
Sample Number:	NT09040405	**Location:**	Waihao Downs
Date Collected:	4/4/2009	**Formation:**	Otekaike Lst

Hand Specimen Description

Colour	**Induration**	**Bedding and Sedimentary Structures**		**Grainsize**
Green to white	Friable			Fine
Grain or matrix supported	**Sorting**	**Roundness**	**Sphericity - shape**	**Biologic binding**
Grain	Moderate			No
Textural Name:	**Grainstone**	**Notes:**	Normal grading from high to low glauconite.	

Thin Section Description

Matrix	**Percentage /100**
Clastics: Quartz, biotite	3%
Cement	25%
Mud	0%
Bioclasts	57%
Authigenic minerals: Glauconite	15%

Foraminifera	**Percentage /100**
Planktic	76% (n=69)
Benthic	24% (n=22)

Bioclasts	**Percentage of identified/total**
Foraminifera	57%/20%
Bryozoans	<1%/<1%
Echinoderms	14%/5%
Algae	0%/0%
Molluscs	29%/10%
Brachiopods	0%/0%
Barnacles	0%/0%
Sponge spicules	0%/0%
Worm Tubes	0%/0%
Unidentified bioclasts	65%

Notes from thin section:	Glauconite grains appear in bands throughout the section, ranging from 2% to 35%, some showing iron staining. Quartz clasts range also between 1-5%, and follow the same pattern as the glauconite. Single bryozoan has glauconite within its pores. Red iron secondary mineralisation in bands and isolated clasts of unidentified material, and appears porous.

Stratigraphic Column:	NT09/01		
Sample Number:	NT09040501	**Location:**	Waihao Downs
Date Collected:	4/5/2009	**Formation:**	Otekaike Lst

Hand Specimen Description

Colour	**Induration**	**Bedding and Sedimentary Structures**		**Grainsize**
Brownish-green	Unconsolidated			Fine to medium
Grain or matrix supported	**Sorting**	**Roundness**	**Sphericity - shape**	**Biologic binding**
Grain	Moderate			No
Textural Name:	**Packstone**	**Notes:**		

Thin Section Description

Matrix	**Percentage /100**
Clastics:	5%
Cement	3%
Mud	7%
Bioclasts	45%
Authigenic minerals:	40%

Foraminifera	**Percentage /100**
Planktic	38% (n=44)
Benthic	62% (n=72)

Bioclasts	**Percentage of identified/total**
Foraminifera	50%/20%
Bryozoans	0%/0%
Echinoderms	50%/20%
Algae	0%/0%
Molluscs	0%/0%
Brachiopods	0%/0%
Barnacles	0%/0%
Sponge spicules	0%/0%
Worm Tubes	0%/0%
Unidentified bioclasts	60%

Notes from thin section:	Loose sediments in resin. Calcite cement is seen as minor overgrowth around echinoid fragments, although the values given here are a minimum due to the nature of this slide. Mud values are estimated from small sediment clumps but are averaged for the slide, making this a minimum value also. Glauconite is mostly rounded grains with some intraclast growth. Minor hematite alteration in some clasts around the intraclast glauconite. Small rounded phosphate grains rare. Benthics are coiled (planar, trochospiral), with some uniserials. Planar coiled are the dominant morphology. Tests are predominantly microcrystalline, with a few hyalines. Unidentified bioclasts are lots of broken shell fragments that are too small to identify.

Stratigraphic Column:	NT09/01		
Sample Number:	NT09040502	**Location:**	Waihao Downs
Date Collected:	4/5/2009	**Formation:**	Otekaike Lst

Hand Specimen Description

Colour	**Induration**	**Bedding and Sedimentary Structures**		**Grainsize**
Yellowish-white and green	Indurated			Very fine to fine
Grain or matrix supported	**Sorting**	**Roundness**	**Sphericity - shape**	**Biologic binding**
Matrix	Moderate			No
Textural Name:	**Wackestone**	**Notes:**		

Thin Section Description

Matrix	**Percentage /100**
Clastics: Quartz (angular - sub-angular), minor biotite	3%
Cement	15%
Mud	15%
Bioclasts	47%
Authigenic minerals: Glauconite	20%

Foraminifera	**Percentage /100**
Planktic	57% (n=45)
Benthic	43% (n=34)

Bioclasts	**Percentage of identified/total**
Foraminifera	28%/17%
Bryozoans	2%/1%
Echinoderms	50%/30%
Algae	0%/0%
Molluscs	20%/12%
Brachiopods	0%/0%
Barnacles	0%/0%
Sponge spicules	0%/0%
Worm Tubes	0%/0%
Unidentified bioclasts	40%

Notes from thin section:	Loose sediments in resin. Blocky sparry calcite cement both around and within clasts. Glauconite grains are rounded to sub-rounded. Some glauconitised biotites. Benthics are coiled (planar, trochospiral), biserial, and uniserial. Tests are mostly microcrystalline with some hyalines. Shells show heavy boring.

Stratigraphic Column:	NT09/01		
Sample Number:	NT09040507	**Location:**	Waihao Downs
Date Collected:	5/4/2009	**Formation:**	Otekaike Lst

Hand Specimen Description

Colour	**Induration**	**Bedding and Sedimentary Structures**		**Grainsize**
Greenish-grey	Friable			Fine
Grain or matrix supported	**Sorting**	**Roundness**	**Sphericity - shape**	**Biologic binding**
Grain	Well			No
Textural Name: **Packstone**		**Notes:**		

Thin Section Description

Matrix	**Percentage /100**
Clastics: Quartz (95%), biotite, plagioclase feldspar, amphibole, isotropics	20%
Cement	10%
Mud	30%
Bioclasts	25%
Authigenic minerals: Glauconite	15%

Foraminifera	**Percentage /100**
Planktic	16% (n=26)
Benthic	84% (n=139)

Bioclasts	**Percentage of identified/total**
Foraminifera	94%/75%
Bryozoans	0%/0%
Echinoderms	1%/1%
Algae	0%/0%
Molluscs	5%/2%
Brachiopods	0%/0%
Barnacles	0%/0%
Sponge spicules	0%/0%
Worm Tubes	0%/0%
Unidentified bioclasts	22%

Notes from thin section:	Quartz clasts are sub-angular to angular and most appear to have a rim of calcite cement. Quartz is the vast majority of clasts, with only very minor contributions from the other minerals listed. Very equigranular. Foram tests are mixed with muds, and some a broken. Molluscs are few and broken, with majority being bivalves with only one observed mostly intact gastropod.

Stratigraphic Column:	NT09/01		
Sample Number:	NT09040508	**Location:**	Waihao Downs
Date Collected:	4/5/2009	**Formation:**	Otekaike Lst

Hand Specimen Description

Colour	**Induration**	**Bedding and Sedimentary Structures**		**Grainsize**
Brownish-green	Unconsolidated			Fine to medium
Grain or matrix supported	**Sorting**	**Roundness**	**Sphericity - shape**	**Biologic binding**
Grain	Moderate			No
Textural Name:	**Packstone**	**Notes:**		

Thin Section Description

Matrix	**Percentage /100**
Clastics: Quartz (angular - sub-rounded)	4%
Cement	2%
Mud	2%
Bioclasts	32%
Authigenic minerals: Glauconite (94%), phosphate (6%)	60%

Foraminifera	**Percentage /100**
Planktic	24% (n=40)
Benthic	76% (n=126)

Bioclasts	**Percentage of identified/total**
Foraminifera	76%/45%
Bryozoans	1%/1%
Echinoderms	20%/12%
Algae	0%/0%
Molluscs	3%/2%
Brachiopods	0%/0%
Barnacles	0%/0%
Sponge spicules	0%/0%
Worm Tubes	0%/0%
Unidentified bioclasts	40%

Notes from thin section:	Loose sediment in resin. Calcite blocky overgrowths on echinoid fragments. Matrix estimates are minimums due to the nature of the slide. Glauconite is very abundant, and present mostly as rounded grains with some small amounts of intraclast formation. Rounded phosphate grains present also. Benthics are coiled (planar, trochospiral), biserial, and uniserial. Tests are mostly microcrystalline with some hyalines, including a few large hyaline tests. Few large quartz agglutinates observed. Molluscs are heavily bored and fragmented. Unidentifed bioclasts appear to be small bored shell fragments.

Stratigraphic Column: NT09/01

Sample Number: NT09040511 **Location:** Waihao Downs

Date Collected: 4/5/2009 **Formation:** Otekaike Lst

Thin Section Description

Matrix	Percentage /100
Clastics: Quartz (angular - sub-angular) (98%), biotite (2%)	20%
Cement	7%
Mud	15%
Bioclasts	33%
Authigenic minerals: Glauconite (95%), hematite (5%)	25%

Foraminifera	Percentage /100
Planktic	41% (n=67)
Benthic	59% (n=94)

Bioclasts	Percentage of identified/total
Foraminifera	88%/70%
Bryozoans	0%/0%
Echinoderms	5%/4%
Algae	0%/0%
Molluscs	7%/6%
Brachiopods	0%/0%
Barnacles	0%/0%
Sponge spicules	0%/0%
Worm Tubes	0%/0%
Unidentified bioclasts	20%

Notes from thin section:	Loose sediment in resin. Calcite cement is blocky within some bioclasts as well as forming bioclast overgrowth. Glauconite grains are rounded to sub-angular, with both mature and fresh glauconite. Hematite formed within some bioclasts. Benthics are trochospirally and planar coiled, uniserial, with most appearing to be broken and microcrystalline.

Stratigraphic Column:	NT09/01		
Sample Number:	NT10061401	**Location:**	Waihao
Date Collected:	6/14/2010	**Formation:**	Otekaike Lst

Hand Specimen Description

Colour	**Induration**	**Bedding and Sedimentary Structures**		**Grainsize**
Greenish-yellowish-white	Very well indurated			Fine
Grain or matrix supported	**Sorting**	**Roundness**	**Sphericity - shape**	**Biologic binding**
Grain	Well			No
Textural Name:	**Packstone**	**Notes:**	Cemented	

Thin Section Description

Matrix	**Percentage /100**
Clastics: Quartz (angular-subrounded)	2%
Cement	36%
Mud	23%
Bioclasts	34%
Authigenic minerals: Glauconite (85%), hematite (14%), phosphate (1%)	5%

Foraminifera	**Percentage /100**
Planktic	43% (n=68)
Benthic	57% (n=92)

Bioclasts	**Percentage of identified/total**
Foraminifera	85%/40%
Bryozoans	0%/0%
Echinoderms	10%/5%
Algae	0%/0%
Molluscs	5%/2%
Brachiopods	0%/0%
Barnacles	0%/0%
Sponge spicules	0%/0%
Worm Tubes	0%/0%
Unidentified bioclasts	53%

Notes from thin section:	Poor quality slide. Glauconite grains very from 1%-10% as they are found in zones of concentration. Mottly interior in xpl, with some showing some hematite alteration. Most benthics are micritic, with some hyaline calcitic and at least one observed agglutinate. One encrusting benthic on mollusc fragment. Some benthics as well as planktics have their chambers hematite/glauconite or micrite filled, while others are spar filled. Benthics are uniserial, coil, rotalid, and biserial, with some minor encrusting.

Stratigraphic Column:	NT09/01		
Sample Number:	NT10061402	**Location:**	Waihao
Date Collected:	6/14/2010	**Formation:**	Otekaike Lst

Hand Specimen Description

Colour	Induration	Bedding and Sedimentary Structures		Grainsize
Yellowy-cream	Very well indurated			Fine to medium
Grain or matrix supported	**Sorting**	**Roundness**	**Sphericity - shape**	**Biologic binding**
Grain	Moderate			No
Textural Name:		**Notes:**		

Thin Section Description

Matrix	Percentage /100
Clastics: Quartz, biotite,	2%
Cement	50%
Mud	5%
Bioclasts	28%
Authigenic minerals: Glauconite	15%

Foraminifera	Percentage /100
Planktic	41% (n=77)
Benthic	59% (n=110)

Bioclasts	Percentage of identified/total
Foraminifera	70%/20%
Bryozoans	0%/0%
Echinoderms	27%/15%
Algae	0%/0%
Molluscs	3%/<1%
Brachiopods	0%/0%
Barnacles	0%/0%
Sponge spicules	0%/0%
Worm Tubes	0%/0%
Unidentified bioclasts	65%

Notes from thin section:	Glauconitised biotites. Quartz is subangular to angular. Uniform extinction calcite cements in some places. ~25% of benthic tests are disarticulated. Minor amount of benthics hyaline (<5%). Some benthics agglutinated? Benthic tests involute coil (majority), uniserial, biserial, very minor trochoid. Foram's sparry cement filled with most having multiple extinctions within the tests. Echinoderm fragments overgrown by sparry cement in equal extinction. Identified molluscs are mostly pteropods

Stratigraphic Column: NT09/01

Sample Number: NT10061403 **Location:** Waihao

Date Collected: 6/14/2010 **Formation:** Otekaike Lst

Thin Section Description

Matrix	Percentage /100
Clastics: Quartz (95%) (angular - sub-angular), biotite (5%)	2%
Cement	14%
Mud	8%
Bioclasts	30%
Authigenic minerals: Glauconite (99%), phosphate (1%)	46%

Foraminifera	Percentage /100
Planktic	34% (n=52)
Benthic	66% (n=101)

Bioclasts	Percentage of identified/total
Foraminifera	59%/44%
Bryozoans	0%0%
Echinoderms	40%/30%
Algae	0%0%
Molluscs	1%/1%
Brachiopods	0%0%
Barnacles	0%0%
Sponge spicules	0%0%
Worm Tubes	0%0%
Unidentified bioclasts	25%

Notes from thin section:	Loose sediment and clasts in resin. Lots of rounded to sub-rounded glauconite clasts, with a small amount of intraclast growth. Calcite cement is blocky and forms the majority of the matrix that is holding the clumps of sediment in this slide together, as well as overgrowths on echinoid fragments. Benthics are coiled (planar), biserial and uniserial. Tests are microcrystalline and hyaline.

Stratigraphic Column:	NT09/01		
Sample Number:	NT10061404	**Location:**	Waihao
Date Collected:	6/14/2010	**Formation:**	Otekaike Lst

Hand Specimen Description

Colour	**Induration**	**Bedding and Sedimentary Structures**		**Grainsize**
Yellow-cream	Indurated			Fine
Grain or matrix supported	**Sorting**	**Roundness**	**Sphericity - shape**	**Biologic binding**
Grain	Well			No
Textural Name:	**Packstone**	**Notes:**		

Thin Section Description

Matrix	**Percentage /100**
Clastics: Quartz, minor biotite	3%
Cement	35%
Mud	15%
Bioclasts	30%
Authigenic minerals: Glauconite (83%), Phosphate (2%), some hematite (15%)	17%

Foraminifera	**Percentage /100**
Planktic	29% (n=38)
Benthic	71% (n=93)

Bioclasts	**Percentage of identified/total**
Foraminifera	75%/45%
Bryozoans	0%/0%
Echinoderms	20%/13%
Algae	0%/0%
Molluscs	5%/2%
Brachiopods	0%/0%
Barnacles	0%/0%
Sponge spicules	0%/0%
Worm Tubes	0%/0%
Unidentified bioclasts	40%

Notes from thin section:	Phosphatised glauconites. Appears to have an alignment fabric, with majority of elongate bioclasts/clasts aligned. Glauconitised benthic test chambers in some specimens. Some hematite alteration. Benthics are rotalid, biserial, involute coil, uniserial, and miliolid (?). Micritic calcite tests with occasional hyaline. Echinoid fragments are commonly overgrown by syn-extinctional sparry cement. Mollusc fragments are too small to distinguish between gastropods/bivalves.

Stratigraphic Column:	NT09/01		
Sample Number:	NT10061408	**Location:**	Waihao
Date Collected:	6/14/2010	**Formation:**	Otekaike Lst

Hand Specimen Description

Colour	**Induration**	**Bedding and Sedimentary Structures**		**Grainsize**
Greenish-white	Friable			Fine
Grain or matrix supported	**Sorting**	**Roundness**	**Sphericity - shape**	**Biologic binding**
Matrix	Well			No
Textural Name:	**Wackestone**	**Notes:**	Muscovite?	

Thin Section Description

Matrix	**Percentage /100**
Clastics: Quartz (angular-subangular)	5%
Cement	10%
Mud	20%
Bioclasts	40%
Authigenic minerals: Glauconite (95%), phosphate (5%)	25%

Foraminifera	**Percentage /100**
Planktic	49% (n=52)
Benthic	51% (n=55)

Bioclasts	**Percentage of identified/total**
Foraminifera	40%/20%
Bryozoans	<1%/<1%
Echinoderms	0%/0%
Algae	0%/0%
Molluscs	3%/1%
Brachiopods	0%/0%
Barnacles	0%/0%
Sponge spicules	0%/0%
Worm Tubes	0%/0%
Unidentified bioclasts	79%

Notes from thin section:	Slightly smaller section due to a broken slide end. Very micritic section. Glauconites are well rounded and there appear to be no remnant glauconitised biotites in this section, with most glauconites the largest grains in the sample. Some phosphate rounded nodules. Strong micrite growth may be obscuring identification of some benthic forams, causing a higher than may be present ratio in favour of planktics. Some benthic tests are glauconite filled. Identified benthic tests are biserial, uniserial, and evolute coil, with nearly all being micritic.

Stratigraphic Column:	NT09/01		
Sample Number:	NT10061411	**Location:**	Waihao
Date Collected:	6/14/2010	**Formation:**	Otekaike Lst

Hand Specimen Description

Colour	**Induration**	**Bedding and Sedimentary Structures**		**Grainsize**
Greeny-grey	Friable			Fine
Grain or matrix supported	**Sorting**	**Roundness**	**Sphericity - shape**	**Biologic binding**
Matrix	Well			No
Textural Name:	**Wackestone**	**Notes:**		

Thin Section Description

Matrix	**Percentage /100**
Clastics: Quartz (angular to subangular), minor biotite	7%
Cement	13%
Mud	35%
Bioclasts	10%
Authigenic minerals: Glauconite, phosphate	35%

Foraminifera	**Percentage /100**
Planktic	82% (n=75)
Benthic	18% (n=17)

Bioclasts	**Percentage of identified/total**
Foraminifera	100%/60%
Bryozoans	0%/0%
Echinoderms	0%/0%
Algae	0%/0%
Molluscs	0%/0%
Brachiopods	0%/0%
Barnacles	0%/0%
Sponge spicules	0%/0%
Worm Tubes	0%/0%
Unidentified bioclasts	40%

Notes from thin section:	Poor quality thin section. Benthic forams obscured by micrite, possibly skewing the count in favour of the planktics. Biotites being glauconitised. Phosphatised glauconites minor, while most glauconite grains are rounded-subrounded and show mottly internal structure in xpl. Benthics are calcitic (hyalite and micritic), rotalid (?), uniserial, biserial.

Stratigraphic Column:	NT09/01		
Sample Number:	NT10061412	**Location:**	Waihao
Date Collected:	6/14/2010	**Formation:**	Otekaike Lst

Hand Specimen Description

Colour	**Induration**	**Bedding and Sedimentary Structures**		**Grainsize**
Greeny-grey	Friable			Fine
Grain or matrix supported	**Sorting**	**Roundness**	**Sphericity - shape**	**Biologic binding**
Matrix	Well			No
Textural Name:	**Wackestone**	**Notes:**		

Thin Section Description

Matrix	**Percentage /100**
Clastics: Quartz (angular-subrounded), minor biotite	8%
Cement	16%
Mud	16%
Bioclasts	10%
Authigenic minerals: Glauconite (96%), phosphate (4%)	50%

Foraminifera	**Percentage /100**
Planktic	69% (n=29)
Benthic	31% (n=13)

Bioclasts	**Percentage of identified/total**
Foraminifera	99%/29%
Bryozoans	0%/0%
Echinoderms	0%/0%
Algae	0%/0%
Molluscs	1%/<1%
Brachiopods	0%/0%
Barnacles	0%/0%
Sponge spicules	0%/0%
Worm Tubes	0%/0%
Unidentified bioclasts	71%

Notes from thin section:	Poor quality thin section. Glauconite is mottly in cross polars, and many have a ppl light rind that is mottly black/white in xpl (spar/micrite on rims?). Some heamatised glauconites? Sparry cement and micrite have formed between glauconite grains. Density of glauconite grains and micrite filling the interstices make it hard to identify benthic forams, which may skew results towards planktics. Hard to identify accuratly most bioclasts due to mud content. Many benthic foram tests are broken. Observed benthics are uniserial, biserial, trochoid (and rotalids?) with all those observed being calcareous walled (mostly micritic, some hyaline). One large gastropod fragment, sparry cement filled

Stratigraphic Column:	NT09/01		
Sample Number:	NT10061413	**Location:**	Waihao
Date Collected:	6/14/2010	**Formation:**	Otekaike Lst

Hand Specimen Description

Colour	**Induration**	**Bedding and Sedimentary Structures**		**Grainsize**
Greenish-white	Very well indurated			Fine
Grain or matrix supported	**Sorting**	**Roundness**	**Sphericity - shape**	**Biologic binding**
Grain	Well			No
Textural Name:	**Packstone**	**Notes:**	Shell fragments.	

Thin Section Description

Matrix	**Percentage /100**
Clastics: Quartz, biotite	2%
Cement	35%
Mud	13%
Bioclasts	35%
Authigenic minerals: Glauconite	15%

Foraminifera	**Percentage /100**
Planktic	31% (n=56)
Benthic	69% (n=124)

Bioclasts	**Percentage of identified/total**
Foraminifera	72%/30%
Bryozoans	<1%/<1%
Echinoderms	15%/7%
Algae	0%/0%
Molluscs	13%/6%
Brachiopods	<1%/<1%
Barnacles	0%/0%
Sponge spicules	0%/0%
Worm Tubes	0%/0%
Unidentified bioclasts	57%

Notes from thin section:	Quartz dominant clastic, subangular. Some glauconite has grown inside/around various benthic forams. Some glauconite grains show internal structure of original glauconitised grains. Benthics are involute coil, trochoid, biserial, uniserial. Vast majority of benthic tests are microgranular, with some uniserial tests appearing hyaline. Some benthic tests disarticulated. Single bryozoan fragment. Minor psuedopunctate brachiopod fragments. Shell fragments common, with molluscs represented predominantly by bivalve fragments, with minor pteropods.

Stratigraphic Column: NT09/02

Sample Number: NT09040512 **Location:** Waitaki River Maori Rock Art

Date Collected: 4/5/2009 **Formation:** Otekaike Lst

Hand Specimen Description

Colour	Induration	Bedding and Sedimentary Structures		Grainsize
Greenish-white	Friable			Fine
Grain or matrix supported	**Sorting**	**Roundness**	**Sphericity - shape**	**Biologic binding**
Matrix	Well			No
Textural Name:	**Wackestone**	**Notes:**		

Thin Section Description

Matrix	Percentage /100
Clastics: Quartz (angular-subangular)	7%
Cement	10%
Mud	45%
Bioclasts	28%
Authigenic minerals: Glauconite	10%

Foraminifera	Percentage /100
Planktic	45% (n=80)
Benthic	55% (n=99)

Bioclasts	Percentage of identified/total
Foraminifera	70%/35%
Bryozoans	0%/0%
Echinoderms	15%/8%
Algae	0%/0%
Molluscs	10%/5%
Brachiopods	5%/2%
Barnacles	0%/0%
Sponge spicules	0%/0%
Worm Tubes	0%/0%
Unidentified bioclasts	50%

Notes from thin section:	Moderate amount of plucked and resin filled holes in this section. Glauconite and echinoid fragments have sparry cement rims. Benthic tests are coil, rotalid, biserial, uniserial, with most being micritic calcite, and minority being hyaline. Some possible agglutinated tests, but difficult to confirm due to the nature of the cement/micritic matrix.

Stratigraphic Column:	NT09/02		
Sample Number:	NT09040513	**Location:**	Waitaki River Maori Rock Art
Date Collected:	4/5/2009	**Formation:**	Otekaike Lst

Hand Specimen Description

Colour	**Induration**	**Bedding and Sedimentary Structures**		**Grainsize**
White	Indurated			Very fine to fine
Grain or matrix supported	**Sorting**	**Roundness**	**Sphericity - shape**	**Biologic binding**
Grain	Moderate			No
Textural Name:	**Packstone**	**Notes:**		

Thin Section Description

Matrix	**Percentage /100**
Clastics: Quartz	5%
Cement	10%
Mud	35%
Bioclasts	35%
Authigenic minerals: Hematite (30%), glauconite (70%)	15%

Foraminifera	**Percentage /100**
Planktic	38% (n=27)
Benthic	62% (n=44)

Bioclasts	**Percentage of identified/total**
Foraminifera	78%/45%
Bryozoans	0%/0%
Echinoderms	20%/9%
Algae	0%/0%
Molluscs	2%/1%
Brachiopods	0%/0%
Barnacles	0%/0%
Sponge spicules	0%/0%
Worm Tubes	0%/0%
Unidentified bioclasts	45%

Notes from thin section:	Glauconite is altering with heamatite. Some large echinoid fragments alongside a few large shell pieces, with smaller echinoid fragments with sparry cement overgrowths in syn-extinction. Benthics are biserial, uniserial, coil, rotalid, trochoid. Benthic tests are ~70% micritic - ~30% hyaline.

Stratigraphic Column:	NT09/02		
Sample Number:	NT10061514	**Location:**	Waitaki River Maori Rock Art
Date Collected:	5/15/2010	**Formation:**	Otekaike Lst

Hand Specimen Description

Colour	Induration	Bedding and Sedimentary Structures		Grainsize
Yellowish-white	Friable			Fine
Grain or matrix supported	**Sorting**	**Roundness**	**Sphericity - shape**	**Biologic binding**
Grain	Well			No
Textural Name:	**Packstone**	**Notes:**		

Thin Section Description

Matrix	Percentage /100
Clastics: Quartz (angular-subangular)	5%
Cement	17%
Mud	35%
Bioclasts	40%
Authigenic minerals: Glauconite (65%), hematite (35%)	3%

Foraminifera	Percentage /100
Planktic	37% (n=41)
Benthic	63% (n=70)

Bioclasts	Percentage of identified/total
Foraminifera	91%/45%
Bryozoans	0%/0%
Echinoderms	8%/4%
Algae	0%/0%
Molluscs	1%/<1%
Brachiopods	0%/0%
Barnacles	0%/0%
Sponge spicules	0%/0%
Worm Tubes	0%/0%
Unidentified bioclasts	51%

Notes from thin section:	Benthic tests are coil, biserial, uniserial, with most tests micritic-hyaline, and minor agglutinateds. Some tests are hematite filled. Some slightly larger echinoid fragments, but majority of material is v.fine and broken.

Stratigraphic Column: NT09/03

Sample Number: NT09040514 **Location:** Earthquakes

Date Collected: **Formation:** Tapui Sandstone

Hand Specimen Description

Colour	Induration	Bedding and Sedimentary Structures		Grainsize
White	Friable			Silt
Grain or matrix supported	**Sorting**	**Roundness**	**Sphericity - shape**	**Biologic binding**
	Well			No
Textural Name:	**Siltstone**	**Notes:**		

Thin Section Description

Matrix	Percentage /100
Clastics: Quartz larger (rounded - sub-rounded) smaller (angular - sub-rounded), minor biotite	95%
Cement	0%
Mud	0%
Bioclasts	0%
Authigenic minerals: Glauconite (10%), hematite (90%)	5%

Foraminifera	Percentage /100
Planktic	n/a
Benthic	n/a

Bioclasts	Percentage of identified/total
Foraminifera	n/a
Bryozoans	n/a
Echinoderms	n/a
Algae	n/a
Molluscs	n/a
Brachiopods	n/a
Barnacles	n/a
Sponge spicules	n/a
Worm Tubes	n/a
Unidentified bioclasts	n/a

Notes from thin section:	Loose sediment in resin. Quartz is bimodal, with some polycrystalline quartz grains. Some clasts of grains grouped together. Few rounded glauconite grains. Hematite alteration is some locations around glauconite and some quartz grains. A couple of possible rounded to sub-rounded igneous clasts. No observed bioclasts. Some opaques, rounded - angular.

Stratigraphic Column:	NT09/03		
Sample Number:	NT09040515	**Location:**	Earthquakes
Date Collected:	4/5/2009	**Formation:**	Tapui Sandstone (upper contact)

Hand Specimen Description

Colour	**Induration**	**Bedding and Sedimentary Structures**		**Grainsize**
Greeny-orange	Friable			Fine to medium
Grain or matrix supported	**Sorting**	**Roundness**	**Sphericity - shape**	**Biologic binding**
Grain	Moderate			No
Textural Name:	**Grainstone**	**Notes:**		

Thin Section Description

Matrix	**Percentage /100**
Clastics: Quartz	83%
Cement	0%
Mud	0%
Bioclasts	0%
Authigenic minerals: Glauconite (60%), hematite (40%)	17%

Foraminifera	**Percentage /100**
Planktic	n/a
Benthic	n/a

Bioclasts	**Percentage of identified/total**
Foraminifera	n/a
Bryozoans	n/a
Echinoderms	n/a
Algae	n/a
Molluscs	n/a
Brachiopods	n/a
Barnacles	n/a
Sponge spicules	n/a
Worm Tubes	n/a
Unidentified bioclasts	n/a

Notes from thin section:	Loose sediment in resin. Quartz is bimodal, with large rounded to sub-rounded grains and smaller angular grains. Glauconite grains are rounded to sub-rounded. Glauconite appears to be quite mature. Hematite is present as heavy alteration around groupings of quartz grains. No obvious bioclasts.

Stratigraphic Column: NT09/03

Sample Number: NT09040516 **Location:** Earthquakes

Date Collected: 4/5/2009 **Formation:** Tapui Sandstone

Thin Section Description

Matrix	Percentage /100
Clastics: Quartz (sub-rounded - rounded)	20%
Cement	0%
Mud	0%
Bioclasts	0%
Authigenic minerals: Hematite	80%

Foraminifera	Percentage /100
Planktic	n/a
Benthic	n/a

Bioclasts	Percentage of identified/total
Foraminifera	n/a
Bryozoans	n/a
Echinoderms	n/a
Algae	n/a
Molluscs	n/a
Brachiopods	n/a
Barnacles	n/a
Sponge spicules	n/a
Worm Tubes	n/a
Unidentified bioclasts	n/a

Notes from thin section:	Very poor quality slide with massive hematite weathering, producing almost opaque grains. Quartz grains are relatively large, and some show good rounding. Hematite covers all other clasts and textures.

Stratigraphic Column:	NT09/03		
Sample Number:	NT09040517	**Location:**	Earthquakes
Date Collected:	4/5/2009	**Formation:**	Ototara Lst

Hand Specimen Description

Colour	**Induration**	**Bedding and Sedimentary Structures**		**Grainsize**
Yellowish-white	Indurated			Very fine to fine
Grain or matrix supported	**Sorting**	**Roundness**	**Sphericity - shape**	**Biologic binding**
Matrix	Well			No
Textural Name:	**Wackestone**	**Notes:**		

Thin Section Description

Matrix	**Percentage /100**
Clastics: Small Quartz grains (angular - sub-rounded), biotite	30%
Cement	0%
Mud	50%
Bioclasts	10%
Authigenic minerals: Glauconite (90%), hematite (10%)	10%

Foraminifera	**Percentage /100**
Planktic	88% (n=37)
Benthic	12% (n=5)

Bioclasts	**Percentage of identified/total**
Foraminifera	68%/34%
Bryozoans	0%/0%
Echinoderms	0%/0%
Algae	0%/0%
Molluscs	25%/12%
Brachiopods	0%/0%
Barnacles	0%/0%
Sponge spicules	2%/1%
Worm Tubes	0%/0%
Unidentified bioclasts	50%

Notes from thin section:	Micritic slide with some hematite alteration. Quartzose. The few observed benthics are uniserial and coiled trochospiral, with tests being microcrystalline and hyaline. All foram tests in this sample are very small, with common hematite in the chambers. Glauconite grains are rounded to sub-angular, with common glauconitised biotites. Hematite alteration relatively common of matrix and within bioclast voids. Shell fragments show heavy abrasion and/or borings. Most unidentified bioclasts are small shell fragments. Mollusc pieces appear to be both fragments of gastropods and bivalves. Glauconitised radiolarians.

Stratigraphic Column:	NT09/03		
Sample Number:	NT09040518	**Location:**	Earthquakes
Date Collected:	4/5/2009	**Formation:**	Kokoamu Greensand (in burrows in Ototara)

Hand Specimen Description

Colour	**Induration**	**Bedding and Sedimentary Structures**		**Grainsize**
Greenish-orange	Unconsolidated			Fine
Grain or matrix supported	**Sorting**	**Roundness**	**Sphericity - shape**	**Biologic binding**
Grain	Well			No
Textural Name:	**Packstone**	**Notes:**		

Thin Section Description

Matrix	**Percentage /100**
Clastics: Quartz (angular - sub-rounded) (90%), some biotite lathes (10%)	20%
Cement	0%
Mud	20%
Bioclasts	25%
Authigenic minerals: Glauconite, hematite	35%

Foraminifera	**Percentage /100**
Planktic	56% (n=54)
Benthic	44% (n=43)

Bioclasts	**Percentage of identified/total**
Foraminifera	100%/60%
Bryozoans	0%/0%
Echinoderms	0%/0%
Algae	0%/0%
Molluscs	0%/0%
Brachiopods	0%/0%
Barnacles	0%/0%
Sponge spicules	0%/0%
Worm Tubes	0%/0%
Unidentified bioclasts	40%

Notes from thin section:	Loose sediment in resin. Micrite estimate is taken from larger clumps of sediment and extrapolated. Rounded glauconite grains, most showing some hematisation, with some heavy. Glauconitised biotite lathes. Benthics are coiled (planar, trochospiral), and biserial. Tests are microcrystalline with a couple of hyalines. One larger quartz agglutinate benthic observed. Unidentified bioclasts appear to be shell fragments.

Stratigraphic Column:	NT09/03		
Sample Number:	NT09040520	**Location:**	Earthquakes Kokoamu
Date Collected:	4/5/2010	**Formation:**	Greensand/Otekaike Lst transition

Hand Specimen Description

Colour	**Induration**	**Bedding and Sedimentary Structures**		**Grainsize**
Yellowish-green	Friable			Fine to very-fine
Grain or matrix supported	**Sorting**	**Roundness**	**Sphericity - shape**	**Biologic binding**
Grain	Well			No
Textural Name:	**Packstone**	**Notes:**		

Thin Section Description

Matrix	**Percentage /100**
Clastics: Quartz (angular - sub-rounded), minor biotite	17%
Cement	0%
Mud	40%
Bioclasts	8%
Authigenic minerals: Glauconite (95%), hematite (5%)	35%

Foraminifera	**Percentage /100**
Planktic	41% (n=7)
Benthic	59% (n=10)

Bioclasts	**Percentage of identified/total**
Foraminifera	100%/50%
Bryozoans	0%/0%
Echinoderms	0%/0%
Algae	0%/0%
Molluscs	0%/0%
Brachiopods	0%/0%
Barnacles	0%/0%
Sponge spicules	0%/0%
Worm Tubes	0%/0%
Unidentified bioclasts	50%

Notes from thin section:	Loose sediment in resin. Glauconite grains are rounded to sub-rounded, with some glauconitised biotite. Some hematite alteration of matrix. Benthics are coiled (planar, trochospiral) and uniserial. Tests are microcrystalline with a couple of hyalines. Unidentified bioclasts are small shell fragments.

Stratigraphic Column:	NT09/03		
Sample Number:	NT09040521	**Location:**	Earthquakes
Date Collected:	4/5/2009	**Formation:**	Otekaike Lst

Hand Specimen Description

Colour	**Induration**	**Bedding and Sedimentary Structures**		**Grainsize**
White-cream	Friable			Fine
Grain or matrix supported	**Sorting**	**Roundness**	**Sphericity - shape**	**Biologic binding**
Matrix	Well			No
Textural Name:	**Wackestone**	**Notes:**		

Thin Section Description

Matrix	**Percentage /100**
Clastics: Quartz (angular - subrounded)	5%
Cement	10%
Mud	40%
Bioclasts	40%
Authigenic minerals: Glauconite (96%), hematite (3%), phosphate (1%)	5%

Foraminifera	**Percentage /100**
Planktic	38% (n=85)
Benthic	62% (n=138)

Bioclasts	**Percentage of identified/total**
Foraminifera	88%/57%
Bryozoans	0%/0%
Echinoderms	10%/7%
Algae	0%/0%
Molluscs	2%/1%
Brachiopods	0%/0%
Barnacles	0%/0%
Sponge spicules	0%/0%
Worm Tubes	0%/0%
Unidentified bioclasts	35%

Notes from thin section:	More mature glauconites, mostly rounded grains, some phosphatised or hematised. Some hematite/glauconite formed intraclast in forams. Most benthic tests are microcrystalline with some hyaline, and minor agglutinates. Benthic test forms are uniserial, coil, biserial, with some tests disarticulated. Hematite appears to be in situ formation.

Stratigraphic Column: NT09/04

Sample Number: NT09040601 **Location:** Landon Creek

Date Collected: 4/6/2009 **Formation:** Ototara Lst

Hand Specimen Description

Colour	Induration	Bedding and Sedimentary Structures		Grainsize
White-cream	Friable			Fine to medium
Grain or matrix supported	**Sorting**	**Roundness**	**Sphericity - shape**	**Biologic binding**
Grain	Poor			No
Textural Name:	**Packstone**	**Notes:**		

Thin Section Description

Matrix	Percentage /100
Clastics: Quartz	<1%
Cement	5%
Mud	20%
Bioclasts	74%
Authigenic minerals: Glauconite (60%), phosphate (40%)	1%

Foraminifera	Percentage /100
Planktic	0% (n=0)
Benthic	100% (n=27)

Bioclasts	Percentage of identified/total
Foraminifera	30%/25%
Bryozoans	50%/43%
Echinoderms	20%/17%
Algae	0%/0%
Molluscs	0%/0%
Brachiopods	0%/0%
Barnacles	0%/0%
Sponge spicules	0%/0%
Worm Tubes	0%/0%
Unidentified bioclasts	15%

Notes from thin section:	Quite a number of plucked holes in this thin section. Poor section. Glauconite is found as grains and also intraclast in foram test chambers. Benthics are nummilites, biserial, uniserial, and coil. Echinoid fragments have spar overgrowth. Some bryozoans show zooecial diaphragms.

Stratigraphic Column:	NT09/04		
Sample Number:	NT09040602	**Location:**	Landon Creek
Date Collected:	4/6/2009	**Formation:**	Ototara Lst

Hand Specimen Description

Colour	**Induration**	**Bedding and Sedimentary Structures**		**Grainsize**
Cream	Friable			Fine to medium
Grain or matrix supported	**Sorting**	**Roundness**	**Sphericity - shape**	**Biologic binding**
Grain	Poor			No
Textural Name:	**Packstone**	**Notes:**		

Thin Section Description

Matrix	**Percentage /100**
Clastics: Quartz (angular)	Trace
Cement	6%
Mud	17%
Bioclasts	75%
Authigenic minerals: Glauconite (40%), hematite (60%)	2%

Foraminifera	**Percentage /100**
Planktic	1% (n=1)
Benthic	99% (n=74)

Bioclasts	**Percentage of identified/total**
Foraminifera	60%/40%
Bryozoans	20%/15%
Echinoderms	20%/15%
Algae	0%/0%
Molluscs	0%/0%
Brachiopods	0%/0%
Barnacles	0%/0%
Sponge spicules	0%/0%
Worm Tubes	0%/0%
Unidentified bioclasts	30%

Notes from thin section:	Poor section, has a number of plucked holes and appears to be quite weathered/altered. Glauconite is mature rounded grains. Hematite is found as alteration rims on clasts. Some dolomite replacement of cements (?). Benthics are nummulites, rotallid trochospiral, coil, uniserial, biserial, with the vast majority microcrystalline with some minor hyaline tests. Echinoid fragments overgrown with cement.

Stratigraphic Column:	NT09/04		
Sample Number:	NT09040603	**Location:**	Landon Creek
Date Collected:	4/6/2009	**Formation:**	Ototara Lst

Hand Specimen Description

Colour	**Induration**	**Bedding and Sedimentary Structures**		**Grainsize**
Orangy-cream	Friable			Fine to medium
Grain or matrix supported	**Sorting**	**Roundness**	**Sphericity - shape**	**Biologic binding**
Grain	Moderate			No
Textural Name:	**Packstone**	**Notes:**		

Thin Section Description

Matrix	**Percentage /100**
Clastics:	None
Cement	7%
Mud	10%
Bioclasts	80%
Authigenic minerals: Glauconite (5%), hematite (95%)	3%

Foraminifera	**Percentage /100**
Planktic	0% (n=0)
Benthic	100% (n=31)

Bioclasts	**Percentage of identified/total**
Foraminifera	43%/21%
Bryozoans	25%/8%
Echinoderms	30%/10%
Algae	0%/0%
Molluscs	2%/1%
Brachiopods	0%/0%
Barnacles	0%/0%
Sponge spicules	0%/0%
Worm Tubes	0%/0%
Unidentified bioclasts	60%

Notes from thin section:	Very poor and weathered/altered section. Number of plucked holes, and section may be slightly too thick to show detail in clasts. Identification of some bioclasts is very difficult due to the thickness of the section and the alteration. Glauconite grains (very few) are rounded and mature. Hematite is present as weathering/alteration rinds on clasts and in interstices, and can be found in localised concentrations. Benthics are biserial, uniserial, rotallid (trochospiral), nummulites, and coil, with most tests microcrystalline, and some hyaline. Isopachous cement common on clasts rims and on bioclast void spaces. Echinoid spines and plates overgrown with calcite cement.

Stratigraphic Column:	NT09/04		
Sample Number:	NT09040604	**Location:**	Landon Creek
Date Collected:	4/6/2009	**Formation:**	Ototara Lst (at karst surface)

Hand Specimen Description

Colour	**Induration**	**Bedding and Sedimentary Structures**		**Grainsize**
Orangy-cream	Indurated			Fine to medium
Grain or matrix supported	**Sorting**	**Roundness**	**Sphericity - shape**	**Biologic binding**
Grain	Poor			No
Textural Name:	**Packstone**	**Notes:**		

Thin Section Description

Matrix	**Percentage /100**
Clastics:	None
Cement	4%
Mud	20%
Bioclasts	70%
Authigenic minerals: Hematite (75%), Phosphate (25%)	6%

Foraminifera	**Percentage /100**
Planktic	2% (n=1)
Benthic	98% (n=56)

Bioclasts	**Percentage of identified/total**
Foraminifera	50%/34%
Bryozoans	25%/18%
Echinoderms	25%/18%
Algae	0%/0%
Molluscs	0%/0%
Brachiopods	0%/0%
Barnacles	0%/0%
Sponge spicules	0%/0%
Worm Tubes	0%/0%
Unidentified bioclasts	30%

Notes from thin section:	Sparry calcite cement present on most echinoid fragments. Dolomite (?) Hematite is found as rim growths on bioclasts, while phosphate appears as rounded grains. Benthics are biserial, nummulites, rotalid trochospiral, and coils. All are microcrystalline, with some rotallids being hyaline alongside all nummulites.

Stratigraphic Column:	NT09/04		
Sample Number:	NT09040606	**Location:**	Landon Creek Ototara Lst (Karst contact clast)
Date Collected:	4/6/2009	**Formation:**	

Hand Specimen Description

Colour	**Induration**	**Bedding and Sedimentary Structures**		**Grainsize**
Brownish-cream	Indurated			Fine to medium
Grain or matrix supported	**Sorting**	**Roundness**	**Sphericity - shape**	**Biologic binding**
Grain	Poor			No
Textural Name:	**Packstone**	**Notes:**		

Thin Section Description

Matrix	**Percentage /100**
Clastics: Quartz (95% of grains on hematised end of section)	1%
Cement	10%
Mud	39%
Bioclasts	40%
Authigenic minerals: Hematite (80%), phosphate (19%), glauconite (1%)	10%

Foraminifera	**Percentage /100**
Planktic	0% (n=0)
Benthic	100% (n=60)

Bioclasts	**Percentage of identified/total**
Foraminifera	60%/50%
Bryozoans	20%/17%
Echinoderms	15%/13%
Algae	0%/0%
Molluscs	0%/0%
Brachiopods	0%/0%
Barnacles	0%/0%
Sponge spicules	0%/0%
Worm Tubes	0%/0%
Unidentified bioclasts	20%

Notes from thin section:	Poor sample with many plucked holes in the section. Shows signs of weathering. Hematite is altering clasts and is primarily forming around and over clasts, commonly from the outside in, with some clasts only partially altered. Mud is found as both clasts and interstices fill of roughly equal proportions. Clasts are subrounded to rounded, and spherical to rod shaped. Benthic tests are coil, biserial, trochispiral? and uniserial, with mostly microcrystalline tests, a number of hylaines, and some agglutinates. Some rotalids. Echinoid fragments show spar overgrowths.

Stratigraphic Column:	NT09/04		
Sample Number:	NT09040607	**Location:**	Landon Creek Kokoamu
Date Collected:	4/6/2009	**Formation:**	Greensand

Hand Specimen Description

Colour	**Induration**	**Bedding and Sedimentary Structures**		**Grainsize**
Yellowish-brown	Friable			Fine to medium
Grain or matrix supported	**Sorting**	**Roundness**	**Sphericity - shape**	**Biologic binding**
Grain	Moderate			No
Textural Name:	**Packstone**	**Notes:**		

Thin Section Description

Matrix	**Percentage /100**
Clastics: Quartz (angular - sub-rounded), rounded limestone clasts, one rounded igneous clast	6%
Cement	6%
Mud	12%
Bioclasts	31%
Authigenic minerals: Glauconite (65%), phosphate (5%), hematite (30%)	45%

Foraminifera	**Percentage /100**
Planktic	83% (n=67)
Benthic	17% (n=14)

Bioclasts	**Percentage of identified/total**
Foraminifera	43%/30%
Bryozoans	10%/7%
Echinoderms	40%/28%
Algae	0%/0%
Molluscs	7%/5%
Brachiopods	0%/0%
Barnacles	0%/0%
Sponge spicules	0%/0%
Worm Tubes	0%/0%
Unidentified bioclasts	30%

Notes from thin section:	Loose sediment in resin. Some rounded limestone clasts, and one vesicular igneous clast. Glauconite grains are well rounded. Hematite has formed on matrix as dark growth and coating on some glauconite grains. Phosphate found as well rounded grains. Benthics are coiled (trochospiral, planar), and uniserial. Tests are microcrystalline with a few hyalines.

Stratigraphic Column:	NT09/04		
Sample Number:	NT09040608	**Location:**	Landon Creek
Date Collected:	4/6/2009	**Formation:**	Otekaike Lst

Hand Specimen Description

Colour	Induration	Bedding and Sedimentary Structures		Grainsize
Orangy-cream	Indurated			Fine to medium
Grain or matrix supported	**Sorting**	**Roundness**	**Sphericity - shape**	**Biologic binding**
Grain	Moderate			No
Textural Name:	**Packstone**	**Notes:**		

Thin Section Description

Matrix	Percentage /100
Clastics: Quartz, extraclasts	Qtz - 2%, Extraclasts - 1%
Cement	2%
Mud	6%
Bioclasts	81%
Authigenic minerals: Glauconite (70%), phosphate (5%), hematite (25%)	8%

Foraminifera	Percentage /100
Planktic	18% (n=22)
Benthic	82% (n=102)

Bioclasts	Percentage of identified/total
Foraminifera	39%/27%
Bryozoans	6%/4%
Echinoderms	30%/21%
Algae	18%/13%
Molluscs	4%/3%
Brachiopods	3%/2%
Barnacles	0%/0%
Sponge spicules	0%/0%
Worm Tubes	0%/0%
Unidentified bioclasts	30%

Notes from thin section:	Extraclast (~3mm) with significant micrite content, yellowed carbonate matrix, some bioclast material, has burrows/cracks penetrating from one side of the clast, and is hematised in the middle but predominantly on the outside of the clast. At least one lump of glauconite where the grains interlock to form one larger (~2mm) clast with spar between each of the smaller clasts and rimming the whole; the internal grains are sunangular to subrounded while the clast itself is subrounded. Phosphate grains range from the same size to four times the size of the glauconite grains. Some glauconite has formed in benthic foram test chambers. Benthics are microcrystalline mostly, with some hyaline and several agglutinates. Tests are coil, biserial, uniserial, with hyaline rotallids. Some shell fragments show signs of boring. Echinoid fragments commonly overgrown by sparry cement. Some mollusc fragments neomorphosed to sparry cement.

Stratigraphic Column:	NT09/04		
Sample Number:	NT09040609	**Location:**	Landon Creek
Date Collected:	4/6/2009	**Formation:**	Gee Greensand

Hand Specimen Description

Colour	**Induration**	**Bedding and Sedimentary Structures**		**Grainsize**
Greeny-orange	Friable			Fine to medium
Grain or matrix supported	**Sorting**	**Roundness**	**Sphericity - shape**	**Biologic binding**
Grain	Moderate			No
Textural Name:	**Grainstone**	**Notes:**		

Thin Section Description

Matrix	**Percentage /100**
Clastics: Quartz (angular)	3%
Cement	6%
Mud	1%
Bioclasts	60%
Authigenic minerals: Glauconite (90%), hematite (10%)	30%

Foraminifera	**Percentage /100**
Planktic	45% (n=30)
Benthic	55% (n=37)

Bioclasts	**Percentage of identified/total**
Foraminifera	25%/10%
Bryozoans	10%/4%
Echinoderms	40%/16%
Algae	0%/0%
Molluscs	20%/8%
Brachiopods	5%/2%
Barnacles	0%/0%
Sponge spicules	0%/0%
Worm Tubes	0%/0%
Unidentified bioclasts	60%

Notes from thin section:	Loose sediment in resin. Quite heavily altered sample, with hematite common. Calcite cement only forms around echinoid fragments. Very difficult to determine the mud content due to the loose sediment nature of the slide and heavy alteration present. Glauconite grains are rounded to sub-rounded, with glauconitisation of some bioclasts, noticibly inside echinoid fragments. Hematite alteration common on most clasts and the matrix, however its presence has been calculated as low due to its altered nature, rather than its replacement nature. Benthics are biserial, uniserial, coiled (planar, trochospiral) and milliolid. Tests are microcrystalline and hyaline, with one quartz agglutinate uniserial. Can be difficult to find forams in this sample. Glauconite often formed inside foram tests. Heavy abrasion and boring of a large component of these bioclasts. Molluscs are both bivalves and gastropods. Echinoids are spines and plates, with plates rounded to angular.

Stratigraphic Column:	NT09/06		
Sample Number:	NT09040804	**Location:**	Gee's Point
Date Collected:	4/8/2009	**Formation:**	Ototara Lst

Hand Specimen Description

Colour	**Induration**	**Bedding and Sedimentary Structures**		**Grainsize**
Yellow-cream	Friable			Fine to medium
Grain or matrix supported	**Sorting**	**Roundness**	**Sphericity - shape**	**Biologic binding**
Grain	Poor			No
Textural Name:	**Packstone**	**Notes:**		

Thin Section Description

Matrix	**Percentage /100**
Clastics: Quartz (angular)	3%
Cement	4%
Mud	24%
Bioclasts	65%
Authigenic minerals: Glauconite (85%), hematite (15%)	4%

Foraminifera	**Percentage /100**
Planktic	14% (n=13)
Benthic	86% (n=83)

Bioclasts	**Percentage of identified/total**
Foraminifera	30%/12%
Bryozoans	46%/14%
Echinoderms	30%/12%
Algae	0%/0%
Molluscs	4%/2%
Brachiopods	0%/0%
Barnacles	0%/0%
Sponge spicules	0%/0%
Worm Tubes	0%/0%
Unidentified bioclasts	60%

Notes from thin section:	Calcite cement is mostly overgrowth on echinoid fragments. Significant glauconite formation within foram tests. Rounded to sub-rounded glauocnite grains. Some hematite alteration, especially on one side of this sample (not taken into account in this instance). Benthics are coiled (planar, trochospiral), biserial, uniserial, and rotalid. Most tests are microcrystalline and hyaline, with some larger quartz agglutinate biserials.

Stratigraphic Column:	NT09/06		
		Location:	Gee's Point
Sample Number:	NT09040805		
		Formation:	Tuff cone/Ototara interface - clast from contact
Date Collected:	4/8/09		

Thin Section Description

Matrix	Percentage /100
Clastics: Pyroxenes, isotropics.	98%
Cement	0%
Mud	1%
Bioclasts	1%
Authigenic minerals: Glauconite	0%

Foraminifera	Percentage /100
Planktic	0% (n=0)
Benthic	100% (n=1)

Bioclasts	Percentage of identified/total
Foraminifera	100%/100%
Bryozoans	0%/0%
Echinoderms	0%/0%
Algae	0%/0%
Molluscs	0%/0%
Brachiopods	0%/0%
Barnacles	0%/0%
Sponge spicules	0%/0%
Worm Tubes	0%/0%
Unidentified bioclasts	0%

Notes from thin section:	Poor slide, heavily weathered and plucked. Volcanic clasts, all sub-angular to sub-rounded. Hematite alteration around some of the clasts. Most have fractures running through them. One lone benthic coiled foram inside void space. Possibly some minor micrite in the fractures of a large pyroxene.

Stratigraphic Column: NT09/06

Sample Number: NT09040806 **Location:** Gee's Point

Date Collected: 4/8/09 **Formation:** Ototara Lst

Thin Section Description

Matrix	Percentage /100
Clastics: Quartz (angular)	1%
Cement	2%
Mud	32%
Bioclasts	60%
Authigenic minerals: Glauconite (10%), hematite (90%)	5%

Foraminifera	Percentage /100
Planktic	20% (n=15)
Benthic	80% (n=61)

Bioclasts	Percentage of identified/total
Foraminifera	25%/15%
Bryozoans	10%/6%
Echinoderms	0%/0%
Algae	0%/0%
Molluscs	40%/24%
Brachiopods	25%/15%
Barnacles	0%/0%
Sponge spicules	0%/0%
Worm Tubes	0%/0%
Unidentified bioclasts	40%

Notes from thin section:	Loose sediment in resin. Neomorphosed mollusc fragments. Punctate brachiopods. Some heavy borings on some shells. Matrix taken from larger clasts within the resin. Hematite altered muds. Few sub-rounded glauconites. Benthics are coiled (planar, trochospiral), uniserial, biserial. Tests are microcrystalline with a few hyalines. Borings in shells show hematite and glauconite within them. Some shell fragments are very large. Most unidentified bioclasts are broken shell material.

Stratigraphic Column:	NT09/06		
Sample Number:	NT09040807A	**Location:**	Gee's Point
Date Collected:	4/8/09	**Formation:**	Ototara Lst (karst boundary)

Thin Section Description

Matrix	Percentage /100
Clastics: Quartz (angular-subrounded)	1%
Cement	7%
Mud	10%
Bioclasts	77%
Authigenic minerals: Glauconite (88%), phosphate (2%), hematite (10%)	5%

Foraminifera	Percentage /100
Planktic	Clean Lst: 9% (n=4), Gl Lst: 52% (n=14)
Benthic	Clean Lst: 91% (n=40), Gl Lst: 48% (n=13)

Bioclasts	Percentage of identified/total
Foraminifera	21%/14%
Bryozoans	60%/35%
Echinoderms	15%/9%
Algae	0%/0%
Molluscs	3%/2%
Brachiopods	1%/<1%
Barnacles	0%/0%
Sponge spicules	0%/0%
Worm Tubes	0%/0%
Unidentified bioclasts	40%

Notes from thin section:	Thicker section. Glauconite is rounded to subrounded and found as grains as well as inside foram test chambers, although predominantly the latter. It ranges in concentration over the clast from ~1% to ~20%. Cements are isopachous to blocky spar, and form on the rims and chambers of bioclasts. Virtually all planktics in this slide were found in the higher glauconite section of the karst, indicating that this is a seperate deposit boundary. Benthic tests are predominantly microcrystalline, with occasional hyalines. Morphologies include involute coils, uniserial, biserial, rotallid (trochospiral), and nummulites. Mullusc fragments show neomorphism to blocky calcite,.

Stratigraphic Column:	NT09/06		
Sample Number:	NT09040807B	**Location:**	Gee's Point
Date Collected:	4/8/09	**Formation:**	Kokoamu Greensand (karst boundary)

Thin Section Description

Matrix	Percentage /100
Clastics: Quartz (Ot = angular-subrounded, Gsnd = rounded-subangular)	<1%/2%
Cement	3%/2%
Mud	10%/25%
Bioclasts	86%/56%
Authigenic minerals: Glauconite	1%/15%

Foraminifera	Percentage /100 Lst/Gsnd
Planktic	11% (n=5)/ 40% (n=22)
Benthic	89% (n=42)/ 60% (n=33)

Bioclasts	Percentage of identified/total Lst/Gsnd
Foraminifera	20%/16%; 57% /51%
Bryozoans	45%/36%; 10%/8%
Echinoderms	15%/12%; 30%/24%
Algae	20%/16%; 1%/1%
Molluscs	0%/0%; 2%/1%
Brachiopods	0%/0%; 0%/0%
Barnacles	0%/0%; 0%/0%
Sponge spicules	0%/0%; 0%/0%
Worm Tubes	0%/0%; 0%/0%
Unidentified bioclasts	20%; 15%

Notes from thin section:	This slide contains a contact between clean Ototara Lst and greensand infill of the karst. The only apparent differences between the two lithologies is the appearance of glauconite and quartz grains in the latter. Here the two have been classed seperatly, while they were done together in NT09040807A. Glauconite in the clean section is present as rounded-subrounded grains or infill, while in the greensand it is dominantly rounded to subrounded grains with some infill. Ototara Lst benthics are coil, trochospiral, biserial, uniserial. Tests are mostly microcrystalline with some hyalines. Gsnd benthics are coils, uniserial, trochospiral. Most tests microcrystalline, with some hyaline. Coralline algae consists of broken subrounded fragments.

Stratigraphic Column:	NT09/06		
Sample Number:	NT09040808G	**Location:**	Gee's Point
Date Collected:	4/8/09	**Formation:**	Otekaike Lst

Hand Specimen Description

Colour	**Induration**	**Bedding and Sedimentary Structures**		**Grainsize**
Greenish-white	Very well indurated			Fine to medium
Grain or matrix supported	**Sorting**	**Roundness**	**Sphericity - shape**	**Biologic binding**
Grain	Moderate			No
Textural Name:	**Packstone**	**Notes:**	Glauconitic, fossiliferous, one ribbed bivalve.	

Thin Section Description

Matrix	**Percentage /100**
Clastics: Quartz (angular-subangular, 90%), rounded carbonate lithics (10%)	2%
Cement	3%
Mud	30%
Bioclasts	45%
Authigenic minerals: Glauconite (75%), hematite (20%), phosphate (5%)	20%

Foraminifera	**Percentage /100**
Planktic	57% (n=101)
Benthic	43% (n=76)

Bioclasts	**Percentage of identified/total**
Foraminifera	81%/58%
Bryozoans	2%/1%
Echinoderms	15%/10%
Algae	0%/0%
Molluscs	2%/1%
Brachiopods	0%/0%
Barnacles	0%/0%
Sponge spicules	0%/0%
Worm Tubes	0%/0%
Unidentified bioclasts	30%

Notes from thin section:	Quartz clasts range from 1-3%, with the higher concentrations being found alongside increased concentrations of glauconite grains. The glauconite grains are rounded to sub-rounded, with some forming in foram chambers, while others are hematised, and range from 5%-30% concentrations. Hematite is present as an alteration product and occurs around authigenic clasts and bioclasts. Phosphate clasts are well-rounded. Benthics are primarily microcrystalline, with some hyalines. Tests are uniserial, coil, biserial, trochospiral (rotallid). Benthic tests may be obscured by high mud content. Large mollusc fragment showing neomorphism and boring into the shell filled with micrite and glauconite grains.

Stratigraphic Column:	NT09/06		
Sample Number:	NT09040808L	**Location:**	Gee's Point
Date Collected:	4/8/09	**Formation:**	Ototara Lst

Hand Specimen Description

Colour	**Induration**	**Bedding and Sedimentary Structures**		**Grainsize**
Cream	Very well indurated			Fine to coarse
Grain or matrix supported	**Sorting**	**Roundness**	**Sphericity - shape**	**Biologic binding**
Grain	Poor			No
Textural Name:	**Packstone**	**Notes:**		

Thin Section Description

Matrix	**Percentage /100**
Clastics: Quartz (95%), lithic clasts (5% - 1 observed clast)	1%
Cement	7%
Mud	20%
Bioclasts	65%
Authigenic minerals: Glauconite (20%), phosphate (40%), hematite (40%)	7%

Foraminifera	**Percentage /100**
Planktic	29% (n=36)
Benthic	71% (n=88)

Bioclasts	**Percentage of identified/total**
Foraminifera	36%/29%
Bryozoans	35%/28%
Echinoderms	15%/12%
Algae	7%/5%
Molluscs	5%/4%
Brachiopods	2%/2%
Barnacles	0%/0%
Sponge spicules	0%/0%
Worm Tubes	0%/0%
Unidentified bioclasts	20%

Notes from thin section:	Lithic clasts appear to be Lst fragments, and contain forams and bioclast material. Rounded glauconite grains, all of which appear to be phosphatised or hematised, with some intraclast formation within bioclast void spaces, with some beginning to form within echinoid fragments. Blocky and isopachous cements common both around and within clasts. Benthic tests are biserial, uniserial, coiled, nummulites, trochospiral. Tests are mostly microcrystalline with some hyaline, including nummulites. Rare quartz agglutinate/micrite biserials. Shell fragments are neomorphosed into blocky cements, retaining a microcrystalline rim. Gastropod:bivalvae ratio isnt determinable, although one fragment may be a gastropod, most likely bivavle due to gentle curved shapes.

Stratigraphic Column:	NT09/06		
Sample Number:	NT09040809	**Location:**	Gee's Point
Date Collected:	4/8/09	**Formation:**	Otekaike Lst

Hand Specimen Description

Colour	**Induration**	**Bedding and Sedimentary Structures**		**Grainsize**
White (black flecks)	Very well indurated			Fine to medium
Grain or matrix supported	**Sorting**	**Roundness**	**Sphericity - shape**	**Biologic binding**
Grain	Moderate			No
Textural Name:	**Packstone**	**Notes:**		

Thin Section Description

Matrix	**Percentage /100**
Clastics: Quartz (angular-subangular, 99%), feldspar(?)(euhedral, 1%)	1%
Cement	10%
Mud	5%
Bioclasts	69%
Authigenic minerals: Glauconite (98%), phosphate (2%)	15%

Foraminifera	**Percentage /100**
Planktic	38% (n=46)
Benthic	62% (n=74)

Bioclasts	**Percentage of identified/total**
Foraminifera	25%/15%
Bryozoans	2%/1%
Echinoderms	30%/20%
Algae	0%/0%
Molluscs	0%/0%
Brachiopods	0%/0%
Barnacles	0%/0%
Sponge spicules	0%/0%
Worm Tubes	0%/0%
Unidentified bioclasts	64%

Notes from thin section:	Poor section, quite a thick cut causing some difficulty identifying the darker clasts. Some plucked holes in slide. Glauconite grains are rounded to subrounded and either spherical or rodlike. Phosphate grains are subrounded, with common darker centre to the grain. Glauconite distribution is not even. Spary calcite cement (mostly blocky, with some drusy) filling most interstices of clasts. Thickness of slide may conceal some microcrystalline benthic tests causing an increase in the relative number of planktics. Benthic tests are uniserial, biserial, coil, rotallid (trochospiral), with most being microcrystalline with a few hyaline uniserial/biserial tests. Unidentified bioclasts contain a number of shell fragments that can't be identified due to thickness of slide.

Stratigraphic Column:	NT09/06		
Sample Number:	NT09040811	**Location:**	Gee's Point
Date Collected:	4/8/09	**Formation:**	Gee Greensand

Hand Specimen Description

Colour	**Induration**	**Bedding and Sedimentary Structures**		**Grainsize**
Whitish-green	Friable			Fine to medium
Grain or matrix supported	**Sorting**	**Roundness**	**Sphericity - shape**	**Biologic binding**
Grain	Moderate			No
Textural Name:	**Packstone**	**Notes:**		

Thin Section Description

Matrix	**Percentage /100**
Clastics: Quartz	2%
Cement	2%
Mud	20%
Bioclasts	56%
Authigenic minerals: Glauconite (50%), hematite (50%)	20%

Foraminifera	**Percentage /100**
Planktic	46% (n=58)
Benthic	54% (n=68)

Bioclasts	**Percentage of identified/total**
Foraminifera	73%/44%
Bryozoans	5%/3%
Echinoderms	20%/13%
Algae	0%/0%
Molluscs	1%/<1%
Brachiopods	1%/<1%
Barnacles	0%/0%
Sponge spicules	0%/0%
Worm Tubes	0%/0%
Unidentified bioclasts	40%

Notes from thin section:	Altered slide, with a fair bit of hematite alteration of grains and bioclasts. Significant formation of hematite/glauconite inside foram test chambers. Bioturbation? Benthics are microcrystalline and hyaline, with the latter more abundant, although the mud content may be obscuring further microcrystalline tests. Test morphologies include involute coils, uniserial, biserial.

Stratigraphic Column:	NT09/06		
Sample Number:	NT09040815	**Location:**	Gee's Point
Date Collected:	4/8/09	**Formation:**	Ototara Lst (lithified)

Hand Specimen Description

Colour	**Induration**	**Bedding and Sedimentary Structures**		**Grainsize**
Cream	Very well indurated			Fine to coarse
Grain or matrix supported	**Sorting**	**Roundness**	**Sphericity - shape**	**Biologic binding**
Grain	Poor			No
Textural Name:	**Packstone**	**Notes:**	Fossiliferous	

Thin Section Description

Matrix	**Percentage /100**
Clastics: Quartz	Trace
Cement	20%
Mud	5%
Bioclasts	72%
Authigenic minerals: Glauconite (40%), hematite (60%)	3%

Foraminifera	**Percentage /100**
Planktic	10% (n=6)
Benthic	90% (n=57)

Bioclasts	**Percentage of identified/total**
Foraminifera	25%/17%
Bryozoans	55%/36%
Echinoderms	10%/6%
Algae	5%/3%
Molluscs	5%/3%
Brachiopods	0%/0%
Barnacles	0%/0%
Sponge spicules	0%/0%
Worm Tubes	0%/0%
Unidentified bioclasts	35%

Notes from thin section:	Isopachous and blocky cement. Glauconite appears to be primarily forming as intraclasts within foram test chambers, bryozoan zooecia and the like, with some rounded grains. Hematite occurs as an alteration product on glauconite clasts and bioclasts in concentrated areas of the slide. Benthic tests are biserial, coiled, uniserial, and predominantly microcrystalline with some hyalines. Algae is branching corraline. Mollusc fragments are not further identifiable, and all seem to show calcite replacement from aragonite.

Stratigraphic Column:	NT09/06		
Sample Number:	NT10061612	**Location:**	Gee's Point
Date Collected:	6/16/10	**Formation:**	Ototara Lst

Hand Specimen Description

Colour	**Induration**	**Bedding and Sedimentary Structures**		**Grainsize**
Browny-yellowy-cream	Very well indurated			Fine to medium
Grain or matrix supported	**Sorting**	**Roundness**	**Sphericity - shape**	**Biologic binding**
Grain	Moderate			No
Textural Name:	**Packstone**	**Notes:**	Cemented, phosphate coating	

Thin Section Description

Matrix	**Percentage /100**
Clastics: Quartz (angular)	1%
Cement	2%
Mud	5%
Bioclasts	52%
Authigenic minerals: Glauconite (2%), hematite (13%), phosphate (85%)	40%

Foraminifera	**Percentage /100**
Planktic	5% (n=2)
Benthic	95% (n=38)

Bioclasts	**Percentage of identified/total**
Foraminifera	38%/23%
Bryozoans	50%/35%
Echinoderms	5%/3%
Algae	5%/3%
Molluscs	2%/1%
Brachiopods	0%/0%
Barnacles	0%/0%
Sponge spicules	0%/0%
Worm Tubes	0%/0%
Unidentified bioclasts	35%

Notes from thin section:	Highly altered section. Quartz grains are primarily present in the localised areas of heavy hematite alteration. Cements are primarily blocky spar and found only in very localised, less altered regions of the slide. Phosphate is present as some rounded grains, but primarily seems to be present as alteration of the matrix (?). Hematite occurs in localised concentrations of Fe-altered material, where also the quartz grains appear to be clustered. Benthics are biserial, uniserial, nummulites, coiled, miliolid, and trochosprial (rotalid). Tests are dominantly microcrystalline. Algae are branching corraline. Bored shell material. Mulluscan material is calcite neomorphosed.

Stratigraphic Column:	NT09/06		
Sample Number:	NT10061613	**Location:**	Gee's Point
Date Collected:	6/16/10	**Formation:**	Gee Greensand

Hand Specimen Description

Colour	**Induration**	**Bedding and Sedimentary Structures**		**Grainsize**
Greeny-yellowy-brown	Friable			Fine to coarse
Grain or matrix supported	**Sorting**	**Roundness**	**Sphericity - shape**	**Biologic binding**
Grain	Poor			No
Textural Name:	**Packstone**	**Notes:**	Fossiliferous, bryozoan-rich	

Thin Section Description

Matrix	**Percentage /100**
Clastics: Quartz (angular-subangular)	1%
Cement	4%
Mud	10%
Bioclasts	65%
Authigenic minerals: Glauconite (20% lightly altered), hematite (80% altered glauconite)	20% (glauconite/ hematite grains/ infill)

Foraminifera	**Percentage /100**
Planktic	43% (n=21)
Benthic	57% (n=28)

Bioclasts	**Percentage of identified/total**
Foraminifera	47%/19%
Bryozoans	10%/4%
Echinoderms	40%/16%
Algae	0%/0%
Molluscs	1%/<1%
Brachiopods	2%/1%
Barnacles	0%/0%
Sponge spicules	0%/0%
Worm Tubes	0%/0%
Unidentified bioclasts	60%

Notes from thin section:	Significant alteration in this sample with moderate plucking from slide. Substantial glauconite precipitation inside bioclasts and in some cases total growth over echinoid fragments and other bioclasts. Glauconite also found as rounded and fractured grains with glauconite overgrowths. Significant hematite alteration, primarily over the glauconite. Many of the clasts are micritised and are difficult to identify. Benthics are difficult to identify due to disarticulation of tests and micrite/hematite content. Test morphologies are uniserial, coil, biserial, and nummulites. Most tests are microcrystalline with some hyalines. In most places the planktics are obscured while in others they were easy to locate. Brachiopod shows psuedopunctae.

Stratigraphic Column:	NT09/06		
Sample Number:	NT10061614	**Location:**	Gee's Point
Date Collected:	6/16/10	**Formation:**	Gee Greensand

Hand Specimen Description

Colour	**Induration**	**Bedding and Sedimentary Structures**		**Grainsize**
Greenish-white	Friable			Fine to coarse
Grain or matrix supported	**Sorting**	**Roundness**	**Sphericity - shape**	**Biologic binding**
Grain	Poor			No
Textural Name:	**Grainstone**	**Notes:**		

Thin Section Description

Matrix	**Percentage /100**
Clastics: Quartz, (angular)	Trace
Cement	3%
Mud	1%
Bioclasts	76%
Authigenic minerals: Glauconite (25%), hematite (75%)	20%

Foraminifera	**Percentage /100**
Planktic	35% (n=8)
Benthic	65% (n=15)

Bioclasts	**Percentage of identified/total**
Foraminifera	28%/16%
Bryozoans	12%/7%
Echinoderms	55%/34%
Algae	0%/0%
Molluscs	3%/2%
Brachiopods	2%/1%
Barnacles	0%/0%
Sponge spicules	0%/0%
Worm Tubes	0%/0%
Unidentified bioclasts	40%

Notes from thin section:	Poor section, significant plucking due to large grainsize. Glauconite grains are rounded, and all appear to be altered by hematite formation. Hematite has formed in strong concentrations, including over glauconite grains and echinoid fragments, either partially or completly. Forams are very hard to identify in this slide due to heavy alteration. Benthics are biserial, rotallid (trochospiral), and coil. Most benthics are microcrystalline or hyaline, with one observed agglutinate.

Stratigraphic Column:	NT09/06		
Sample Number:	NT10061615	**Location:**	Gee's Point
Date Collected:	6/16/10	**Formation:**	Ototara Lst

Hand Specimen Description

Colour	**Induration**	**Bedding and Sedimentary Structures**		**Grainsize**
Cream	Very well indurated			Fine to coarse
Grain or matrix supported	**Sorting**	**Roundness**	**Sphericity - shape**	**Biologic binding**
Grain	Poor			No
Textural Name:	**Packstone**	**Notes:**		

Thin Section Description

Matrix	**Percentage /100**
Clastics:	None
Cement	10%
Mud	40%
Bioclasts	48%
Authigenic minerals: Glauconite (25%), hematite (75%)	2%

Foraminifera	**Percentage /100**
Planktic	5% (n=2)
Benthic	95% (n=39)

Bioclasts	**Percentage of identified/total**
Foraminifera	23%/19%
Bryozoans	40%/35%
Echinoderms	15%/12%
Algae	20%/17%
Molluscs	2%/2%
Brachiopods	0%/0%
Barnacles	0%/0%
Sponge spicules	0%/0%
Worm Tubes	0%/0%
Unidentified bioclasts	15%

Notes from thin section:	Lithified lst section with isopachous and blocky cements around and within most clasts, with drak micrite filling in interstices between cemented clasts. Minor intraclast glauconite formation, and some localised hematite alteration of clasts. Benthics are miliolid, uniserial, biserial, coiled, trichoidal, nummulites, with most tests being microcrystalline alongside some hyalines. Planktics may have been somewhat obscured by the volume of cements.

Stratigraphic Column:	NT09/06		
Sample Number:	NT10061616	**Location:**	Gee's Point
Date Collected:	6/16/10	**Formation:**	Gee Greensand

Hand Specimen Description

Colour	**Induration**	**Bedding and Sedimentary Structures**		**Grainsize**
Greeny-brown	Friable			Fine to medium
Grain or matrix supported	**Sorting**	**Roundness**	**Sphericity - shape**	**Biologic binding**
Grain	Moderate			No
Textural Name:	**Packstone**	**Notes:**	Glauconite-rich	

Thin Section Description

Matrix	**Percentage /100**
Clastics: Quartz (angular to subangular)	2%
Cement	3%
Mud	30%
Bioclasts	50%
Authigenic minerals: Glauconite (80%), hematite (20%)	15%

Foraminifera	**Percentage /100**
Planktic	61% (n=84)
Benthic	39% (n=54)

Bioclasts	**Percentage of identified/total**
Foraminifera	75%/44%
Bryozoans	5%/3%
Echinoderms	20%/13%
Algae	0%/0%
Molluscs	0%/0%
Brachiopods	0%/0%
Barnacles	0%/0%
Sponge spicules	0%/0%
Worm Tubes	0%/0%
Unidentified bioclasts	40%

Notes from thin section:	Some plucking in slide. Glauconite grains are rounded to subangular, with some showing internal fracturing, and occasional intraclast formation. Hematite has formed almost exclusively over glauconite grains. Benthics are microcrystalline with a few hyaline, and few agglutinates. Tests are biserial, involute coil, uniserial. Micrite volumes may be obscuring a number of microcrytalline benthics. Some indistinguishable shell material included in the unidentified bioclasts.

Stratigraphic Column:	NT09/06		
Sample Number:	OT1	**Location:**	Gee's Point
Date Collected:	7/5/12	**Formation:**	Ototara Limestone

Thin Section Description

Matrix	Percentage /100
Clastics: Quartz	0%
Cement	8%
Mud	40%
Bioclasts	49%
Authigenic minerals: Glauconite (10%), hematite (90%)	3%

Bioclasts	Percentage of identified/total
Foraminifera	15%/14%
Bryozoans	49%/47%
Echinoderms	18%/17%
Algae	15%/14%
Molluscs	0%/0%
Brachiopods	3%/3%
Barnacles	0%/0%
Sponge spicules	0%/0%
Worm Tubes	0%/0%
Unidentified bioclasts	5%

Notes from thin section:	Very mud-rich slide. Cement forms as isopachous or blocky spar overgrowths, or replacement of echinoids. Hematisation of some probable glauconite, mostly as interspace precipitation. Significant amounts of corraline algae, bryozoan and echinoid fragments. Some large benthic forams. Some punctate brachiopod fragments. Rounded algal fragments. Some borings. Large bioclastic fragments throughout.

Stratigraphic Column:	NT09/07		
Sample Number:	NT10061605	**Location:**	Alma Pillow Lavas
Date Collected:	6/16/10	**Formation:**	Ototara Lst

Hand Specimen Description

Colour	**Induration**	**Bedding and Sedimentary Structures**		**Grainsize**
Yellowish-white	Very well indurated			n/a
Grain or matrix supported	**Sorting**	**Roundness**	**Sphericity - shape**	**Biologic binding**
n/a	n/a			Yes
Textural Name:	**Bindstone**	**Notes:**	Algal balls.	

Thin Section Description

Matrix	**Percentage /100**
Clastics: Rounded carbonate clasts	3%
Cement	10%
Mud	10%
Bioclasts	76%
Authigenic minerals: Glauconite (20%), phosphate(40%), hematite (40%)	1%

Foraminifera	**Percentage /100**
Planktic	0% (n=0)
Benthic	100% (n=13)

Bioclasts	**Percentage of identified/total**
Foraminifera	3%/3%
Bryozoans	5%/5%
Echinoderms	0%/0%
Algae	85%/75%
Molluscs	5%/5%
Brachiopods	0%/0%
Barnacles	2%/2%
Sponge spicules	0%/0%
Worm Tubes	0%/0%
Unidentified bioclasts	10%

Notes from thin section:	This is an unusual slide, with large amounts of algae, large neomorphosed mollusc, and carbonate extraclasts included. Looks to have geopetal fabric within void spaces. Bryozoans encrusting algae. Algae itself appears to be encrusting clasts, while within the encrusted fill there are coralline algae fragments. Mixed phosphate and isotropics clasts, as well as some hematised glauconite (?). Forams almost entirely found within clast material that has been encrusted with algae. Benthics are biserial, trochospiral, coils with most being microcrystalline and a couple of hyalines. Cements are large and blocky, trending into micrite within geopetal fabrics. Large neomorphosed mollusc shell that is forming the centre of a large portion of the slide that has been encrusted by the algae.

Stratigraphic Column:	NT09/07		
Sample Number:	NT10061606	**Location:**	Alma Pillows
Date Collected:	6/16/10	**Formation:**	Ash beds overlying pillows

Hand Specimen Description

Colour	**Induration**	**Bedding and Sedimentary Structures**		**Grainsize**
Greeny-brown	Friable			Fine to medium
Grain or matrix supported	**Sorting**	**Roundness**	**Sphericity - shape**	**Biologic binding**
Grain	Moderate			No
Textural Name:	**Agglomerate (packstone)**	**Notes:**		

Thin Section Description

Matrix	**Percentage /100**
Clastics: Amphibole, biotite, extraclasts, isotropics	45%
Cement	8%
Mud	7%
Bioclasts	0%
Authigenic minerals: Glauconite (hematised)	40%

Foraminifera	**Percentage /100**
Planktic	n/a
Benthic	n/a

Bioclasts	**Percentage of identified/total**
Foraminifera	n/a
Bryozoans	n/a
Echinoderms	n/a
Algae	n/a
Molluscs	n/a
Brachiopods	n/a
Barnacles	n/a
Sponge spicules	n/a
Worm Tubes	n/a
Unidentified bioclasts	n/a

Notes from thin section:	Volcanic ash with carbonate cements. One side of the slide is predominantly angular-subangular glauconite (?) grains in a micritic (with some cement) matrix, alongside some (amphibole) clasts. Larger clasts tend to have a micritic rind around them, with hematite alteration from the outside of the grains towards the centre. The other half of the slide seems to be predominantly angular to subrounded clasts of volcanic (some show feldspar lathes) origin, some showing vesicles, or half vesicles where the clasts has been broken. A number have a cement rind to them that is distinct from the blocky cement filling the interstices between the clasts. Hematite alteration around clasts and over cement in some places. No fossils have been observed.

Stratigraphic Column:	NT09/07		
Sample Number:	NT10061609	**Location:**	Alma Pillow Lavas
Date Collected:	6/16/10	**Formation:**	Ototara Lst (onlapping tuff)

Hand Specimen Description

Colour	**Induration**	**Bedding and Sedimentary Structures**		**Grainsize**
Orangey-brown	Friable			Fine to very coarse
Grain or matrix supported	**Sorting**	**Roundness**	**Sphericity - shape**	**Biologic binding**
Grain	Very poor			No
Textural Name:	**Rudstone**	**Notes:**	Fossiliferous	

Thin Section Description

Matrix	**Percentage /100**
Clastics: Quartz (angular)	Trace
Cement	15%
Mud	5%
Bioclasts	77%
Authigenic minerals: Glauconite (20%), phosphate (80%)	3%

Foraminifera	**Percentage /100**
Planktic	0% (n=0)
Benthic	100% (n=25)

Bioclasts	**Percentage of identified/total**
Foraminifera	5%/5%
Bryozoans	60%/57%
Echinoderms	12%/11%
Algae	18%/17%
Molluscs	2%/2%
Brachiopods	2%/2%
Barnacles	1%/1%
Sponge spicules	0%/0%
Worm Tubes	0%/0%
Unidentified bioclasts	5%

Notes from thin section:	Poor slide with significant plucking. Glauconite and phosphate is mostly of clasts, including being present as growth inside echinoid fragments and inside bioclast chambers. Microcrystalline calcite cement overgrowths in syn extinction with echinoid fragments. Isopachous cements inside some bioclast chambers and off some bioclasts rims. Benthics are uniserial, rotallid, trochospiral, biserial, and coiled. Tests are nearly all microcrystalline, with one observed hyaline trochospiral. Coralline algae fragments.

Stratigraphic Column:	NT09/07		
Sample Number:	NT10061610	**Location:**	Alma Pillow Lavas
Date Collected:	6/16/10	**Formation:**	Ototara Lst

Hand Specimen Description

Colour	**Induration**	**Bedding and Sedimentary Structures**		**Grainsize**
Yellowish-white	Indurate			Silt to fine
Grain or matrix supported	**Sorting**	**Roundness**	**Sphericity - shape**	**Biologic binding**
Matrix	Moderate			No
Textural Name:	**Wackestone**	**Notes:**	Fossiliferous	

Thin Section Description

Matrix	**Percentage /100**
Clastics:	None
Cement	3%
Mud	40%
Bioclasts	56%
Authigenic minerals: Glauconite (15%), phosphate (85%)	1%

Foraminifera	**Percentage /100**
Planktic	1% (n=1)
Benthic	99% (n=97)

Bioclasts	**Percentage of identified/total**
Foraminifera	18%/15%
Bryozoans	65%/59%
Echinoderms	15%/14%
Algae	2%/2%
Molluscs	0%/0%
Brachiopods	0%/0%
Barnacles	0%/0%
Sponge spicules	0%/0%
Worm Tubes	0%/0%
Unidentified bioclasts	10%

Notes from thin section:	Average quality slide, with some plucking present, and some dirty fragments in some parts. There appears to be an alignment fabric in the clasts. Cements are syn-extinctional blocky overgrowths on enchinoid clasts or drusy/blocky growths on the chambers/rims of other bioclasts. Benthic test morphologies are trochospiral, coil, uniserial and some nummulites. Tests are predominantly microcrystalline with some trochosprials and all nummulites being hyaline. Some shell fragments, but indistinct.

Stratigraphic Column:	NT09/07		
Sample Number:	NT10061608	**Location:**	Alma Pillow Lavas
Date Collected:	6/16/10	**Formation:**	Deborah/Waireka Volcanics

Thin Section Description

Matrix	Percentage /100
Clastics: Igneous clasts (angular) and tuff	80%
Cement	20%
Mud	0%
Bioclasts	0%
Authigenic minerals: Glauconite	0%

Foraminifera	Percentage /100
Planktic	n/a
Benthic	n/a

Bioclasts	Percentage of identified/total
Foraminifera	n/a
Bryozoans	n/a
Echinoderms	n/a
Algae	n/a
Molluscs	n/a
Brachiopods	n/a
Barnacles	n/a
Sponge spicules	n/a
Worm Tubes	n/a
Unidentified bioclasts	n/a

Notes from thin section:	Loose sediments in resin. Fissures through clasts of tuff that contain spary cement. Isolated calcite pockets throughout also. Biotite crystals within igneous clastes. Void spaces infilled with calcite.

Stratigraphic Column:	NT09/07		
Sample Number:	NT10061603	**Location:**	Alma Pillow Lavas
Date Collected:	6/16/10	**Formation:**	Ototara Lst

Hand Specimen Description

Colour	**Induration**	**Bedding and Sedimentary Structures**		**Grainsize**
Brownish-white	Indurated			Fine to coarse
Grain or matrix supported	**Sorting**	**Roundness**	**Sphericity - shape**	**Biologic binding**
Grain	Poor			Yes
Textural Name:	**Bindstone**	**Notes:**	Algal balls	

Thin Section Description

Matrix	**Percentage /100**
Clastics: Igneous clasts (rounded)	Trace
Cement	15%
Mud	15%
Bioclasts	69%
Authigenic minerals: Hematite	1%

Foraminifera	**Percentage /100**
Planktic	6% (n=1)
Benthic	94% (n=17)

Bioclasts	**Percentage of identified/total**
Foraminifera	3%/3%
Bryozoans	10%/10%
Echinoderms	0%/0%
Algae	87%/82%
Molluscs	0%/0%
Brachiopods	0%/0%
Barnacles	0%/0%
Sponge spicules	0%/0%
Worm Tubes	0%/0%
Unidentified bioclasts	5%

Notes from thin section:	Algal ball section over volcanic clasts. Small remnant of the volcanic clasts (mafic) shown in slide but not included in this description. Apparent geopetal texture within some voids between algae layers, with spary cement at one end and micrite at the other. Very good blocky calcite cement occuring between algae layers, often abutting micrite. Some minor hematite occuring around the edges of the slide. Forams and any other bioclastic material is found within the micrite between algae layers. Banded encrusting red algae, with some void space containing fragments of algae also. Bethics are nummulites, biserial, and coiled (planar, trochospiral). Tests are mostly microcrystalline with some hyalines.

Stratigraphic Column:	NT09/08		
Sample Number:	NT09060901	**Location:**	Prydes Gully Quarry
Date Collected:	6/9/09	**Formation:**	Otekaike Lst

Hand Specimen Description

Colour	**Induration**	**Bedding and Sedimentary Structures**		**Grainsize**
Greenish-white	Indurated			Fine
Grain or matrix supported	**Sorting**	**Roundness**	**Sphericity - shape**	**Biologic binding**
Grain	Well			No
Textural Name:	**Packstone**	**Notes:**	Glauconitic (25%)	

Thin Section Description

Matrix	**Percentage /100**
Clastics: Quartz (angular), biotite - trace (euhedral)	7%
Cement	2%
Mud	10%
Bioclasts	71%
Authigenic minerals: Glauconite	10%

Foraminifera	**Percentage /100**
Planktic	30% (n=46)
Benthic	70% (n=109)

Bioclasts	**Percentage of identified/total**
Foraminifera	75%/60%
Bryozoans	0%/0%
Echinoderms	25%/20%
Algae	0%/0%
Molluscs	0%/0%
Brachiopods	0%/0%
Barnacles	0%/0%
Sponge spicules	0%/0%
Worm Tubes	0%/0%
Unidentified bioclasts	20%

Notes from thin section:	Syn-extinctional blocky cement overgrowths on echinoid fragments. Bored shell fragments. Glauconite grains are sub-rounded to subangular with some intraclast growth inside bioclast void space. Some glauconitised biotite crystals. Benthic tests are coil, biserial, uniserial. Some planktics may be obscured in the micrite matrix. Benthic tests are mostly microcrystalline, with some hyalines. One larger quartz agglomerate uniserial benthic present.

Stratigraphic Column:	NT09/09		
Sample Number:	NT09060902	**Location:**	Tokarahi-Ngapara Rd cliffs
Date Collected:	6/9/09	**Formation:**	Otekaike Lst

Hand Specimen Description

Colour	**Induration**	**Bedding and Sedimentary Structures**		**Grainsize**
White	Indurated			Very fine to fine
Grain or matrix supported	**Sorting**	**Roundness**	**Sphericity - shape**	**Biologic binding**
Grain	Well			No
Textural Name:	**Packstone**	**Notes:**	Shell fragments.	

Thin Section Description

Matrix	**Percentage /100**
Clastics:	3%
Cement	3%
Mud	20%
Bioclasts	69%
Authigenic minerals:	5%

Foraminifera	**Percentage /100**
Planktic	32% (n=39)
Benthic	68% (n=83)

Bioclasts	**Percentage of identified/total**
Foraminifera	83%/42%
Bryozoans	0%/0%
Echinoderms	15%/8%
Algae	0%/0%
Molluscs	1%/<1%
Brachiopods	1%/<1%
Barnacles	0%/0%
Sponge spicules	0%/0%
Worm Tubes	0%/0%
Unidentified bioclasts	50%

Notes from thin section:	Quite a dirty slide. Glauconite grains are subangular to rounded with some intraclast formation. Benthic tests are coiled, uniserial, trochospiral, biserial with mostly microcrystalline tests and some hyalines. Syn-exticntional cements on echinoid fragments.

Stratigraphic Column:	NT09/09		
Sample Number:	NT09060903	**Location:**	Tokarahi-Ngapara Rd Cliffs
Date Collected:	6/9/09	**Formation:**	Otekaike Lst

Hand Specimen Description

Colour	**Induration**	**Bedding and Sedimentary Structures**		**Grainsize**
Yellowish-white	Well			Fine-medium
Grain or matrix supported	**Sorting**	**Roundness**	**Sphericity - shape**	**Biologic binding**
Matrix	Well			No
Textural Name:	**Wackestone**	**Notes:**		

Thin Section Description

Matrix	**Percentage /100**
Clastics: Quartz (angular-sub angular), trace biotites	2%
Cement	30%
Mud	10%
Bioclasts	55%
Authigenic minerals: Glauconite	3%

Foraminifera	**Percentage /100**
Planktic	30% (n=24)
Benthic	70% (n=78)

Bioclasts	**Percentage of identified/total**
Foraminifera	49%/24%
Bryozoans	0%/0%
Echinoderms	50%/25%
Algae	0%/0%
Molluscs	0%/0%
Brachiopods	1%/1%
Barnacles	0%/0%
Sponge spicules	0%/0%
Worm Tubes	0%/0%
Unidentified bioclasts	50%

Notes from thin section:	Micritic-rich section, making some bioclast identification difficult. Blocky cement overgrowths around most clasts. Glauconite grains are rounded to subangular with some inside bioclast chambers as intraclast growth. Some glauconitised biotites. Benthic tests are uniserial, coiled, biserial, and trochosprial. Tests are predominantly microcrystalline for benthics, with a few hyalines. Numerous broken tests. Lots of broken, unidentified bioclastic material - some clear undiscernable shell pieces - some micritisation.

Stratigraphic Column:	NT09/09		
Sample Number:	NT09060904	**Location:**	Tokarahi-Ngapara Rd Cliffs
Date Collected:	6/9/09	**Formation:**	Otekaike Lst

Thin Section Description

Matrix	Percentage /100
Clastics: Quartz (angular - sub-rounded)	5%
Cement	Trace
Mud	30%
Bioclasts	57%
Authigenic minerals: Glauconite (50%), hematite (50%)	8%

Foraminifera	Percentage /100
Planktic	37% (n=74)
Benthic	63% (n=127)

Bioclasts	Percentage of identified/total
Foraminifera	41%/14%
Bryozoans	3%/1%
Echinoderms	45%/16%
Algae	0%/0%
Molluscs	10%/4%
Brachiopods	1%/<1%
Barnacles	0%/0%
Sponge spicules	0%/0%
Worm Tubes	0%/0%
Unidentified bioclasts	65%

Notes from thin section:	Some plucking in this slide. Small traces of cement on rims of echinoid fragments. Glauconite grains (rounded - sub-rounded) as well as intraclast growth within bioclasts. Common hematite alteration of glauconite as well as some localised matrix. Benthics are coiled (planar, trochospiral), uniserial, and biserial. Tests are microcrystalline and hyaline, with a few larger hyaline benthic tests. Micritic matrix may have obscured some tests in a few locations on the slide. One punctate brachiopod fragment. Some borings evident on shell fragments. Unidentified bioclasts are shell fragments.

Stratigraphic Column:	NT09/10		
Sample Number:	NT09060905	**Location:**	Anatini
Date Collected:	6/9/09	**Formation:**	Otekaike Lst

Hand Specimen Description

Colour	**Induration**	**Bedding and Sedimentary Structures**		**Grainsize**
Cream	Indurated			Fine
Grain or matrix supported	**Sorting**	**Roundness**	**Sphericity - shape**	**Biologic binding**
Grain	Well			No
Textural Name:	**Packstone**	**Notes:**		

Thin Section Description

Matrix	**Percentage /100**
Clastics: Quartz (angular-subrounded)	1%
Cement	7%
Mud	25%
Bioclasts	64%
Authigenic minerals: Glauconite (80%) (rounded to subangular), hematite (20%)	3%

Foraminifera	**Percentage /100**
Planktic	42% (n=73)
Benthic	58% (n=101)

Bioclasts	**Percentage of identified/total**
Foraminifera	70%/29%
Bryozoans	0%/0%
Echinoderms	30%/11%
Algae	0%/0%
Molluscs	0%/0%
Brachiopods	0%/0%
Barnacles	0%/0%
Sponge spicules	0%/0%
Worm Tubes	0%/0%
Unidentified bioclasts	60%

Notes from thin section:	Some plucking, and a fairly micritic slide. Glauconite is present as grains and also as intraclast growth, with some hematisation of the latter. Benthics are coiled, trochospiral, uniserial, biserial and triserial. Most benthic tests are microcrystalline with some hylines present. Calcite cement overgrowths on echinoid fragments, with some isopachous cement inside and rimming various bioclasts.

Stratigraphic Column:	NT09/10		
Sample Number:	NT10061514	**Location:**	Anatini
Date Collected:	6/15/10	**Formation:**	Otekaike Lst

Hand Specimen Description

Colour	Induration	Bedding and Sedimentary Structures		Grainsize
Yellowish-white	Friable			Fine
Grain or matrix supported	**Sorting**	**Roundness**	**Sphericity - shape**	**Biologic binding**
Grain	Well			No
Textural Name:	**Packstone**	**Notes:**	Shell fragments	

Thin Section Description

Matrix	Percentage /100
Clastics: Quartz (subrounded - angular)	2%
Cement	8%
Mud	30%
Bioclasts	58%
Authigenic minerals: Glauconite, hematite (trace), phosphate (trace)	2%

Foraminifera	Percentage /100
Planktic	59% (n=86)
Benthic	41% (n=61)

Bioclasts	Percentage of identified/total
Foraminifera	78%/39%
Bryozoans	2%/1%
Echinoderms	20%/10%
Algae	0%/0%
Molluscs	0%/0%
Brachiopods	0%/0%
Barnacles	0%/0%
Sponge spicules	0%/0%
Worm Tubes	0%/0%
Unidentified bioclasts	50%

Notes from thin section:	Heavily micitised section, makes some bioclast identification difficult. Glauconite is present as rounded grains and intraclast formation. Some hematite and phosphate alteration of glauconite has occured. Blocky cement overgrowths on bioclasts (enchinoids), with some isopachous cement inside tests. Benthic tests are biserial, uniserial, coiled, trochospiral. Microcrystalline and hyaline tests seen in similiar proportions, although it is likely that the number of microcrystalline benthic tests observed is lower than actual due to the micrite matrix ad general dirtiness of the slide. This may artificially increase the planktic ratio somewhat. Lots of bioclasts fragments, including indistinct shell pieces.

Stratigraphic Column:	NT09/10		
Sample Number:	NT10061515	**Location:**	Anatini
Date Collected:	6/15/10	**Formation:**	Otekaike Lst

Hand Specimen Description

Colour	**Induration**	**Bedding and Sedimentary Structures**		**Grainsize**
Cream	Friable			Fine
Grain or matrix supported	**Sorting**	**Roundness**	**Sphericity - shape**	**Biologic binding**
Matrix	Well			No
Textural Name:	**Wackestone**	**Notes:**		

Thin Section Description

Matrix	**Percentage /100**
Clastics: Quartz (angular)	2%
Cement	2%
Mud	30%
Bioclasts	63%
Authigenic minerals: Glauconite	3%

Foraminifera	**Percentage /100**
Planktic	44% (n=58)
Benthic	56% (n=74)

Bioclasts	**Percentage of identified/total**
Foraminifera	89%/36%
Bryozoans	0%/0%
Echinoderms	10%/4%
Algae	0%/0%
Molluscs	1%/<1%
Brachiopods	0%/0%
Barnacles	0%/0%
Sponge spicules	0%/0%
Worm Tubes	0%/0%
Unidentified bioclasts	60%

Notes from thin section:	Rather micritised slide. Minor cement overgrowths on some clasts, predominantly rim blocky cements with some very minor isopachous calcite observed inside foram test chambers. Most glauconite is found as intraclast growth. Benthic tests are coiled, trichospiral, uniserial, involute coil, and biserial. Most benthic tests are microcrystalline, with some hyalines. Miciritc alteration and some plucking may be obscuring some forams of both types. Lots of broken shell material and micritised bioclasts.

Stratigraphic Column:	NT09/10		
Sample Number:	NT10061516	**Location:**	Anatini
Date Collected:	6/15/10	**Formation:**	Otekaike Lst

Hand Specimen Description

Colour	**Induration**	**Bedding and Sedimentary Structures**		**Grainsize**
Cream	Friable			Fine to medium
Grain or matrix supported	**Sorting**	**Roundness**	**Sphericity - shape**	**Biologic binding**
Grain	Moderate			No
Textural Name:	**Packstone**	**Notes:**		

Thin Section Description

Matrix	**Percentage /100**
Clastics: Quartz (angular to subangular)	1%
Cement	8%
Mud	25%
Bioclasts	64%
Authigenic minerals: Glauconite (95%), hematite (5%)	2%

Foraminifera	**Percentage /100**
Planktic	46% (n=88)
Benthic	54% (n=105)

Bioclasts	**Percentage of identified/total**
Foraminifera	74%/43%
Bryozoans	0%/0%
Echinoderms	25%/16%
Algae	0%/0%
Molluscs	0%/0%
Brachiopods	1%/1%
Barnacles	0%/0%
Sponge spicules	0%/0%
Worm Tubes	0%/0%
Unidentified bioclasts	40%

Notes from thin section:	Micritic slide with some obscured bioclasts. Glauconite is rounded grains or intraclast growth with some minor hematite alteration is some places. Benthics are uniserial, coiled, trochospiral, and biserial. Tests are mostly microcrystalline and some hyalines. A number of broken tests are present. Blocky calcite cements overgrowing numerous clasts. One large piece of punctate brachiopod.

Stratigraphic Column: NT09/11

Sample Number: NT09061008 **Location:** Raupo Creek

Date Collected: 6/10/09 **Formation:** Tapui Sandstone

Thin Section Description

Matrix	Percentage /100
Clastics: Quartz (angular - sub-angular)	82%
Cement	0%
Mud	15%
Bioclasts	0%
Authigenic minerals: Glauconite (50%), hematite (50%)	3%

Foraminifera	Percentage /100
Planktic	n/a
Benthic	n/a

Bioclasts	Percentage of identified/total
Foraminifera	n/a
Bryozoans	n/a
Echinoderms	n/a
Algae	n/a
Molluscs	n/a
Brachiopods	n/a
Barnacles	n/a
Sponge spicules	n/a
Worm Tubes	n/a
Unidentified bioclasts	n/a

Notes from thin section:	Loose sediment in resin. Glauconite is rounded grains. Some minor hematite alteration of glauconites and matrix. Clay/mud forming matrix between quartz grains.

Stratigraphic Column:	NT09/11		
Sample Number:	NT09061005	**Location:**	Raupo Creek
Date Collected:	6/10/09	**Formation:**	Tapui Sandstone

Hand Specimen Description

Colour	**Induration**	**Bedding and Sedimentary Structures**		**Grainsize**
Yellowish-brown	Unconsolidated			Silt
Grain or matrix supported	**Sorting**	**Roundness**	**Sphericity - shape**	**Biologic binding**
Matrix	Very well			No
Textural Name:	**Mudstone**	**Notes:**		

Thin Section Description

Matrix	**Percentage /100**
Clastics: Quartz (sub-rounded - angular)	83%
Cement	0%
Mud	14%
Bioclasts	0%
Authigenic minerals: Glauconite	3%

Foraminifera	**Percentage /100**
Planktic	n/a
Benthic	n/a

Bioclasts	**Percentage of identified/total**
Foraminifera	n/a
Bryozoans	n/a
Echinoderms	n/a
Algae	n/a
Molluscs	n/a
Brachiopods	n/a
Barnacles	n/a
Sponge spicules	n/a
Worm Tubes	n/a
Unidentified bioclasts	n/a

Notes from thin section:	Loose sediment in resin. Quartz sands with pockets of clay. No observed bioclasts. Glauconite grains are rounded to sub-rounded and evenly dispersed.

Stratigraphic Column:	NT09/12		
Sample Number:	NT09061011	**Location:**	Fuchsia Creek
Date Collected:	6/10/09	**Formation:**	Taratu Formation

Hand Specimen Description

Colour	Induration	Bedding and Sedimentary Structures		Grainsize
White	Friable			Silt
Grain or matrix supported	**Sorting**	**Roundness**	**Sphericity - shape**	**Biologic binding**
n/a	Well			No
Textural Name:	**Siltstone**	**Notes:**		

Thin Section Description

Matrix	Percentage /100
Clastics: Quartz (angular - sub-rounded)	100%
Cement	0%
Mud	0%
Bioclasts	0%
Authigenic minerals:	0%

Foraminifera	Percentage /100
Planktic	n/a
Benthic	n/a

Bioclasts	Percentage of identified/total
Foraminifera	n/a
Bryozoans	n/a
Echinoderms	n/a
Algae	n/a
Molluscs	n/a
Brachiopods	n/a
Barnacles	n/a
Sponge spicules	n/a
Worm Tubes	n/a
Unidentified bioclasts	n/a

Notes from thin section:	Loose sediment in resin. Appears to be just small angular - sub-rounded quartz grains. No apparent matrix preservation. No bioclasts.

Stratigraphic Column:	NT09/13		
Sample Number:	NT09061015	**Location:**	Fuchsia Creek Road-cut
Date Collected:	6/10/09	**Formation:**	Taratu Formation

Hand Specimen Description

Colour	**Induration**	**Bedding and Sedimentary Structures**		**Grainsize**
White	Friable			Silt
Grain or matrix supported	**Sorting**	**Roundness**	**Sphericity - shape**	**Biologic binding**
n/a	Well			No
Textural Name:	**Siltstone**	**Notes:**	Siliciclastic	

Thin Section Description

Matrix	**Percentage /100**
Clastics: Quartz (angular - sub-rounded)	99%
Cement	0%
Mud	0%
Bioclasts	0%
Authigenic minerals: Glauconite	1%

Foraminifera	**Percentage /100**
Planktic	n/a
Benthic	n/a

Bioclasts	**Percentage of identified/total**
Foraminifera	n/a
Bryozoans	n/a
Echinoderms	n/a
Algae	n/a
Molluscs	n/a
Brachiopods	n/a
Barnacles	n/a
Sponge spicules	n/a
Worm Tubes	n/a
Unidentified bioclasts	n/a

Notes from thin section:	Loose sediment in resin. Sub-angular to sub-rounded glauconite grains.

Stratigraphic Column: NT09/14

Sample Number: NT09061201 **Location:** Trig Z

Date Collected: 6/12/09 **Formation:** Otekaike Lst

Thin Section Description

Matrix	Percentage /100
Clastics: Quartz (angular - sub-rounded)	10%
Cement	0%
Mud	15%
Bioclasts	65%
Authigenic minerals: Glauconite	10%

Foraminifera	Percentage /100
Planktic	35% (n=64)
Benthic	65% (n=110)

Bioclasts	Percentage of identified/total
Foraminifera	80%/28%
Bryozoans	0%/0%
Echinoderms	2%/1%
Algae	0%/0%
Molluscs	15%/5%
Brachiopods	3%/1%
Barnacles	0%/0%
Sponge spicules	0%/0%
Worm Tubes	0%/0%
Unidentified bioclasts	65%

Notes from thin section:	Loose sediment in resin. Mud estimates are taken from large sediment clumps within the resin. Glauconite grains are sub-angular to sub-rounded with somewhat lesser amounts of intraclast growth. Benthics are coiled (planar, trochospiral), uniserial, and biserial. Tests are microcrystalline and hyaline. Mollusc and brachiopod fragments are often small, with some showing borings. Unidentified bioclasts are mostly shell fragments.

Stratigraphic Column: NT09/14

Sample Number: NT09061205 **Location:** Trig Z

Date Collected: 6/12/09 **Formation:** Otekaike Lst

Thin Section Description

Matrix	Percentage /100
Clastics: Quartz (angular)	4%
Cement	Trace
Mud	5%
Bioclasts	84%
Authigenic minerals: Glauconite (90%), hematite (10%)	7%

Foraminifera	Percentage /100
Planktic	26% (n=38)
Benthic	74% (n=110)

Bioclasts	Percentage of identified/total
Foraminifera	57%/11%
Bryozoans	0%/0%
Echinoderms	10%/2%
Algae	0%/0%
Molluscs	30%/6%
Brachiopods	3%/1%
Barnacles	0%/0%
Sponge spicules	0%/0%
Worm Tubes	0%/0%
Unidentified bioclasts	80%

Notes from thin section:	Loose sediment in resin. Glauconite grains are rounded to sub-angular. Some glauconite formed within bioclast void spaces, as well as glauconitisation of the rims of mollusc fragments. Some hematite alteration of matrix and glauconite grains. Benthics are coiled (planar, trochospiral), uniserial, and biserial. Tests are mostly microcrystalline with some hyalines and a couple of quartz agglutinates. Some large benthics. Large prismatic and cross-laminated mollusc fragments, with some showing heavy boring and glauconite fill of boreholes. Mollusc appear to be a mix of dominantly bivalves, with at least one scaphopod and gastropod. Some larger echinoid plate fragments, although most are small. One larger punctate brachiopod fragment. Unidentifed bioclasts are small shell fragments and other amorphous fragments.

Stratigraphic Column:	NT09/14		
Sample Number:	NT09061206	**Location:**	Trig Z
Date Collected:	6/12/09	**Formation:**	Otekaike Lst

Hand Specimen Description

Colour	**Induration**	**Bedding and Sedimentary Structures**		**Grainsize**
Yelloish-white	Friable			Fine
Grain or matrix supported	**Sorting**	**Roundness**	**Sphericity - shape**	**Biologic binding**
Grain	Well			No
Textural Name:	**Packstone**	**Notes:**	Bioturbation	

Thin Section Description

Matrix	**Percentage /100**
Clastics: Quartz (angular-subangular)	7%
Cement	trace
Mud	30%
Bioclasts	43%
Authigenic minerals: Glauconite (25%), hematite (75%)	20%

Foraminifera	**Percentage /100**
Planktic	60% (n=101)
Benthic	40% (n=67)

Bioclasts	**Percentage of identified/total**
Foraminifera	90%/54%
Bryozoans	0%/0%
Echinoderms	0%/0%
Algae	0%/0%
Molluscs	3%/2%
Brachiopods	7%/4%
Barnacles	0%/0%
Sponge spicules	0%/0%
Worm Tubes	0%/0%
Unidentified bioclasts	40%

Notes from thin section:	Very micritic slide, with significant hematite alteration that makes it harder to identify bioclasts. Glauconite is present as grains and as intraclast growth, with most being hematised. Hematisation of around 20% of the clasts and surrounding micrite content, varying in intensity from light to heavy. Benthics are coiled, uniserial, biserial, trochospiral and milioloid. Benthic tests are predominantly microcrystalline with a few hyalines. Micrite matrix may be obscuring some benthics, skewing the ratio towards the planktics. Some broken shell peices, including some neomorphosed mollusc fragments.

Stratigraphic Column: NT09/14

Sample Number: NT09061207 **Location:** Trig Z

Date Collected: 6/12/09 **Formation:** Otekaike Lst

Thin Section Description

Matrix	Percentage /100
Clastics: Quartz (angular - rounded)	5%
Cement	Trace
Mud	45%
Bioclasts	40%
Authigenic minerals: Glauconite	10%

Foraminifera	Percentage /100
Planktic	38% (n=49)
Benthic	62% (n=79)

Bioclasts	Percentage of identified/total
Foraminifera	63%/25%
Bryozoans	2%/1%
Echinoderms	0%/0%
Algae	0%/0%
Molluscs	30%/12%
Brachiopods	5%/2%
Barnacles	0%/0%
Sponge spicules	0%/0%
Worm Tubes	0%/0%
Unidentified bioclasts	60%

Notes from thin section:	Quartz grains are bimodal, with some larger rounded grains. Some minor blocky spar cement, observed within foram tests. Loose sediment in resin. Rounded glauconite grains and intraclast growth within bioclasts. Coiled (planar, trochospiral), uniserial, with one possible milliolid. Tests are microcrystalline with some hyalines. Some large benthics. Punctate brachiopods. Some heavy borings in mollusc shells. Some shells are large fragments. Glauconitisation within borings.

Stratigraphic Column:	NT09/14		
Sample Number:	NT10012201	**Location:**	Trig Z
Date Collected:	1/22/10	**Formation:**	Gee Greensand

Thin Section Description

Matrix	Percentage /100
Clastics: Quartz (angular - sub-rounded)	25%
Cement	0%
Mud	5%
Bioclasts	0%
Authigenic minerals: Glauconite (85%), hematite (15%)	70%

Foraminifera	Percentage /100
Planktic	n/a
Benthic	n/a

Bioclasts	Percentage of identified/total
Foraminifera	0%/0%
Bryozoans	0%/0%
Echinoderms	0%/0%
Algae	0%/0%
Molluscs	100%/60%
Brachiopods	0%/0%
Barnacles	0%/0%
Sponge spicules	0%/0%
Worm Tubes	0%/0%
Unidentified bioclasts	40%

Notes from thin section:	Loose sediment in resin. Matrix is hard to identify as it is nearly all hematite altered, as well as this slide is set in resin with a matrix that is probably unidicative of the in situ lithology. Glauconite grains are bimodal, with the larger being rounded and the smaller being rounded to sub-rounded. Bioclasts are almost totally absent, but what is there appears to be mollusc fragments with prismatic structure.

Stratigraphic Column:	NT09/14		
Sample Number:	NT10012202	**Location:**	Trig Z
Date Collected:	1/22/10	**Formation:**	Otekaike Lst

Thin Section Description

Matrix	Percentage /100
Clastics: Quartz (99%) (angular-rounded), biotite (1%)	40%
Cement	0%
Mud	15%
Bioclasts	0%
Authigenic minerals: Glauconite, hematite	45%

Foraminifera	Percentage /100
Planktic	n/a
Benthic	n/a

Bioclasts	Percentage of identified/total
Foraminifera	n/a
Bryozoans	n/a
Echinoderms	n/a
Algae	n/a
Molluscs	n/a
Brachiopods	n/a
Barnacles	n/a
Sponge spicules	n/a
Worm Tubes	n/a
Unidentified bioclasts	n/a

Notes from thin section:	Loose sediment in resin. Glauconite is sub-rounded to rounded clasts, with a significant amount of interclast growth as matrix. Hematite as formed on some of this, as well as a few grains that have heavy hematite alteration to the degree that they are now isotropic. No obvious bioclasts. Matrix appears to be mostly glauonitised micrite muds.

Stratigraphic Column:	NT09/14		
Sample Number:	NT10012203	**Location:**	Trig Z
Date Collected:	1/22/10	**Formation:**	Otekaike Lst

Thin Section Description

Matrix	Percentage /100
Clastics: Quartz (sub-rounded - sub-angular)	6%
Cement	1%
Mud	7%
Bioclasts	46%
Authigenic minerals: Glauconite (97%), hematite (3%)	40%

Foraminifera	Percentage /100
Planktic	29% (n=38)
Benthic	71% (n=93)

Bioclasts	Percentage of identified/total
Foraminifera	30%/11%
Bryozoans	3%/1%
Echinoderms	0%/0%
Algae	0%/0%
Molluscs	47%/16%
Brachiopods	14%/5%
Barnacles	3%/1%
Sponge spicules	3%/1%
Worm Tubes	0%/0%
Unidentified bioclasts	65%

Notes from thin section:	Loose sediment in resin. Matrix estimates are based solely on remnant attached to clasts due to the loose grain nature of the slide. Hematite found primarily as altered matrix around glauconite grains within one clast. Hematite grains are rounded to sub-rounded and relatively fresh. Benthics are coiled (planar, trochospiral), uniserial, and biserial. Most are microcrystalline with a few hyalines, and some larger quartz agglutinates. Some shell fragments are glauconitised and bored. One observed radiolarian. Large amounts of shell fragments within unidentified bioclasts.

Stratigraphic Column: NT09/14

Sample Number: NT10012207 **Location:** Trig Z

Date Collected: 1/22/10 **Formation:** Otekaike Lst

Thin Section Description

Matrix	Percentage /100
Clastics: Quartz (angular - sub-rounded)	5%
Cement	0%
Mud	10%
Bioclasts	65%
Authigenic minerals: Glauconite (75%), hematite (25%)	20%

Foraminifera	Percentage /100
Planktic	60% (n=109)
Benthic	40% (n=74)

Bioclasts	Percentage of identified/total
Foraminifera	80%/20%
Bryozoans	2%/1%
Echinoderms	12%/3%
Algae	0%/0%
Molluscs	2%/1%
Brachiopods	4%/1%
Barnacles	0%/0%
Sponge spicules	0%/0%
Worm Tubes	0%/0%
Unidentified bioclasts	74%

Notes from thin section:	Loose sediment in resin. Matrix estimation is difficult due to the nature of the slide, with values being a minimum or not represented at all. Glauconite is mostly sub-rounded grains with some intraclast growth. Some hematisation has occured, heavy on some grains. Chambers of foram tests are often heavily hematised. There is a micritic clast within the slide that contains a higher planktic to benthic ratio than the slide as a whole (9:1). Benthics are coiled (planar), biserial, uniserial, with possibly one milliod. Tests are mostly microcrystalline, with some hyaline biserials, and one larger quartz agglutinate benthic. Hematite alteration on edge of large echinoid fragments. Unidentified bioclasts are mostly shell fragments. Micritisation in this slide makes some identification difficult.

Stratigraphic Column:	NT09/14		
Sample Number:	NT10061501	**Location:**	Trig Z
Date Collected:	6/15/10	**Formation:**	Otekaike Lst

Thin Section Description

Matrix	Percentage /100
Clastics: Quartz (angular)	40%
Cement	0%
Mud	0%
Bioclasts	2%
Authigenic minerals: Glauconite, hematite	58%

Foraminifera	Percentage /100
Planktic	n/a
Benthic	n/a

Bioclasts	Percentage of identified/total
Foraminifera	0%/0%
Bryozoans	0%/0%
Echinoderms	0%/0%
Algae	0%/0%
Molluscs	100%/100%
Brachiopods	0%/0%
Barnacles	0%/0%
Sponge spicules	0%/0%
Worm Tubes	0%/0%
Unidentified bioclasts	0%

Notes from thin section:	Loose sediment in resin. Glauconites are rounded grains, with some in situ growth between clasts. Hematite alteration of some clasts and matrix, with some very heavy. The few bioclasts are altered with glauconite and hematite. Nature of the slide makes matrix estimate very difficult. Mollusc fragment shows crossed-laminar wall structure.

Stratigraphic Column:	NT09/14		
Sample Number:	NT10061503	**Location:**	Trig Z
Date Collected:	6/15/10	**Formation:**	Otekaike Lst

Thin Section Description

Matrix	Percentage /100
Clastics: Quartz (98%) (angular to sub-angular), biotite (2%)	40%
Cement	0%
Mud	25%
Bioclasts	0%
Authigenic minerals: Glauconite (73%), hematite (25%), phosphate (2%)	35%

Foraminifera	Percentage /100
Planktic	n/a
Benthic	n/a

Bioclasts	Percentage of identified/total
Foraminifera	n/a
Bryozoans	n/a
Echinoderms	n/a
Algae	n/a
Molluscs	n/a
Brachiopods	n/a
Barnacles	n/a
Sponge spicules	n/a
Worm Tubes	n/a
Unidentified bioclasts	n/a

Notes from thin section:	Loose sediment in resin. Glauconite grains sub-rounded to angular. Hematite alteration of some glauconites and some matrix concentrations. No obvious bioclasts present.

Stratigraphic Column:	NT09/14		
Sample Number:	NT10061504	**Location:**	Trig Z
Date Collected:	6/15/10	**Formation:**	Otekaike Lst

Hand Specimen Description

Colour	Induration	Bedding and Sedimentary Structures		Grainsize
Orangey-brown	Friable			Fine
Grain or matrix supported	**Sorting**	**Roundness**	**Sphericity - shape**	**Biologic binding**
Grain	Well			No
Textural Name:	**Grainstone**	**Notes:**		

Thin Section Description

Matrix	Percentage /100
Clastics: Quartz (angular)	2%
Cement	0%
Mud	0%
Bioclasts	30%
Authigenic minerals: Hematite	68%

Foraminifera	Percentage /100
Planktic	not counted - see notes
Benthic	not counted - see notes

Bioclasts	Percentage of identified/total
Foraminifera	not counted - see notes
Bryozoans	not counted - see notes
Echinoderms	not counted - see notes
Algae	not counted - see notes
Molluscs	not counted - see notes
Brachiopods	not counted - see notes
Barnacles	not counted - see notes
Sponge spicules	not counted - see notes
Worm Tubes	not counted - see notes
Unidentified bioclasts	not counted - see notes

Notes from thin section:	Loose sediment in resin. Heavily altered and weathered slide. Small quartz clasts may be greater in number, but weathering is obscuring them. There are a number of forams present within the slide, although any count would be inaccurate due to the weathered and obscured nature of the slide. Both benthics and planktics were observed, with benthic test morphologies consisting of uniserials, biserials, coiled planar and trochospirals. Tests are both microcrystalline and hyaline. Some mollusc fragments.

Stratigraphic Column:	NT09/14		
Sample Number:	NT10061505	**Location:**	Trig Z
Date Collected:	6/15/10	**Formation:**	Otekaike Lst

Hand Specimen Description

Colour	**Induration**	**Bedding and Sedimentary Structures**		**Grainsize**
Cream-yellow	Friable			Fine
Grain or matrix supported	**Sorting**	**Roundness**	**Sphericity - shape**	**Biologic binding**
Grain	Well			No
Textural Name:	**Packstone**	**Notes:**		

Thin Section Description

Matrix	**Percentage /100**
Clastics: Quartz (angular - sub-angular)	7%
Cement	1%
Mud	25%
Bioclasts	50%
Authigenic minerals: Glauconite (85%), hematite (15%)	17%

Foraminifera	**Percentage /100**
Planktic	48% (n=96)
Benthic	52% (n=104)

Bioclasts	**Percentage of identified/total**
Foraminifera	92%/32%
Bryozoans	0%/0%
Echinoderms	0%/0%
Algae	0%/0%
Molluscs	5%/2%
Brachiopods	2%/1%
Barnacles	0%/0%
Sponge spicules	0%/0%
Worm Tubes	1%/<1%
Unidentified bioclasts	0%/0%

Notes from thin section:	Loose sediment in resin. Cement is in very small amounts as a slim rim on some clasts. Due to the nature of this slide the matrix values are a minimum. Glauconite is present as sub-rounded to sub-angular grains with significant intraclast growth. Some hematite alteration of intraclast glauconite. Benthics are biserial, coiled (planar), and uniserial. Tests are microcrystalline and hyaline with some larger benthics. A few quartz agglutinates. One piece of flabellum. Unidentified bioclasts are mostly shell fragments.

Stratigraphic Column:	NT09/14		
Sample Number:	NT10061506	**Location:**	Trig Z
Date Collected:	6/15/10	**Formation:**	Otekaike Lst

Hand Specimen Description

Colour	**Induration**	**Bedding and Sedimentary Structures**		**Grainsize**
Brownish-green	Unconsolidated			Very fine to fine
Grain or matrix supported	**Sorting**	**Roundness**	**Sphericity - shape**	**Biologic binding**
Grain	Well			No
Textural Name:	**Packstone**	**Notes:**		

Thin Section Description

Matrix	**Percentage /100**
Clastics: Quartz (angular)	7%
Cement	2%
Mud	15%
Bioclasts	46%
Authigenic minerals: Glauconite (97%), hematite (3%)	30%

Foraminifera	**Percentage /100**
Planktic	35% (n=42)
Benthic	65% (n=78)

Bioclasts	**Percentage of identified/total**
Foraminifera	64%/16%
Bryozoans	1%/<1%
Echinoderms	7%/2%
Algae	0%/0%
Molluscs	20%/5%
Brachiopods	5%/1%
Barnacles	3%/1%
Sponge spicules	0%/0%
Worm Tubes	0%/0%
Unidentified bioclasts	75%

Notes from thin section:	Loose sediment in resin. Matrix volumes are estimates based on the more cohesive clumps of sediment set in the resin and averaged over the slide. Glauconite grains are rounded to sub-rounded and appear to be bimodal in size. There is also some intraclast growth. Hematite occurs as heavy localised alteration around some clasts. Benthics are coiled (planar), uniserial, and biserial. Tests are microcrystalline and hyaline. Molluscs show cross lamination. Some lamination apparent within the larger clasts.

Stratigraphic Column:	NT09/14		
Sample Number:	NT10061507	**Location:**	Trig Z
Date Collected:	6/16/10	**Formation:**	Otekaike Lst

Hand Specimen Description

Colour	**Induration**	**Bedding and Sedimentary Structures**		**Grainsize**
Yellowish-cream	Indurated			Fine
Grain or matrix supported	**Sorting**	**Roundness**	**Sphericity - shape**	**Biologic binding**
Grain	Well			No
Textural Name:	**Packstone**	**Notes:**	Fossiliferous with shell fragments (and small whole shells).	

Thin Section Description

Matrix	**Percentage /100**
Clastics: Quartz (angular)	5%
Cement	0%
Mud	25%
Bioclasts	60%
Authigenic minerals: Glauconite (65%), hematite (35%)	10%

Foraminifera	**Percentage /100**
Planktic	44% (n=42)
Benthic	56% (n=53)

Bioclasts	**Percentage of identified/total**
Foraminifera	85%/25%
Bryozoans	0%/0%
Echinoderms	10%/3%
Algae	0%/0%
Molluscs	0%/0%
Brachiopods	5%/2%
Barnacles	0%/0%
Sponge spicules	0%/0%
Worm Tubes	0%/0%
Unidentified bioclasts	70%

Notes from thin section:	Very micritic and dirty slide. No obvious cements. Glauconite is present as grains and intraclast growth inside bioclasts. Some hematisation has occured around glauconites. Benthic tests are coiled, uniserial, and biserial. Tests are microcrystalline, hyaline and a few agglutinates. Tests are commonly disarticulated, and micrite matrix makes microcrystalline tests occasionally obscured. Bioclasts are commonly small and broken fragments, with most appearing to be broken shell fragments. Some punctate brachiopod pieces.

Stratigraphic Column:	NT09/14		
Sample Number:	NT10061508	**Location:**	Trig Z
Date Collected:	6/15/10	**Formation:**	Otekaike Lst

Thin Section Description

Matrix	Percentage /100
Clastics: Quartz (angular - sub-angular)	2%
Cement	0%
Mud	25%
Bioclasts	58%
Authigenic minerals: Glauconite (50%), hematite (50%)	15%

Foraminifera	Percentage /100
Planktic	28% (n=48)
Benthic	72% (n=124)

Bioclasts	Percentage of identified/total
Foraminifera	81%/16%
Bryozoans	2%/<1%
Echinoderms	7%/2%
Algae	0%/0%
Molluscs	7%/2%
Brachiopods	3%/<1%
Barnacles	0%/0%
Sponge spicules	0%/0%
Worm Tubes	0%/0%
Unidentified bioclasts	80%

Notes from thin section:	Loose sediment and sediment clasts in resin. Glauconite is both grains and intraclast growth with most altered by hematite to some degree. Hematite alteration on some micrite matrix. Benthics are coiled (planar, trochospiral), uniserial, and biserial. Microcrystalline tests with some hyalines. A few larger benthics, with at least one agglutinate. One piece of mollusc identifiable as a gastropod by the fragment's shape. Brachiopods show punctae. Crossed-laminar wall structure on one mollusc fragment that has been slightly hematised. Micritised slide making smaller fragmented bioclast identification difficult. Most fragments appear to be small shell fragments.

Stratigraphic Column:	NT09/14		
Sample Number:	NT10061509	**Location:**	Trig Z
Date Collected:	6/15/10	**Formation:**	Otekaike Lst

Hand Specimen Description

Colour	**Induration**	**Bedding and Sedimentary Structures**		**Grainsize**
Orangey-white	Friable			Fine
Grain or matrix supported	**Sorting**	**Roundness**	**Sphericity - shape**	**Biologic binding**
Grain	Well			No
Textural Name:	**Packstone**	**Notes:**	Fossiliferous.	

Thin Section Description

Matrix	**Percentage /100**
Clastics: Quartz (angular - subrounded)	7%
Cement	trace
Mud	30%
Bioclasts	53%
Authigenic minerals: Glauconite (80%), hematite (20%)	10%

Foraminifera	**Percentage /100**
Planktic	38% (n=46)
Benthic	62% (n=74)

Bioclasts	**Percentage of identified/total**
Foraminifera	80%/40%
Bryozoans	0%/0%
Echinoderms	10%/5%
Algae	0%/0%
Molluscs	10%/5%
Brachiopods	0%/0%
Barnacles	0%/0%
Sponge spicules	0%/0%
Worm Tubes	0%/0%
Unidentified bioclasts	50%

Notes from thin section:	Mature glauconite rounded grains and some intraclast growth in bioclasts, with some hematitic alteration. Some glauconitisation of echinoid fragment centres. Benthics are trochospiral (rotallid), biserial, uniserial, and coiled. Tests are microcrystalline, hyaline and a few larger quartz agglutinates. Unidentified bioclasts are mostly shell fragments.

Stratigraphic Column:	NT10/02		
Sample Number:	NT10012008	**Location:**	Campbell's Bay
Date Collected:	1/20/10	**Formation:**	Ototara Lst

Hand Specimen Description

Colour	**Induration**	**Bedding and Sedimentary Structures**		**Grainsize**
White	Indurated			Fine to coarse
Grain or matrix supported	**Sorting**	**Roundness**	**Sphericity - shape**	**Biologic binding**
Grain	Very poor			No
Textural Name:	**Packstone**	**Notes:**		

Thin Section Description

Matrix	**Percentage /100**
Clastics: Quartz (60%), igneous lithics and one quartz grain lithic (40%)	4%
Cement	0%
Mud	25%
Bioclasts	61%
Authigenic minerals: Glauconite (70%), hematite (5%), phosphate (25%)	10%

Foraminifera	**Percentage /100**
Planktic	77% (n=87)
Benthic	23% (n=26)

Bioclasts	**Percentage of identified/total**
Foraminifera	20%/16%
Bryozoans	40%/33%
Echinoderms	25%/19%
Algae	5%/4%
Molluscs	10%/8%
Brachiopods	0%/0%
Barnacles	0%/0%
Sponge spicules	0%/0%
Worm Tubes	0%/0%
Unidentified bioclasts	20%

Notes from thin section:	Micritic-rich slide. Glauconite is mostly found as intraclast growths with occasional slight hematisation and some rounded grains. Phosphate is present as some clasts and also intraclast growth. Benthic tests are coiled and biserial. Similar proportions of microcrystalline and hyaline tests, with a number partly obscured. The micrite content may be reducing the number of identified microcrystalline tests. Bored and broken shell fragments, a number of which are partly or wholly neomorphosed.

Stratigraphic Column:	NT10/02		
Sample Number:	NT10012009	**Location:**	Campbell's Beach
Date Collected:	1/20/10	**Formation:**	Ototara

Hand Specimen Description

Colour	**Induration**	**Bedding and Sedimentary Structures**		**Grainsize**
Greenish-yellowish-white	Very well indurated			Fine to medium
Grain or matrix supported	**Sorting**	**Roundness**	**Sphericity - shape**	**Biologic binding**
Grain	Moderate			No
Textural Name:	**Packstone**	**Notes:**	Clear boundary between greensand and limestone on the karsted contact. Descriptions for Greensand presented as NT10012009A.	

Thin Section Description

Matrix	**Percentage /100**
Clastics: Quartz (angular-subrounded), igneous clast	3%
Cement	2%
Mud	20%
Bioclasts	65%
Authigenic minerals: Glauconite (85%), phosphate (10%), hematite (5%)	10%

Foraminifera	**Percentage /100**
Planktic	68% (n=89
Benthic	32% (n=42

Bioclasts	**Percentage of identified/total**
Foraminifera	57%/39%
Bryozoans	15%/11%
Echinoderms	15%/11%
Algae	3%/2%
Molluscs	10%/7%
Brachiopods	0%/0%
Barnacles	0%/0%
Sponge spicules	0%/0%
Worm Tubes	0%/0%
Unidentified bioclasts	30%

Notes from thin section:	This slide contains karst contact between Ototara Lst and greensand infill, and is split accordingly. In Ototara glauconite is present as both grains (so quite large, and rounded) as well as intraclast growth, with some minor hematisation. Phosphate present as rounded grains and some intraclast growth. Benthics in Ototara are biserial, uniserial, coiled, milliolid, and trochospiral. Similar numbers of hyaline and microcyrstalline, although the micritic content of the slide may be obscuring a number of microscrystalline tests. Broken mollusc pieces have been extrensively bored and infilled with glauconite. Determination between bivalve and gastropod cannot be observed.

Stratigraphic Column:	NT10/02		
Sample Number:	NT10012009A	Location:	Campbells Beach
Date Collected:	1/20/10	Formation:	Gee Greensand

Hand Specimen Description

Colour	**Induration**	**Bedding and Sedimentary Structures**		**Grainsize**
Greenish-white	Very well indurated			Fine to medium
Grain or matrix supported	**Sorting**	**Roundness**	**Sphericity - shape**	**Biologic binding**
Grain	Moderate			No
Textural Name:	**Packstone**	**Notes:**		

Thin Section Description

Matrix	**Percentage /100**
Clastics: Quartz (angular and bigger than Ototara)	2%
Cement	1%
Mud	20%
Bioclasts	52%
Authigenic minerals: Glauconite (80%), phosphate (10%), hematite (10%)	25%

Foraminifera	**Percentage /100**
Planktic	63% (n=61)
Benthic	37% (n=36)

Bioclasts	**Percentage of identified/total**
Foraminifera	73%/56%
Bryozoans	2%/1%
Echinoderms	15%/11%
Algae	0%/0%
Molluscs	10%/7%
Brachiopods	0%/0%
Barnacles	0%/0%
Sponge spicules	0%/0%
Worm Tubes	0%/0%
Unidentified bioclasts	25%

Notes from thin section:	Greensand is very micritic with some clasts obscured, while cement is drusy and observed only in cavities. Benthics are uniserial, coiled, trochospiral, biserial and milliolid. Tests are microcrystalline and hyaline in similar proportions, but heavily micritic matrix may have obscured many. Glauconite is mostly rounded grains with some intraclasts formation. Phosphate is present as rounded clasts that are on the whole larger than the glauconite. Bored and glauconite infilled shell fragments.

Stratigraphic Column:	NT10/02		
Sample Number:	NT10012007	Location:	Campbells Beach
Date Collected:	1/20/10	Formation:	Ototara Lst

Thin Section Description

Matrix	Percentage /100
Clastics: Quartz (angular), one larger igneous clasts (sub-rounded)	3%
Cement	1%
Mud	34%
Bioclasts	55%
Authigenic minerals: Glauconite	7%

Foraminifera	Percentage /100
Planktic	73% (n=58)
Benthic	27% (n=17)

Bioclasts	Percentage of identified/total
Foraminifera	20%/17%
Bryozoans	46%/39%
Echinoderms	10%/8%
Algae	8%/7%
Molluscs	15%/13%
Brachiopods	1%/1%
Barnacles	0%/0%
Sponge spicules	0%/0%
Worm Tubes	0%/0%
Unidentified bioclasts	15%

Notes from thin section:	Loose sediment and groupings of sediment in resin. Quartz fragments are very small. Some remnant blocky calcite cement around some echinoid fragments. Micrite percentages taken as estimate from whole sediment clumps within the resin. Glauconite is mostly intraclast growth, with some formed within echinoid fragments, but not yet on the rims. Some rounded grains of glauconite. Benthics are coiled (planar, trochospiral), and biserial. Tests appear to be solely microcrystalline. One possible quartz agglutinate. Some shell fragments show heavy boring.

Stratigraphic Column:	NT10/02		
Sample Number:	NT10012012	**Location:**	Campbells Beach
Date Collected:	2/20/10	**Formation:**	Gee Greensand

Hand Specimen Description

Colour	**Induration**	**Bedding and Sedimentary Structures**		**Grainsize**
Brownish-green	Friable			Fine
Grain or matrix supported	**Sorting**	**Roundness**	**Sphericity - shape**	**Biologic binding**
Grain	Well			No
Textural Name:	**Packstone**	**Notes:**	Glauconite-rich	

Thin Section Description

Matrix	**Percentage /100**
Clastics: Quartz (angular)	2%
Cement	0%
Mud	30%
Bioclasts	28%
Authigenic minerals: Glauconite	40%

Foraminifera	**Percentage /100**
Planktic	75% (n=83)
Benthic	25% (n=28)

Bioclasts	**Percentage of identified/total**
Foraminifera	82%/66%
Bryozoans	0%/0%
Echinoderms	10%/8%
Algae	0%/0%
Molluscs	5%/4%
Brachiopods	3%/2%
Barnacles	0%/0%
Sponge spicules	0%/0%
Worm Tubes	0%/0%
Unidentified bioclasts	20%

Notes from thin section:	Loose sediment in resin. Mud estimate is taken from clumps of sediment preserved within the resin. Glauconite is present as large rounded to sub-angular grains with some small amounts of intraclast growth (including some observed in the centre of an echinoid fragment. Estimate of glauconite percentage may be high due to presistance of this type of mineral within a loose sediment slide such as this. Benthics are uniserial, millioid, and coiled (planer, trochospiral). Tests are microcrystalline with a few hyalines, and a couple of larger benthics. Mollusc fragment is heavily bored.

Stratigraphic Column:	NT10/02		
Sample Number:	NT10012011	**Location:**	Campbells Beach
Date Collected:	1/20/10	**Formation:**	Otekaike/Ototara Lst (karsted)

Thin Section Description

Matrix	Percentage /100
Clastics: Quartz (sub-rounded - angular) (70%), one large angular amphibole and a couple of rounded mafic clasts (30%)	4%
Cement	13%
Mud	38%
Bioclasts	30%
Authigenic minerals: Glauconite	15%

Foraminifera	Percentage /100
Planktic	82% (n=116)
Benthic	18% (n=26)

Bioclasts	Percentage of identified/total
Foraminifera	43%/32%
Bryozoans	30%/22%
Echinoderms	25%/19%
Algae	0%/0%
Molluscs	2%/2%
Brachiopods	0%/0%
Barnacles	0%/0%
Sponge spicules	0%/0%
Worm Tubes	0%/0%
Unidentified bioclasts	25%

Notes from thin section:	Calcite cement observed to be filling void space, particularly within bioclasts. Commonly blocky, becoming more so into each void. Where micrite and cements fill the same void there is a probable geopetal fabric. Glauconite commonly rounded to sub-rounded, some showing to be quite mature. Tests are coiled (trochospiral), uniserial and biserial. Most benthic tests are microcrystalline with some hyalines. Some larger benthics. Glauconite growth within bioclast tests.

Stratigraphic Column:	NT10/03		
Sample Number:	NT10011913	**Location:**	Kakanui River mouth
Date Collected:	1/19/10	**Formation:**	Ototara Lst syn-volcanics

Thin Section Description

Matrix	Percentage /100
Clastics: Igneous clasts, and crystals of biotite, pyroxene, amphibole.	100%
Cement	0%
Mud	0%
Bioclasts	0%
Authigenic minerals: Glauconite	0%

Foraminifera	Percentage /100
Planktic	n/a
Benthic	n/a

Bioclasts	Percentage of identified/total
Foraminifera	n/a
Bryozoans	n/a
Echinoderms	n/a
Algae	n/a
Molluscs	n/a
Brachiopods	n/a
Barnacles	n/a
Sponge spicules	n/a
Worm Tubes	n/a
Unidentified bioclasts	n/a

Notes from thin section:	Igneous clasts and crystals set in glassy groundmass. All clasts and crystals have a glassy rim.

Stratigraphic Column: NT10/03

Sample Number: NT10011915 Location: Kakanui River mouth

Date Collected: 1/19/10 Formation: Ototara Lst

Thin Section Description

Matrix	Percentage /100
Clastics: igneous clasts (mostly vesicular), crystals (some quite large) of biotite, amphibole, pyroxene. Small detrital quartz (5%)	27%
Cement	7%
Mud	42%
Bioclasts	15%
Authigenic minerals: Glauconite, hematite, phosphate	9%

Foraminifera	Percentage /100
Planktic	18% (n=21)
Benthic	82% (n=94)

Bioclasts	Percentage of identified/total
Foraminifera	81%/73%
Bryozoans	7%/6%
Echinoderms	10%/9%
Algae	0%/0%
Molluscs	2%/2%
Brachiopods	0%/0%
Barnacles	0%/0%
Sponge spicules	0%/0%
Worm Tubes	0%/0%
Unidentified bioclasts	10%

Notes from thin section:	Igneous clasts in a micritic/bioclasts matrix. Some alteration and obscuration of some clasts. Many benthic forams have their tests filled with glauconite, while most clasts are rimmed with blocky and drusy calcite cement. Some parts of the slide are more heavily cemented than others. Cements appear to have formed in cracks within the matrix. Some igneous clasts contain infills of blocky cement. Benthics are involute coil, uniserial, biserial, and trochospiral, with microcrystalline tests dominant, some hyalines and a few agglutinates. Shell fragments, with one neomorhposed mollusc fragment that has been altered.

Stratigraphic Column:	NT10/03		
Sample Number:	NT10011917	**Location:**	Kakanui River Mouth
Date Collected:	1/19/10	**Formation:**	Ototara Lst (tuffaceous)

Thin Section Description

Matrix	Percentage /100
Clastics: Quartz (angular-rounded) (20%), mafic clasts (large amphiboles, biotites, opaques, rounded-angular)(80%).	19%
Cement	3%
Mud	30%
Bioclasts	38%
Authigenic minerals: Glauconite (85%), hematite (15%)	10%

Foraminifera	Percentage /100
Planktic	55% (n=46)
Benthic	45% (n-37)

Bioclasts	Percentage of identified/total
Foraminifera	15%/9%
Bryozoans	10%/6%
Echinoderms	40%/24%
Algae	10%/6%
Molluscs	25%/15%
Brachiopods	0%/0%
Barnacles	0%/0%
Sponge spicules	0%/0%
Worm Tubes	0%/0%
Unidentified bioclasts	40%

Notes from thin section:	Cements are only observed around echinoid fragments. Micrite mud dominant matrix, with some hematisation. Benthics are coiled (planar, trochospiral), and biserial. Tests are mostly microcrystalline with some hyalines. Vast majority of bioclasts show strong abrasion/boring/alteration (suggesting reworking). Borings and abrasions are commonly filled with glauconite/hematite alteration. Echinoid fragments are plates and commonly rounded, with some spine transects. Branching corraline red algae, commonly showing abrasion/alteration.

Stratigraphic Column: NT10/04

Sample Number: NT10012014 **Location:** Old Rifle Butts

Date Collected: 1/20/10 **Formation:** Ototara Lst

Thin Section Description

Matrix	Percentage /100
Clastics: Quartz (angular) (2%), mafic clasts (angular, one very large) (98%).	10%
Cement	30%
Mud	15%
Bioclasts	40%
Authigenic minerals: Glauconite (10%), hematite (90%)	5%

Foraminifera	Percentage /100
Planktic	13% (n=2)
Benthic	87% (n=14)

Bioclasts	Percentage of identified/total
Foraminifera	13%/7%
Bryozoans	40%/24%
Echinoderms	7%/5%
Algae	20%/12%
Molluscs	0%/0%
Brachiopods	0%/0%
Barnacles	0%/0%
Sponge spicules	0%/0%
Worm Tubes	20%/12%
Unidentified bioclasts	40%

Notes from thin section:	Calcite cements are blocky and isopachous, and form as matrix and intraclastly in bioclast voids. Commonly more blocky in centre of voids, with smaller growth on the void boundary. Few rounded glauconites. Hematite alteration common in matrix and around igneous clasts. Benthic are coiled (planar, trochospiral), biserial, uniserial, and nummulites. Tests are microcrystalline and hyaline. Apparent geopetal fabric within bioclast void space between micrite and cement.

Stratigraphic Column: NT10/04

Sample Number: NT10012015 **Location:** Old Rifle Butts

Date Collected: 1/20/10 **Formation:** Ototara Lst

Thin Section Description

Matrix	Percentage /100
Clastics:	0%
Cement	15%
Mud	5%
Bioclasts	80%
Authigenic minerals: Glauconite	Trace

Foraminifera	Percentage /100
Planktic	12% (n=4)
Benthic	88% (n=30)

Bioclasts	Percentage of identified/total
Foraminifera	3%/2%
Bryozoans	63%/50%
Echinoderms	12%/10%
Algae	15%/12%
Molluscs	7%/6%
Brachiopods	0%/0%
Barnacles	0%/0%
Sponge spicules	0%/0%
Worm Tubes	0%/0%
Unidentified bioclasts	20%

Notes from thin section:	Loose sediment in resin. One observed glauconite is on a small glauconitised bryozoan fragment. Blocky cement overgrowths around primarily echinoid fragments, with isopachous formations within most bioclast internal void spaces. Benthics are biserial, uniserial, and coiled (trochospiral, planar involute). Tests are almost exclusively microcrystalline, with a few larger than most. Corraline branching algae.

Stratigraphic Column: NT10/04

Sample Number: NT10012016 **Location:** Old Rifle Butts

Date Collected: 1/20/10 **Formation:** Ototara Lst

Thin Section Description

Matrix	Percentage /100
Clastics: Quartz (angular) (10%), mafic clasts (vesiculated, sub-rounded to angular) (90%)	35%
Cement	3%
Mud	10%
Bioclasts	32%
Authigenic minerals: Glauconite (10%), hematite (90%)	20%

Foraminifera	Percentage /100
Planktic	30% (n=5)
Benthic	70% (n=12)

Bioclasts	Percentage of identified/total
Foraminifera	17%/7%
Bryozoans	70%/28%
Echinoderms	3%/1%
Algae	3%/1%
Molluscs	7%/3%
Brachiopods	0%/0%
Barnacles	0%/0%
Sponge spicules	0%/0%
Worm Tubes	0%/0%
Unidentified bioclasts	60%

Notes from thin section:	Loose sediment in resin. Poor section as hematite altered and broken up. Calcite cement only observed as blocky/isopachous within bioclast void space (forams mostly). Rounded to sub-angular glauconite, with heavy hematite alteration in the matrix, which is presumably micrite although cannot be confirmed in most places. Heavy boring and abrasion of bioclasts with alteration filling borings. Benthics are coiled (planar and trochospiral) and uniserial. The few tests observed were all microcrystalline.

Stratigraphic Column:	NT10/04		
Sample Number:	NT10012017	**Location:**	Old Rifle Butts
Date Collected:	1/20/10	**Formation:**	Ototara Lst (rhodolith bed)

Hand Specimen Description

Colour	**Induration**	**Bedding and Sedimentary Structures**		**Grainsize**
Cream	Very well indurated			Very fine
Grain or matrix supported	**Sorting**	**Roundness**	**Sphericity - shape**	**Biologic binding**
n/a	n/a			Yes
Textural Name:	**Bindstone**	**Notes:**	Large rhodolith.	

Thin Section Description

Matrix	**Percentage /100**
Clastics: Quartz	Trace
Cement	20%
Mud	7%
Bioclasts	70%
Authigenic minerals: Glauconite (15%), hematite (80%), phosphate (5%)	3%

Foraminifera	**Percentage /100**
Planktic	6% (n=3)
Benthic	94% (n=47)

Bioclasts	**Percentage of identified/total**
Foraminifera	4%/3%
Bryozoans	10%/9%
Echinoderms	5%/4%
Algae	80%/73%
Molluscs	1%/1%
Brachiopods	0%/0%
Barnacles	0%/0%
Sponge spicules	0%/0%
Worm Tubes	0%/0%
Unidentified bioclasts	10%

Notes from thin section:	Algal balls with large amounts of encrusting algae (minor branching corraline algae) with lots of bryozoan fragments. Slide contains algal ball matrix interface. Benthic tests are biserial, coil, trochospiral, and uniserial. Tests are microcrystalline and hyaline. Blocky calcite cement overgrowths on bioclast fragments and inside cavities.

Stratigraphic Column:	NT10/04		
Sample Number:	NT10012018	**Location:**	Old Rifle Butts
Date Collected:	1/20/10	**Formation:**	Gee Greensand (brachiopod-rich bed)

Thin Section Description

Matrix	Percentage /100
Clastics: Quartz (angular)	2%
Cement	1%
Mud	0%
Bioclasts	52%
Authigenic minerals: Glauconite (70%), hematite (30%)	45%

Foraminifera	Percentage /100
Planktic	62% (n=53)
Benthic	38% (n=33)

Bioclasts	Percentage of identified/total
Foraminifera	35%/16%
Bryozoans	10%/5%
Echinoderms	30%/13%
Algae	0%/0%
Molluscs	0%/0%
Brachiopods	25%/11%
Barnacles	0%/0%
Sponge spicules	0%/0%
Worm Tubes	0%/0%
Unidentified bioclasts	55%

Notes from thin section:	Loose sediment in resin. Heavily hematite altered slide. Traces of isopachous calcite cement around some echinoid clasts. The nature of this slide as sediment in resin alongside the heavy alteration makes the identification of mud/cement almost impossibly. Values given are minimums. Glauconite grains are rounded to sub-rounded, with lots of intraclast growth on fragments, including the centre and whole of echinoid fragments. Hematite alteration is very heavy, and occurs often around the rim of glauconite grains, as well as heavily on clumps of sediment and around bioclasts. The hematite percantages given here are in relation to glauconite alteration only to preserve the ratios between the different components of the slide. Benthics are coiled (planar, trochospiral), uniserial, and biserial. Tests are microcrystalline and hyaline. Altered nature of this slide may be obscuring some of the darker benthics. Some large brachiopod fragments with clear punctae. Some shell fragments are showing a lot of boring.

Stratigraphic Column: NT10/04

Sample Number: NT10012019 **Location:** Old Rifle Butts

Date Collected: 1/20/10 **Formation:** Gee Greensand

Thin Section Description

Matrix	Percentage /100
Clastics: Quartz (rounded - angular)	7%
Cement	0%
Mud	7%
Bioclasts	36%
Authigenic minerals: Glauconite (90%), hematite (10%)	50%

Foraminifera	Percentage /100
Planktic	70% (n=100)
Benthic	30% (n=43)

Bioclasts	Percentage of identified/total
Foraminifera	88%/47%
Bryozoans	1%/1%
Echinoderms	3%/2%
Algae	0%/0%
Molluscs	5%/3%
Brachiopods	0%/0%
Barnacles	0%/0%
Sponge spicules	0%/0%
Worm Tubes	0%/0%
Unidentified bioclasts	45%
Radiolarians	3%/2%

Notes from thin section:	Poor quality slide. Glauconite grains are rounded to sub-rounded with some showing fracturing. Some intraclast growth within bioclasts. Some heavy hematite alteration of micrite matrix and around most glauconite grains. Benthics are uniserial, biserial, and coiled (planar, trochospiral). Tests are microcrystalline and hyaline. Some borings in shell fragments. Unidentified bioclasts are generally shell fragments.

Stratigraphic Column: NT10/06

Sample Number: NT10012103 **Location:** Awamoko Creek

Date Collected: 1/21/10 **Formation:** Raki Siltstone

Thin Section Description

Matrix	Percentage /100
Clastics: Small angular quartz grains (95%), biotite (5%)	37%
Cement	0%
Mud	17%
Bioclasts	0%
Authigenic minerals: Glauconite (90%), hematite (10%)	46%

Foraminifera	Percentage /100
Planktic	n/a
Benthic	n/a

Bioclasts	Percentage of identified/total
Foraminifera	n/a
Bryozoans	n/a
Echinoderms	n/a
Algae	n/a
Molluscs	n/a
Brachiopods	n/a
Barnacles	n/a
Sponge spicules	n/a
Worm Tubes	n/a
Unidentified bioclasts	n/a

Notes from thin section:	Sediment and sediment clasts in resin. Very glauconite rich slide, with grains appearing as rounded to sub-angular grains, some that may be glauconitised biotites. Some show darker centres, and often sharply become lighter towards the grain rim. Weathered slide. Matrix is difficult to distinguish as it mixes heavily with the resin, but appears to be a muddy silt mix. Evenly dispersed with quartz grains, and all show a slight alignment fabric. No bioclasts observed within this slide.

Stratigraphic Column:	NT10/06		
Sample Number:	NT10012104	**Location:**	Awamoko Creek
Date Collected:	1/21/10	**Formation:**	Kokoamu Greensand

Hand Specimen Description

Colour	**Induration**	**Bedding and Sedimentary Structures**		**Grainsize**
Orangey-brown	Unconsolidated			Fine to very fine
Grain or matrix supported	**Sorting**	**Roundness**	**Sphericity - shape**	**Biologic binding**
Grain	Moderate			No
Textural Name:	**Packstone**	**Notes:**		

Thin Section Description

Matrix	**Percentage /100**
Clastics: Quartz (rounded - angular)	2%
Cement	6%
Mud	20%
Bioclasts	2%
Authigenic minerals: Glauconite (87%), phosphate (3%), hematite (10%)	70%

Foraminifera	**Percentage /100**
Planktic	0% (n=0)
Benthic	100% (n=2)

Bioclasts	**Percentage of identified/total**
Foraminifera	70%/35%
Bryozoans	0%/0%
Echinoderms	0%/0%
Algae	0%/0%
Molluscs	30%/15%
Brachiopods	0%/0%
Barnacles	0%/0%
Sponge spicules	0%/0%
Worm Tubes	0%/0%
Unidentified bioclasts	50%

Notes from thin section:	Loose sediment in resin. Calcite cement is observed in clasts of spar with few other matrial included, and tends to be polycrystalline. Micrite is present in small collections as remnant matrix around clasts. Glauconite is rounded to sub-rounded, with some glauconitised biotites. Some rounded phosphates. Some hematite alteration of glauconite as well as of the matrix. The two benthic tests are planar coiled and unserial, with both microcrystalline. Very few bioclasts.

Stratigraphic Column: NT10/06

Sample Number: NT10012105 **Location:** Awamoko Creek

Date Collected: 1/21/10 **Formation:** Otekaike Lst

Hand Specimen Description

Colour	Induration	Bedding and Sedimentary Structures		Grainsize
Greenish-orange	Indurated			Fine to medium
Grain or matrix supported	**Sorting**	**Roundness**	**Sphericity - shape**	**Biologic binding**
Grain	Moderate			No
Textural Name:	**Packstone**	**Notes:**		

Thin Section Description

Matrix	Percentage /100
Clastics: Quartz (angular), minor biotite	4%
Cement	2%
Mud	5%
Bioclasts	29%
Authigenic minerals: Glauconite (94%), hematite (5%), phosphate (1%)	60%

Foraminifera	Percentage /100
Planktic	38% (n=43)
Benthic	62% (69)

Bioclasts	Percentage of identified/total
Foraminifera	88%/53%
Bryozoans	0%/0%
Echinoderms	10%/6%
Algae	0%/0%
Molluscs	2%/1%
Brachiopods	0%/0%
Barnacles	0%/0%
Sponge spicules	0%/0%
Worm Tubes	0%/0%
Unidentified bioclasts	40%

Notes from thin section:	Highly glauconitic slide with rounded glauconite grains dominant with some intraclast growths. Glauconite also appears to have grown into the matrix. Isopachous calcite cement rims on most glauconite grains. Some hematite alteration of glauconite. Biotites have been partially glauconitised. Glauconite appears to be quite mature. Benthics are coiled, biserial, uniserial and trochospiral. Tests are microcyrstalline and hyaline. Phosphate clast is angular. Shell fragments have been bored and infilled.

Stratigraphic Column:	NT10/06		
Sample Number:	NT10012106	**Location:**	Awamoko Creek
Date Collected:	1/21/10	**Formation:**	Otekaike Lst

Hand Specimen Description

Colour	Induration	Bedding and Sedimentary Structures		Grainsize
Yellowish-cream	Indurated			Fine
Grain or matrix supported	**Sorting**	**Roundness**	**Sphericity - shape**	**Biologic binding**
Matrix	Well			No
Textural Name:	**Wackestone**	**Notes:**	Very weathered.	

Thin Section Description

Matrix	Percentage /100
Clastics: Quartz (angular-subangular), v. minor plagioclase	25%
Cement	Trace
Mud	40%
Bioclasts	25%
Authigenic minerals: Glauconite (80%), hematite (15%), phosphate (5%)	10%

Foraminifera	Percentage /100
Planktic	40% (n=75)
Benthic	60% (n=114)

Bioclasts	Percentage of identified/total
Foraminifera	93%/56%
Bryozoans	0%/0%
Echinoderms	5%/3%
Algae	0%/0%
Molluscs	2%/1%
Brachiopods	0%/0%
Barnacles	0%/0%
Sponge spicules	0%/0%
Worm Tubes	0%/0%
Unidentified bioclasts	40%

Notes from thin section:	Glauconite is present as rounded grains and some intraclast formation, and some minor rounded phosphate calsts. Some hematite alteration within localised areas of the matrix and around quartz grains. Benthics are coiled, uniserial, biserial, and trochospiral. Tests are hyaline and microcrystalline. Shell fragments have some borings.

Stratigraphic Column: NT10/06

Sample Number: NT10012107 **Location:** Awamoko Creek

Date Collected: 1/21/10 **Formation:** Otekaike Lst

Thin Section Description

Matrix	Percentage /100
Clastics: Quartz (angular - sub-angular)	25%
Cement	0%
Mud	15%
Bioclasts	35%
Authigenic minerals: Glauconite (50%), hematite (50%)	25%

Foraminifera	Percentage /100
Planktic	39% (n=84)
Benthic	61% (n=133)

Bioclasts	Percentage of identified/total
Foraminifera	90%/32%
Bryozoans	0%/0%
Echinoderms	1%/<1%
Algae	0%/0%
Molluscs	9%/3%
Brachiopods	0%/0%
Barnacles	0%/0%
Sponge spicules	0%/0%
Worm Tubes	0%/0%
Unidentified bioclasts	65%

Notes from thin section:	Loose sediment in resin. Hematite is present as alteration within matrix, while glauconite grains are either rounded to sub-rounded and relatively fresh, or appear intergrown with quartz grains. Benthics are biserial, uniserial, and coiled (planar, trochospiral). Tests are microcrystalline and hyaline. Bioclastic content is very fragmentory.

Stratigraphic Column: NT10/07

Sample Number: NT10012601 **Location:** Tokarahi Cliffs

Date Collected: 1/26/10 **Formation:** Otekaike Lst

Hand Specimen Description

Colour	Induration	Bedding and Sedimentary Structures		Grainsize
Yellowish-white	Moderate			Fine sand
Grain or matrix supported	**Sorting**	**Roundness**	**Sphericity - shape**	**Biologic binding**
Grain	Moderate			No
Textural Name:	**Packstone**	**Notes:**		

Thin Section Description

Matrix	Percentage /100
Clastics: Quartz (subrounded - angular)	4%
Cement	1%
Mud	40%
Bioclasts	50%
Authigenic minerals: Glauconite	5%

Foraminifera	Percentage /100
Planktic	39% (n=60)
Benthic	61% (n=96)

Bioclasts	Percentage of identified/total
Foraminifera	88%/62%
Bryozoans	2%/1%
Echinoderms	10%/7%
Algae	0%/0%
Molluscs	0%/0%
Brachiopods	0%/0%
Barnacles	0%/0%
Sponge spicules	0%/0%
Worm Tubes	0%/0%
Unidentified bioclasts	30%

Notes from thin section:	Micritic-rich slide. Glauconite present mostly as intraclast fill with some rounded to subangular grains. Benthics are coiled, uniserial, biserial, trochospiral (rotallid). Tests are microcrystalline primarily with lesser numbers of hyalines. Most of the unidentified bioclasts appear to be small broken shell fragments that are indeterminate. Bryozoans represented by a couple of branching pieces.

Stratigraphic Column:	NT10/07		
Sample Number:	NT10012602	**Location:**	Tokarahi Cliffs
Date Collected:	1/26/10	**Formation:**	Otekaike Lst

Thin Section Description

Matrix	Percentage /100
Clastics: Quartz (angular - sub-angular), minor biotite lathes. One large micrite clast	5%
Cement	1%
Mud	14%
Bioclasts	50%
Authigenic minerals: Glauconite (99%), hematite (1%)	30%

Foraminifera	Percentage /100
Planktic	36% (n=94)
Benthic	64% (n=94)

Bioclasts	Percentage of identified/total
Foraminifera	42%/17%
Bryozoans	3%/1%
Echinoderms	45%/18%
Algae	0%/0%
Molluscs	10%/4%
Brachiopods	0%/0%
Barnacles	0%/0%
Sponge spicules	0%/0%
Worm Tubes	0%/0%
Unidentified bioclasts	60%

Notes from thin section:	Loose sediment in resin. Estimates taken from more consolidated clusters in the slide. Calcite cement is observed only as blocky overgrowth on small echinoid fragments. One large angular micritic clast with one glauconite grain inside and small calcitic fragments. Glauconite grains are rounded with some fracturing, as well as intraclast growth within bioclasts. Glauconitised biotites. Some very minor hematisation of glauconite grains and intraclast growth, often very localised. Benthics are coiled (planar, trochospiral), uniserial, and biserial. Most tests are microcrystalline, but there are some hyalines. Some larger benthics, and some broken tests. Shell fragments show borings, some heavy. Echinoid fragments are all plates of small size and somewhat dusty. Unidentified bioclasts are usually shell fragments.

Stratigraphic Column:	NT10/08		
Sample Number:	NT10012603	**Location:**	Tokarahi Sill
Date Collected:	1/26/10	**Formation:**	Tapui Sst

Hand Specimen Description

Colour	**Induration**	**Bedding and Sedimentary Structures**		**Grainsize**
Brownish-green	Unconsolidated			Very fine to fine
Grain or matrix supported	**Sorting**	**Roundness**	**Sphericity - shape**	**Biologic binding**
Grain	Well			No
Textural Name:	**Siltstone**	**Notes:**	Siliciclastic.	

Thin Section Description

Matrix	**Percentage /100**
Clastics: Quartz (angular) (95%), biotite (angular) (5%)	95%
Cement	0%
Mud	0%
Bioclasts	0%
Authigenic minerals: Glauconite (5%), hematite (95%)	5%

Foraminifera	**Percentage /100**
Planktic	n/a
Benthic	n/a

Bioclasts	**Percentage of identified/total**
Foraminifera	n/a
Bryozoans	n/a
Echinoderms	n/a
Algae	n/a
Molluscs	n/a
Brachiopods	n/a
Barnacles	n/a
Sponge spicules	n/a
Worm Tubes	n/a
Unidentified bioclasts	n/a

Notes from thin section:	Loose sediment in resin. Quartz-rich sediment with biotite lathes, and localised heavy hematite alteration around grains. No observed bioclasts. A few sub-rounded glauconite grains.

Stratigraphic Column:	NT10/09		
Sample Number:	NT10012607	**Location:**	Elephant Rocks
Date Collected:	1/26/10	**Formation:**	Otekaike Lst

Hand Specimen Description

Colour	**Induration**	**Bedding and Sedimentary Structures**		**Grainsize**
Yellow-cream	Indurated			Fine
Grain or matrix supported	**Sorting**	**Roundness**	**Sphericity - shape**	**Biologic binding**
Matrix	Well			No
Textural Name:	**Wackestone**	**Notes:**		

Thin Section Description

Matrix	**Percentage /100**
Clastics: Quartz (angular-subangular)	1%
Cement	5%
Mud	20%
Bioclasts	67%
Authigenic minerals: Glauconite (30%), hematite (70%)	7%

Foraminifera	**Percentage /100**
Planktic	31% (n=54)
Benthic	69% (n=89)

Bioclasts	**Percentage of identified/total**
Foraminifera	80%/24%
Bryozoans	0%/0%
Echinoderms	20%/6%
Algae	0%/0%
Molluscs	0%/0%
Brachiopods	0%/0%
Barnacles	0%/0%
Sponge spicules	0%/0%
Worm Tubes	0%/0%
Unidentified bioclasts	70%

Notes from thin section:	Glauconite rounded grains alongside intraclasts within bioclast cavities. Hematite alteration of micrite matrix and some minor rim alteration of glauconite grains. Benthics are biserial, uniserial, trochpspiral and coiled. Tests are hyaline and microcrystalline. Calcite cement overgrowths on echinoid fragments. Broken small shell fragments with some borings.

Stratigraphic Column:	NT10/13		
Sample Number:	NT10061611	**Location:**	Browns Road
Date Collected:	6/16/10	**Formation:**	Ototara Lst

Hand Specimen Description

Colour	**Induration**	**Bedding and Sedimentary Structures**		**Grainsize**
Creamish-white	Indurated			Fine to coarse
Grain or matrix supported	**Sorting**	**Roundness**	**Sphericity - shape**	**Biologic binding**
Grain	Poor			No
Textural Name:	**Rudstone**	**Notes:**	Fossiliferous, bryozoan-rich.	

Thin Section Description

Matrix	**Percentage /100**
Clastics:	0%
Cement	5%
Mud	15%
Bioclasts	78%
Authigenic minerals: Glauconite, hematite	2%

Foraminifera	**Percentage /100**
Planktic	16% (n=10)
Benthic	84% (n=54)

Bioclasts	**Percentage of identified/total**
Foraminifera	28%/21%
Bryozoans	60%/44%
Echinoderms	7%/5%
Algae	2%/2%
Molluscs	1%/1%
Brachiopods	0%/0%
Barnacles	2%/2%
Sponge spicules	0%/0%
Worm Tubes	0%/0%
Unidentified bioclasts	25%

Notes from thin section:	This slide is mostly large bioclast pieces, and as such as been somewhat plucked. Section that is mostly unplucked has a mostly mictritic matrix, suggesting that same for the whole slide and thus the mud content may well be higher. Cements are primarily blocky overgrowths around bioclasts in singular extinction, with some isopachous cements as small rims around and within bioclasts. Glauconite is present as both mature grains and intrclast growth, with some hematite alterations. Some of the planktics are large micritised globorotalids. Benthics are dominated by large cyclina tests, with some coils, trochospiral, and nummulites (micritised). All tests are microcrystalline. Some indestinguishable shell fragments.

Stratigraphic Column:	NT10/14		
Sample Number:	NT10061702	**Location:**	Simpson Property Cliffs
Date Collected:	6/17/10	**Formation:**	Otekaike Lst

Hand Specimen Description

Colour	**Induration**	**Bedding and Sedimentary Structures**		**Grainsize**
Orangey-greeny-cream	Indurated			Fine to medium
Grain or matrix supported	**Sorting**	**Roundness**	**Sphericity - shape**	**Biologic binding**
Grain	Moderate			No
Textural Name:	**Packstone**	**Notes:**		

Thin Section Description

Matrix	**Percentage /100**
Clastics: Quartz (angulra to subangular), glauconitised biotite	10%
Cement	20%
Mud	7%
Bioclasts	43%
Authigenic minerals: Glauconite (89%), hematite (9%), phosphate (2%)	20%

Foraminifera	**Percentage /100**
Planktic	25% (n=50)
Benthic	75% (n=147)

Bioclasts	**Percentage of identified/total**
Foraminifera	83%/66%
Bryozoans	0%/0%
Echinoderms	10%/8%
Algae	2%/2%
Molluscs	0%/0%
Brachiopods	5%/4%
Barnacles	0%/0%
Sponge spicules	0%/0%
Worm Tubes	0%/0%
Unidentified bioclasts	20%

Notes from thin section:	Rounded glauconite grains with some intraclast growth. Some glauconite intraclast growth of echinoid fragments. Phosphate grains rounded to subangular. Hematite alteration of matrix in some minor localised parts of the slide. Blocky calcite cement in matrix. Benthics are coiled, uniserial, biserial, with significant trochospirals, with milliolids. Benthics are mostly microcrystalline, with some hyalines and a few large agglutinates. Large hinged brachiopod valves. Some pieces of corraline algae.

Stratigraphic Column:	NT10/14		
Sample Number:	NT10061704	**Location:**	Simpson Property Cliffs
Date Collected:	6/17/10	**Formation:**	Otekaike Lst

Hand Specimen Description

Colour	**Induration**	**Bedding and Sedimentary Structures**		**Grainsize**
Greenish-white	Very well indurated			Fine
Grain or matrix supported	**Sorting**	**Roundness**	**Sphericity - shape**	**Biologic binding**
Grain	Well			No
Textural Name:	**Packstone**	**Notes:**	Cemented and glauconitic.	

Thin Section Description

Matrix	**Percentage /100**
Clastics: Quartz (angular), minor biotite	5%
Cement	20%
Mud	5%
Bioclasts	50%
Authigenic minerals: Glauconite(95%), hematite (4%), phosphate (1%)	20%

Foraminifera	**Percentage /100**
Planktic	36% (n=65)
Benthic	64% (n=117)

Bioclasts	**Percentage of identified/total**
Foraminifera	57%/37%
Bryozoans	0%/0%
Echinoderms	35%/23%
Algae	0%/0%
Molluscs	5%/3%
Brachiopods	3%/2%
Barnacles	0%/0%
Sponge spicules	0%/0%
Worm Tubes	0%/0%
Unidentified bioclasts	35%

Notes from thin section:	Glauconite is present as rounded grains with some very minor intraclast formation. Some localised hematite alteration of matrix and around clasts. Blocky calcite cement overgrowths around some clasts forming matrix. Benthics are biserial, coiled, uniserial, and trochospiral. Tests are microcrystalline and hyaline. Large mollusc fragment has a micrite concentration against one side that may indicate some geopetal structure. Molluscs are smooth bivalve fragments.

Stratigraphic Column:	NT10/14		
Sample Number:	NT10061706	**Location:**	Simpson Property Cliffs
Date Collected:	6/17/10	**Formation:**	Otekaike Lst

Hand Specimen Description

Colour	**Induration**	**Bedding and Sedimentary Structures**		**Grainsize**
Grey-cream	Very well indurated			Fine
Grain or matrix supported	**Sorting**	**Roundness**	**Sphericity - shape**	**Biologic binding**
Grain	Well			No
Textural Name:	**Packstone**	**Notes:**	Cemented.	

Thin Section Description

Matrix	**Percentage /100**
Clastics: Quartz (angular), minor glauconitised biotites	2%
Cement	35%
Mud	10%
Bioclasts	43%
Authigenic minerals: Glauconite	10%

Foraminifera	**Percentage /100**
Planktic	22% (n=40)
Benthic	78% (n=140)

Bioclasts	**Percentage of identified/total**
Foraminifera	46%/23%
Bryozoans	0%/0%
Echinoderms	50%/25%
Algae	0%/0%
Molluscs	3%/1%
Brachiopods	1%/1%
Barnacles	0%/0%
Sponge spicules	0%/0%
Worm Tubes	0%/0%
Unidentified bioclasts	50%

Notes from thin section:	Blocky cement forming the majority of the matrix in this slide. Most of the glauconite present as rounded grains, with minor intraclast formation within benthic tests. Few glauconitised biotites. Benthics are coiled, uniserial, biserial, and trochospiral. Tests are mostly microcrystalline, with some hyalines. Unidentified bioclasts appear to be broken shell material.

Stratigraphic Column:	NT10/14		
Sample Number:	NT10061707	**Location:**	Simpson Property Cliffs
Date Collected:	6/17/10	**Formation:**	Otekaike Lst

Hand Specimen Description

Colour	**Induration**	**Bedding and Sedimentary Structures**		**Grainsize**
Greenish-yellowish-white	Very well indurated			Fine to medium
Grain or matrix supported	**Sorting**	**Roundness**	**Sphericity - shape**	**Biologic binding**
Grain	Moderate			No
Textural Name:	**Packstone**	**Notes:**	Glauconitic, muscovite (?), cemented, shell fragments.	

Thin Section Description

Matrix	**Percentage /100**
Clastics: Quartz (angular)	2%
Cement	20%
Mud	5%
Bioclasts	63%
Authigenic minerals: Glauconite (90%), hematite (6%), phosphate (4%)	10%

Foraminifera	**Percentage /100**
Planktic	26% (n=52)
Benthic	74% (n=147)

Bioclasts	**Percentage of identified/total**
Foraminifera	57%/34%
Bryozoans	0%/0%
Echinoderms	40%/24%
Algae	0%/0%
Molluscs	3%/2%
Brachiopods	0%/0%
Barnacles	0%/0%
Sponge spicules	0%/0%
Worm Tubes	0%/0%
Unidentified bioclasts	40%

Notes from thin section:	Rounded and subrounded glauconite grains, with a few intergrown with bioclasts. Some glauconite intraclast growth. Some very localised hematite alteration around single bioclasts. Some rounded to angular phosphate grains. Benthics are biserial, coiled, trochospiral, and milliolid. Mostly microcrystalline, with some hyalines and a few larger biserial quartz agglutinates. A few large coiled benthics. Large neomorphosed mollusc fragment. Some large echinoid fragments. Possibly a piece of corraline red algae, but is too micritised to determine the presence of characteristic texture.

Stratigraphic Column:	NT10/14		
Sample Number:	NT10061708	**Location:**	Simpson Property Cliffs Kokoamu
Date Collected:	6/17/10	**Formation:**	Greensand/Otekaike Lst

Hand Specimen Description

Colour	**Induration**	**Bedding and Sedimentary Structures**		**Grainsize**
Greeny-orange	Unconsolidated			Fine
Grain or matrix supported	**Sorting**	**Roundness**	**Sphericity - shape**	**Biologic binding**
Grain	Well			No
Textural Name:	**Packstone**	**Notes:**		

Thin Section Description

Matrix	**Percentage /100**
Clastics: Quartz (97%) (angular - sub-angular), biotite (3%)	10%
Cement	1%
Mud	23%
Bioclasts	25%
Authigenic minerals: Glauconite	41%

Foraminifera	**Percentage /100**
Planktic	71% (n=144)
Benthic	29% (n=60)

Bioclasts	**Percentage of identified/total**
Foraminifera	96%/72%
Bryozoans	0%/0%
Echinoderms	1%/1%
Algae	0%/0%
Molluscs	3%/2%
Brachiopods	0%/0%
Barnacles	0%/0%
Sponge spicules	0%/0%
Worm Tubes	0%/0%
Unidentified bioclasts	25%

Notes from thin section:	Loose sediment in resin. Calcite cement is present in very small amounts within a few bioclasts as tiny crystals forming a lining. Matrix estimates are a minimum and are based on some inclusive clasts within the resin. Benthics are coiled (planar, trochospiral), uniserial. Tests are microscrystalline, with one quartz agglutinate uniserial. Some larger benthic. Planktic forams are often very small. Large rounded glauconite grains, alongside small rounded to sub-angular grains. The few mollusc fragments are heavily bored and not very big.

Stratigraphic Column: NT10/14

Sample Number: NT10061709 **Location:** Simpson Property Cliffs

Date Collected: 6/17/10 **Formation:** Otekaike Lst

Hand Specimen Description

Colour	Induration	Bedding and Sedimentary Structures		Grainsize
Cream	Friable			Fine
Grain or matrix supported	**Sorting**	**Roundness**	**Sphericity - shape**	**Biologic binding**
Grain	Well			No
Textural Name:	**Packstone**	**Notes:**		

Thin Section Description

Matrix	Percentage /100
Clastics: Quartz (angular-rounded)	3%
Cement	1%
Mud	40%
Bioclasts	51%
Authigenic minerals: Glauconite (95%), hematite (5%)	5%

Foraminifera	Percentage /100
Planktic	45% (n=89)
Benthic	55% (n=107)

Bioclasts	Percentage of identified/total
Foraminifera	78%/47%
Bryozoans	0%/0%
Echinoderms	20%/12%
Algae	0%/0%
Molluscs	2%/1%
Brachiopods	0%/0%
Barnacles	0%/0%
Sponge spicules	0%/0%
Worm Tubes	0%/0%
Unidentified bioclasts	40%

Notes from thin section:	Very micritic and dirty slide. Minor spots of calcite cement remain on rims of some clasts, although there may have been more that has been removed or obscured in the slide. Glauconite is present primarily as intraclast growth in bioclast chambers (with some have been hematised), as well as some rounded grains. Benthics are uniserial, biserial, trochospiral, and coiled. Tests are dominantly microcrystalline with some hyalines. A few larger quartz allutinate tests and large hyaline benthics. Micritic matrix may be obscuring some microcrytalline tests, this scewing the ratio towards the planktics. Some large echinoid fragments.

Stratigraphic Column:	NT10/14		
Sample Number:	NT10061710	**Location:**	Simpson Property Cliffs
Date Collected:	6/17/10	**Formation:**	Otekaike Lst

Hand Specimen Description

Colour	**Induration**	**Bedding and Sedimentary Structures**		**Grainsize**
Light brown	Indurated			Fine
Grain or matrix supported	**Sorting**	**Roundness**	**Sphericity - shape**	**Biologic binding**
Grain	Well			No
Textural Name:	**Packstone**	**Notes:**		

Thin Section Description

Matrix	**Percentage /100**
Clastics: Quartz (angular)	7%
Cement	1%
Mud	35%
Bioclasts	52%
Authigenic minerals: Glauconite (95%), hematite (5%)	5%

Foraminifera	**Percentage /100**
Planktic	35% (n=39)
Benthic	65% (n=74)

Bioclasts	**Percentage of identified/total**
Foraminifera	69%/28%
Bryozoans	0%/0%
Echinoderms	30%/12%
Algae	0%/0%
Molluscs	1%/<1%
Brachiopods	0%/0%
Barnacles	0%/0%
Sponge spicules	0%/0%
Worm Tubes	0%/0%
Unidentified bioclasts	60%

Notes from thin section:	Micritic-rich slide. Glauconite rounded grains, with intraclast growth inside foram tests. Some hematisation of localised bioclasts and matrix. Benthics are coiled, biserial, trochospiral, and uniserial. Mostly microcrystalline tests with some hyalines. A few large biserial quartz agglutinate benthics. Some large hyaline trochospiral benthics also. A few large echinoid plate fragments. One mollusc fragment. Unidentified bioclasts are shell fragments.

Stratigraphic Column:	NT10/14		
Sample Number:	NT10061711	**Location:**	Simpson Property Cliffs
Date Collected:	6/17/10	**Formation:**	Otekaike Lst

Hand Specimen Description

Colour	**Induration**	**Bedding and Sedimentary Structures**		**Grainsize**
Yellowish-white	Very well indurated			Fine
Grain or matrix supported	**Sorting**	**Roundness**	**Sphericity - shape**	**Biologic binding**
Grain	Well			No
Textural Name:	**Packstone**	**Notes:**		

Thin Section Description

Matrix	**Percentage /100**
Clastics: Quartz (angular)	1%
Cement	35%
Mud	5%
Bioclasts	56%
Authigenic minerals: Glauconite (75%), hematite (25%)	3%

Foraminifera	**Percentage /100**
Planktic	29% (n=52)
Benthic	71% (n=127)

Bioclasts	**Percentage of identified/total**
Foraminifera	55%/17%
Bryozoans	0%/0%
Echinoderms	40%/12%
Algae	0%/0%
Molluscs	0%/0%
Brachiopods	5%/1%
Barnacles	0%/0%
Sponge spicules	0%/0%
Worm Tubes	0%/0%
Unidentified bioclasts	70%

Notes from thin section:	Glauconite is present as grains with some intraclast growth. Hematite alteration has occured mostly on the intraclast glauconite. Benthics are biserial, coiled, trochospiral, and uniserial. Tests are mostly microcrystalline, with some hyalines and some larger quartz agglutinates. One micritic planktic test is present also. Cements are blocky and form around bioclasts and their interstices. Often in single extinction crystals. Echinoid fragments are both small fragments with calcite cement overgrowths and large plates running through the whole slide. Brachipod pieces have psudopunctae. Most unidentified bioclasts appear to be shell fragments.

Stratigraphic Column:	NT10/14		
Sample Number:	NT10061712	**Location:**	Simpson Property Cliffs
Date Collected:	6/17/10	**Formation:**	Otekaike Lst

Hand Specimen Description

Colour	**Induration**	**Bedding and Sedimentary Structures**		**Grainsize**
Whitish-cream	Very well indurated			Fine to medium
Grain or matrix supported	**Sorting**	**Roundness**	**Sphericity - shape**	**Biologic binding**
Grain	Moderate			No
Textural Name:	**Grainstone**	**Notes:**	Shell fragments.	

Thin Section Description

Matrix	**Percentage /100**
Clastics: Quartz (angular to subangular), minor biotite crystals.	1%
Cement	30%
Mud	2%
Bioclasts	64%
Authigenic minerals: Glauconite (90%), hematite (10%)	3%

Foraminifera	**Percentage /100**
Planktic	35% (n=71)
Benthic	65% (n=130)

Bioclasts	**Percentage of identified/total**
Foraminifera	52%/26%
Bryozoans	2%/1%
Echinoderms	40%/20%
Algae	0%/0%
Molluscs	2%/1%
Brachiopods	4%/2%
Barnacles	0%/0%
Sponge spicules	0%/0%
Worm Tubes	0%/0%
Unidentified bioclasts	50%

Notes from thin section:	Very cemented matrix. Blocky calcite cement forming matrix and bioclast infills. Calcite cement overgrowths around echinoid fragments in syn-extinction. Some bioclast chambers are showing geopetal texture with blocky calcite cement forming alongside micrite. Rounded glauconite grains with some intraclast growth. Some minor localised hematite alteration of intraclast glauconite. Benthics are coiled, uniserial, triserial, and trochospiral. Some larger quartz agglutinate and hyaline benthic tests, but most are smaller microcrystalline and hyaline. Brachiopod valve has psuedopunctae filled with hematite. Large echinoid plate fragments. Mollusc appears to be a gastropod. Unidentified bioclasts appear to be shell fragments that cannot be determined as either brachiopod or mollusc etc.

Stratigraphic Column:	NT10/14		
Sample Number:	NT10061713	**Location:**	Simpson Property Cliffs
Date Collected:	6/17/10	**Formation:**	Otekaike Lst

Hand Specimen Description

Colour	**Induration**	**Bedding and Sedimentary Structures**		**Grainsize**
Yellowy-cream	Indurated			Silt to fine
Grain or matrix supported	**Sorting**	**Roundness**	**Sphericity - shape**	**Biologic binding**
Grain	Moderate			No
Textural Name:	**Packstone**	**Notes:**	One prominany ribbed bivalve.	

Thin Section Description

Matrix	**Percentage /100**
Clastics: Quartz (angular), some minor glauconitised biotite	5%
Cement	9%
Mud	32%
Bioclasts	51%
Authigenic minerals: Glauconite	3%

Foraminifera	**Percentage /100**
Planktic	34% (n=57)
Benthic	66% (n=113)

Bioclasts	**Percentage of identified/total**
Foraminifera	90%/36%
Bryozoans	0%/0%
Echinoderms	10%/4%
Algae	0%/0%
Molluscs	0%/0%
Brachiopods	0%/0%
Barnacles	0%/0%
Sponge spicules	0%/0%
Worm Tubes	0%/0%
Unidentified bioclasts	60%

Notes from thin section:	Micritic slide. Cements are blocky calcite in the matrix. Glauconite is mostly just rounded grains, although there are some bioclasts with glauconite formed in their chambers. Benthics are coiled, uniserial, trochospiral, and biserial. Most tests are microcrystalline with some hyalines and quartz agglutinates. Echinoids are mostly broken fragments with some larger plate pieces.

Stratigraphic Column:	NT10/03		
Sample Number:	NT10061802	**Location:**	Roy Farm
Date Collected:	6/18/10	**Formation:**	Ototara Lst

Hand Specimen Description

Colour	**Induration**	**Bedding and Sedimentary Structures**		**Grainsize**
Orangey-cream	Very well indurated			Medium to coarse
Grain or matrix supported	**Sorting**	**Roundness**	**Sphericity - shape**	**Biologic binding**
Grain	Moderate			No
Textural Name:	**Packstone**	**Notes:**	Cemented.	

Thin Section Description

Matrix	**Percentage /100**
Clastics: Rounded igneous clasts	2%
Cement	45%
Mud	10%
Bioclasts	40%
Authigenic minerals: Glauconite (23%), hematite (75%), phosphate (2%)	3%

Foraminifera	**Percentage /100**
Planktic	4% (n=1)
Benthic	96% (n=27)

Bioclasts	**Percentage of identified/total**
Foraminifera	10%/9%
Bryozoans	34%/33%
Echinoderms	10%/9%
Algae	44%/42%
Molluscs	2%/2%
Brachiopods	0%/0%
Barnacles	0%/0%
Sponge spicules	0%/0%
Worm Tubes	0%/0%
Unidentified bioclasts	5%

Notes from thin section:	Highly cemented. Calcite cement is isopachous rimming around bioclasts with blocky cement filling the matrix interstices. Micritic muds are found mostly inside zooecia of bryozoans or in other cavities of the various bioclasts. Some appears to have been left uncemented in the interstices between cement growth, where the micrite shows no drusy rims suggesting that they are not clasts, but remnant mud matrix. Glauconite is only seen as intraclasts within bioclast cavities, with most having been hematised lightly to heavily, with one algae fragment totally hematised. One observed phosphate occurence inside bioclast. Benthics are nummulites, coiled, uniserial, and biserial. A number of large hyaline and microcrystalline benthics. Algae is encrusting and braching corraline.

Stratigraphic Column:	NT10/15		
Sample Number:	NT10061803	**Location:**	Roy Farm
Date Collected:	6/18/10	**Formation:**	Ototara Lst

Hand Specimen Description

Colour	**Induration**	**Bedding and Sedimentary Structures**		**Grainsize**
White	Friable			Silt
Grain or matrix supported	**Sorting**	**Roundness**	**Sphericity - shape**	**Biologic binding**
Matrix	Well			No
Textural Name:	**Mudstone**	**Notes:**	Bioclast-free, clay-like.	

Thin Section Description

Matrix	**Percentage /100**
Clastics:	0%
Cement	2%
Mud	96%
Bioclasts	0%
Authigenic minerals: Hematite	2%

Foraminifera	**Percentage /100**
Planktic	n/a
Benthic	n/a

Bioclasts	**Percentage of identified/total**
Foraminifera	n/a
Bryozoans	n/a
Echinoderms	n/a
Algae	n/a
Molluscs	n/a
Brachiopods	n/a
Barnacles	n/a
Sponge spicules	n/a
Worm Tubes	n/a
Unidentified bioclasts	n/a

Notes from thin section:	Very miciritc section with very small localised occurenced of hematite alteration and minor calcite cement.

Stratigraphic Column:	NT10/15		
Sample Number:	NT10061804	**Location:**	Roy Farm
Date Collected:	6/18/10	**Formation:**	Ototara Lst

Hand Specimen Description

Colour	**Induration**	**Bedding and Sedimentary Structures**		**Grainsize**
Yellowy-cream	Fine to coarse			Fine to coarse
Grain or matrix supported	**Sorting**	**Roundness**	**Sphericity - shape**	**Biologic binding**
Grain	Poor			No
Textural Name:	**Grainstone**	**Notes:**		

Thin Section Description

Matrix	**Percentage /100**
Clastics: Quartz (angular)	Trace
Cement	20%
Mud	1%
Bioclasts	74%
Authigenic minerals: Glauconite (50%), hematite (50%)	5%

Foraminifera	**Percentage /100**
Planktic	6% (n=6)
Benthic	94% (n=91)

Bioclasts	**Percentage of identified/total**
Foraminifera	25%/21%
Bryozoans	25%/21%
Echinoderms	10%/8%
Algae	30%/26%
Molluscs	7%/6%
Brachiopods	2%/2%
Barnacles	1%/1%
Sponge spicules	0%/0%
Worm Tubes	0%/0%
Unidentified bioclasts	15%

Notes from thin section:	Somewhat dirty and heavily plucked slide. Cement is blocky in the matrix and shows isopachous needle habit around bioclasts, with syn-extinctional growth around large echinoid fragments. Glauconite is present almost entirely as intraclast growth within bioclasts, with some minor grain presence. Hematisation has occured in roughly half of the glauconite present. Benthics are coiled (including involute), milliolid, biserial, uniserial, and trochospiral. Tests are mostly microcrystalline with hyalines included. Some larger tests, including quartz agglutinates. Molluscs are both gastropod and lots of bivalve pieces, most of which retain original crystal structure with no alteration. Algae is both encrusting and branching corraline, with most of it broken into small pieces, while some encrusting examples are still found attached to bryozoan and mollusc fragments. Possible barnacle fragment.

Stratigraphic Column:	NT10/15		
Sample Number:	NT10061805	**Location:**	Roy Farm
Date Collected:	6/18/10	**Formation:**	Ototara Lst

Hand Specimen Description

Colour	**Induration**	**Bedding and Sedimentary Structures**		**Grainsize**
Orangey-cream	Very well indurated			Fine to coarse
Grain or matrix supported	**Sorting**	**Roundness**	**Sphericity - shape**	**Biologic binding**
Grain	Poor			No
Textural Name:	**Packstone**	**Notes:**	Cemented.	

Thin Section Description

Matrix	**Percentage /100**
Clastics: Quartz	trace
Cement	50%
Mud	5%
Bioclasts	40%
Authigenic minerals: Glauconite (40%), hematite (60%)	5%

Foraminifera	**Percentage /100**
Planktic	4% (n=4)
Benthic	96% (n=88)

Bioclasts	**Percentage of identified/total**
Foraminifera	30%/27%
Bryozoans	15%/13%
Echinoderms	7%/6%
Algae	45%/41%
Molluscs	3%/3%
Brachiopods	0%/0%
Barnacles	0%/0%
Sponge spicules	0%/0%
Worm Tubes	0%/0%
Unidentified bioclasts	10%

Notes from thin section:	Highly calcite cemented slide - equant spar drusy mosaic. Glauconite is present almost entirely as intraclast growth within bryozoan and foram cavities. The grains that have formed are present in a localised part of the slide, where nearly all have been heavily hematised. Hematisation has occured to a lesser degree in most glauconite content. Benthics are coiled, biserial, uniserial, trochospiral, nummulites, and milliolid. Tests are hyaline and microcrystalline with one mixed agglutinate biserial, with a number of large benthics. Algae consist of large and small pieces of both encrusting and branching corraline red algae.

Stratigraphic Column:	NT10/15		
Sample Number:	NT10061806	**Location:**	Roy Farm
Date Collected:	6/18/10	**Formation:**	Ototara Lst (mixed tuff lapilli)

Thin Section Description

Matrix	Percentage /100
Clastics: Igneous vesicular clasts (95%), pyroxene crystals (5%)	75%
Cement	15%
Mud	10%
Bioclasts	0%
Authigenic minerals:	0%

Foraminifera	Percentage /100
Planktic	n/a
Benthic	n/a

Bioclasts	Percentage of identified/total
Foraminifera	n/a
Bryozoans	n/a
Echinoderms	n/a
Algae	n/a
Molluscs	n/a
Brachiopods	n/a
Barnacles	n/a
Sponge spicules	n/a
Worm Tubes	n/a
Unidentified bioclasts	n/a

Notes from thin section:	Vesicular igneous clasts in a blocky calcite matrix. Significant hematite alteration of clasts. Some cement has formed in vesicles.

Stratigraphic Column:	NT10/16		
Sample Number:	NT10061808	**Location:**	Forresters
Date Collected:	6/18/10	**Formation:**	Oamaru Diatomite?

Hand Specimen Description

Colour	**Induration**	**Bedding and Sedimentary Structures**		**Grainsize**
Grey	Indurated			Very fine to silt
Grain or matrix supported	**Sorting**	**Roundness**	**Sphericity - shape**	**Biologic binding**
Matrix	Moderate			No
Textural Name:	**Mudstone**	**Notes:**	Slaked mudstone appearance. Bioturbated.	

Thin Section Description

Matrix	**Percentage /100**
Clastics: Quartz	1%
Cement	15%
Mud	83%
Bioclasts	1%
Authigenic minerals: Glauconite	Trace

Foraminifera	**Percentage /100**
Planktic	0% (n=0)
Benthic	100% (n=8)

Bioclasts	**Percentage of identified/total**
Foraminifera	89%/89%
Bryozoans	0%/0%
Echinoderms	0%/0%
Algae	0%/0%
Molluscs	0%/0%
Brachiopods	0%/0%
Barnacles	0%/0%
Sponge spicules	0%/0%
Worm Tubes	0%/0%
Unidentified bioclasts	11%/11%

Notes from thin section:	Very fine-grained slide. Dominantly one component (brown angular isotropic grains). Some small benthic forams (uniserial and biserial) observed, but generally there is little bioclast material. A couple of glauconite grains. Small drusy calcite cement crystals present, but do not appear to be growing off any nucleus.

Stratigraphic Column:	NT10/16		
Sample Number:	NT10061809	**Location:**	Forresters Oamaru
Date Collected:	6/18/10	**Formation:**	Diatomite

Hand Specimen Description

Colour	**Induration**	**Bedding and Sedimentary Structures**		**Grainsize**
Brown	Friable			Clay to fine
Grain or matrix supported	**Sorting**	**Roundness**	**Sphericity - shape**	**Biologic binding**
Matrix	Moderate			No
Textural Name:	**Mudstone**	**Notes:**	Diatomite.	

Thin Section Description

Matrix	**Percentage /100**
Clastics: Quartz (very small subangular grains)	4%
Cement	0%
Mud	50%
Bioclasts	31%
Authigenic minerals: Glauconite	15%

Foraminifera	**Percentage /100**
Planktic	43% (n=46)
Benthic	57% (n=61)

Bioclasts	**Percentage of identified/total**
Foraminifera	7%/7%
Bryozoans	0%/0%
Echinoderms	0%/0%
Algae	0%/0%
Molluscs	1%/1%
Brachiopods	0%/0%
Barnacles	0%/0%
Sponge spicules	33%/31%
Worm Tubes	0%/0%
Radiolarians	59%/56%
Unidentified bioclastics	5%

Notes from thin section:	Loose sediments in resin. Glauconite is rounded to subangular grains. Lots of sponge spicule fragments, and radiolarians are seen only as hexagonal grid patterns at 40x zoom in the mud matrix. A few radiolarian tests appear to have been glauconitised. Some glauconite formed within foram tests. Benthics are coiled, uniserial, and biserial. Tests are hyaline and microcrystalline with no large tests. Uniserials appear to be all hyaline and small.

Stratigraphic Column:	NT10/15		
Sample Number:	NT10061810	**Location:**	Forresters Oamaru
Date Collected:	6/18/10	**Formation:**	Diatomite

Hand Specimen Description

Colour	Induration	Bedding and Sedimentary Structures		Grainsize
Brown	Friable			Silt to fine
Grain or matrix supported	**Sorting**	**Roundness**	**Sphericity - shape**	**Biologic binding**
Matrix	Moderate			No
Textural Name:		**Notes:**	Diatomite.	

Thin Section Description

Matrix	Percentage /100
Clastics: Very small quartz (angular)	1%
Cement	3%
Mud	80%
Bioclasts	6%
Authigenic minerals: Glauconite (90%), phosphate (10%)	10%

Foraminifera	Percentage /100
Planktic	36% (n=17)
Benthic	64% (n=30)

Bioclasts	Percentage of identified/total
Foraminifera	20%/18%
Bryozoans	0%/0%
Echinoderms	0%/0%
Algae	0%/0%
Molluscs	0%/0%
Brachiopods	0%/0%
Barnacles	0%/0%
Sponge spicules	70%/63%
Worm Tubes	0%/0%
Radiolarians	10%/9%
Unidentified bioclastics	10%

Notes from thin section:	Very micritic section. Glauconite rounded grains, with some intraclast growth within test chambers, sponge spicule interiors, and overgrown on radioalrians. A few rounded phosphate clasts. Benthics are microcrystalline and hyaline, with one larger quartz agglutinate. Tests are coiled, biserial, and uniserial. Heavily micritic matrix obscuring a number of benthic tests, skewing the ratio in favour of planktics. Lots of broken sponge spicules.

Stratigraphic Column:	NT10/16		
Sample Number:	NT10061811	**Location:**	Forresters
Date Collected:	6/18/10	**Formation:**	Ototara Lst

Hand Specimen Description

Colour	**Induration**	**Bedding and Sedimentary Structures**		**Grainsize**
Greenish-white	Indurated			Fine
Grain or matrix supported	**Sorting**	**Roundness**	**Sphericity - shape**	**Biologic binding**
Grain	Well			No
Textural Name:	**Packstone**	**Notes:**	Cemented.	

Thin Section Description

Matrix	**Percentage /100**
Clastics: Quartz	5%
Cement	40%
Mud	10%
Bioclasts	40%
Authigenic minerals: Glauconite (85%), phosphate (15%)	5%

Foraminifera	**Percentage /100**
Planktic	8% (n=7)
Benthic	92% (n=78)

Bioclasts	**Percentage of identified/total**
Foraminifera	14%/11%
Bryozoans	15%/12%
Echinoderms	15%/12%
Algae	50%/40%
Molluscs	0%/0%
Brachiopods	0%/0%
Barnacles	0%/0%
Sponge spicules	5%/4%
Worm Tubes	0%/0%
Radiolarians	1%/1%
Unidentified bioclastics	20%

Notes from thin section:	Apparent alignment fabric in this slide showing bedding. Quartz is concentrated in layers that are more plucked. Glauconite present as grains and intraclast growth. Some phosphate grains. Calcite cement is drusy around bioclasts with blocky matrix interstices. Benthics are coiled, uniserial, trochospiral, and biserial. Tests are mostly microcrystalline with some hyalines. Planktic tests may have been obscured by calcite matrix. Algae are fragmented branching corraline.

Stratigraphic Column:	NT10/16		
Sample Number:	NT10061812	**Location:**	Forresters
Date Collected:	6/18/10	**Formation:**	Ototara Lst

Hand Specimen Description

Colour	**Induration**	**Bedding and Sedimentary Structures**		**Grainsize**
Yellowish-white	Indurated			Fine
Grain or matrix supported	**Sorting**	**Roundness**	**Sphericity - shape**	**Biologic binding**
Grain	Well			No
Textural Name:	**Packstone**	**Notes:**		

Thin Section Description

Matrix	**Percentage /100**
Clastics:	trace
Cement	10%
Mud	40%
Bioclasts	49%
Authigenic minerals: Glauconite (85%), phosphate (15%)	1%

Foraminifera	**Percentage /100**
Planktic	6% (n=4)
Benthic	94% (n=67)

Bioclasts	**Percentage of identified/total**
Foraminifera	30%/20%
Bryozoans	50%/32%
Echinoderms	14%/9%
Algae	5%/3%
Molluscs	1%/1%
Brachiopods	0%/0%
Barnacles	0%/0%
Sponge spicules	0%/0%
Worm Tubes	0%/0%
Unidentified bioclasts	35%

Notes from thin section:	Rather dirty and micritic section. Glauconite rounded grains and intraclast growth, with a few rounded phosphate clasts. Bethics are uniserial, trochospiral, biserial, milliolid and coiled. Most tests are microcrystalline, with some hyalines. Algae are encrusting.

Stratigraphic Column:	NT10/17		
Sample Number:	NT10061813	**Location:**	Bains
Date Collected:	6/18/10	**Formation:**	Diatomite

Hand Specimen Description

Colour	**Induration**	**Bedding and Sedimentary Structures**		**Grainsize**
Light brown	Friable			Clay
Grain or matrix supported	**Sorting**	**Roundness**	**Sphericity - shape**	**Biologic binding**
Matrix	Well			No
Textural Name:	**Mudstone**	**Notes:**	Diatomite.	

Thin Section Description

Matrix	**Percentage /100**
Clastics: Quartz, one quartz arenite clast	1%
Cement	0%
Mud	96%
Bioclasts	2%
Authigenic minerals: Glauconite (75%), hematite (25%)	1%

Foraminifera	**Percentage /100**
Planktic	n/a
Benthic	n/a

Bioclasts	**Percentage of identified/total**
Foraminifera	0%/0%
Bryozoans	0%/0%
Echinoderms	0%/0%
Algae	0%/0%
Molluscs	0%/0%
Brachiopods	0%/0%
Barnacles	0%/0%
Sponge spicules	70%/70%
Worm Tubes	0%/0%
Radiolarians	30%/30%
Unidentified bioclastics	0%

Notes from thin section:	Very fine grained diatomite with intersperced sponge spicules and radiolarians. Sub-angular glauconite with some hematite alteration. One clasts that appears to be a sub-rounded quartz arenite with a glauconite grain included. No forams observed, with only a few radiolarians sighted due to nature of the fine matrix. One radiolarian showing complete hexagonally textured frustule.

Stratigraphic Column:	NT10/17		
Sample Number:	NT10061815	**Location:**	Bains
Date Collected:	6/18/10	**Formation:**	Waiareka-Deborah Volcanics

Hand Specimen Description

Colour	Induration	Bedding and Sedimentary Structures		Grainsize
Browny-green	Indurated			Fine
Grain or matrix supported	**Sorting**	**Roundness**	**Sphericity - shape**	**Biologic binding**
Grain	Well			No
Textural Name:	**Tuff (packstone)**	**Notes:**	Tuff.	

Thin Section Description

Matrix	Percentage /100
Clastics:	20%
Cement	0%
Mud	78%
Bioclasts	1%
Authigenic minerals:	1%

Foraminifera	Percentage /100
Planktic	0% (n=0)
Benthic	100% (n=3)

Bioclasts	Percentage of identified/total
Foraminifera	100%/100%
Bryozoans	0%/0%
Echinoderms	0%/0%
Algae	0%/0%
Molluscs	0%/0%
Brachiopods	0%/0%
Barnacles	0%/0%
Sponge spicules	0%/0%
Worm Tubes	0%/0%
Unidentified bioclasts	0%

Notes from thin section:	Igneous tuff deposit with minor igneous vesicular clasts that show flow banding in the vesiculated glass. Some hematisation of the matrix. Some rounded glauconite grains in matrix. A couple of uniserial benthics observed, with one completed hematised. Igneous nature of matrix and clasts makes bioclast ID very difficult.

Stratigraphic Column:	NT10/17		
Sample Number:	NT10061816	**Location:**	Bains
Date Collected:	6/18/10	**Formation:**	Waiareka-Deborah Volcanics

Thin Section Description

Matrix	Percentage /100
Clastics: Vesicular igneous clasts	50%
Volcanic glass	50%
Mud	0%
Bioclasts	0%
Authigenic minerals: Glauconite	0%

Foraminifera	Percentage /100
Planktic	n/a
Benthic	n/a

Bioclasts	Percentage of identified/total
Foraminifera	n/a
Bryozoans	n/a
Echinoderms	n/a
Algae	n/a
Molluscs	n/a
Brachiopods	n/a
Barnacles	n/a
Sponge spicules	n/a
Worm Tubes	n/a
Unidentified bioclasts	n/a

Notes from thin section:	Igneous clasts in volcanic glass. Vesicular with flow textures. One basalt clasts with neddlelike euhedral feldspars.

Stratigraphic Column:	NT10/18		
Sample Number:	NT10071301	**Location:**	Teschemaker Volcanics
Date Collected:	7/13/10	**Formation:**	Waiareka-Deborah Volcanics)

Thin Section Description

Matrix	Percentage /100
Clastics: Quartz, amphibole, mafic clasts including one scoria clast. Glass.	80%
Cement	0%
Mud	0%
Bioclasts	0%
Authigenic minerals: Hematite	20%

Foraminifera	Percentage /100
Planktic	n/a
Benthic	n/a

Bioclasts	Percentage of identified/total
Foraminifera	n/a
Bryozoans	n/a
Echinoderms	n/a
Algae	n/a
Molluscs	n/a
Brachiopods	n/a
Barnacles	n/a
Sponge spicules	n/a
Worm Tubes	n/a
Unidentified bioclasts	n/a

Notes from thin section:	Loose sediments set in resin. Hematite altered tuff deposit with some remnant mafic crystals (amphibole) and occasional quartz grain. Very difficult to identify much from this slide. One vesicular basalt clast. Isotropic glass mixed in with resin.

Stratigraphic Column:	NT10/18		
Sample Number:	NT10071302	**Location:**	Teschemaker Volcanics
Date Collected:	7/13/10	**Formation:**	Waiareka-Deborah Volcanics

Thin Section Description

Matrix	Percentage /100
Clastics: Mafic angular clasts (99%), Quartz (1%) (small grains found in mafic clasts)	100%
Cement	0%
Mud	0%
Bioclasts	0%
Authigenic minerals:	0%

Foraminifera	Percentage /100
Planktic	n/a
Benthic	n/a

Bioclasts	Percentage of identified/total
Foraminifera	n/a
Bryozoans	n/a
Echinoderms	n/a
Algae	n/a
Molluscs	n/a
Brachiopods	n/a
Barnacles	n/a
Sponge spicules	n/a
Worm Tubes	n/a
Unidentified bioclasts	n/a

Notes from thin section:	Loose angular clasts in resin.

Stratigraphic Column:	NT10/19		
Sample Number:	NT10071401	**Location:**	Kakanui River Section
Date Collected:	7/14/10	**Formation:**	Ototara Lst

Hand Specimen Description

Colour	**Induration**	**Bedding and Sedimentary Structures**		**Grainsize**
White	Friable			Fine to medium
Grain or matrix supported	**Sorting**	**Roundness**	**Sphericity - shape**	**Biologic binding**
Grain	Poorly sorted			No
Textural Name:	**Packstone**	**Notes:**		

Thin Section Description

Matrix	**Percentage /100**
Clastics: Quartz	2%
Cement	<1%
Mud	30%
Bioclasts	67%
Authigenic minerals: Glauconite (30%), phosphate (70%)	1%

Foraminifera	**Percentage /100**
Planktic	17% (n=4)
Benthic	83% (n=19)

Bioclasts	**Percentage of identified/total**
Foraminifera	5%/3%
Bryozoans	85%/56%
Echinoderms	7%/4%
Algae	0%/0%
Molluscs	3%/2%
Brachiopods	0%/0%
Barnacles	0%/0%
Sponge spicules	0%/0%
Worm Tubes	0%/0%
Unidentified bioclasts	35%

Notes from thin section:	Loose sediment in resin. Calcite matrix is present in very small amounts as traces of blocky cement within a few bryozoan walls. Significant amounts of micritic mud matrix. Minor glauconite grains and intraclast growths. Angular to rounded phosphate grains. Benthics are coiled, biserial and uniserial. Loose sediment nature of this slide and the large amounts of micrite matrix make foram identification difficult. Tests are microcrystalline, with one large benthic hyaline test. One ostracod.

Stratigraphic Column:	NT10/19		
Sample Number:	NT10071402	**Location:**	Kakanui River Section
Date Collected:	7/14/10	**Formation:**	Ototara Lst

Hand Specimen Description

Colour	**Induration**	**Bedding and Sedimentary Structures**		**Grainsize**
Greenish-white	Inudrated			Fine to medium
Grain or matrix supported	**Sorting**	**Roundness**	**Sphericity - shape**	**Biologic binding**
Grain	Moderate			No
Textural Name:	**Packstone**	**Notes:**	Fossiliferous, bryozoans.	

Thin Section Description

Matrix	**Percentage /100**
Clastics: Quartz (angular), small angular igneous clasts	7%
Cement	2%
Mud	25%
Bioclasts	51%
Authigenic minerals: Glauconite (85%), hematite (15%)	15%

Foraminifera	**Percentage /100**
Planktic	42% (n=53)
Benthic	58% (n=74)

Bioclasts	**Percentage of identified/total**
Foraminifera	10%/9%
Bryozoans	56%/50%
Echinoderms	10%/9%
Algae	20%/18%
Molluscs	4%/4%
Brachiopods	0%/0%
Barnacles	0%/0%
Sponge spicules	0%/0%
Worm Tubes	0%/0%
Unidentified bioclasts	10%

Notes from thin section:	Moderatly plucked slide. Calcite cement observed within bioclast void space. Most plucked out. Sub-angular to rounded glauconite grains. Mature and fresh glauconite grains and intraclast growth. Some hematite alteration of glauconite and igneous clasts. Benthics are biserial, uniserial, coiled (planar, trochospiral), and milliolid. Some larger quartz agglutinate benthics. Tests are mostly microcrystalline, with some hyalines. Corraline encrusting and branching red algae. Some shell fragments show boring.

Stratigraphic Column:	NT10/19		
Sample Number:	NT10071403	**Location:**	Kakanui River Section
Date Collected:	7/14/10	**Formation:**	Ototara Lst

Hand Specimen Description

Colour	**Induration**	**Bedding and Sedimentary Structures**		**Grainsize**
Cream-white	Indurated			Very fine to medium
Grain or matrix supported	**Sorting**	**Roundness**	**Sphericity - shape**	**Biologic binding**
Grain	Poor			No
Textural Name:	**Packstone**	**Notes:**	Bryozoans.	

Thin Section Description

Matrix	**Percentage /100**
Clastics: Quartz (angular)	1%
Cement	20%
Mud	4%
Bioclasts	72%
Authigenic minerals: Glauconite	3%

Foraminifera	**Percentage /100**
Planktic	30% (n=21)
Benthic	70% (n=50)

Bioclasts	**Percentage of identified/total**
Foraminifera	4%/3%
Bryozoans	57%/48%
Echinoderms	15%/13%
Algae	20%/17%
Molluscs	3%/3%
Brachiopods	1%/1%
Barnacles	0%/0%
Sponge spicules	0%/0%
Worm Tubes	0%/0%
Unidentified bioclasts	15%

Notes from thin section:	Calcite cements are blocky around echinoid fragments, while being isopachous within and around most other bioclasts, particularly within bryozoan void space (although resin has filled most of these). Glauconite is primarily intraclast growth of bioclasts, with some more mature rounded grains present also. Benthics are coiled (planar, trochospiral), uniserial, and biserial. Tests are microcrystalline with a few hyalines. Some relatively large benthic uniserials. Algae are branching corraline.

Stratigraphic Column:	NT10/19		
Sample Number:	NT10071404	**Location:**	Kaknui River Section
Date Collected:	7/14/10	**Formation:**	Ototara Lst

Hand Specimen Description

Colour	**Induration**	**Bedding and Sedimentary Structures**		**Grainsize**
Greenish-yellow	Friable			Fine to medium
Grain or matrix supported	**Sorting**	**Roundness**	**Sphericity - shape**	**Biologic binding**
Grain	Moderate			No
Textural Name:	**Packstone**	**Notes:**		

Thin Section Description

Matrix	**Percentage /100**
Clastics: Quartz (angular - subangular)	10%
Cement	0%
Mud	5%
Bioclasts	38%
Authigenic minerals: Glauconite, hematite	47%

Foraminifera	**Percentage /100**
Planktic	22% (n=38)
Benthic	78% (n=132)

Bioclasts	**Percentage of identified/total**
Foraminifera	53%/47%
Bryozoans	17%/15%
Echinoderms	22%/20%
Algae	3%/3%
Molluscs	4%/4%
Brachiopods	1%/1%
Barnacles	0%/0%
Sponge spicules	0%/0%
Worm Tubes	0%/0%
Unidentified bioclasts	10%

Notes from thin section:	Sample is made from unconsolidated sediments set in resin. Large amount of hematite alteration is within the matrix and is probably altered micrite. Glauconite is present both as rounded clasts and within bioclast chambers. Some glauconitisation present within echinoid fragments. Benthics are uniserial, biserial, and coiled (trochospiral and planar). Benthics are mostly microcrystalline, with some hyalines and some larger agglutinates. Neomorphosed and unaltered mollusc fragments with some showing borings.

Stratigraphic Column:	NT10/19		
Sample Number:	NT10071405	**Location:**	Kakanui River Section
Date Collected:	7/14/10	**Formation:**	Ototara Lst

Hand Specimen Description

Colour	**Induration**	**Bedding and Sedimentary Structures**		**Grainsize**
Cream	Indurated			Fine to coarse
Grain or matrix supported	**Sorting**	**Roundness**	**Sphericity - shape**	**Biologic binding**
Grain	Poor			No
Textural Name:	**Packstone**	**Notes:**	Fossiliferous, bryozoans.	

Thin Section Description

Matrix	**Percentage /100**
Clastics: Quartz (sub-angular - angular), one small angular igneous clast	3%
Cement	10%
Mud	25%
Bioclasts	59%
Authigenic minerals: Glauconite (70%), hematite (10%), phosphate (20%)	3%

Foraminifera	**Percentage /100**
Planktic	58% (n=26)
Benthic	42% (n=19)

Bioclasts	**Percentage of identified/total**
Foraminifera	5%/5%
Bryozoans	58%/52%
Echinoderms	15%/13%
Algae	20%/18%
Molluscs	2%/2%
Brachiopods	0%/0%
Barnacles	0%/0%
Sponge spicules	0%/0%
Worm Tubes	0%/0%
Unidentified bioclasts	10%

Notes from thin section:	Calcite cement is blocky around echinoid fragments as well as inside some shell remnant fragments. Isopachous elsewhere, including relatively heavily inside some bryozoan zooecia. Rounded phosphate and glauconite grains. Some alteration of matrix and glauconite grains by hematite. Benthics are biserial, uniserial, and coiled (trochospiral, planar). Tests are mostly microcrystalline, with some hyalines. One large ribbed trochosprial hyaline benthic observed. One quartz agglutinate benthic.

Stratigraphic Column:	NT10/19		
Sample Number:	NT10071406	**Location:**	Kakanui River Section
Date Collected:	7/14/10	**Formation:**	Ototara Lst

Hand Specimen Description

Colour	**Induration**	**Bedding and Sedimentary Structures**		**Grainsize**
Greenish-yellow	Friable			Grain
Grain or matrix supported	**Sorting**	**Roundness**	**Sphericity - shape**	**Biologic binding**
Moderate	Moderate			No
Textural Name:	**Packstone**	**Notes:**	Heavily bioturbated carbonate sands.	

Thin Section Description

Matrix	**Percentage /100**
Clastics: Quartz (angular-subrounded) (90%), mafic clasts and amphibole (10%)	10%
Cement	1%
Mud	5%
Bioclasts	59%
Authigenic minerals: Glauconite (95%), hematite (5%)	25%

Foraminifera	**Percentage /100**
Planktic	28% (n=51)
Benthic	72% (n=131)

Bioclasts	**Percentage of identified/total**
Foraminifera	80%/32%
Bryozoans	5%/2%
Echinoderms	10%/4%
Algae	0%/0%
Molluscs	3%/1%
Brachiopods	1%/<1%
Barnacles	0%/0%
Sponge spicules	1%/<1%
Worm Tubes	0%/0%
Unidentified bioclasts	61%

Notes from thin section:	Loose sediment in resin. Glauconite content is both as rounded grains and intraclast growth. Estimating mud and cement percentages is innacurate due to the nature of the resinous slide. Benthics are coiled (trochospiral and planar), uniserial, and biserial. Tests are microcrystalline with some hyalines, and at least one large agglutinate. Some lagre benthics present. Brachiopod fragments shows punctae. Bored shell fragments.

Stratigraphic Column:	NT10/19		
Sample Number:	NT10071407	**Location:**	Kakanui River Section
Date Collected:	7/14/10	**Formation:**	Ototara Lst

Hand Specimen Description

Colour	**Induration**	**Bedding and Sedimentary Structures**		**Grainsize**
Greenish-yellow	Friable	Normal grading		Fine to coarse
Grain or matrix supported	**Sorting**	**Roundness**	**Sphericity - shape**	**Biologic binding**
Grain	Moderate			No
Textural Name:	**Packstone**	**Notes:**	Normal grading, flame structures, echinoid spine.	

Thin Section Description

Matrix	**Percentage /100**
Clastics: Quartz, two igneous clasts. Some biotite lathes.	5%
Cement	2%
Mud	20%
Bioclasts	48%
Authigenic minerals: Glauconite (96%), phosphate (2%), hematite (2%)	25%

Foraminifera	**Percentage /100**
Planktic	24% (n=29)
Benthic	76% (n=90)

Bioclasts	**Percentage of identified/total**
Foraminifera	59%/38%
Bryozoans	15%/10%
Echinoderms	6%/4%
Algae	5%/3%
Molluscs	15%/10%
Brachiopods	0%/0%
Barnacles	0%/0%
Sponge spicules	0%/0%
Worm Tubes	0%/0%
Unidentified bioclasts	35%

Notes from thin section:	Loose sediment and sediment clumps in resin. Some small spary cement in bioclast voids or around a few clasts. Some micrite inside bioclast voids as well as forming the matrix. Glauconite forms many rounded to sub-angular grains, with lots of intraclast growth in bioclasts, as well as forming within shell borings and on echinoid fragment rims. Phosphate observed as a couple of elongated rounded grains. Hematite forms on the rims of a couple of glauconite grains. Some foram tests chambers are filled with dark hematite. Benthics are coiled (trochospiral, planar), uniserial, and biserial. Tests are mostly microcrystalline, with a few hyalines. Some larger benthic tests observed. Some shell fragments show heavy borings, both small and large. Large echinoid plate fragments. Two larger corraline red algae fragments.

Stratigraphic Column:	NT10/19		
Sample Number:	NT10071408	**Location:**	Kakanui River Section
Date Collected:	7/14/10	**Formation:**	Ototara Lst

Hand Specimen Description

Colour	**Induration**	**Bedding and Sedimentary Structures**		**Grainsize**
Whitish-cream	Friable			Silt
Grain or matrix supported	**Sorting**	**Roundness**	**Sphericity - shape**	**Biologic binding**
Matrix	Well			No
Textural Name:	**Mudstone**	**Notes:**		

Thin Section Description

Matrix	**Percentage /100**
Clastics: Quartz (angular) (5%), igneous clasts (sub-rounded) (95%)	2%
Cement	5%
Mud	85%
Bioclasts	5%
Authigenic minerals: Hematite (85%), glauconite (15%)	3%

Foraminifera	**Percentage /100**
Planktic	35% (n=9)
Benthic	65% (n=17)

Bioclasts	**Percentage of identified/total**
Foraminifera	95%/86%
Bryozoans	0%/0%
Echinoderms	0%/0%
Algae	0%/0%
Molluscs	5%/4%
Brachiopods	0%/0%
Barnacles	0%/0%
Sponge spicules	0%/0%
Worm Tubes	0%/0%
Unidentified bioclasts	10%

Notes from thin section:	Loose sediment in resin. Very poor quality slide. Calcite cement observed as small blocky fills within circular or bioclast (shell) shaped voids. Micrite is by far the dominant material here. Hematite altered igneous clasts, with some alteration of unidentified clasts. Minor glauconite observed within foram test. Benthics are uniserial, and coiled (planar, trochospiral). Tests are mostly hyaline, with microcrystallines present but probably obscured by matrix. All foram tests are very small. Unidentified bioclasts are fragmented shell material or cement filled voids.

Stratigraphic Column:	NT10/19		
Sample Number:	NT10071409	**Location:**	Kakanui River Section
Date Collected:	7/14/10	**Formation:**	Deborah Volcanics

Hand Specimen Description

Colour	**Induration**	**Bedding and Sedimentary Structures**		**Grainsize**
Yellowish-green	Indurated			Fine to very fine
Grain or matrix supported	**Sorting**	**Roundness**	**Sphericity - shape**	**Biologic binding**
Grain	Well			No
Textural Name:	**Tuff (packstone)**	**Notes:**	Tuffaceous with some glauconite. Faint lamination.	

Thin Section Description

Matrix	**Percentage /100**
Clastics: Igneous minerals and clasts (30%) - tuff (70%)	84%
Cement	15%
Mud	0%
Bioclasts	Trace
Authigenic minerals: Glauconite	1%

Foraminifera	**Percentage /100**
Planktic	0% (n=0)
Benthic	100% (n=1)

Bioclasts	**Percentage of identified/total**
Foraminifera	100%/100%
Bryozoans	0%/0%
Echinoderms	0%/0%
Algae	0%/0%
Molluscs	0%/0%
Brachiopods	0%/0%
Barnacles	0%/0%
Sponge spicules	0%/0%
Worm Tubes	0%/0%
Unidentified bioclasts	0%

Notes from thin section:	Rounded to sub-rounded glauconite grains. Significant amounts of euhedral biotite lathes, with some pyroxene. Some sub-rounded igneous clasts. One observed coiled planar microcrystalline benthic foram. Some locations in the slide show blocky calcite cement (large portions of the matrix have been plucked off the slide).

Stratigraphic Column:	NT10/19		
Sample Number:	NT10071410	**Location:**	Kakanui River Section
Date Collected:	7/14/10	**Formation:**	Ototara Lst

Hand Specimen Description

Colour	**Induration**	**Bedding and Sedimentary Structures**		**Grainsize**
Yellowish-white	Friable			Fine to coarse
Grain or matrix supported	**Sorting**	**Roundness**	**Sphericity - shape**	**Biologic binding**
Grain	Very poor			No
Textural Name:	**Packstone**	**Notes:**	Observed bryozoan.	

Thin Section Description

Matrix	**Percentage /100**
Clastics: Quartz (angular), a few rounded to sub-rounded igneous clasts	2%
Cement	2%
Mud	7%
Bioclasts	81%
Authigenic minerals: Glauconite (80%), hematite (15%), phosphate (5%)	8%

Foraminifera	**Percentage /100**
Planktic	10% (n=7)
Benthic	90% (n=61)

Bioclasts	**Percentage of identified/total**
Foraminifera	10%/10%
Bryozoans	47%/45%
Echinoderms	12%/11%
Algae	12%/11%
Molluscs	3%/3%
Brachiopods	15%/14%
Barnacles	1%/1%
Sponge spicules	0%/0%
Worm Tubes	0%/0%
Unidentified bioclasts	5%

Notes from thin section:	Glauconite present mostly as intraclast growth within bioclast void space, as well as within shell borings. Some rounded to sub-angular grains. Glauconitisation of some echinoid fragments. Hematite alteration in some places of glauconite grains. Rounded phosphate grains. Calcite cement is observed only as thin rims within bioclast chambers, with the rest filled by resin. Benthics are coiled (planar, trochospiral), uniserial, and biserial. Tests are predominantly microcrystalline, with some hyalines (mostly biserials). A few larger benthics, with one observed quartz agglutinate. Most shelly bioclasts fragments (bivalves and echinoid fragments) are heavily bored. Corraline branching as well as encrusting red algae.

Stratigraphic Column:	NT10/19		
Sample Number:	NT10071411	**Location:**	Kakanui River Section
Date Collected:	7/14/10	**Formation:**	Ototara Lst

Hand Specimen Description

Colour	**Induration**	**Bedding and Sedimentary Structures**		**Grainsize**
Yellowish-white	Friable			Silt to very fine
Grain or matrix supported	**Sorting**	**Roundness**	**Sphericity - shape**	**Biologic binding**
Matrix	Moderate			No
Textural Name:	**Wackestone**	**Notes:**		

Thin Section Description

Matrix	**Percentage /100**
Clastics: Quartz (angular), one large igneous clast	5%
Cement	0%
Mud	70%
Bioclasts	15%
Authigenic minerals: Glauconite (70%), hematite (30%)	10%

Foraminifera	**Percentage /100**
Planktic	29% (n=25)
Benthic	71% (n=60)

Bioclasts	**Percentage of identified/total**
Foraminifera	34%/32%
Bryozoans	0%/0%
Echinoderms	0%/0%
Algae	0%/0%
Molluscs	1%/1%
Brachiopods	0%/0%
Barnacles	0%/0%
Sponge spicules	65%/62%
Worm Tubes	0%/0%
Unidentified bioclasts	5%

Notes from thin section:	Poor muddy slide. Glauconite grains are rounded, but also commonly form as intraclast growth in bioclast void space. Hematite alteration of some glauconite, and also formation predominantly around sponge spicules. Benthics are coiled (planar, trochospiral), uniserial, biserial, and milliolid. Micritic matrix makes identification of microcrystalline foram tests difficult.

Stratigraphic Column:	NT10/20		
Sample Number:	NT10071501	**Location:**	Teschemaker
Date Collected:	7/15/10	**Formation:**	Ototara Lst

Hand Specimen Description

Colour	**Induration**	**Bedding and Sedimentary Structures**		**Grainsize**
Cream	Friable			Silt to medium
Grain or matrix supported	**Sorting**	**Roundness**	**Sphericity - shape**	**Biologic binding**
Matrix	Moderate			No
Textural Name:	**Wackestone**	**Notes:**		

Thin Section Description

Matrix	**Percentage /100**
Clastics: Quartz (angular), one igneous clast	1%
Cement	1%
Mud	40%
Bioclasts	53%
Authigenic minerals: Glauconite (60%), hematite (30%), phosphate (10%)	5%

Foraminifera	**Percentage /100**
Planktic	14% (n=13)
Benthic	86% (n=79)

Bioclasts	**Percentage of identified/total**
Foraminifera	20%/14%
Bryozoans	55%/39%
Echinoderms	10%/7%
Algae	5%/3%
Molluscs	10%/7%
Brachiopods	0%/0%
Barnacles	0%/0%
Sponge spicules	0%/0%
Worm Tubes	0%/0%
Unidentified bioclasts	30%

Notes from thin section:	Quartz fragments are very small. Calcite cement present as small overgrowths on echinoid fragments, with some isopachous spar. Glauconite grains are rounded and commonly altered with hematite. Rounded phosphate grains. Glauconite intraclasts formation is common. Benthics are uniserial, biserial, coiled (planar, trochospiral), and milliolid. Tests are mostly microcrystalline, with some hyalines. Shell fragments show boring. Bioclasts appear to show parallel alignment.

Stratigraphic Column:	NT10/20		
Sample Number:	NT10071502	**Location:**	Teschemaker
Date Collected:	7/15/10	**Formation:**	Ototara Lst

Hand Specimen Description

Colour	**Induration**	**Bedding and Sedimentary Structures**		**Grainsize**
Yellowish-white	Indurated			Fine to medium
Grain or matrix supported	**Sorting**	**Roundness**	**Sphericity - shape**	**Biologic binding**
Grain	Moderate			No
Textural Name:	**Packstone**	**Notes:**		

Thin Section Description

Matrix	**Percentage /100**
Clastics: Quartz (angular)	Trace
Cement	7%
Mud	15%
Bioclasts	74%
Authigenic minerals: Glauconite (10%), hematite (90%)	4%

Foraminifera	**Percentage /100**
Planktic	4% (n=1)
Benthic	96% (n=22)

Bioclasts	**Percentage of identified/total**
Foraminifera	2%/2%
Bryozoans	87%/74%
Echinoderms	5%/4%
Algae	1%/1%
Molluscs	5%/4%
Brachiopods	0%/0%
Barnacles	0%/0%
Sponge spicules	0%/0%
Worm Tubes	0%/0%
Unidentified bioclasts	15%

Notes from thin section:	Calcite cement is small-scale blocky within bryzoan zooecia and some echinoid overgrowth. A few rounded glauconite grains. Very heavy hematite alteration in a couple of locations, becoming less as it radiates out. Benthics are uniserial, coiled (planar, trochospiral), and biserial. Microcrystalline and hyaline tests. Shell fragments show signs of borings. Most unidentified material is shell fragment.

Stratigraphic Column:	NT10/20		
Sample Number:	NT10071503	**Location:**	Teschemaker
Date Collected:	7/15/10	**Formation:**	Ototara Lst

Hand Specimen Description

Colour	**Induration**	**Bedding and Sedimentary Structures**		**Grainsize**
Yellowish-white	Indurated			Fine to very fine
Grain or matrix supported	**Sorting**	**Roundness**	**Sphericity - shape**	**Biologic binding**
Matrix	Well			No
Textural Name:	**Wackestone**	**Notes:**	One distinct bivalve shell.	

Thin Section Description

Matrix	**Percentage /100**
Clastics: Quartz (angular)	Trace
Cement	1%
Mud	40%
Bioclasts	58%
Authigenic minerals: Glauconite (40%), phosphate (10%), hematite (50%)	1%

Foraminifera	**Percentage /100**
Planktic	18% (n=26)
Benthic	82% (n=122)

Bioclasts	**Percentage of identified/total**
Foraminifera	56%/45%
Bryozoans	30%/24%
Echinoderms	10%/8%
Algae	0%/0%
Molluscs	2%/2%
Brachiopods	2%/2%
Barnacles	0%/0%
Sponge spicules	0%/0%
Worm Tubes	0%/0%
Unidentified bioclasts	19%

Notes from thin section:	Quite a micritic slide. Very small traces of isopachous calcite cement to be found within a few bioclast void spaces. A couple of blocky remnants near echinoid fragments. Minor glauconite rounded grains, most showing hematite alteration. Some hematite alteration of matrix. Minor glauconite growth observed within bioclast chambers/zooecia. One grain of phosphate (rounded) observed. Benthics are uniserial, biserial, coiled (planar, trochospiral), and milliolid. Tests are a mix of microcrystalline and hyaline. Micritic matrix does make foram identification somewhat difficult.

Stratigraphic Column:	NT10/20		
Sample Number:	NT10071504	**Location:**	Teschemaker
Date Collected:	7/15/10	**Formation:**	Ototara Lst

Hand Specimen Description

Colour	**Induration**	**Bedding and Sedimentary Structures**		**Grainsize**
White	Inudrated			Fine to very coarse
Grain or matrix supported	**Sorting**	**Roundness**	**Sphericity - shape**	**Biologic binding**
Grain	Very poor			No
Textural Name:	**Packstone**	**Notes:**	Very fossiliferous.	

Thin Section Description

Matrix	**Percentage /100**
Clastics: Quartz (angular)	Trace
Cement	3%
Mud	15%
Bioclasts	81%
Authigenic minerals: Glauconite (20%), hematite (80%)	1%

Foraminifera	**Percentage /100**
Planktic	6% (n=3)
Benthic	94% (n=49)

Bioclasts	**Percentage of identified/total**
Foraminifera	13%/10%
Bryozoans	70%/53%
Echinoderms	7%/5%
Algae	8%/6%
Molluscs	2%/1%
Brachiopods	0%/0%
Barnacles	0%/0%
Sponge spicules	0%/0%
Worm Tubes	0%/0%
Unidentified bioclasts	25%

Notes from thin section:	Calcite cement forms as a thin blocky rim around echinoids, with some small isopachous cements around and within bioclasts. Glauconite present as very minor intraclast growths. Hematite growth in a few locations, some heavy. Hematite alteration of glauconite. Benthics are coiled (planar, trochospiral), uniserial, and biserial. Tests are mostly microcrystalline, with some hyalines. Shell fragments show borings. Encrusting corraline algae.

Stratigraphic Column: NT10/20

Sample Number: NT10071505 **Location:** Teschemaker

Date Collected: 7/15/10 **Formation:** Ototara Lst

Thin Section Description

Matrix	Percentage /100
Clastics: Quartz (angular), igneous clast (angular)	1%
Cement	3%
Mud	25%
Bioclasts	70%
Authigenic minerals: Glauconite (70%), hematite (30%)	1%

Foraminifera	Percentage /100
Planktic	0% (n=0)
Benthic	100% (n=21)

Bioclasts	Percentage of identified/total
Foraminifera	5%/4%
Bryozoans	88%/70%
Echinoderms	5%/4%
Algae	0%/0%
Molluscs	2%/2%
Brachiopods	0%/0%
Barnacles	0%/0%
Sponge spicules	0%/0%
Worm Tubes	0%/0%
Unidentified bioclasts	20%

Notes from thin section:	Calcite cement as thin overgrowths on echinoid fragments. Some very minor drusy growths around bioclasts. Rounded glauconite grains with some intraclast growth. Hematite alteration on some glauconite. Igneous clast is hematite altered, and mafic. Benthics are coiled (planar, trochospiral), uniserial, and biserial. Tests are microcrystalline with some hyalines.

Stratigraphic Column:	NT10/20		
Sample Number:	NT10071507	**Location:**	Teschemaker
Date Collected:	7/15/10	**Formation:**	Ototara Lst

Hand Specimen Description

Colour	**Induration**	**Bedding and Sedimentary Structures**		**Grainsize**
Yellowish-white	Friable			Fine to medium
Grain or matrix supported	**Sorting**	**Roundness**	**Sphericity - shape**	**Biologic binding**
Grain	Moderate			No
Textural Name:	**Packstone**	**Notes:**	Fossiliferous.	

Thin Section Description

Matrix	**Percentage /100**
Clastics: Igneous clasts (sub-angular)	1%
Cement	7%
Mud	20%
Bioclasts	71%
Authigenic minerals: Glauconite (20%), hematite (80%)	1%

Foraminifera	**Percentage /100**
Planktic	8% (n=1)
Benthic	92% (n=12)

Bioclasts	**Percentage of identified/total**
Foraminifera	7%/7%
Bryozoans	75%/71%
Echinoderms	15%/14%
Algae	1%/1%
Molluscs	2%/2%
Brachiopods	0%/0%
Barnacles	0%/0%
Sponge spicules	0%/0%
Worm Tubes	0%/0%
Unidentified bioclasts	5%

Notes from thin section:	Calcite cement is blocky as both overgrowths on echinoid fragments, as well as intraclast formation, primarily within bryozoan zooecia. One sub-rounded grain of glauconite observed, with some minor and localised hematite alteration in selected locales of the matrix. Benthics are biserial, coiled (trochospiral, planar), and nummulites. Tests are microcrystalline and hyaline, with some larger benthics, including hyaline nummulites. Some tests may have been obscured by the micritic matrix and the large number of bryozoans. Shell fragments show signs of boring. Nearly all bryozoans are branching, but one specimen appears to be encrusting.

Stratigraphic Column:	NT10/20		
Sample Number:	NT10071508	**Location:**	Teschemaker
Date Collected:	7/15/10	**Formation:**	Ototara Lst

Hand Specimen Description

Colour	Induration	Bedding and Sedimentary Structures		Grainsize
Yellowish-white	Indurated			Fine to medium
Grain or matrix supported	**Sorting**	**Roundness**	**Sphericity - shape**	**Biologic binding**
Grain	Poor			No
Textural Name:	**Packstone**	**Notes:**	Bryozoans.	

Thin Section Description

Matrix	Percentage /100
Clastics:	0%
Cement	3%
Mud	12%
Bioclasts	75%
Authigenic minerals: Glauconite (10%), hematite (80%), phosphate (10%)	10%

Foraminifera	Percentage /100
Planktic	6% (n=2)
Benthic	94% (n=33)

Bioclasts	Percentage of identified/total
Foraminifera	15%/13%
Bryozoans	69%/59%
Echinoderms	10%/8%
Algae	0%/0%
Molluscs	6%/5%
Brachiopods	0%/0%
Barnacles	0%/0%
Sponge spicules	0%/0%
Worm Tubes	0%/0%
Unidentified bioclasts	15%

Notes from thin section:	Loose sediment in resin. Calcite cement is commonly isopachous within bioclast voids, with some minor blocky occurences. Rounded glauconite and phosphate grains. Hematite alteration common of matrix and around some bioclasts, and is interspersed throughout the slide as thin vinears. Benthics are discocyclina, uniserial, and coiled (planar, trochospiral). Tests are microcrystalline and hyaline. Some larger hyaline coiled trochospirals. Discocyclina are large. Shell fragments show borings. Bryozoans are fenestrate and branching (mostly the latter). Some pockets of micrite containing many bioclast fragments.

Stratigraphic Column:	NT10/20		
Sample Number:	NT10071509	**Location:**	Teschemaker
Date Collected:	7/15/10	**Formation:**	Ototara Lst

Hand Specimen Description

Colour	**Induration**	**Bedding and Sedimentary Structures**		**Grainsize**
Whitish	Indurated			Fine
Grain or matrix supported	**Sorting**	**Roundness**	**Sphericity - shape**	**Biologic binding**
Grain	Well			No
Textural Name:	**Packstone**	**Notes:**	Fossiliferous.	

Thin Section Description

Matrix	**Percentage /100**
Clastics: Quartz (angular)	Trace
Cement	4%
Mud	20%
Bioclasts	71%
Authigenic minerals: Glauconite (60%), hematite (40%)	5%

Foraminifera	**Percentage /100**
Planktic	9% (n=7)
Benthic	91% (n=71)

Bioclasts	**Percentage of identified/total**
Foraminifera	10%/6%
Bryozoans	72%/42%
Echinoderms	5%/3%
Algae	4%/3%
Molluscs	8%/5%
Brachiopods	1%/1%
Barnacles	0%/0%
Sponge spicules	0%/0%
Worm Tubes	0%/0%
Unidentified bioclasts	40%

Notes from thin section:	Calcite cement is present as slim overgrowths on echinoid fragments, as well as small-scale isopachous cement within bioclasts. Some bryozoan zooecia contain blocky cements. Glauconite grains are rounded sub-angular, with some intraclast growth. Glauconite seems mature and has some hematite alteration. Benthics are coiled (planar, trochospiral), uniserial, and biserial. Tests are mostly microcrystalline, with some hyalines. Algae is encrusting and branching corraline. Appears to be some alignment fabric of bioclasts.

Stratigraphic Column:	NT10/21		
Sample Number:	NT10071901	**Location:**	Ross Farm
Date Collected:	7/19/10	**Formation:**	Ototara Lst

Hand Specimen Description

Colour	**Induration**	**Bedding and Sedimentary Structures**		**Grainsize**
Greenish-white	Friable			Very fine to fine
Grain or matrix supported	**Sorting**	**Roundness**	**Sphericity - shape**	**Biologic binding**
Matrix	Moderate			No
Textural Name:	**Wackestone**	**Notes:**		

Thin Section Description

Matrix	**Percentage /100**
Clastics: Quartz (angular - sub-rounded), minor euhedral biotite	35%
Cement	0%
Mud	35%
Bioclasts	5%
Authigenic minerals: Glauconite	25%

Foraminifera	**Percentage /100**
Planktic	40% (n=8)
Benthic	60% (n=12)

Bioclasts	**Percentage of identified/total**
Foraminifera	95%/48%
Bryozoans	0%/0%
Echinoderms	0%/0%
Algae	0%/0%
Molluscs	5%/2%
Brachiopods	0%/0%
Barnacles	0%/0%
Sponge spicules	0%/0%
Worm Tubes	0%/0%
Unidentified bioclasts	50%

Notes from thin section:	Glauconite grains are rounded to sub-rounded. Benthics are coiled (planar, trochospiral), biserial, and uniserial. Tests are microcrystalline and hyaline. Forams are unusually small, and difficult to identify due to nature of the slide. Possible radiolarian. Unidentified bioclasts are small shell fragments. Appears to have some alignment fabric of clastics.

Stratigraphic Column: NT10/21

Sample Number: NT10071902 **Location:** Ross Farm

Date Collected: 7/19/10 **Formation:** Ototara Lst

Hand Specimen Description

Colour	Induration	Bedding and Sedimentary Structures		Grainsize
Yellowish/white	Friable			Silt to very fine
Grain or matrix supported	**Sorting**	**Roundness**	**Sphericity - shape**	**Biologic binding**
Matrix	Moderate			No
Textural Name:	**Wackestone**	**Notes:**		

Thin Section Description

Matrix	Percentage /100
Clastics: Quartz (angular), some biotite	40%
Cement	0%
Mud	28%
Bioclasts	7%
Authigenic minerals: Glauconite (85%), hematite (15%)	25%

Foraminifera	Percentage /100
Planktic	69% (n=18)
Benthic	31% (n=8)

Bioclasts	Percentage of identified/total
Foraminifera	85%/77%
Bryozoans	0%/0%
Echinoderms	0%/0%
Algae	0%/0%
Molluscs	15%/13%
Brachiopods	0%/0%
Barnacles	0%/0%
Sponge spicules	0%/0%
Worm Tubes	0%/0%
Unidentified bioclasts	10%

Notes from thin section:	Quartz-rich slide, although grains are small. Glauconites are rounded - sub-rounded grains as well as a good proportion of glauconitised biotites, with some grains enclosing quartz grains. Hematite is localised alteration of matrix. Forams that have microcrystalline tests would be very hard to identify in this muddy matrix. This may cause a higher than expected planktic ratio. Coiled benthic tests. Mollusc fragments are bored.

Stratigraphic Column:	NT10/21		
Sample Number:	NT10071904	**Location:**	Ross Farm Kokoamu
Date Collected:	7/19/10	**Formation:**	Greensand

Hand Specimen Description

Colour	**Induration**	**Bedding and Sedimentary Structures**		**Grainsize**
Green	Friable			Fine to medium
Grain or matrix supported	**Sorting**	**Roundness**	**Sphericity - shape**	**Biologic binding**
Grain	Moderate			No
Textural Name:	**Packstone**	**Notes:**	Fossiliferous, glauconitic.	

Thin Section Description

Matrix	**Percentage /100**
Clastics: Quartz (50%), limestone clast (50%)	6%
Cement	Trace
Mud	3%
Bioclasts	16%
Authigenic minerals: Glauconite (94%), hematite (1%), phosphate (5%)	75%

Foraminifera	**Percentage /100**
Planktic	22% (n=12)
Benthic	78% (n=43)

Bioclasts	**Percentage of identified/total**
Foraminifera	35%/23%
Bryozoans	0%/0%
Echinoderms	25%/16%
Algae	0%/0%
Molluscs	40%/26%
Brachiopods	0%/0%
Barnacles	0%/0%
Sponge spicules	0%/0%
Worm Tubes	0%/0%
Unidentified bioclasts	35%

Notes from thin section:	Loose sediment in resin. Large limestone clast is planktic-rich, with some quartz grains, and ~10% glauconite, with a fine micrite matrix and no obvious cements. In the body of this slide the micrite matrix is lower than the actual value due to the inability to preserve it in the resin. The small pockets of matrix show dense micrite between clasts. Glauconite and phosphate grains rounded to sub-rounded. Minor glauconite within foram tests. Glauconite estimates may be high due to low matrix content. Minor hematite alteration of glauconite. Some glauconitised biotites. Benthics uniserial, and coiled (planar, trochospiral). Tests are mostly microcrystalline, with some hyaline. One possible quartz agglutinate benthic. Foram ratios may be skewed due to the nature of the slide and preferential benthic preservation. Shell and echinoid fragments in this slide are very large. Some shells show moderate boring.

Stratigraphic Column:	NT10/21		
Sample Number:	NT10071906	**Location:**	Ross Farm Kokoamu Greensand/Otekaike
Date Collected:	7/19/10	**Formation:**	Lst

Hand Specimen Description

Colour	**Induration**	**Bedding and Sedimentary Structures**		**Grainsize**
Greenish-yellow	Friable			Fine
Grain or matrix supported	**Sorting**	**Roundness**	**Sphericity - shape**	**Biologic binding**
Grain	Well			No
Textural Name:	**Packstone**	**Notes:**		

Thin Section Description

Matrix	**Percentage /100**
Clastics: Quartz, minor biotite	2%
Cement	Trace
Mud	8%
Bioclasts	50%
Authigenic minerals: Glauconite (98%), hematite (2%)	40%

Foraminifera	**Percentage /100**
Planktic	43% (n=55)
Benthic	57% (n=72)

Bioclasts	**Percentage of identified/total**
Foraminifera	65%/20%
Bryozoans	0%/0%
Echinoderms	30%/9%
Algae	0%/0%
Molluscs	5%/1%
Brachiopods	0%/0%
Barnacles	0%/0%
Sponge spicules	0%/0%
Worm Tubes	0%/0%
Unidentified bioclasts	70%

Notes from thin section:	Loose sediment in resin. Small traces of spar cement. Nature of the slide makes matrix estimates difficult. Micrite estimate is probably lower than actual, but was observed in small matrix clusters and one larger clast. Rounded to sub-rounded glauconite grains, with some glauconitised biotites. Some hematite alteration of glauconites, primarily around the edge of a few grains. No observed intraclast growth of glauconite. Benthics are coiled (trochospiral, coiled), uniserial, and biserial. Tests are microcrystalline and hyaline. Shells show some borings. Most unidentified bioclasts are either shell fragments, or so altered as to be indistiguishable.

Stratigraphic Column:	NT10/21		
Sample Number:	NT10071907	**Location:**	Ross Farm
Date Collected:	7/19/10	**Formation:**	Kokoamu-Otekaike

Hand Specimen Description

Colour	**Induration**	**Bedding and Sedimentary Structures**		**Grainsize**
Yellowish-green	Friable			Fine
Grain or matrix supported	**Sorting**	**Roundness**	**Sphericity - shape**	**Biologic binding**
Grain	Well			No
Textural Name:	**Grainstone**	**Notes:**	Glauconite-rich.	

Thin Section Description

Matrix	**Percentage /100**
Clastics: Quartz	1%
Cement	0%
Mud	0%
Bioclasts	19%
Authigenic minerals: Glauconite (98%), phosphate (2%)	80%

Foraminifera	**Percentage /100**
Planktic	20% (n=6)
Benthic	80% (n=24)

Bioclasts	**Percentage of identified/total**
Foraminifera	50%/20%
Bryozoans	2%/1%
Echinoderms	40%/16%
Algae	3%/1%
Molluscs	5%/2%
Brachiopods	0%/0%
Barnacles	0%/0%
Sponge spicules	0%/0%
Worm Tubes	0%/0%
Unidentified bioclasts	60%

Notes from thin section:	Loose sediment in resin. Overwhelmingly glauconitic sample, with all present as well rounded grains and relatively fresh. Some phosphate grains. Benthics are coiled (trochospiral), uniserial, and biserial. Tests are mostly microcrystalline with some hyalines. A few large benthics. One good sized fragment of branching corraline algae. Shell fragments are heavily bored.

Stratigraphic Column:	NT10/21		
Sample Number:	NT10071907a	**Location:**	Ross Farm
Date Collected:	7/19/10	**Formation:**	Kokoamu-Otekaike

Hand Specimen Description

Colour	**Induration**	**Bedding and Sedimentary Structures**		**Grainsize**
Yellowish-green	Friable			Fine
Grain or matrix supported	**Sorting**	**Roundness**	**Sphericity - shape**	**Biologic binding**
Grain	Well			No
Textural Name:	**Grainstone**	**Notes:**		

Thin Section Description

Matrix	**Percentage /100**
Clastics: Quartz (angular - sub-angular), minor biotite	3%
Cement	2%
Mud	5%
Bioclasts	45%
Authigenic minerals: Glauconite (98%), phosphate (2%)	45%

Foraminifera	**Percentage /100**
Planktic	40% (n=50)
Benthic	60% (n=75)

Bioclasts	**Percentage of identified/total**
Foraminifera	40%/20%
Bryozoans	0%/0%
Echinoderms	45%/23%
Algae	0%/0%
Molluscs	15%/7%
Brachiopods	0%/0%
Barnacles	0%/0%
Sponge spicules	0%/0%
Worm Tubes	0%/0%
Unidentified bioclasts	50%

Notes from thin section:	Loose sediment in resin. Some calcite cement formed around echinoid fragments. Nature of slide makes any identification of matrix difficult. Glauconite grains are rounded to sub-rounded. Sub-rounded phosphate grains. Benthics are uniserial, biserial, and coiled (planar, trochospiral). Tests are microcrystalline with some hyalines. Shell fragments commonly show boring.

Stratigraphic Column:	NT10/21		
Sample Number:	NT10071910	**Location:**	Ross Farm
Date Collected:	7/19/10	**Formation:**	Otekaike Lst

Hand Specimen Description

Colour	Induration	Bedding and Sedimentary Structures		Grainsize
Cream-white	Very well indurated			Fine to medium
Grain or matrix supported	**Sorting**	**Roundness**	**Sphericity - shape**	**Biologic binding**
Grain	Moderate			No
Textural Name:	**Packstone**	**Notes:**	Fossiliferous, cemented.	

Thin Section Description

Matrix	Percentage /100
Clastics: Quartz (angular - sub-angular)	3%
Cement	17%
Mud	10%
Bioclasts	60%
Authigenic minerals: Glauconite	10%

Foraminifera	Percentage /100
Planktic	24% (n=35)
Benthic	76% (n=111)

Bioclasts	Percentage of identified/total
Foraminifera	37%/9%
Bryozoans	0%/0%
Echinoderms	55%/14%
Algae	1%/<1%
Molluscs	7%/2%
Brachiopods	0%/0%
Barnacles	0%/0%
Sponge spicules	0%/0%
Worm Tubes	0%/0%
Unidentified bioclasts	75%

Notes from thin section:	Calcite cement formed as blocky textures both as overgrowths on bioclasts (commonly echinoid fragments) as well as inside bioclast void space. Well developed, although not usually in large continuous crystals as there is a lot of material in this slide. Glauconite grains are mostly rounded, with some elongate. Glauconite intraclast growth is also present, although in less numbers than those in grain form. Benthics are uniserial, coiled (planar, trochospiral), uniserial, and milliolid. Tests are microcrystalline and hyaline, with one large uniserial quartz agglutinate. Some larger benthic tests. Fragments of corraline branching algae. Shell fragments show some heavy boring, some infilled with glauconite. Most unidentifed bioclasts are shell fragments.

Stratigraphic Column:	NT10/21		
Sample Number:	NT10071911	**Location:**	Ross Farm
Date Collected:	7/19/10	**Formation:**	Gee Greensand

Hand Specimen Description

Colour	**Induration**	**Bedding and Sedimentary Structures**		**Grainsize**
Greenish-orange	Friable			Fine
Grain or matrix supported	**Sorting**	**Roundness**	**Sphericity - shape**	**Biologic binding**
Grain	Well			No
Textural Name:	**Packstone**	**Notes:**	Weathered, glauconitic.	

Thin Section Description

Matrix	**Percentage /100**
Clastics: Quartz (angular - sub-rounded)	10%
Cement	3%
Mud	20%
Bioclasts	33%
Authigenic minerals: Glauconite, hematite	34%

Foraminifera	**Percentage /100**
Planktic	54% (n=111)
Benthic	46% (n=96)

Bioclasts	**Percentage of identified/total**
Foraminifera	83%/66%
Bryozoans	0%/0%
Echinoderms	7%/6%
Algae	0%/0%
Molluscs	10%/8%
Brachiopods	0%/0%
Barnacles	0%/0%
Sponge spicules	0%/0%
Worm Tubes	0%/0%
Unidentified bioclasts	20%

Notes from thin section:	Loose sediment in resin, with estimates taken from larger clumps within the resin matrix. Some blocky overgrowth on echinoid fragments. Glauconite grains are rounded to sub-rounded with some intraclast growth. Strong hematite alteration of matrix, as well as heavy intraclast hematisation of planktic test chambers. Benthics are uniserial, biserial, and coiled (planar, trochospiral). Tests are microcrystalline with some hyalines, as well as at least one quartz agglutinate. Molluscs are present as bored fragments. Bioclasts are heavily fragmented, although forams are generally intact.

Stratigraphic Column:	NT10/21		
Sample Number:	NT10071912	**Location:**	Ross Farm
Date Collected:	7/19/10	**Formation:**	Gee Greensand

Hand Specimen Description

Colour	**Induration**	**Bedding and Sedimentary Structures**		**Grainsize**
Light brown	Unconsolidated			Fine to silt
Grain or matrix supported	**Sorting**	**Roundness**	**Sphericity - shape**	**Biologic binding**
Matrix	Moderate			No
Textural Name:	**Mudstone**	**Notes:**		

Thin Section Description

Matrix	**Percentage /100**
Clastics: Quartz	2%
Cement	7%
Mud	74%
Bioclasts	5%
Authigenic minerals: Glauconite (60%), hematite (40%)	12%

Foraminifera	**Percentage /100**
Planktic	42% (n=16)
Benthic	58% (n=22)

Bioclasts	**Percentage of identified/total**
Foraminifera	99%/49%
Bryozoans	0%/0%
Echinoderms	0%/0%
Algae	0%/0%
Molluscs	1%/1%
Brachiopods	0%/0%
Barnacles	0%/0%
Sponge spicules	0%/0%
Worm Tubes	0%/0%
Unidentified bioclasts	50%

Notes from thin section:	Loose sediments in resin. Not a good quality slide. Matrix estimation is difficult and values given are only a minimum based on clasts set in resin. Glauconite grains are rounded with a number of them hematised. Benthics are uniserial and biserial with one observed planar coiled. Tests are mostly microcrystalline with a few hyalines. No large benthics. Dense matrix nature of this slide makes accurate bioclast identification difficult.

Stratigraphic Column: NT10/21

Sample Number: NT12070501 **Location:** Ross Farm

Date Collected: 7/5/12 **Formation:** Kokoamu/Otekaike

Thin Section Description

Matrix	Percentage /100
Clastics: Quartz	1%
Cement	4%
Mud	5%
Bioclasts	65%
Authigenic minerals: Glauconite	25%

Notes from thin section:	Blocky cements around bioclasts. Some replacement of echinoid fragments. Glauconite is light green sub-rounded to sub-angular peloids, with common cracking and healing of grains. Intergrown grains. Quartz are angular silt sized. Very broken up section of bioclasts. Difficult to determine types. Mostly forams, mixed planktic:benthic. Some echinoid fragments.

Stratigraphic Column: NT10/21

Sample Number: NT12070504 **Location:** Ross Farm

Date Collected: 7/5/12 **Formation:** Kokoamu/Otekaike

Thin Section Description

Matrix	Percentage /100
Clastics: Quartz	3%
Cement	0%
Mud	0%
Bioclasts	10%
Authigenic minerals: Glauconite (97%), Phosphate (3%)	87%

Notes from thin section:	Very glauconitic slide. Some muddy pellets. Glauconite pelloids contain micaceous angular grains, rounded to sub-rounded peloids with common cracking and intergrowth. Quartz angular and silty. Some porosity. Phosphate grains rounded to sub-angular. Most glauconite grains appear autochthonous. Few echinoid plate fragments. Most bioclasts heavily fragmented.

Stratigraphic Column: NT10/21

Sample Number: NT12070502 **Location:** Ross Farm

Date Collected: 7/5/12 **Formation:** Kokoamu/Otekaike

Thin Section Description

Matrix	Percentage /100
Clastics: Quartz	1%
Cement	Trace
Mud	2%
Bioclasts	12%/95%
Authigenic minerals: Glauconite	85% (in glauconitic section)/ 2% (unglauconitic section)

Notes from thin section:	This slide has a mix of glauconitic and non-glauconitic areas that appear to be actual and not induced by thin sectioning. Glauconite has grown around or bounded by bioclasts. Some cracking of peloids, rounded to sub-rounded, with commong sympathetic boundaries of grains. Bioclasts are heavily broken and reworked.

Stratigraphic Column: NT10/21

Sample Number: NT12070503 **Location:** Ross Farm

Date Collected: 7/5/12 **Formation:** Kokoamu/Otekaike

Thin Section Description

Matrix	Percentage /100
Clastics: Quartz	Trace
Cement	3%
Mud	1%
Bioclasts	81%
Authigenic minerals: Glauconite	15%

Notes from thin section:	Glauconite is often in situ, sympathetic boundaries of peloids. Cracking common. Glaucony is present mostly in one half of the slide. Non-glauconitic side has most of the cement, which occurs around a few bioclasts. Very broken up bioclastic assemblage. Echinoid fragments, forams, appears to be similar amounts of benthics and planktics.

Stratigraphic Column:	NT10/22		
Sample Number:	NT10072101	**Location:**	McCulloch Farm
Date Collected:	7/21/10	**Formation:**	Raki Siltstone

Hand Specimen Description

Colour	**Induration**	**Bedding and Sedimentary Structures**		**Grainsize**
Yellowish-cream	Indurated			Fine
Grain or matrix supported	**Sorting**	**Roundness**	**Sphericity - shape**	**Biologic binding**
Matrix	Well			No
Textural Name:	**Packstone**	**Notes:**		

Thin Section Description

Matrix	**Percentage /100**
Clastics: Quartz (angular)	4%
Cement	0%
Mud	61%
Bioclasts	0%
Authigenic minerals: Glauconite (70%), hematite (30%)	35%

Foraminifera	**Percentage /100**
Planktic	n/a
Benthic	n/a

Bioclasts	**Percentage of identified/total**
Foraminifera	n/a
Bryozoans	n/a
Echinoderms	n/a
Algae	n/a
Molluscs	n/a
Brachiopods	n/a
Barnacles	n/a
Sponge spicules	n/a
Worm Tubes	n/a
Unidentified bioclasts	n/a

Notes from thin section:	Loose sediment clumps in resin. Alignment fabric in matrix. Apparent swirling of matrix around larger glauconite grains. Very heavy hematite alteration through fractures and in some locations of the matrix. Quartz grains are very small and evenly spread through slide. Matrix is a brown micrite (?) mud mix. Glauconite grains appear to form preferential layers, although is still relatively dispersed, and are well-rounded.

Stratigraphic Column:	NT10/22		
Sample Number:	NT10072102	**Location:**	McCulloch Farm
Date Collected:	7/21/10	**Formation:**	Raki Siltstone

Hand Specimen Description

Colour	**Induration**	**Bedding and Sedimentary Structures**		**Grainsize**
Yellowish-brown	Indurated			Very fine to fine
Grain or matrix supported	**Sorting**	**Roundness**	**Sphericity - shape**	**Biologic binding**
Grain	Moderate			No
Textural Name:	**Packstone**	**Notes:**	Highly weathered.	

Thin Section Description

Matrix	**Percentage /100**
Clastics: Quartz angular - sub-angular), minor biotite (euhedral lathes common)	25%
Cement	0%
Mud	45%
Bioclasts	0%
Authigenic minerals: Glauconite	30%

Foraminifera	**Percentage /100**
Planktic	n/a
Benthic	n/a

Bioclasts	**Percentage of identified/total**
Foraminifera	n/a
Bryozoans	n/a
Echinoderms	n/a
Algae	n/a
Molluscs	n/a
Brachiopods	n/a
Barnacles	n/a
Sponge spicules	n/a
Worm Tubes	n/a
Unidentified bioclasts	n/a

Notes from thin section:	Poor slide with significant sections plucked. Significant hematite alteration. Appears to be a lineation fabric within the matrix and quartz grains. Glauconite grains are rounded to sub-rounded and relatively evenly distributed. Some glauconitised biotite. No observed bioclastic material.

Stratigraphic Column:	NT10/22		
Sample Number:	NT10072103	**Location:**	McCulloch Farm
Date Collected:	7/21/10	**Formation:**	Otekaike Lst

Hand Specimen Description

Colour	**Induration**	**Bedding and Sedimentary Structures**		**Grainsize**
Greenish-white	Very well indurated			Fine to granule
Grain or matrix supported	**Sorting**	**Roundness**	**Sphericity - shape**	**Biologic binding**
Grain	Moderate			No
Textural Name:	**Packstone**	**Notes:**	Very fossiliferous, whole shells, sub-rounded to sub-angular lithics. Yellow weathering, and cemented.	

Thin Section Description

Matrix	**Percentage /100**
Clastics: Quartz (sub-rounded - angular) (40%), sedimentary clasts (60%)	7%
Cement	10%
Mud	5%
Bioclasts	43%
Authigenic minerals: Glauconite (90%), hematite (10%)	35%

Foraminifera	**Percentage /100**
Planktic	50% (n=47)
Benthic	50% (n=47)

Bioclasts	**Percentage of identified/total**
Foraminifera	47%/16%
Bryozoans	2%/1%
Echinoderms	42%/15%
Algae	0%/0%
Molluscs	7%/2%
Brachiopods	2%/1%
Barnacles	0%/0%
Sponge spicules	0%/0%
Worm Tubes	0%/0%
Unidentified bioclasts	65%

Notes from thin section:	Weathered fractures. One large and several smaller rounded clasts of quartz-rich glauconitic material (very much like NT10072102 at this site). Calcite cement is blocky as overgrowths on bioclasts, commonly echinoid fragments. Micrite as matrix as well as intraclast in foram tests. Glauconite grains are unevenly disperesed, and range from ~5% - 50% in localised concetrations. Grains are well rounded with fracturing common. Hematite alteration of some fractured glauconite grains. Heavy hematite alteration along post-depositional fractures that cut through glauconite grains. Benthics are uniserial, and coiled (trochosprial, planar). Tests are a mix of microcrystalline and hyaline. A couple of larger hyaline benthics. Matrix partially obscures some tests. Heavy borings on some shell fragments. Echinoid plates and spines.

Stratigraphic Column:	NT10/22		
Sample Number:	NT10072104	**Location:**	McCulloch Farm
Date Collected:	7/21/10	**Formation:**	Otekaike Lst

Hand Specimen Description

Colour	**Induration**	**Bedding and Sedimentary Structures**		**Grainsize**
White with black specks	Very well undurated			Fine
Grain or matrix supported	**Sorting**	**Roundness**	**Sphericity - shape**	**Biologic binding**
Grain	Well			No
Textural Name:	**Packstone**	**Notes:**	Cemented.	

Thin Section Description

Matrix	**Percentage /100**
Clastics: Quartz (angular - sub-angular)	3%
Cement	17%
Mud	10%
Bioclasts	55%
Authigenic minerals: Glauconite (90%), hematite (5%), phosphate (5%)	15%

Foraminifera	**Percentage /100**
Planktic	32% (n=39)
Benthic	68% (n=85)

Bioclasts	**Percentage of identified/total**
Foraminifera	50%/15%
Bryozoans	0%/0%
Echinoderms	30%/9%
Algae	0%/0%
Molluscs	20%/6%
Brachiopods	0%/0%
Barnacles	0%/0%
Sponge spicules	0%/0%
Worm Tubes	0%/0%
Unidentified bioclasts	70%

Notes from thin section:	Calcite cement is blocky spar around bioclasts, mostly echinoid fragments. Some small blocky spar found within bioclasts. Rounded glauconite grains with some intraclast formation within bioclasts. Some minor localised hematite alteration of some larger shell fragments, with some dense alteration around some glauconite grains (including through grain fractures) and their surrounding matrix. Benthics are coiled (planar, trochospiral), uniserial, and biserial. Tests are microcrystalline and hyaline. Some shell fragments show borings. Unidentified bioclasts are either shell fragments or are too highly broken and degraded to identify.

Stratigraphic Column:	NT10/22		
Sample Number:	NT10072105	**Location:**	McCulloch Farm
Date Collected:	7/21/10	**Formation:**	Otekaike Lst

Hand Specimen Description

Colour	Induration	Bedding and Sedimentary Structures		Grainsize
Greenish-white	Indurated			Fine to medium
Grain or matrix supported	**Sorting**	**Roundness**	**Sphericity - shape**	**Biologic binding**
Grain	Moderate			No
Textural Name:	**Packstone**	**Notes:**		

Thin Section Description

Matrix	Percentage /100
Clastics: Quartz (sub-rounded - angular)	5%
Cement	8%
Mud	15%
Bioclasts	57%
Authigenic minerals: Glauconite (87%), hematite (3%), phosphate (10%)	15%

Foraminifera	Percentage /100
Planktic	27% (n=53)
Benthic	73% (n=142)

Bioclasts	Percentage of identified/total
Foraminifera	55%/22%
Bryozoans	0%/0%
Echinoderms	25%/10%
Algae	0%/0%
Molluscs	20%/8%
Brachiopods	0%/0%
Barnacles	0%/0%
Sponge spicules	0%/0%
Worm Tubes	0%/0%
Unidentified bioclasts	60%

Notes from thin section:	Calcite cement is commonly blocky around echinoid fragments. Glauconite grains are rounded to sub-rounded with some fracturing. Some glauconitisation of echinoid fragments, with the centres showing the piont of origin and exhibiting heavier alteration, radiating out to the rims. Phosphate clasts are sub-angular. Hematite alteration of a couple of glauconite grains, and minor alteration of localised matrix. Benthics are coiled (planar, trochospiral), uniserial, and biserial. Tests are microcrystalline and hyaline. A few larger hyaline trochispirals with ribbed test.

Stratigraphic Column:	NT10/22		
Sample Number:	NT10072106	**Location:**	McCulloch Farm
Date Collected:	7/21/10	**Formation:**	Otekaike Lst

Hand Specimen Description

Colour	**Induration**	**Bedding and Sedimentary Structures**		**Grainsize**
Greenish-white	Indurated			Fine to medium
Grain or matrix supported	**Sorting**	**Roundness**	**Sphericity - shape**	**Biologic binding**
Grain	Moderate			No
Textural Name:	**Packstone**	**Notes:**	Shell fragments.	

Thin Section Description

Matrix	**Percentage /100**
Clastics: Quartz (sub-rounded - angular)	5%
Cement	8%
Mud	8%
Bioclasts	59%
Authigenic minerals: Glauconite (98%), hematite (2%)	20%

Foraminifera	**Percentage /100**
Planktic	24% (n=52)
Benthic	76% (n=165)

Bioclasts	**Percentage of identified/total**
Foraminifera	53%/19%
Bryozoans	7%/2%
Echinoderms	30%/11%
Algae	0%/0%
Molluscs	10%/3%
Brachiopods	0%/0%
Barnacles	0%/0%
Sponge spicules	0%/0%
Worm Tubes	0%/0%
Unidentified bioclasts	65%

Notes from thin section:	Calcite cements are blocky around echinoid fragments, and for small drusy textures around and within other clasts. Minor hematite alteration of a few glauconite grains. Glauconite itself forms some intraclast growth, but is mostly rounded to sub-rounded grains (some exhibiting fracturing). Benthics are biserial, uniserial, and coiled (planar, trochospiral). Most are microcrystalline, with some hyalines. Some are larger tests. Large amounts of broken shell material. Small scaphopod.

Stratigraphic Column: NT10/22

Sample Number: NT10072107 **Location:** McCulloch Farm

Date Collected: 7/21/10 **Formation:** Otekaike Lst

Thin Section Description

Matrix	Percentage /100
Clastics: Quartz (sub-rounded - sub-angular)	2%
Cement	25%
Mud	2%
Bioclasts	67%
Authigenic minerals: Glauconite	4%

Foraminifera	Percentage /100
Planktic	26% (n=25)
Benthic	74% (n=70)

Bioclasts	Percentage of identified/total
Foraminifera	55%/14%
Bryozoans	0%/0%
Echinoderms	40%/10%
Algae	0%/0%
Molluscs	5%/1%
Brachiopods	0%/0%
Barnacles	0%/0%
Sponge spicules	0%/0%
Worm Tubes	0%/0%
Unidentified bioclasts	75%

Notes from thin section:	Sparry calcite cement around bioclasts and clastics. Glauconite grains are rounded to sub-rounded, with some glauconite present as intraclast growth within bioclasts. Benthics are coiled (planar, trochospiral), uniserial, and biserial. Tests are microcrystalline and hyaline. One probably fragment of a quartz agglitinate larger benthic test. Unidentified bioclastics are mostly shell fragments.

Stratigraphic Column:	NT10/22		
Sample Number:	NT10072108	**Location:**	McCulloch Farm
Date Collected:	7/21/10	**Formation:**	Otekaike Lst

Hand Specimen Description

Colour	**Induration**	**Bedding and Sedimentary Structures**		**Grainsize**
Yellowish-cream	Friable			Fine
Grain or matrix supported	**Sorting**	**Roundness**	**Sphericity - shape**	**Biologic binding**
Matrix	Well			No
Textural Name:	**Wackestone**	**Notes:**	Fossiliferous inclusion; Bioclasts.	

Thin Section Description

Matrix	**Percentage /100**
Clastics: Quartz (angular - sub-angular)	7%
Cement	5%
Mud	20%
Bioclasts	61%
Authigenic minerals: Glauconite (90%), hematite (10%)	7%

Foraminifera	**Percentage /100**
Planktic	31% (n=46)
Benthic	69% (n=105)

Bioclasts	**Percentage of identified/total**
Foraminifera	64%/32%
Bryozoans	1%/1%
Echinoderms	20%/10%
Algae	0%/0%
Molluscs	15%/7%
Brachiopods	0%/0%
Barnacles	0%/0%
Sponge spicules	0%/0%
Worm Tubes	0%/0%
Unidentified bioclasts	50%

Notes from thin section:	Heavily micritic slide. Calcite cement is blocky as overgrowths on echinoid fragments. Some isopachous cement present on bioclasts. Rounded glauconite grains as well as intraclast growth within bioclasts. Minor hematite alteration. Benthics are biserial, uniserial, and coiled (planar, trochospiral). Tests are microcrystalline and hyaline. Most unidentified bioclasts are small shell fragments.

Stratigraphic Column:	NT10/23		
Sample Number:	NT10072109	**Location:**	Limeworks
Date Collected:	7/21/10	**Formation:**	Otekaike Lst

Hand Specimen Description

Colour	**Induration**	**Bedding and Sedimentary Structures**		**Grainsize**
Greenish-cream	Indurated			Fine
Grain or matrix supported	**Sorting**	**Roundness**	**Sphericity - shape**	**Biologic binding**
Grain	Well			No
Textural Name:	**Packstone**	**Notes:**	Highly fossiliferous (shelly material), fragmented shells aligned to a horizon.	

Thin Section Description

Matrix	**Percentage /100**
Clastics: Quartz (angular), minor biotite	10%
Cement	5%
Mud	15%
Bioclasts	45%
Authigenic minerals: Glauconite	25%

Foraminifera	**Percentage /100**
Planktic	18% (n=36)
Benthic	82% (n=166)

Bioclasts	**Percentage of identified/total**
Foraminifera	53%/37%
Bryozoans	1%/1%
Echinoderms	35%/25%
Algae	0%/0%
Molluscs	10%/7%
Brachiopods	0%/0%
Barnacles	0%/0%
Sponge spicules	0%/0%
Worm Tubes	0%/0%
Unidentified bioclasts	30%

Notes from thin section:	Calcite cement is primarily blocky as overgrowths on what appear to be echinoid fragments predominantly. Commonly fractured, rounded to sub-rounded glauconite grains. Benthics are biserial, uniserial, coiled (planar, trochospiral), and milliolid. Tests are microcrystalline with some hyalines. Shell fragments show some heavy boring.

Stratigraphic Column:	NT10/23		
Sample Number:	NT10072110	**Location:**	Limeworks
Date Collected:	7/21/10	**Formation:**	Otekaike Lst

Hand Specimen Description

Colour	**Induration**	**Bedding and Sedimentary Structures**		**Grainsize**
Greenish-yellow	Friable			Fine
Grain or matrix supported	**Sorting**	**Roundness**	**Sphericity - shape**	**Biologic binding**
Grain	Well			No
Textural Name:	**Packstone**	**Notes:**	Shell fragments.	

Thin Section Description

Matrix	**Percentage /100**
Clastics: Quartz (angular - sub-rounded)	15%
Cement	3%
Mud	12%
Bioclasts	50%
Authigenic minerals: Glauconite (94%), hematite (5%), phosphate (1%)	20%

Foraminifera	**Percentage /100**
Planktic	26% (n=63)
Benthic	74% (n=184)

Bioclasts	**Percentage of identified/total**
Foraminifera	40%/16%
Bryozoans	1%/<1%
Echinoderms	44%/18%
Algae	0%/0%
Molluscs	15%/6%
Brachiopods	0%/0%
Barnacles	0%/0%
Sponge spicules	0%/0%
Worm Tubes	0%/0%
Unidentified bioclasts	60%

Notes from thin section:	Calcite cement observed as blocky, sometimes thin, overgrowths around echinoid fragments. Micrite found as matrix, but also inside foram tests, filling them. Micrite is dense in some locales, while being quite sparse in others. Glauconite grains are commonly rounded, but show a spectrum to sub-angular. Some minor intraclast growth of glauconite, commonly around or along the rims of quartz grains and within foram tests. Some minor hematite alteration of gluaconite grains and localised matrix. One rounded phosphate grain observed. Benthics are uniserial, biserial, and coiled (planar, trochospiral). Tests are a mix of microcrystalline and hyaline, with a few larger hyaline benthics. Some shell fragments show borings. Most unidentified bioclastic material is small and fragmented shells.

Stratigraphic Column:	NT10/23		
Sample Number:	NT10072111	**Location:**	Limeworks
Date Collected:	7/21/10	**Formation:**	Otekaike Lst

Hand Specimen Description

Colour	Induration	Bedding and Sedimentary Structures		Grainsize
Cream with black flecks	Indurated			Fine
Grain or matrix supported	**Sorting**	**Roundness**	**Sphericity - shape**	**Biologic binding**
Grain	Well			No
Textural Name:	**Packstone**	**Notes:**		

Thin Section Description

Matrix	Percentage /100
Clastics: Quartz (angular - sub-angular), minor biotite	5%
Cement	7%
Mud	20%
Bioclasts	53%
Authigenic minerals: Glauconite	15%

Foraminifera	Percentage /100
Planktic	44% (n=121)
Benthic	56% (n=155)

Bioclasts	Percentage of identified/total
Foraminifera	60%/24%
Bryozoans	0%/0%
Echinoderms	30%/12%
Algae	0%/0%
Molluscs	10%/4%
Brachiopods	0%/0%
Barnacles	0%/0%
Sponge spicules	0%/0%
Worm Tubes	0%/0%
Unidentified bioclasts	60%

Notes from thin section:	Calcite cement is found as blocky overgrowths on echinoid fragments. Glauconite grains are rounded to sub-angular. Some intraclast formation of glauconite. Benthics are uniserial, biserial, coiled (planar, trochospiral) and milliolid. Tests are microcrystalline with some hyalines. Glauconitised biotites. Most unidentified bioclasts are shell fragments. Shell fragments show borings.

Stratigraphic Column:	NT10/23		
Sample Number:	NT10072112	**Location:**	Limeworks
Date Collected:	7/21/10	**Formation:**	Otekaike Lst

Hand Specimen Description

Colour	**Induration**	**Bedding and Sedimentary Structures**		**Grainsize**
Greenish-white	Indurated			Fine to medium
Grain or matrix supported	**Sorting**	**Roundness**	**Sphericity - shape**	**Biologic binding**
Grain	Moderate			No
Textural Name:	**Packstone**	**Notes:**	Glauconitic, large shell fragments.	

Thin Section Description

Matrix	**Percentage /100**
Clastics: Quartz (angular - sub-angular)	5%
Cement	20%
Mud	25%
Bioclasts	38%
Authigenic minerals: Glauconite (98%), phosphate (2%)	12%

Foraminifera	**Percentage /100**
Planktic	43% (n=121)
Benthic	57% (n=164)

Bioclasts	**Percentage of identified/total**
Foraminifera	60%/24%
Bryozoans	0%/0%
Echinoderms	35%/14%
Algae	0%/0%
Molluscs	5%/2%
Brachiopods	0%/0%
Barnacles	0%/0%
Sponge spicules	0%/0%
Worm Tubes	0%/0%
Unidentified bioclasts	60%

Notes from thin section:	Calcite cement is primarily blocky around echinoid clasts, with some isopachous cements around and within bioclasts. Glauconite grains are rounded to sub-rounded, with minor intraclast growth. A few rounded phosphate grains. Benthics are uniserial, biserial, and coiled (planar, trochospiral). Tests are mostly microcrystalline with some hyalines. Shell fragments show borings. Most unidentified bioclasts are micritic amorphous fragments, commonly with blocky cement overgrowths.

Stratigraphic Column:	NT10/24		
Sample Number:	NT10072302	**Location:**	Thousand Acre Rd Waiareka-Deborah
Date Collected:	7/23/10	**Formation:**	Volcanics

Thin Section Description

Matrix	Percentage /100
Clastics: igneous clasts and crystals (90%), calcite clast fragments (10%)	97%
Cement	0%
Mud	0%
Bioclasts	3%
Authigenic minerals: Glauconite	0%

Foraminifera	Percentage /100
Planktic	n/a
Benthic	n/a

Bioclasts	Percentage of identified/total
Foraminifera	0%/0%
Bryozoans	100%/100%
Echinoderms	0%/0%
Algae	0%/0%
Molluscs	0%/0%
Brachiopods	0%/0%
Barnacles	0%/0%
Sponge spicules	0%/0%
Worm Tubes	0%/0%
Unidentified bioclasts	0%

Notes from thin section:	Loose tuff sediment in resin. Igneous clasts are weathered with a rind (palagonite?) around most of them. Significant visiculation, with some shattered showing half vesicles. Some mafic crystals (pyroxene). One large bryozoan fragment within the matrix. Fragments of calcite clasts.

Stratigraphic Column:	NT10/24		
Sample Number:	NT10072303	**Location:**	Thousand Acre Rd
Date Collected:	7/23/10	**Formation:**	Veining within tuff deposit (Waiareka-Deborah Volcanics)

Thin Section Description

Matrix	Percentage /100
Clastics: Igneous (50%) and calcite clasts (50%).	97%
Cement	0%
Mud	0%
Bioclasts	3%
Authigenic minerals: Glauconite	0%

Foraminifera	Percentage /100
Planktic	n/a
Benthic	n/a

Bioclasts	Percentage of identified/total
Foraminifera	0%/0%
Bryozoans	100%/100%
Echinoderms	0%/0%
Algae	0%/0%
Molluscs	0%/0%
Brachiopods	0%/0%
Barnacles	0%/0%
Sponge spicules	0%/0%
Worm Tubes	0%/0%
Unidentified bioclasts	0%

Notes from thin section:	Loose sediment in resin. Igneous and blocky calcite clasts. Weathering around the ignous clasts, while the carbonates remain relatively fresh. Some veining within igneous fragments, as well as some vesiculation. Brittle deformation feature within one carbonate clast showing fractured offset of a prominent band. Hematite alteration of mafic clasts.

Stratigraphic Column: NT10/24

Sample Number: NT10072304 **Location:** Thousand Acre Road

Date Collected: 7/23/10 **Formation:** Ototara Lst

Hand Specimen Description

Colour	Induration	Bedding and Sedimentary Structures		Grainsize
Greenish-cream	Indurated			Fine to medium
Grain or matrix supported	**Sorting**	**Roundness**	**Sphericity - shape**	**Biologic binding**
Grain	Moderate			No
Textural Name:	**Packstone**	**Notes:**		

Thin Section Description

Matrix	Percentage /100
Clastics: Quartz, numerous igneous clasts, minor limestone clasts	15%
Cement	15%
Mud	15%
Bioclasts	35%
Authigenic minerals: Glauconite (85%), hematite (10%), phosphate (5%)	20%

Foraminifera	Percentage /100
Planktic	60% (n=134)
Benthic	40% (n=91)

Bioclasts	Percentage of identified/total
Foraminifera	89%/62%
Bryozoans	1%/1%
Echinoderms	2%/2%
Algae	0%/0%
Molluscs	7%/4%
Brachiopods	0%/0%
Barnacles	0%/0%
Sponge spicules	1%/1%
Worm Tubes	0%/0%
Unidentified bioclasts	30%

Notes from thin section:	Limestone fragment contains planktic forams. Igneous clasts are often heavily hematite altered, and contain vesicles. Some of the larger quartz grains are polycrystalline in XPL. Hematite alteration around subgrain rims. Blocky calcite cement forms as matrix. Glauconite grains are rounded, with some showing hematite alteration beginning at the rims. Phosphate clasts are also rounded. Hematite alteration is predominantly on igneous clasts, but is also present on some glauconites. Benthics are coiled (planar), biserial, uniserial, and milliolid. Tests are mostly microcrystalline with some minor hyaline component. Nature of micritic matrix obscures good benthic identification and may skew the ratio in favour of the planktics somewhat more than otherwise would be the case. Shell fragments are commonly heavily bored.

Stratigraphic Column:	NT10/24		
Sample Number:	NT10072305	**Location:**	Thousand Acre Rd
Date Collected:	7/23/10	**Formation:**	Otekaike Lst

Hand Specimen Description

Colour	**Induration**	**Bedding and Sedimentary Structures**		**Grainsize**
Whitish-green	Friable			Fine to medium
Grain or matrix supported	**Sorting**	**Roundness**	**Sphericity - shape**	**Biologic binding**
Grain	Moderate			No
Textural Name:	**Packstone**	**Notes:**		

Thin Section Description

Matrix	**Percentage /100**
Clastics: Quartz (sub-angular-sub-rounded)	3%
Cement	15%
Mud	2%
Bioclasts	45%
Authigenic minerals: Glauconite (78%), hematite (20%), phosphate (2%)	35%

Foraminifera	**Percentage /100**
Planktic	36% (n=38)
Benthic	64% (n=68)

Bioclasts	**Percentage of identified/total**
Foraminifera	56%/22%
Bryozoans	4%/2%
Echinoderms	40%/16%
Algae	0%/0%
Molluscs	0%/0%
Brachiopods	0%/0%
Barnacles	0%/0%
Sponge spicules	0%/0%
Worm Tubes	0%/0%
Unidentified bioclasts	60%

Notes from thin section:	Loose sediment in resin. Calcite cement overgrowths, primarily on echinoid fragments, and small-scale isopachous rims on most other clasts, although not common on glauconites. Glauconite grains are rounded with some intraclast growth. Some clasts and grains show heavy hematite alteration. A few rounded phosphate clasts. Benthics are biserial, coiled (planar, trochospiral), and uniserial. Tests are mostly microcrystalline, with no large benthics. Unidentified bioclasts are small shell pieces.

Stratigraphic Column: NT10/24

Sample Number: NT10072306 **Location:** Thousand Acre Rd

Date Collected: 7/23/10 **Formation:** Ototara Lst

Hand Specimen Description

Colour	Induration	Bedding and Sedimentary Structures		Grainsize
Yellowish-white	Very well indurated			Fine to coarse
Grain or matrix supported	**Sorting**	**Roundness**	**Sphericity - shape**	**Biologic binding**
Grain	Poor			No
Textural Name:	**Packstone**	**Notes:**		

Thin Section Description

Matrix	Percentage /100
Clastics: Quartz (sub-angular - rounded)	1%
Cement	20%
Mud	5%
Bioclasts	64%
Authigenic minerals: Glauconite	10%

Foraminifera	Percentage /100
Planktic	32% (n=37)
Benthic	68% (n=78)

Bioclasts	Percentage of identified/total
Foraminifera	22%/18%
Bryozoans	40%/32%
Echinoderms	35%/28%
Algae	0%/0%
Molluscs	3%/2%
Brachiopods	0%/0%
Barnacles	0%/0%
Sponge spicules	0%/0%
Worm Tubes	0%/0%
Unidentified bioclasts	20%

Notes from thin section:	Calcite cement is blocky. Mud is found only within clast cavities. Glauconite is primarily rounded to sub-rounded grains, with some intraclast growth. Benthics are coiled (trochospiral, planar), biserial, and uniserial, with the trochospiral tests being dominant. Tests are microcrystalline and hyaline, with a few larger benthics present. Some echinoid fragments are well-rounded.

Stratigraphic Column: NT10/24

Sample Number: NT10072307 **Location:** Thousand Acre Road

Date Collected: 7/23/10 **Formation:** Ototara Lst

Hand Specimen Description

Colour	Induration	Bedding and Sedimentary Structures		Grainsize
White with black flecks	Very well indurated			Fine to medium
Grain or matrix supported	**Sorting**	**Roundness**	**Sphericity - shape**	**Biologic binding**
Grain	Moderate			No
Textural Name:	**Packstone**	**Notes:**	Cemented.	

Thin Section Description

Matrix	Percentage /100
Clastics: Quartz (sub-rounded - sub-angular)	2%
Cement	24%
Mud	7%
Bioclasts	44%
Authigenic minerals: Glauconite (80%), hematite (15%), phosphate (3%)	23%

Foraminifera	Percentage /100
Planktic	30% (n=47)
Benthic	70% (n=109)

Bioclasts	Percentage of identified/total
Foraminifera	67%/40%
Bryozoans	8%/5%
Echinoderms	15%/9%
Algae	0%/0%
Molluscs	8%/5%
Brachiopods	0%/0%
Barnacles	0%/0%
Sponge spicules	2%/1%
Worm Tubes	0%/0%
Unidentified bioclasts	40%

Notes from thin section:	Quartz grains are larger than in most samples, being only slightly smaller than most bioclasts. Calcite cements are well formed as matrix and occur as blocky and drusy types around bioclasts and authigentic grains. Glauconites are mature and fresh rounded grains, with only minor intraclast growth. Some smaller glauconitised echinoid fragments. Phosphates are also rounded grains. Hematite is present on some heavily altered glauconite grains. Benthics are coiled (trochospiral, planar), uniserial, milliolid, and biserial. Tests are a mix of microcrystalline and hyaline, and are often relatively large, including a few larger planktics also. One observed radiolarian. Mollusc fragments are often bored. One juvenile gastropod.

Stratigraphic Column:	NT10/25		
Sample Number:	NT10072308	**Location:**	Maheno Cliffs
Date Collected:	7/23/10	**Formation:**	Ototara Lst

Hand Specimen Description

Colour	**Induration**	**Bedding and Sedimentary Structures**		**Grainsize**
Greenish-yellow	Friable			Fine to silt
Grain or matrix supported	**Sorting**	**Roundness**	**Sphericity - shape**	**Biologic binding**
Matrix	Moderate			No
Textural Name:	**Wackestone**	**Notes:**		

Thin Section Description

Matrix	**Percentage /100**
Clastics: Igneous clasts, minor angular quartz	10%
Cement	0%
Mud	40%
Bioclasts	20%
Authigenic minerals: Glauconite (50%), hematite (47%), phosphate (3%)	30%

Foraminifera	**Percentage /100**
Planktic	4% (n=2)
Benthic	96% (n=50)

Bioclasts	**Percentage of identified/total**
Foraminifera	90%/72%
Bryozoans	0%/0%
Echinoderms	7%/6%
Algae	0%/0%
Molluscs	3%/2%
Brachiopods	0%/0%
Barnacles	0%/0%
Sponge spicules	0%/0%
Worm Tubes	0%/0%
Unidentified bioclasts	20%

Notes from thin section:	Very clayey and weathered slide. Ingneous clasts are angular, which are plagioclase-rich and commonly vesiculated. Glauconite is rounded to sub-angular grains, as well as intraclast growth within bioclasts. Hematite alteration very widespread within matrix as well as on glauconite clasts. Few rounded phosphates. Benthics are coiled (planar, trochospiral), uniserial, and biserial. Tests are nearly all microcrystalline. Quartz agglutinate benthics. Unidentified bioclasts are shell fragments.

Stratigraphic Column:	NT10/25		
Sample Number:	NT10072309	**Location:**	Maheno Cliffs
Date Collected:	7/23/10	**Formation:**	Ototara Lst

Hand Specimen Description

Colour	**Induration**	**Bedding and Sedimentary Structures**		**Grainsize**
Yellowish-white	Indurated			Fine to medium
Grain or matrix supported	**Sorting**	**Roundness**	**Sphericity - shape**	**Biologic binding**
Grain	Moderate			No
Textural Name:	**Packstone**	**Notes:**	Bryozoans.	

Thin Section Description

Matrix	**Percentage /100**
Clastics: Igneous clasts (rounded - sub-angular) (98), quartz (angular - sub-angular) (2%)	7%
Cement	8%
Mud	20%
Bioclasts	55%
Authigenic minerals: Glauconite (40%), hematite (60%)	10%

Foraminifera	**Percentage /100**
Planktic	6% (n=2)
Benthic	94% (n=32)

Bioclasts	**Percentage of identified/total**
Foraminifera	10%/8%
Bryozoans	32%/27%
Echinoderms	15%/13%
Algae	20%/17%
Molluscs	15%/13%
Brachiopods	2%/2%
Barnacles	2%/2%
Sponge spicules	0%/0%
Worm Tubes	4%/3%
Unidentified bioclasts	15%

Notes from thin section:	Igneous clasts are mafic and plagioclase-rich, some showing strong vesiculation. Calcite cement is mostly blocky within bioclasts, as well as overgrowth on clasts. Some minor drusy. Micrite mud is commonly seen mixed with cements as matrix, as well as in some bioclast chambers. Glauconite present primarily as intraclast growth, in some cases entirely filling benthic foram chambers. Glauconite grains also present and are rounded. Hematite alteration of matrix is common, and heavy in some locales. Some hematited glauconite. Benthics are coiled (planar, trochospiral), biserial, uniserial, and nummulites. Tests are microcrystalline and hyaline, with some larger benthics. Algae appear to be encrusting and branching coralline red. Bryozoans are branching.

Stratigraphic Column:	NT10/25		
Sample Number:	NT10072310	**Location:**	Maheno Cliffs
Date Collected:	7/23/10	**Formation:**	Ototara Lst

Thin Section Description

Matrix	Percentage /100
Clastics: Igneous clasts (angular - sub-rounded) (70%), quartz (angular) (30%)	5%
Cement	1%
Mud	50%
Bioclasts	24%
Authigenic minerals: Glauconite (80%), hematite (15%), phosphate (5%)	20%

Foraminifera	Percentage /100
Planktic	0% (n=0)
Benthic	100% (n=54)

Bioclasts	Percentage of identified/total
Foraminifera	30%/24%
Bryozoans	55%/44%
Echinoderms	10%/8%
Algae	0%/0%
Molluscs	5%/4%
Brachiopods	0%/0%
Barnacles	0%/0%
Sponge spicules	0%/0%
Worm Tubes	0%/0%
Unidentified bioclasts	20%

Notes from thin section:	Loose sediment in resin. Not a very clear slide as it consists of small sediment clumps that are weathered and micritised. Igneous clasts are commonly plagioclase-rich mafics. Calcite cement is small scale isopachous within some bioclasts. Nature of slide may have removed some cements. Matrix is a mix of micrite mud and clays that look similar to that which was obserbved within diatomites in this area. Glauconite is mostly found as intraclast growth within bioclast void space, as well as some angular to rounded grains. Rounded phosphate grains. Hematite alteration of some matrix and glauconite. Benthics are uniserial, biserial, and coiled (coiled, trochospiral). Tests are mostly microcrystalline with some hyalines. Some larger benthics. One uniserial quartz agglutinate benthic foram.

Stratigraphic Column:	NT10/25		
Sample Number:	NT10072311	**Location:**	Maheno Cliffs
Date Collected:	7/23/10	**Formation:**	Ototara Lst

Hand Specimen Description

Colour	**Induration**	**Bedding and Sedimentary Structures**		**Grainsize**
Greenish-cream	Indurated			Fine to medium
Grain or matrix supported	**Sorting**	**Roundness**	**Sphericity - shape**	**Biologic binding**
Grain	Poor			No
Textural Name:	**Packstone**	**Notes:**		

Thin Section Description

Matrix	**Percentage /100**
Clastics: Quartz (angular) (20%), Igneous clasts (angular - sub-rounded) (80%)	5%
Cement	10%
Mud	10%
Bioclasts	65%
Authigenic minerals: Glauconite (10%), hematite (70%), phosphate (20%)	10%

Foraminifera	**Percentage /100**
Planktic	3% (n=3)
Benthic	97% (n=85)

Bioclasts	**Percentage of identified/total**
Foraminifera	15%/14%
Bryozoans	40%/38%
Echinoderms	15%/14%
Algae	25%/24%
Molluscs	5%/5%
Brachiopods	0%/0%
Barnacles	0%/0%
Sponge spicules	0%/0%
Worm Tubes	0%/0%
Unidentified bioclasts	5%

Notes from thin section:	Igneous clasts are plagioclase-rich (1-2mm) and vesicular. Clacite cement is blocky around echinoids and within bioclast chambers. Some isopachous cement in bryozoan and foram chambers/zooecia. Glauconite intraclast growth with some mature grains. Rounded phosphate grains. Some heavy hematite alteration of glauconite and matrix. Common around igneous clasts. Benthics are biserial, coiled (planar, trochospiral), nummulites, and uniserial. Tests are microcrystalline and hyaline. Large nummulites and trochospiral hyaline benthics. Algae are corraline branching red algae. Shells show some boring. Some mollusc fragments are possible gastropods.

Stratigraphic Column:	NT10/25		
Sample Number:	NT10072312	**Location:**	Maheno Cliffs
Date Collected:	7/23/10	**Formation:**	Ototara Lst

Hand Specimen Description

Colour	**Induration**	**Bedding and Sedimentary Structures**		**Grainsize**
Whitish-grey	Friable			Silt to fine
Grain or matrix supported	**Sorting**	**Roundness**	**Sphericity - shape**	**Biologic binding**
Matrix	Well			No
Textural Name:	**Wackestone**	**Notes:**		

Thin Section Description

Matrix	**Percentage /100**
Clastics:	2%
Cement	0%
Mud	58%
Bioclasts	25%
Authigenic minerals:	15%

Foraminifera	**Percentage /100**
Planktic	16% (n=14)
Benthic	84% (n=75)

Bioclasts	**Percentage of identified/total**
Foraminifera	81%/69%
Bryozoans	15%/12%
Echinoderms	2%/2%
Algae	0%/0%
Molluscs	2%/2%
Brachiopods	0%/0%
Barnacles	0%/0%
Sponge spicules	0%/0%
Worm Tubes	0%/0%
Unidentified bioclasts	15%

Notes from thin section:	Loose sediment in resin. Matrix shows some alignment fabric. Matrix is mix between micrite and clays. Glauconite is both sub-rounded grains and intraclast growth, with hematite alteration of intraclast glauconites and mafic clasts. Benthics are coiled (planar and trochospiral), milliolid, uniserial and biserial. Benthic tests are microcrystalline and hyaline, with some larger tests and a couple of larger agglutinates.

Stratigraphic Column: NT10/25

Sample Number: NT10072313 **Location:** Maheno Cliffs

Date Collected: 7/23/10 **Formation:** Ototara Lst

Hand Specimen Description

Colour	Induration	Bedding and Sedimentary Structures		Grainsize
White	Friable			Silt to fine
Grain or matrix supported	**Sorting**	**Roundness**	**Sphericity - shape**	**Biologic binding**
Matrix	Moderate			No
Textural Name:	**Wackestone**	**Notes:**		

Thin Section Description

Matrix	Percentage /100
Clastics: Quartz, mafic clasts (2 clasts)	2%
Cement	5%
Mud	25%
Bioclasts	62%
Authigenic minerals: Glauconite (85%), hematite (15%)	6%

Foraminifera	Percentage /100
Planktic	3% (n=2)
Benthic	97% (n=59)

Bioclasts	Percentage of identified/total
Foraminifera	15%/10%
Bryozoans	78%/55%
Echinoderms	7%/5%
Algae	0%/0%
Molluscs	0%/0%
Brachiopods	0%/0%
Barnacles	0%/0%
Sponge spicules	0%/0%
Worm Tubes	0%/0%
Unidentified bioclasts	30%

Notes from thin section:	Loose sediment in resin. Glauconite is sub-angular grains with most as intraclast growth. Matrix values are a minimum due to the nature of the slide. Calcite cement is small-scale isopachous inside bioclasts. Benthics are coiled (planar, trochospiral), uniserial and biserial. Some larger coiled benthics. Tests are microcrystalline with some hyaline biserials.

Stratigraphic Column: NT10/25

Sample Number: NT10072314 **Location:** Maheno Cliffs

Date Collected: 7/23/10 **Formation:** Ototara Lst

Hand Specimen Description

Colour	Induration	Bedding and Sedimentary Structures		Grainsize
Yellowish-grey	Friable			Silt
Grain or matrix supported	**Sorting**	**Roundness**	**Sphericity - shape**	**Biologic binding**
Matrix	Well			No
Textural Name:	**Wackestone**	**Notes:**		

Thin Section Description

Matrix	Percentage /100
Clastics: Quartz (very small grains)	4%
Cement	0%
Mud	55%
Bioclasts	37%
Authigenic minerals: Glauconite (40%), hematite (60%)	4%

Foraminifera	Percentage /100
Planktic	18% (n=12)
Benthic	82% (n=56)

Bioclasts	Percentage of identified/total
Foraminifera	20%/17%
Bryozoans	75%/64%
Echinoderms	5%/4%
Algae	0%/0%
Molluscs	0%/0%
Brachiopods	0%/0%
Barnacles	0%/0%
Sponge spicules	0%/0%
Worm Tubes	0%/0%
Unidentified bioclasts	15%

Notes from thin section:	Loose sediments in resin. Muds appear to be a mix of micrite and clay. Matrix estimations are a minimum value and are taken from clast content set in resin. Some alignment fabric observed within the larger clasts. Subrounded to rounded clasts of glauconite, with intraclast growth inside bioclast chambers. Hematite alteration of intraclast glauconites and some matrix alteration. Benthics are coiled (planar and trochospiral), biserial, and uniserial. Tests are microcrystalline with some hyalines. A few larger benthics.

Stratigraphic Column:	NT10/25		
Sample Number:	NT10072315	**Location:**	Maheno Cliffs
Date Collected:	7/23/10	**Formation:**	Ototara Lst

Hand Specimen Description

Colour	**Induration**	**Bedding and Sedimentary Structures**		**Grainsize**
Cream	Indurated			Fine to coarse
Grain or matrix supported	**Sorting**	**Roundness**	**Sphericity - shape**	**Biologic binding**
Grain	Poor			No
Textural Name:	**Packestone**	**Notes:**	Colour change within sample showing a darker horizon along a planar contact. Bryozoan-rich.	

Thin Section Description

Matrix	**Percentage /100**
Clastics: Quartz, one small igneous clast (angular)	Trace
Cement	10%
Mud	15%
Bioclasts	74%
Authigenic minerals: Glauconite (10), hematite (60%), phosphate (30%)	1%

Foraminifera	**Percentage /100**
Planktic	21% (n=6)
Benthic	79% (n=23)

Bioclasts	**Percentage of identified/total**
Foraminifera	5%/5%
Bryozoans	77%/73%
Echinoderms	7%/7%
Algae	10%/9%
Molluscs	1%/1%
Brachiopods	0%/0%
Barnacles	0%/0%
Sponge spicules	0%/0%
Worm Tubes	0%/0%
Unidentified bioclasts	5%

Notes from thin section:	Calcite cement is blocky within most bryozoan zooecia, with some isopachous cements. Significant plucking has occured however. Some localised hematite alteration, one sub-angular phosphate clast, and minor glauconite that has been heavily altered by hematite. Benthics are uniserial, biserial, coiled (planar, trochospiral), and one nummulites. Tests are mostly microcrystalline with a few hyalines. Some are relatively large, including the partly obscured single nummulites.

Stratigraphic Column:	NT10/25		
Sample Number:	NT10072316	**Location:**	Maheno Cliffs
Date Collected:	7/23/10	**Formation:**	Ototara Lst

Hand Specimen Description

Colour	**Induration**	**Bedding and Sedimentary Structures**		**Grainsize**
Cream	Indurated			Fine to medium
Grain or matrix supported	**Sorting**	**Roundness**	**Sphericity - shape**	**Biologic binding**
Grain	Moderate			No
Textural Name:	**Packstone**	**Notes:**	Fossiliferous, bryozoans.	

Thin Section Description

Matrix	**Percentage /100**
Clastics:	Trace
Cement	8%
Mud	17%
Bioclasts	74%
Authigenic minerals:	1%

Foraminifera	**Percentage /100**
Planktic	4% (n=2)
Benthic	96% (n=51)

Bioclasts	**Percentage of identified/total**
Foraminifera	25%/23%
Bryozoans	43%/39%
Echinoderms	15%/13%
Algae	12%/11%
Molluscs	5%/4%
Brachiopods	0%/0%
Barnacles	0%/0%
Sponge spicules	0%/0%
Worm Tubes	0%/0%
Unidentified bioclasts	10%

Notes from thin section:	Calcite cements are blocky overgrowths around echinoid fragments, with isopachous cement within bioclast chambers and rims. Glauconite is intraclast formation, with some hematite alteration of clasts and matrix. Benthics are uniserial, biserial, coiled (planr, trochospiral), and nummulites. Tests are microcrystalline with some hyalines. Nummulites are large and hyaline.

Stratigraphic Column:	NT10/27		
Sample Number:	NT10081702	**Location:**	Otekaieke Settlement
Date Collected:	8/17/10	**Formation:**	Otekaike Lst

Hand Specimen Description

Colour	**Induration**	**Bedding and Sedimentary Structures**		**Grainsize**
Whitish-cream	Friable			Fine
Grain or matrix supported	**Sorting**	**Roundness**	**Sphericity - shape**	**Biologic binding**
Grain	Well			No
Textural Name:	**Grainstone**	**Notes:**		

Thin Section Description

Matrix	**Percentage /100**
Clastics: Quartz (angular-subrounded)	10%
Cement	3%
Mud	<1%
Bioclasts	80%
Authigenic minerals: Glauconite (85%), hematite (10%), phosphate (5%)	7%

Foraminifera	**Percentage /100**
Planktic	35% (n=75)
Benthic	65% (n=143)

Bioclasts	**Percentage of identified/total**
Foraminifera	98%/59%
Bryozoans	0%/0%
Echinoderms	0%/0%
Algae	0%/0%
Molluscs	2%/1%
Brachiopods	0%/0%
Barnacles	0%/0%
Sponge spicules	0%/0%
Worm Tubes	0%/0%
Unidentified bioclasts	40%

Notes from thin section:	Loose sediments set in resin with almost no matrix preserved. Cement is calcite isopachous around and within some clasts, with percentage not representative of original sample. Angular phosphate clasts. Some micrite muds within clasts, although again this is not representative of the original sample due to the nature of the loose sediment. Glauconite is present mostly as rounded grains and quite fresh, with some formation within clasts where hematisation is also found. One radiolarian and one ostracod. Benthics are uniserial, coiled (trochospiral and planar), biserial, and milliolid. Tests are microcrystalline and hyaline.

Stratigraphic Column:	NT10/27		
Sample Number:	NT10081703	**Location:**	Otekaieke Settlement
Date Collected:	8/17/10	**Formation:**	Otekaike Lst

Hand Specimen Description

Colour	**Induration**	**Bedding and Sedimentary Structures**		**Grainsize**
Yellowish-cream	Friable			Fine to silt
Grain or matrix supported	**Sorting**	**Roundness**	**Sphericity - shape**	**Biologic binding**
Grain	Well			No
Textural Name:	**Packstone**	**Notes:**		

Thin Section Description

Matrix	**Percentage /100**
Clastics: Quartz (angular - sub-rounded), minor biotite	10%
Cement	1%
Mud	35%
Bioclasts	34%
Authigenic minerals: Glauconite (70%), hematite (30%)	20%

Foraminifera	**Percentage /100**
Planktic	51% (n=105)
Benthic	49% (n=100)

Bioclasts	**Percentage of identified/total**
Foraminifera	58%/35%
Bryozoans	0%/0%
Echinoderms	10%/6%
Algae	0%/0%
Molluscs	30%/18%
Brachiopods	2%/1%
Barnacles	0%/0%
Sponge spicules	0%/0%
Worm Tubes	0%/0%
Unidentified bioclasts	40%

Notes from thin section:	Loose sediment in resin. A few small occurences of blocky spar cement. Small sub-rounded to rounded grains of glauconite, although most glauconite is present as intraclast growth. Some shows hematite alterations, while others appear to be glauconitised biotites. Benthics are biseriall, uniserial, and coiled (planar, trochospiral). Tests are mostly microcrystalline, with some hyalines. Some tests obscured by the matrix. Shells show some minor boring. Unidentified bioclasts are shell fragments.

Stratigraphic Column:	NT10/27		
Sample Number:	NT10081705	**Location:**	Otekaieke Settlement
Date Collected:	8/17/10	**Formation:**	Otekaike Lst

Hand Specimen Description

Colour	**Induration**	**Bedding and Sedimentary Structures**		**Grainsize**
Yellowish-cream	Friable			Fine to very fine
Grain or matrix supported	**Sorting**	**Roundness**	**Sphericity - shape**	**Biologic binding**
Grain	Well			No
Textural Name:	**Packstone**	**Notes:**	Shell fragments.	

Thin Section Description

Matrix	**Percentage /100**
Clastics: Quartz (subrounded - subangular)	7%
Cement	1%
Mud	20%
Bioclasts	52%
Authigenic minerals: Glauconite	20%

Foraminifera	**Percentage /100**
Planktic	48% (n=104)
Benthic	52% (n=112)

Bioclasts	**Percentage of identified/total**
Foraminifera	88%/35%
Bryozoans	0%/0%
Echinoderms	1%/<1%
Algae	0%/0%
Molluscs	1%/<1%
Brachiopods	9%/4%
Barnacles	0%/0%
Sponge spicules	1%/1%
Worm Tubes	0%/0%
Unidentified bioclasts	60%

Notes from thin section:	Loose sediment set in resin. Mud and cement estimates are based on the sediment shown in the resin without an accompanying matrix, making these estimates a minumum value. Cement is present as small crystals of calcite forming microscale isopachous remants on the interior of foram test chambers. Muds are shown as the matrix within the larger sediment clumps within the resin. Glauconite is both grains (sub-angular to rounded) and intraclast growth, with grains appearing to be dominant. Benthics are coiled (planar, trochospiral), uniserial, milliolid and biserial. Benthic tests are mostly microcrystalline with a few hyalines. One large trochospiral hyaline benthic observed. Punctae on brachoipod fragments. Cross lamina wall-structure observed in a mollusc fragment.

Stratigraphic Column:	NT10/27		
Sample Number:	NT10081706	**Location:**	Otekaieke Settlement
Date Collected:	8/17/10	**Formation:**	Otekaike Lst

Hand Specimen Description

Colour	**Induration**	**Bedding and Sedimentary Structures**		**Grainsize**
Whitish-yellow	Friable			Fine
Grain or matrix supported	**Sorting**	**Roundness**	**Sphericity - shape**	**Biologic binding**
Grain	Well			No
Textural Name:	**Packstone**	**Notes:**		

Thin Section Description

Matrix	**Percentage /100**
Clastics: Quartz (angular - sub-rounded)	7%
Cement	1%
Mud	37%
Bioclasts	40%
Authigenic minerals: Glauconite (60%), hematite (35%), phosphate (5%)	15%

Foraminifera	**Percentage /100**
Planktic	52% (n=111)
Benthic	48% (n=102)

Bioclasts	**Percentage of identified/total**
Foraminifera	91%/55%
Bryozoans	1%/<1%
Echinoderms	3%/2%
Algae	0%/0%
Molluscs	5%/3%
Brachiopods	0%/0%
Barnacles	0%/0%
Sponge spicules	0%/0%
Worm Tubes	0%/0%
Unidentified bioclasts	40%

Notes from thin section:	Micritised slide. Glauconite grains are rounded, but more commonly found as intraclast growth. Often hematised. Some minor blocky cement. Phosphate is minor sub-rounded fragments. Benthics are uniserial, biserial, and coiled (trochosprial, planar). Tests are mostly microcrystalline, with a few hyalines. Micritic matrix makes identification of microcrystalline benthics more difficult. Most unidentified bioclastic material appears to be broken shell fragments from bivalves.

Stratigraphic Column:	NT10/28		
Sample Number:	NT10081801	**Location:**	Meek Rd Quarry
Date Collected:	8/18/10	**Formation:**	Ototara Lst

Hand Specimen Description

Colour	**Induration**	**Bedding and Sedimentary Structures**		**Grainsize**
Cream-white	Indurated			Fine to medium
Grain or matrix supported	**Sorting**	**Roundness**	**Sphericity - shape**	**Biologic binding**
Grain	Moderate			No
Textural Name:	**Packstone**	**Notes:**	Bryozoan-rich.	

Thin Section Description

Matrix	**Percentage /100**
Clastics:	0%
Cement	7%
Mud	7%
Bioclasts	83%
Authigenic minerals: Glauconite (5%), phosphate (15%), hematite (80%)	3%

Foraminifera	**Percentage /100**
Planktic	6% (n=2)
Benthic	94% (n=30)

Bioclasts	**Percentage of identified/total**
Foraminifera	3%/3%
Bryozoans	40%/36%
Echinoderms	12%/11%
Algae	37%/33%
Molluscs	8%/7%
Brachiopods	0%/0%
Barnacles	0%/0%
Sponge spicules	0%/0%
Worm Tubes	0%/0%
Unidentified bioclasts	10%

Notes from thin section:	Calcite cements are blocky overgrowths around echinoid fragments, while being present as small scall isopachous rims within and around other bioclasts. Hematite alteration of localised portions of the matrix. Sub-angular clasts of phosphate, and one observed sub-rounded glauconite grain. Benthics are uniserial, biserial, coiled (planar, trochospiral), and milliolid. Tests are mostly microcrystalline, with a few hyalines. Nature of matrix and bioclasts may obscure some foram observation. Encrusting with some corraline branching algae, attaching to bioclast fragments, in some cases enclosing them. Shell fragments show signs of boring. One probable gastropod.

Stratigraphic Column:	NT10/28		
Sample Number:	NT10081802	**Location:**	Meek Rd Quarry
Date Collected:	8/18/10	**Formation:**	Ototara Lst

Hand Specimen Description

Colour	**Induration**	**Bedding and Sedimentary Structures**		**Grainsize**
Yellowish-white	Indurated			Fine to coarse
Grain or matrix supported	**Sorting**	**Roundness**	**Sphericity - shape**	**Biologic binding**
Grain	Very poor			No
Textural Name:	**Packstone**	**Notes:**	Echinoid plate, bryozoan-rich.	

Thin Section Description

Matrix	**Percentage /100**
Clastics: Quartz. One sub-rounded igneous clast	1%
Cement	8%
Mud	5%
Bioclasts	82%
Authigenic minerals: Glauconite (2%), hematite (94%), phosphate (4%)	4%

Foraminifera	**Percentage /100**
Planktic	15% (n=5)
Benthic	85% (n=28)

Bioclasts	**Percentage of identified/total**
Foraminifera	3%/3%
Bryozoans	55%/49%
Echinoderms	10%/9%
Algae	30%/27%
Molluscs	2%/2%
Brachiopods	0%/0%
Barnacles	0%/0%
Sponge spicules	0%/0%
Worm Tubes	0%/0%
Unidentified bioclasts	10%

Notes from thin section:	Glauconite is only observed as one small grain. Hematite is dispersed throughout the slide at random locations, and is seen to alter matrix in small clusters. Phosphate is seen as a couple of sub-rounded grains, and is altered by hematite. Blocky calcite cement overgrowths around echinoid fragments. Some isopachous rims. Benthics are coiled (planar, trochospiral), and uniserial. Tests are mostly microcrystalline, with some hyaline. Dominant bryozoan assemblage may have obscured some foram observation. Encrusting and branching corraline algae.

Stratigraphic Column:	NT10/28		
Sample Number:	NT10081803	**Location:**	Meek Rd Quarry
Date Collected:	8/18/10	**Formation:**	Ototara Lst

Hand Specimen Description

Colour	**Induration**	**Bedding and Sedimentary Structures**		**Grainsize**
Orangey-brown	Unconsolidated			Clay to fine
Grain or matrix supported	**Sorting**	**Roundness**	**Sphericity - shape**	**Biologic binding**
Matrix	Poor			No
Textural Name:	**Wackestone**	**Notes:**	Echinoid spine.	

Thin Section Description

Matrix	**Percentage /100**
Clastics: Quartz, mafic clasts (1 clast)	1%
Cement	8%
Mud	55%
Bioclasts	30%
Authigenic minerals: Glauconite (5%), hematite (95%)	6%

Foraminifera	**Percentage /100**
Planktic	n/a
Benthic	n/a

Bioclasts	**Percentage of identified/total**
Foraminifera	0%/0%
Bryozoans	5%/4%
Echinoderms	95%/86%
Algae	0%/0%
Molluscs	0%/0%
Brachiopods	0%/0%
Barnacles	0%/0%
Sponge spicules	0%/0%
Worm Tubes	0%/0%
Unidentified bioclasts	10%

Notes from thin section:	Loose sediment in resin. Calcite cements are overgrowths on echinoid fragments. Muds are mix of clays and micrite. There are pockets of clay clasts. Hematite alteration on most of the matrix, with some clasts heavily altered. One pocket of quartz rich clay. Matrix alteration makes identification of forams or other small bioclast fragments difficult.

Stratigraphic Column: NT10/28

Sample Number: NT10081804 **Location:** Meek Rd Quarry

Date Collected: 8/18/10 **Formation:** Ototara Lst

Thin Section Description

Matrix	Percentage /100
Clastics: Quartz (angular-subrounded)(95%), biotite (5%),	50%
Cement	0%
Mud	30%
Bioclasts	0%
Authigenic minerals: Glauconite (15%), hematite (55%), phosphate (30%)	20%

Foraminifera	Percentage /100
Planktic	n/a
Benthic	n/a

Bioclasts	Percentage of identified/total
Foraminifera	n/a
Bryozoans	n/a
Echinoderms	n/a
Algae	n/a
Molluscs	n/a
Brachiopods	n/a
Barnacles	n/a
Sponge spicules	n/a
Worm Tubes	n/a
Unidentified bioclasts	n/a

Notes from thin section:	Loose sediments set in resin. Phosphate, hematite and glauconititic grains, mostly rounded with some more angular. A lot of the hematisation has occured to grains and the matrix, with some very heavily (opaque) altered clasts. Micrite muds are present mostly as matrix within individual sediment grains set in the resin, while most clasts are resin filled with some probable clays and micrite as the matrix.

Stratigraphic Column:	NT10/28		
Sample Number:	NT10081805	**Location:**	Meek Rd Quarry
Date Collected:	8/18/10	**Formation:**	Ototara Lst

Hand Specimen Description

Colour	**Induration**	**Bedding and Sedimentary Structures**		**Grainsize**
White	Friable			Fine to coarse
Grain or matrix supported	**Sorting**	**Roundness**	**Sphericity - shape**	**Biologic binding**
Grain	Poor			No
Textural Name:	**Packstone**	**Notes:**	Fossiliferous, bryozoan-rich.	

Thin Section Description

Matrix	**Percentage /100**
Clastics: Quartz (angular)	1%
Cement	8%
Mud	15%
Bioclasts	72%
Authigenic minerals: Glauconite (10%), hematite (90%)	4%

Foraminifera	**Percentage /100**
Planktic	4% (n=1)
Benthic	96% (n=23)

Bioclasts	**Percentage of identified/total**
Foraminifera	3%/3%
Bryozoans	70%/60%
Echinoderms	10%/8%
Algae	10%/8%
Molluscs	7%/6%
Brachiopods	0%/0%
Barnacles	0%/0%
Sponge spicules	0%/0%
Worm Tubes	0%/0%
Unidentified bioclasts	15%

Notes from thin section:	Quartz clasts, although few in number, appear in small groupings. Calcite cements are blocky overgrowths on echinoid fragments and small-scale blocky formations within bioclast void spaces. Glauconite grains (few in number) are rounded and appear mature. Some minor intraclast growth. Hematite alteration of matrix and bioclasts is localised and dispersed throughout slide. Benthics are coiled (planar, trochospiral), and uniserial. Tests are microcrystalline with some hyalines. Micritic matrix made foram identification and observation difficult. Mollusc fragments show some borings.

Stratigraphic Column:	NT10/28		
Sample Number:	NT10081806	**Location:**	Meek Rd Quarry
Date Collected:	8/18/10	**Formation:**	Ototara Lst

Hand Specimen Description

Colour	Induration	Bedding and Sedimentary Structures		Grainsize
White	Friable			Fine to medium
Grain or matrix supported	**Sorting**	**Roundness**	**Sphericity - shape**	**Biologic binding**
Grain	Moderate			No
Textural Name:	**Packstone**	**Notes:**	Bryozoans.	

Thin Section Description

Matrix	Percentage /100
Clastics: Quartz (angular)	Trace
Cement	7%
Mud	7%
Bioclasts	85%
Authigenic minerals: Glauconite (30%), hematite (70%)	1%

Foraminifera	Percentage /100
Planktic	12% (n=3)
Benthic	88% (n=21)

Bioclasts	Percentage of identified/total
Foraminifera	3%/3%
Bryozoans	55%/52%
Echinoderms	10%/10%
Algae	30%/28%
Molluscs	2%/2%
Brachiopods	0%/0%
Barnacles	0%/0%
Sponge spicules	0%/0%
Worm Tubes	0%/0%
Unidentified bioclasts	5%

Notes from thin section:	Quite micritic slide with plucking common from bioclast void space. Quartz grains only noted in one matrix locality where slide had been plucked and thinned. Calcite cements are blocky as overgrowths on some echinoid fragments, as well as small scale isopachous rims around and within some bioclasts, although plucking appears to have reduced this. One rounded grain of glauconite, with a few spots of isolated hematite alteration on shell fragments. Benthics are uniserial and coiled (planar). Tests are microcrystalline. The nature of the matrix and numerous bryozoans make foram indentification difficult. Algae is mostly encrusting, with some branching corraline.

Stratigraphic Column:	NT10/28		
Sample Number:	NT10081807	**Location:**	Meek Rd Quarry
Date Collected:	8/18/10	**Formation:**	Ototara Lst

Hand Specimen Description

Colour	**Induration**	**Bedding and Sedimentary Structures**		**Grainsize**
White	Indurated			Fine to medium
Grain or matrix supported	**Sorting**	**Roundness**	**Sphericity - shape**	**Biologic binding**
Grain	Moderate			No
Textural Name:	**Packstone**	**Notes:**	Weathering rind. Bryozoans.	

Thin Section Description

Matrix	**Percentage /100**
Clastics:	0%
Cement	10%
Mud	15%
Bioclasts	71%
Authigenic minerals: Glauconite (20%), hematite (80%)	4%

Foraminifera	**Percentage /100**
Planktic	5% (n=1)
Benthic	95% (n=18)

Bioclasts	**Percentage of identified/total**
Foraminifera	5%/3%
Bryozoans	83%/62%
Echinoderms	10%/8%
Algae	1%/1%
Molluscs	1%/1%
Brachiopods	0%/0%
Barnacles	0%/0%
Sponge spicules	0%/0%
Worm Tubes	0%/0%
Unidentified bioclasts	25%

Notes from thin section:	Loose sediments in resin. Poor quality slide as most of the slide is dark and drab. Calcite cement is present as overgrowths on echinoid fragments and as blocky infill and small crystalline rims on most clasts. Due to the nature of this slide being within resin it is only a minimum value given for muds and cements as the matrix is not present in the proper proportions. Hematite appears to only be as a weathering product on mixed composition grains and doesn't appear to be preferentially altering anything in particular. Difficult to determine mud content and foram ratios accuratly due to the nature of the slide. Few subrounded glauconite grains. Benthics are uniserial and coiled (planar and trochospiral). Observed tests are all microcrystalline. Probable encrusting algae, but difficult to confirm.

Stratigraphic Column: NT10/28

Sample Number: NT10081808 **Location:** Meeks Rd Quarry

Date Collected: 8/18/10 **Formation:** Ototara Lst

Thin Section Description

Matrix	Percentage /100
Clastics:	0%
Cement	4%
Mud	30%
Bioclasts	62%
Authigenic minerals: Glauconite (5%), hematite (93%), phosphate (2%)	4%

Foraminifera	Percentage /100
Planktic	0% (n=0)
Benthic	100% (n=25)

Bioclasts	Percentage of identified/total
Foraminifera	9%/6%
Bryozoans	80%/56%
Echinoderms	10%/7%
Algae	2%/1%
Molluscs	1%/<1%
Brachiopods	0%/0%
Barnacles	0%/0%
Sponge spicules	0%/0%
Worm Tubes	0%/0%
Unidentified bioclasts	30%

Notes from thin section:	Loose sediment/sediment clasts in resin. Very micritic slide. Cements are blocky overgrowths on echinoid fragments, with some minor isopachous growths within bryozoan walls. Few rounded glauconite grains, with hematised growths within some bioclasts. Hematite alteration on some sediment clasts' matrix. Angular phosphate clast. Benthics are coiled (trochospiral and planer) and uniserial. Tests are microcrystalline. Due to highly micritic martix it is difficult to identify foram tests. Algae appear to be small fragments of encrusting corraline red algae.

Stratigraphic Column: NT10/28

Sample Number: NT10081809 **Location:** Meek Rd Quarry

Date Collected: 8/18/10 **Formation:** Ototara Lst

Thin Section Description

Matrix	Percentage /100
Clastics: Quartz (angular)	1%
Cement	5%
Mud	4%
Bioclasts	75%
Authigenic minerals: Glauconite (60%), hematite (37%), phosphate (3%)	15%

Foraminifera	Percentage /100
Planktic	10% (n=6)
Benthic	90% (n=52)

Bioclasts	Percentage of identified/total
Foraminifera	18%/7%
Bryozoans	54%/22%
Echinoderms	15%/6%
Algae	10%/4%
Molluscs	3%/1%
Brachiopods	0%/0%
Barnacles	0%/0%
Sponge spicules	0%/0%
Worm Tubes	0%/0%
Unidentified bioclasts	60%

Notes from thin section:	Loose sediments set in resin. Cement and mud estimates are based on that seen with clasts, and will be under what would be seen in outcrop due to the loss of matrix in the uncosolidated sediments seen here. Calcite cements are blocky overgrowths on clasts or small scale isopachous rims around and within some bioclasts. Glauconite is both as intraclast growth and rounded grains, with most appearing fresh and some more fractured and mature. Hematite is alteration of clasts and some localised clast rim matrix, with some very heavy (almost opaque). Phosphate is angular and not very common. Benthics are coiled (trochospiral, planar), and uniserial. Tests are microcrystalline and hyaline, but the nature of the slide makes test identification difficult. Mollusc fragment shows extensive boring. Algae are present as fragments of branching corraline red algae.

Stratigraphic Column:	NT10/28		
Sample Number:	NT10081810	**Location:**	Meek Rd Quarry
Date Collected:	8/18/10	**Formation:**	Ototara Lst

Hand Specimen Description

Colour	**Induration**	**Bedding and Sedimentary Structures**		**Grainsize**
White-cream	Indurated			Fine to medium
Grain or matrix supported	**Sorting**	**Roundness**	**Sphericity - shape**	**Biologic binding**
Grain	Moderate			No
Textural Name:	**Packstone**	**Notes:**	Fossiliferous	

Thin Section Description

Matrix	**Percentage /100**
Clastics:	0%
Cement	5%
Mud	7%
Bioclasts	86%
Authigenic minerals: Glauconite, hematite	2%

Foraminifera	**Percentage /100**
Planktic	4% (n=1)
Benthic	96% (n=24)

Bioclasts	**Percentage of identified/total**
Foraminifera	15%/14%
Bryozoans	35%/33%
Echinoderms	20%/19%
Algae	25%/24%
Molluscs	5%/5%
Brachiopods	0%/0%
Barnacles	0%/0%
Sponge spicules	0%/0%
Worm Tubes	0%/0%
Unidentified bioclasts	5%

Notes from thin section:	Calcite cement is blocky overgrowths on echinoid fragments. Glauconite grains are sub-angular with some hematite alteration. Some hematite alteration in localised matrix. Benthics are coiled (planar, trochospiral), uniserial and biserial. Tests are microcrystalline with some hyalines. Shells show some signs of boring. Algae appear as encrusting red. Bryozoans appear to be all branching.

Stratigraphic Column:	NT10/28		
Sample Number:	NT10081811	**Location:**	Meek Rd Quarry
Date Collected:	8/18/10	**Formation:**	Ototara Lst

Hand Specimen Description

Colour	**Induration**	**Bedding and Sedimentary Structures**		**Grainsize**
White	Indurated			Fine to medium
Grain or matrix supported	**Sorting**	**Roundness**	**Sphericity - shape**	**Biologic binding**
Grain	Moderate			No
Textural Name:	**Packstone**	**Notes:**	Fossiliferous.	

Thin Section Description

Matrix	**Percentage /100**
Clastics: Quartz (angular), igneous clasts (sub-rounded)	1%
Cement	5%
Mud	20%
Bioclasts	67%
Authigenic minerals: Glauconite (35%), hematite (40%), phosphate (25%)	7%

Foraminifera	**Percentage /100**
Planktic	0% (n=0)
Benthic	100% (n=48)

Bioclasts	**Percentage of identified/total**
Foraminifera	26%/22%
Bryozoans	30%/25%
Echinoderms	20%/17%
Algae	20%/17%
Molluscs	3%/3%
Brachiopods	0%/0%
Barnacles	1%/1%
Sponge spicules	0%/0%
Worm Tubes	0%/0%
Unidentified bioclasts	15%

Notes from thin section:	Some plucking of slide. Calcite cements are blocky around echinoid fragments, with some intraclast formation within bioclasts. Mature glauconite intraclast formation. Phosphate intraclast growth within bioclast void space and some rounded grains. Hematite alteration in localised matrix/clast clusters, some very heavy. Benthics are uniserial, coiled (planar, trochospiral), nummulites, biserial, and milliolid. Tests are dominantly microcrystalline, with some hyalines. Some boring on shell fragments. Corraline branching red algae.

Stratigraphic Column:	NT10/28		
Sample Number:	NT10081812	**Location:**	Meek Rd Quarry
Date Collected:	8/18/10	**Formation:**	Ototara Lst

Hand Specimen Description

Colour	**Induration**	**Bedding and Sedimentary Structures**		**Grainsize**
Yellowish-white	Indurated			Fine to medium
Grain or matrix supported	**Sorting**	**Roundness**	**Sphericity - shape**	**Biologic binding**
Grain	Moderate			No
Textural Name:	**Packstone**	**Notes:**	Whole brachiopods.	

Thin Section Description

Matrix	**Percentage /100**
Clastics: Quartz	Trace
Cement	4%
Mud	4%
Bioclasts	77%
Authigenic minerals: Glauconite (35%), hematite (50%), phosphate (15%)	15%

Foraminifera	**Percentage /100**
Planktic	0% (n=0)
Benthic	100% (n=44)

Bioclasts	**Percentage of identified/total**
Foraminifera	15%/7%
Bryozoans	65%/33%
Echinoderms	20%/10%
Algae	0%/0%
Molluscs	0%/0%
Brachiopods	0%/0%
Barnacles	0%/0%
Sponge spicules	0%/0%
Worm Tubes	0%/0%
Unidentified bioclasts	50%

Notes from thin section:	Loose sediment in resin. Determining the amount of mud and cement is difficult with the numbers given a minimum. Calcite cements are blocky overgrowths on echinoid fragments, as well as small fragments attacched to rims and void spaces of clasts. Glauconite grains are mature and fresh, showing rounded to sub-angular clasts as well as intra clast formation. Hematite is mostly as alteration of clasts with some glauconite alteration. Phosphate grains appear to be altered glauconites. Benthics are coiled (trochospiral, planar), uniserial, and milliolid. Tests are microcrystalline, with some larger benthics.

Stratigraphic Column:	NT10/29		
Sample Number:	NT10082101	**Location:**	Devil's Bridge Road
Date Collected:	8/21/10	**Formation:**	Ototara Lst

Hand Specimen Description

Colour	**Induration**	**Bedding and Sedimentary Structures**		**Grainsize**
Yellow-cream	Friable			Silt to fine
Grain or matrix supported	**Sorting**	**Roundness**	**Sphericity - shape**	**Biologic binding**
Grain	Moderate			No
Textural Name:	**Packstone**	**Notes:**		

Thin Section Description

Matrix	**Percentage /100**
Clastics: Quartz (angular)	1%
Cement	5%
Mud	25%
Bioclasts	66%
Authigenic minerals: Glauconite (70%), hematite (20%), phosphate (10%)	3%

Foraminifera	**Percentage /100**
Planktic	12% (n=7)
Benthic	88% (n=52)

Bioclasts	**Percentage of identified/total**
Foraminifera	25%/18%
Bryozoans	43%/30%
Echinoderms	20%/14%
Algae	7%/5%
Molluscs	5%/3%
Brachiopods	0%/0%
Barnacles	0%/0%
Sponge spicules	0%/0%
Worm Tubes	0%/0%
Unidentified bioclasts	30%

Notes from thin section:	Quartz clasts are very small and well dispersed. Calcite cement is blocky as overgrowths on echinoids fragments, with some isopachous rims on bioclasts. Glauconite is present as rounded grains as well intraclast growth within bioclasts, primarily bryozoans. Minor phosphate grains. Hematite alteration of some matrix and glauconite. Benthics are uniserial, coiled (planar, trochospiral), and biserial. Tests are microcrystalline with minor hyalines. Some larger benthics. Borings in some shell fragements.

Stratigraphic Column:	NT10/29		
Sample Number:	NT10082102	**Location:**	Devil's Bridge Road
Date Collected:	8/21/10	**Formation:**	Ototara Lst

Hand Specimen Description

Colour	**Induration**	**Bedding and Sedimentary Structures**		**Grainsize**
Yellow-cream	Friable			Very fine to medium
Grain or matrix supported	**Sorting**	**Roundness**	**Sphericity - shape**	**Biologic binding**
Grain	Moderate			No
Textural Name:	**Packstone**	**Notes:**		

Thin Section Description

Matrix	**Percentage /100**
Clastics: Quartz (angular)	Trace
Cement	5%
Mud	25%
Bioclasts	55%
Authigenic minerals: Glauconite (88%), hematite (10%), phosphate (2%)	15%

Foraminifera	**Percentage /100**
Planktic	14% (n=18)
Benthic	86% (n=111)

Bioclasts	**Percentage of identified/total**
Foraminifera	24%/19%
Bryozoans	35%/28%
Echinoderms	25%/20%
Algae	3%/3%
Molluscs	10%/8%
Brachiopods	3%/3%
Barnacles	0%/0%
Sponge spicules	0%/0%
Worm Tubes	0%/0%
Unidentified bioclasts	19%

Notes from thin section:	Calcite cement is blocky overgrowths around echinoid fragments. Glauconite is found as intraclast growth of both fresh and mature material. Some hematite alteration of glauconite. Benthics are uniserial, biserial, milliolid, and coiled (planar, trochospiral). Tests are microcrystalline and hyaline. Shell fragments show heavy borings.

Stratigraphic Column:	NT10/30		
Sample Number:	NT10082201	**Location:**	Devil's Bridge Wetlands
Date Collected:	8/22/10	**Formation:**	Ototara Lst

Hand Specimen Description

Colour	**Induration**	**Bedding and Sedimentary Structures**		**Grainsize**
Yellowish-white	Indurated			Fine to medium
Grain or matrix supported	**Sorting**	**Roundness**	**Sphericity - shape**	**Biologic binding**
Grain	Moderate			No
Textural Name:	**Packstone**	**Notes:**		

Thin Section Description

Matrix	**Percentage /100**
Clastics: Quartz	Trace
Cement	10%
Mud	5%
Bioclasts	80%
Authigenic minerals: Glauconite (5%), hematite (85%), phosphate (10%)	5%

Foraminifera	**Percentage /100**
Planktic	3% (n=2)
Benthic	97% (n=74)

Bioclasts	**Percentage of identified/total**
Foraminifera	10%/7%
Bryozoans	25%/19%
Echinoderms	30%/23%
Algae	30%/23%
Molluscs	5%/3%
Brachiopods	0%/0%
Barnacles	0%/0%
Sponge spicules	0%/0%
Worm Tubes	0%/0%
Unidentified bioclasts	25%

Notes from thin section:	Quite micritic slide. Calcite cement is blocky around echinoid fragments, while showing isopachous rims within and around a number of other mixed clast types. Very little glauconite present, while hematite forms as alteration on matrix and heavily on some grains. Phosphate is present as rounded grains. Benthics are coiled (planar, trochospiral), uniserial, and biserial. Tests are microcrystalline and hyaline. Micritic nature of the matrix may be obscuring some tests. Shell fragments show signs of boring, and are very disarticulated. One partially intact gastropod.

APPENDIX E - FRED FILES AND REVISED BIOSTRATIGRAPHY

This appendix presents a summary of data gathered from the Fossil Record Electronic Database (FRED) provided by GNS (www.fred.org.nz). The information provided is based on the palaeontological data from the Database, and is arranged by stratigraphic location (Appendix A). It includes the FRED file number, formation, any comments provided on the file, and who collected the samples the file refers to.

Ages given in **bold** were confirmed by author during this study; ages which are italicised were unable to be confirmed and are questionable; all other ages were of recent publication and did not require revision. Age ranges of foraminifera were confirmed or revised using Hornibrook et al. (1989).

Note: Measurements (in the 'Comment' column) are given in both metric and imperial based on their original descriptions.

FRF #	Unit	Comments	Collector (year)	Age	Reference for dating	Revised age
			NT09/01 Waihao			
J40/f0179	Otekaike	5 m below base Takoma Zst.	1993 (Batt)	**Waitakian (25.2-21.7)**		
J40/f0180	Otekaike	10 m below base Tokama Zst. From lens of rich GL material.	1993 (Batt)	**Duntroonian (27.3 - 25.2)**		
J40/f8747	Otekaike	15.2 m above top Waihao Greensand Bed.	1965 (Riddolls)	Waitakian (25.2-21.7)	Scott, G.H.	**Waitakian - Otaian**
J40/f8748	Otekaike	Pinnacle Gully (West and parallel to Mt Harris Rd).	1965 (Riddolls)	Duntroonian - Waitakian (27.3-21.7)	Scott, G.H.	**Waitakian - Otaian**
J40/f8749	Otekaike	Pinnacle Gully (West and parallel to Mt Harris Rd).	1965 (Riddolls)	Waitakian (25.2-21.7)	Scott, G.H.	**Waitakian - Otaian**
J40/f0190	Kokoamu	2 m below resistant Otekaike layer.	1993 (Jones)	Whaingaroan - Duntroonian (34.3-25.2)		
J40/f0191	Kokoamu	1.5 m above first nodular layer in calcareous sandy limestone 14.5 m below base scoured channel cross-bedded limestone.	1993 (Jones)	Duntroonian (27.3-25.2)		
J40/f8750	Otekaike?	24 – 30 m above top Waihao Greensand Bed. Top of limestone escarpment.	1965? (Scott, G.H.)	*Duntroonian? - Waitakian (27.3-21.7)*		
J40/f8752	Otekaike?	4.6 m above top Waihao Greensand Bed.	1965? (Scott, G.H.)	**Whaingaroan - Duntroonian (34.3-25.2)**		

FRF #	Unit	Comments	Collector (year)	Age	Reference for dating	Revised age
NT09/02 Waitaki Rock Art						
I40/f9384	Otekaike		1934 collection	**Waitakian (25.2-21.7)**	ID by Finlay, date unknown	
NT09/03 Earthquakes						
I41/f7547	Kokoamu	Fillings of borings below greensand.	Collector not recorded (1947)	*Duntroonian? (27.3-25.2)*	ID by Finlay, date unknown	
I41/f7548	Ototara	Immediately below bored zone.	Collector not recorded (1947); Hornibrook, date unknown	**Whaingaroan (34.3-27.3)**	ID by Finlay, date unknown	
I41/f7704	Kokoamu	Above bored greensand.	Hornibrook (1986)	Duntroonian (27.3-25.2)		
I41/f7707	Otekaike	From large fallen block.	Hornibrook (1986)	Duntroonian (27.3-25.2)		
I41/f7709	Ototara	2.1 m below top Ototara.	Hornibrook (1965)	**Whaingaroan (34.3-27.3)**		
NT09/04 Landon Creek						
J41/f9527	Kokoamu	0.9 m above top Ototara.	Flemming collection (1947)	Duntroonian (27.3-25.2)	ID by Finlay, date unknown	**Duntroonian - Waitakian**
J41/f9528	Kokoamu		Gage collection (1947)	*Duntroonian (27.3-25.2)*	ID by Finlay, date unknown	
J41/f9530	Ototara	Limestone block from karst contact.	Gage collection (1947)	Whaingaroan-Duntroonian (34.3-25.2)	Finlay ID, date unknown	**Whaingaroan**
J41/f9607	Gee	Underlain by blocky Otekaike Limestone.	Hornibrook (1964)	**Otaian (21.7-19.0)**		
J41/f9509	Ototara	Poor sample.	Gage collection (1947)	Duntroonian - Waitakian (27.3-21.7)	ID Finlay, date unknown	**Waitakian - Altonian (no Duntroonian indicators)**
NT09/06 Gee's Point						
J42/f6558	Kokoamu?	Gl limestone filling borings in Ototara karst	Gage collection (1947)	**Duntroonian - Waitakian (27.3-21.7)**	Finlay ID, date unknown; ID Hornibrook; date unknown	
J42/f6556	Gee	At base of Gee	Gage collection (1947)	**Waitakian (25.2-21.7)**	ID Finlay, date unknown	
NT09/07 Alma						
J41/f8602	Ototara		Gage collection (1947)	Whaingaroan (34.3-27.3)	Hornibrook ID, date unknown	**Kaiatan - Lower Whaingaroan**
NT10/02 Campbells						
J42/f0220	Otekaike	0.2 m above top of Ototara.	Batt (1993)	Waitakian (25.2-21.7)		
J42/f6542	Gee	0.91 m above base Gee.	Gage collection (1947); Hornibrook (1962)	Waitakian (25.2-21.7)	ID Finlay, date unknown	**Waitakian - Otaian**
J42/f6543	Gee	0.61 m above base Gee.	Gage collection (1947)	**Waitakian (25.2-21.7)**	ID Finlay, date unknown	

FRF #	Unit	Comments	Collector (year)	Age	Reference for dating	Revised age
NT10/04 Old Rifle Butts						
J41/f0249	Gee	0.5 m above top of Ototara.	Batt (1993)	No age given		**Early-mid Waitakian**
J41/f8553	Ototara	Matrix of conglomerate immediately above Waiareka tuffs.	Marwick collection (1947); Hornibrook (1961)	*Runangan (36.0-34.3)*	ID Finlay date unknown	**Whaingaroan**
J41/f8554	Ototara	2.74 m above base Ototara.	Gage collection (1947)	Runangan - Whaingaroan (26.0-27.3)	ID Finlay date unknown	**Whaingaroan**
J41/f8797	Gee	Upper part of Greensand.	Marwick collection (1947)	**Otaian (21.7-19.0)**	ID Finlay date unknown	
NT10/06 Awamoko						
J41/f6533	Otekaike?	Marl 4.6 m above top of Waitakian Limestone	Marwick collection (1947)	Waitakian (25.2-21.7)	ID Finlay date unknown	**Waitakian - Otaian**
NT10/16 Forresters						
J41/f8095	Ototara/ Waiareka	From 3 ft above base Waiareka Volcanics; Abundant polyzoa in tuff.	Edwards collection (1966)	Kaiatan (37.0-36.0)	ID Finlay date unknown	**Runangan**
J41/f8096	Oamaru Diatomite	Obvious sponge spicules.	Hornibrook collection (1966)	*Runangan (36.0-34.3)*	ID Hornibrook date unknown	
J41/f8097	Ototara (lower)	0.9 m below top of limestone as exposed; No Planktics.	Edwards collection (1966)	*Whaingaroan (34.3-27.3)*	ID Hornibrook date unknown	
J41/f8994	Ototara?	4.9 m below base Ototara Limestone.	Edwards collection (1965)	Runangan? (36.0-34.3)	ID Hornibrook no date	**Runangan - Whaingaroan**
J41/f8995	Ototara? Diatomite?	0.9 m below base Ototara Limestone.	Edwards collection (1965)	Runangan (36.0-34.3)	ID Hornibrook no date	**Runangan - Whaingaroan**
NT10/17 Bains						
J41/f8092	Ototara	Base of limestone at south end of section	Hornibrook collection (1966)	**Runangan (36.0-34.3)**	ID Hornibrook no date	
J41/f8963	Waiareka	Taken by core, base of section; Good radiolarian.	Edwards collection (1965)	**Runangan (36.0-34.3)**	ID unknown	
J41/f8971	Waiareka; Diatomite?	From trench below limestone scarp. Abundant sponge spicules.	Edwards collection (1965)	Runangan (36.0-34.3)	ID Hornibrook no date	**Upper Porangan - Runangan**
NT10/19 Kakanui						
J42/f0090	Ototara	10m above base Ototara, 3m below exposed; top Ototara.	Hoskins (1982)	Whaingaroan (34.3-27.3)		
NT10/20 Teschemakers						
J41/f8591	Ototara	2 ft above exposed base of limestone.	Gage collection (1947)	**Runangan (36.0-34.3)**	ID Hornibrook no date	

FRF #	Unit	Comments	Collector (year)	Age	Reference for dating	Revised age
			NT10/21 Ross Farm			
J40/f8505	Ototara	2.55 m below base limestone.	Gage collection (1947); Hornibrook no date	Whaingaroan (34.3-27.3)	ID Finlay no date	**Upper Runangan - lower Whaingaroan**
			NT10/23 Limeworks			
I41/f7582	Otekaike	10.7 m above base limestone.	Gage collection (1947)	Waitakian (25.2-21.7)	ID Finlay no datge	**Uppermost Whaingaroan - Pareora Series**
			NT10/24 Thousand Acre Road			
J41/F8944	Otekaike	Just above Deborah Volcanics; Mapped at Ototara by Gage.	Coombs collection (1965)	Duntroonian (27.3-25.2)	ID Hornibrook no date	**Upper Whaingaroan, Duntroonian - Pareora Series**
			NT10/25 Maheno			
J42/f0003	Ototara	Marl overlain by bryozoan Ototara; Maheno Marl.	Nazifral collection (1976)	**Runangan (36.0-34.3)**	No date or author of ID	
J42/f0004	Ototara	Bed immediately overlain by Marl.	Sikumbang (1976)	**Runangan (36.0-34.3)**		
			NT10/27 Otekaieke			
I40/f9538	Otekaike	Gully at rear of special school.	Marwick collection (1947)	**Waitakian (25.2-21.7)**	ID Finlay no date	
I40/F9711	Ototara	150 yards upstream from bridge near special school.	Gage collection (1947)	**Whaingaroan (34.3-27.3)**	ID Hornibrook no date	
			NT10/28 Meeks Road Quarry			
J41/f0081 A	Ototara	Tuffaceous band Weston Quarry, ~1.35 m from top of quarry face. Tuffaceous sediment from volcanic event which occurred during limestone bryozoan reef development.	Collector not recorded	**Runangan (36.0 - 34.3 Ma)**	ID Lamb 1982	
J41/f0081	Ototara	Tuffaceous lens in Totara Limestone in disused Weston Quarry = Thomson's type locality for Stethothyris uttleyi.	Lee collection (1978)	*Runangan (36.0 - 34.3 Ma)*	No ID date	
J41/f8089	Ototara		Gage collection (1947)	Whaingaroan (34.3 - 27.3 Ma)	ID Hornibrook	**Teurian, Kaiatan - Upper Whaingaroan**
J41/f8622	Ototara	Old building-stone quarry, Weston. From tuffaceous brachiopod band.	Gage collection (1947)	Whaingaroan (34.3 - 27.3 Ma)	ID Hornibrook date unknown	**Teurian, Kaiatan - Upper Whaingaroan**

FRF #	Unit	Comments	Collector (year)	Age	Reference for dating	Revised age
J41/f8921	Ototara	Old stone quarry, Weston. 6 inch tuffaceous bed in limestone, with plentiful Stethothyris uttleyi (type locality). Obvious Stethothyris uttleyi (R.S. Allan), polyzoa. Thought to be basal part of limestone as exposed at Jackson's Paddock with S. uttleyi (103) and not exposed at Taylors Quarry. According to Park (Bull. 20:55, 73) is 40 ft of limestone exposed - the brachiopods are from 26 ft above the exposed base (Old Stone Quarry).	Collection Hornibrook (1964)	*Whaingaroan (34.3 - 27.3 Ma)*	ID Hornibrook	
NT10/29 Devil's Bridge Road						
J41/f8666	Ototara		Gage collection (1947)	Kaiatan? (37.0 - 36.0 Ma)	Finlay ID date unknown	**Whaingaroan**
NT10/30 Wetlands						
J41/f8569	Ototara		Collector not recorded (1975?)	*Runangan (36.0 - 34.3 Ma)*		Questionable Runangan.
From collections listed in Gage (1957) associated with the Tapui Glauconitic Sandstone, Raki Siltstone and Rifle Butts Formation						
	Raki Siltstone	All these sample from Gage (1957)	Gage (1957); Finlay, Karrer, Stache, Lalicker, d'Orb, Parr, Reuss	**Kaiatan**		
	Tapui Glauconitic Sandstone	All these sample from Gage (1957); Maheno and Kakanui sites	Finlay; Stache; d'Orb; Reuss	**Bortonian**		
	Rifle Butts Formation	From Gage (1957)	Finlay; Reuss; Cushman; D'Orb	**Altonian**		

APPENDIX F – STABLE ISOTOPE GEOCHEMISTRY

This appendix presents the results from stable isotope geochemistry carried out at the University of Canterbury. For methodology, refer to Chapter 7. Samples NT1-NT9 refer to individual samples of phosphate nodules from Gee's Point locality (NT09/06).

Sample Number	$\delta^{13}C$ (‰V-PDB)	σ	$\delta^{18}O$ (‰V-PDB)	σ
NT1.1	0.70	0.09	2.69	0.09
NT1.2	0.66	0.03	1.98	0.08
NT1.3	0.89	0.10	2.09	0.14
NT1.4	0.86	0.18	2.66	0.32
NT1.5	0.65	0.05	2.15	0.07
Average:	*0.75*	*0.09*	*2.32*	*0.14*
NT2.1	0.04	0.13	1.89	0.21
NT2.2	-0.18	0.11	1.84	0.10
NT2.3	0.05	0.12	2.40	0.20
NT2.4	0.11	0.10	1.77	0.10
NT2.5	0.03	0.12	1.77	0.11
Average:	*0.01*	*0.11*	*1.93*	*0.14*
NT3.1	-0.24	0.07	1.59	0.10
NT3.2	-0.08	0.08	1.72	0.09
NT3.3	-0.41	0.15	2.10	0.16
NT3.4	-0.33	0.06	1.53	0.06
NT3.5	-0.36	0.06	1.72	0.07
Average:	*-0.29*	*0.08*	*1.73*	*0.10*
NT4.1	-0.11	0.10	1.42	0.10
NT4.2	-0.10	0.08	1.87	0.11
NT4.3	-0.09	0.02	1.63	0.05
NT4.4	-0.17	0.02	1.18	0.04
NT4.5	-0.04	0.04	1.81	0.03
Average:	*-0.10*	*0.05*	*1.58*	*0.07*
NT5.1	0.32	0.04	2.00	0.03
NT5.2	0.34	0.07	2.10	0.05
NT5.3	0.41	0.12	1.97	0.14
NT5.4	0.52	0.12	2.13	0.12
NT5.5	0.26	0.08	1.50	0.11
Average:	*0.37*	*0.09*	*1.94*	*0.09*

Sample Number	$\delta^{13}C$ (‰V-PDB)	σ	$\delta^{18}O$ (‰V-PDB)	σ
NT6.1	-0.01	0.10	1.59	0.05
NT6.2	-0.16	0.07	2.09	0.05
NT6.3	-0.28	0.03	1.86	0.03
NT6.4	-0.19	0.06	1.52	0.06
NT6.5	0.13	0.06	2.29	0.06
Average:	*-0.10*	*0.06*	*1.87*	*0.05*
NT7.1	-0.27	0.11	1.30	0.08
NT7.2	-0.47	0.03	1.02	0.02
NT7.3	-0.26	0.07	1.51	0.07
NT7.4	-0.33	0.04	1.44	0.06
NT7.5	-0.39	0.04	2.07	0.02
Average:	*-0.34*	*0.06*	*1.47*	*0.05*
NT8.1	0.39	0.04	2.44	0.03
NT8.2	0.54	0.06	2.06	0.10
NT8.3	0.45	0.04	2.41	0.04
NT8.4	0.39	0.12	2.16	0.11
NT8.5	0.54	0.07	1.86	0.12
Average:	*0.47*	*0.06*	*2.19*	*0.08*
NT9.1	0.60	0.10	1.99	0.12
NT9.2	0.64	0.07	2.51	0.07
NT9.3	0.44	0.10	1.97	0.13
NT9.4	0.62	0.07	2.38	0.10
NT9.5	0.49	0.11	2.37	0.13
Average:	*0.56*	*0.09*	*2.25*	*0.11*